(ISSN 0161-8202)

Journal of ARACHNOLOGY

PUBLISHED BY THE AMERICAN ARACHNOLOGICAL SOCIETY

VOLUME 46 2018 NUMBER 1

The *Journal of Arachnology* (ISSN 0161-8202), a publication devoted to the study of Arachnida, is published three times each year by *The American Arachnological Society*. **Memberships (yearly):** Membership is open to all those interested in Arachnida. A subscription to the *Journal of Arachnology* and annual meeting notices are included with membership in the Society. Regular, $55; Students, $30; Institutional, $125. Inquiries should be directed to the Membership Secretary (see below). **Back Issues:** James Carrel, 209 Tucker Hall, Missouri University, Columbia, Missouri 65211-7400 USA. Telephone: (573) 882-3037. **Undelivered Issues:** Allen Press, Inc., 810 E. 10th Street, P.O. Box 368, Lawrence, Kansas 66044 USA.

Cover photo: Male holotype of *Pseudocellus olmeca* sp. nov., one of two new, sympatric species of *Pseudocellus* Platnick, 1980 described from the state of Veracruz, Mexico. The name is dedicated to the Olmec people, whose civilization flourished in Meso-America from ca. 1500 BCE to 400 BCE. See page 114; photo by Alejandro Valdez-Mondragón.

Publication date: 17 April 2018

♾ **This paper meets the requirements of ANSI/NISO Z39.48-1992 (Permanence of Paper).**

2018. Journal of Arachnology 46:1–6

Aspects of courtship risks and mating success in the dimorphic jumping spider, *Maevia inclemens* (Araneae: Salticidae)

David L. Clark[1], **Lyle A. Simmons**[1,2] and **Richard G. Bowker**[1]: [1]Biology Department, Alma College, Alma, MI 48801, U.S.A., E-mail: clarkd@alma.edu [2]College of Literature, Science, and Arts, University of Michigan, Ann Arbor, MI 48109, U.S.A.

Abstract. The jumping spider *Maevia inclemens* (Walckenaer, 1837) is unusual because there are two male types, tufted (T) and gray (G). We investigated the risks of predation associated with the different courtship strategies by testing the response of the predatory jumping spider *Phidippus audax* (Hentz, 1845) to T and G courtship display, to ascertain if the two morphs were equally noticeable. We then tested the courting responses of T and G in the presence of a conspecific mate and a potential predator (*P. audax*). For the first experiment, we used computer-animation techniques to present two different views of courting males: *face-on* view as a female might see a courting male; and *45°-above* view as may be seen from the perspective of a predator hunting in the vegetation. Visual orientation distance to the courting male images was used as an estimate of predation risk. Results demonstrated that risk of visual detection was not equal for the males; *P. audax* oriented to G at significantly greater distances than to T. From the *45°-above* view, the apparent size of courting G males measured approximately three times greater than that of T males, suggesting that from this point of view, T may be less conspicuous to predators. In our second experiment, T and G responded differently when courting a conspecific female if a live predator had recently been or remained in view of the male. Fewer G males courted than T males and the courtship latency was significantly longer for G than for T. The visibility of T and G males to both females and potential predators may help to understand how these different, but equally successful, courtship strategies are maintained.

Keywords: Predation risk, predator attraction, male dimorphism, video playback, computer animated stimuli

Male courtship displays have evolved to attract female attention and this can ultimately lead to successful mating (Darwin 1871; Andersson 1994; Busso & Rabosky 2016). However, the obvious benefits of courtship are not without risk. Conspicuous male displays and coloration may be energetically costly, attract predators, or reduce opportunities for escape from hungry conspecific females (Moodie 1972; Haas 1976; Daly 1978; Burk 1982; Gwynne 1989; Lima & Dill 1990; Magnhagen 1991; Candolin & Voigt 1998; Fowler-Finn & Hebets 2011; Marshall et al. 2015; Clark et al. 2016). Courting males of some species may reduce how detectable they are to a potential predator by decreasing the intensity of their courtship display (Hastings 1991; Fuller & Berglund 1996), or switching to alternative reproductive strategies (Cade 1979; Lloyd 1984; Godin 1995). For very small species such as spiders, conspicuous male displays seem particularly risky. Clark et al. (2016) found that courting male wolf spiders *Schizocosa ocreata* (Hentz, 1844) have a higher risk of visual detection by predatory toads than do non-courting (walking) males. In jumping spiders (Salticidae), Bulbert et al. (2015) demonstrated that female *Cosmophasis umbratica* Simon, 1903 are more attracted to males that reflect UV; however, the predatory jumping spider *Portia labiata* (Thorell, 1887) uses UV reflectance to cue in on prey, putting UV attractive males at higher risk of predation.

Species exhibiting polymorphism, or the presence of at least two variants within a population, are relatively common in nature (Gray & McKinnon 2007). Polymorphic species can be useful for investigating the evolution of male traits because different selection pressures are likely to have favored the different male variants within the population (Clark & Morjan 2001). Here, we explore how predation risk may have influenced the evolution of different courtship displays in the dimorphic jumping spider, *Maevia inclemens* (Walckenaer, 1837).

Maevia inclemens is an unusual jumping spider (Salticidae) because there are two male morphs that are strikingly distinct not only in morphology but also in courtship behavior (Clark 1994). The tufted (T) male morph has a black body, three rows of setae on the anterior cephalothorax, black pedipalps and white legs. After orienting to the female, the T male generally begins courting by standing up in place, assuming a stilting posture approximately 9 cm from her. He then begins wagging his abdomen side-to-side and simultaneously waving the first pair of legs back and forth vigorously towards her. The gray (G) male morph lacks the tufts but has a white stripe above the eyes; the body and legs are striped and the pedipalps are bright orange in color. The G male initiates courtship much closer to the female (about 3 cm) by lowering his body to the substratum, pointing the first two pair of walking legs forward in a triangle-like configuration, and sidling back and forth (Clark & Uetz 1993; Clark 1994). Although males differ dramatically in behavior and morphology, a receptive female generally mates with the first male that attracts her attention without preferring one male type over the other (Clark & Uetz 1992).

Although we still do not understand the selection pressures that produced two completely different male strategies for female attraction (see Busso & Rabosky 2016 for a recent review), cannibalistic predation pressure from females may have been important in the evolution of the male dimorphism for *M. inclemens*. In a study testing female *M. inclemens* attraction to male courtship behavior, Clark & Morjan (2001) found a trade-off between the benefits of attracting her attention at a distance and initiating courtship in close proximity to the female. Whereas T males have the advantage of female attraction at greater distances than G males, T males

courting within 4 cm of the female experienced a higher risk of attack than the G males courting within the same proximity. These results support the hypothesis that predation pressure from cannibalistic females may impose different risks for the dimorphic males.

These small male spiders live in a world of multiple predation risks, including conspecific females, heterospecific spiders and other predatory invertebrates and vertebrates. However, it is still unknown if the different courtship displays also attract the attention of nearby predators. Might a predatory spider respond differently to these displaying males, and conversely might the males alter their behaviors when they sense a nearby threat? If male courtship display reduces effort or increases the success of attracting a female, the cost of courtship display can be measured by the conspicuousness to predators and the alteration of behavior in response to a potential predator. To explore how the risk of predation may have selected for different courtship behaviors in *M. inclemens,* we used a two-fold approach. First, we examined the responses of a predatory heterospecific jumping spider, *Phidippus audax* (Hentz, 1845), to courting male *M. inclemens* (both T & G) to determine if the male morphs were equally attractive to the predator. Second, we explored the influences of the presence of a predatory spider on the courting activities of male *M. inclemens* (both T & G).

METHODS

Mature male and female *M. inclemens* and mature female *P. audax* were collected by hand and sweep net in May–June of 1995 in southwestern Ohio, at the Cincinnati Nature Center in Clermont Co., OH, U.S.A. The daring or bold jumping spider, *P. audax* (Araneae: Salticidae), is a known araneophagic species (Edwards & Jackson 1993) and was chosen as the potential predator for this study because they occur sympatrically with *M. inclemens* and have been seen to prey upon them in the field (Clark, unpublished data). All spiders were maintained in the laboratory at Alma College, housed in circular plastic deli containers measuring 12 cm (diam) x 4 cm (height). A diet of domestic crickets, *Acheta domesticus* (Linnaeus, 1758), obtained from Flukers Cricket Farm (Portland, LA) and fruit flies (*Drosophila* sp.) cultured at Alma College was provided weekly, and water was available *ad libitum*. Voucher specimens of *M. inclemens and P. audax* are on deposit at University of Cincinnati and Alma College. To ensure that the predators were hungry and therefore more likely to respond to prey, each *P. audax* was food deprived for two days prior to being used in an experiment. All *P. audax* used throughout these experiments were adult and similar in size. Since male jumping spiders rarely court heterospecifics and since salticids are known to respond appropriately to computer-animated stimuli (hereafter CAS) (Clark & Uetz 1990, 1992, 1993), female *P. audax* were shown CAS sequences of each male morph (T and G) performing its morph-specific phase I courtship display (see Clark 1994). Specifically, both face-on and 45°-above view CAS were created of courting T and G males, for a total of four stimuli to be shown to the predator test subjects (see video S1 Gray-3D, online at http://dx.doi.org/101636/JoA-S-16-029.s1 and video S2 Tuft-3D, online at http://dx.doi.org/101636/JoA-S-16-029.s2). Although similar in physical size, when T and G court they assume different postures and initiate courtship at different distances from the female. The T male stands up, making himself appear as large as possible, but courts further from the female. The G male crouches, minimizing his apparent size, and courts more closely to the female. At their morph-specific courting distance, they present essentially the same size visual image (=visual target area) to the female (see Clark & Uetz 1993).

Construction of computer-animated courtship displays.—*Face-on computer-animated stimuli (CAS):* Face-on CAS were constructed by digitizing raw video footage of courting males of T and G morphs in phase I courtship display (see Clark & Uetz 1990, 1992, 1993 for details on constructing and appropriately sizing video stimuli). Each CAS sequence was standardized by placing the courting male against a plain background (Pantone 312 CVU), and then set to the mean movement rate of live courting males: T morph ($n = 8$): leg waves, $\bar{X} = 10.37$/sec, $SD = 1.7$; abdominal swings, $\bar{X} = 2.5$/sec, $SD = 0.75$; pedipalp waves, $\bar{X} = 4.3$/sec, $SD = 1.1$; G morph ($n = 8$): sidle back and forth, $\bar{X} = 14.25$ mm/sec, $SD = 3.1$. The individual video frames were sequenced into a QuickTime movie loop with pixel dimensions of 640 (w) x 480 (h) and a frame rate of 29.97 frames per second. Each CAS was then downloaded to a Panasonic AG-1970 videocassette recorder (VCR) and stored on separate S-VHS tapes. Finally, the courting male CAS were presented life-size on a Sony Watchman (FDL 310) mini-television.

45°-above view computer-animated stimuli: Since a predatory spider may be hunting in the vegetation somewhere above the courting male, we constructed 3-dimensional CAS that simulated the view a predator would see from a 45° angle above the T and G morphs performing phase I courtship displays. These life-size animations were created using Swivel 3D Professional (v 2.0.4) by first building a 3-D skeleton over raw video footage of courting males and then superimposing digital "skins" on the skeleton. The "skins" used color patterns derived from photos of live T and G males. Morph-specific postures and movements (set to the average display movements described above for the *Face-on* CAS) were animated and then rotated to create the 45°-above view CAS.

Visual target area.—Although the T and G males are similar in absolute size, both their courting postures (stilting or body-lowered) as well as the angle from which they are viewed (*Face-on* and *45°-above*) change their apparent sizes (i.e., the visual target area). The CAS were carefully scaled to reflect these morph-specific differences. The visual target area was estimated from digital still photographs of courting males using NIH Image (v 1.59) (Fig. 1). Eight different males of each morph were photographed in a slightly different position of their morph-specific phase I courtship display. Using NIH Image and a mm ruler size standard, the perimeter of each male was traced and the visual target area of the image was estimated. To be consistent, eight different positions of the 3D computer-animated male stimuli were digitally "captured" using the camera snapshot mode in Swivel and the area was estimated from jpeg pictures using NIH Image.

Experiment I: Predator attraction to male *M. inclemens* morph-specific courtship behaviors.—*Predator to prey orientation distance:* Ten female predators (*P. audax*) were randomly assigned to view each of the four stimuli ($n = 40$ trials). All

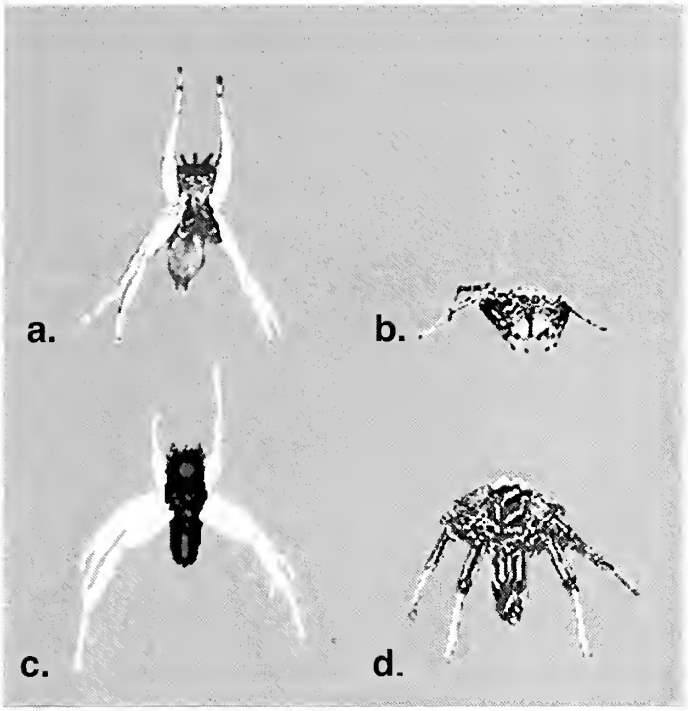

Figure 1.—Views of the video stimuli used to test predator orientation response: face-on view (a) tufted morph phase I courtship posture; (b) gray morph phase I courtship posture; 45°-view (c) tufted morph; (d) gray morph.

trials were videotaped from above using a Panasonic HD 5100HS video camera and recorded on a VCR. Each *P. audax* (predator) was scored for the furthest distance at which it oriented to the courting male *M. inclemens* stimulus.

Spiders were placed in a covered rectangular plastic viewing container measuring 5.3 cm (l) x 4.1 cm (w) x 2.7 cm (h) with a thin glass front (0.6 mm). To present the video stimuli to the test subjects, a Sony Watchman (FDL-310) television was fixed to one end of a 75 cm long runway that was marked off in 1 cm increments. The spider was placed on the runway outside of its visual response range of the stimulus (60 cm). The CAS was then started and the cover of the viewing container was removed. The test spider was given one minute to visually orient to the CAS. If no response occurred within the allotted time, the cover was replaced and the viewing container was moved closer to the CAS in 10 cm increments. When a visual orientation did occur, the viewing container was covered, moved back 10 cm, then uncovered again and moved ahead incrementally 1 cm at a time until visual orientation occurred. This technique allowed us to determine the maximum visual orientation distance (to the nearest cm).

Experiment II: Male *M. inclemens* courtship while in the presence of a potential predator.—Three experimental treatments were designed to determine how the presence of a potential predator might influence the initiation of courtship behavior for male T and G *M. inclemens*: (a) control—no predator present; (b) visual exposure to the predator for three minutes followed by removal of the predator from view; and (c) sustained visual exposure to the predator.

An arena measuring 20 cm (l) x 8 cm (w) x 4 cm (h) with removable partitions on either side of the middle compartment was constructed. The middle compartment (compartment B) was separated from the end compartments (A and C) by 0.6-mm glass and the inner walls were lightly coated with petroleum jelly to prevent the spiders from escaping. To elicit courtship behavior, a female *M. inclemens* was anesthetized with CO_2, affixed to a cardboard strip using non-toxic wax adhesive and placed in the center of compartment A of the arena. A total of five females were used as stimuli and were released unharmed after the experiments were conducted. For the predator, 10 different adult female *P. audax* were used throughout these experiments. Fifteen males of each morph were randomly assigned to one of the three experimental treatments (T, $n = 45$; G, $n = 45$); males were tested one time and not repeated throughout the experiment. For all treatments, the *M. inclemens* female was placed in compartment A, the *M. inclemens* male (either T or G morph) was placed in compartment B and the predator (*P. audax*) was placed in compartment C. In compartment B, the paper was changed between each new male tested. The number of males that courted and the courtship latency (= time to initiate courtship once the male visually oriented to the female) was recorded for each experimental treatment.

Treatment 1 (control): A female was placed in the center of compartment A behind a partition and a male was placed in compartment B. After a three-minute acclimation period, the partition was removed and the male courtship behavior was scored.

Treatment 2: A female was placed in compartment A behind the partition, the male was placed in compartment B and a predator was placed in compartment C. The experiment began by removing the partition between compartments of the male (B) and the predator (C), so that the predator was in full view of the male. After three minutes, the partition between B and C was lowered and the partition between the male and the female was raised.

Treatment 3: The procedure was the same as treatment 2, except the partition between the male and predator remained open so that the predator was in full view of the male at all times. After three minutes, the partition between A and B was removed and courtship was scored. For all treatments, males were given a maximum of five minutes to respond.

RESULTS

Experiment I: Predator attraction to male *M. inclemens* morph-specific courtship behaviors.—*Predator-prey orientation distance:* The predator, *P. audax*, visually oriented to the face-on view of the G male at a significantly greater distance than to the face-on view of the T male ($\bar{X} \pm$ SE: G = 21.7 cm ± 0.51; T = 12.5 cm ± 0.67; *t*-test: $t_{18} = 10.85$; $P < 0.0001$; Fig. 2). Likewise, the predator visually oriented to the 45°-view of the G male at a significantly greater distance than to the 45°-view of the T male ($\bar{X} \pm$ SE: G = 35.7 cm ± 1.63; T = 12.8 cm ± 0.61; *t*-test: $t_{18} = 13.13$; $P < 0.0001$; Fig. 2). The predator also responded to the 45°-above view of G at greater mean distances compared to the face-on view of the G male (*t*-test: $t_{18} = 8.17$; $P < 0.0001$; Fig. 2). However, when the mean response distance to the face-on view of T was compared to the 45°-view of T, mean predator orientation distances did not differ significantly (*t*-test: $t_{18} = 0.33$, NS; Fig. 2).

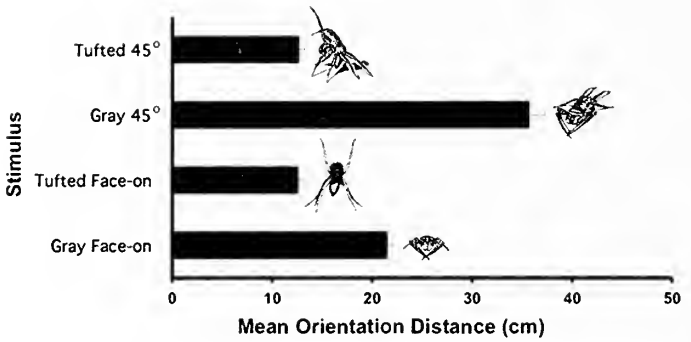

Figure 2.—Mean orientation distance of the predator *P. audax* in response to face-on and 45° views of *M. inclemens* male courtship behavior.

Experiment II: Male *M. inclemens* courtship while in the presence of a potential predator.—*Treatment 1 (control – no predator present):* The number of T and G males that courted (T = 13 (87%); G = 14 (93%)) did not differ in control treatment 1 (chi square test: $\chi^2_1 = 0.037$, NS; Fig. 3a). The numbers of males that courted in treatments 2 and 3 were compared to the number of similar males that courted in the control treatment 1.

Treatment 2 (3-minute visual exposure to predator, then removal of predator from view): The number of courting T males in treatment 2 did not differ significantly from controls (T = 6 (46%): chi square test: $\chi^2_1 = 2.5$, NS; Fig. 3a). However, the number of G males that courted was significantly lower than the controls (G = 3 (21%); chi square test: $\chi^2_1 = 7.1$, $P < 0.008$; Fig. 3a).

Treatment 3 (3-minute visual exposure to the predator, predator remains in view): The number of T males that courted in treatment 3 was significantly lower than the number of T males that courted in the controls (T = 4 (30%): chi square test: $\chi^2_1 = 4.7$, $P < 0.03$; Fig. 3a). Likewise, the number of G males that courted in treatment 3 was significantly lower than the number of G males that courted in the controls (G = 2 (14%); chi square test: $\chi^2_1 = 9.0$, $P < 0.003$; Fig. 3a).

Courtship latency time: For treatment 1 (no exposure to a potential predator), there was no significant difference in the latency time to courting of T and G after visually orienting to the female ($\bar{X} \pm$ SE: T = 5.3 sec ± 0.97; G = 5.5 sec ± 0.88; t-test: $t_{25} = 0.08$, NS; Fig. 3b). For treatment 2 (3-minute exposure to the predator, predator not in view), there was a significant difference in courtship latency between T and G males ($\bar{X} \pm$ SE: T = 33.0 sec ± 1.9; G = 51 sec ± 2.8; *t*-test: $t_7 = 5.08$, $P < 0.01$; Fig. 3b). Likewise, for treatment 3 (3-minute exposure to the predator, predator remains in view) the courtship latency was significantly longer for G males than it was for T males ($\bar{X} \pm$ SE: T = 27.25 sec ± 2.8; G = 41.5 ± 4.5; *t*-test: $t_4 = 2.78$, $P < 0.05$; Fig. 3b).

Prey visual target sizes.—By altering posture, the males can make themselves appear larger or smaller. To explore how this may influence the predator's responses, the visual target areas of the males in the different stimuli were compared. There was no significant difference between the mean areas of the face-on view of the T morph and the 3-dimensional 45°-view of the T morph ($\bar{X} \pm$ SE: T face-on = 21.04 ± 0.53; 45° = 21.48 ± 0.2; *t*-test: $t_8 = 0.76$; NS; Fig. 1a, c). However, the area of the face-on

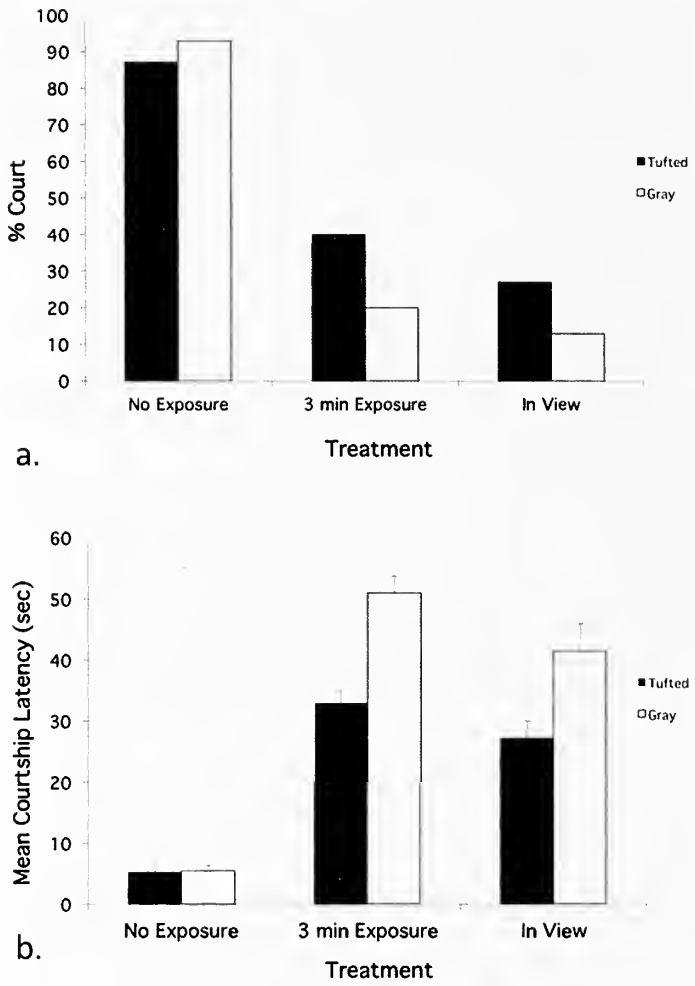

Figure 3.—Courtship response of *M. inclemens* males in the presence of a *P. audax* potential predator; (a) percent of the males that courted after exposure to the predator; (b) mean courtship latency after exposure to the predator.

view of the G morph was significantly smaller than the area of 3-dimensional 45°-view of the G morph ($\bar{X} \pm$ SE: G face-on = 10.6 ± 0.17; G 45° = 32.6 ± 0.29; *t*-test: $t_8 = 63.7$, $P < 0.0001$; Fig. 1b, d).

DISCUSSION

Several studies have demonstrated that male courtship displays not only attract female attention (Houde 1987; Houde & Endler 1990; Andersson 1994; Godin & Briggs 1996) but also may garner unwelcome attention from predators (Burk 1982; Lima & Dill 1990; Magnhagen 1991; Sih 1994; Candolin 1997; Clark et al. 2016). In this study, we demonstrated that the uniquely dimorphic *M. inclemens* males that differ in coloration, presence/absence of tufts, courtship postures, movements and courting distances from the female (Clark & Uetz 1993; Clark 1994; Clark & Morjan 2001), also differ in visual detectability to a potential predator, a large jumping spider, *P. audax*. Although the *P. audax* in our experimental trials did not directly feed on *Maevia* test subjects, we believe that visual detection is the likely first phase of a predatory sequence; thus detectability is a legitimate measurement of

predation risk. The G morph with its side-to-side movement attracted the predator's attention at significantly greater distances than did the stationary, stilting and leg-waving, courting posture of the T morph. The differences in visual detectability were also dependent on the perspective from which the predator viewed the displaying males. The predator visually oriented to the face-on view of the G morph display at approximately twice the distance at which it orients to the T morph display. This suggests that the G male display is more conspicuous than the display of the T male. However, neither would typically present a face-on view to a potential predator, consequently the 45° above-view of the courting male provides a more realistic view that a potential predator might see. From this perspective, the predator oriented to the displaying G male at approximately three times the distance that it oriented to the T morph. This difference may likely be due to two factors: the three-fold larger apparent size due to posture affecting visual target; and, to the sweeping, side-to-side movements of the G male. The result is that G male is more conspicuous to the predator than the T male; similarly, at close distances, the G male is also more conspicuous to the conspecific female (Clark & Morjan 2001).

Jumping spiders are known to have excellent visual acuity (Blest 1985; Forster 1985) and the males of *M. inclemens* should easily notice a nearby predator orienting to them. To determine if male morphs respond differently in the presence of a potential predator, we conducted an experiment with live test subjects and varied the duration of visual exposure to a live potential predator. When the predator was absent, approximately 90% of males tested (both morphs) courted the female within 5 seconds of visually orienting to her. This is consistent with previous observations of courtship tendencies by the two male morphs, and supports the hypothesis that the "first male" the female notices has the mating advantage (Clark & Uetz 1992). However, when the predator was visually present, the courting activities of both T and G males changed. If first exposed to a potential predator before presentation of the female, fewer males courted and of those that did court, the latency to courtship display was longer than that of the controls. Dynamic changes in male behavior have been demonstrated in other species where males are known to adjust their behavior when a potential predator has been detected nearby. For example, some males adjust their courtship behavior by courting less actively (Candolin 1997; Godin & MacAulay 1997; Candolin & Voigt 1998). Such a change in behavior is not without cost and the dilemma is that males that court less actively in the presence of predators are also less attractive to females (Candolin 1997; Godin & MacAulay 1997), and males that court for a longer time to compensate for less activity, run the risk of being more conspicuous to predators (Burk 1982; Lima & Dill 1990; Magnhagen 1991).

In this study, we showed that the two male morphs responded differently to the presence of a potential predator. Fewer G males courted after predator exposure than T males. Of those G males that did finally court, they took significantly longer to initiate courtship than the T males. Being more conspicuous to females at relatively close distances has obvious advantages for the G morph; conversely being more conspicuous to potential predators has serious disadvantages for the G morph, and this may help us understand why G males tend to initiate courtship in close proximity to the female. Courting close to the female and attracting her attention quickly reduces the risk of visual detection by a potential predator. Furthermore, being in close proximity to the female significantly reduces the distance, or "travel time" to approach the female to mate. While we do not fully understand the mechanisms that might favor the "close to female" courtship behavior of the G males, T males are at higher risk of being preyed upon by females at closer range than are G males (Clark & Morjan 2001). Furthermore, Clark & Morjan (2001) suggested that courting G males might be more adroit than T males at escaping predation from the females, perhaps due to the G males' orange pedipalps, which may suppress the females' predation tendencies (see also Clark & Uetz 1993). By courting further from the female, the less-conspicuous-to-potential-predators T males can reduce their risk from hungry conspecific females and still optimize their mating opportunities. By assuming a stationary pose at a safe distance from the female, the risk of detection by a potential predator is relatively low, while at the same time being relatively conspicuous to, and safe from, the predatory advances of a conspecific female.

The interrelationships among posture, behavior, courting distance, lack of female preference, and predation risk management ultimately lead to equal courtship success for the two male *M. inclemens* morphs. This is helpful for understanding how the balance between the two morphs might be maintained. However, the evolution of these traits still remains elusive.

ACKNOWLEDGMENTS

This research was supported by grants from the National Science Foundation (IBN-93-07056) and Alma College professional development. We would like to thank Carrie Morjan and Brandon Biesiadecki for assistance in the field and laboratory. Special thanks to George Uetz for advise and insightful suggestions. We appreciate the helpful contributions of two reviewers.

LITERATURE CITED

Andersson, M. 1994. Sexual Selection. Princeton University Press, Princeton, New Jersey.

Blest, A.D. 1985. The fine structure of spider photoreceptors in relation to function. Pp. 80–102. *In* Neurobiology of Arachnids (F.G. Barth, ed.). Springer-Verlag, New York.

Bulbert, M.W., J.C. O'Hanlon, S. Zappettini, S. Zhang & D. Li. 2015. Sexually selected UV signals in the tropical ornate jumping spider, *Cosmophasis umbratica* may incur costs from predation. Ecology and Evolution 5:914–920.

Burk, T. 1982. Evolutionary significance of predation on sexually signaling males. Florida Entomologist 65:90–104.

Busso, J.P. & A.R.D. Rabosky. 2016. Disruptive selection on male reproductive polymorphism in a jumping spider, *Maevia inclemens*. Animal Behaviour 120:1–10.

Cade, W. 1979. The evolution of alternative male reproductive strategies in field crickets. Pp. 343–380. *In* Sexual Selection and Reproductive Competition in Insects (M.S. Blum, N.A. Blum, eds.). Academic Press, New York.

Candolin, U. 1997. Predation risk affects courtship and attractiveness

of competing threespine stickleback males. Behavioral Ecology and Sociobiology 41:81–87.

Candolin, U. & H.-R. Voigt. 1998. Predator induced nest site preference: safe nests allow courtship in sticklebacks. Animal Behaviour 56:1205–1211.

Clark, D.L. 1994. Sequence analysis of courtship behavior in the dimorphic jumping spider, *Maevia inclemens*. Journal of Arachnology 22:94–107.

Clark, D.L. & C.L. Morjan. 2001. Attracting female attention: the evolution of dimorphic courtship displays in the jumping spider *Maevia inclemens* (Araneae: Salticidae). Proceedings of the Royal Society B 268:2461–2465.

Clark, D.L. & G.W. Uetz. 1990. Video image recognition by the jumping spider *Maevia inclemens*. Animal Behaviour 40:884–890.

Clark, D.L. & G.W. Uetz. 1992. Morph-independent mate selection in a dimorphic jumping spider: demonstration of movement bias in female choice using video-controlled courtship behavior. Animal Behaviour 43:247–254.

Clark, D.L. & G.W. Uetz. 1993. Signal efficacy and the evolution of male dimorphism, Proceedings of the National Academy of Sciences 90:11954–11957.

Clark, D.L., C. Kizer Zeeff, A. Karson, J.A. Roberts & G.W. Uetz. 2016. Risky courtship: background contrast, ornamentation, and display behavior of wolf spiders affect visual detection by toad predators. Ethology 122:364–375.

Daly, M. 1978. The cost of mating. American Naturalist 112:771–774.

Darwin, C. 1871. The Descent of Man and Selection in Relation to Sex. John Murray, London.

Edwards, G.B. & R.R. Jackson. 1993. Use of prey-specific predatory behavior by North American jumping spiders (Araneae, Salticidae) of the genus *Phidippus*. Journal of Zoology, London 229:709–716.

Forster, L.M. 1985. Target discrimination in jumping spiders. Pp. 250–274. *In* Neurobiology of Arachnids (F.G. Barth, ed.). Springer-Verlag, New York.

Fowler-Finn, K. & E. Hebets. 2011. The degree of response to increased predation risk corresponds to male secondary sexual traits. Behavioral Ecology 22:268–275.

Fuller, R. & A. Berglund. 1996. Behavioural responses of a sex-role reversed pipefish to a gradient of perceived predation risk. Behavioral Ecology 7:69–75.

Godin, J.-G.J. 1995. Predation risk and alternative mating tactics in male Trinidadian guppies (*Poecilia reticulata*). Oecologia 103:224–229.

Godin, J.-G.J. & S.E. Briggs. 1996. Female mate choice under predation risk in the guppy. Animal Behaviour 51:117–130.

Godin, J.-G.J. & A. MacAulay. 1997. Predator-mediated changes in male courtship affect female mate choice in sticklebacks. Advances in Ethology 32:205.

Gray, S.M., & J.S. McKinnon. 2007. Linking color polymorphism maintenance and speciation. Trends in Ecology & Evolution 22:71–79.

Gwynne, D.T. 1989. Does copulation increase the risk of predation? Trends in Ecology and Evolution 4:54–56.

Haas, R. 1976. Sexual selection in *Nothobranchius guentheri* (Pisces: Cyprinodontidae). Evolution 30:614–622.

Hastings, P.A. 1991. Flexible responses to predators in a marine fish. Ethology, Ecology and Evolution 3:177–184.

Houde, A.E. 1987. Mate choice based upon naturally occurring color pattern variation in a guppy population. Evolution 41:1–10.

Houde, A.E. & J.A. Endler. 1990. Correlated evolution of female mating preferences and male color patterns in the guppy *Poecilia reticulata*. Science 248:1405–1408.

Lima, S.L. & L.M. Dill. 1990. Behavioral decisions made under the risk of predation: a review and prospectus. Canadian Journal of Zoology 68:619–640.

Lloyd, J.E. 1984. On deception, a way of all flesh, and firefly signaling and systematics. Oxford Surveys in Evolutionary Biology 1:48–84.

Magnhagen, C. 1991. Predation risk as a cost of reproduction. Trends in Ecology and Evolution 6:183–186.

Marshall, K.L.A., K.E. Philpot & M. Stevens. 2015. Conspicuous male coloration impairs survival against avian predators in Aegean wall lizards, *Podarcis erhardii*. Ecology and Evolution 5:4115–4131.

Moodie, G.E.E. 1972. Predation, natural selection and adaptation in an unusual threespine stickleback. Heredity 28:155–167.

Sih, A. 1994. Predation risk and the evolutionary ecology of reproductive behaviour. Journal of Fish Biology 45:111–130.

Manuscript received 25 April 2016, revised 5 July 2017.

2018. Journal of Arachnology 46:7–12

Flying sand-dwelling spiders: aerial dispersal in *Allocosa marindia* and *Allocosa senex* (Araneae: Lycosidae)

Ana Carlozzi[1], **Leticia Bidegaray-Batista**[2,1], **Ivan González-Bergonzoni**[1] and **Anita Aisenberg**[1]: [1]Laboratorio de Etología, Ecología y Evolución, Instituto de Investigaciones Biológicas Clemente Estable, Avenida Italia 3318, CP 11600, Montevideo, Uruguay; [2]Departamento de Biodiversidad y Genética, Instituto de Investigaciones Biológicas Clemente Estable, Avenida Italia 3318, CP 11600, Montevideo, Uruguay. E-mail: anita.aisenberg@gmail.com

Abstract. Aerial dispersal in spiders or ballooning is typically considered to occur during the day by juvenile instars or small-sized adults. *Allocosa marindia* Simó, Lise, Pompozzi & Laborda, 2017 and *Allocosa senex* (Mello-Leitão, 1945) are two nocturnal wolf spiders that inhabit coastal sandy beaches of South America. As mothers of both species emerge from the burrows during the night to disperse the spiderlings, we expected that aerial dispersal of spiderlings could occur during that period. Our aim was to test ballooning occurrence in both species during day and night under laboratory conditions, using as a positive control, the wolf spider *Schizocosa malitiosa* (Tullgren, 1905). We examined ballooning behavior of once-molted spiderlings of *A. marindia*, *A. senex* and *S. malitiosa*, under diurnal and nocturnal conditions, recording observations in a container with grasses and sand as substrate. We exposed the spiderlings to air flow and recorded occurrences of climbing the grass, dropping on dragline and tip-toeing (pre-ballooning behaviors). The three species performed pre-ballooning behaviors during the day but also in the night, and the occurrences of these behaviors varied both within and among species. More events of pre-ballooning behavior were observed during the day than during the night. However, we found differences in the number of events of tip-toeing and dropping on dragline according to the time of the day. We discuss the possibility that microhabitat conditions could affect ballooning propensity particularly in the three coastal wolf spiders.

Keywords: Ballooning, wolf spider, tip-toe, drop on dragline, coastal environment

Aerial dispersal is a central trait affecting the life history of spider species (Bonte & Dahirel 2017). Along with other biotic and abiotic factors, aeronautic behavior can shape species distributions and population structures (Muñoz et al. 2004; Papadopoulou et al. 2009; Gillespie et al. 2012). It allows species to colonize remote habitats and experience rapid range shifts during unfavorable environmental conditions (Muñoz et al. 2004; Papadopoulou et al. 2009; Peterson 2009; Gillespie et al. 2012; Travis et al. 2013).

Ballooning is commonly known as the mechanism for aerial dispersal in spiders (Foelix 2011). By means of silk threads, spiders can travel throughout the air, moving from few meters to many kilometers away from their birth site (Decae 1987; Weyman et al. 2002; Bell et al. 2005; Bonte 2013). This behavior is widespread among araneomorph spiders and has rarely been described in mygalomorphs (Decae 1987; Bell et al. 2005; Coddington 2005; Ferretti et al. 2013). With few exceptions (Weyman et al. 2002; A. Aisenberg, pers. obs.), aerial dispersal is restricted to juvenile instars or to spiders with small adult sizes (e.g., linyphiids) (Greenstone et al. 1987; Weyman 1993). In general, ballooning occurs during daylight in warm dry days, and when wind speed is low (< 3 m/s) (Richter 1970; Vugts & Van Wingerden 1976; Bishop 1990; Greenstone 1990; Weyman 1993; Duffey 1998; Reynolds et al. 2007).

The most frequently known pre-ballooning behavior is the stereotypical 'tip-toeing' (i.e., after climbing to a high point the spider places itself in front of an air stream, stretches the legs, raises the opisthosoma and produces silk threads until taking-off) (Richter 1970; Decae 1987). Another mechanism is the 'dropping on dragline', during which the spider climbs to a high point, drops from attached lines of silk and swings in the wind. When the silk lines break, the spider becomes airborne (see Decae 1987, Eberhard 1987 for other pre-ballooning behaviors).

As with any other dispersal mechanism, ballooning will help to avoid inbreeding, competition for resources, and unfavorable environmental conditions (Decae 1987; Bonte et al. 2006). Moreover, other factors like starvation and overcrowding have also shown to stimulate ballooning behaviors (Duffey 1998; Mestre & Bonte 2012; Bonte 2013). However, because spiders can control when to balloon but not where they are going to land, aerial dispersal has a potential cost of landing in unsuitable habitats. Hence, the performance of ballooning will depend of the trade-off between costs and benefits (Bell et al. 2005; Bonte 2013). Theoretical and empirical studies in several organisms have shown that the temporality of the habitat and its spatial distribution are main factors shaping dispersal strategies (Southwood 1962; McPeek & Holt 1992; Travis & Dytham 1999). Thus, unpredictable and unstable habitats may select for higher dispersal rates either in continuous or fragmented areas (Southwood 1962; McPeek & Holt 1992; Travis & Dytham 1999; Travis et al. 2013). Studies of spiders agree with those predictions (see Richter 1970; Greenstone 1982; Bonte et al. 2006, for examples of lycosids of the genus *Pardosa* C.L. Koch, 1847). In addition, Bonte et al. (2003b) showed that ballooning in spiders is negatively related to habitat specialization in fragmented habitats.

The nocturnal sand-dwelling wolf spiders *Allocosa marindia* Simó, Lise, Pompozzi & Laborda, 2017 and *A. senex* (Mello-Leitão, 1945) are distributed throughout the coasts of rivers, lakes and the ocean shores of Argentina, Brazil and Uruguay (Capocasale 1990). Both species are strictly associated with sandy coastal shores and are considered good bio-indicators of

those environments (Ghione et al. 2013). They construct burrows in the sand where they shelter during the cold months and during daylight, becoming active during the summer nights (Costa 1995; Costa et al. 2006). Both species exhibit a reversal in sex roles and sexual size dimorphism expected in spiders; thus, females are smaller than males and they seek and initiate courtship (Aisenberg et al. 2007; Aisenberg & Costa 2008). Mating occurs inside male burrows and females lay their egg-sac there, exiting during the night when it is time for progeny dispersal (Aisenberg 2014), with the spiderlings on their dorsum as it is typical for this family (Foelix 2011). These species have sympatric distributions, but *A. senex* is most frequently found in open sandy areas with scarce psammophile native vegetation, whereas *A. marindia* is associated with sandy areas showing greater abundance of native and exotic vegetation (Costa et al. 2006; Aisenberg et al. 2009, 2011; Ghione et al. 2013). Moreover, the two species differ in the continuity of their distributions: *A. senex* has a continuous distribution whereas *A. marindia* shows a more irregular and patchy distribution throughout the coastline of Uruguay (Bidegaray-Batista, pers. obs.). Due to their extraordinary morphological, ecological and behavioral adaptations to inhabit sandy coasts, both species are promising models to study ballooning propensity and shed light on the evolution of dispersal strategies in spiders.

Here, we study the propensity to exhibit ballooning behavior during day and night in *A. marindia* and *A. senex* under laboratory conditions. As a positive control, we examined ballooning behavior in the similar-sized wolf spider *Schizocosa malitiosa* (Tullgren, 1905), which inhabits neighboring anthropic habitats and shows high propensity for aerial dispersal (Capocasale & Costa 1975; Carlozzi et al. 2014). We predicted that both *Allocosa* would exhibit ballooning behavior during the night, when the dispersal of spiderlings occurs in nature. We also expected to find differences in ballooning occurrence between the three species, accordingly to the degree of stability of their microhabitats. As both *Allocosa* species inhabit sand coastal habitats which are considered unpredictable and unstable, we predicted higher ballooning propensity in these species compared to *S. malitiosa*.

METHODS

During February 2014, we collected 4 females of *A. marindia*, 5 females of *A. senex* and 4 females of *S. malitiosa* carrying spiderlings on the dorsum. *Allocosa* females were collected at San José de Carrasco, Canelones, Uruguay (34°50′46.71″S, 55°58′17.65″W), while the females of *S. malitiosa* were collected at Marindia, Canelones, Uruguay (34°46′52.15″S, 55°49′30.18″W).

We maintained the females with their progeny under laboratory conditions in individual cylindrical containers of 6.7 cm diameter and 7.5 cm height, with sand as substrate and water provision. We waited until the spiderlings molted and descended from their mother on their own initiative. Then we separated the spiderlings in small groups for the trials. We formed groups of 5 in *A. marindia*, and of 3 in *A. senex* and *S. malitiosa*. We decided to form larger groups in *A. marindia* because they showed lower activity than the other species, making them easier to record in a higher number (A. Carlozzi, unpublished data).

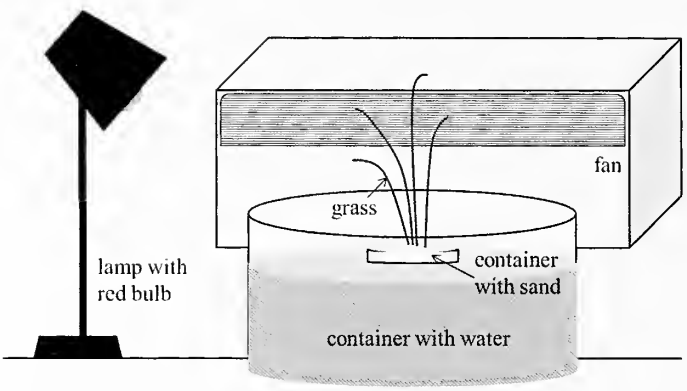

Figure 1.—Experimental set-up.

We followed the experimental design described by Richter (1970) (Fig. 1). Each group of individuals was placed in a cylindrical plastic container of 7 cm diameter and 10 cm height, with sand as substrate and four leaves of *Panicum racemosum* grass (Poaceae). The container was centered inside a bowl of 21 cm diameter and 10.5 cm height with water, to prevent potential escape of the spiderlings. We generated a continuous airflow at a rate that averaged 2.47 ± 0.16 m/sec. We measured the airflow with a handheld digital anemometer (Benetech GM816), at the middle of the grass that was closer to the airflow device. The air was generated by a fan directed upwards at an angle of 45° (Fig. 1). This breeze speed has been indicated as adequate for displaying ballooning by spiderlings of other wolf spider species (Richter 1970; Greenstone 1982). Each trial was run for 15 minutes after placing each group of spiderlings at the sand of the container.

We performed trials during the day between 12 am and 9 pm, and during the night between 9.30 pm and 6.30 am, under a 40 watt red light bulb. All the trials were carried out during summer of the Southern Hemisphere. We tested a total of 60 spiderlings of *A. marindia* (25 spiderlings at diurnal and 35 at nocturnal trials), 135 of *A. senex* (75 spiderlings at diurnal and 60 at nocturnal trials), and 132 of *S. malitiosa* (75 spiderlings at diurnal and 57 at nocturnal trials). The age of the spiderlings, measured in days since leaving the mother's dorsum, was 5.77 ± 3.71 days (range: 1–13). Temperature and humidity data under laboratory conditions are summarized in Table 1.

For each trial, we recorded by direct observation the number of occurrences of the behaviors: climbing the grass, tip-toeing, dropping on dragline and ballooning. We compared the total number of events of climbing the grass, dropping on dragline and tip-toeing between diurnal and nocturnal trials, and between species. Also, we tested for significant interactions among the behaviors and time of the day, and among the behaviors and species identity, using generalized linear mixed-effects models under a negative binomial distribution. The species identity, trial time (day vs. night) and its interaction were set as fixed-effect factors while the variable 'mother' was set as a random factor (because maternal effects have been shown to affect ballooning behavior, Mestre & Bonte 2012). Furthermore, to test for changes in the prevalence of dropping on dragline or tip-

Table 1.—Temperature and humidity conditions during the experimental trials for each species, during the day and night. All data are presented as mean values with their corresponding standard deviations.

	Temperature (°C)	Humidity (%)
A. marindia	Day: 27.40 ± 1.14	Day: 65.56 ± 4.29
	Night: 26.94 ± 0.11	Night: 72.30 ± 5.50
A. senex	Day: 26.61 ± 1.21	Day: 73.20 ± 6.70
	Night: 26.59 ± 0.48	Night: 75.00 ± 2.90
S. malitiosa	Day: 31.19 ± 2.90	Day: 70.60 ± 4.83
	Night: 33.00 ± 0.00	Night: 74.80 ± 4.55

toeing events in each trial in the different species and according to the time of the day, we built a mixed-effects binomial model, considering each of the species, timing (day vs. night) and its interaction as fixed-effect factors and the variable 'mother' as a random factor.

Temperature was added as a fixed-effect continuous factor to all the full models created in order to disregard any effect of this variable in our results. The general procedure was to build full models (including all potential effects) and compare these models to reduced models (removing one factor at a time) using likelihood ratio tests (e.g., Zuur et al. 2009). In case of finding differences between the species or an interaction between time and species, we performed multiple comparison post hoc tests. The modelling was made using the glmer function in lme4 package (Bates et al. 2015) in R software (R core Team 2016). The selection of the probability distribution in which to frame our analysis and accomplishment of assumptions were performed following standardized methods for generalized linear models (Zuur et al. 2009).

Voucher specimens were deposited in the collection of Sección Entomología, Facultad de Ciencias, Uruguay.

RESULTS

We summarize data about the total number of events in which the pre-ballooning behaviors "dropping on dragline" and "tip-toeing" were followed by ballooning in Table 2. Temperature did not affect the total number of pre-ballooning behaviors (pooling dropping on dragline plus tip-toeing events) observed (likelihood ratio test: $Chisq = 2.58$, df = 1, $P = 0.11$). We observed higher counts of pre-ballooning behaviors per trial during the day (mean ± SD = 2.7 ± 2.4) than during night (mean ± SD = 2.1 ± 1.2) (likelihood ratio test: $Chisq = 25.7$, df = 3, $P = 1.1 \times 10^{-5}$), and a different number of pre-ballooning behaviors per trial were displayed

Table 2.—Total number of events in which the pre-ballooning behaviors dropping on dragline (DD) and tip-toeing (TT) were followed by ballooning (B) for each species and diurnal/nocturnal trials. Total number of trials is shown in parentheses.

Species	DD + B Diurnal trials	DD + B Nocturnal trials	TT + B Diurnal trials	TT + B Nocturnal trials
A. senex	7 (25)	4 (20)	3 (25)	1 (20)
A. marindia	1 (5)	3 (7)	0 (5)	0 (7)
S. malitiosa	7 (25)	10 (19)	9 (25)	1 (19)

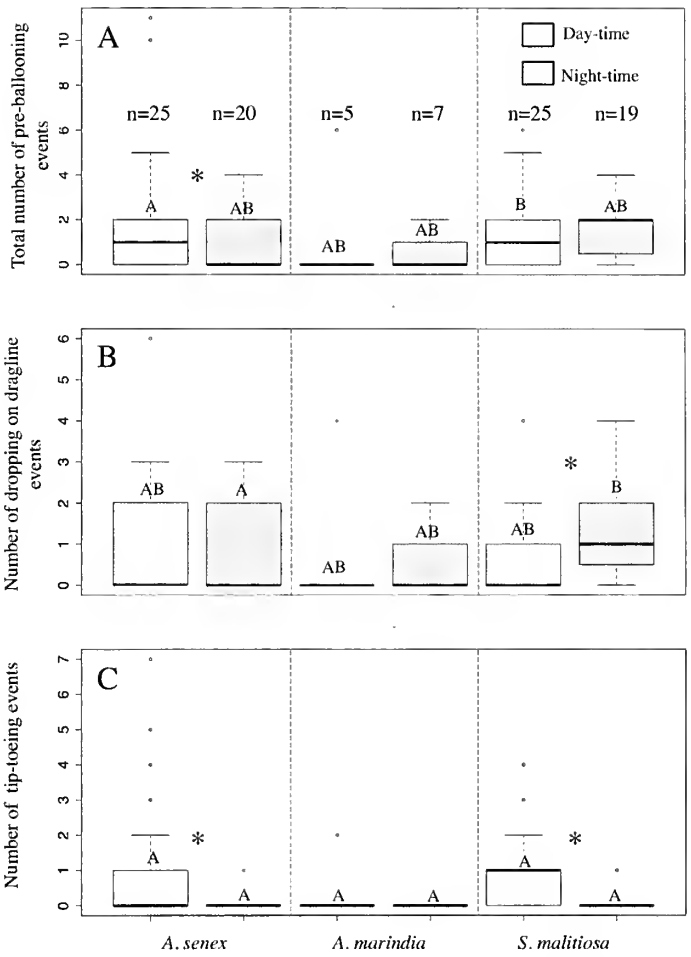

Figure 2.—Box and whiskers plots of the total number of pre-ballooning events per trial: (A) dropping on dragline + tip-toeing, (B) dropping on dragline events, and (C) tip-toeing events, recorded for *A. senex*, *A. marindia*, and *S. malitiosa* during day and night trials (shown by light and dark boxes, respectively). The total number of trials in each treatment (n) is shown in panel A, above each box. Open circles represent outliers. The results of mixed-effects negative binomial models testing effects of species and trial times are summarized in the plots as follows: in each panel, significant differences between species are represented by different letters; significant differences between day and night trials are indicated by an asterisk within each species in each panel. Only statistical differences in which $P < 0.05$ are reported in the graph.

between species (likelihood ratio test: $Chisq = 20.3$, df = 4, $P = 0.0005$). Furthermore, day-night effects depended on the species (significant interaction, likelihood ratio test: $Chisq = 11.0$, df = 2, $P = 0.004$). During the day *A. senex* produced more pre-ballooning behaviors per trial than *S. malitiosa* (posthoc comparison: $Z = -2.85$, $P = 0.01$), whereas the number of pre-ballooning behaviors per trial in *A. marindia* did not differ from the others ($Z = -0.19$, $P = 0.18$ compared with *A. senex* and $Z = -1.7$, $P = 0.84$ compared with *S. malitiosa*). However, during the night, the number of pre-ballooning events per trial was similar between all the species (*A. senex* versus *A. marindia:* $Z = -0.55$, $P = 0.57$; *A. senex* versus *S. malitiosa:* $Z = 1.3$, $P = 0.46$; and *A. marindia* versus *S. malitiosa:* $Z = 1.4$, $P = 0.46$) (Fig. 2). *Allocosa senex*

performed significantly higher number of pre-ballooning behaviors during the day trials (2.9 ± 3.0 events) than during the night trials (1.9 ± 1.2 events) (posthoc comparison: $Z = -3.71$, $P = 0.0002$) (Fig. 2). However, *A. marindia* and *S. malitiosa* did not show significant differences between day and night trials (posthoc tests: $Z = -1.0$, $P = 0.31$ and $Z = 0.01$, $P = 0.99$, respectively).

We did not find statistical differences in the number of climbing the grass events observed between species (likelihood ratio test: $Chisq = 3.6$, df = 2, $P = 0.16$). Trial time and this behavior was not related to temperature in our dataset (likelihood ratio test: $Chisq = 0.52$, df = 1, $P = 0.46$).

We observed more dropping on dragline events per trial during the night (mean ± SD = 1.0 ± 1.1) than during the day (mean ± SD = 0.8 ± 1.3) (likelihood ratio test: $Chisq = 12.2$, df = 3, $P = 0.007$). However, this behavior differed between species (likelihood ratio test: $Chisq = 14.3$, df = 4, $P = 0.006$), as the day–night differences depended on the species (significant interaction on likelihood ratio test $Chisq = 12.2$, df = 2, $P = 0.002$). While during the night all the species displayed similar numbers of dropping on dragline events per trial (posthoc tests: *A. senex* versus *A. marindia:* $Z = -0.7$, $P = 0.47$; *A. senex* versus *S. malitiosa:* $Z = 1.5$, $P = 0.31$; and *A. marindia* versus *S. malitiosa:* $Z = 1.6$, $P = 0.31$), during the day *S. malitiosa* tended to perform more dropping on dragline than *A. senex* (note the marginal *P* value in posthoc tests: *A. senex* versus *A. marindia:* $Z = -1.0$, $P = 0.56$; *A. senex* versus *S. malitiosa:* $Z = -2.1$, $P = 0.09$; and *A. marindia* versus *S. malitiosa:* $Z = -0.4$, $P = 0.68$). Moreover, *A. senex* showed a tendency (note the marginal *P* value) to make more dropping on dragline during the day than during the night ($Z = -1.8$, $P = 0.06$), while *S. malitiosa* showed the opposite pattern with more dropping on dragline events observed during the night ($Z = 2.54$, $P = 0.01$). *Allocosa marindia* did not show significant differences in this behavior between day and night ($Z = -1.2$, $P = 0.24$) (Fig. 2).

Opposite to the pattern of dropping on dragline behaviors, the tip-toeing events occurred in higher numbers per trial during the day (mean ± SD = 0.87 ± 1.5) than during the night (mean ± SD = 0.08 ± 0.28) (likelihood ratio test: $Chisq = 44.2$, df = 1, $P = 2.9 \times 10^{-11}$). Although initially the likelihood ratio test suggested differences between species (likelihood ratio test: $Chisq = 7.6$, df = 2, $P = 0.02$), posthoc comparisons did not show differences between any of the species (posthoc tests: *A. senex* versus *A. marindia:* $Z = -1.5$, $P = 0.36$; *A. senex* versus *S. malitiosa:* $Z = -1.4$, $P = 0.36$; *and A. marindia* versus *S. malitiosa:* $Z = 0.8$, $P = 0.41$). This is likely attributed to the fact that there is only one observation of night tip-toeing in one trial for *A. senex*, one for *S. malitiosa*, and none for *A. marindia* (Fig. 2).

Consistent with the aforementioned patterns, we found that individuals performed a higher proportion of dropping on dragline per trial (implying a lower proportion of tip-toeing) during the night (mean ± SD = 93.2 ± 0.84 %) than during the day (mean ± SD = 49.9 ± 1.6 %)) ($Chisq = 33.6$, df = 1, $P = 6.5 \times 10^{-9}$). However there were no significant differences between the species ($Chisq = 0.5562$, df = 2, $P = 0.75$) or a significant interaction between time and species ($Chisq = 0.26$, df = 2, $P = 0.87$).

DISCUSSION

Our results showed that *A. marindia*, *A. senex* and *S. malitiosa* can perform ballooning behavior during the day but also during night hours. Interestingly, although adults and juveniles of both *Allocosa* species are inside their burrows during the day (Costa 1995), our results suggest that once-molted spiderlings would balloon or at least be able to balloon also during the day. This aerial dispersal ability found in both *Allocosa* species is in agreement with recent phylogeographic studies, which revealed an absence of genetic differentiation and high connectivity among populations of both species (Bidegaray-Batista et al. 2017; Postiglioni 2015). However, pre-ballooning frequencies varied both within and among species and also between day and night.

Though the three wolf spiders inhabit the sandy coasts of Uruguay, *A. senex* is more common in sand dunes with scarce native vegetation, while *A. marindia* is more frequent in sandy areas with higher abundance of native and exotic vegetation (including shrubs and trees), and *S. malitiosa* inhabits continuous areas with more vegetation and human constructions (Costa et al. 2006; Ghione et al. 2013). Microhabitat characteristics such as the vegetation coverage could negatively affect the incidence and speed of air currents perceived by the spiderlings, determinant factors for triggering ballooning behavior (Weyman et al. 2002). *Allocosa senex* showed higher number of pre-ballooning events compared to *S. malitiosa* during the day, but did not show differences with *A. marindia*. The high occurrence of ballooning in *A. senex* during the day could be related with the harshness and unpredictability of their habitat (Aisenberg 2014; Jorge et al. 2015), characteristics that can promote aerial dispersal in spiders (Southwood 1962; Greenstone 1982; Bell et al. 2005). On the other hand, the degree of continuity or fragmentation of the habitat can determine the possibilities of aerial dispersal of a spider species, population or individual (Bonte et al. 2006). Moreover, species showing a strict association with a certain habitat (in our case *Allocosa*) are expected to show lower frequencies of aerial dispersal compared to species with more generalist distributions (Bonte et al. 2003b). These two last hypotheses do not agree with the results of the present study. Hypotheses of how habitat fragmentation, harshness or stability can affect ballooning occurrence in spiders can be difficult to test and interpret in contexts in which more than one of those characteristics apply, as occurs in our situation, so results should be analyzed cautiously.

In the present study, carried out under controlled laboratory conditions, the three species were able to balloon at night, under red light. According to a recent study by Postiglioni et al. (2017), *Allocosa* balloons at night also in the field. According to this, light conditions would not be the main factor triggering ballooning occurrence in *A. senex*, *A. marindia* and *S. malitiosa*. However, most studies testing aerial dispersal in spiders have been carried out during daylight (Richter 1970; Yeargan 1975; Greenstone 1982, 1990; Suter 1999). Moreover, Bishop (1990) performed a field study to test spider aerial dispersal by placing sticky traps in a forest canopy and found that ballooning occurred only during the day. Though thermal conditions and the appropriate air flow necessary for ballooning diminish after sunset, the night would not prevent the occurrence of ballooning (Weyman et

al. 2002). The meteorological conditions determining ballooning occurrence in both *Allocosa* species and in *S. malitiosa* remain to be further studied.

Though both tip-toeing and dropping on dragline have been reported as pre-ballooning behaviors (Decae 1987; Barth et al. 1991), we found differences in the number of events of those behaviors between the day and the night. In this study, we found more dropping on dragline events during the night and more tiptoeing during the day. Dropping on dragline is a pre-ballooning behavior, but it can also occur in other contexts to avoid predation, when the spider starts to build a web, or as a consequence of overcrowding. However, the three spiders tested in this study are wolf spiders that do not construct webs or perform pre-bridging behavior. Moreover, as we show in Table 2, dropping on dragline was followed by ballooning in some observations, corroborating that this behavior was not misunderstood as pre-ballooning behavior. The dissimilarities in the number of events of tip-toeing and dropping on dragline according to the time of the day remain to be further studied.

Other factors that can affect aerial dispersal behavior in spiders are the individual nutrition status, mother condition, feeding history and temperature breeding conditions during juvenile stages (Bonte et al. 2003a; Mestre & Bonte 2012). In the current study, we did not control those variables, the body size and weight of the spiderlings or of their mothers, so the influences of those characteristics in *A. marindia*, *A. senex* or *S. malitiosa* remain to be studied further. Moreover, despite that the trials for *A. marindia* contained five individuals versus three individuals in the rest of groups this did not translate into more ballooning events observed in the trials of *A. marindia*, disregarding a potential increase in the number of observed ballooning per trial with increasing number of individuals. Though aerial dispersal in spiders is an extraordinary phenomenon, much work still needs to be done in order to determine the factors triggering this behavior.

ACKNOWLEDGMENTS

We thank Fernando G. Costa for his help with the experimental design and fruitful discussions. Andrea Albín, Matilde Carballo, Tomás Casacuberta, Marcelo Casacuberta, Macarena González, Estefanía Stanley and Rodrigo Postiglioni, for their help during fieldwork. We also acknowledge editor Thomas Jones, Dries Bonte, one anonymous reviewer and the editor for their comments which improved the final version of the manuscript. We acknowledge financial support by Programa Acortando Distancias (ANII-ANEP). AA, LB and IGB thank the Sistema Nacional de Investigación (ANII) and Programa de Desarrollo de las Ciencias Básicas, UdelaR, Uruguay.

LITERATURE CITED

Aisenberg, A. 2014. Adventurous females and demanding males: sex role reversal in a neotropical spider. Pp. 163–182. *In* Sexual Selection: Perspectives and Models from the Neotropics (R. Macedo & G. Machado, eds), Elsevier, USA.

Aisenberg, A. & F.G. Costa. 2008. Reproductive isolation and sex-role reversal in two sympatric sand-dwelling wolf spiders of the genus *Allocosa*. Canadian Journal of Zoology 86:648–658.

Aisenberg, A., C. Viera & F.G. Costa. 2007. Daring females, devoted males, and reversed sexual size dimorphism in the sand-dwelling spider *Allocosa brasiliensis* (Araneae, Lycosidae). Behavioral Ecology and Sociobiology 62:29–35.

Aisenberg, A., M. González, A. Laborda, R. Postiglioni & M. Simó. 2009. Reversed cannibalism, foraging, and surface activities of *Allocosa alticeps* and *Allocosa brasiliensis*: two wolf spiders from coastal sand dunes. Journal of Arachnology 37:135–138.

Aisenberg, A., M. Simó & C. Jorge 2011. Spider as a model towards the conservation of coastal sand dunes in Uruguay. Pp. 75–93. *In* Sand Dunes: Conservation, Shapes/Types and Desertification (J.A. Murphy, ed.), NOVA Science Publishers, USA.

Barth, F.G., S. Komarek, J.A. Humphrey & B. Treidler. 1991. Drop and swing dispersal behavior of a tropical wandering spider: experiments and numerical model. Journal of Comparative Physiology A 169:313–322.

Bates, D., M. Mächler, B. Bolker & S. Walker. 2015. Fitting linear mixed-effects models using lme4. Journal of Statistical Software 67:1–48.

Bell, J.R., D.A. Bohan, E.M. Shaw & G.S. Weyman. 2005. Ballooning dispersal using silk: world fauna, phylogenies, genetics and models. Bulletin of Entomological Research 95:69–114.

Bidegaray-Batista, L., Arnedo M., Carlozzi A., Jorge C., Pliscoff P., Postiglioni R., Simó M., A. Aisenberg. 2017. Dispersal strategies, genetic diversity and distribution: implications for conservation in two South American sand-dwelling wolf spiders (Araneae, Lycosidae). Pp. 109–135. In: Behaviour and Ecology of Spiders. Contributions from the Neotropical Region (Viera C. & M. Gonzaga, eds.). Springer Nature, Cham, Switzerland.

Bishop, L. 1990. Meteorological aspects of spider ballooning. Environmental Entomology 19:1381–1387.

Bonte, D. 2013. Cost-benefit balance of dispersal and the evolution of conditional dispersal strategies in spiders. Pp. 67–78. *In* Spider Ecophysiology. (W. Nentwig, ed.). Springer, Heidelberg New York Dordrecht London.

Bonte, D. & M. Dahirel. 2017. Dispersal: a central and independent trait in life history. Oikos 126:472–479.

Bonte, D., I. Deblauwe & J.P. Maelfait. 2003a. Environmental and genetic background of tiptoe-initiating behaviour in the dwarf spider *Erigone atra*. Animal Behaviour 66:169–174.

Bonte, D., N. Vandenbroecke, L. Lens & J.-P. Maelfait. 2003b. Low propensity for aerial dispersal in specialist spiders from fragmented landscapes. Proceedings of the Royal Society of London B: Biological Sciences 270:1601–1607.

Bonte, D., J.V. Borre, L. Lens & J.-P. Maelfait. 2006. Geographical variation in wolf spider dispersal behaviour is related to landscape structure. Animal Behaviour 72:655–662.

Capocasale, R.M. 1990. Las especies de la subfamilia Hippasinae de America del Sur (Araneae, Lycosidae). Journal of Arachnology 18:131–141.

Capocasale, R.M. & F. Costa. 1975. Descripcion de los biotopos y caracterización de los habitats de *Lycosa malitiosa* Tullgren (Araneae, Lycosidae) en Uruguay. Vie Milieu 25:1–15.

Carlozzi, A., F.G. Costa, L. Bidegaray-Batista, R. Postiglioni & A. Aisenberg. 2014. Arañas que vuelan en la costa: estudios de dispersión en *Allocosa brasiliensis* y *Allocosa alticeps* (Araneae: Lycosidae). Tercer Congreso Uruguayo de Zoología, Montevideo, Uruguay.

Coddington, J.A. 2005. Phylogeny and classification of spiders. Pp. 18–24. *In* Spiders of North America: An Identification Manual (D. Ubick, P. Paquin, P. E. Cushing & V. Roth, eds). American Arachnological Society.

Costa, F.G. 1995. Ecología y actividad diaria de las arañas de la arena *Allocosa* spp. (Araneae, Lycosidae) en Marindia, localidad costera del sur del Uruguay. Revista Brasilera de Biología 55:457–466.

Costa, F.G., M. Simó, A. Aisenberg, R. Menafra, L. Rodríguez-Gallego, F. Scarabino et al. 2006. Composición y ecología de la fauna epígea de Marindia (Canelones, Uruguay) con especial

énfasis en las arañas: un estudio de dos años con trampas de intercepción. Pp. 427–436. *In* Bases para la Conservación y el Manejo de la Costa Uruguaya (R. Menafra, L. Rodríguez-Gallego, F. Scarabino & D. Conde, eds). Vida Silvestre Uruguay, Montevideo.

Decae, A.E. 1987. Dispersal: ballooning and other mechanisms. Pp. 348–356. *In* Spider Ecophysiology. (W. Nentwig, ed.). Springer, Heidelberg New York Dordrecht London.

Duffey, E. 1998. Aerial dispersal in spiders. Pp. 187–191. *In* Proceedings of the 17th European Colloquium of Arachnology, Edinburgh. (P. Selden, ed.). British Arachnological Society, Burnham Beeches, Bucks.

Eberhard, W.G. 1987. How spiders initiate airborne lines. Journal of Arachnology 15:1–9.

Ferretti, N., G. Pompozzi, S. Copperi & L. Schwerdt. 2013. Aerial dispersal by *Actinopus* spiderlings (Araneae: Actinopodidae). Journal of Arachnology 41:407–408.

Foelix, R.F. 2011. Biology of Spiders. Oxford University Press, New York.

Ghione, S., M. Simó, A. Aisenberg & F.G. Costa. 2013. *Allocosa brasiliensis* (Araneae, Lycosidae) as a bioindicator of coastal sand dunes in Uruguay. Arachnology 16:94–98.

Gillespie, R.G., B.G. Baldwin, J.M. Waters, C.I. Fraser, R. Nikula & G.K. Roderick. 2012. Long-distance dispersal: a framework for hypothesis testing. Trends in Ecology and Evolution 27:47–56.

Greenstone, M.H. 1982. Ballooning frequency and habitat predictability in two wolf spider species (Lycosidae: *Pardosa*). Florida Entomologist 65:83–89.

Greenstone, M. 1990. Meteorological determinants of spider ballooning: the roles of thermals vs. the vertical windspeed gradient in becoming airborne. Oecologia 84:164–168.

Greenstone, M.H., C.E. Morgan, A. L. Hultsch, R.A. Farrow & J. Dowse. 1987. Ballooning spiders in Missouri, USA, and New South Wales, Australia: family and mass distributions. Journal of Arachnology 15:163–170.

Jorge, C., Á. Laborda, M. Alves Días, A. Aisenberg & M. Simó. 2015. Habitat preference and effects of coastal fragmentation in the sand-dwelling spider *Allocosa brasiliensis* (Lycosidae, Allocosinae). Open Journal of Animal Sciences 5:309–324.

McPeek, M.A. & R.D. Holt. 1992. The evolution of dispersal in spatially and temporally varying environments. American Naturalist 140:1010–1027.

Mestre, L. & D. Bonte. 2012. Food stress during juvenile and maternal development shapes natal and breeding dispersal in a spider. Behavioral Ecology 23:759–764.

Muñoz, J., Á.M. Felicísimo, F. Cabezas, A.R. Burgaz & I. Martínez. 2004. Wind as a long-distance dispersal vehicle in the Southern Hemisphere. Science 304:1144–1147.

Papadopoulou, A., I. Anastasiou, B. Keskin & A.P. Vogler. 2009. Comparative phylogeography of tenebrionid beetles in the Aegean archipelago: the effect of dispersal ability and habitat preference. Molecular Ecology 18:2503–2517.

Peterson, A.T. 2009. Phylogeography is not enough: The need for multiple lines of evidence. Frontiers of Biogeography 1:19–25.

Postiglioni, R. 2015. Estructuración genética y variación morfológica en ambientes fluviales y oceánico-estuarinos en la araña *Allocosa brasiliensis* (Lycosidae) del sur de Uruguay. Master dissertation thesis, Programa de Desarrollo de las Ciencias Básicas, UdelaR, Uruguay.

Postiglioni, R., A. Aisenberg, A. Carlozzi & L. Bidegaray-Batista. 2017. The dark side of ballooning: nocturnal aerial dispersal in wolf spiders from the South American coastline. Arachnology 17(4):1–5.

R Core Team. 2016. R: A language and environment for statistical computing. R Foundation for Statistical Computing, Vienna, Austria. Available online at http://www.R-project.org/.

Reynolds, A.M., D.A. Bohan & J.R. Bell. 2007. Ballooning dispersal in arthropod taxa: conditions at take-off. Biology Letters 3:237–240.

Richter, C.J.J. 1970. Aerial dispersal in relation to habitat in eight wolf spider species (*Pardosa*, Araneae, Lycosidae). Oecologia 5:200–214.

Southwood, T.R.E. 1962. Migration of terrestrial arthropods in relation to habitat. Biological Reviews 37:171–211.

Suter, R.B. 1999. An aerial lottery: the physics of ballooning in a chaotic atmosphere. Journal of Arachnology 27:281–293.

Travis, J.M. & C. Dytham. 1999. Habitat persistence, habitat availability and the evolution of dispersal. Proceedings of the Royal Society of London B: Biological Sciences 266:723–728.

Travis, J.M., M. Delgado, G. Bocedi, M. Baguette, K. Bartón, D. Bonte, et al. 2013. Dispersal and species' responses to climate change. Oikos 122:1532–1540.

Vugts, H.F. & W.K.R.E. Van Wingerden. 1976. Meteorological aspects of aeronautic behaviour of spiders. Oikos 27:433–444.

Weyman, G.S. 1993. A review of the possible causative factors and significance of ballooning in spiders. Ethology Ecology and Evolution 5:279–291.

Weyman, G., K. Sunderland & P. Jepson. 2002. A review of the evolution and mechanisms of ballooning by spiders inhabiting arable farmland. Ethology Ecology and Evolution 14:307–326.

Yeargan, K.V. 1975. Factors influencing the aerial dispersal of spiders (Arachnida: Araneida). Journal of the Kansas Entomological Society 48:403–408.

Zuur, A.F., E.N. Ieno, N.J. Walker, G.M. Smith & A.A. Saveliev. 2009. Mixed Effects Models and Extensions in Ecology with R. New York: Springer.

Manuscript received 31 March 2017, revised 1 August 2017.

2018. Journal of Arachnology 46:13–20

Vertical distribution of wandering spiders in Central America

Witold Lapinski[1] and **Marco Tschapka**[1,2]: [1] Institute of Evolutionary Ecology and Conservation Genomics, University of Ulm, Albert-Einstein-Allee 11, 89069 Ulm, Germany; E-mail: wito.l@gmx.de; [2] Smithsonian Tropical Research Institute, P.O. Box 0843-03092, Balboa Ancón, República de Panamá

Abstract. We examined patterns of vertical distribution within an assemblage of seven species of large wandering spiders in a lowland rainforest on the Caribbean slope of Costa Rica. Over 16 months, 22 trees were surveyed regularly at night, up to a height of 43 m, using a rope climbing technique. Local climate and canopy microclimate exhibited only weak seasonal fluctuations. There was a distinct vertical segregation between ground-dwelling and arboreal species. The arboreal species used almost the entire available height range, whereby immature *Cupiennius coccineus* F.O.P.-Cambridge, 1901 occupied higher parts of the trees than adults. The two most abundant arboreal species differed also in their use of arboreal microhabitats: while *Cu. coccineus* occurred most frequently on trunk bark and on epiphyte leaves, the smaller *Ctenus* sp. 4 was more restricted to trunk bark. We detected effects of structural complexity of the host trees but no effects of canopy microclimate or of local climate on vertical distribution of *Cu. coccineus*, by far the most abundant arboreal species. The differences in vertical distribution both between age classes of *Cu. coccineus*, and between *Cu. coccineus* and the smaller *Ctenus* sp. 4 suggest size-dependent habitat segregation in arboreal species along the vertical axis, which might diminish cannibalism and/or intra-guild predation. Moreover, the wide range of vertical distribution of arboreal spiders suggests that they may connect the understory and canopy food webs.

Keywords: Canopy, Costa Rica, Ctenidae, epiphyte, tree

Rainforest canopies are fascinating but still poorly studied habitats. Since the pioneering days of canopy biology, the access techniques have been improved and now allow more thorough and sophisticated analyses of the processes in the tree tops (Mitchell et al. 2002; Lowman et al. 2013). In tropical forest canopies the bulk of arthropods is formed by insects and spiders (Basset 2001). Comprising 4.6–10.2% of all arthropod individuals, spiders exhibit high relative abundance in tropical forest canopies (Russel-Smith & Stork 1994; Floren & Deeleman-Reinhold 2005; Gurgel-Gonçalves et al. 2006; Marques et al. 2006). Mass-collecting by fogging is the most common technique to assess abundance and species diversity of canopy arthropods (Basset 2001). However, due to its destructive character, this technique is not suitable to examine ecological traits of target species that need repeated surveying in the canopy. Here, an inexpensive rope climbing technique (see Jepson 2000; Barker & Standridge 2002) provides more flexible survey possibilities as it allows observations on any tree at any height except for the outermost crown regions of climbed trees.

The ecology of most tropical spiders is still understudied. Large, wandering araneomorph spiders are often common in the tropics and may form assemblages of seven or more species (Höfer et al. 1994; Gasnier et al. 2002; Lapinski & Tschapka 2013). Observations on habitat use outside the canopy within a guild of araneomorph wandering spiders in a Costa Rican lowland rainforest revealed the existence of three distinct subguilds (Lapinski & Tschapka 2013). The **semi-aquatic species** *Ancylometes bogotensis* (Keyserling, 1877) (Ctenidae) and *Trechalea tirimbina* Silva & Lapinski, 2012 (Trechaleidae) were strongly associated with bodies of water. The **forest-ground dwellers** *Ctenus curvipes* (Keyserling, 1881), *Ctenus sinuatipes* F.O.P.-Cambridge, 1897, and *Ctenus* sp. 3 (Ctenidae) roamed the forest floor and climbed only occasionally into the lower vegetation. The **vegetation dwellers** *Cupiennius coccineus* F.O.P.-Cambridge, 1901, *Cupiennius getazi* Simon, 1891, and *Phoneutria boliviensis* (F.O.P.-Cambridge, 1897) (Ctenidae) were found almost exclusively on plants. In the latter subguild, *Cu. coccineus* was most abundant in the forest and was also found to climb on trees, while the latter two species were found mainly on tall vegetation in treeless areas. Distinct differences in desiccation resistance among the species were related to habitat microclimate. Vegetation-dwelling species experienced drier and more variable microclimate than ground-dwelling and semi-aquatic species. Accordingly, vegetation dwellers showed higher desiccation resistance than species from the other two subguilds (Lapinski & Tschapka 2014). Differences in the ability to adhere to smooth surfaces and the corresponding morphological traits also matched the ecological preferences of these species (Lapinski & Tschapka 2013; Lapinski et al. 2015). All this provides evidence that species traits play a key role in shaping community structure (Kneitel & Chase 2004).

So far, ecology of large wandering spiders was mostly observed on and close to the forest floor (Höfer et al. 1994; Gasnier et al. 2002; Torres-Sánchez & Gasnier 2010). Thus, almost nothing is known about the vertical distribution of these spiders, its seasonal fluctuations or its underlying causes. To fill this gap, we surveyed 22 trees from ground to the canopy in a lowland rainforest at the Reserva Biológica Tirimbina on the Caribbean slope of Costa Rica.

We hypothesized that the known vegetation-dwelling species occur even higher than estimated and that the canopy would harbour additional species. We expected that arboreal species would be segregated vertically and that vertical distribution would depend on local climate or microclimate. Moreover, more heterogeneous habitats provide more shelters and food for any type of animals, both prey and predators. Therefore, arboreal wandering spider species should occur at greater heights and in greater densities on structurally complex host trees with many epiphytes than on less complex trees with few epiphytes.

METHODS

Study area.—Fieldwork was carried out from September 2010 to February 2012 at the Reserva Biológica Tirimbina (RBT; 10°24′ N, 84°07′ W, 180 – 220 m asl), Heredia Province, Costa Rica. Mean annual temperature is 25.3°C and mean annual precipitation is 3,777 mm. RBT includes very humid tropical pre-montane forest and transitions to very humid tropical forest. Eighty-five percent of the reserve's forest is classified as primary forest. RBT also encompasses areas of secondary forest of various age classes. The trees surveyed on an island in the Sarapiquí river were in old growth secondary forest, while the rest of the surveyed trees were in primary forest (see Fig. S1, online at http://dx.doi.org/10.1636/JoA-S-16-033.S1). Forest canopy height in the area ranged between 30 and 40 m, with emergent trees up to *ca.* 50 m. For a more detailed description, see Lapinski & Tschapka (2013).

Fieldwork.—Most fieldwork was conducted in the western part of RBT. We surveyed 22 trees belonging to 12 different species once per month (except December 2010 and March 2011), using rope climbing technique (Jepson 2000; Barker & Standridge 2002). A table of tree species and their characteristics is available online at http://dx.doi.org/10.1636/JoA-S-16-033.S3. As spiders are not usually host-tree specific, we surveyed suitable trees from different species (Sorensen 2003 and references therein). Selection criteria of suitable trees were (1) accessibility by an arrow shot from the ground in order to install a climbing rope and (2) height at least that of the surrounding canopy. Spiders were surveyed at night on trunks and central portions of the crown of each selected tree and its surrounding vegetation, from ground level to *ca.* 3 m above the branch to which the climbing rope was attached. Data were taken within a survey radius of approximately five meters and only during the ascension to prevent repeated sampling. Prior to ascension, we also searched for 15 minutes for spiders on the forest ground and in the understory vegetation within a 5-meter radius around the climbed tree, to collect data on spiders roaming the lower strata of the forest. Active spiders of different instars were recorded during 152 surveys, from 1830 – 0415 h. All spiders encountered at the entrance or outside of their day shelters were considered to be active. Only large araneomorph species with an adult body length ≥17 mm were included, to reduce a potential size-driven bias while searching for the spiders on the trees. These species were known from previous studies at RBT (Lapinski & Tschapka 2013, 2014; Lapinski et al. 2015) and thus could be identified in the field without the necessity of capturing and killing them. Even juveniles could be reliably identified in the field, as we had previous experience with captive individuals. We distinguished the following instar categories: subadult or adult, large juvenile (i.e., ≥0.5 the body length of adults), and small juvenile (<0.5 the body length of adults of the respective species). As the smallest juveniles (spiderlings ≤3 mm body length) could not be reliably located and identified in the field, they were omitted from our surveys. Spiders at greater distance from the climbing observer were identified using binoculars (Pentax 8x36 DCF HS). Spiders were never observed to flee when illuminated by head lamp or when a branch was shaken by the climber's movements. Voucher specimens of two previously unidentified species were preserved in ethanol (70%) and after successful identification will be deposited in the Museo de Zoología, Escuela de Biología, Universidad de Costa Rica, San José, Costa Rica.

For each individual spider sighting, the following parameters were recorded: date, time, tree individual, tree species, species of the spider, sex, instar, height above ground using a measuring tape (to the nearest 0.1 m), microhabitat (for categories, see Fig. 4). Tree species were identified using Condit et al. (2011) and with the help of the local botanist José Angel González Ramírez. To assess the influence of microclimate fluctuations on the vertical distribution of the spiders during the study period, data loggers (Hobo Pro v2, temperature/relative air humidity, Onset Computer Corporation, Cape Cod, MA, U.S.A.) were installed on three trees at 1 m and 28 m above ground on the northern side of the tree trunks (see supplementary material Table S3). Temperature (°C) and relative air humidity (%) were recorded hourly from 1 Oct 2010 to 27 Feb 2012 (for details see Lapinski & Tschapka 2014). Since the data loggers provide the exact time point of logging, temperature and relative air humidity-values were related to the full hour of encounter of each spider individual. Vapor pressure deficit is the force that drives evaporation (Anderson 1936; Gates 1980) and, therefore, we calculated vapor pressure deficit from the recorded temperature and relative air humidity data using the equation of Allen et al. (2005). Additionally, precipitation data obtained from the RBT meteorological unit were used to relate changes of local climate with vertical distribution patterns of the spiders.

Statistical tests.—In both inter- and intraspecific analyses, all instars were included unless otherwise indicated. We used SigmaStat (Version 3.5) for all univariate analyses and stepwise forward and multiple linear regressions. We tested for interspecific differences in the use of substrate type and microhabitat (nominal variables) with a Chi-square (χ^2) test. Continuous non-normally distributed variables were analyzed with Kruskal-Wallis one way ANOVA on ranks using Dunn's *post-hoc* test for unequal sample size. To make the vertical distribution of the spiders on trees of different height comparable, relative height of the spiders (rHS) on the respective tree was calculated (with values ranging between 0 and 1) and used instead of absolute height of the spiders above ground. Similarly, instead of absolute height of the lowest branch of a tree, its relative height (values between 0 and 1) was used for the analyses, the higher the value, the smaller the crown height relative to total tree height. To better visualize the vertical distribution of the two most common arboreal species, data on the relative height above ground of all observed individuals (all instars) were assembled in classes (0.0–0.2, 0.21–0.4, ...0.81–1.0). We tested with a Chi-square for differences in the absolute numbers encountered in the classes.

Cupiennius coccineus was the by far most abundant arboreal species ($n = 880$) and we used the species' data as an example to explore the vertical distribution of large wandering spiders. To obtain densities of *Cu. coccineus* per surveyed tree, we divided abundance by total tree height, since due to varying structural complexity of the trees, no area values could be calculated. In order to explore which variables may affect density and vertical distribution of *Cu. coccineus* data were $\log_{10}(x+1)$ – transformed and then standardized. We used only the standardized data that we entered into stepwise forward

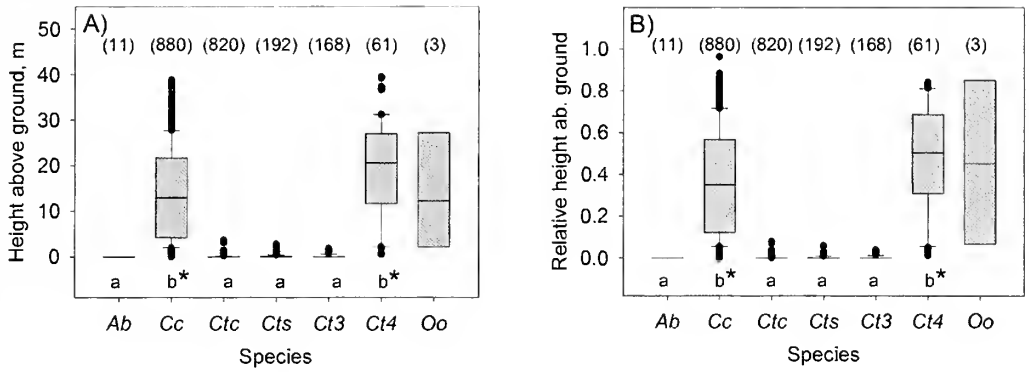

Figure 1.—Vertical distribution of wandering spiders at RBT expressed by (A) absolute height of the spiders above ground and (B) height of the spiders relative to the total height of the trees. Different letters below the boxes indicate significant differences in the *post hoc* test of Kruskal-Wallis ANOVA, asterisks point to significant difference in Mann-Whitney test, figures in parentheses above the boxes give the sample size. Horizontal lines in the boxes represent the median, boxes are from Q_{25} to Q_{75}, error bars from Q_{10} to Q_{90}, full circles are outliers. Species abbreviations: *Ab* = *Ancylometes bogotensis*, *Cc* = *Cupiennius coccineus*, *Ctc* = *Ctenus curvipes*, *Cts* = *Ctenus sinuatipes*, *Ct3*, *Ct4* = *Ctenus* sp. 3 and 4, respectively, *Oo*=*Olios obtusus*.

and then multiple linear regressions. We used only the data obtained on the climbed trees because structural characteristics of neighbouring vegetation were not assessed. Two approaches were applied. (1) To examine which structural variables may affect mean density of *Cu. coccineus* per survey on each tree we conducted stepwise forward linear regression. The number of tree individuals was the sample size ($n = 20$). Following independent variables were entered: diameter of tree trunk at breast height (DBH), tree height, relative height of the lowest branch, total number of holes (both on trunk and in the crown), and total number of epiphytes (both on trunk and in the crown) (see supplementary Table S4, available online at http://dx.doi.org/10.1636/JoA-S-16-033.S4). Subsequently, based on the results from that stepwise regression, we entered only those independent variables that may significantly contribute to the prediction of density of *Cu. coccineus*: DBH, relative height of the lowest branch, and total number of holes. The remaining independent variables did not add significantly to the prediction of density and were omitted from the multiple linear regression.

(2) To investigate how vertical distribution (i.e., relative height of spider above ground) may be affected we applied stepwise forward regression and subsequently multiple linear regression as described above. The difference was that each individual *Cu. coccineus* was treated as case and each tree was considered a replicate. Hence, in addition to the structural variables of the trees (DBH, height of tree, relative height of the lowest branch, number of epiphytes on the trunk, number of epiphytes in the crown, number of holes in the trunk, and number of holes within the crown), we were able to include instar, and vapor pressure deficit at 28 m above ground during the hour of spider encounter. Sample size was reduced from $n = 880$ to $n = 551$ individual observations made during the period from which microclimate data were available. First, we ran a stepwise forward regression on all variables and based on the results from that we entered only the following independent variables into a multiple linear regression: instar, DBH, height of tree, relative height of lowest branch, and number of epiphytes in the crown.

RESULTS

Twenty-two trees belonging to 12 species with a total height ranging from 26 to 47 m were regularly surveyed. Two trees (sp. 1, sp. 2) could not be identified because leaves and flowers could not be reached. We had to exclude two trees early during the study due to tree fall of neighboring trees that altered the site characteristics. Data already collected at these trees prior to the tree fall were included for assessing overall vertical distribution of the spider species (Figs. 1–3), the use of microhabitats and substrate types by the arboreal species (Fig. 4), and the seasonal fluctuations of vertical distribution of *Cu. coccineus* (Fig. 5).

Vertical distribution of the assemblage.—Data from 2136 individual observations from seven wandering spider species were recorded. Not a single individual of *Cu. getazi* and *P. boliviensis* was found within the forest. We found *Ancylometes bogotensis* only rarely because these spiders live mainly on banks of creeks and only three trees were close enough to water. *Ctenus curvipes*, *Ct. sinuatipes*, and *Ctenus* sp. 3 (Ctenidae) occurred mainly on or very close to the ground, rarely higher than 1 m (Fig. 1). *Cupiennius coccineus* and two previously undescribed species, *Ctenus* sp. 4 (Ctenidae) and *Olios obtusus* F.O. Pickard-Cambridge, 1900 (Sparassidae), were found almost exclusively on vegetation using almost the entire height range. *Cupiennius coccineus* and *Ctenus* sp. 4 occurred significantly higher than *A. bogotensis*, *Ct. curvipes*, *Ct. sinuatipes*, and *Ctenus* sp. 3 (Figs. 1 A, B, Kruskal-Wallis ANOVA, $P \leq 0.001$, for height of spider: $H_5 = 1755.2$, for relative height of spider: $H_5 = 1756.3$, Dunn's *post-hoc* test, $P < 0.05$). During all nocturnal tree surveys, only three individuals of *O. obtusus* were found, but during the walks to the surveyed trees several additional individuals were observed on understory vegetation, supporting the assignment of this species to the vegetation-dwelling subguild.

Vertical segregation of arboreal species.—The vertical distribution of *Cu. coccineus* and *Ctenus* sp. 4 overlapped strongly at intermediate heights (Fig. 2, all instars considered). However, *Cu. coccineus*, was more strongly represented in the lowest class of relative height, while *Ctenus* sp. 4 was more frequently found in the higher parts of the trees (Chi-squared

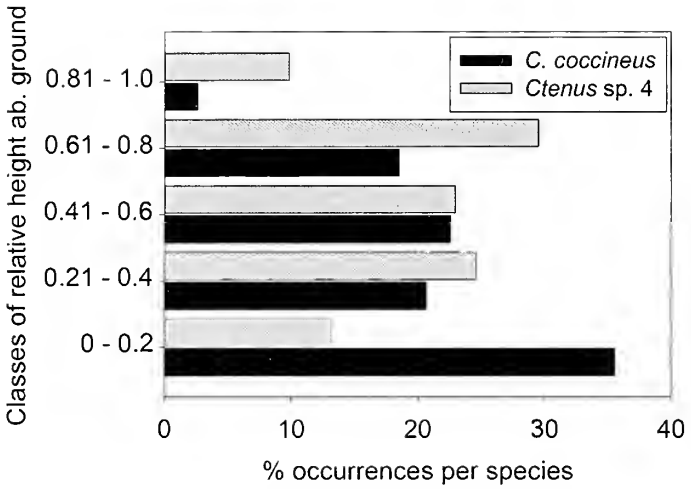

Figure 2.—Percentage of occurrences in different classes of relative height of spider above ground showing the vertical distribution of the arboreal *Cupiennius coccineus* ($n = 880$) and *Ctenus* sp. 4 ($n = 61$).

test, $\chi^2 = 22.08$, df = 4, $P \leq 0.001$). Subadult/adult *Cu. coccineus* occurred significantly lower than both large and small juveniles, although the vertical distribution of all instars strongly overlapped (Fig. 3A, Kruskal-Wallis ANOVA, $P \leq 0.001$, $H_2 = 32.3$, Dunn's *post-hoc* test, $P < 0.05$). In *Ctenus* sp. 4, we found no such differences among the instars (Fig. 3B, Kruskal-Wallis ANOVA, $P = 0.628$, $H_2 = 0.93$).

Arboreal microhabitats.—*Cupiennius coccineus* and *Ctenus* sp. 4 differed significantly in microhabitat and substrate preferences (Fig. 4 A,B). Tree trunks and epiphytes on tree trunks were preferred by *Cu. coccineus* while *Ctenus* sp. 4 showed a more pronounced preference for tree trunks (Chi-squared test, $\chi^2 = 140.2$, df = 10, $P \leq 0.001$). Accordingly, *Cu. coccineus* preferred bark and leaf substrates, and *Ctenus* sp. 4 was mostly found on bark and moss (Chi-squared test, $\chi^2 = 133.6$, df = 7, $P \leq 0.001$)

Seasonality.—Local climate at RBT showed no pronounced seasonality between September 2010 and February 2012. The two phases of reduced precipitation and higher vapour pressure deficit in April 2011 and February 2012 did not coincide with a clear change in vertical distribution of *Cu. coccineus* (Fig. 5). However, the position on the trees was significantly lower in September 2010 than in April 2011 (Kruskal-Wallis ANOVA, $P = 0.041$, $H_{15} = 25.7$, Dunn's *post-hoc* test, $P < 0.05$). In *Ct. curvipes*, *Ct. sinuatipes*, and *Ctenus* sp. 3, relative height of spiders was consistently below 0.1 and vertical distribution did not differ significantly among months (Kruskal-Wallis-ANOVA, $P = 0.704$, $H_{15} = 11.7$; $P = 0.162$, $H_{15} = 20.3$; and $P = 0.304$, $H_{15} = 17.2$, respectively). Sample size of *Ctenus* sp. 4 was too low to analyze seasonality in vertical distribution of that species.

The arboreal *Cupiennius coccineus*.—Because *Cu. coccineus* was by far the most abundant species on trees, we examined the variables affecting its density and vertical distribution in more detail. Density of *Cu. coccineus* varied significantly among individual trees and showed considerable variation among surveys (Kruskal-Wallis ANOVA on ranks $H_{19} = 133.03$, $P \leq 0.001$; see Fig. S2, available online at http://dx.doi.org/10.1636/JoA-S-16-033.S2).

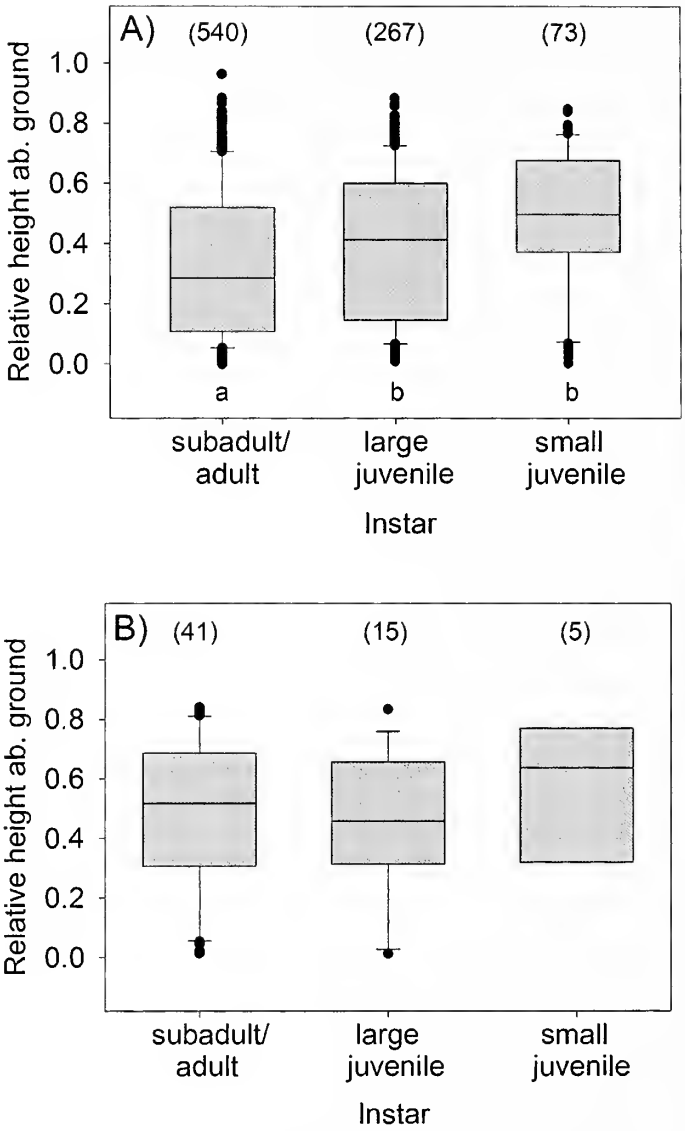

Figure 3.—Vertical distribution of different instars of (A) *Cupiennius coccineus* and (B) *Ctenus* sp.4. Instar abbreviations: sa/a=subadult/adult females and males, j2=large juveniles, j1=small juveniles. Different letters below the boxes indicate significant differences, figures in parentheses above the boxes show sample size. Horizontal lines in the boxes represent the median, boxes are from Q_{25} to Q_{75}, error bars from Q_{10} to Q_{90}, full circles are outliers.

Density of *Cu. coccineus* increased with the diameter at breast height, the relative height of the lowest branch and the number of holes (multiple linear regression, Table 1). The relative height of *Cu. coccineus* on trees was lower for late than for young instars, and decreased with tree diameter and the height of the lowest branch. It increased with height of the tree and with the number of epiphytes in the canopy (multiple linear regression, Table 2). The effect of instar and epiphytes is congruent with intraspecific differences in vertical distribution (Fig. 3) and microhabitat and substrate use (Fig. 4).

DISCUSSION

We explored the distribution of seven large araneomorph wandering spiders in a Costa Rican rainforest along vertical

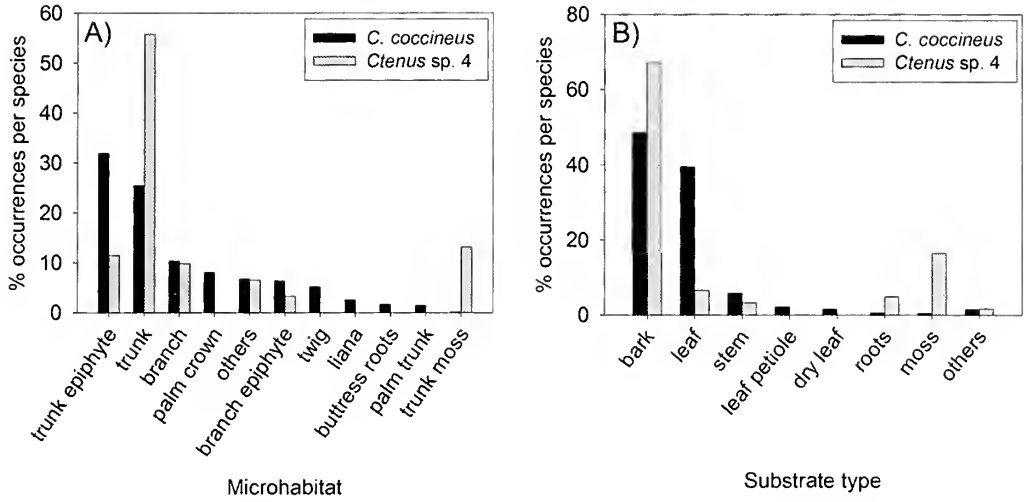

Figure 4.—Use of (A) microhabitats and (B) substrate types by the arboreal species *Cupiennius coccineus* ($n = 880$) and *Ctenus* sp. 4 ($n = 61$).

transects (i.e., trees). Lapinski & Tschapka (2013) suggested that the large wandering spiders at the study site may differ significantly in their vertical distribution, with *Cu. coccineus* being the most common arboreal species. However, these data were obtained mainly from the ground and surveys were limited mostly to a maximum height of 5 m. The current study overcomes these limitations and presents a more complete picture of a guild of large wandering spiders in a Neotropical rainforest. It confirms that *Ancylometes bogotensis*, *Ct. sinuatipes*, *Ct. curvipes* and *Ctenus* sp. 3 are indeed restricted to the forest ground and lower understory. The vegetation-dwelling subguild of large araneomorph wandering spiders, consisting of *Cu. coccineus*, *Cu. getazi*, and *P. boliviensis* (Lapinski & Tschapka 2013) is extended by two rare medium-sized species: *Ctenus* sp. 4 (Ctenidae) and *O. obtusus* (Sparassidae), which, together with *Cu. coccineus*, are rather arboreal and use nearly the entire height range. The data confirm our hypotheses that the known vegetation-dwelling species occur even higher than had been estimated and that the canopy would harbour additional species. However, more

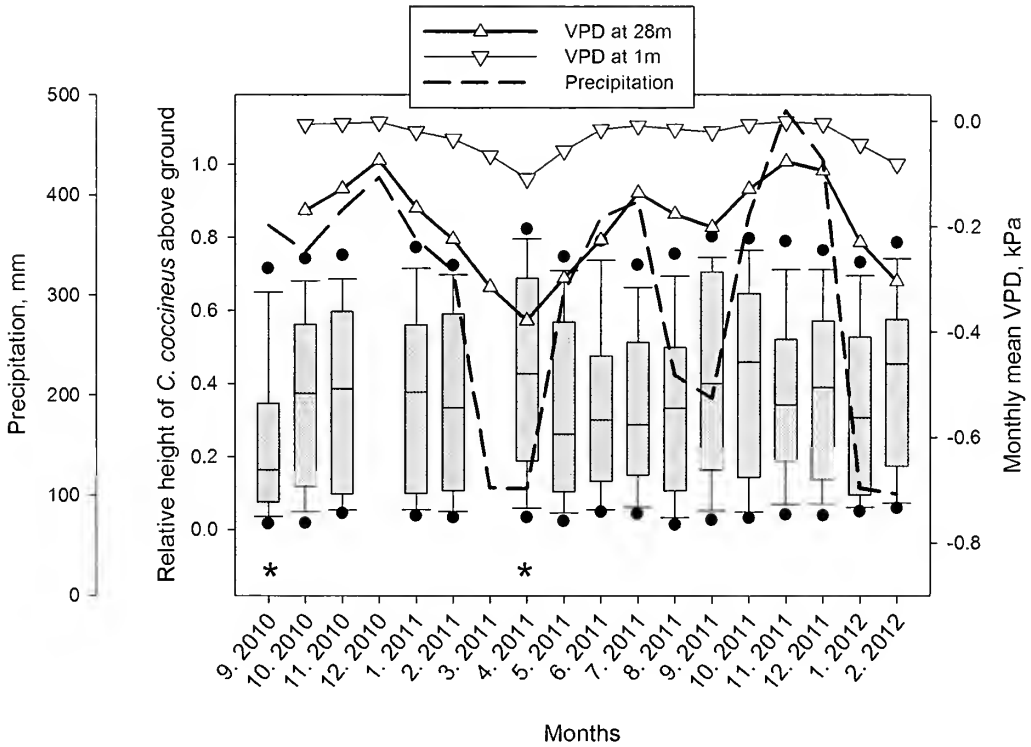

Figure 5.—Seasonal fluctuations of vapor pressure deficit (VPD) 1m and 28 m above the ground, precipitation, and relative height above ground (rHS) of *Cupiennius coccineus* (box plots, all instars included). Asterisks indicate significantly lower positions of *Cu. coccineus* relative to the remaining months. Horizontal lines in the boxes represent the median, boxes are from Q_{25} to Q_{75}, error bars from Q_{10} to Q_{90}, full circles are outliers within 5%- and 95%-percentiles.

Table 1.—Results of multiple regression analysis with density of *Cupiennius coccineus* on $n = 20$ trees as dependent variable and DBH, relative height of lowest branch, and total number of holes as independent variables. For definitions and details of variables see Table S4, available online at http://dx.doi.org/10.1636/JoA-S-16-033.S4.

	Coefficient	Std. Error	t	P	VIF
Constant	-7.97E-16	0.13	-6.16E-15	1	
DBH	0.69	0.15	4.71	<0.001	1.22
rel. height lowest branch	0.58	0.15	3.82	0.002	1.31
total number of holes	0.44	0.15	2.89	0.011	1.31
Analysis of Variance:					
	DF	SS	MS	F	P
Regression	3	13.64	4.55	13.57	<0.001
Residual	16	5.36	0.33		
Total	19	19	1		
R = 0.85	$R^2 = 0.72$	Adj $R^2 = 0.67$			
SE of estimate = 0.58					

data on the ecology of the apparently rare *O. obtusus* are needed. In Puerto Rico, an *Olios* species was the most abundant large wandering spider on low understory vegetation (Formanowicz et al. 1981). The arboreal katydid *Philophyllia ingens* (Tettigoniidae) showed a similarly wide range of vertical distribution with conspicuous movements upwards at dawn and downwards starting at noon (Fornoff et al. 2012). Because we did not find any single individual of *Cu. getazi* and *P. boliviensis* within the forest at any height, our suggestion that these vegetation dwelling species are restricted to early succession habitats is corroborated (Lapinski & Tschapka 2013). However, the cause for the habitat segregation among *Cu. coccineus* on the one hand, and *Cu. getazi* and *P. boliviensis* on the other hand remains unclear.

In ecological networks of wooded savannah of central Kenya, mainly ground-dwelling rather than arboreal predators couple food webs of canopy and grass strata by feeding on ground-dwelling as well as on fallen arboreal animals (Pringle & Fox-Dobbs 2008). In structurally much more complex rainforest networks, however, arboreal generalist predators with a broad range of vertical distribution and microhabitats, such as the common *Cu. coccineus*, appear to be the more efficient link between the understory and the canopy of the forest. These spiders may feed on occasionally climbing ground-dwelling prey, on understory residents and on canopy specialists. Both in Ecuador and in Costa Rica, the rainforest canopy and understory have distinct assemblages of fruit-feeding butterflies of the family Nymphalidae (DeVries et al. 2011). Through their wide vertical range, the studied arboreal spiders might exploit both understory and canopy Lepidoptera, and probably also other insects that segregate similarly along the vertical axis. Additionally, the spiders might be preyed upon by both understory and canopy predators, thus being an integral part of a complex network.

Microclimate may affect habitat use via physiology (Kneitel & Chase 2004; Morin 2011) and vertical distribution of generalist predators may mainly depend on their tolerance to environmental conditions (Basset et al. 2003). Thus, the pattern of vertical distribution at Reserva Biológica Tirimbina (RBT) can be largely explained by the interaction between spider physiology and the microclimate gradient along the vertical axis. Like other forests (Parker & Brown 2000; Madigosky 2004), the forest at RBT shows a gradient of decreasing temperature, increasing relative air humidity, and decreasing variation of both from the forest canopy to the ground (Lapinski & Tschapka 2014). Accordingly, the semi-aquatic and ground-dwelling species at RBT had lower desiccation resistance than vegetation-dwelling species, with *Cu. coccineus* showing the lowest susceptibility to water loss (Lapinski & Tschapka 2014). Similar links between physiology

Table 2.—Results of multiple regression analysis with relative height of ($n = 551$) *Cupiennius coccineus* on $n = 20$ trees as dependent variable and instar, DBH, height of tree, relative height of lowest branch, and number of epiphytes in the crown as independent variables. For definitions and details of variables see Table S4, available online at http://dx.doi.org/10.1636/JoA-S-16-033.S4.

	Coefficient	Std. Error	t	P	VIF
Constant	8.70E-03	0.04	2.20E-01	0.825	
instar	-0.18	0.04	-4.67	<0.001	1
DBH	-0.35	0.06	-5.57	<0.001	2.52
height of tree	0.46	0.07	6.64	<0.001	3.16
rel. height lowest branch	-0.16	0.07	-2.55	0.011	2.71
epiphytes in crown	0.18	0.05	3.81	<0.001	1.31
Analysis of Variance:					
	DF	SS	MS	F	P
Regression	5	88.54	17.71	20.92	<0.001
Residual	545	461.39	0.85		
Total	550	549.93	1		
R = 0.40	$R^2 = 0.16$	Adj $R^2 = 0.15$			
SE of estimate = 0.92					

and habitat use were found in other animal taxa, such as ants (Hood & Tschinkel 1990), frogs (e.g., Buttemer 1990; Young et al. 2005), and lizards (Eynan & Dmi'el 1993). Furthermore, we expected vertical distribution of arboreal species to depend on fluctuations of local climate or microclimate, which was not confirmed. Vapor pressure deficit during spider encounters did not add significantly to predict relative height of *Cu. coccineus* and seasonal fluctuations of precipitation at RBT were too weak to cause significant seasonal differences in vertical distribution in that species. This may result from its high desiccation resistance (Lapinski & Tschapka 2014); thus, even higher on the trees the microclimate may still be suitable for the species throughout the entire study period at the study site. In contrast, the three ground-dwelling *Ctenus* species occurred on or near the forest ground during the entire study period, even during wetter periods. This suggests that, due to their low tolerance to desiccation, the microclimate already becomes unfavourable for these species at low heights. Similarly, there was no significant effect of weekly rainfall on the activity density of spiders on lower parts of tree trunks in central Amazonia (Gasnier et al. 1995).

Moreover, microhabitat choice and hence vertical distribution of the studied spiders was also linked to morphology, with relatively bigger tarsal claw tufts (bearing adhesive setae) in the vegetation-dwelling than in the ground-dwelling species. The semi-aquatic species even lack these adhesive structures completely (Lapinski et al. 2015). These morphological characteristics result in better adhesion capabilities on smooth surfaces such as leaves or insect cuticle in the vegetation-dwelling compared to ground-dwelling and semi-aquatic species (Lapinski & Tschapka 2013). Similar relations between morphology, microhabitat choice, and vertical distribution are well documented for example in *Anolis* lizards (Polychrotidae, Elstrott & Irschick 2004) and in arboreal carabid beetles (Ober 2003).

The data only partially confirm our hypothesis that arboreal species are segregated vertically. Despite considerable overlap, the subtle differences in vertical distribution and microhabitat preferences together with low densities may reduce cannibalism, intraguild predation and competition among the instars of *Cu. coccineus* and the smaller *Ctenus* sp. 4. In this context, intraspecific differences in habitat use of the different instars have been observed, for example, in the predatory aquatic bug *Notonecta hoffmani* (Notonectidae, reviewed by Morin 2011), the theraphosid *Ephebopus murinus* (Walckenaer, 1937) (Marshall & West, 2008), and the co-occurring ctenid wandering spiders *Phoneutria fera* Perty, 1833, and *Phoneutria reidyi* (F.O.P.-Cambridge, 1897) (Torres-Sánchez & Gasnier 2010).

The results corroborate our expectation that on structurally more complex host trees, arboreal wandering spider species should also occur in greater heights and in greater densities than on less complex trees. The amount of epiphytes in the crown may affect vertical distribution of *Cu. coccineus* and thus form key components of the microhabitats, representing refuge sites for both the spiders and for their potential prey. Total number of holes may influence density of that species on the host trees. High complexity of vegetation may enhance densities of arthropods through providing both predators and their prey with shelter and food (Halaj et al. 1998; Stunz et al. 2002; Teixeira de Souza & Martins 2004). Experiments revealed the importance of structural complexity of plants for vertical distribution of spiders (Scheidler 1990), and for abundance and diversity of both spiders and potential prey arthropods (Halaj et al. 2000). Structurally complex canopies may also maintain higher densities of arthropods. High availability of shelters may lower predation on arthropods by actively hunting predators such as ants and birds because they need longer to find prey than in microhabitats with low structural complexity and hence low availability of shelters (Šipoš & Kindlmann 2012). High occurrence of epiphytes may not only enhance the structural complexity of trees but also the food supply for insects through vegetative parts, inflorescences and the associated fauna (Teixeira da Souza & Martins 2004).

In conclusion, our results demonstrate clear segregation between tree- and ground-dwelling species of large araneomorph wandering spider species in the rainforest, with only weak vertical segregation between arboreal species, which were used almost the entire height range. Vertical distribution of species may be the result of species-specific interactions between morphology and physiology on the one hand and microclimate and structural parameters of the host trees on the other. Given the wide range of vertical distribution of the studied arboreal spiders, they may couple the ecological networks of rainforest understory and canopy. Well planned long-term experiments are needed to investigate in more detail the factors promoting the observed dominance of *Cu. coccineus*, the role structural parameters play in microhabitat choice and vertical distribution within rainforests, and the coupling potential of these generalist predators. Similar surveys at other tropical sites are necessary to allow generalizations about the causes of vertical distribution of generalist arthropod predators.

ACKNOWLEDGMENTS

The Ministerio de Ambiente, Energía y Telecomunicaciones (MINAET) kindly granted us the permission to conduct the field work in Costa Rica. The friendly assistance of Javier Guevara (MINAET) is greatly appreciated. We are very grateful to all staff members at the Reserva Biológica Tirimbina for all their friendliness, support and for allowing us to realize this project at the station. Many thanks to José Angel González Ramírez (Organization for Tropical Studies) for identification of some trees and to Simone Blomenkamp for creating the map of RBT and assistance during tree preparation. Thanks to the editor and two anonymous reviewers for their suggestions which helped very much to improve the manuscript.

LITERATURE CITED

Allen, R.G., I.A. Walter, R. Elliott, T. Howell, D. Itenfisu & M. Jensen. 2005. The ASCE standardized reference evapotranspiration equation. Pp. 11–15. *In* Task Committee on Standardization of Reference Evapotranspiration of the Environmental and Water Resources Institute of the American Society of Civil Engineers. Reston, Virginia, USA.

Anderson, D.B. 1936. Relative humidity or vapor pressure deficit. Ecology 17:277–282.

Barker, M. & N. Standridge. 2002. Ropes as a mechanism for canopy

access. Pp. 13–23. *In* The Global Canopy Handbook. Techniques of Access and Study in the Forest Roof. (A.W. Mitchell, K. Secoy, T. Jackson (eds.)). Global Canopy Programme, Oxford, UK.

Basset, Y. 2001. Invertebrates in the canopy of tropical rain forests. How much do we really know? Plant Ecology 153:87–107.

Basset, Y., P.M. Hammond, H. Barrios, J.D. Holloway & S.E. Miller. 2003. Vertical stratification of arthropod assemblages. Pp. 17–27. *In* Arthropods of Tropical Forests: Spatio-temporal Dynamics and Resource Use in the Canopy. (Y. Basset, V. Novotny, S. E. Miller & R.L. Kitching (eds.)). Cambridge University Press, Cambridge, UK.

Buttemer, W.A. 1990. Effect of temperature on evaporative water loss of the Australian tree frogs *Litoria caerulea* and *Litoria chloris*. Physiological Zoology 63:1043–1057.

Condit, R., R. Pérez & N. Daguerre. 2011. Trees of Panama and Costa Rica. Princeton Field Guides. Princeton University Press, Princeton, New Jersey, USA.

DeVries, P. J., L.G. Alexander, I.A. Chacón & J.A. Fordyce. 2011. Similarity and difference among rainforest fruit-feeding butterfly communities in Central and South America. Journal of Animal Ecology 81:472–482.

Elstrott, J. & D.J. Irschick. 2004. Evolutionary correlations among morphology, habitat use and clinging performance in Carribean *Anolis* lizards. Biological Journal of the Linnean Society 83:389–398.

Eynan, M. & R. Dmi'el. 1993. Skin resistance to water loss in agamid lizards. Oecologia 95:290–294.

Floren, A. & C. Deeleman-Reinhold. 2005. Diversity of arboreal spiders in primary and disturbed tropical forests. Journal of Arachnology 33:323–333.

Formanowicz, D.R. Jr., M.M. Stewart, K. Townsend, F.H. Pough & P.F. Brussard. 1981. Predation by giant crab spiders on the Puerto Rican frog *Eleutherodactylus coqui*. Herpetologica 37:125–129.

Fornoff, F., D.K.N. Dechmann & M. Wikelski. 2012. Observation of movement and activity via radio-telemetry reveals diurnal behavior of the Neotropical katydid *Philophyllia ingens* (Orthoptera: Tettigoniidae). Ecotropica 18:27–34.

Gasnier, T.R., A.C. Azevedo, M.P. Torres-Sánchez & H. Höfer. 2002. Adult size of eight hunting spider species in central Amazonia: Temporal variations and sexual dimorphisms. Journal of Arachnology 30:146–154.

Gasnier, T.R., H. Höfer & A.D. Brescovit. 1995. Factors affecting the "activity density" of spiders on tree trunks in an Amazonian rainforest. Ecotropica 1:69–77.

Gates, D. M. 1980. Biophysical Ecology. Springer-Verlag, New York, USA.

Gurgel-Gonçalves, R., A.R.T. Palma, P.C. Motta, M.E. Bar & C.A.C. Cuba. 2006. Arthropods associated with the crown of *Mauritia flexuosa* (Arecaceae) palm trees in three different environments from Brazilian cerrado. Neotropical Entomology 35:302–312.

Halaj, J., D.W. Ross & A.R. Moldenke. 1998. Habitat structure and prey availability as predictors of the abundance and community organization of spiders in western Oregon forest canopies. Journal of Arachnology 26:203–220.

Halaj, J., D.W. Ross & A.R. Moldenke. 2000. Importance of habitat structure to the arthropod food-web in Douglas-fir canopies. Oikos 90:139–152.

Höfer, H., A.D. Brescovit & T.R. Gasnier. 1994. The wandering spiders of the genus *Ctenus* (Ctenidae: Araneae) of Reserva Adolfo Ducke, a rainforest reserve in central Amazonia. Andrias 13:81–98.

Hood, W.G. & W.R. Tschinkel. 1990. Desiccation resistance in arboreal and terrestrial ants. Physiological Entomology 15:23–35.

Jepson, J. 2000. The Tree Climber's Companion. A Reference and Training Manual for Professional Tree Climbers. 2nd ed. Beaver Tree Publishing, Longville, U.S.A.

Kneitel, J.M. & J.M. Chase. 2004. Trade-offs in community ecology: linking spatial scales and species coexistence. Ecology Letters 7:69–80.

Lapinski, W. & M. Tschapka. 2013. Habitat use in an assemblage of Central American wandering spiders. Journal of Arachnology 41:151–159.

Lapinski, W. & M. Tschapka. 2014. Desiccation resistance reflects patterns of microhabitat choice in a Central-American assemblage of wandering spiders. Journal of Experimental Biology 217:2789–2795.

Lapinski, W., P. Walther & M. Tschapka. 2015. Morphology reflects microhabitat preferences in an assemblage of Neotropical wandering spiders. Zoomorphology, DOI 10.1007/s00435-015-0257-8

Lowman, M.D., T.D. Schowalter & J.F. Franklin. 2013. Methods in Forest Canopy Research. University of California Press, Berkeley, Los Angeles, U.S.A., London, UK.

Madigosky, S.R. 2004. Tropical microclimatic considerations. Pp. 24–48. *In* Forest Canopies. 2nd ed.,(M.D. Lowman, H.B. Rinker, eds.). Elsevier Academic Press, San Diego, U.S.A.

Marques, M.I., J. Adis, G.B. dos Santos & L.D. Battirola. 2006. Terrestrial arthropods from tree canopies in the Pantanal of Matto Grosso, Brazil. Revista Brasileira de Entomologia 50:257–267.

Marshall, S.D. & R. West. 2008. An ontogenetic shift in habitat use by the Neotropical tarantula *Ephebopus murinus* (Araneae, Theraphosidae, Aviculariinae). Bulletin of the British Arachnological Society 14:280–284.

Mitchell, A.W., K. Secoy & T. Jackson (eds.). 2002. The Global Canopy Handbook. Techniques of Access and Study in the Forest Roof. Global Canopy Programme, Oxford, UK.

Morin, P.J. 2011. Community Ecology. Wiley-Blackwell, Chichester, UK.

Ober, K. 2003. Arboreality and morphological evolution in ground beetles (Carabidae: Harpalinae): testing the taxon pulse model. Evolution 57:1343–1358.

Parker, G.G. & M J. Brown. 2000. Forest canopy stratification – is it useful? American Naturalist. 155:473–484.

Pringle, R.M. & K. Fox-Dobbs. 2008. Coupling of canopy and understory food webs by ground-dwelling predators. Ecology Letters 11:1328–1337.

Russell-Smith, A. & N.E. Stork. 1994. Abundance and diversity of spiders from the canopy of tropical rainforests with particular reference to Sulawesi, Indonesia. Journal of Tropical Ecology 10:545–558.

Scheidler, M. 1990. Influence of habitat structure and vegetation architecture on spiders. Zoologischer Anzeiger 225:333–340.

Šipoš, J. & P. Kindlmann. 2012. Effects of the canopy complexity of trees on the rate of predation of insects. Journal of Applied Entomology 137:445–451.

Sorensen, L.L. 2003. Stratification of the spider fauna in a Tanzanian forest. Pp. 92–101. *In* Arthropods of Tropical Forests: Spatio-temporal Dynamics and Resource Use in the Canopy. (Y. Basset, V. Novotny, S.E. Miller, R.L. Kitching, eds.). Cambridge University Press, Cambridge, UK.

Stunz, S., C. Ziegler, U. Simon & G. Zotz. 2002. Diversity and structure of the arthropod fauna within three canopy epiphyte species in central Panama. Journal of Tropical Ecology 18:161–176.

Teixeira da Souza, A.L. & R.P. Martins. 2004. Distribution of plant dwelling spiders: inflorescences versus vegetative branches. Australian Ecology 29:342–349.

Torres-Sánchez, M.P. & T.R. Gasnier. 2010. Patterns of abundance, habitat use and body size structure of *Phoneutria reidyi* and *P. fera* (Araneae: Ctenidae) in a Central Amazonian rainforest. Journal of Arachnology 38:433–440.

Young, J.E., K.A. Christian, S. Donnellan, C.R. Tracy & D. Parry. 2005. Comparative analysis of cutaneous evaporative water loss in frogs demonstrates correlation with ecological habits. Physiological and Biochemical Zoology 78:847–856.

Manuscript received 31 May 2016, revised 21 July 2017.

2018. Journal of Arachnology 46:21–25

Daily pattern of locomotor activity of the synanthropic spiders *Loxosceles laeta* and *Scytodes globula*

Rigoberto Solís[1], **Ana Alfaro**[1], **Bernardo Segura**[1], **Lucila Moreno**[2] and **Mauricio Canals**[3]: [1]Departamento de Ciencias Biológicas Animales, Facultad de Ciencias Veterinarias y Pecuarias, Universidad de Chile; E-mail: rsolis@uchile.cl; [2]Departamento de Zoología. Facultad de Ciencias Naturales y Oceanográficas. Universidad de Concepción; [3]Departamento de Medicina y Programa de Salud Ambiental, Escuela de Salud Pública, Facultad de Medicina, Universidad de Chile.

Abstract. The locomotor activity of the Chilean recluse spider *Loxosceles laeta* (Nicolet, 1849), and the spitting spider, *Scytodes globula* Nicolet, 1849, were studied in the laboratory under controlled conditions (LD 12:12). In Chile, these are two common synanthropic spiders which share a microhabitat and show extensive thermal niche overlap. Although no systematic studies have been performed, it has been reported that they have nocturnal habits. Here we confirmed strictly nocturnal activity for *S. globula* and mainly nocturnal but with some degree of diurnal activity for the Chilean recluse spider. Also, *S. globula* showed a bimodal pattern of activity while *L. laeta* had a unimodal one. The similarity of the use of space and time make the interaction of these spiders inside homes highly probable.

Keywords: Circadian rhythm, niche, overlap, behavior

In Chile, there are two common synanthropic spiders: *Loxosceles laeta* (Nicolet, 1849) and *Scytodes globula* Nicolet, 1849. The former species has been associated with necrotic arachnidism in this country; because of its araneophagic behavior, the latter has been considered as a natural predator of *L. laeta* (Fernandez et al. 2002; Canals et al. 2015a). In spite of its medical and ecological importance, there is scarce information about the behavior of these species. These spiders show similar physiological performance under the same thermal and humidity experimental conditions (Canals et al. 2013, 2015b) which may explain their presence in the same places in homes. However, they differ in trophic exploitation because *S. globula* is mainly an araneophagic spider while *L. laeta* shows a wider prey spectrum (Nentwig 2013). As a consequence, these spiders may use time differently, with *L. laeta* having a less restricted degree of activity than *S. globula*. In addition, preliminary data indicate they also differ in the photic sensibility threshold which produces inhibition of their movements of reaction (unpublished data).

An important amount of documentary evidence indicate that diel rhythms of locomotor activity in spiders are linked to an endogenous rhythm (Cloudsley-Thompson 2013). This activity also appears to be synchronized to the light-dark cycle, with light intensity being an important temporal environmental cue (Cloudsley-Thompson 2000). Because time is an important axis of the niche which may make possible the spatial coexistence of species, this study helps to understand the dynamics of the interaction of two synanthropic species in Chile. Here we report differences in locomotor behavior between the species maintained under an experimental light-dark cycle.

METHODS

Adult specimens of *S. globula* and *L. laeta* used in this study were caught inside houses, abandoned warehouses and other dark and little-disturbed synanthropic settings. In the laboratory, spiders were kept in plastic 750 ml screw cap bottles with a light-dark cycle of 12:12. The temperature was maintained at 20 ± 2° C during the stay in the laboratory and the experiments, which in a previous study was found to be the preferred temperature of these species (Alfaro et al. 2013). Throughout the study, the spiders were fed with larval stages of *Tenebrio molitor* twice a month and watered using a spray bottle twice per week.

Locomotor activity of 18 individuals (5 males and 13 females) of *S. globula* and 18 individuals of *L. laeta* (9 males and 9 females) was recorded. Seven days before the start of the activity recordings, spiders were transferred to an arena for habituation. The arena consisted of a white plastic circular container (19.5 cm diameter and 5 cm deep) covered by a glass plate.

The measurements were made inside an experimental chamber (0.6 m wide x 1.3 m long x 1.5 m high), where the same maintenance cycle of light: dark (12 hours light and 12 hours dark) was applied. As a source of light, a 40 W bulb with tungsten filament produced 20 lux intensity. In order not to alter the behavior of individuals during the dark phase of the cycle, an infrared light was used (Canals et al. 1997), and the recordings were made with the "nightshot" function of a SONY HDR-CX 700 digital video camera for infrared lighting for night vision. To our knowledge there is no previous information on the sensitivity of spiders to infrared light, and available evidence describe maximal sensitivities at wavelengths lower than 600 nm (Foelix 2011). In agreement with these observations, we did not detect any behavioral changes in the species we used under IR.

All spiders were recorded in photophase first and then in scotophase. After the diurnal activity was recorded, the L:D cycle was inverted in the experimental chamber in order to match the natural cycle and our work schedule, because the nightshot function needs to be activated manually. The experimental subject was exposed to the new cycle for at least seven days with the new cycle before its nocturnal locomotor activity was recorded. Available evidence indicates that invertebrates are able to synchronize to a new L:D cycle very rapidly (Ortega-Escobar 2002; Mistlberger & Rusak 2005). Thus, locomotor activity during photophase and scotophase

Table 1.—Average of movement events (ME) and distance walked (DW) during 12 hours of light (L) and 12 hours of dark (D) by *Scytodes globula* and *Loxosceles laeta*

	ME (*n*)		DW (cm)	
	L	D	L	D
S. globula				
Males	67 ± 18	1009 ± 461	18 ± 6	222 ± 117
Females	35 ± 30	1101 ± 324	9 ± 6	553 ± 231
All individuals	45 ± 21	1092 ± 257	12 ± 6	443 ± 161
Proportion of activity (%)	4.1	95.9	2.6	97.4
L. laeta				
Males	723 ± 304	1619 ± 540	535 ± 355	845 ± 262
Females	803 ± 281	2441 ± 540	274 ± 389	424 ± 332
All individuals	763 ± 200	2132 ± 355	407 ± 186	635 ± 147
Proportion of activity (%)	26.4	73.6	39	61

of each individual was recorded only for one 12-hour period, the last of the seven days of acclimation to the normal or inverted cycle L:D.

Locomotor activity was measured as the number of movement events (ME) of the spider in the arena during the scotophase and photophase. The criterion for movement was a position shift not less than the body length of the spider. In each phase, the activity was recorded continuously with the camera connected to a Noldus Ethovision system (Noldus Information Technology, Wageningen, The Netherlands) using a sampling rate of one frame per second. Variables measured were number of movement events (ME) and total distance walked (DW) by the spider during recordings. To discern a temporal pattern of activity, the number of movements per hour was plotted both in the light and dark phases. To compare between phases, species and sex, a factorial analysis of variance was performed.

Frequency histograms were constructed for total ME per hour for each species and the overlap resulting of the temporal use of the time axis was calculated using Pianka's index (Pianka 1973):

$$O_{jk} = \frac{\sum_i p_{ij} p_{ik}}{\sqrt{\sum_i p_{ij}^2 \sum_i p_{ik}^2}}.$$

O_{jk} is index of overlap (0 to 1) of species "j" and "k", and p_{ij} is the proportion of use for species "j" in hour "i". In addition, the activity histogram recorded in the night phase was analyzed looking for unimodality *vs.* multimodality using the Hartigan test (Hartigan & Hartigan 1985).

Table 2.—Multiple comparisons of ME and DW between species in both phases of L:D cycle. Same letters indicate absence of differences.

	ME		DW	
	L	D	L	D
L. laeta	a	b	ad	b
S. globula	c	d	c	d

The data required transformation to (log(x+1)) in order to satisfy normality and homoscedasticity assumptions. To verify the parametric assumptions, Shapiro-Wilk and Bartlett tests were applied. In addition, an ANOVA for repeated measures was performed with ME.

RESULTS

The analyses of the number of movement events of the spiders indicated that both species are nocturnal, with significant differences in the total number of movements during the dark and light periods of the cycle ($F_{1,60} = 50.37$, $P < 0.001$); sex differences were not significant ($F_{1,60} = 2.14$, $P = 0.14$). However, differences were found between species ($F_{1,60} = 28.52$, $P < 0.001$) and there was a significant interaction between cycle and species ($F_{1,60} = 6.57$, $P = 0.012$) (Table 1).

A multiple comparison test showed both species being more active during the night phase and *L. laeta* more active than *S. globula* during both phases of the light-dark cycle ($P < 0.05$; Tukey test) (Table 2).

The repeated measures analysis was consistent with the previous analysis and differences between species were detected (Λ-Wilk = 0.569, $F_{12,49} = 3.1$, $P = 0.003$), a L:D cycle effect (Λ-Wilk = 0.499, $F_{12,49} = 4.1$, $P = 0.0002$), absence of sexual differences (Λ-Wilk = 0.788, $F_{12,49} = 1.1$, $P = 0.38$), and interactions ($P > 0.05$) (Fig. 1).

The activity of *S. globula* was bimodal (D = 0.0689, $P = 0.0008$), while the activity of *L. laeta* was unimodal (D = 0.0714, $P = 0.1643$) (see Fig. 1).

The analysis of distance walked (DW) also showed differences between the two species, with *L. laeta* wandering a significantly greater distance than *S. globula* ($F_{1,60} = 26.29$, $P << 0.001$), with the largest distances traveled during the light phase ($F_{1,60} = 31.42$, $P << 0.001$), without sex differences ($F_{1,60} = 1.13$, $P = 0.29$) or interaction between phases of the L:D cycle or species ($F_{1,60} = 8.16$, $P = 0.006$). Multiple comparisons showed that both species traveled a greater distance in the scotophase, and with *L. laeta* roaming more actively than *S. globula* in both phases (Tables 1, 2).

The value of Pianka's index was OJK= 0.739, which indicates considerable overlap in the temporal use of the time axis by both species.

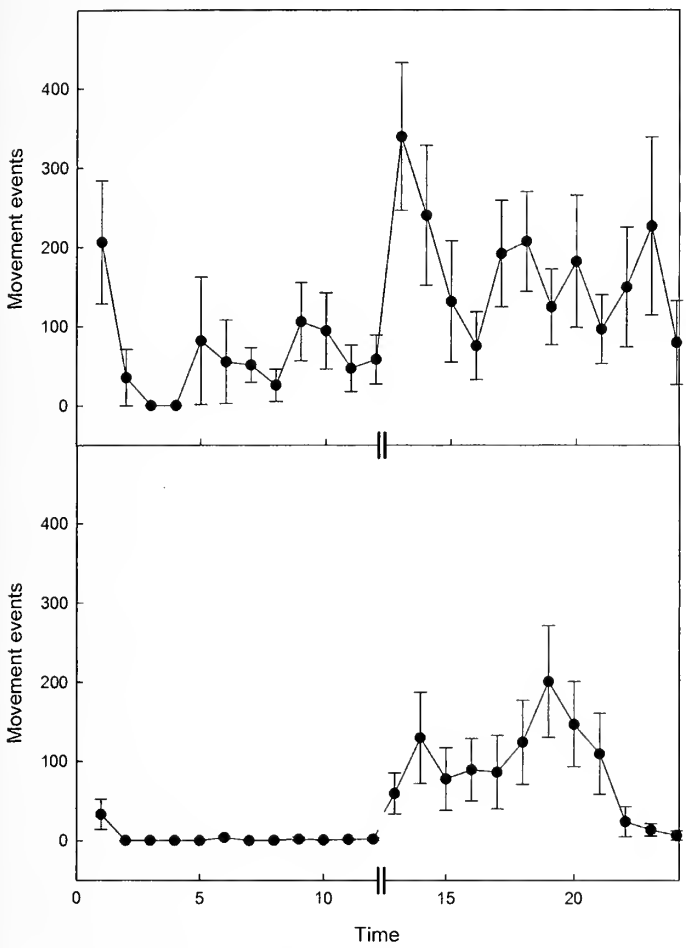

Figure 1.—Activity pattern of *Loxosceles laeta* (upper) and *Scytodes globula* (lower) measured as number of movement events (ME) during a L:D/12:12 cycle. X-axis is measured in hours; vertical bars indicate onset of the 12-hour dark period.

DISCUSSION

Although there are previous reports pointing to *L. laeta* and *S. globula* as nocturnal species, there are no previous systematic studies of the chronobiology of these species. In this study, both species entrained to a circadian cycle light: dark (12:12), and their locomotor activity was mainly restricted to the dark phase. Also, no differences in activity between males and females were observed even when experiments were performed in the reproductive period. This contrasts with previous reports showing greater cursorial activity of males than females, which has been attributed to the active search for these during reproductive period (Gonzaga et al. 2007). However, differences were observed in the proportion of activity of the spider species during the photophase, with 4.1% and 26.4% for *S. globula* and *L. laeta,* respectively.

The negligible diurnal activity of *S. globula* agrees with that reported for other nocturnal spiders such as araneomorph species of the genus *Cupiennius* Simon, 1891, in which only 4.1% of the activity of males and 8.7% of female activity occurs during the day (Ortega-Escobar 2002). However, the low level of diurnal activity of *S. globula* contrasts with that almost six times greater exhibited by *L. laeta.* Activity during daylight hours in predominantly nocturnal species has been previously described in spiders. For example, a study on *Tetragnatha montana* Simon, 1874, and *Dolomedes fimbriatus* (Clerck, 1757) based on field observations showed that both species can extend their activity in daylight hours, especially in times of food shortage (Horn 1969).

Even though both species studied here developed their main activity during dark period, they differed in the degree of nocturnality, with *S. globula* showing a strong nocturnal periodicity and with *L. laeta,* a statistically significant nocturnality accompanied by some degree of activity during the light hours. This is in agreement with the assertion of individuals of other species of spiders which are not purely nocturnal or diurnal (Suter & Benson 2014) and the reported behavior of individuals of the brown recluse spider (*L. reclusa* Gertsch & Mulaik, 1940) which were observed active during the day, specially in darker places of a home (Cramer 2015). Moreover, the difference might also be attributable to different foraging strategies of these species. The spitting spider *S. globula* is more sedentary and employs a "sit and wait" strategy (Suter & Stratton 2005, 2009) which has been also described in the brown recluse spiders (Cramer 2015). Nevertheless, the Chilean recluse spider is probably a species which roams actively looking for prey and not only feeding on those who fall into their irregular webs (Suter & Stratton 2005, 2009). Furthermore, spiders of the genus *Loxosceles* Heiniken & Lowe, 1832, capture invertebrates in their webs or during ambulation (Fischer et al. 2006) and also use the strategy of cannibalism and consumption of dead prey in their path (Sandidge 2003; Fischer et al. 2006; Cramer 2008; Vetter 2011; Souza-Silva & Ferreira 2014). However, scavenging seems to be an opportunistic behavior which occurs under unusual circumstances only (Cramer 2008).

Overall, the difference of diurnal activity between the synanthropic species studied here is consistent with the common finding of the Chilean recluse spider wandering around during daylight hours while *S. globula* remains motionless in its typical rest position (Suter & Stratton 2005, 2009) in human habitations during the same period.

Another difference observed between *L. laeta* and *S. globula* was the shape of the nocturnal activity curves. *Scytodes globula* was bimodal with peaks of activity 2 and 7 hours after the beginning of the scotophase. This bimodal activity pattern has been described in some crepuscular mygalomorph spiders (Cloudsley-Thompson 2013). However, the activity of *L. laeta* during the dark phase was unimodal, reaching a maximum at the very beginning of the scotophase and maintaining sustained activity throughout this phase. A similar pattern has been recorded in *L. reclusa* (Cramer 2015).

The Chilean recluse spider may have higher energy requirements than *S. globula* because of its greater mass and more active strategy of foraging in environments of low prey availability such as anthropogenic environments (Schochat et al. 2004; Van Nuland & Whitlow 2014). This fact together with a higher response threshold to light intensity might drive the extended activity to daylight. Species with some degree of diurnal activity are expected to have a higher threshold of light intensity than those having strictly nocturnal activity. Preliminary data show that this is the case for *L. laeta* and *S. globula,* with light intensity thresholds producing a decrease or

cessation of activity significantly at greater than 20 lux for the Chilean recluse spider and *S. globula* stopping its activity long before reaching that value (unpublished data). Whatever the reason, comparatively *L. laeta* shows physiological characteristics such as less sensitivity to the thermal environment and a higher rate of water loss which made this species more self-reliant than *S. globula* (Canals et al. 2015c).

Both species studied here show an extensive and remarkable thermal niche overlap (Alfaro et al. 2013) which implies that their micro-habitats are also similar (Canals & Solís 2013) and increases the probability of meeting and competitive interactions. Taken together, these facts and the results of the daily pattern of locomotor activity studied here, it is very possible that niche overlap encircle many other niche variables determining strong competitive interactions between Chilean recluse spider and *S. globula* spiders, especially in domestic environments. Nevertheless, the diurnal activity presented by individuals of *L. laeta* may decrease the probability of encounter with the strongly nocturnal araneophagic *S. globula*.

Spiders in our experimental arena faced an unusual environment, bare and without shelter, very different to those where these species are commonly found. Clearly, this fact preclude direct extrapolation to human-structured environment where some metrics like movement events may be lower, because availability of many places to hide. However, in spite of this, our results give strong evidence of real differences in locomotor activities between both species and the way this activity develops during light and dark periods.

Previous studies contributed information about the use of space ("where") by these spiders that would help to increase the efficiency of sanitary control (Vetter & Rust 2008, 2010). Complementarily, the knowledge of the use of time by these synanthropic species helps to understand "when" it is most likely these species will interact and improve measures of control.

LITERATURE CITED

Alfaro, C., C. Veloso, H. Torres-Contreras, R. Solís & M. Canals. 2013. Thermal niche overlap of the spider of the nook *Loxosceles laeta* (Araneae: Sicariidae) and its possible predator, the tiger spider *Scytodes globula* (Scytodidae). Journal of Thermal Biology 38:502–507.

Canals, M. & R. Solís. 2013. Is the tiger spider *Scytodes globula* an effective predator of the brown recluse spider *Loxosceles laeta*? Revista Médica de Chile 141:805–807.

Canals, M., C. Alfaro, C. Veloso, H. Torres-Contreras & R. Solís. 2013. Tolerancia a la desecación y sobreposición del nicho térmico entre la araña del rincón *Loxosceles laeta* y un posible control biológico, la araña tigre *Scytodes globula*. Revista Ibero-Latinoamericana de Parasitología 72:52–60.

Canals, M., N. Arriagada & R. Solís. 2015a. Interactions between the Chilean recluse spider (Araneae: Sicariidae) and an araneophagic spitting spider (Araneae: Scytodidae). Journal of Medical Entomology 52:109–116.

Canals, M., C. Veloso & R. Solís. 2015b. Adaptation of the spiders to the environment: the case of some Chilean species. Frontiers in Physiology 6:220. doi: 10.3389/fphys.2015.00220

Canals, M., C. Veloso, L. Moreno & R. Solís. 2015c. Low metabolic rates in primitive hunters and weaver spiders. Physiological Entomology 40:232–238.

Canals, M., R. Solís, J. Valderas, M. Ehrenfeld & P.E. Cattan. 1997. Preliminary studies on temperature selection and activity cycle of Chilean vectors of the Chagas disease. Journal of Medical Entomology 34:11–17.

Cloudsley-Thompson, J.L. 2000. Biological rhythms in Arachnida (excluding Acari). Memorie della Societa Entomologica Italiana 78:251–273.

Cloudsley-Thompson, J.L. 2013. The biorhythms of spiders. Pp. 371–379. *In* Spider Ecophysiology. (W. Nentwig, ed.). Spinger-Verlag, Heidelberg.

Cramer, K.L. 2008. Are brown recluse spiders, *Loxosceles reclusa* (Araneae, Sicariidae) scavengers? The influence of predator satiation, prey size, and prey quality. Journal of Arachnology 36:140–144.

Cramer, K.L. 2015. Activity patterns of synanthropic population of the brown recluse spider, *Loxosceles reclusa* (Araneae: Sicariidae), with observations on feeding and mating. Journal of Arachnology 43:67–71.

Fernandez, D., L. Ruz & H. Toro. 2002. Aspectos de la biología de *Scytodes globula* Nicolet, 1949 (Aranae: Scytodidae), un activo depredador de Chile Central. Acta Entomológica Chilena 26:17–25.

Fischer, M.L., J. Vasconcellos-Neto & L. Gonzaga. 2006. The prey and predators of *Loxosceles intermedia* Mello-Leitao 1934 (Araneae, Sicariidae). Journal of Arachnology 34:485–488.

Foelix, R.F. 2011. Biology of Spiders. 3rd ed. Oxford University Press, New York.

Gonzaga, M.O., A.J. Santos & H.F. Japyassu. 2007. Ecologia e comportamento de aranhas. Editora Intereciencia. Sao Paulo.

Hartigan, J.A. & P.M. Hartigan 1985. The dip test of unimodality. Annals of Statistics 13:70–84.

Horn, E. 1969. 24-hour cycles of locomotor and food activity of *Tetragnatha montana* Simon (Araneae, Tetragnathidae) and *Dolomedes fimbriatus* (Clerck) (Araneae, Pisauridae). Ekologia Polska A 17:533–549.

Mistlberger, R. & B. Rusak. 2005. Biological rhythms and importance. Pp. 71–96. *In* The Behavior of Animals: Mechanisms, Function, and Evolution. (J. Bolhuis & L. Giraldeau, eds.). Blackwell Publishing, New York.

Nentwig, W. 2013. Spider Ecophysiology. Springer Verlag, Berlin Heidelberg

Ortega-Escobar, J. 2002. Circadian rhythms of locomotor activity in *Lycosa tarantula* (Araneae, Lycosidae) and the pathways of ocular entrainment. Biological Rhythm Research 33:561–576.

Pianka, E. 1973. The structure of lizard communities. Annual Review of Ecology and Systematics 4:53–74.

Sandidge, J.S. 2003. Arachnology: scavenging by brown recluse spiders. Nature 426:30.

Shochat, E., W.L. Stefanov, M.E.A. Whitehouse & S.H. Faeth. 2004. Urbanization and spider diversity: influences of human modification of habitat structure and productivity. Ecological Applications 14:268–280.

Souza-Silva, M & R.L. Ferreira. 2014. *Loxosceles* spiders (Araneae: Sicariidae) preying on invertebrates in Brazilian caves. Speleobiology Notes 6:27–32.

Suter, R.B. & K. Benson. 2014. Nocturnal, diurnal, crepuscular: activity assessments of Pisauridae and Lycosidae. Journal of Arachnology 42:178–191.

Suter, R.B. & G.E. Stratton. 2005. *Scytodes* vs. *Schizocosa*: predatory techniques and their morphological correlates. Journal of Arachnology 33:7–15.

Suter, R.B. & G.E. Stratton. 2009. Spitting performance parameters and their biomechanical implications in the spitting spider *Scytodes thoracica*. Journal of Insect Science 9:1–15.

Van Nuland, M.E. & W.L. Whitlow. 2014. Temporal effects on biodiversity and composition of arthropod communities along an urban-rural gradient. Urban Ecosystems 17:1047–1060.

Vetter, R.S. 2011. Scavenging by spiders (Araneae) and its relationship to pest management of the brown recluse spider. Journal of Economic Entomology 104:986 989.

Vetter, R.S. & M.K. Rust. 2008. Refugia preferences by the spiders *Loxosceles reclusa* and *Loxosceles laeta* (Araneae: Sicariidae). Journal of Medical Entomology 45:36 41.

Vetter, R.S. & M.K. Rust. 2010. Influence of spider silk on refugia preferences of the recluse spiders *Loxosceles reclusa* and *Loxosceles laeta* (Araneae: Sicariidae). Journal of Economic Entomology 103:808 815.

Manuscript received 23 September 2016, revised 27 June 2017.

2018. Journal of Arachnology 46:26–30

Circadian rhythms of locomotor activity in *Metazygia wittfeldae* (Araneae: Araneidae)

Thomas C. Jones[1], **Rebecca J. Wilson**[1] and **Darrell Moore**[1]: [1]Department of Biological Sciences, East Tennessee State University, Box 70703, Johnson City, TN 37614 USA. E-mail: jonestc@etsu.edu

Abstract. Internal clocks, or circadian rhythms, are nearly ubiquitous across taxa (e.g., animals, plants, fungi, and cyanobacteria), and it is widely believed that a biological clock benefits organisms by enabling them to schedule behavioral and physiological changes in anticipation of predictable changes in environmental conditions. Theory and evidence suggest it is important that the internal clock resonate closely with the 24-h daily cycle. Recently, however, *Cyclosa turbinata* (Walckenaer, 1841) (Araneidae) was revealed to have a circadian clock with a period of about 19 h, which was presumed to be anomalous. Here, we report on the behavioral rhythms of a nocturnal orbweaver, *Metazygia wittfeldae* (McCook, 1894), from the same family. Under laboratory conditions of a 12:12 h light:dark cycle, we found that locomotor activity initiates shortly after dark, reaching a peak early in the dark phase, continuing at a lower level throughout the remaining dark phase, and then diminishing shortly after lights-on. Locomotor activity continued to cycle under constant dark conditions with a mean free-running period of 22.7 h. We also found a second component in the free-running activity (mean 11.5 h) which correlated very tightly with the free-running period. Thus, *M. wittfeldae* has what can be considered a typical circadian clock resonating with the 24-h day. Notably, however, there were two outliers close to the 19-h period observed in *C. turbinata*, suggesting that there may be sufficient variation in clock period among araneid spiders upon which selection could act leading to the short-period clocks in *C. turbinata*.

Keywords: Behavioral rhythm, circadian clock, chronoecology

Endogenous clocks, or circadian rhythms, are nearly ubiquitous among animal taxa (Johnson & Kondo 2001), and it is widely believed that the advantage of having an internal clock allows individuals to anticipate daily environmental changes and schedule behavioral and physiological changes appropriately. Circadian rhythms are detected as oscillations in behavior or physiology, with periods of approximately 24 h that persist in the absence of external cues (i.e., 'free-running'). Another property of circadian rhythms is that they are entrainable by external cues, such as changes in light levels over the course of a day, keeping biological changes synchronized with daily environmental changes. In spiders, circadian rhythms in locomotor activity have been described in several families including Lycosidae (Ortega-Escobar 2002), Ctenidae (Seyfarth 1980), and Linyphiidae and Theridiidae (Suter 1993). Circadian oscillations also are reported in visual sensitivity (Yamashita & Nakamura 1999), and in antipredator behavior (Jones et al. 2011) of spiders in the family Araneidae.

In all of the studies of spiders listed above, the reported circadian periods are 'typical' (i.e., within two hours of the natural 24-h daily cycle). Theory predicts that appropriate anticipation and scheduling of biological changes require that the circadian clock resonate closely with the natural 24-h cycle, and this has been supported empirically (Woelfle et al. 2004; Spoelstra et al. 2016). Recently, however, it was reported that *Cyclosa turbinata* (Walckenaer, 1841) (Araneidae) has an exceptionally short-period clock regulating locomotor activity (Moore et al. 2016). With a mean free-running period (FRP) of activity of 18.5 h, *C. turbinata* has the shortest known naturally-occurring circadian period, comparable to 20-h and 18-h mutants in hamsters (Konopka & Benzer 1971; Monecke et al. 2011), the 19-h per^S mutant in *Drosophila* (Ralph & Menaker 1988), and 19-h laboratory strains of the adzuki bean beetle (Harano & Miyatake 2010). The short-period clock in *C. turbinata* was presumed to be unusual given general circadian theory and previous studies of spiders (Moore et al. 2016). However, to our knowledge, there are no other reports of circadian periods in araneid spiders, so we do not yet know if *C. turbinata* is, in fact, exceptional. We begin to address this in the present study by examining diel and circadian patterns of locomotor activity in another araneid spider *Metazygia wittfeldae* (McCook, 1894).

METHODS

Study species.—*Metazygia wittfeldae* is an orbweaver common to the eastern US (Bradley 2013). The species is described as nocturnal, building or replacing its orb after dark, foraging through the night, and then hiding in a retreat during the day (Levi 1977). We collected adult females from their webs at night in Washington Co. TN, in late April 2017. Care of the animals followed ASAB/ABS guidelines, and the animals were released near the site of collection following experiments.

Locomotor activity.—To observe entrainment to the laboratory LD 12:12 environment, activity monitoring began within 24 h of collection. Individuals were placed in 25 mm diameter X 100 mm length, clear glass tubes and inserted into a locomotor activity monitor (model LAM25, Trikinetics Inc., Waltham, Massachusetts). Activity within each tube was measured *via* interruption of three infrared beams transmitting through the midpoint of the tube: each interruption was registered as an event. Events were counted in 1-min bins and analyzed using Clocklab Analysis 6 Software (Actimetrics, Wilmette, IL, U.S.A.). Activity was depicted graphically by double-plotted actograms to facilitate visual recognition of periods. Significant periods were detected using two different periodogram analyses, chi-square and Lomb-Scargle. The chi-square periodogram (Sokolove & Bushell 1978) is broadly applicable for analyzing circadian data. Using a form of Fourier spectral analysis, the Lomb-Scargle periodogram is

better suited to analyze records with large or frequent gaps (Van Dongen et al. 1999). The use of these two complementary methods, rather than just one, provides additional support for determinations of period. Because of the sparse nature of activity bouts exhibited by these spiders, we accepted circadian periodicities only if indicated by both methods.

Spiders ($n = 43$) were monitored in a temperature-controlled environmental chamber (24 ± 0.5 °C) under a light-dark cycle of 12 hours of light and 12 hours of dark (LD 12:12) for five days and then under constant darkness (DD) for ten days thereafter. Lights-on occurred at 07:00 h and lights-off at 19:00 h. Light during photophase was provided by four vertically mounted, 32 W fluorescent tubes; the illuminance was approximately 1400–1600 lux at the level of the activity monitor. Six spiders were excluded from the analyses because they did not perform locomotor activity in all five days of LD entrainment.

RESULTS

Entrainment profiles.—Nearly all of the spiders analyzed ($n = 37$) performed locomotor activity throughout the 5 days of LD 12:12 h entrainment. Locomotor activity in these animals was almost exclusively nocturnal with a DiNoc ratio (daytime activity – nighttime activity/ total activity; Suter & Benson, 2014) very close to -1 (mean = -0.96, SEM = 0.006). In each day of entrainment, activity began about 30 min after lights off, peaking 1–2 h into scotophase, then continuing at a lower level throughout scotophase, before tapering off to nothing an hour after lights on (Fig. 1). Overall activity was higher in the first night of entrainment than in subsequent nights. Aside from the initial peak of activity in early scotophase, there were no consistent patterns thereafter. The onset of activity after lights out became remarkably precise after two days of entrainment (mean delay for entrainment days 3–5 = 31.39 min, SEM = 1.27 min; Fig. 2). No correlation was detected between an individual's delay in onset of activity after lights-off in LD and its free-running period.

Circadian free-runs.—Of the 37 spiders analyzed, 28 exhibited free-running periods that were significant at $P < 0.001$, for both chi-square and Lomb-Scargle periodograms (Mean FRP = 22.7 h, SEM = 0.24 h). Actograms revealed that, in most individuals, the main burst of free-running activity under constant dark (DD) conditions extrapolates back to the peak of activity in early scotophase of entrainment (Fig. 3). Also, the onset of free-running activity was very precise for many individuals, resulting in remarkably straight (as visualized on the actograms) free-runs and distinctly sharp primary peaks in the periodograms.

In 18 individuals, a second periodicity was identified in the free-runs which was significant at $P < 0.001$, for both chi-square and Lomb-Scargle periodograms (Fig. 3a–d). The mean FRP of these second components was 11.47 h (SEM = 0.1 h), which is nearly exactly half the FRP of the main component. Moreover, the main FRP and second components were highly correlated within individuals (Spearman rank-order correlation: $r_s = 0.985$, df = 16, $P < 0.000001$). This second component is particularly distinct in some of the actograms (Fig. 3a–c), and, by inspection, it extrapolates back to late scotophase of the LD 12:12 entrainment. However, we do not detect any peaks of activity under LD 12:12 that would correspond to this second component, even when considering only individuals in which periodogram analyses showed a significant second component under DD.

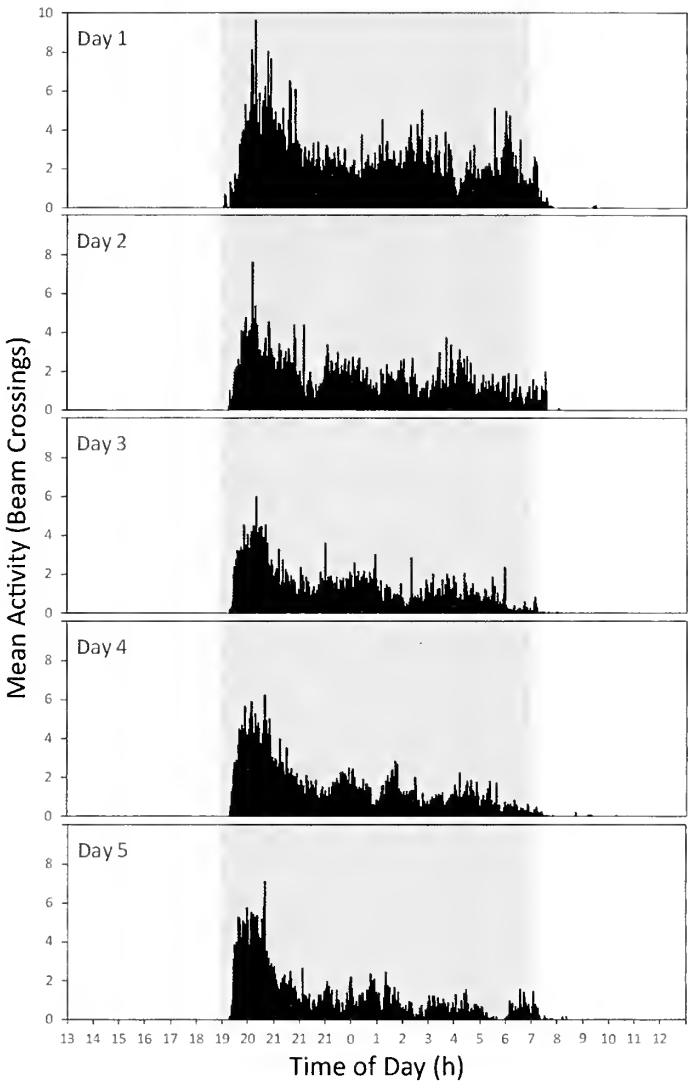

Figure 1.—Pattern of entrainment to LD 12:12 h cycle, showing mean activity levels of 37 individuals, in 1-min bins, for five consecutive days of exposure to the light-dark cycle. Shading indicates scotophase.

The majority of FRPs calculated for *M. wittfeldae* fell within a left-skewed distribution between 21.5 and 23.8 h (Fig. 4). However, there were two outliers with distinctly shorter FRPs of 18.75 and 19.53 h. The actogram and periodogram for one of these outliers are illustrated in Fig. 3e. Interestingly, the FRPs of these two outliers fall within the distribution of 'exceptionally short' free-running periods (Fig. 4) described for *C. turbinata* (Moore et al. 2016).

DISCUSSION

Locomotor activity in the nocturnally foraging *M. wittfeldae* was almost exclusively nocturnal under LD 12:12 conditions, the only exception being that some activity persisted up to an hour after lights on. This contrasts with what was found for eight non-web building species of

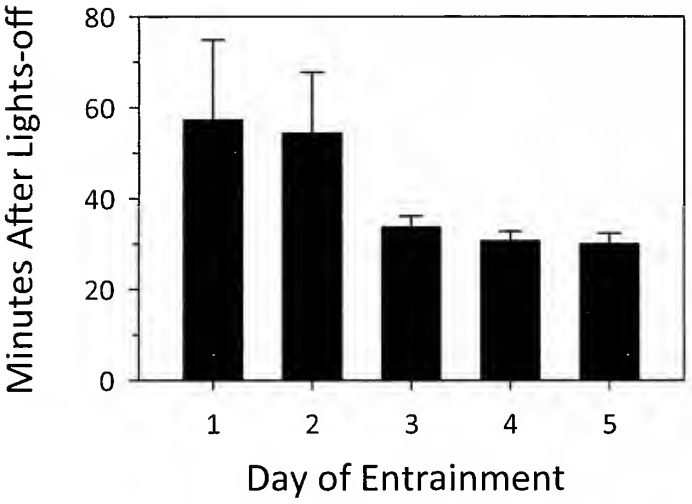

Figure 2.—Delay (in minutes) between lights-off and the beginning of locomotor activity each day for five consecutive days of exposure to the LD 12:12 h cycle. Bars show means (+ SE). Only spiders that exhibited activity during scotophase for all five days ($n = 34$) were included in the analysis.

Lycosidae and Pisauridae (Suter & Benson 2014), in which seven species were predominantly nocturnal and one predominantly diurnal but, in all species, activity was distributed throughout the LD cycle (the most extreme mean DiNoc ratio being -0.528). The nocturnal LD 12:12 activity patterns we found for *M. wittfeldae* were more similar to another araneid spider, *C. turbinata,* which has a mean DiNoc ratio of -0.79 (Moore et al. 2016).

Metazygia wittfeldae builds its web after dusk and forages only during the night (Levi 1977), while *C. turbinata* replaces its web pre-dawn and forages throughout the day and night (Moore et al. 2016). It is curious, therefore, that both species show predominantly nocturnal patterns of locomotor activity. Moreover, there is a question as to what laboratory locomotor activity represents in orb-weaving spiders which, in natural conditions, remain motionless unless capturing prey or working on their webs. Generally, in the circadian literature, locomotor activity is interpreted as an indication of underlying neurological arousal (Brady 1981). This interpretation is compelling for animals such as rodents which do, in fact, move around their environment during periods of arousal. It also seems to fit the natural behavior of wandering spiders which move about their environment when foraging, such as the lycosids and pisaurids studied by Suter & Benson (2014). It is clear from the distinctly non-random entrainment and free-running patterns that locomotor activity represents something biologically real in araneid spiders (Moore et al. 2016; this study). The idea that locomotor activity represents general neurological arousal at night in these spiders is supported by the observation that *C. turbinata* is more likely to attack a prey stimulus at night than during the day (Watts et al. 2014) and that *Larinioides cornutus* (Clerck, 1757) is generally bolder at night than in the day (Jones et al. 2011). From our own observations of several araneid species refusing to build webs in large cages (which are presumably more natural than activity monitor tubes), we speculate that what we measure as

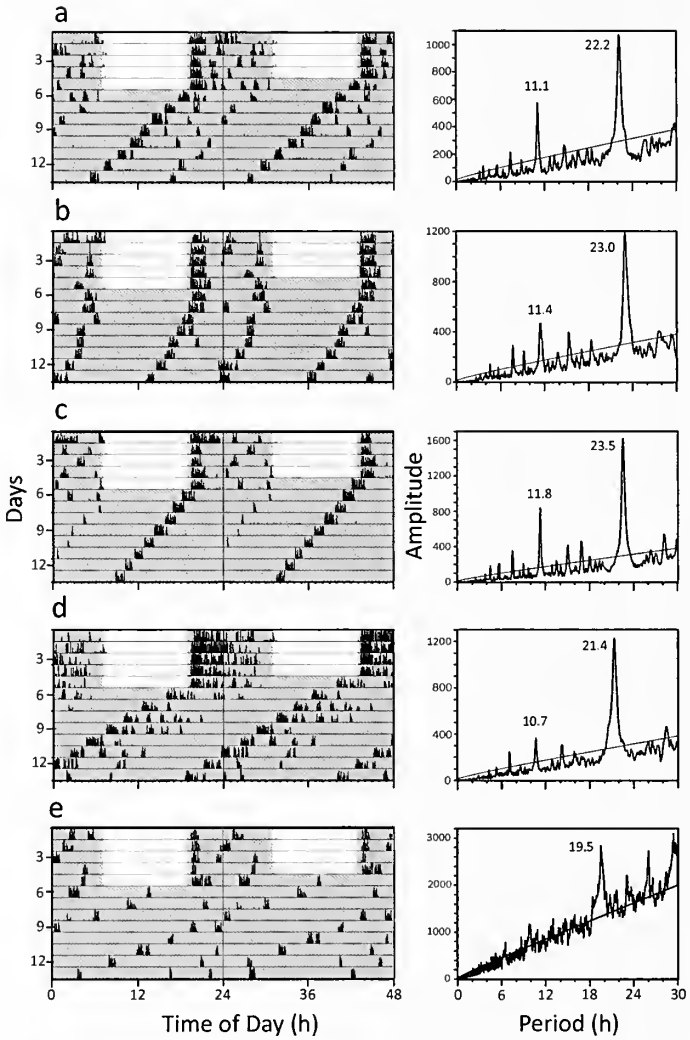

Figure 3.—Double-plotted actograms, each with its accompanying periodogram, illustrating entrainment and free-running locomotor activity in five different individuals of *Metazygia wittfeldae*. Actograms (left panels) depict the timing of activity for five consecutive days under a LD 12:12 h cycle, followed by constant dark (DD) conditions thereafter. Dark periods are represented by gray background. Chi-square periodograms (right panels) indicate significant periodicities ($P < 0.001$) of locomotor activity under DD (FRPs in hours are indicated adjacent to significant peaks). Individuals a-e show particularly strong second components of activity at about half the period of the main component under DD, while in d, the second component is less pronounced, but still significant. Individual e is an example of a short-period outlier.

locomotor activity corresponds to exploratory behavior which is observed almost exclusively at night.

The average free-running period of *M. wittfeldae* was 22.7 h, suggesting that this species has a 'typical' circadian clock resonating adaptively with the 24-h day (Ouyang et al. 1998; Johnson & Kondo 2001; Woelfle et al. 2004; Spoelstra et al. 2016). These data from an araneid spider, and previous studies on non-araneid species (Seyfarth 1980; Suter 1993; Ortega-Escobar 2002), support the hypothesis that the short-period clock (mean 18.5 h) of *C. turbinata* is, in fact, unusual. *Metazygia wittfeldae* now is the closest relative to *Cyclosa* Menge, 1866 for which an FRP is known, but as yet, this does

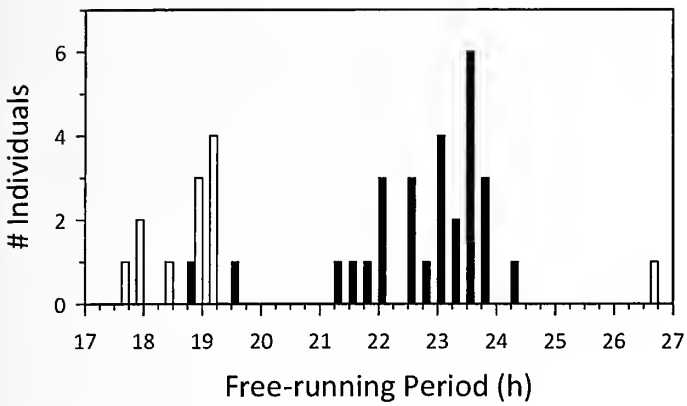

Figure 4.—Frequency distribution of circadian free-running periods of locomotor activity under DD conditions for two species of araneids: *Metazygia wittfeldae* (filled bars) and *Cylosa turbinata* (open bars; Moore et al. 2016).

not give much insight as to where, in the phylogeny of Araneidae, a short-period clock evolved. In an older morphological phylogeny (Scharff & Coddington 1997), *Metazygia* F. O. Pickard-Cambridge, 1904 and *Cyclosa* appear fairly closely related within Araneidae, but nevertheless are in a clade of 18 genera. Unfortunately for this work, *Metazygia* is not included in more recent molecular phylogenies of Araneidae (Dimitrov et al. 2016; Wheeler et al. 2016).

Two aspects of the free-running locomotor activity in *M. wittfeldae* were notable. First was the precise regularity of the onset of activity under constant conditions (Fig. 3). This, coupled with the precise delay of the onset of activity in LD (Figs. 1 & 2), suggests that locomotor activity is tightly regulated by the circadian clock in this species. Second was the presence of a second component of free-running activity, the periodicity of which appeared to be precisely half that of the primary FRP. This second component (appearing in 18 of the 28 individuals for which significant FRPs were obtained) suggests a single oscillator with two active phases or perhaps two separate but tightly coupled oscillators. A similar bimodality in locomotor activity, in which the components maintain a 180° phase difference under constant conditions, occurs in the cockroach *Leucophaea maderae* (Fabricius, 1781). Because the two components free-ran with the same period, they were interpreted as outputs of a single circadian oscillator (Wiedenmann 1980). Despite the fact that the second component in *M. wittfeldae* extrapolated back to a phase position in late scotophase, we did not detect any corresponding peak in locomotor activity at this phase under LD 12:12. This is in contrast to what was found in *C. turbinata*, in which there was a second peak of locomotor activity under LD 12:12 which corresponded to the timing of web-replacement behavior (Moore et al. 2016). Interestingly, however, *C. turbinata* did not have a second component of activity in the free-runs. Future work will look for correlations with the second component in the natural behavior and boldness of *M. wittfeldae*.

The primary objective of this study was to examine the entrainment and free-running patterns of locomotor behavior, with a particular interest of providing a comparison with *C. turbinata* and its short-period circadian clock. Thus, it is remarkable that, while most individuals of *M. wittfeldae* had typical FRPs close to 24 h, two outliers had short FRPs similar to those of *C. turbinata* (Fig. 4). However, the variation in FRPs does not appear continuous, in that the short-period outliers in *M. wittfeldae*, and the distribution of FRPs in *C. turbinata*, are distinctly separate from the main FRP distribution of *M. wittfeldae* (Fig. 4). This is inconsistent with a quantitative trait, and may indicate that there is an associated mutation such as those leading to short circadian clocks in the per^s mutant in *Drosophila* (Konopka & Benzer 1971), and the *tau* and super duper mutants in hamsters (Ralph & Menaker 1988; Monecke et al. 2011). Future studies will focus on the evolution of circadian clocks in Araneidae, and the molecular mechanisms underlying variation in FRPs.

ACKNOWLEDGMENTS

We gratefully acknowledge support from the National Science Foundation (IOS grant no. 1257133). We thank the ETSU Department of Biological Sciences for logistical support. We also thank A. Roberts and two anonymous reviewers for constructive criticisms of the manuscript, M. Entling, R. Vetter, and D. Smith for editing the manuscript, and A. deMarco for help with spider collection.

LITERATURE CITED

Bradley, R.A. 2013. Common Spiders of North America. University of California Press, Los Angeles.

Brady, J. 1981. Behavioral rhythms in invertebrates. Pp. 125–144. *In* Handbook of Behavioral Neurobiology, Vol. 4, Biological Rhythms. (J. Aschoff, ed.). Plenum Press, New York.

Dimitrov, D., L.R. Benavides, M.A. Arnedo, G. Giribet, C.E. Griswold, N. Scharff et al. 2016. Rounding up the usual suspects: a standard target-gene approach for resolving the interfamilial phylogenetic relationships of ecribellate orb-weaving spiders with a new family-rank classification (Araneae, Arancoidea). Cladistics 33:221–250.

Harano, T. & T. Miyatake. 2010. Genetic basis of incidence and period length of circadian rhythm for locomotor activity in populations of a seed beetle. Heredity 105:268–273.

Johnson, C.H. & T. Kondo. 2001. Circadian rhythms in unicellular organisms. Pp. 61–78. *In* Circadian Clocks, Vol. 12. (J.S. Takahashi, F.W. Turek, R.Y. Moore, eds.). Kluwer Academic/Plenum Publishers, New York.

Jones, T.C., T.S. Akoury, C.K. Hauser & D. Moore. 2011. Evidence of circadian rhythm in antipredator behavior in the orb-weaving spider *Larinioides cornutus*. Animal Behaviour 82:549–555.

Konopka, R.J. & S. Benzer. 1971. Clock mutants of *Drosophila melanogaster*. Proceedings of the National Academy of Sciences U.S.A. 68:2112–2116.

Levi, H.W. 1977. The American orb-weaver genera, *Cyclosa*, *Metazygia* and *Eustala* north of Mexico (Araneae, Araneidae). Bulletin of the Museum of Comparative Zoology 148:61–127.

Monecke, S., J.M. Brewer, S. Krug & E.L. Bittman. 2011. Duper: A mutation that shortens hamster circadian period. Journal of Biological Rhythms 26:283–292.

Moore, D., J.C. Watts, A. Herrig & T.C. Jones. 2016. Exceptionally short-period circadian clock in *Cyclosa turbinata*: regulation of locomotor and web-building behavior in an orb-weaving spider. Journal of Arachnology 44:388–396.

Ortega-Escobar, J. 2002. Circadian rhythms of locomotor activity in *Lycosa tarantula* (Araneae, Lycosidae) and the pathways of ocular entrainment. Biological Rhythms Research 33:561–576.

Ouyang, Y., C.R. Anderson, T. Kondo, S.S. Golden & C.H. Johnson. 1998. Resonating circadian clocks enhance fitness in cyanobacteria. Proceedings of the National Academy of Sciences, USA 195:8660–8664.

Ralph, M.R. & M. Menaker. 1988. A mutation of the circadian system in golden hamsters. Science 241:1225–1227.

Scharff, N. & J. A. Coddington. 1997. A phylogenetic analysis of the orb-weaving spider family Araneidae (Arachnida, Araneae). Zoological Journal of the Linnean Society 120:355–434.

Seyfarth, E.A. 1980. Daily patterns of locomotor activity in a wandering spider. Physiological Entomology 5:199–206.

Sokolove, P.G. & W.N. Bushell. 1978. The chi square periodogram: its utility for analysis of circadian rhythms. Journal of Theoretical Biology 72:131–160.

Spoelstra, K., M. Wikelski, S. Daan, A.S.I. Loudon & M. Hau. 2016. Natural selection against a circadian clock gene mutation in mice. Proceedings of the National Academy of Sciences, USA 113:686–691.

Suter, R.B. 1993. Circadian rhythmicity and other patterns of spontaneous motor activity in *Frontinella pyramitela* (Linyphiidae) and *Argyrodes trigonum* (Theridiidae). Journal of Arachnology 21:6–22.

Suter, R.B. & K. Benson. 2014. Nocturnal, diurnal, crepuscular: activity assessments of Pisauridae and Lycosidae. Journal of Arachnology 42:178–191.

Van Dongen, H.P.A., E. Olofsen, J.H. Van hartevelt & E.W. Kruyt. 1999. A procedure for multiple period searching in unequally spaced time-series with the Lomb-Scargle method. Biological Rhythm Research 30:149–177.

Watts, J.C., A. Herrig, W.D. Allen & T.C. Jones. 2014. Diel patterns of foraging aggression and antipredator behaviour in the trashline orb-weaving spider, *Cyclosa turbinata*. Animal Behaviour 94:79–86.

Wiedenmann, G. 1980. Two peaks in the activity rhythm of cockroaches controlled by one circadian pacemaker. Journal of Comparative Physiology 137:249–254.

Wheeler W.C., J.A. Coddington, L.M. Crowley, D. Dimitrov, P.A. Goloboff, C.E. Griswold et al. 2016. The spider tree of life: phylogeny of Araneae based on target-gene analyses from an extensive taxon sampling. Cladistics (online only). DOI: 10.1111/cla.12182.

Woelfle, M.A., Y. Ouyang, K. Phanvijhitsiri & C.H. Johnson. 2004. The adaptive value of circadian clocks: an experimental assessment in cyanobacteria. Current Biology 14:1481–1486.

Yamashita, S. & T. Nakamura. 1999. Circadian oscillation of sensitivity of spider eyes: diurnal and nocturnal spiders. Journal of Experimental Biology 202:2539–2542.

Manuscript received 25 May 2017, revised 18 August 2017.

2018. Journal of Arachnology 46:31–34

Changing oviposition times of the crab spider *Misumena vatia* (Thomisidae) correlate with climate change

Douglass H. Morse: Department of Ecology & Evolutionary Biology, Box G-W, Brown University, Providence, RI 02912 USA. E-mail: d_morse@brown.edu

Abstract. The crab spider *Misumena vatia* (Clerck, 1757) (Thomisidae) is an important sit-and-wait predator at flowers visited by nectar or pollen-seeking insects. Typically, female *M. vatia* molt into their adult stage when many insect-attracting flowers come into bloom, and the spiders quickly gain weight leading up to oviposition. Between 1979 and 2010, the first spider ovipositions shifted one month earlier, from late July to late June, at my study site in coastal Maine, USA, in accordance with a concurrent temperature increase of ca. 0.44°C and a lengthening growing season. Flowering times of the spiders' most important hunting site, common milkweed *Asclepias syriaca*, as well as recruitment dates of their most important prey, bumblebees *Bombus* spp., to flowering milkweed, advanced as well. The shift in spider oviposition times increased the feasibility of second broods, though I found no successful second broods in the field, and the success of such broods would be problematic because of heavy overwintering losses. Differing rates of change of spider, milkweed and bumblebee activity indicated decreasing synchrony among these species; in particular, lessening future hunting opportunities for the spiders.

Keywords: Global warming, egg-laying, growing season, seasonal change, sit-and-wait predator

Recent years have seen increased interest and concern about the effects of climate change on the phenology of animals and plants (Parmesan 2006; Thackeray et al. 2010; Bewick et al. 2016). Changes in seasonality may produce shifts in life cycles that conflict with the currently existing environmental regime, and if they do not match those of interacting species, further problems may arise (Memmott et al. 2007; Johansson et al. 2015). Mean temperature changes may also play a dominant role in shifting habitat ranges and geographic distributions of populations (Primack et al. 2009; Mason et al. 2015), though I will focus here on changes within a site.

In spite of the currently perceived importance of documented climatic change and much anecdotal information for many groups of organisms, rather few long-term measures of organismal response to yearly change currently exist over multiple trophic levels (Clark & May 2002; LeRoy et al. 2013). To the best of my knowledge no such information exists for spiders. However, in the process of a long-term study of the crab spider *Misumena vatia* (Clerck, 1757) (Thomisidae) in coastal Maine, USA (Morse 1979, 2007, 2014), I maintained large populations of adult females over a 32-year period (1979–2010) that allowed me to record initial dates of oviposition for each year. For 16 of these years, I also obtained initial flowering dates of their most important hunting site, inflorescences of common milkweed *Asclepias syriaca*, which attract great numbers of large insects that provide the main resources for *Misumena* reproduction (Morse 1982a; Morse & Fritz 1982). For most of the flowering years I also recorded the dates at which bumblebees, the spiders' most important prey, first recruited to the milkweed flowers. This body of information allowed me to establish whether the activity patterns of these three species shifted in accordance with the changing seasons and whether any such changes affected their relationship to each other. In turn, the results allowed me to assess the effects of climate change on these species over the period of study, as well as to project likely future consequences for their relationships.

METHODS

Misumena vatia is a small sit-and-wait predator that typically hunts on flowers. Females weigh from 35–55 mg upon reaching adulthood, usually in the early summer following hatching in late summer two years earlier. They average 220 mg at laying their single clutch of eggs, with a range of 115 mg to over 400 mg. Their single clutch weighs approximately 65% of their mass immediately prior to egg laying (Morse 2007).

Each year, I maintained 50 or more field-collected adult females in order to gather various life history variables on the population and to obtain young for a wide range of experiments reported elsewhere. I collected the spiders in fields and roadsides at and near the Darling Marine Center, South Bristol, Lincoln County, Maine, U.S.A. (43°57′N, 69°33′W), mostly from common milkweed and pasture rose *Rosa carolina*, with smaller numbers from ox-eye daisy *Leucanthemum vulgare*, common buttercup *Ranunculus acris*, cow vetch *Vicia cracca* and red clover *Trifolium pratense*. I sampled these adults independently of mass, but the sample size ensured that they included individuals likely to become among the earliest ovipositers. I maintained them in 7-dram vials (5 cm long, 3 cm diameter) at ambient temperature and natural day length in an unheated laboratory and fed them moths or large flies every other day. Generally these spiders will not take large prey on successive days (Morse 2007), so the feeding regime resembled that obtained at a high-quality hunting site like that of common milkweed.

The spiders typically refuse to feed one to two days before laying. At that point, I placed them on a milkweed leaf in the field, which resembled a natural nest site, and enclosed the plant with a loosely fitting nylon tricot bag. Most individuals laid either the following night or one night later. I resorted to the field regime because these spiders appeared reluctant to lay in the vials where they could not construct a normal nest. The bags themselves do not significantly affect the temperature within (Morse 1994a). I checked the spiders daily to ensure an accurate laying date.

Additionally, I recorded first observations of egg masses while conducting unrelated fieldwork between 1980 and 1994. They provided a comparison between laying dates in the field and those in the standardized routine described above.

I also recorded the initial flowering dates of milkweed, the most important hunting site for *Misumena* in my study area, during the 16 years (1979–1994) for which I possessed data on the spiders' oviposition date. A perennial, common milkweed grows in clones that vary greatly in size, but that routinely attract large numbers of bees, moths and butterflies when in bloom (Morse 1982a, 2007). Milkweed stems vary from 80–120 cm in height and bear multiple round inflorescences (umbels) that bloom sequentially (Morse 1985). A large clone may remain in flower for three weeks or more.

For 11 of these years (1979–1991, data missing for 1989 and 1990) I also recorded the dates at which bumblebees first recruited to milkweed. Bumblebees, mostly *Bombus terricola* and *B. vagans*, were the most common large diurnal insects that visited milkweed flowers and made up by far the spiders' most important prey (Morse & Fritz 1982).

The vicinity of the study site has undergone measurable climatic change over the 32-year period of data gathering. Using the estimate of Jacobson et al. (2009) of a 0.25° F/decade increase in temperature for coastal Maine in 1975–2009, a period similar to that of this 1979–2010 study, I estimated that the mean temperature of the study area increased 0.44°C between 1979 and 2010, a rate that considerably exceeds the estimated global rate for the entire twentieth century of 0.6°C (Houghton et al. 2001). Precipitation also increased by 6.50 cm during this time (Jacobson et al. 2009). Fernandez et al. (2015) also noted that the warm season in this area (defined as days with a mean daily temperature above 0° C) increased by two weeks over the past century, with both earlier spring and later fall seasons. Increase in winter temperatures exceeded the increase in summer temperatures.

Initially I ran one-way ANOVAs between each one of the three variables (oviposition of spiders, flowering of milkweeds, and recruitment of bumblebees) against the ongoing years to search for whether these variables exhibited systematic change over the period of the study. I first ran these variables separately because of the different lengths of data runs for each of them. In addition to the three separate analyses, I ran a three-way ANOVA that incorporated data from the 11 years (1979 through 1991) for which I possessed data sets for crab spiders, milkweeds, and bumblebees. Analyses were carried out in R Version 2.13.0 (R Development Core Team 2011).

RESULTS

The initial date of oviposition shifted earlier by approximately one month over the 32-year period from 1979 to 2010 (Fig. 1). Although exhibiting considerable year-to-year differences, the highly significant slope moved consistently toward earlier laying dates ($R^2 = 0.524$, $F_{1,30} = 35.05$, $P < 0.0001$ in a one-way ANOVA), as did dates of the egg masses found in the field ($R^2 = 0.828$, $F_{1,13} = 62.56$, $P < 0.0001$ in a one-way ANOVA: Fig. 2). Flowering dates of the milkweed from 1979 to 1994 generally resembled the oviposition pattern of the spiders ($R^2 = 0.334$, $F_{1,14} = 7.03$, $P = 0.019$ in a one-way ANOVA, although considerably weaker. Similarly, recruitment dates of the bumblebees to the milkweed flowers shifted earlier over the period of 1979 to 1991 ($R^2 = 0.485$, $F_{1,9} = 8.46$, $P = 0.017$ in a one-way ANOVA.

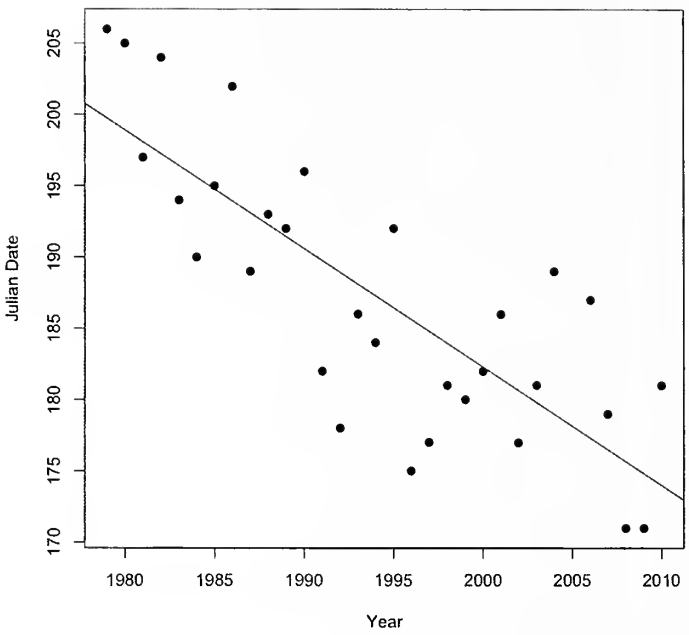

Figure 1.—Change in first oviposition date of field-collected crab spiders *Misumena vatia* from 1979 through 2010. Julian date 170 = 20 June; Julian date 205 = 25 July.

During 1979–1991, when I obtained data on oviposition times of spiders, flowering times of milkweed, and recruitment times of bumblebees (Table 1), the overall relationship among these variables was significant ($R^2 = 0.945$, $F_{3,7} = 25.51$, $P = 0.011$ in a three-way ANOVA), with significant contributions of both oviposition time and flowering time. Recruitment date was not significant, but interactions between oviposition time and flowering time and between flowering time and recruitment time suggested further differences among the three variables (Table 1). The slope of oviposition date over the 1979–1991 period ($R^2 = 0.534$) closely resembled that measure for the entire 32-year period.

DISCUSSION

The initial laying date of crab spiders shifted nearly a month earlier (from late July to late June) during this 32-year analysis. The field-laid broods exhibited an even stronger change during the 15 years in which I recorded them, although a likely outlier contributed to this difference. The procedures used in the two measures also differed significantly, preventing a direct comparison. However, results of the field-laid sample resemble the primary analysis in showing a strong shift toward earlier initial laying dates over time.

This shift to earlier laying dates should enhance overwintering survival of the resulting offspring. Middle and late instars overwinter more successfully than early instars (Morse 2007, 2012). However, the factor most important to the spiders, namely the recruitment of bees to milkweed flowers, should depend to some degree on flowering time, though not in the simplest way, because bumblebees do not recruit to the very earliest milkweed flowers, perhaps because the bees at that time are foraging for pollen to supply the colony's brood

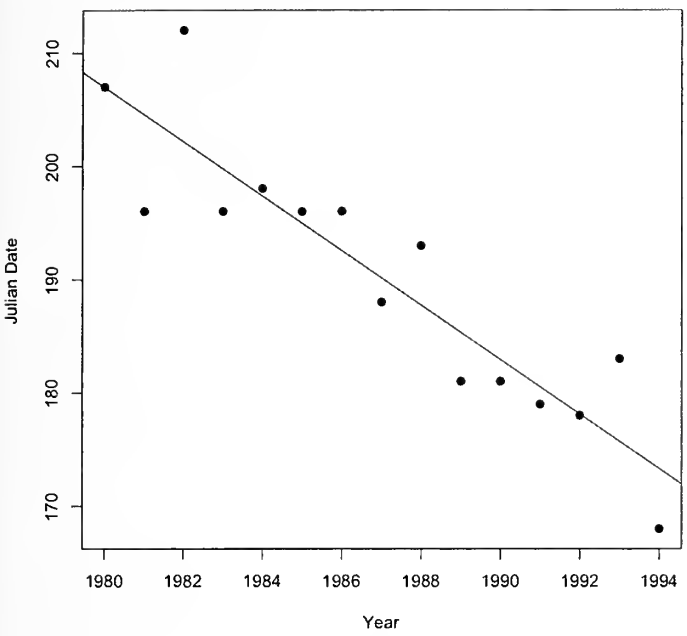

Figure 2.—Change in date of the first crab spider *Misumena vatia* egg masses found in the field from 1980 through 1994. Note the differences in x and y labels in Figure 1 and Figure 2.

(Morse 1982a, 2007). They cannot obtain pollen from milkweeds, because milkweed encapsulates its pollen in pollinia that pollinators can transmit, but cannot exploit (Woodson 1954; Morse 1985). Nevertheless, the bumblebees' recruitment time was significantly related to flowering time, though the significant lag in recruitment to milkweed deprives them of a considerable amount of nectar (Morse 1982b). This lag deprives the spiders as well, since it curtails their time to forage profitably at a highly attractive hunting site (Morse & Fritz 1982).

In the initial years of this census, spiders had little opportunity to produce a second brood due to time limitations, but by the end of the census period oviposition had moved earlier enough to provide the opportunity for a second brood. Indeed, the appearance of several second nests subsequent to rearing a successful first brood suggests the ability to rear a second brood at the study site. Rapid weight gains of females following removal from their first brood followed by supplementary feeding demonstrated that these spiders can produce a second brood if time allows (Morse 1994b), although over the study period I did not find a successful second brood in the field.

Possible advantages of a second brood are open to question because of the stage at which a brood would reach overwintering. A second brood that emerged just before the end of summer would experience a greater overwintering loss than members of first broods, since even members of the latest first broods experience a much lower overwintering success than older juveniles (Morse 1993, 2012). In an analogous situation, Neff & Simpson (1992) found that occasional second broods of the anthophorid bee *Diadasia rinconis* usually failed because of the lack of an adequate flower source. The timing might thus lead second *Misumena* broods into a developmental trap, in which a vulnerable instar reaches

Table 1.—Results from three-way ANOVA of year vs. oviposition date*flowering date*recruitment date over 1979–1991 period.

	Df	Sum Sq	Mean Sq	F value	Pr(>F)
Oviposition date	1	86.340	86.340	117.3094	0.001684 **
Flowering date	1	9.352	9.352	12.7071	0.037694 *
Recruitment date	1	3.525	3.525	4.7898	0.116412
Oviposition date: flowering date	1	2.921	2.921	3.9693	0.140368
Oviposition date: recruitment date	1	8.495	8.495	11.5418	0.042545 *
Flowering date: recruitment date	1	19.209	19.209	26.0999	0.014509 *
Oviposition date: flowering date: recruitment date	1	1.585	1.585	2.1540	0.238493
Residuals	3	2.208	0.736		

the season's end in a stage unfavorable for or fatal to survival (Fielding 2006; Van Dyck et al. 2015).

The lengthened season might appear to provide the opportunity for the spiders to reproduce a year earlier: that is, rather than overwintering a second time, to reproduce the season following their birth. Such offspring, however, would face the problem of immediately encountering the winter, which brings with it low survival rates, especially to the earlier instars conventionally produced (from 3rd year females). Any possible survivors should, however, enhance the fitness of their parents, although producing a second brood might entail countering costs for them, such as increased predation on their first broods resulting from a decreased period of guarding.

The relationship of the ongoing years with spider oviposition, milkweed flowering, and bumblebee recruitment suggests that changing conditions over the study period have affected all of these factors. Regressions for the three species were roughly similar, but if played out over longer periods, their synchrony would decline significantly (Bale et al. 2002). Oviposition date was weakly affected by recruitment date, a reflection of the bumblebees' importance as a food source for the spiders, in spite of the lack of a significant interaction between oviposition and flowering dates. This pattern reflects the response of the spiders directly to their prey, rather than to the flowers themselves, as reported earlier (Morse & Fritz 1982). The one-way analyses confirmed this difference: oviposition and flowering regressions were 0.524 and 0.334, respectively. If continued, this trend would progressively force the spiders to find sites other than milkweed for hunting. Flowering date significantly affected recruitment date; thus the two factors remained relatively in step, perhaps because the bumblebees' nectar sources became available earlier as well. These results all indicate ongoing changes, some of which will continue to decrease the synchrony of these species (Barton et al. 2009; Laws & Joern 2013).

Over the period presented here I have also kept less extended phenological data for several other species in the study area that are minimally related or unrelated to the spider-milkweed-bumblebee system, but show similar trends: emergence dates of adult Japanese beetles *Popilia japonica*, flight dates of Harris' checkerspot butterfly *Chlosyne harrisii*, and eclosion dates of the fern moth *Herpetogramma thieseusalis* (Crambidae), the moth's common parasitoid wasp

Alabagrus texanus (Braconidae), and its hyperparasitoid *Aprostocetus* sp. (Eulophidae) (D.H. Morse unpubl. data). Thus, although *Misumena*, milkweed, and bumblebees have demonstrated striking shifts in phenology, they do not appear unusual in their pattern of change.

In conclusion, I have demonstrated long-term shifts in the oviposition times of crab spiders *Misumena vatia* that parallel patterns of climate change. The lengthening of the season increases the feasibility of becoming double-brooded, although such a second brood would face extreme difficulties. This change in oviposition time parallels changes of other species upon which the spiders depend, but the differences in rate of change among these species suggests that the spiders' relationship with them will shift over time and result in future dependence on other species.

ACKNOWLEDGMENTS

A generation of Brown University undergraduates assisted in the collection and care of the spiders. Several US National Science Foundation grants supported this work. I thank the Darling Marine Center of the University of Maine for use of the study site and K.J. Eckelbarger, T.E. Miller, L. Healy, and other staff members for facilitating fieldwork on the premises.

LITERATURE CITED

Bale, J.S., G.J. Masters, I.D. Hodkinson, C. Awmack, T.M. Bezemer, V.K. Brown et al. 2002. Herbivory in global climate change research: direct effects of rising temperature on insect herbivores. Global Change Biology 8:1–16.

Barton, B.T., A.P. Beckerman & O.J. Schmitz. 2009. Climate warming strengthens indirect interactions in an old-field food web. Ecology 90:2346–2351.

Bewick, S., R.S. Cantrell, C. Cosner & W.F. Fagan. 2016. How resource phenology affects consumer population dynamics. American Naturalist 187:151–166.

Clark, J.A. & R.M. May. 2002. Taxonomic bias in conservation research. Science 297:191b–192b.

Fernandez, I.J., C.V. Schmitt, S.D. Birkel, E. Stancioff, A.J. Pershing, J.T. Kelley et al. 2015. Maine's Climate Future: 2015 Update. University of Maine, Orono, Maine.

Fielding, D. 2006. Optimal diapause strategies of a grasshopper, *Melanoplus sanguinipes*. Journal of Insect Science 6:2.

Houghton, J.T., Y. Ding, D.J. Griggs, M. Noguer, P.J. van der Linden, D. Xiaosu et al. Climate Change 2001: The Scientific Basis. Cambridge University Press, Cambridge, UK.

Jacobson, G., I. Fernandez, S. Jain, K. Maasch, P. Mayewski & S. Norton. 2009. Maine's climate yesterday, today, and tomorrow. Pp. 8–16. *In* Maine's Climate Future: an Initial Assessment. (G.L. Jacobson, I.J. Fernandez, P.A. Mayewski & C.V. Schmitt, eds.) University of Maine, Orono, Maine.

Johansson, J., N.P. Kristensen, J.-Å. Nilsson & N. Jonzén. 2015. The eco-evolutionary consequences of interspecific phenological asynchrony – a theoretical perspective. Oikos 124:102–112.

Laws, A.N. & A. Joern. 2013. Predator-prey interactions in a grassland food chain vary with temperature and food quality. Oikos 122:977–986.

LeRoy, B., M. Paschetta, A. Canad, M. Bakkenes, M. Isaia & F. Ysnel. 2013. First assessment of effects of global change on threatened spiders: potential impacts on *Dolomedes okabtarius* (Clerck) and its conservation plans. Biological Conservation 161:155–163.

Mason, S.C., G. Palmer, R. Fox, S. Gillings, J.K. Hill, C.D. Thomas et al. 2015. Geographical range margins of many taxonomic groups continue to shift polewards. Biological Journal of the Linnean Society 115:586–597.

Memmott, J., P.G. Craze, N.M. Waser & M.V. Price. 2007. Global warming and the disruption of plant-pollinator interactions. Ecology Letters 10:710–717.

Morse, D.H. 1979. Prey capture by the crab spider *Misumena calycina* (Araneae: Thomisidae) Oecologia 39:309–319.

Morse, D.H. 1982a. The turnover of milkweed pollinia on bumble bees, and implications for outcrossing. Oecologia 53:187–196.

Morse, D.H. 1982b. Behavior and ecology of bumble bees. Pp. 245–322. *In* Social Insects, vol. 3. (H.R. Hermann, ed.). Academic Press, New York.

Morse, D.H. 1985. Milkweeds and their visitors. Scientific American 253(1):112–119.

Morse, D.H. 1993. Some determinants of dispersal in crab spiderlings. Ecology 74:427–432.

Morse, D.H. 1994a. The role of self-pollen in the female reproductive success of common milkweed (*Asclepias syriaca*: Aselepiadaceae). American Journal of Botany 81:322–330.

Morse, D.H. 1994b. Numbers of broods produced by the crab spider *Misumena vatia* (Araneae, Thomisidae). Journal of Arachnology 22:195–199.

Morse, D.H. 2007. Predator Upon a Flower: Life History and Fitness in a Crab Spider. Harvard University Press, Cambridge, MA.

Morse, D.H. 2012. Reproductive output of female sit-and-wait spiders: the relative impacts of mating failure, natural enemies and resource availability. Entomologia Experimentalis et Applicata 146:141–148.

Morse, D.H. 2014. Locomotor performance of adult male crab spiders, with implications for the importance of small size. Evolutionary Ecology 28:23–36.

Morse, D.H. & R.S. Fritz. 1982. Experimental and observational studies of patch-choice at different scales by the crab spider *Misumena vatia*. Ecology 63:172–182.

Neff, J.L. & B.B. Simpson. 1992. Partial bivoltinism in a ground-nesting bee: the biology of *Diadasia rinconis* in Texas (Hymenoptera, Anthophoridae). Journal of the Kansas Entomological Society 65:377–392.

Parmesan, C. 2006. Ecological and evolutionary responses to recent climate change. Annual Review of Ecology, Evolution, and Systematics 37:637–669.

Primack, R.B., I. Ibàñez, H. Higuchi, S.D. Lee, A.J. Miller-Rushing, A.M. Wilson et al. 2009. Spatial and interspecific variability in phenological responses to warming temperatures. Biological Conservation 142:2569–2577.

R Development Core Team. 2011. R: a language and environment for statistical computing. R Foundation for Statistical Computing. Vienna, Austria.

Thackeray, S.J., T.H. Sparks, M. Frederiekson, S. Burthe, P.J. Bacon, J.R. Bell et al. 2010. Trophic level asynchrony in rates of phenological change for marine, freshwater and terrestrial environments. Global Change Biology 16:3304–3313.

Van Dyck, H., D. Bonte, R. Puls, K. Gotthard & D. Maes. 2015. The lost generation hypothesis: could climate change drive ectotherms into a developmental trap? Oikos 124:54–61.

Woodson, R.E. 1954. The North American species of *Asclepias*. Annals of the Missouri Botanical Garden 41:1–211.

Manuscript received 3 June 2017, revised 10 October 2017.

2018. Journal of Arachnology 46:35–39

The egg sac of *Benoitia lepida* (Araneae: Agelenidae): structure, placement and the function of its layers

Soren Toft[1] and **Yael Lubin**[2]: [1]Department of Bioscience, Aarhus University, Ny Munkegade 116, DK-8000 Århus C, Denmark; E-mail: soeren.toft@bios.au.dk ; [2]Blaustein Institutes for Desert Research, Ben-Gurion University of the Negev, Sede Boqer Campus, Midreshet Ben-Gurion, 8499000, Israel

Abstract. We describe the remarkable egg sac of *Benoitia lepida* (O.P.-Cambridge, 1876) (Agelenidae) from the Negev Desert, Israel. It consists of four layers: (from outside) a papery envelope, an outer loose silk layer, a "dirt layer", and an inner flocculent silk layer surrounding the eggs. The dirt layer consists of loess soil, and may include stones, snail shells, or twigs from the surroundings. Some sacs hang from a silken string over the female's web sheet, attached to barrier threads or overhanging vegetation. In these "hanging sacs", the outer papery wall is shiny white and covers the inner layers completely. Other sacs ("attached sacs") are attached to a top branch of a shrub, away from the female's web. These sacs often have little or no outer papery envelope; the outer silk wrapping encloses the branch, and the sac may be dull brown in color. We studied the species at two sites; at one the hanging sac type predominated, while at the other the attached type was most common. A field experiment revealed that the dirt layer is effective in protecting the sacs against predation from ants but had no effect on spider predators of the egg sacs.

Keywords: Egg cocoon, manipulative experiment, anti-predatory function, Negev desert

Spider eggs are covered with silk, which forms an egg sac (Foelix 2011). Most egg sacs have a layer of flocculent silk surrounding the eggs. Apart from that, the structure of the sac varies among species depending on the environment in which they are positioned and the dangers they meet from oviposition until emergence of the young (Austin 1985). Suspension in the air on silken strings, strong paper-like surfaces, and other elaborate structures have evolved presumably to protect against egg predators and parasitoids as well as fluctuating climatic conditions (Foelix 2011). Experimental studies have confirmed the anti-predatory function of egg sac structures, while their role in protection against the climate may be minor if any (Christenson & Wenzl 1980; Austin 1985; Hieber 1985, 1992a,b).

The spider *Benoitia lepida* (O. Pickard-Cambridge, 1876) was extremely common throughout the summer months in many parts of the Negev Desert, Israel, when the present studies were performed (1990–91). However, in recent years their numbers have diminished for unknown reasons, and lately it has been difficult to find them. Their funnel webs are placed at the base of shrubs (Fig. 1A). At some localities (e.g., near Sede Boqer in the Negev desert highlands, 30°51′8.27″N 34°47′0.24″E), egg sacs were seen suspended among the barrier threads over the female's web (Fig. 1B). These egg sacs were shiny white and could be observed from a long distance. By opening some of the sacs, we observed a multilayered structure, one of the layers composed of loess soil and often including stones, fragments of snail shells (Fig. 2). On a few occasions, however, we found the egg sac firmly attached to a branch at the top of the shrub (Fig. 2B), with no connection to the female's web. These sacs were usually dull in color but had the same multilayered structure. Our interest in these egg sacs was further enhanced when at a different locality at a distance of less than 50 km (Borot Loz, 30°30′48″N 34°36′32″E), we found that most females produced sacs of the attached type. These initial observations raised several questions, some of which will be dealt with here. First, what is the significance of the layers of the egg sac, in particular the layer with dirt and stones (hereafter named "dirt layer")? Does the high visibility of the sacs increase the danger of bird predation? Before dealing with these questions we describe the structure of the egg sacs and how they are positioned at our two study sites.

The hanging type of egg sac (Figs. 1B, 2A) is typically drop-shaped (length 8–10 mm, diameter 6–7 mm) and situated at the end of a silken string of variable length (from < 1 cm to c. 20 cm). The string and the egg sac itself are typically shiny white and clearly observable even at 5–10 m distance. The sac is nearly always suspended from the barrier threads above the female's web. Up to five egg sacs were seen above a single web. A few very thin threads attached along the string connect it with other barrier threads or with branches of the nearby shrub. These threads keep the sac in a fixed position and prevent it from swinging in the wind and being blown into the branches.

An egg sac consists of four layers (Fig. 2). The shiny white surface is due to a thin papery envelope. Below this is a thin outer, loose layer of silk enclosing the thick dirt layer. The dirt layer may consist of loess soil particles, small stones (some up to one third the length of the egg sac; Fig. 2E), pieces of snail shells, feces of desert snails (mainly *Sphincterochila boissieri* (Charpentier) and of isopods *Hemilepistes reaumuri* (H. Milne-Edwards) (Fig. 2G)), and small twigs, all tightly packed around the inner silk layer and held together by means of silk threads. Surrounding the eggs, the inner silk layer consists of loose flocculent silk. The inner silk layer is continuous with the string, while the outer three layers are packed around both (Fig. 2H).

The attached sacs were usually attached to the side of a vertical branch near the top of the shrub, usually near the center. They were connected to the branch in two ways: by a short string at the top (like a hanging sac) and by a layer of swathing silk that surrounds both the sac and the branch (Fig. 2B). Attached sacs were usually larger and more irregular in appearance than hanging sacs because a section of the branch was included in the wrapped silk. The multilayered structure is the same, except that attached sacs were often light brown in color. This was due to a thinner outer loose silk layer and a

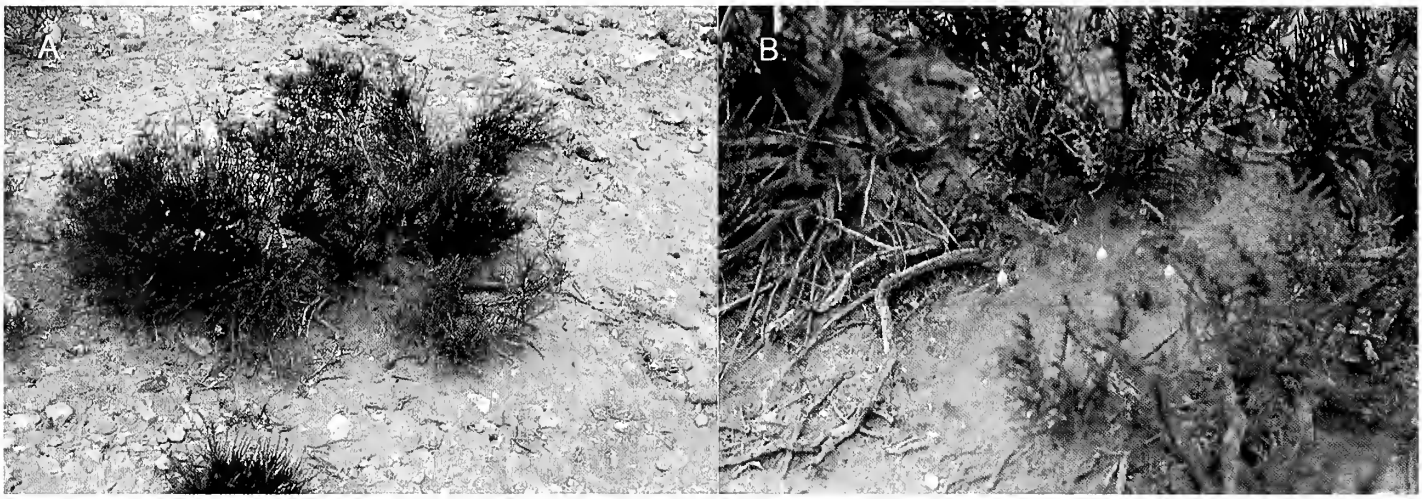

Figure 1.—A. *Benoitia lepida* web at the base of a shrub. B. egg sacs (seen as white spots) hanging above the female's web.

thinner, less papery envelope which allowed the dirt layer to be visible through it. At our Sede Boqer study site, hanging sacs constituted 97% and attached sacs 3%. At Borot Loz, the corresponding values were 24% and 76%.

We hypothesized that the peculiar egg sac structure, and in particular the dirt layer, is an adaptation against egg predators. In the field, we had observed several types of predators attacking the egg sacs: ants (*Tapinoma* sp.) and spiders (*Poecilochroa senilis* (O. Pickard-Cambridge, 1872) or *Cheiracanthium* sp.) might enter sacs and eat the eggs or young; the larvae of *Mercetina matritensis* Bolivar & Pieltain, 1934 (Hymenoptera: Chalcidoidea: Eupelmidae) develop within the egg sac and consume the eggs. To test this hypothesis, we conducted two field experiments, the first designed to examine the role of the different egg sac layers, and a second to determine if the shiny white outer layer is attractive to birds.

METHODS

Skewer experiment.—We manipulated egg sacs by removing a small piece of one or more layers from the egg sac to form a "window" on its side, judged to be a maximum of one sixth of the total surface area. The operation was performed with fine scissors under the dissection microscope.

The main experiment at the Sede Boqer site in 1991 consisted of three treatments: 1) removal of the papery + outer silk layer; 2) removal of the papery + outer silk layer +

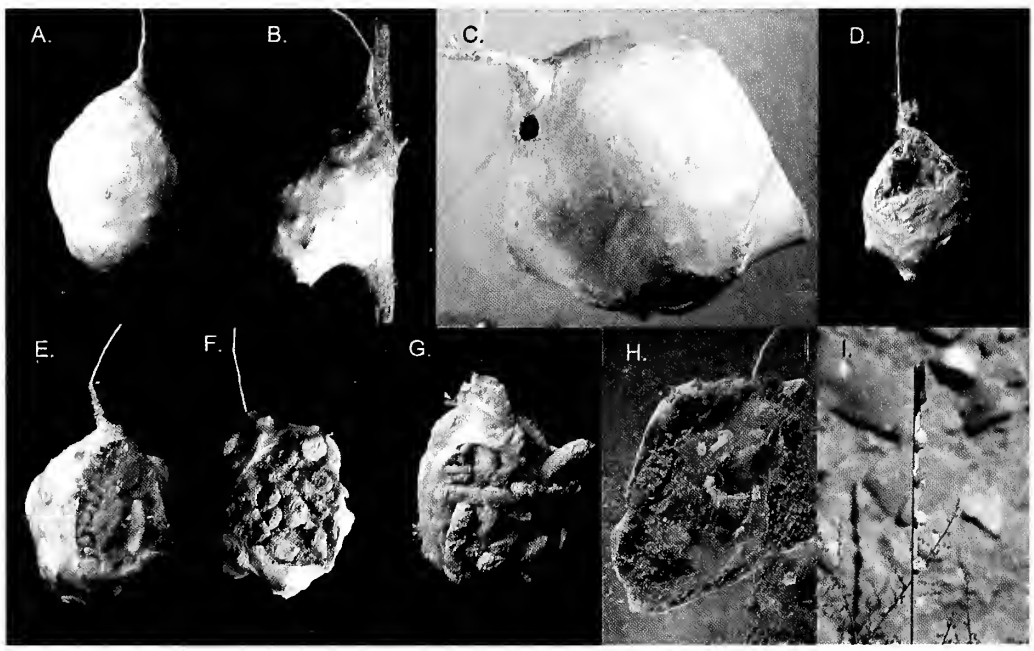

Figure 2.—*Benoitia lepida* egg sacs. A. a typical hanging sac. B. an attached sac. C. a hanging sac with exit hole from which the young have emerged. D. a hanging sac attacked by *Poecilochroa senilis*. E-F. hanging sacs with stones in dirt layer. G. hanging sac with isopod (*Hemilepistes reaumuri*) feces in dirt layer. H. hanging sac with sand grains in dirt layer; egg shells and exuviae can be seen within the inner flocculent silk layer. I. the skewer experiment: four egg sacs (3 manipulated egg sacs and a control) glued to a skewer and placed in a shrub.

the dirt layer; 3) removal of the papery+ outer silk layer + dirt layer + inner silk layer. Control sacs were sham operated, i.e., they were opened all way through to the inner silk layer and closed again. This served two purposes: first, to make sure the operation itself was not harmful to the eggs; second, to check the age of the sacs. Only sacs in which the eggs had not visibly started development were used. In this way, they were all of approximately the same age, and they would not hatch untimely.

Control and experimental sacs were glued to the side of thin wooden skewers (ca. 25 cm long) at the top end, one below another with 2–3 cm between them (Fig. 2I). The control sacs were attached such that the glue closed the sacs. The order of the treatments along the skewer was randomized and the skewers with attached sacs were positioned in low shrubs of *Artemisia sieberi* Besser, near the eastern side of each shrub (the predominant side on which *B. lepida* webs were located).

In a preliminary experiment in 1990 at Sede Boqer, only one treatment was used: removal of papery + outer silk layer + dirt layer. Thus, each skewer had a manipulated and a control sac glued to it, and all skewers were placed in a shrub on the south-facing slope. The experiment began on 10 August 1990 and the sacs were inspected four times over a period of one month.

In 1991, two experiments were performed at two sites in the Negev desert, beginning on 24 July and lasting one month, during which the egg sacs were inspected five times. One experiment with two treatment groups (removal of papery + outer silk + dirt layers and control) was performed at Borot Loz. The other experiment was performed at Sede Boqer, with a control group and all three treatment groups as described above.

The fate of the sacs was recorded when a predation effect was visible or when it had hatched. The following categories were distinguished: **sac hatched**- young presumably dispersed, no evidence of predation, the sac had a small exit hole (Fig. 2C) and the number of egg shells and exuviae from first spiderling instar inside were the same; **ant predation**- ants were present inside the egg sac and most or all eggs were consumed; **empty**- sac empty except perhaps for a few egg shells, presumed to have been preyed on by ants; **spider predation**- a large hole was visible (Fig. 2D) and some hatching may have occurred, but few spiderling exuviae were visible; and **preyed on by *M. matritensis***- the pupal case of the wasp remained inside the egg sac.

Bird predation experiment.—The visibility of the shiny white hanging egg sacs suggested that predation by birds is of no concern. We tested this assumption by means of a brief pilot experiment: in the yard behind the research institute buildings at Sede Boqer, two groups of 10 egg sacs were laid out on the ground, one group in the open, the other in the shade below trees. Flocks of house sparrows (*Passer domesticus* L.) as well as other garden birds occurred abundantly here. These birds were not likely to have had any experience with *B. lepida* egg sacs as the spider did not occur inside the village. After two days of exposure, the two plots with egg sacs were baited with bread crumbs. The egg sacs were examined after an additional two days.

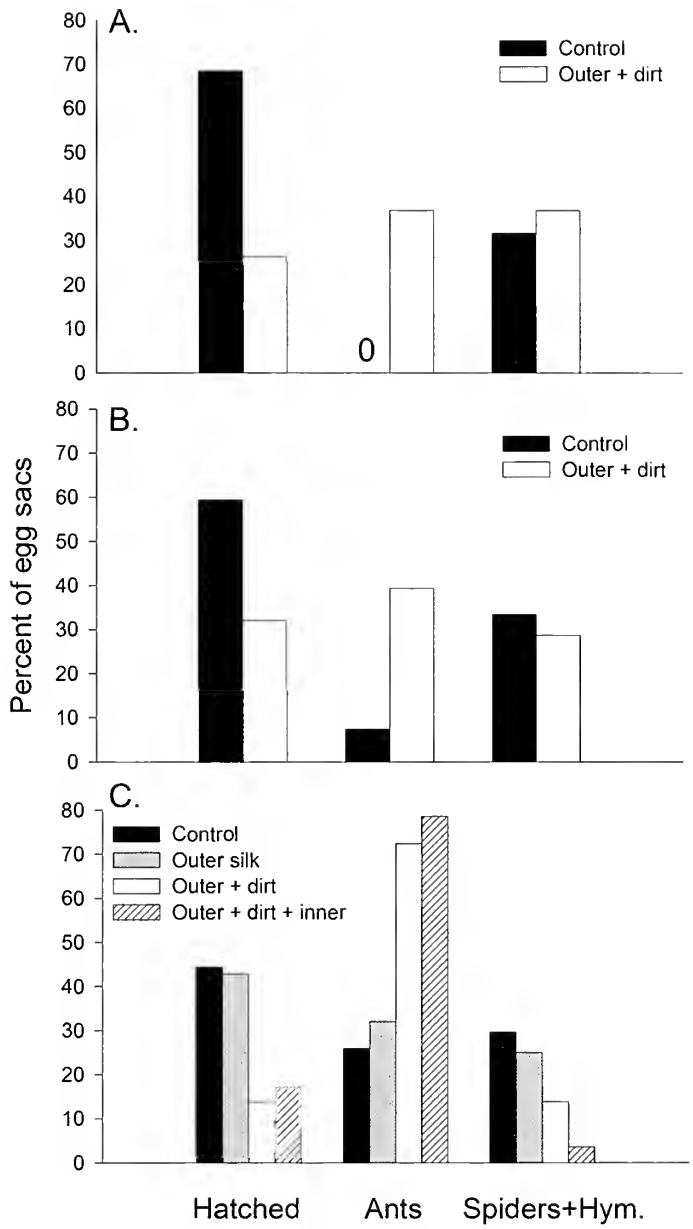

Figure 3.—Skewer experiment. Percent of egg sacs hatched, attacked by ants, or attacked by spiders or hymenopteran egg predators. A. Preliminary experiment, Sede Boqer 1990 (Control, $n = 19$; outer silk + dirt removed, $n = 19$). B. Borot Loz 1991 (Control, $n = 27$; outer silk + dirt removed, $n = 28$). C. Sede Boqer 1991 (control, $n = 27$; outer silk removed, $n = 28$; outer silk + dirt removed, $n = 29$; outer silk + dirt + inner silk removed, $n = 28$).

RESULTS

Skewer experiment.—In both the preliminary experiment in Sede Boqer (1990) and the experiment at Borot Loz (1991), significantly more manipulated sacs were attacked by ants or were emptied of eggs than control sacs ($\chi^2_2 = 10.63$, $P = 0.0053$, and $\chi^2_2 = 8.23$, $P = 0.016$, respectively; Fig. 3A,B). In both cases, there was no difference between the controls and manipulated sacs in the frequency of attacks by spiders and hymenopterans. In the second experiment at Sede Boqer, there were significant differences between the four groups ($\chi^2_6 =$

25.44, $P = 0.0005$). There was no difference between the control sacs and those from which only the papery + outer silk layer had been removed, whereas removal of the dirt layer and of the dirt layer + inner silk layer both resulted in significantly greater frequencies of attacks by ants ($\chi^2_2 = 24.15$, $P < 0.001$; Fig. 3C). Thus, it was removal of the dirt layer that made the sacs more susceptible to ant attacks, and there was no evidence that any of the silk layers contributed to the level of protection. When the outer layers + dirt were removed, seemingly there was reduced predation from spiders in the 1991 experiment (Fig. 3C); however, this may be due to the fact that a large number of the manipulated sacs (>70%) were quickly attacked by ants, and few were left intact.

Bird predation experiment.—After two days, none of the egg sacs had been touched. During the following two days, all the bread crumbs had been eaten, but still none of the egg sacs had been touched. Seemingly, they had not even been tested by the birds as they were still in the exact spots where they were laid out.

DISCUSSION

In many respects, our study is comparable to that of Hieber (1992b). He considered two orb-web spiders (Araneidae) whose egg sacs consist of multiple layers and are suspended in the air by silk threads. Hieber found that the suspension system and outer egg sac cover mainly functioned to prevent predation from ants, whereas the inner flocculent silk layer (the one directly surrounding the eggs) reduced the access for egg laying of specialized egg predators whose larvae develop in the egg sac (ichneumonids, mantispids). Similarly, we never observed ants accessing a hanging egg sac or even moving out onto the barrier threads of *B. lepida*'s web. However, even if made accessible to ants as in the skewer experiments, predation from ants on intact egg sacs was low (Fig. 3). The experiment demonstrated that the dirt layer effectively prevented access into the egg sac by ants, whereas this layer had no effect on predation from spiders.

Contrary to Hieber (1992b), we did not find any effects of the outer papery silk cover and also no effects of the inner flocculent silk layer with respect to predation risk. If they have any, more experiments focused on these layers may be needed.

In designing the pilot bird predation experiment, we assumed, following Hieber (1992b), that the barrier threads of the web were no obstacle to bird predation. From observations of many hundreds of webs, we have never seen any sign of disturbance from animals the size of birds, lizards or small mammals. Thus, we tested whether the egg sacs themselves provide any signals of being potential food to birds. Since the egg sacs were not even tested by the birds, they may rather signal not being food. The lack of interest cannot be due to negative experiences, e.g., with the dirt layer, as the birds were unlikely to have had any experience with these egg sacs before. Not all spider egg sacs are free from bird predation. Lockley & Young (1993) found a high frequency of house sparrow damage to egg sacs of *Argiope aurantia* Lucas, 1833. Barrantes et al. (2013) analyzed the light spectra emitted from the surface silk of egg sacs of spider species from several families. They concluded that reduced conspicuousness is the main function of the wavelength distribution of light reflectance (i.e., egg sac coloration). This cannot be true for the hanging sacs of *B. lepida*, which are so shiny white that conspicuousness must be intended or at least not avoided. Possibly, its high conspicuousness serves a protective function, e.g., signaling being something inedible. A test of this hypothesis should also include, however, an answer to the question why attached sacs are camouflaged and hanging sacs are conspicuous.

Ants constitute the potentially most serious group of egg sac predators in the habitat, but the two adaptations, the hanging sacs and the impenetrable dirt layer, seem to have freed *B. lepida* more or less completely from this danger. Why the species at some localities produce attached sacs predominantly cannot be answered from the results presented here. One of the mechanisms protecting against ants, however, the dirt layer, functions also in the attached sacs.

Suspending the egg sac in the air by means of silk is a widespread phenomenon occurring in species of many families, either by a multitude of threads radiating from the egg sac to surrounding supports (e.g., Araneidae: Hieber 1992a, b; Theridiidae: Bristowe 1956; Uloboridae: Opell 1984), situated within a nest suspended in the web (Theridiidae: Norgaard 1956; Bristowe 1956), or hanging from a single string or stalk (e.g., Agelenidae: Nielsen 1932; Mimetidae: Bristowe 1956; Theridiosomatidae: Hajer et al. 2009; Liocranidae: Holm 1940). Protection from predation, especially from ants, may be a universal function of these traits.

Use of debris or other materials from the surroundings to cover the egg sac can be seen as well in numerous spider families (Nielsen 1932). It is widespread in the family Agelenidae. Already Scheffer (1905) noted about *Agelenopsis naevia* (Walckenaer, 1842) "two silken blankets, with a layer of dirt or wood chippings between" forming the outer cover of the egg sac. *Tegenaria* spp. also may cover their sacs with debris (Nielsen 1932). Egg sacs placed in the open are often covered with debris, which may serve as visual camouflage in addition to physical protection against predators. Hidden sacs as well may be covered with debris (Nielsen 1932). In those cases, a physical protection function against predators may seem the best explanation, though chemical camouflage is also a possibility. In *Tegenaria*, the two traits (egg sacs hanging from a string and covered with debris) may even be combined (Nielsen 1932). A unique feature of the typical *B. lepida* hanging egg sac is that the dirt layer is completely covered by the outer silk layers (papery silk and outer flocculent silk layer) making the dirt layer undetectable from the outside.

ACKNOWLEDGMENTS

We thank the Blaustein Center for Scientific Cooperation for supporting the visit of ST to Sede Boqer. We are indebted to Dr. Gary Gibson, Canada, for identification of *Mercetina matritensis* and to two anonymous reviewers for valuable comments. This is publication no. 931 of the Mitrani Department of Desert Ecology.

LITERATURE CITED

Austin, A.D. 1985. The function of spider egg sacs in relation to parasitoids and predators, with special reference to the Australian fauna. Journal of Natural History 19:359–376.

Barrantes, G., L. Sandoval, C. Sanchez-Quiros, P.-P. Bitton & S.M. Doucet. 2013. Variation and possible function of egg sac coloration in spiders. Journal of Arachnology 41:342–348.

Bristowe, W.S. 1956. The World of Spiders. Collins, London.

Christenson, T.E. & P.A. Wenzl. 1980. Egg-laying of the golden silk spider, *Nephila clavipes* L. (Araneae, Arancidae): functional analysis of the egg sac. Animal Behaviour 28:1110–1118.

Foelix, R. 2011. Biology of Spiders. 3rd ed., Oxford University Press, Oxford.

Hajer, J., J. Maly, L. Hruba & D. Rehakova. 2009. Egg sac silk of *Theridiosoma gemmosum* (Araneae: Theridiosomatidae). Journal of Morphology 270:1269–1283.

Hieber, C.S. 1985. The "insulation" layer in the cocoons of *Argiope aurantia* (Araneae: Arancidae). Journal of Thermal Biology 10:171–175.

Hieber, C.S. 1992a. The role of spider cocoons in controlling desiccation. Oecologia 89:442–448.

Hieber, C.S. 1992b. Spider cocoons and their suspension systems as barriers to generalist and specialist predators. Oecologia 91:530–535.

Holm, Å. 1940. Studien über die Entwicklung und Entwicklungsbiologie der Spinnen. Zoologiska Bidrag från Uppsala 19:1–214.

Lockley, T.C. & O.P. Young. 1993. Survivability of overwintering *Argiope aurantia* (Arancidae) egg cases, with an annotated list of associated arthropods. Journal of Arachnology 21:50–54.

Nielsen, E. 1932. The Biology of Spiders. Levin & Munksgaard, Copenhagen.

Norgaard, E. 1956. Environment and behaviour of *Theridion saxatile*. Oikos 37:41–57.

Opell, B.D. 1984. Eggsac differences in the spider family Uloboridae (Arachnida: Araneae). Transactions of the American Microscopical Society 103:122–129.

Scheffer, T.H. 1905. The cocooning habits of spiders. Kansas University Science Bulletin 3:85–114.

Manuscript received 14 March 2017, revised 19 June 2017.

2018. Journal of Arachnology 46:40–44

Evidence of airborne chemoreception in the scorpion *Paruroctonus marksi* (Scorpiones: Vaejovidae)

Zia Nisani, Arielle Honaker, Victoria Jenne, Felina Loya and **Hoyoung Moon**: Antelope Valley College, Division of Math, Sciences & Engineering, Department of Biological & Environmental Sciences, 3041 West Ave K, Lancaster, CA, 93536 USA; E-mail: znisani@avc.edu

Abstract. Chemically induced predator avoidance behaviors exist in many arthropods. In this paper, we examined the behavioral responses of the desert scorpion, *Paruroctonus marksi* (Haradon, 1984), to airborne chemical cues from a natural predator, the larger scorpion *Hadrurus arizonensis* (Ewing, 1928). We used a Y-shaped, dual-choice olfactometer to test for avoidance behavior in the presence of a known predator, *H. arizonensis*. Prior to this study there has been little research done on chemically induced predator avoidance behaviors in scorpions. The results of this study suggest that *P. marksi* is capable of detecting a predator's airborne cues, though the nature and identity of these cues remain unknown, and it appears that the constellation array of the fixed finger does function in detecting these cues. We also discuss the importance of adaptive predator avoidance behaviors.

Keywords: Arachnid, arthropod, kairomone, pheromone, Y-tube olfactometer

Prey organisms demonstrate a variety of adaptations to defend themselves from predators. These adaptations can include morphological (e.g., spines and armor), biochemical (e.g., repellents, toxins, and resistance to these), behavioral (e.g., fleeing), or life history-based (e.g., delayed hatching) traits. Due to the unforgiving nature of predation, prey organisms are under strong selection to detect and avoid predators (Lima & Dill 1990; Lima 1998a,b). Early detection and recognition of predation risk represent important adaptations of predator avoidance. Thus, an organism will benefit from the use of multiple sensory inputs, including visual, tactile, and chemical cues.

Chemically mediated behaviors that reduce predation risk have received considerable attention among diverse taxonomic groups (for detailed reviews see Kats & Dill 1998; Dicke & Grostal 2001). The majority of studies have documented chemically mediated antipredator behaviors in aquatic organisms, with fewer focusing on terrestrial vertebrates (Hay 2009; Ferrari et al. 2010). Avoidance is often seen when prey are given a choice between an area that contains a predator, or cues of its presence, versus an empty area.

Arthropod prey species can perceive the chemical cues of a potential predator from either direct or indirect sources (Dicke & Grostal 2001). Direct chemical cues produced by the predator (kairomones) can be recognized by the prey. These cues derive from eggs, excreta, pheromones, and other by-products that a prey animal can detect (Nolte et al. 1994; Hoffmeister & Roitberg 1997; Grostal & Dicke 2000; Dicke & Grostal 2001). In scorpions, Miller and Formanowicz (2010) demonstrated that male *Paruroctonus boreus* (Girard, 1854) significantly avoided areas exposed to direct cues from conspecific males. Indirect cues do not come from the predator itself, as they originate from injured or dead conspecifics (Chivers & Smith 1998; Huryn & Chivers 1999; Hoefler et al. 2012). To date, no study has demonstrated that scorpions can use indirect cues.

Scorpions can perceive their environment using multiple sensory systems. In addition to vision, which is well-developed and allows for image formation and identifying subtle changes in light magnitude (Schliwa & Fleissner 1980; Fleissner & Fleissner 2001), scorpions possess an assortment of mechano- and chemoreceptors that provide them with relevant information. For example, trichobothria react to horizontal air streams and possess directional sensitivity (Hoffman 1967). These or other structures might also facilitate detection of substrate vibrations (Brownell & Farley 1979a,b,c; Brownell & van Hemmen 2001). Pectines appear to be involved in chemically-mediated orientation behaviors such as mate recognition and possibly localization of water (Gaffin & Brownell 1992; Gaffin et al. 1992). Fingers of the pedipalps possess a constellation-shaped microscopic array of sensilla that are thought to be involved with chemoreception (Fet et al. 2006a,b).

Chemoreception is well developed in scorpions, but much remains to be learned about the structures, contexts, and behaviors involved. Several studies suggest that male scorpions can use substrate-borne pheromones to locate females (Gaffin & Brownell 1992; Melville et al. 2003; Taylor et al. 2012), but in the only study that examined airborne chemical transmission, males of *Centruroides vittatus* (Say, 1863) showed no tendency to move toward the female, though they responded when they contacted substrate-borne female deposits (Steinmetz et al. 2004). To demonstrate the role of pedipalps in chemoreception, Abushama (1964) offered fivekeeled gold scorpions (*Leiurus quinquestriatus* Hemprich & Ehrenberg, 1829) a choice between a compartment treated with various chemicals (chemical in petri dish) and an untreated compartment (empty petri dish). The scorpions moved away from most treated areas, and selected compartments that were either scent free or had the odor of cockroach (*Periplaneta americana*) prey. However, when the pedipalps (pincers) were painted over, the scorpions demonstrated reduced sensitivity to chemical odors. Abushama (1964) hypothesized that small hairs distributed over the pedipalps might be responsible for detecting airborne chemicals, but no further studies were conducted to support this claim. Fet et al. (2006a,b) subsequently described a constellation-shaped microscopic array of sensilla on the distal external portion of the fixed finger of the pedipalp in several scorpion species

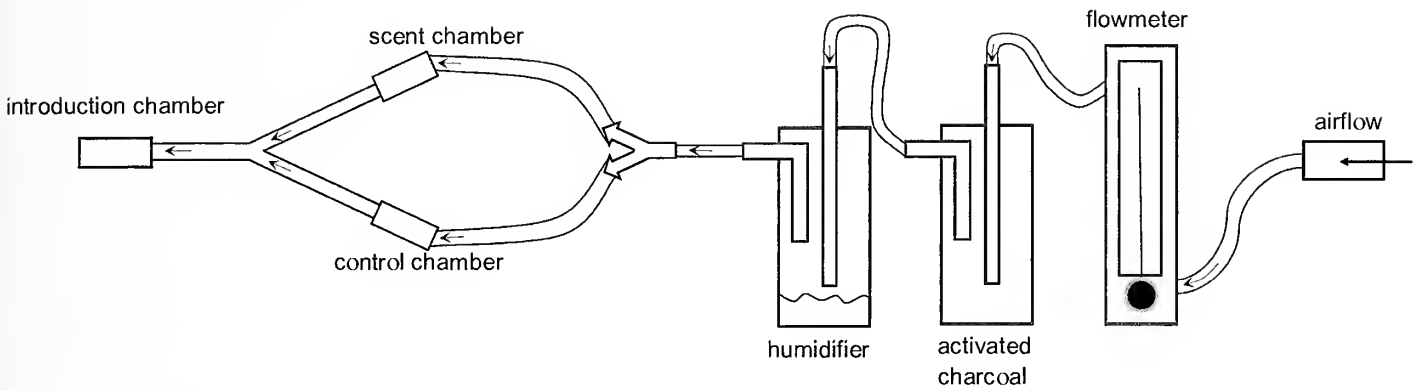

Figure 1.—Schematic of the glass Y-tube olfactometer used to test the response of adult *Paruroctonus marksi* scorpions to volatiles of *Hadrurus arizonensis* (predator). Test subjects were placed into the Introduction chamber from which they locomoted to the Y-intersection and then selected a Y-arm to enter. Arrows indicate the direction of airflow. See Methods for dimensions and further explanation.

(including *Paruroctonus*), and suggested that these structures serve a chemosensory role.

The purpose of the present study was to test two hypotheses. First, we hypothesized that the scorpion *Paruroctonus marksi* (Haradon, 1984) can detect the presence of a known scorpion predator (*H. arizonensis* (Ewing, 1928)) using airborne predator-derived chemical cues. We used a Y-tube olfactometer that provided simultaneous discrimination between two chemical environments, and quantified ambulatory behaviors that might be associated with the sampling of the airborne chemicals. Second, we hypothesized that constellation array sensilla on the pedipalp fingers are used to detect chemicals.

METHODS

Research animals.—We collected all specimens of *P. marksi* (mean prosoma and mesosoma combined 1.35 ± 1.19 cm) and *H. arizonensis* (3.5 cm) scorpions (all adult females) during mid-July and August at a single location in Lancaster, California (34°38′36" N, 118°11′38" W), using UV light. We used a single *H. arizonensis* (predator) for all trials. We housed *P. marksi* scorpions individually in clear plastic containers measuring 13 x 12 x 10 cm (L x W x H), and *H. arizonensis* in a 31 x 19 x 12 cm clear plastic container, with all containers having a sand substrate and a wet sponge. Scorpions were kept at 21–23°C and 55–60% relative humidity under a 12:12 h light:dark cycle. Scorpions were fed an appropriate-sized cricket once a week.

Olfactometer.—We examined the olfactory responses of *P. marksi* toward predator (*H. arizonensis*) odors using a Y-shaped glass tube olfactometer (3 cm inner diameter) with a long (11 cm) introduction arm and two short (7 cm) "choice" arms (Fig. 1). The angle between the two short arms was 65°. An introduction glass chamber (5 cm long with diameter of 2 cm) and two scent source glass chambers (11 cm long with diameter of 2 cm) were attached to the proximal end of the introduction tube and the distal ends of the choice arms, respectively; a fine mesh was located at 8 cm where the scent (marble, predator, or crickets) was placed behind it. The chambers could be disassembled for cleaning between trials. Airflow (250 ml/min) generated by the laboratory's pressurized air system was purified via passage through activated charcoal (6–14 mesh) and then humidified to carry airborne chemicals more efficiently by passage through a bottle containing deionized water before entering the scent source chambers at the distal ends of the two choice arms. Before conducting the experiment, we visualized the airflow using dry ice in water to ensure that there was negligible air mixing at the Y-junction of the long arm of the olfactometer.

Behavioral assays.—For each trial, we first set up the two scent source chambers and turned on the airflow. Next, we placed a single specimen of *P. marksi* into the introduction chamber and connected the chamber to the proximal end of the long arm. The scorpion was then given 5 minutes to ambulate toward the Y junction and choose which arm to enter. If the scorpion remained in the long arm, it was recorded as No Response. Upon entering either of the short arms, the scorpion was given 1 additional minute before the choice was recorded. The test scorpions were small enough that they could turn around in the tubes, so if the scorpion entered an arm and then exited within the 1 minute time frame, the behavior was recorded. Two scorpions that showed No Response (did not leave the introduction chamber or stayed motionless in the long arm) were retested 10 days later. In addition to recording the choice of arms entered, we also noted the behavior exhibited by the scorpions.

Trials were conducted between the hours of 1900 and 2100 in a dimly lit room. To minimize the effect of any directional bias, we alternated the odor conditions of the right and left arms every three trials. In a supplemental trial, we confirmed the absence of a directional bias in 13 scorpions tested with both chambers empty (binomial test: $P = 1.00$). The scent chambers and Y-tube were cleaned with isopropyl alcohol and deionized water between trials.

Experiment 1.—We conducted two sets of trials to test whether *P. marksi* avoided the odors of a scorpion predator. For the predator scent trials, we placed a scorpion predator (*H. arizonensis*) in one scent source chamber and left the other chamber empty as a control. The *H. arizonensis* in the scent chamber was immobile and could not be seen through the fine mesh, thereby eliminating visual cues. We then tested the behavioral choices of 25 *P. marksi* scorpions. Because the scorpions might respond to non-chemical cues of the predator, such as altered airflow, we repeated the experiment with another 21 *P. marksi* scorpions, but substituted a presumably

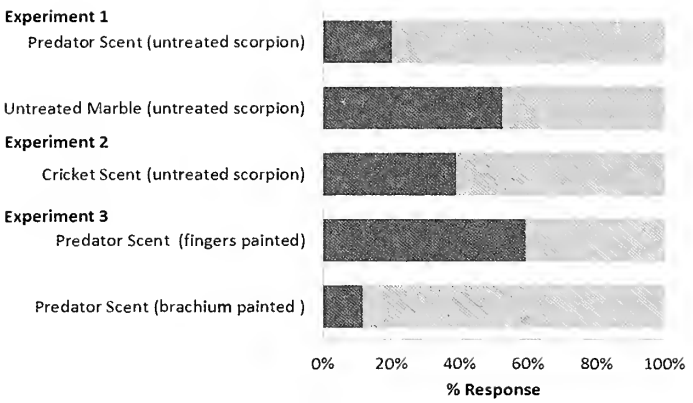

Figure 2.—Response of *Paruroctonus marksi* scorpions to various treatment groups in the Y-tube olfactometer. The light and dark areas of each bar represent, respectively, the percentage of scorpions that selected the arm containing a control odor (empty chamber) or an odor source (live *Hadrurus arizonensis* scorpion as a predator or a marble as a control). In Experiment 1 the scorpions avoided the predator scent odor but not the marble (control) while in Experiment 2 there was no significant response to Cricket odor, suggesting use of chemoreception for predator avoidance. In Experiment 3 the scorpions with sensilla-free brachium of the pedipalps painted over (as a control) avoided the predator scent, whereas those with the sensilla-bearing fingers of the pedipalps painted over showed no avoidance, suggesting a role a chemoreception for the sensilla of the pedipalp fingers.

chemically inert object, a glass marble (about 14 mm), in place of the predator odor. The presence of the *H. arizonensis* and marble did not disrupt airflow into the olfactometer.

Experiment 2.—We conducted 18 trials to test whether *P. marksi* responded to the non-predator odors (crickets). Each trial was conducted as described above with 5 crickets placed in the scent chamber. The presence of the crickets did not disrupt airflow into the olfactometer.

Experiment 3.—We conducted two more sets of trials to determine whether the constellation array of *P. marksi* plays a role in detecting predator odors. In the first trial, we tested 26 *P. marksi* with the aforementioned predator versus control conditions (Experiment 1) after painting the fingers of their pedipalps (Treated group) with non-toxic nail polish. We assumed this treatment impeded chemical detection of the predator scent. We then repeated the trial with another 26 scorpions having only the brachium (first segment before the chela) painted (Control group). No mortality was seen in the nail polish painted scorpions.

Data analysis.—For each experiment, we conducted a 2×2 (trial $\times$ choice) chi-square test (Zar 1996) to determine whether *P. marksi* choices were non-random. But for experiment 2, we conducted a 2×3 chi-square test. We computed phi (φ) as a measure of effect size, with values of $\sim$0.1, $\sim$0.3, and $\geq$0.5 deemed as small, medium, and large effects, respectively (Cohen 1988). We then tested simple main effects with a binomial test (Zar 1996). We used SPSS 13.0 for Windows (SPSS Inc, Chicago, IL, USA) with alpha set at 0.05.

RESULTS

Experiment 1.—The two trials testing predator scent and an airflow control yielded contrasting results ($\chi^2 = 5.28$, df = 1, asymptotic $P = 0.022$, $\varphi = 0.34$). Thus, the scorpions responded differently to the cues of a predator and an inanimate object. Scorpions given the choice between the scent of a predator versus no odor avoided the predator scent by selecting the arm of the control chamber (80.0%, $n = 25$, binomial asymptotic $P = 0.004$; see Fig. 2), whereas those given the choice between the marble versus no odor selected the arm of the control chamber at random (52.0%, $n = 21$; binomial asymptotic $P = 1.00$; Fig. 2).

Experiment 2.—There was no difference when it came to choosing between crickets (39%) versus no odor (61%) source ($n = 18$; binomial asymptotic $P = 0.48$; Fig. 2). Although experiment 2 was run separately from experiment 1, it was done in an identical manner, so we combined the trial to those of experiment 1 to run a 2×3 chi-square test, which showed contrasting results ($\chi 2 = 8.58$, df =2, $P = 0.014$, $\varphi = 0.37$). Therefore, the scorpions responded differently to the cues of a predator, a non-predator (cricket), and an inanimate object.

Experiment 3.—The two trials testing sensory deprivation and its control likewise yielded contrasting results ($\chi^2 = 13.12$, df = 1, asymptotic $P < 0.001$, $\varphi = 0.50$). Thus, the scorpions responded differently depending on which portion of the chelae was painted. Scorpions that had their pedipalp fingers painted exhibited no predator avoidance (40.7%, $n = 27$; binomial asymptotic $P = 1.00$; Fig. 2), whereas control scorpions that had their brachium painted exhibited predator avoidance by preferentially selecting the arm of the control chamber (88.5%, $n = 26$; binomial asymptotic $P < 0.001$; Fig. 2).

Behavioral observations.—In all trials after a short pause in the introduction chamber, the scorpions slowly walked through the long arm of the Y-tube. Walking was interrupted with intermittent pauses before reaching the Y-junction. While traveling in the long arms, the scorpions repeatedly waved their pedipalps up and down. When the scorpions paused, the pedipalps were either kept in the up or down position until locomotion resumed. These behaviors were observed in all the trials regardless of scorpions being treated (painted or not) and type of odor source used. The scorpions that selected the side containing the predator generally exhibited a typical defensive posture with the metasoma arched above the body. In the trials in which scorpions selected the marble, empty, or cricket chambers, none of the scorpions exhibited a defensive posture and assumed a resting posture with the body resting low and legs withdrawn.

DISCUSSION

The results of this study suggest that *P. marksi* is capable of detecting a predator's airborne cues, though the nature and identity of these cues remain unknown. However, it is logical to conclude that airborne chemical cues may play a role in predator avoidance in this scorpion. Furthermore, the data suggest that the constellation array of *P. marksi* may play a role in allowing these scorpions to detect predator's airborne cues. We acknowledge that more studies, especially neuro-ethological studies, might shed more light on scorpion's use of airborne cues in avoiding redators.

Due to high densities, scorpions comprise an important food source for diverse predators. Polis et al. (1981) documented that the predators of scorpions were mainly

other scorpions, followed by vertebrates and other invertebrates. Among scorpions, *H. arizonensis* is a frequent intraguild predator, with 30% of its diet composed of scorpions (Polis & McCormick 1987). Additional studies have also demonstrated that scorpion-scorpion predation is very common (Polis 1979; Polis & McCormick 1987). Therefore, being able to detect scorpion and other potential predators should feature prominently in the above-ground foraging behavior of scorpions.

Many studies have shown that the nature of chemical cues from predators can depend on the identity of the prey that is consumed (Chivers & Mirza 2001; Hoefler et al. 2012). We doubt the possibility that prior meals of *H. arizonensis* would serve as an indirect cue because both scorpion species used in this study were fed crickets for two months prior to the behavioral assay. Thus, the source of the airborne cues detected by *P. marksi* likely came directly from *H. arizonensis* itself.

Recent studies suggest that scorpions can use chemical cues in conspecific avoidance (Miller & Formanowicz 2010) and mate tracking (Gaffin & Brownell 1992; Melville et al. 2003; Steinmetz et al. 2004; Taylor et al. 2012). Miller & Formanowicz (2010) demonstrated that males of *Paruroctonus boreus* in an open Y-maze avoided areas exposed to other males of the same population. Furthermore, male *P. boreus* spent significantly more time in areas that previously contained females from the same population than in areas exposed to females from different populations. Taylor et al. (2012) used cuticular extracts from female *P. utahensis* (Williams, 1968) applied to the sand of the arena floor to induce pre-courtship behavior in males, thus demonstrating the existence of female pheromones. These studies highlight the importance of substrate-borne chemical cues in mate localization by male scorpions; however, the presence of airborne chemical cues was not eliminated, though its role in mate tracking was discounted (Steinmetz et al. 2004).

When studying the response of *L. quinquestriatus* to airborne chemical cues (naphthalene, cockroaches or conspecific scorpions), Abushama (1964) reported that scorpions placed in the preference chamber performed a stereotypical movement with raised pedipalps. When the appendages were painted over, this behavioral sensitivity to chemical cues was reduced. Abushama hypothesized that the pedipalps might be used as sense organs to detect airborne cues. We observed similar behavior in the present study. When *P. marksi* scorpions traveled in the long arm of the Y-tube, they ambulated while raising their pedipalps up and down repeatedly. Furthermore, the up-and-down movement of the pedipalps was exhibited most prominently at the junction of the Y-tube, suggesting a chemosensory function.

Fet et al. (2006a,b) described a constellation-shaped microscopic array of sensilla on the distal external portion of the fixed finger of the pedipalp in several scorpion species (including *Paruroctonus*). They hypothesized that the constellation array is a chemosensory structure possibly analogous to the palpal organ and Haller's organ on tarsi I in ticks. In our study, painting of the pedipalps blocked *P. marksi* discrimination between predator and control odors, whereas painting of the brachia did not alter avoidance of the predator. Thus, our results suggest that *P. marksi* uses this constellation array of pedipalp sensilla (or a yet unidentified structure) to detect the odors of predators.

To the best of our knowledge, this study is the first demonstration of scorpions using kairomones in predator avoidance. We do not know whether *P. marksi* detected *H. arizonensis* pheromones or other yet to be identified chemicals, and thus we recognize the need for further study to identify the source and nature of these airborne chemical cues.

ACKNOWLEDGMENTS

The authors thank Dr. Les Uhazy and Prof. Christos Valiotis for their support of the Antelope Valley College Undergraduate Research Initiative (AVC-URI). We also thank Dr. Arie van der Meijden and Ms. Diana Pedroso for donating some of the collected scorpions. Finally, we are grateful to Drs. Les Uhazy, William Hayes, and Allen Cooper for their constructive comments and Dr. William Kitto with advising on statistical analyses. This project was performed by Arielle Honaker, Victoria Jenne, Felina Loya, and Hoyoung Moon as part of the AVC-URI, and was supported by United States Department of Education grant P031C110009-13.

LITERATURE CITED

Abushama, F.T. 1964. On the behaviour and sensory physiology of the scorpion *Leiurus quinquestriatus* (H. & E.). Animal Behaviour 12:140–153.

Brownell, P.H. & R.D. Farley. 1979a. Detection of vibrations in sand by tarsal sense organs of the nocturnal scorpion, *Paruroctonus mesaensis*. Journal of Comparative Physiology A 131:23–30.

Brownell, P.H. & R.D. Farley. 1979b. Orientation to vibrations in sand by the nocturnal scorpion, *Paruroctonus mesaensis*: mechanism of target localization. Journal of Comparative Physiology A 131:31–38.

Brownell, P.H. & R.D. Farley. 1979c. Prey localization behaviour of the nocturnal scorpion, *Paruroctonus mesaensis*: orientation to substrate vibrations. Animal Behaviour 27:185–193.

Brownell, P.H. & J.L. van Hemmen. 2001. Vibration sensitivity and a computational theory for prey-localizing behavior in sand scorpions. American Zoologist 41:1229–1240.

Chivers, D.P. & R.S. Mirza. 2001. Predator diet cues and the assessment of predation risk by aquatic vertebrates: a review and prospectus. Pp. 277–284. *In* Chemical Signals in Vertebrates, Vol. 9. (A. Marchlewska-Koj, J.J. Lepri & D. Muller-Schwarze, eds.). Plenum, New York, New York.

Chivers, D.P. & R.J.F. Smith. 1998. Chemical alarm signaling in aquatic predator-prey systems: a review and prospectus. Ecoscience 5:338–352.

Cohen, J. 1988. Statistical Power Analysis for the Behavioral Sciences. 2nd edition. Lawrence Erlbaum Associated, Inc., USA.

Dicke, M. & P. Grostal. 2001. Chemical detection of natural enemies by arthropods: an ecological perspective. Annual Review of Ecology & Systematics 32:1–23.

Ferrari, M.C.O., B.D. Wisenden & D.P. Chivers. 2010. Chemical ecology of predator–prey interactions in aquatic ecosystems: a review and prospectus. Canadian Journal of Zoology 88:698–724.

Fet, V., M.S. Brewer, M.E. Soleglad & D.P.A. Neff. 2006a. Constellation array: a new sensory structure in scorpions (Arachnida: Scorpiones). Boletin Sociedad Entomologica Aragonesa 38:269–278.

Fet, V., M.E. Soleglad, M.S. Brewer, D.P.A. Neff & M.L. Norton. 2006b. Constellation array in scorpion genera *Paruroctonus*,

Sueringurus, *Vejovoidus*, and *Paravaejovis* (Scorpiones: Vaejovidae). Euscorpius #41:1–15.

Fleissner, G. & G. Fleissner. 2001. Night vision in desert scorpions. Pp. 317–324. *In* Scorpions 2001; In Memoriam Gary A Polis (V. Fet, P.A. Selden, eds), Burnham Beeches, Bucks: British Arachnological Society.

Gaffin, D.D. & P.H. Brownell. 1992. Evidence of chemical signaling in the sand scorpion, *Paruroctonus mesaensis* (Scorpionidae: Vaejovidae). Ethology 91:59–69.

Gaffin, D.D., K.L. Wennstrom & P.H. Brownell. 1992. Water detection in the desert sand scorpion, *Paruroctonus mesaenis* (Scorpionida, Vaejovidae). Journal of Comparative Physiology A 170:623–629.

Grostal, P. & M. Dicke. 2000. Recognising one's enemies: a functional approach to risk assessment by prey. Behavioral Ecology & Sociobiology 47:258–264.

Hay, M.E. 2009. Marine chemical ecology: chemical signals and cues structure marine populations, communities, and ecosystems. Annual Review of Marine Science 1:193–212.

Hoefler, C.D., L.C. Durso & K.D. McIntyre. 2012. Chemical-mediated predator avoidance in the European house cricket (*Acheta domesticus*) is modulated by predator diet. Ethology 118:431–437.

Hoffmann, C. 1967. Bau und Funktion der Trichobothrien von *Euscorpius carpathicus* L. Zeitschrift für vergleichende Physiologie 54:290–352.

Hoffmeister, T.S. & B.D. Roitberg. 1997. Counterespionage in an insect herbivore-parasitoid system. Naturwissenschaften 84:117–119.

Huryn, A.D. & D.P. Chivers. 1999. Contrasting behavioral responses by detritivorous and predatory mayflies to chemicals released by injured conspecifics and their predators. Journal of Chemical Ecology 25:2729–2740.

Kats, L.B. & L.M. Dill. 1998. The scent of death: chemosensory assessment of predation risk by prey animals. Ecoscience 5:361–394.

Lima, S.L. 1998a. Stress and decision making under the risk of predation: recent developments from behavioral, reproductive, and ecological perspectives. Advances in the Study of Behavior 27:215–290.

Lima, S.L. 1998b. Nonlethal effects in the ecology of predator-prey interactions: what are the ecological effects of antipredator decision-making? American Naturalist 153:649–659.

Lima, S.L. & L.M. Dill. 1990. Behavioral decisions made under the risk or predation: a review and prospectus. Canadian Journal of Zoology 68:619–640.

Melville, J.M., S.K. Tallarovic & P.H. Brownell. 2003. Evidence of mate trailing in the giant hairy desert scorpion, *Hadrurus arizonensis* (Scorpionida, Iuridae). Journal of Insect Behavior 16:97–115.

Miller, A.L. & D.R. Formanowicz. 2010. Friend or foe: behavioral responses to conspecifics in the northern scorpion, *Paruroctonus boreus* (Scorpionida: Vaejovidae). Journal of Ethology 29:251–256.

Nolte, D.L., J.R. Mason, G. Epple, E. Aronov & D.L. Campbell. 1994: Why are predator urines aversive to prey? Journal of Chemical Ecology 20:1505–1516.

Polis, G.A. 1979. Prey and feeding phenology of desert sand scorpion *Paruroctonus mesaensis* (Scorpionidae: Vaejovidae). Journal of Zoology – London 188:333–346.

Polis, G.A. & S.J. McCormick. 1987. Intraguild predation and competition among desert scorpions. Ecology 68:332–343.

Polis, G.A., W.D. Sissom & S.J. McCormick. 1981. Predators of scorpions: field data and a review. Journal of Arid Environments 4:309–326.

Schliwa, M. & G. Fleissner. 1980. The lateral eyes of the scorpion, *Androctonus australis*. Cell and Tissue Research 206:95–114.

Steinmetz, S.B., K.C. Bost & D.D. Gaffin. 2004. Response of male *Centruroides vittatus* (Scorpiones: Buthidae) to aerial and substrate-borne chemical signals. Euscorpius #12:1–6.

Taylor, M.S., C.R. Cosper & D.D. Gaffin. 2012. Behavioral evidence of pheromonal signaling in desert scorpion *Paruroctonus utahensis*. Journal of Arachnology 40:240–244.

Zar, J.H. 1996. Biostatistical Analysis, 3rd edition. Prentice Hall, Engelwood Cliffs, New Jersey.

Manuscript received 12 December 2016, revised 25 August 2017.

2018. Journal of Arachnology 46:45–49

Small pholcids (Araneae: Synspermiata) with big surprises: the lowest diploid number in spiders with monocentric chromosomes

Rafael Lucena Lomazi[1], **Douglas Araujo**[2], **Leonardo Sousa Carvalho**[3,4] and **Marielle Cristina Schneider**[1]: [1]Universidade Federal de São Paulo, UNIFESP, Departamento de Ciências Biológicas, Av. Prof. Artur Riedel, 275, 09972-270, Diadema, São Paulo, Brazil. E-mail: marielle.unifesp@gmail.com; [2]Universidade Federal de Mato Grosso do Sul, UFMS, Setor de Biologia Geral, Instituto de Biociências, Cidade Universitária, Bairro Universitário, 79070-900, Campo Grande, Mato Grosso do Sul, Brazil. [3]Universidade Federal do Piauí, UFPI, Campus Amílcar Ferreira Sobral, Departamento de Ciências Biológicas, BR 343, km 3.5, Bairro Meladão, 64800-000, Floriano, Piauí, Brazil. [4]Pós-Graduacão em Zoologia, Universidade Federal de Minas Gerais, Belo Horizonte, MG, Brazil.

Abstract. Even though less than 2% of pholcid species have been karyotyped, previous studies documented a wide diversity of diploid numbers and sex chromosome systems. Here, we increase the number of native Brazilian cytogenetically investigated pholcid species from three to eight and discuss implications of chromosome evolution in this group. The species analyzed here share a X0/XX sex chromosome system and biarmed chromosomes, but vary in diploid numbers, i.e., $2n♂ = 17$ in *Mesabolivar spinulosus* (Mello-Leitão, 1939) and *Mesabolivar togatus* (Keyserling, 1891), $2n♂ = 15$ in *Carapoia* sp., and $2n♂ = 9$ in *Micropholcus piaui* Huber, Carvalho & Benjamin, 2014 and *Micropholcus ubajara* Huber, Carvalho & Benjamin, 2014. Chromosomal data indicate that most *Mesabolivar* species share a $2n♂ = 17$, X0, while *Mesabolivar luteus* shares with *Carapoia* sp. a $2n♂ = 15$, X0. This lends further support to the idea that *M. luteus* is in fact misplaced and more closely related to *Carapoia* González-Sponga, 1998. The diploid number of the two *Micropholcus* species is the lowest reported so far for spiders with monocentric chromosomes. The $2n♂ = 9$, differs strongly from the $2n♂ = 17$ previously reported for *Micropholcus fauroti* (Simon, 1887). As the number of autosomes of *M. piaui* and *M. ubajara* is exactly half of that found in *M. fauroti*, we hypothesize that the reduction occurred by an "all or nothing" fusion event. The low diploid number observed in *M. piaui* and *M. ubajara* is the first morphological synapomorphy that would support the establishment of a new genus to allocate the New World *Micropholcus* species.

Keywords: Karyotype, meiosis, Modisiminae, Pholcinae, sex chromosome system

Knowledge regarding spider cytogenetics has grown considerably in recent years; however, less than 2% of the ca. 47,000 described species are karyotyped so far (Araujo et al. 2017; World Spider Catalog 2017). In spite of this, there is a huge variation in the diploid number, from $2n♂ = 7$, in the dysderid *Dasumia carpatica* (Kulczyński, 1882) and the segestriid *Ariadna lateralis* Karsch, 1881 (Suzuki 1950, 1954; Kořínková & Král 2013), to $2n♂ = 128$, in the ctenizid *Cyclosoma siameusis* Schwendinger, 2005 (Král et al. 2013). In general, lower diploid numbers are found in araneomorphs whilst higher diploid numbers prevail in non-araneomorphs (see Araujo et al. 2017).

The Pholcidae is the ninth and second most diverse family among Araneae and Synspermiata spiders, respectively, with about 1600 species and 80 genera (World Spider Catalog 2017). However, only 19 species belonging to eight genera were cytogenetically studied, with the diploid number varying from $2n♂ = 15$ to $2n♂ = 32$. The X0 sex chromosome system (SCS) predominates within the pholcids, occurring in 13 species, followed by the X_1X_20, X_1X_2Y and XY systems. Similar to most Synspermiata spiders, the chromosomes are, in general, biarmed (see Araujo et al. 2017).

Huber (2011), taking into account several phylogenetic hypotheses, updated a classification of pholcids in five subfamilies: Ninetinae, Arteminae, Modisiminae, Smeringopinae and Pholcinae. This classification was latter corroborated by molecular phylogenies (Dimitrov et al. 2013). Among these subfamilies, only Ninetinae has no cytogenetic data (see Araujo et al. 2017), but many gaps remain, even in the other subfamilies, which are underrepresented in this type of study. For Neotropical pholcids, there are cytogenetics data published for only three native species, all of them belonging to the genus *Mesabolivar* González-Sponga, 1998 (see Araujo et al. 2017): *M. brasiliensis* (Moenkhaus, 1898), *M. cyaneotaeniatus* (Keyserling, 1891) and *M. luteus* (Keyserling, 1891). *Mesabolivar* is a highly species-rich genus with 64 described species and dozens of hitherto undescribed species available in museums, all of them exclusively found in South America (Huber 2015; World Spider Catalog 2017; L.S. Carvalho, pers. obs.). Previous chromosomal studies in the *Mesabolivar* species revealed $2n♂ = 17$, X0 and $2n♂ = 15$, X0, with meta/submetacentric chromosomes (Araujo et al. 2005a; Ramalho et al. 2008).

Here, we provide chromosomal data for five Neotropical pholcid species: three Modisiminae—*Mesabolivar spinulosus* (Mello-Leitão, 1939), *Mesabolivar togatus* (Keyserling, 1891) and *Carapoia* sp.—and two Pholcinae—*Micropholcus piaui* Huber, Carvalho & Benjamin, 2014 and *Micropholcus ubajara* Huber, Carvalho & Benjamin, 2014. The genus *Micropholcus* Deeleman-Reinhold & Prinsen, 1987 (Pholcinae) possesses 16 species, mainly from South America and the Caribbean region (Huber et al. 2014). The only species cytogenetically characterized of this genus is its type-species, the synanthropic pantropical *Micropholcus fauroti* (Simon, 1887), that exhibits $2n♂ = 17$, X0, and metacentric chromosomes in a Brazilian population (Araujo et al. 2005a). *Carapoia* González-Sponga, 1998 (Modisiminae) was never analyzed from the cytogenetic point of view.

METHODS

A total of 38 specimens from the Brazilian fauna were analyzed: 11 individuals (10♂ and 1♀) of *Mesabolivar spinulosus*, from Fazenda Bonito (05°14′S, 41°41′W), municipality of Castelo do Piauí, state of Piauí; two males of *Mesabolivar togatus*, from the municipality of Viçosa (20°45′14″S, 42°52′55″W), state of Minas Gerais; seven specimens (6♂ and 1♀) of an undescribed species of the genus *Carapoia*, from Parque Nacional de Ubajara (03°49′S, 40°59′W), municipality of Ubajara, state of Ceará; 14 topotype specimens of *Micropholcus piani* (10♂and 4♀), from Parque Municipal da Pedra do Castelo (05°12′S, 41°41′W), municipality of Castelo do Piauí, state of Piauí; and four topotype individuals (2♂ and 2♀) of *Micropholcus ubajara*, from Gruta do Morcego Branco, Parque Nacional de Ubajara (03°49′S, 40°59′W), municipality of Ubajara, state of Ceará. After the gonads extraction, the specimens were deposited at Laboratório Especial de Coleções Zoológicas, Instituto Butantan (IBSP, curator A.D. Brescovit), São Paulo, state of São Paulo, and Coleção de História Natural, da Universidade Federal do Piauí (CHNUFPI, curator E.F.B. Lima), Floriano, state of Piauí, Brazil. The collecting permit was issued by the Instituto Chico Mendes de Conservação da Biodiversidade – ICMBio, through the Sistema de Autorização e Informação em Biodiversidade – SISBIO (#39233-1).

The gonads were dissected out and processed for chromosomal preparations, according to Araujo et al. (2005b). The cells were photographed in an Olympus BX51 microscope, using the DP software, or in a Zeiss Axio Imager A2, using the Axio Vision software. In both cases, the total magnification was 1600x. The chromosomal morphology was identified following the proposal of Levan et al. (1964).

RESULTS

All five species analyzed here present a SCS of the X0/XX type, which was confirmed due to the difference of one chromosome between male and female mitotic metaphase cells (except in *Mesabolivar togatus*, in which females were not analyzed), presence of only one chromosomal univalent in male diplotene, and occurrence of the X chromosome in only one pole in metaphase II cells. In the five species, the X chromosome is the largest or nearly the largest element of the karyotype, and all chromosomes are biarmed.

Mitotic metaphase nuclei of *Mesabolivar spinulosus* possess 2n♂ = 17 and 2n♀ = 18 (Fig. 1A), and spermatogonia of *Mesabolivar togatus* has 2n♂ = 17 (Fig. 1B). Male diplotene nuclei of both species revealed eight autosomal bivalents with one or two interstitial or terminal chiasmata, and one sex univalent, which was easily recognized due to its length and configuration (Fig. 2A & B). Male metaphase II cells of two *Mesabolivar* species present n = 8 or n= 8 + X. The chromosome morphology of *M. spinulosus* is metacentric (pairs 1, 2, 4 and X), subtelocentric (pairs 3 and 8), and submetacentric (pairs 5, 6 and 7). *Mesabolivar togatus* presents chromosomes with metacentric (pairs 1, 3–6 and X) and submetacentric (2, 7 and 8) morphology (Fig. 1A & B).

Mitotic metaphase cells of *Carapoia* sp. reveal 2n♂ = 15 (Fig. 1C) and 2n♀ = 16. Male diplotene nuclei show seven autosomal bivalents with one or two terminal or interstitial chiasmata, and one sex univalent (Fig. 2C). Male metaphase II cells possess n = 7 or n= 7 + X (Fig. 2D). The chromosomal morphology is exclusively metacentric (Figs. 1C, 2D).

Mitotic metaphase cells of *Micropholcus piani* and *Micropholcus ubajara* (Pholcinae) present 2n♂ =9 (Fig. 1D & E) and 2n♀ = 10. Male diplotene/metaphase I nuclei showed four autosomal bivalents, with one terminal or interstitial chiasma in *M. piani*, and one or two terminal or interstitial chiasmata in *M. ubajara*. The sex chromosome is univalent, identified due to its positive heteropycnosis (Fig. 2E & F). In both species, male metaphase II nuclei reveal n = 4 or n= 4 + X (Fig. 2G & H). In these species, the chromosomal morphology is exclusively metacentric, except in the submetacentric pair 2 of *M. ubajara* (Fig. 1D & E).

DISCUSSION

The karyotype characteristics (X0 SCS, a large biarmed X chromosome, and biarmed autosomes) observed in the five species studied here are the most common among the Pholcidae (see Araujo et al. 2017). Within *Mesabolivar* (Modisiminae), the 2n♂ = 17, X0 was previously found in *M. brasiliensis* and *M. cyaneotaeniatus* (Ramalho et al. 2008). However, the Pholcidae molecular phylogenetic analyses carried out by Dimitrov et al. (2013) did not recover the monophyly of *Mesabolivar* representatives analyzed.

The phylogenetic position of *M. spinulosus* and *M. togatus* within *Mesabolivar* is unknown as these species were not included in the only available phylogenetic analysis of the Pholcidae (Dimitrov et al. 2013). However, these species, along with *M. brasiliensis, M. cyaneotaeniatus,* (all with 2n♂ = 17), and others, forms a group of *Mesabolivar* species with a "distinctively curved procursus", called "southern group" (Huber 2000). Moreover, these four species of *Mesabolivar* with 2n♂ = 17 present a mixture of meta/submeta/subtelocentrics, or at least meta/submetacentrics, while *M. luteus* presents exclusively metacentric chromosomes, reinforcing that this last species is not closely related to the species with 2n♂ = 17.

Carapoia is the second genus of Modisiminae chromosomally studied, and the results shown herein suggest a close phylogenetic relationship between *M. luteus* and *Carapoia* species based on the chromosome number and morphology. In fact, the generic allocation of *M. luteus* has a long history of uncertainty (see Huber 2000, 2005; Astrin et al. 2007), and the new chromosomal data corroborates the most recent molecular data (Dimitrov et al. 2013) and the female morphology (Huber 2000), pointing towards its position in the genus *Carapoia*.

Interestingly, within pholcids, the karyotype 2n♂ = 15, X0, such as herein observed in *Carapoia* sp., was previously found only in the modisimine *M. luteus* (Araujo et al. 2005a), and in representatives of the arteminae genus *Physocyclus* Simon, 1893 (Cokendolpher & Brown 1985; Cokendolpher 1989; Oliveira et al. 2007; Golding & Paliulis 2011). According to the phylogenetic hypothesis of Dimitrov et al. (2013), Arteminae and Modisiminae are sister clades, but the considerably lack of cytogenetic data prevents any further comparison.

The phylogenetic analysis of Huber et al. (2014) recovered the monophyly of *Micropholcus* species, but with some uncertain relationship between the South American clade,

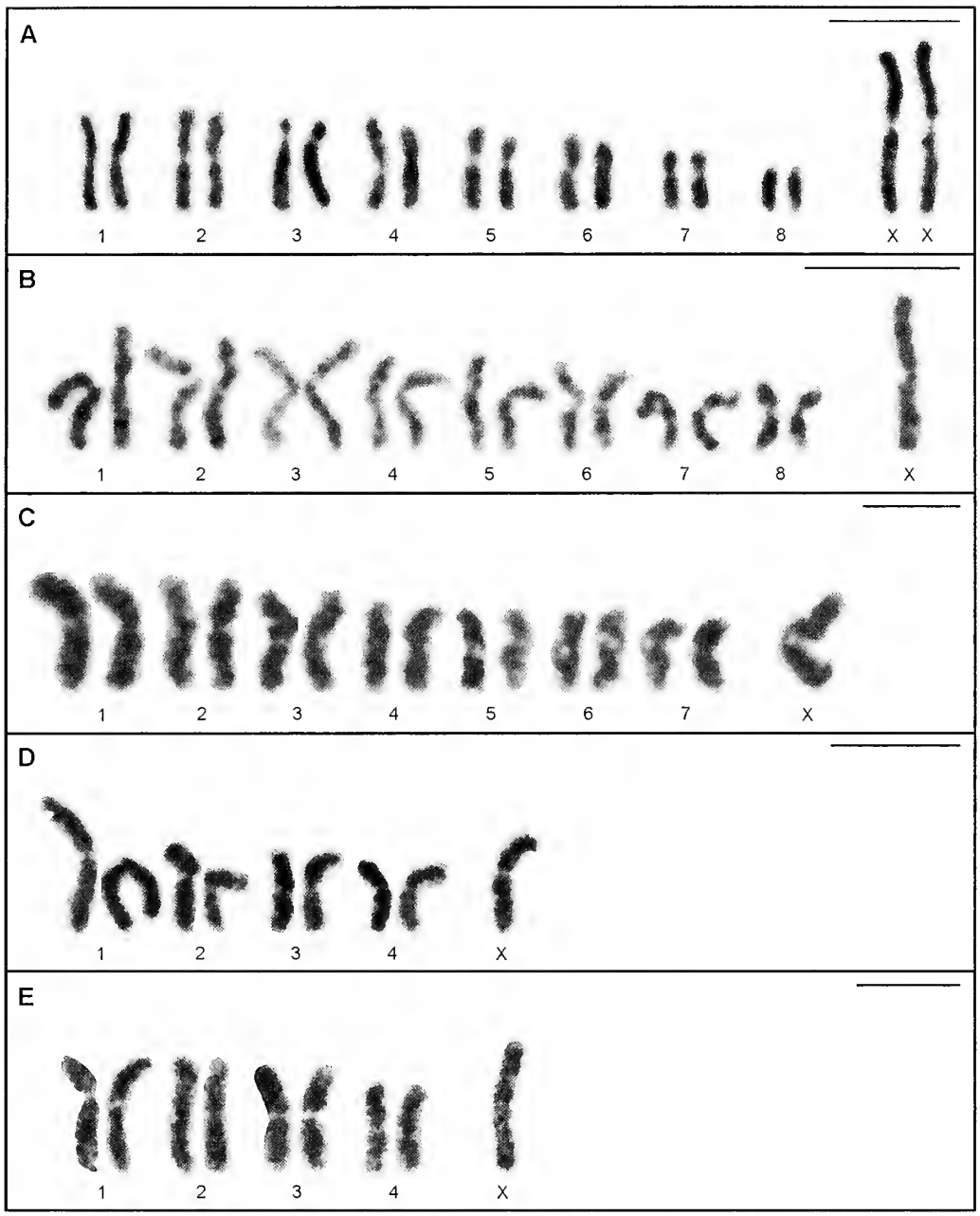

Figure 1.—Karyotypes of five pholcid species. A. *Mesabolivar spinulosus*, 2n♀ = 18, XX. B. *Mesabolivar togatus*, 2n♂ = 17, X0. C. *Carapoia* sp., 2n♂ = 15, X0. D–E. *Micropholcus piaui* and *Micropholcus ubajara*, respectively, 2n♂ = 9, X0. Scale bars = 10 μm.

the Caribbean clade and the *Micropholcus* type-species, the pantropical *M. fauroti*. The chromosomal data obtained in *M. piaui* and *M. ubajara* (2n♂ = 9, X0), both Brazilian species, strongly differ from that of *M. fauroti* (2n♂ = 17, X0) (Araujo et al. 2005a). Huber et al. (2014) placed the New World *Micropholcus* species in this genus mostly because they were not able to find any morphological synapomorphies that would have supported the establishment of a new genus. The lower diploid number observed in *M. piaui* and *M. ubajara* is the first morphological putative synapomorphy that would support a new genus including the New World *Micropholcus* species. Analyses of Caribbean *Micropholcus*, unknown from the cytogenetic point of view, reveals to be important to verify whether a low diploid number is also present in this clade of *Micropholcus*.

The number of autosomes in *M. piaui* and *M. ubajara* (eight) is exactly half of that found in *M. fauroti* (sixteen). Thus, one plausible hypothesis for the origin of the karyotype observed in *M. piaui* and *M. ubajara* is the occurrence of an "all or nothing" fusion event, in which all autosomes from the 2n♂ = 17 = 16 + X0 have fused with each other. This type of mechanism has been proposed to explain the origin of the karyotype of some spider species (Suzuki 1954; Rowell 1990; Stávale et al. 2011). As in all these *Micropholcus* the chromosomes are biarmed, it is possible that tandem fusions, instead of centric fusion, were implied in the process. This rearrangement was preceded or followed by pericentric

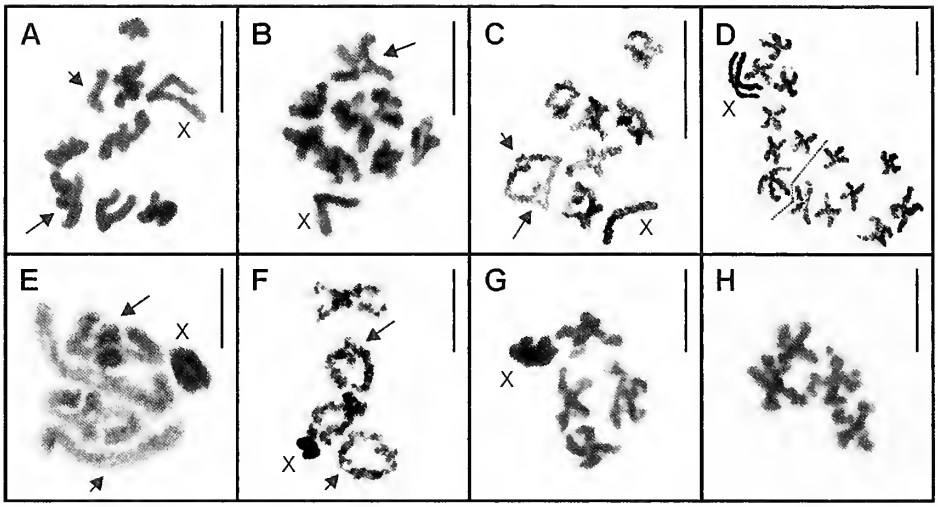

Figure 2.—Male meiotic cells of five pholcid species. A–B. Diplotene nuclei of *Mesabolivar spinulosus* and *Mesabolivar togatus*, respectively, with 8 autosomal bivalents and the X univalent. C. Diplotene of *Carapoia* sp., with 7 autosomal bivalents and one X univalent. D. Metaphase II cells of *Carapoia* sp., n = 7 + X (left pole) and n = 7 (right pole). E–F. Metaphase I and diplotene cells of *Micropholcus piaui* and *Micropholcus ubajara*, respectively, with 4 autosomal bivalents and the X univalent. G–H. Metaphase II nuclei of *Micropholcus piaui*, with n = 4 + X (G) and n = 4 (H). Long arrows = interstitial chiasma, short arrows = terminal chiasma. Scale bars = 10 μm.

inversions, in a way that keep both chromosome arms of each chromosome of similar sizes. The proposition that tandem fusions, instead of centric fusions, occurred in spiders that experienced a reduction in chromosome number and maintenance of chromosomal morphology was already postulated by Král et al. (2006), but referring to acrocentric karyotypes. In the case of *M. piaui* and *M. ubajara*, it is possible that the putative dicentric chromosomes, products of the fusion, undergo an inactivation of one centromere, a process already well documented in several organisms (Stimpson et al. 2012).

The 2n♂ = 9, observed in *M. piaui* and *M. ubajara* is the lowest diploid number recorded for spiders with monocentric chromosomes. Low diploid numbers are found in *Ariadna lateralis* (Segestriidae) and *Dasumia carpatica* (2n♂ = 7), *Dysdera crocata* C.L Koch, 1838 (2n♂ = 8) (Dysderidae), and *Ariadna bosenbergi* Keyserling, 1877 (2n♀ = 8) (Suzuki 1950, 1954; Diaz et al. 2010; Kořínková & Král 2013), however, these species possess holocentric chromosomes.

In conclusion, the present cytogenetical data support a separate evolutionary position of *Mesabolivar luteus* in relation to the remaining *Mesabolivar* representatives and show that, within the Pholcidae, the 2n♂ = 15, X0 is present only in the sister subfamilies Modisiminae and Arteminae. Moreover, we could show the lowest diploid number in spiders with monocentric chromosomes, 2n = 9. Thus, our findings raise questions on the evolution of the low diploid number in the genus *Micropholcus*, requiring further investigation in Caribbean species or hitherto undescribed Old World species.

ACKNOWLEDGMENTS

This work is part of LSC's Ph.D. thesis and part of the Programa de Pesquisas em Biodiversidade do Semiárido (CNPq 558317/2009-0 and 457471/2012-3). This research was supported by Fundação de Amparo à Pesquisa do Estado de São Paulo, FAPESP (2011/21643-1 and 2012/10679-8). We are grateful to Bernhard A. Huber and anonymous referees for their critical reading of the manuscript.

LITERATURE CITED

Araujo, D., A.D. Brescovit, C.A. Rheims & D.M. Cella. 2005a. Chromosomal data of two pholcids (Araneae, Haplogynae): a new diploid number and the first cytogenetical record for the new world clade. Journal of Arachnology 33:591–596.

Araujo, D., D.M. Cella & A.D. Brescovit. 2005b. Cytogenetic analysis of the neotropical spider *Nephilengys cruentata* (Araneomorphae, Tetragnathidae): standard staining, NORs, C-bands and base-specific fluorochromes. Brazilian Journal of Biology 65:193–202.

Araujo, D., M.C. Schneider, E. Paula-Neto & D.M. Cella. 2017. The spider cytogenetic database. Version 5.5. Online at www.arthropodacytogenetics.bio.br/spiderdatabase.

Astrin, J.J., B. Misof & B.A. Huber. 2007. The pitfalls of exaggeration: molecular and morphological evidence suggests *Kaliana* is a synonym of *Mesabolivar* (Araneae: Pholcidae). Zootaxa 1646:17–30.

Cokendolpher, J.C. 1989. Karyotypes of three spider species (Araneae: Pholcidae: *Physocyclus*). Journal of the New York Entomological Society 97:475–478.

Cokendolpher, J. C. & J.D. Brown. 1985. Air-dry method for studying chromosomes of insects and arachnids. Entomological News 96:114–118.

Diaz, M.O., R. Maynard & N. Brum-Zorrilla. 2010. Diffuse centromere and chromosome polymorphism in haplogyne spiders of the families Dysderidae and Segestriidae. Cytogenetic and Genome Research 128:131–138.

Dimitrov, D., J.J. Astrin & B.A. Huber. 2013. Pholcid spider molecular systematics revisited, with new insights into the biogeography and the evolution of the group. Cladistics 29:132–146.

Golding, A.E. & L.V. Paliulis. 2011. Karyotype, sex determination, and meiotic chromosome behavior of two pholcid (Araneomorphae, Pholcidae) spiders: implications for karyotype evolution. PLoS One 6:1–4.

Huber, B.A. 2000. New World pholcid spiders (Araneae: Pholcidae):

a revision at generic level. Bulletin of the American Museum of Natural History 254:1–348.

Huber, B.A. 2005. Revision and cladistic analysis of the spider genus *Carapoia* González-Sponga (Araneae:Pholcidae), with descriptions of new species from Brazil's Atlantic forest. Invertebrate Systematics 19:541–556.

Huber, B.A. 2011. Phylogeny and classification of Pholcidae (Araneae): an update. Journal of Arachnology 39:211–222.

Huber, B.A. 2015. Small scale endemism in Brazil's Atlantic Forest: 14 new species of *Mesabolivar* (Araneae, Pholcidae), each known from a single locality. Zootaxa 3942:1–60.

Huber, B.A., L.S. Carvalho & S.P. Benjamin. 2014. On the New World spiders previously misplaced in *Leptopholcus*: molecular and morphological analyses and descriptions of four new species (Araneae: Pholcidae). Invertebrate Systematics 28:432–450.

Kořínková, T. & J. Král. 2013. Karyotypes, sex chromosomes, and meiotic division in spiders. Pp. 159–171. *In* Spider Ecophysiology (W. Nentwig, ed.). Springer-Verlag, Heidelberg.

Král, J., J. Musilová, F. Štáhlavský, M. Rezác, Z. Akan, R.L. Edwards et al. 2006. Evolution of the karyotype and sex chromosome systems in basal clades of araneomorph spiders (Araneae: Araneomorphae). Chromosome Research 14:859–880.

Král, J., T. Kořínková, L. Krkavcová, J. Musilová, M. Forman, I.M. Ávila Herrera et al. 2013. Evolution of karyotype, sex chromosomes, and meiosis in mygalomorph spiders (Araneae: Mygalomorphae). Biological Journal of the Linnean Society 109:377–408.

Levan, A.K., K. Fredga & A.A. Sandberg. 1964. Nomenclature for centromeric position on chromosomes. Hereditas 52:201–220.

Oliveira, R.M., A.C. Jesus, A.D. Brescovit & D.M. Cella. 2007. Chromosomes of *Crossopriza lyoni* (Blackwall 1867), intraindividual numerical chromosome variation in *Physocyclus globosus* (Taczanowski 1874), and the distribution pattern of NORs (Araneomorphae, Haplogynae, Pholcidae). Journal of Arachnology 35:293–306.

Ramalho, M.O., D. Araujo, M.C. Schneider, A.D. Brescovit & D.M. Cella. 2008. *Mesabolivar brasiliensis* (Moenkhaus 1898) and *Mesabolivar cyaneotaeniatus* (Keyserling 1891) (Araneomorphae, Pholcidae): close relationship reinforced by cytogenetic analyses. Journal of Arachnology 36:453–456.

Rowell, D.M. 1990. Fixed fusion heterozygosity in *Deleua cancerides* Walck. (Araneae: Sparassidae): an alternative to speciation by monobrachial fusion. Genetica 80:139–157.

Stávale, L.M., M.C. Schneider, A.D. Brescovit & D.M. Cella. 2011. Chromosomal characteristics and karyotype evolution of Oxyopidae spiders (Araneae, Entelegynae). Genetics and Molecular Research 10:752–763.

Stimpson, K.M., J.E. Matheny & B.A. Sullivan. 2012. Dicentric chromosomes: unique models to study centromere function and inactivation. Chromosome Research 20:595–605.

Suzuki, S. 1950. Spiders with extremely low and high chromosome numbers. Japanese Journal of Genetics 25:221–222.

Suzuki, S. 1954. Cytological studies in spiders. III. Studies on the chromosomes of fifty-seven species of spiders belonging to seventeen families, with general considerations on chromosomal evolution. Journal of Science of the Hiroshima University, Series B, Division 1 15:23–136.

World Spider Catalog. 2017. World Spider Catalog. Version 18.0. Natural History Museum, Bern. Available online at http://wsc.nmbe.ch/

Manuscript received 5 May 2017, revised 6 October 2017.

2018. Journal of Arachnology 46:50–61

Ontogenetic differences and interspecific variation in the tarsal aggregate pores on leg IV of cosmetid harvestmen (Opiliones: Laniatores)

Victor R. Townsend Jr. and **Trevor J. Maloney**: Department of Biology, Virginia Wesleyan University, 5817 Wesleyan Drive, Virginia Beach, VA 23545 USA; E-mail: vtownsend@vwu.edu

Abstract. Morphological studies of harvestmen usually investigate the structures of adults, seldom including data regarding ontogenetic differences in the microanatomy of the appendages. In gonyleptoidean harvestmen, adults have clusters of pores on the distal-most tarsomeres of legs III and IV that are known as tarsal aggregate pores (TAPs). In gonyleptid harvestmen, these pores occur on the prolateral and retrolateral surfaces as groups adjacent to the tarsal claws. In this study, we used scanning electron microscopy (SEM) to compare the microanatomy of the TAPs occurring on leg IV of adults and antepenultimate nymphs for three common species of Neotropical cosmetid harvestmen, nymphs of an additional seven cosmetid morphospecies, and adults and antepenultimate nymphs of three species of gonyleptoidean harvestmen. The distal tarsomere of leg IV of adult cosmetid harvestmen features two pairs of aggregate pores including dorsal TAPs and ventrolateral vTAPs. The TAPs of cosmetid nymphs have denticulate borders and are not closely associated with trichomes. We observed interspecific variation among cosmetid harvestmen with respect to the number of pores composing the TAPs. The TAPs on the prolateral and retrolateral surfaces occur in similar positions and are generally symmetrical with respect to overall shape and the number of pores. The functional significance of the TAPs and vTAPs of cosmetid harvestmen will require additional empirical evaluation.

Keywords: Glands, Gonyleptoidea, microanatomy, nymph, setae

With more than 700 described species (Medrano & Kury 2016), the Cosmetidae Koch, 1839 represents the third largest family in the order Opiliones, and the second most diverse group in the suborder Laniatores and superfamily Gonyleptoidea (Sharma & Giribet 2011; Pinto-da-Rocha et al. 2012; Giribet & Sharma 2014). Species of cosmetid harvestmen are found from the southern U.S. to Argentina, with the greatest diversity occurring in the forested habitats of Mexico, Central America and northern South America (Kury & Pinto-da-Rocha 2007). The adults of most species are easily differentiated from other gonyleptoideans by the morphology of the pedipalps, which feature flattened femora and patellae and spoon-shaped tibiae (Kury & Pinto-da-Rocha 2007; Pinto-da-Rocha & Hara 2011). In nymphs, these same podomeres are

Table 1.—Comparison of the TAPs and vTAPs of antepenultimate nymphs and adults of gonyleptoidean harvestmen examined in the present study. CR = Costa Rica

	TAP		vTAP	
Species	No. Pores	Type of Border	No. Pores	Type of Border
Cosmetidae				
Cynortula granulata, nymph	7–9	Denticulate	Absent	n/a
Cynortula granulata, adult	8–11	Smooth	4–5	Smooth
Erginulus clavotibialis, nymph	10–13	Denticulate	Absent	n/a
Erginulus clavotibialis, adult	13–15	Smooth	13–14	Smooth
Paecilaema inglei, nymph	7–9	Denticulate	Absent	n/a
Paecilaema inglei, adult	9–11	Smooth	3–4	Smooth
Morphospecies 1 (Belize), nymph	8–9	Denticulate	Absent	n/a
Morphospecies 2 (Belize), nymph	8–10	Denticulate	Absent	n/a
Morphospecies 3 (Belize), nymph	6–8	Smooth	Absent	n/a
Morphospecies 4 (CR), nymph	7–9	Denticulate	Absent	n/a
Morphospecies 5 (CR), nymph	6–9	Smooth	Absent	n/a
Morphospecies 6 (CR), nymph	6–9	Denticulate	Absent	n/a
Morphospecies 7 (CR), nymph	9–12	Smooth	Absent	n/a
Ampycidae				
Glysterus sp., nymph	14–16	Smooth	Absent	n/a
Glysterus sp., adult	13–16	Smooth	3–4	Smooth
Manaosbiidae				
Cranellus montgomeryi, nymph	3–5	Smooth	Absent	n/a
Cranellus montgomeryi, adult	6–9	Smooth	3–4	Smooth
Stygnidae				
Stygnoplus clavotibialis, nymph	10–14	Denticulate	Absent	n/a
Stygnoplus clavotibialis, adult	6–8	Smooth	14–15	Smooth

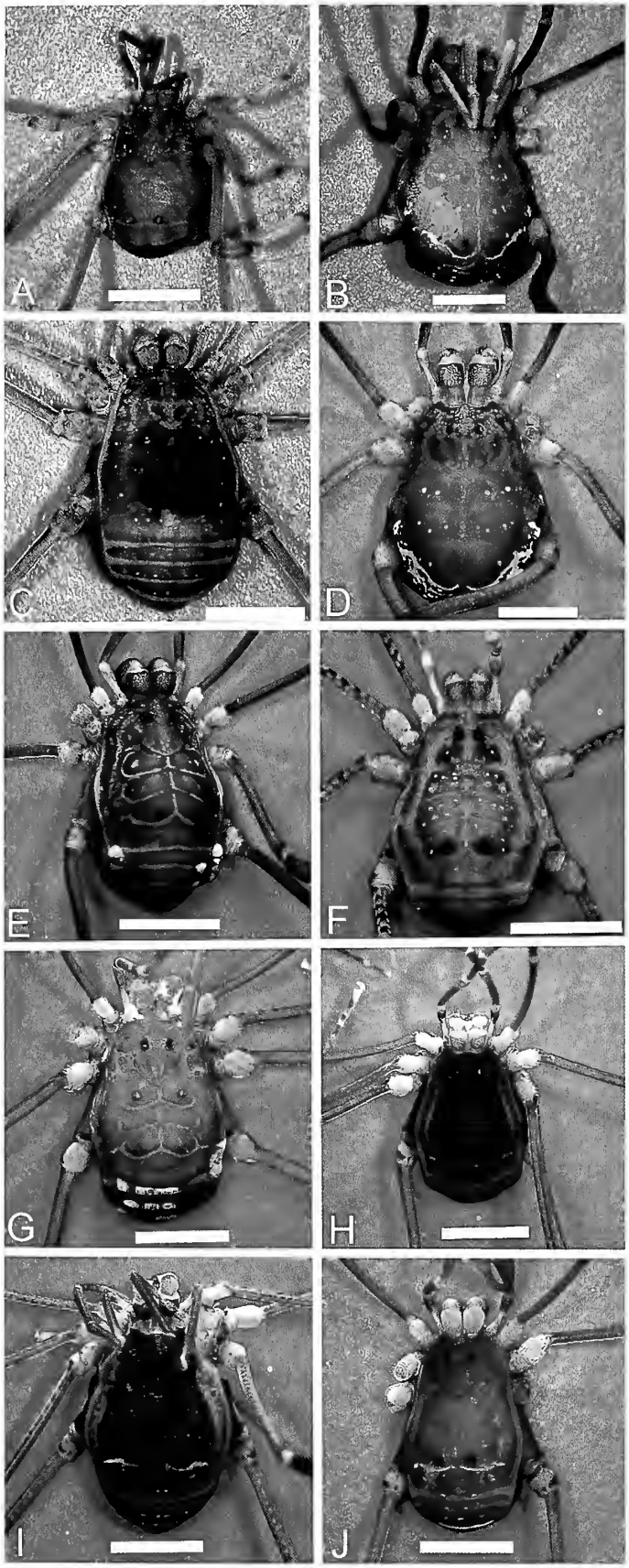

Figure 1.—Light micrographs of the dorsal habitus of cosmetid nymphs (antepenultimates) including (A) *Cynortula granulata*, (B) *Erginulus clavotibialis*, (C) *Paecilaema inglei*, (D–F) morphospecies 1–3 from Bladen Reserve, Belize, and (G-J) morphospecies 4–7 from La Selva Biological Station, Costa Rica. Scale bar = 2 mm.

cylindrical, rather than laterally compressed (Juberthie 1972; Goodnight & Goodnight 1976). The tarsus of the pedipalp of the adult is adorned with a flexible, sclerotized claw, whereas that of the nymph has a slender, elongate pretarsus with a ventral patch of setae (Wolff et al. 2016).

The life history of harvestmen includes three distinct postembryonic stages: larva, nymph (multiple instars) and adult (reviewed by Gnaspini 2007). Although postembryonic development of relatively few species have been studied, cosmetid harvestmen have been observed to have six nymphal instars before the final molt to adulthood (Juberthie 1972; Goodnight & Goodnight 1976). Different ages of nymphs may be distinguished on the basis of body size, the morphology of the pedipalps, and the presence of an arolium (sac-like structure) and pseudonychium (small cuticular process ventral to the arolium) on tarsus III and IV (Muñoz Cuevas 1971). In gonyleptoidean harvestmen, the secondary sexual characteristics of males begin to appear during the antepenultimate nymph (Muñoz Cuevas 1971; Gnaspini 1995; Townsend et al. 2009). The penultimate nymph is distinguished by the absence of the pseudonychium and arolium and the genitalia are not fully formed and functional (Muñoz Cuevas 1971). Temperature affects the rate of growth and it appears to take 4–7 months from hatching for individuals to reach the terminal molt to adulthood (Juberthie 1972; Goodnight & Goodnight 1976; Cokendolpher & Jones 1991). Under captive conditions, adult cosmetid harvestmen have been observed to live 2–3 years (Juberthie 1972; Cokendolpher & Jones 1991).

Relatively little is known about the morphological changes that occur during postembryonic development in cosmetid harvestmen. Like other gonyleptoideans, adult cosmetid harvestmen have clusters of pores with distinct, often sculptured, borders on the distal tarsal segments of legs III and IV that are known as tarsal aggregate pores, or TAPs (Gainett et al. 2014; Rodriguez & Townsend 2015). The TAPs occur as pairs on the dorso-lateral region proximal to the tarsal process, with one cluster on the retrolateral surface and another on the prolateral surface (Willemart et al. 2007, 2009; Ramin et al. 2016). These groups of pores occur in close association with the bases of multiple trichomes (Gainett et al. 2014; Rodriguez & Townsend 2015; Ramin et al. 2016). The TAPs appear to have consistent locations on the surfaces of the distal most tarsomeres of legs III–IV, occurring in the areas bounded by three dorsal setae, termed the S0-S1-S3 triangle (Gainett et al. 2014; Ramin et al. 2016).

In gonyleptoidean harvestmen, the morphology of the TAPs is very similar between tarsi III and IV and does not differ markedly between the prolateral and retrolateral surfaces (Gainett et al. 2014; Ramin et al. 2016). The TAPs of adults are believed to be glandular (Willemart et al. 2007; Gainett et al. 2014; Ramin et al. 2016). The biological role of TAPs has been hypothesized to be that of marking the substrate, with the chemical secretions serving as an aid in navigation (Willemart et al. 2007).

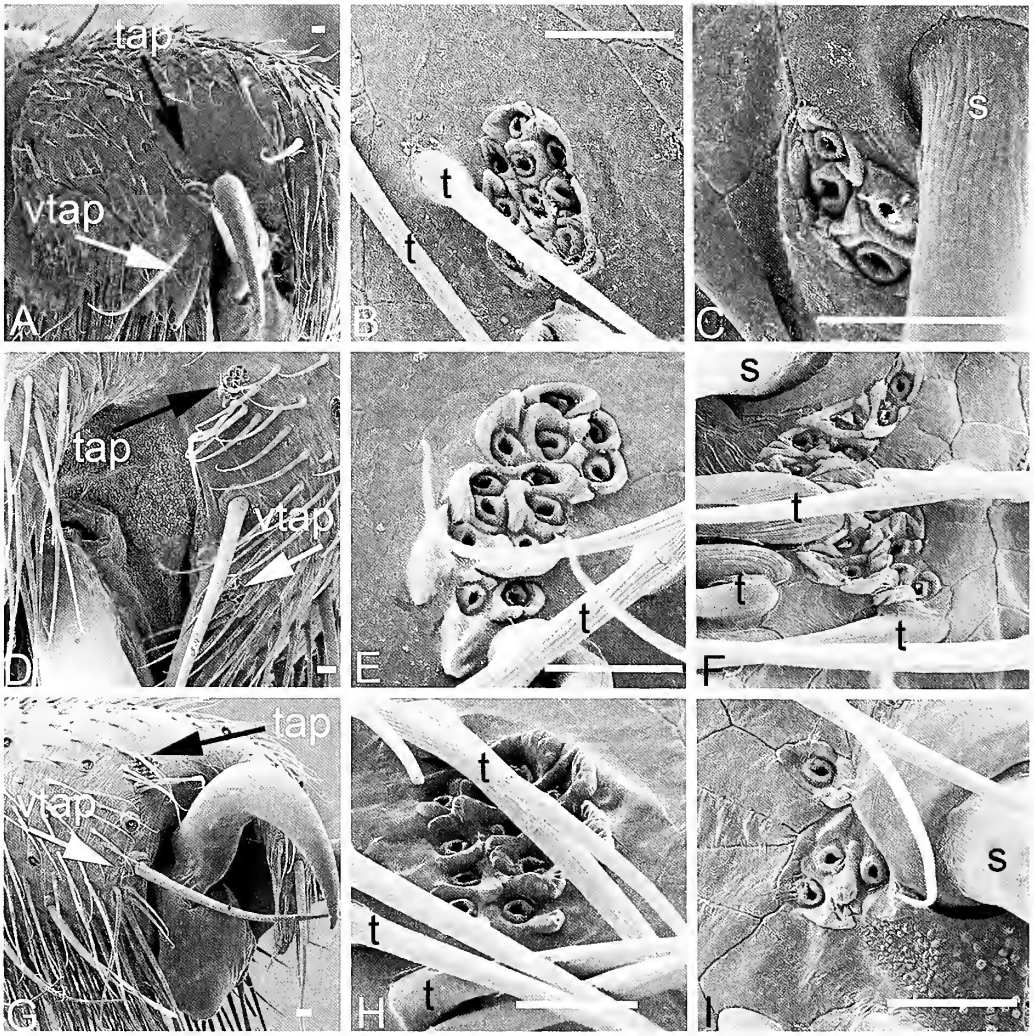

Figure 2.—SEM micrographs of the tarsal aggregate pores (TAPs) and ventral tarsal aggregate pores (vTAPs) on the distal segment of tarsus IV of adult cosmetid harvestmen. (A–C) *Cynortula granulata*: (A) tip of tarsus IV, frontal lateral view. (B) Morphology of the TAP. (C) Morphology of the vTAP. (D–F) *Erginulus clavotibialis*: (D) tip of tarsus IV, frontal view. (E) Morphology of the TAP. (F) Morphology of the vTAP. (G–I) *Paecilaema inglei*: (G) tip of tarsus, lateral view. (H) morphology of the TAP. (I) morphology of the vTAP (I). Scale bar = 10 μm. s = sensillum chaeticum; t = trichome, te = tarsal claw.

While no sexual dimorphism has been observed in the microanatomy of the TAPs (Gainett et al. 2014; Ramin et al. 2016), ontogenetic variation in the distribution and composition of the TAPs has recently been reported for the gonyleptid harvestman *Heteromitobates albiscriptus* (Mello-Leitão, 1932) (Ramin et al. 2016). In this species, TAPs are absent from the tarsi of the first nymph. Beginning in the second nymph, the numbers of pores that constitute the TAPs increase with age (Ramin et al. 2016). Adult *H. albiscriptus* also have two distinct types of TAPs, one pair that are dorsal to the tarsal claws and another pair that are lateral to the tarsal claws and are known as vTAPs (Ramin et al. 2016). Like the more dorsal TAPs, the vTAPs are associated with trichomes and occur in a consistent location, inferior to the dorsal seta known as S2 (Ramin et al. 2016). The vTAPs have only been observed on tarsi III and IV of adults and are not known to occur on the tarsi of nymphs (Ramin et al. 2016). In adult *H. albiscriptus*, there are usually fewer pores associated with the vTAP than with the more dorsal TAP (Ramin et al. 2016). The occurrence of vTAPs in other gonyleptoidean taxa, including the Cosmetidae, has not been investigated.

In this study, we used scanning electron microscopy (SEM) to examine ontogenetic differences in TAPs among cosmetid harvestmen by comparing the morphology of these clusters on tarsi IV of antepenultimate nymphs with those of adults. Specifically, we compared the tarsal morphology of adults and nymphs for the cosmetid harvestmen *Cynortula granulata* Roewer 1912, *Erginulus clavotibialis* (Pickard-Cambridge, 1905) and *Paecilaema inglei* Goodnight & Goodnight, 1947 and those of adults and nymphs for *Cranellus montgomeryi* Goodnight & Goodnight, 1947 (Manaosbiidae), *Glysterus* sp. (Ampycidae) and *Stygnoplus clavotibialis* (Goodnight & Goodnight, 1947) (Stygnidae). For comparative purposes, we also surveyed the morphology of the TAPs on tarsi IV for seven morphospecies of cosmetid nymphs collected from field sites in Belize and Costa Rica.

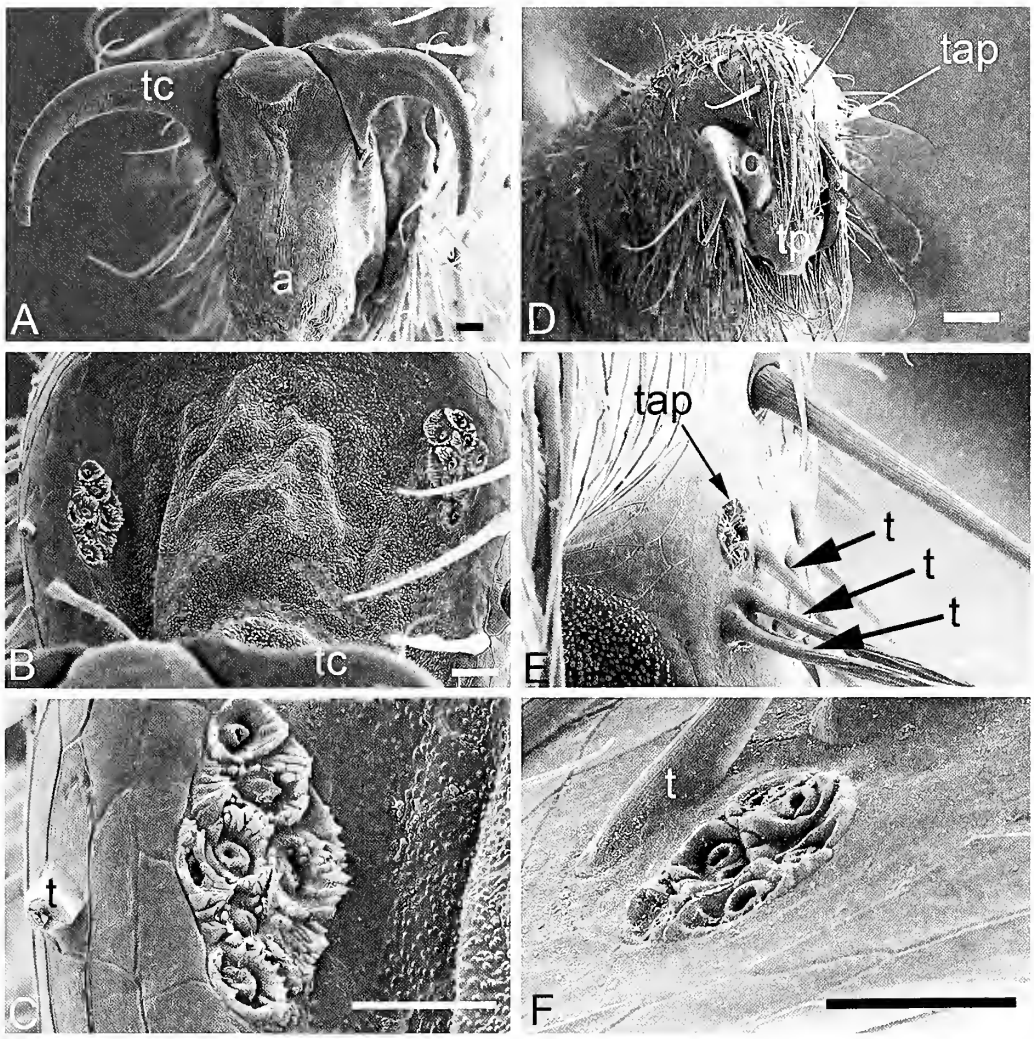

Figure 3.—SEM micrographs of tarsal aggregate pores (TAPs) on tarsus IV of penultimate nymph (A–C) and adult (D–F) *Cynortula granulata* (Cosmetidae). (A) Arolium and tarsal claws, frontal view. (B) Slightly asymmetrical TAPs (shape only) on prolateral and retrolateral surfaces. (C) Surface features of TAP; note sculpturing of borders separating pores. (D) Tarsus with broken claw, tarsal process and TAP, frontal view. (E) TAP with adjacent trichomes. (F) Surface features of TAP; note the reduced sculpturing on the borders surrounding each of pores. Scale bars = 60 μm for D; 10 μm for A–C, E; 5 μm for F. a = arolium, t = trichome, tc = tarsal claws, tp = tarsal process.

METHODS

Owing to ontogenetic variation in the coloration of the body and legs, armature of the dorsal scutum, pedipalps and legs, tarsal morphology and genitalia (present only in adults), it can be challenging to identify to genus or species, the nymphs of laniatorean harvestmen (Townsend et al. 2009), especially from samples collected in Neotropical forests with considerable biodiversity (e.g., the forests at the La Selva Biological Station in Costa Rica are home to 19 species of cosmetid harvestmen: Proud et al. 2012). In this study, we examined the microanatomy of tarsus IV for multiple nymphs (n = 3–6 individuals) and adults (n = 2–3 males and females) of *Cynortula granulata*, *Erginulus clavotibialis*, and *Paecilaema inglei*. Adults and nymphs of these species were previously collected for examination in other studies (Townsend et al. 2008; Walker & Townsend 2014; Townsend et al. 2017). The specimens of *C. granulata* and *P. inglei* were captured by hand in 2005–2007 from forested habitats in the northern and central ranges of Trinidad, West Indies (see Townsend et al. 2008 for specific locations). Adults and nymphs of *Erginulus clavotibialis* were collected from beneath logs and rocks at Clarissa Falls, Cayo District, Belize (17.116° N, 89.120° W; datum: WGS84) in 2012 (Schaus et al. 2013; Townsend et al. 2017). In addition, we examined tarsus IV for multiple individuals (n = 2–5 specimens) of three morphospecies of cosmetid nymphs (Fig. 1D–F) collected by hand from the leaf litter Bladen Reserve, Toledo District, Belize (16°29′60″ N, 88°53′9.6″ W, datum WGS84) in July 2012, and four morphospecies of cosmetid nymphs (Fig. 1G–J) that were captured from leaf litter and vegetation at La Selva Biological Station, Heredia Province, Costa Rica (10°27′20″ N, 84°0′20″ W, datum: WGS84) from 11–24 August 2015. These nymphs were similar in body size to the three known cosmetid species (Fig. 1A–C), but differed from them and each other with respect to dorsal coloration and body shape (Fig. 1D–J). We believe that they represent different species, rather than different instars of nymphs for a single species. However, in

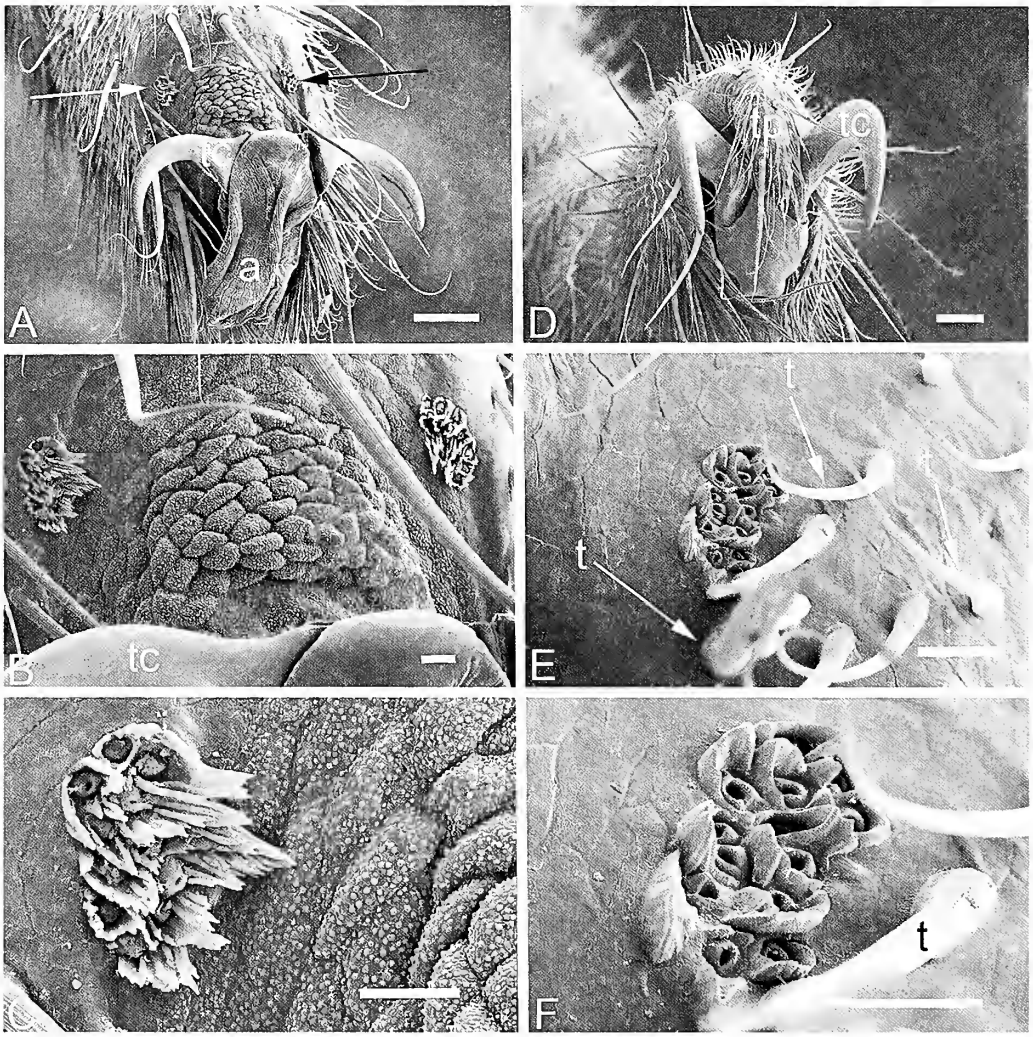

Figure 4.—SEM micrographs of tarsal aggregate pores (TAPs) on tarsus IV of antepenultimate nymph (A–C) and adult (D–F) *Erginulus clavotibialis* (Cosmetidae). (A) Arolium, tarsal claws and TAP (arrows), dorso-frontal view. (B) Asymmetrical TAPs on prolateral and retrolateral surfaces. (C) Surface features of TAP; note morphology of the borders of the pores. (D) Tarsal claws and tarsal process, frontal view. (E) TAP with adjacent trichomes. (F) Surface features of TAP; note increased number of pores and reduction in the size of the borders surrounding the pores. Scale bars = 60 μm for A, D; 15 μm for D–E; 10 μm for C, F. a = arolium, t = trichome, tc = tarsal claws, tp = tarsal process.

the absence of adult characters, we were unable to identify them to species or genus.

Specimens of *Glysterus* sp. were captured by hand from cover objects and from the leaf litter at the La Selva Biological Station, Heredia Province, Costa Rica (10°27′20″ N, 84°0′20″ W, datum: WGS84) in July 2010. Adults and nymphs of *Cranellus montgomeryi* and *Stygnoplus clavotibialis* were collected from Trinidad, West Indies in 2008 (data for specific locations is provided in Rodriguez et al. 2014).

On the basis of their relative body size, dorsal coloration, and the presence of a prominent arolium and pseudonychium on tarsus III and IV (Muñoz Cuevas 1971), we inferred that the cosmetid nymphs that we examined were likely antepenultimate, 5th instars (Fig. 1). Similarly, tarsus III and IV of the nymphs of the non-cosmetid taxa each had a prominent arolium and a well-developed pseudonychium. The degree of their dorsal coloration and relative body size were consistent with 4th or 5th instar nymphs (assuming these species have six nymphal instars, as there are no published postembryonic studies for these taxa). Prior to the removal of leg IV, we photographed nymphs and adults with a Leica EZ4 D stereomicroscope. These images were subsequently processed with Leica Application Suite (LAS) software, version 3.2.1 and Adobe Photoshop CS4 extended software, version 11.0.2.

The right and left tarsi of leg IV of each harvestman were examined by SEM following the process described in Townsend et al. (2009) and Rodriguez et al. (2014). Each leg was removed and ultrasonicated for 1–2 min prior to dehydration. The legs were chemically dried with hexamethyldisilazane (Nation 1983). We dissected each leg at the metatarsus-tibia joint and mounted the distal segments vertically on aluminum stubs with the distal tips of the tarsi visible. The specimens were sputter-coated with 15–30 nm of gold and photographed at accelerating voltages of 5–15 kV with the Hitachi S-3400N SEM on the campus of Virginia Wesleyan College. Unless noted in the figure legend, all SEM micrographs depict the

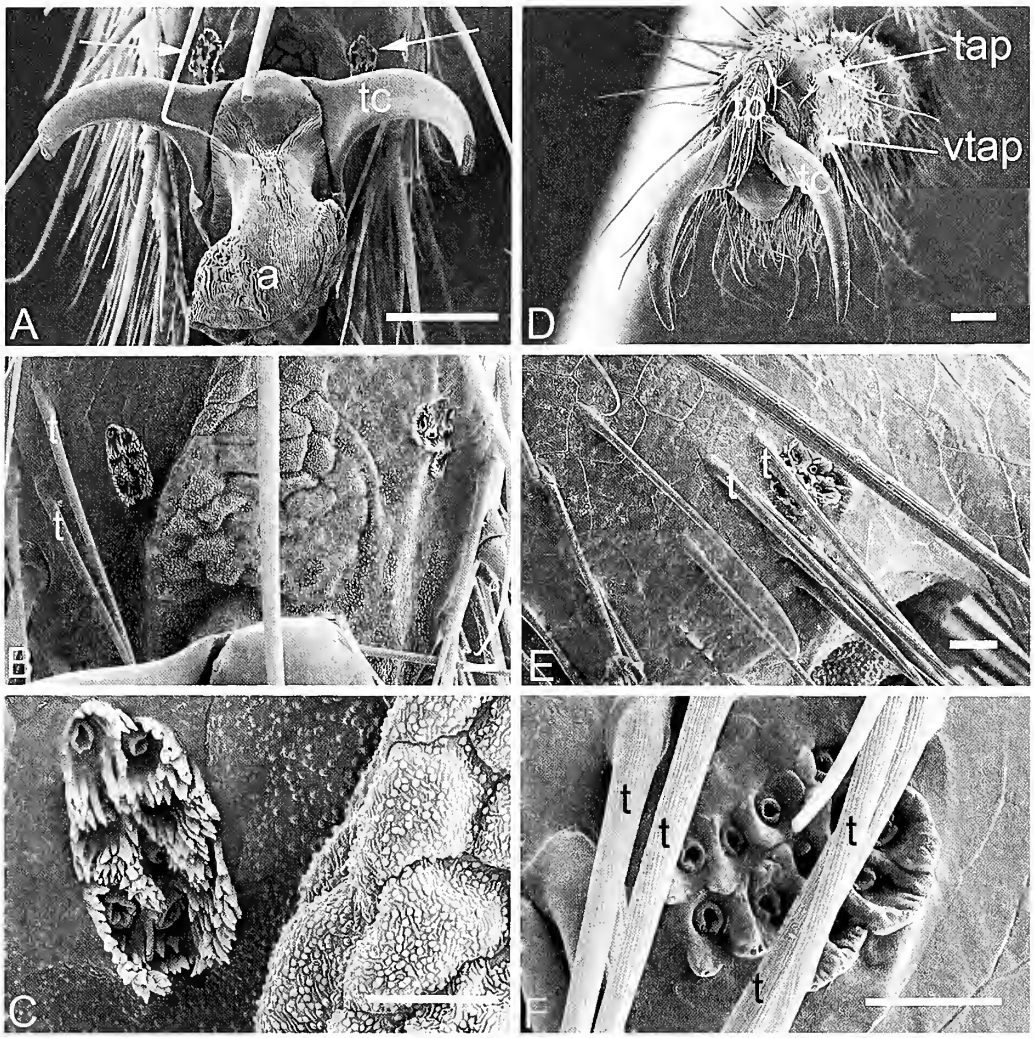

Figure 5.—SEM micrographs of tarsal aggregate pores (TAPs) on tarsus IV of antepenultimate nymph (A–C) and adult (D–F) *Paecilaema inglei* (Cosmetidae). (A) Arolium, tarsal claws and TAPs (arrows), frontal view. (B) Asymmetrical TAPs on prolateral and retrolateral surfaces and their proximity to trichomes. (C) Surface features of TAP; note the texture of the borders of the pores. (D) Tarsal claws, tarsal process, TAP and vTap, frontal view. (E) TAP with adjacent trichomes. (F) Surface features of TAP, note increase in the number of pores and change in the texture of the borders surrounding the pores. Scale bars = 60 μm for A, D; 10 μm for B–C, E–F. a = arolium, t = trichome, tc = tarsal claws, tp = tarsal process.

morphology of the right tarsus. Following the methods of Ramin et al. (2016), we attempted to provide reasonable estimates regarding the numbers of visible pores that comprise the TAPs (and vTAPs) when possible. Owing to the presence of trichomes and sensilla chaetica, we were not always able to view the complete surface of the TAPs, thus our meristic data may slightly under represent the actual number of pores present (Table 1).

Voucher specimens will be deposited into the collections of the American Museum of Natural History (AMNH) and the Universidad de Costa Rica.

RESULTS

TAPs and vTAPs among cosmetid harvestmen.—Adult cosmetid harvestmen have paired TAPs and vTAPs on the distal tarsomere of leg IV (Fig. 2). In *Cynortula granulata* and *Paecialema inglei*, there was a considerable difference in the number of pores between the TAPs and vTAPs (Table 1). In *Erginulus clavotibialis*, we observed a similar number of pores (13–15) present in both clusters. The TAPs of *Cynortula granulata* (Fig. 2A–C) had 8–11 pores (Fig. 2B) and vTAPs had 4–5 pores (Fig. 2C). The TAPs of *Erginulus clavotibialis* (Fig. 2D-F) featured 13–15 pores (Fig. 2E) and the vTAPs had 13–14 pores (Fig. 2F). In *Paecilaema inglei* (Fig. 2G–I), the TAPs were composed of 9–11 pores (Fig. 2H), and there were 3–4 pores associated with vTAPs (Fig. 2I). We observed no striking differences between retrolateral and prolateral clusters with respect to the number of pores constituting the TAPs and vTAPs (Figs. 4B, 5B, 6B). Similarly, we did not observe intersexual variation in the distribution or morphology of the TAPs or vTAPs in the three cosmetid species that we examined.

Ontogenetic variation in TAPs and vTAPS among cosmetid harvestmen.—Tarsus IV of the antepenultimate cosmetid nymph has an arolium (Figs. 3A, 4A, 5A) and pseudonychium between the tarsal claws, whereas tarsus IV of the adult has a

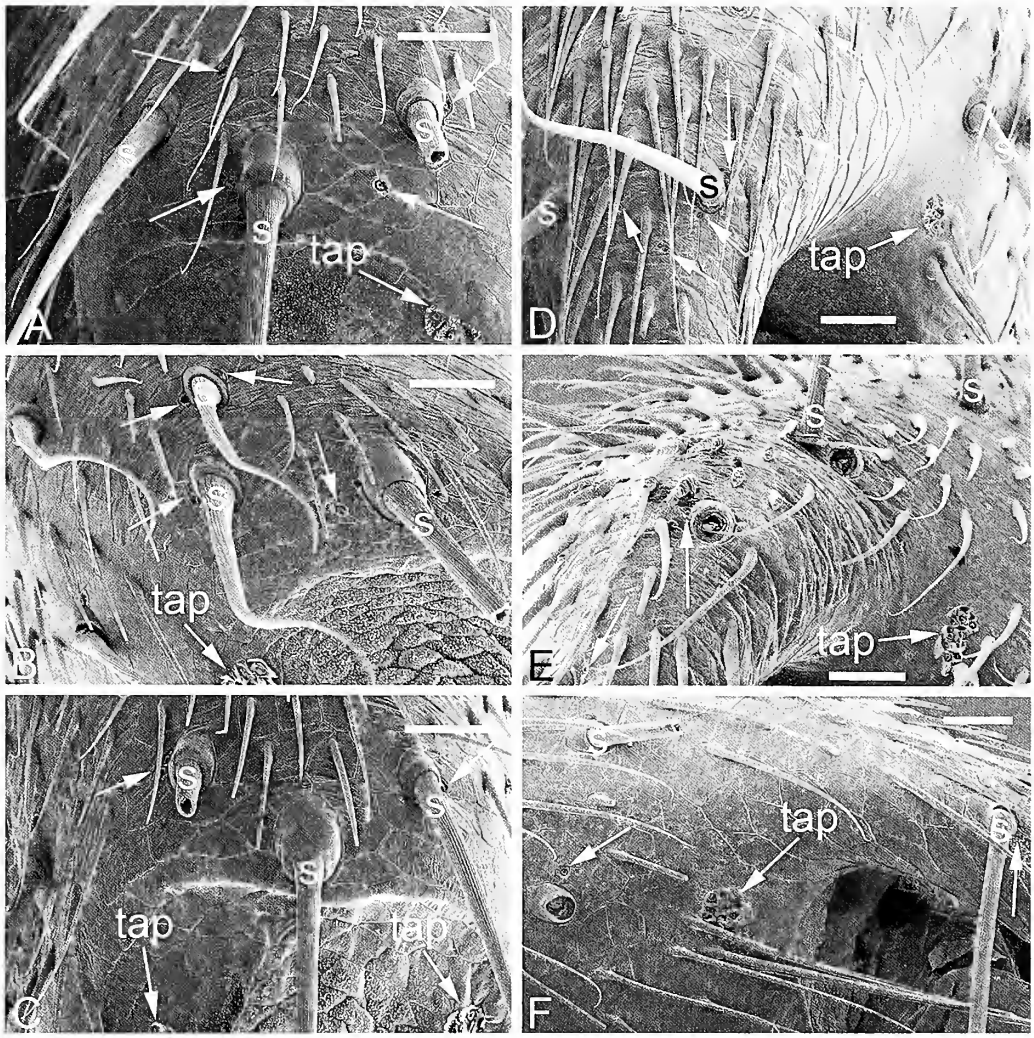

Figure 6.—SEM micrographs of the dorsal surfaces of tarsi IV revealing distribution of the simple pores (arrows), sensilla chaetica (s) and the tarsal aggregated pores (TAPs) on antepenultimate nymph (A-C) and adult (D-F) cosmetid harvestman. *Cynortula granulata*, nymph (A) and adult (D). *Ergiuulus clavotibialis*, nymph (B) and adult (E). *Paecilaema inglei*, nymph (C) and adult (F) Scale bars = 25 μm.

process that originates on the dorsal surface and projects inferiorly between the tarsal claws (Figs. 3D, 4D, 5D). The distal tarsomeres of nymphs feature TAPs on both the prolateral and retrolateral surfaces (Figs. 3–5). In contrast to adults (Fig. 2), vTAPs are absent from the tarsi of nymphs (Table 1). The TAPs of nymphs (Figs. 3B, 4B, 5B) are also not closely associated with the bases of trichomes as they are in the adults (Figs. 3E, F, 4E, F, 5E, F). The pores composing the TAPs of nymphs have sculptured borders (Figs. 3C, 4C, 5C), whereas the borders of the pores of adults (Figs. 3F, 4F, 5F) are much smoother, lacking the irregular, scalloped edges present in nymphs.

Occurrence of single tarsal pores among cosmetid harvestmen.—In addition to the presence of TAPs, we also compared the distribution and morphology of single pores on the distal surfaces of tarsi IV for nymphs and adults of all three species of cosmetid harvestmen (Fig. 6). These pores resemble those found in TAPs and vTAPs with respect to their relative size and the presence of a distinct border. However, in contrast to TAPs and vTAPs, the borders of the single pores were only slightly elevated (Fig. 6A, F) with respect to the surrounding surface of the cuticle and were generally smooth (and not scalloped or denticulate). We found that single pores were most frequently associated with the sensilla chaetica on the dorsal surfaces of the tarsi of nymphs (Fig. 6A–C) and the sensilla chaetica and tarsal processes of adults (Fig. 6D–F). We did not observe any ontogenetic differences between nymphs (Fig. 6A–C) and adults (Fig. 6D–F) with respect to the numbers or distribution of single pores.

Interspecific variation in TAPs among nymphs of cosmetid harvestmen.—We examined the distal tarsomeres of leg IV for seven distinct morphospecies of cosmetid nymphs (Fig. 1D–J), including three morphospecies from Belize (Fig. 7) and four additional morphospecies from Costa Rica (Fig. 8). Individuals of each of these cosmetid harvestmen had TAPs on the prolateral and retrolateral surfaces (Figs. 7A, C, 8A, C, G) that were generally symmetrical in appearance. The TAPs of these nymphs had 6-12 pores in each cluster (Table 1). There was considerable interspecific variation with regards to the sculpturing of the elevated borders surrounding the pores (Figs. 7B, D, F, 8B, D, F, H). In several species (Figs. 7B, D, 8B), the borders had a complex texture of ridges giving the

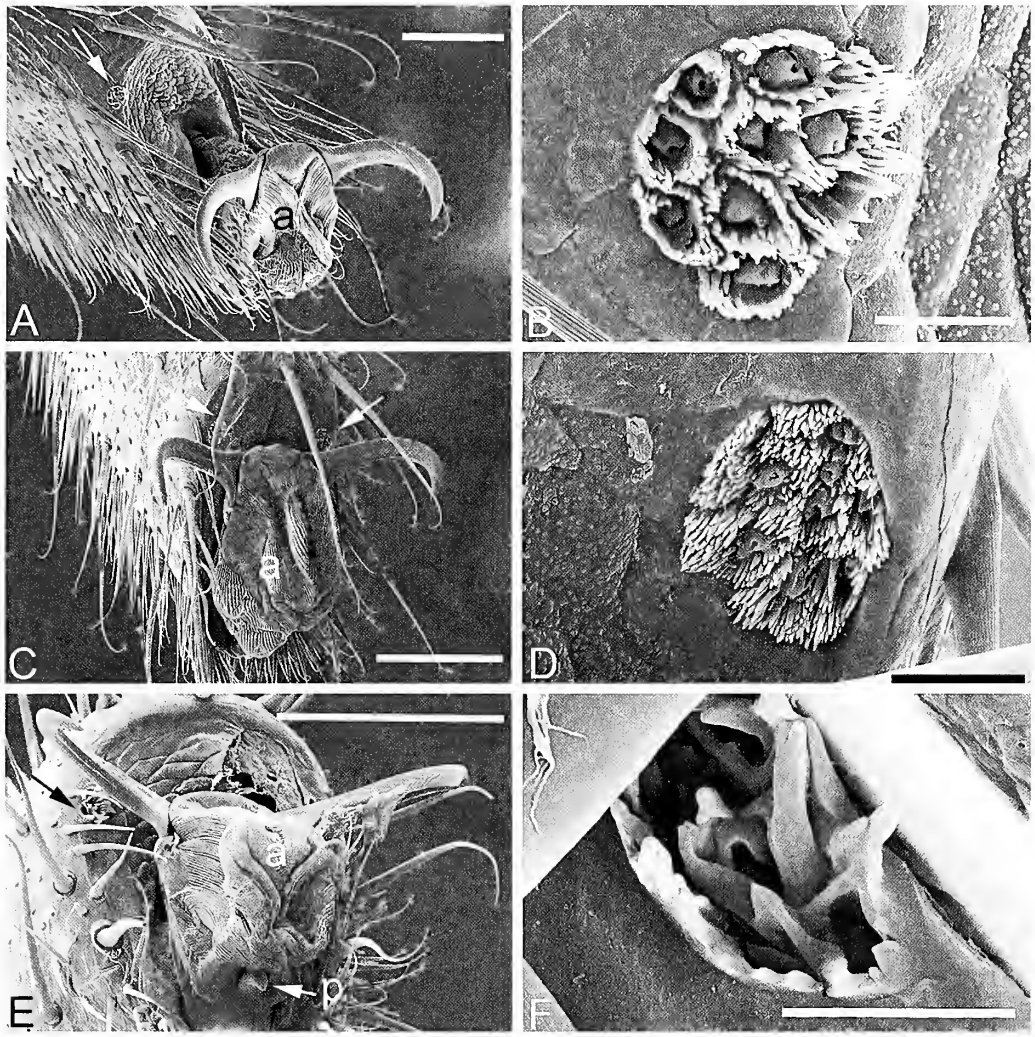

Figure 7.—SEM micrographs of arolium (a) and tarsal aggregate pores (TAPs) on tarsus IV of three morphospecies of cosmetid nymphs from Bladen Reserve, Belize. (A–B) Morphospecies 1: (A) arolium (a), distal tip of tarsus and TAP (arrow), latero-dorsal frontal view. (B) surface features of TAP. (C–D) Morphospecies 2: (C) distal tip of tarsus, frontal view. (D) TAP. (E–F) Morphospecies 3: (E) distal tip of tarsus, arolium, pseudonychium (p), ventro-frontal view. (F) TAP. Scale bars = 100 μm for A, C, E and 10 μm for B, D, F.

TAP a denticulate appearance. In other morphospecies, the borders around the pores were relatively smooth and less irregular (Figs. 7F, 8D, H).

Ontogenetic and interspecific variation in TAPs, single tarsal pores and vTAPs among Gonyleptoidea.—Tarsus IV of the nymphs and adults of *Cranellus montgomeryi* (Manaosbiidae), *Glysterus* sp. (Ampycidae), and *Stygnoplus clavotibialis* (Stygnidae) all had TAPs and single pores, but only those of adults had vTAPs (Figs. 9–11). Single tarsal pores occurred on the dorsal surface of the tarsi of nymphs and were usually associated with the bases of the sockets of large sensilla chaetica (Figs. 9B, C, 10B, 11B). In adults, single tarsal pores were also associated with the bases of large sensilla chaetica (Figs. 9F, 10F) or they occurred near the bases of trichomes on the tarsal process (Fig. 11F). We observed fewer pores in association with the TAPs of nymphs (Fig. 9D) than with those of adults (Fig. 9G) in *C. montgomeryi* (Table 1), but only a slight ontogenetic difference in pore numbers for TAPs between nymphs (Figs. 10D, 11D) and adults (Figs. 10G, 11G) in *Glysterus* sp. and *S. clavotibialis* (Table 1). In *C. montgomeryi* and *Glysterus* sp., there were only 3–4 pores present in the vTAPs (Figs. 9H, 10H), whereas in *S. clavotibialis*, there were 14–15 pores comprising the vTAPs (Fig. 11H). In addition, we found no ontogenetic difference in the morphology of the elevated borders that surrounded the pores between the nymphs (Figs. 9D, 10D) and adults (Figs. 9G, 10G) of *C. montgomeryi* and *Glysterus* sp. The TAPs of the nymphs and adults of *Glysterus* sp. (Figs. 10C, G) as well as those of adult *C. montgomeryi* (Fig. 9G) were associated with the bases of trichomes, whereas those of the nymphs of *C. montgomeryi* were not (Fig. 9C, D). In *S. clavotibialis*, the TAPs were partially obscured by the tarsal process (Fig. 11E) owing to a more medial position of the TAPs than in other gonyleptoidean taxa. This location may have led us to undercount the number of pores associated with the TAP as this was the only species that we examined in which we observed more pores in the TAPs of the nymph than in the adult (Table 1). In this species, there was also an ontogenetic difference in the sculpturing of the elevated borders surrounding the pores of the TAPs (Fig. 11C-H). In the nymphs (Fig.

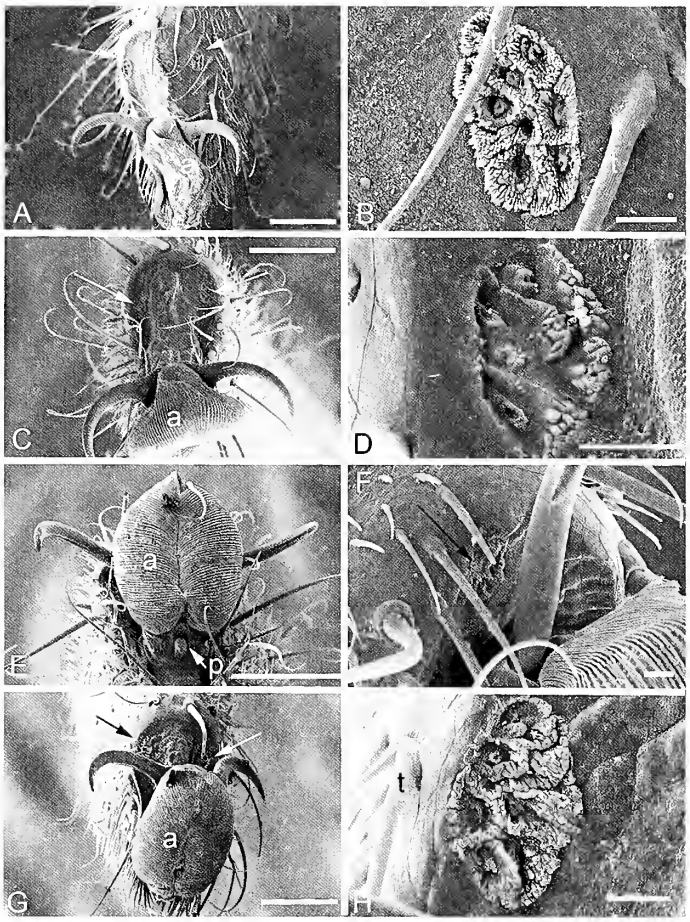

Figure 8.—SEM micrographs of arolium (a) and tarsal aggregate pores (TAPs) on tarsus IV of four morphospecies of cosmetid nymphs from La Selva Station, Costa Rica. (A B) Morphospecies 4: (A) arolium, distal tip of tarsus and position of retrolateral and prolateral TAPs (arrows), frontal view. (B) Surface features of TAP. (C D) Morphospecies 5: (C) arolium, distal tip of tarsus and position of retrolateral and prolateral TAPs (arrows), frontal view. (D) Surface features of TAP. (E F) Morphospecies 6: (E) arolium and pseudonychium (p), ventro-frontal view. (F) TAP (arrow). (G H) Morphospecies 7: (G) arolium, distal tip of tarsus and position of retrolateral and prolateral TAPs, frontal view. (H) Surface features of TAP. Scale bars = 100 μm for A, C, E, G; 10 μm for B, D, F, H.

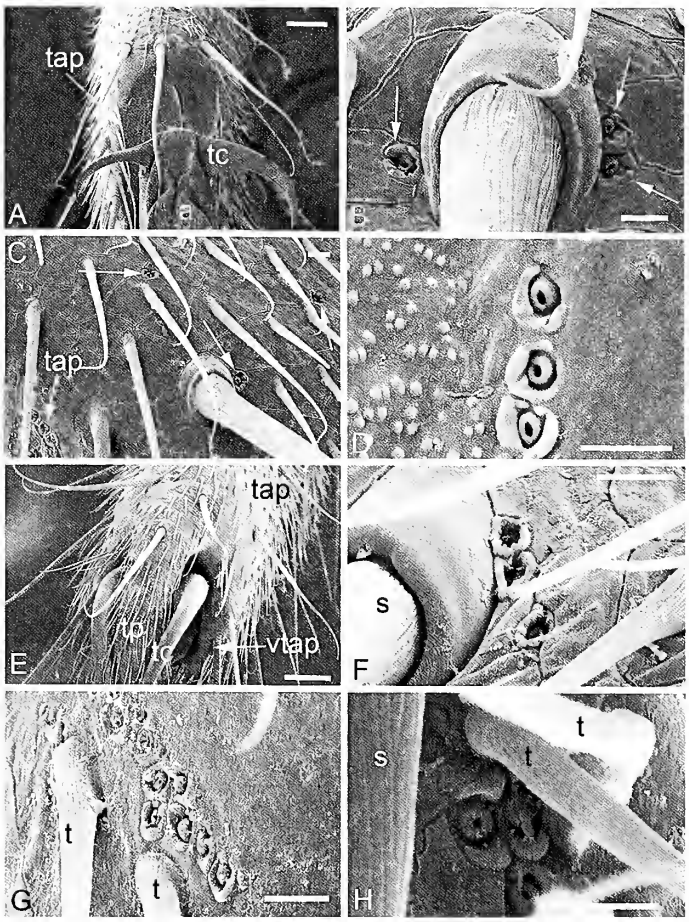

Figure 9.—SEM micrographs of tarsal aggregate pores (TAPs) on tarsus IV of nymph (A D) and adult (E H) of *Cranellus montgomeryi*. (A) Arolium and tarsal claws on the distal tip of tarsus, frontal view. (B) Simple pores (arrows) associated with sensillum chaeticum. (C) Trichomes, sensillum chaeticum, simple pores (arrows) and TAP. (D) Surface features of TAP. (E) Tarsal claws, tarsal process, TAP and vTAP, latero-frontal view. (F) Pores associated with sensillum chaeticum on tarsal process. (G) Surface features of TAP and associated trichomes. (H) Surface features of vTAP. Scale bars = 50 μm for A, E; 5 μm for B D, F H. a = arolium, s = sensillum chaeticum, t = trichome, tc = tarsal claws, tp = tarsal process.

11C, D), the borders were larger and more pointed than those of the adults (Fig. 11G).

We observed no differences between retrolateral and prolateral clusters with respect to the number of pores constituting the TAPs and vTAPs in nymphs and adults of all three non-cosmetid species. Similarly, we did not observe any intersexual differences in the distribution or morphology of the TAPs or vTAPs in these three gonyleptoidean species.

DISCUSSION

Comparative studies of sensory structures (Willemart et al. 2009), pedipalps (Wolff et al. 2016), metatarsal and tarsal sensilla (Gainett et al. 2014, 2017), tegumental glands (Willemart et al. 2010; Proud & Felgenhauer 2011, 2013), ozopores (Gnaspini & Rodrigues 2011), penises (Kury & Villarreal 2015; Kury 2016), and ovipositors (Martens et al. 1981; Walker & Townsend 2014; Townsend et al. 2015; Brooks et al. 2017) have either provided considerable new insights into the natural history of harvestmen or identified novel and informative characters for phylogenetic studies. Among harvestmen, the occurrences of metatarsal paired slits, a proximal tarsomeric gland and tarsal aggregate pores (TAPs) were recognized as diagnostic synapomorphies for the suborder Laniatores (Willemart et al. 2009; Gainett et al. 2014). Recently, Ramin et al. (2016) reported ontogenetic variation in TAPs for the gonyleptid harvestman *Heteromitobates albiscriptus* and also described a new cluster of tarsal pores, the vTAP, which occurs in the adult, but not the nymph. In addition to the Gonyleptidae, our results indicate the vTAPs occur in harvestmen that are members of the families Ampycidae, Cosmetidae, Manaosbiidae and Stygnidae and that vTAPs are also lacking in nymphs of the species that we surveyed. Additional phylogenetic surveys of other gonyleptoidean harvestmen are needed to determine if the

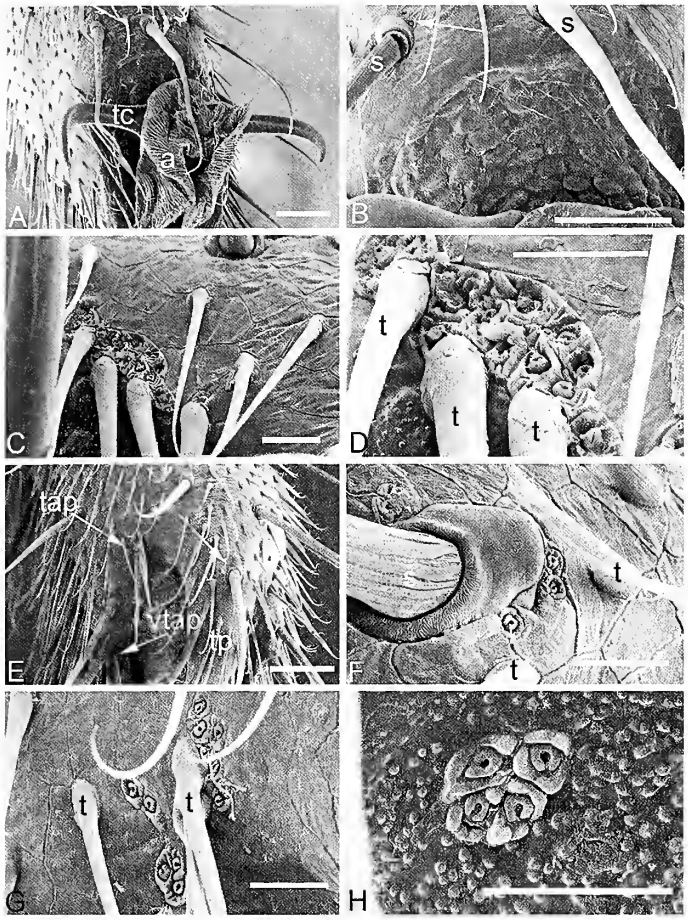

Figure 10.—SEM micrographs of tarsal aggregate pores (TAPs) on tarsus IV of nymph (A–D) and adult (E–H) of *Glysterus* sp. (A) Arolium and tarsal claws on the distal tip of tarsus, latero-frontal view. (B) Simple pores (arrows) associated with sensilla chaetica. (C) Trichomes associated with TAP. (D) Surface features of TAP and associated trichomes. (E) Tarsal claws and tarsal process, dorso-frontal view (F) Pores associated with sensillum chaeticum on tarsal process. (G) Surface features of TAP. (H) Surfaces features of vTAP (ventral tarsal aggregate pores). Scale bars = 50 μm for A, B, E; 10 μm for C–D, F–H. a = arolium, s = sensillum chaeticum, t = trichome, tc = tarsal claws, tp = tarsal process.

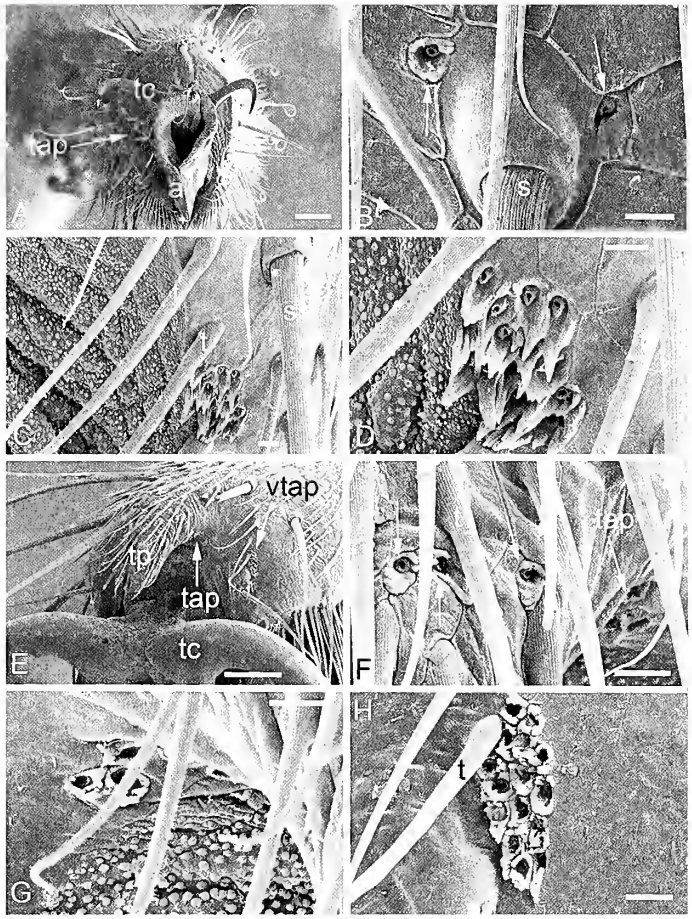

Figure 11.—SEM micrographs of tarsal aggregate pores (TAPs) on tarsus IV of nymph (A–D and adult (E–H) of *Stygnoplus clavotibialis*. (A) Arolium and tarsal claws on the distal tip of tarsus, frontal view. (B) Simple pores (arrows) associated with sensillum chaeticum. (C) Trichomes associated with TAP and ventral tarsal aggregate pores (vTAP). (D) Surface features of TAP. (E) Tarsal claws, tarsal process, TAP and vTAP, dorso-frontal view. (F) Simple pores (arrows) associated with sensilla chaetica on tarsal process. (G) Surface features of TAP. (H) Surface features of vTAP. Scale bars = 50 μm for A, E; 5 μm for B–D, F–H. a = arolium, s = sensillum chaeticum, t = trichome, tc = tarsal claws, tp = tarsal process.

morphology and occurrence of vTAPs are informative characters like TAPS as well as if these clusters of pores only occur in adults of other harvestmen.

The results presented by Ramin et al. (2016) also raise interesting questions concerning the sensory ecology, functional morphology and natural history of the nymphs of harvestmen, highlighting the current paucity of knowledge concerning the biology of this important life history stage. In our study, we observed considerable interspecific and ontogenetic variation in the morphology of the tarsal pores (TAPs and vTAPs) among nymphs and adults of cosmetid harvestmen. As with nymphs of the gonyleptid harvestman *Heteromitobates albiscriptus* (Ramin et al. 2016), cosmetid nymphs lack vTAPS and each TAP has fewer pores than in conspecific adults. In the nymphs of several species, the pores comprising each TAP were generally separated by elevated borders that were denticulate or featured irregular scalloped edges. In contrast, cosmetid adults have a TAP and vTAP on both the prolateral and retrolateral surfaces. The TAPs and vTAPs of cosmetid harvestmen generally occur in the same anatomical locations and are associated with the same setae (S0-S1-S3 and S2, respectively) as those reported for the gonyleptid harvestmen, *H. albiscriptus* (Ramin et al. 2016). As in *H. albiscriptus*, we did not observe any striking asymmetries between tarsal surfaces nor did we observe sexual dimorphism. With the exception of *Erginulus clavotibialis*, there were more pores in the TAP (13–15) than in the vTAP (3–5). The borders of the pores of the TAPs of adults were reduced in prominence and much smoother than those of the nymphs. The functional significance of this ontogenetic difference is not clear, however, this type of variation was not observed for the TAPs of the gonyleptid *H. albiscriptus* (Ramin et al. 2016) or for those of the ampycid *Glysterus* sp. (Table 1) or the manaosbiid *Cranellus montgomeryi* (Table 1). In addition, we also discovered ontogenetic variation with respect to the association of TAPs with trichomes. In adult cosmetid

harvestmen, the TAPs and vTAPs were situated near the bases of multiple trichomes, however, in nymphs, there were no setae in close proximity to the TAPs.

Gainett et al. (2014) reported the widespread occurrence of TAPs among harvestmen in the superfamily Gonyleptoidea. The results of our study indicate that vTAPs may also be common among these harvestmen. In addition to their occurrence in cosmetid harvestmen, we also observed vTAPs on tarsus IV of adults for the ampycid *Glysterus* sp., the manaosbiid *C. montgomeryi* and the stygnid *Stygnoplus clavotibialis*. In *Glysterus* and *C. montgomeryi*, there were more pores in the TAPs than in the vTAPs. However, in *S. clavotibialis*, the vTAPs were more developed and had a much larger number of pores (comparable to those in the TAPs). In *S. clavotibialis*, the pores of the TAPs had elevated, denticulate borders in the nymph that were much shorter in the adult (similar to the pattern that we observed in cosmetid species). In *Glysterus* and *C. montgomeryi*, there was only a subtle difference in the morphology of the border of the pores in the TAPs of nymphs and adults. As with the cosmetid taxa that we observed, the TAPs of nymphs also had fewer pores than those of adults. Unfortunately, our survey featured only 10 species of cosmetid harvestmen and did not include penultimate nymphs, so we are unable to comment on the morphology of the TAPs of these instars. In the gonyleptid *H. albiscriptus*, penultimate nymphs no longer have an arolium or pseudonychium on tarsi III or IV, but also lack vTAPs on their tarsi (Ramin et al. 2016). Additional studies are needed to determine if the same ontogenetic pattern is present in cosmetid harvestmen and other laniatorean taxa.

In addition to clusters of pores (TAPs and vTAPs), we also observed the occurrence of single tarsal pores on the leg IV of all of the gonyleptoidean harvestmen that we surveyed including cosmetid and non-cosmetid taxa and nymphs and adults stages. The morphology of these pores resembles those comprising the TAPs and vTAPs, especially with respect to relative size and the presence of a well-developed, slightly elevated border. We also found that single tarsal pores occurred in close proximity to the sockets and bases of sensilla chaetica and trichomes in both nymphs and adults. The functional significance of these pores is unclear as is the relative contributions of the various tarsal glands of the nymph (single pores and TAPs) and adult (single pores, TAPs and vTAPs) to the chemical marking ability of individuals. Additional studies similar to those of Proud & Felgenhauer (2011, 2013) and Wolff et al. (2016) are needed to investigate the ultrastructure of the tarsal glands on legs III and IV and chemical composition of their secretions, respectively.

There is relatively little published data as to the functional significance of the tarsal glands on legs III and IV of gonyleptoidean harvestmen. Adults have been hypothesized to use glandular secretions to mark the substrate, thereby permitting more efficient navigation through the environment (Ramin et al. 2016). Recent studies have revealed that harvestmen have olfactory setae on the tarsi of leg I–IV (Gainett et al. 2017) and may use chemical cues in conspecific interactions (Willemart & Hebets 2012; Fernandes & Willemart 2014; Murayama & Willemart 2015). Additional ecological experiments are needed to assess how adults and nymphs employ their tarsal glands in the environment and to determine if there is any relationship between ontogenetic differences in the morphology of the tarsal glands and the behavior of nymphs and adults.

ACKNOWLEDGMENTS

We thank Stephen Broadbridge (Caribbean Discovery Tours, Trinidad), Azucena Galvez (Clarissa Falls, Belize), Ronald Vargas and Bernal Matarrita (La Selva Biological Station), Maynard Schaus, Nathaniel Schaus, Ashley Borgard, Sarah Locke, Jeffrey Illinik, and Cynthia Richardson for assistance with logistics and field collections. We thank Justin Bloom, Duncan Miller, Bruce Enzmann, and Mayanni McCourty for help with preparing and photographing samples. Our study was supported by VWC Summer Faculty Development Grant (VRT), a Virginia Foundation of Independent Colleges Mednick Fellowship (VRT) and the VWC Scanning Electron Microscopy Laboratory. Specimens from Costa Rica were collected under scientific passport no. 05953 (VRT) and legally exported in 2008 and 2010. Harvestman from Belize were collected and exported under permit number #CD/60/3/12 (1) from the Belize Ministry of Forestry. The specimens from Trinidad were legally collected and exported under permit numbers 000541 (to VRT in 2005), 001284 (to Daniel Proud in 2006), 001131 (to VRT in 2007), and 001339 (to VRT in 2008) from the Forestry Division of the Ministry of Agriculture, Land and Marine Resources of Trinidad and Tobago. We will deposit voucher specimens in the collections of the Universidad de Costa Rica and AMNH.

LITERATURE CITED

Brooks, E.A., V.R. Townsend, Jr., E.A. Allen & M.A. Tuthill. 2017. Interspecific variation in ovipositor morphology among manaosbiid and nomoclastid harvestmen (Arachnida, Opiliones, Laniatores). Acta Zoologica 98:56–65.

Cokendolpher, J.C. & S.R. Jones. 1991. Karyotype and notes on the male reproductive system and natural history of the harvestman *Vonones sayi* (Simon) (Opiliones, Cosmetidae). Proceedings of the Entomological Society of Washington 93:86–91.

Fernandes, N.S. & R.H. Willemart. 2014. Neotropical harvestmen (Arachnida, Opiliones) use sexually dimorphic glands to spread chemicals in the environment. Comptes Rendus Biologies 337:269–275.

Gainett, G., P. Michalik, C.H.G. Müller, G. Giribet, G. Talarico & R.H. Willemart. 2017. Ultrastructure of chemoreceptive tarsal sensilla in an armored harvestman and evidence of olfaction across Laniatores (Arachnida, Opiliones). Arthropod Structure and Development 46:178–195.

Gainett, G., P.P. Sharma, R. Pinto-da-Rocha, G. Giribet & R.H. Willemart. 2014. Walk it off: Predictive power of appendicular characters toward inference of higher level relationships in Laniatores (Arachnida: Opiliones). Cladistics 30:120–138.

Giribet, G. & P.P. Sharma. 2014. Evolutionary biology of harvestmen (Arachnida, Opiliones). Annual Review of Entomology 60:157–175.

Gnaspini, P. 1995. Reproduction and postembryonic development of *Goniosoma spelaeum*, a cavernicolous harvestman from southeastern Brazil (Arachnida: Opiliones: Gonyleptidae). Invertebrate Reproduction and Development 28:137–151.

Gnaspini, P. 2007. Development. Pp. 455–472. *In* Harvestmen: The Biology of Opiliones. (R. Pinto-da-Rocha, G. Machado and G. Giribet, eds.), Harvard University Press, Cambridge, Massachusetts.

Gnaspini, P. & G.C.S. Rodrigues. 2011. Comparative study of the morphology of the gland opening area among Grassatores harvestmen (Arachnida, Opiliones, Laniatores). Journal of Zoological Systematics and Evolutionary Research 49:273–284.

Goodnight, M.L. & C.J. Goodnight. 1976. Observations on the systematics, development, and habits of *Erginulus clavotibialis* (Opiliones: Cosmetidae). Transactions of the American Microscopy Society 95:654–664.

Juberthie, C. 1972. Reproduction et développement d'un opilon Cosmetidae, *Cynorta cubana* (Banks), de Cuba. Annales de Spéléologie 27:773–785.

Kury, A.B. 2016. A classification of the penial microsetae of Gonyleptoidea (Opiliones: Laniatores). Zootaxa 4179:144–150.

Kury, A.B. & R. Pinto-da-Rocha. 2007. Cosmetidae. Pp. 182–185. *In* Harvestmen: The Biology of Opiliones. (R. Pinto-da-Rocha, G. Machado and G. Giribet, eds.), Harvard University Press, Cambridge, Massachusetts.

Kury, A.B. & O. Villarreal M. 2015. The prickly blade mapped: Establishing homologies and a chaetotaxy for macrosetae of penis ventral plate in Gonyleptoidea (Arachnida, Opiliones, Laniatores). Zoological Journal of the Linnean Society 174:1–46.

Martens, J., U. Hoheisel & M. Götze. 1981. Comparative anatomy of the ovipositors of the Opiliones as a contribution to the Order (Arachnida). Zoologische Jahrbücher Abteilung für Anatomie und Ontogenie der Tiere 105:13–76.

Medrano, M. & A.B. Kury. 2016. Characterization of *Platymessa* with redescription of the type species and a new generic synonymy (Arachnida, Opiliones, Cosmetidae). Zootaxa 4085:52–62. Online at http://doi.org/10.11646/zootaxa.4085.1.2

Muñoz Cuevas, A. 1971. Etude du tarse, de l'apotele et de la formation des griffes au cours du développement postembryonnaire chez *Pachylus quinquavidensis* (Arachnida, Opilions, Laniatores). Bulletin du Muséum National d'historie Naturelle, Paris, series 2, 42:1027–1036.

Murayama, G.P. & R.H. Willemart. 2015. Mode of use of sexually dimorphic glands in a Neotropical harvestman (Arachnida, Opiliones) with parental care. Journal of Natural History 49:1937–1947.

Nation, J.L. 1983. A new method for using hexamethyldisilazane for preparation of soft insect tissue for scanning electron microscopy. Stain Technology 58:347–351.

Pinto-da-Rocha, R. & M.R. Hara. 2011. Redescription of *Platygyndes* Roewer 1943, a false Gonyleptidae (Arachnida, Opiliones, Cosmetidae). ZooKeys 143:1–12. doi:10.3897/zookeys.143.1916.

Pinto-da-Rocha, R., A.R. Benedetti, E.G. de Vasconcelos & M.R. Hara. 2012. New systematic assignments in Gonyleptoidea (Arachnida, Opiliones, Laniatores). ZooKeys 198:25–68.

Proud, D.N. & B.E. Felgenhauer. 2011. Ultrastructure of the sexually dimorphic basitarsal glands of leg I in manaosbiid harvestmen (Opiliones, Laniatores). Journal of Morphology 272:872–882.

Proud, D.N. & B.E. Felgenhauer. 2013. Ultrastructure of the sexually dimorphic tarsal glands and tegumental glands in gonyleptoid harvestmen (Opiliones, Laniatores). Journal of Morphology 274:1203–1215.

Proud, D.N., B. E. Felgenhauer, V.R. Townsend Jr., D.O. Osula, W.O. Gilmore, III, Z.L. Napier et al. 2012. Diversity and habitat use of harvestmen (Arachnida: Opiliones) in a Costa Rican rainforest. ISRN Zoology 1–16. doi:10.5402/2012/549765.

Ramin, A.Z., R.H. Willemart & P. Gnaspini. 2016. Changes in nymphal morphometric values and tarsal microstructures during postembryonic development in the Neotropical harvestman *Heteromitobates albiscriptus* (Opiliones: Gonyleptidae). Journal of Arachnology 44:330–346.

Rodriguez, A.L. & V.R. Townsend, Jr. 2015. Survey of cuticular structures on leg IV of cosmetid harvestmen (Opiliones: Laniatores: Gonyleptoidea). Journal of Arachnology 43:194–206.

Rodriguez, A.L., V.R. Townsend, Jr., M.B. Johnson & T.B. White. 2014. Interspecific variation in the microanatomy of cosmetid harvestmen (Arachnida, Opiliones, Laniatores). Journal of Morphology 275:1386–1405.

Schaus, M.H., V.R. Townsend, Jr. & J.J. Illinik. 2013. Food choice of the Neotropical harvestman *Erginulus clavotibialis* (Opiliones: Laniatores: Cosmetidae). Journal of Arachnology 41:219–221.

Sharma, P.P. & G. Giribet. 2011. The evolutionary and biogeographic history of the armoured harvestmen – Laniatores phylogeny based on ten molecular markers, with the description of two new families of Opiliones (Arachnida). Invertebrate Systematics 25:106–142.

Townsend Jr., V.R., M.S. Bertram & M.A. Milne. 2015. Variation in ovipositor morphology among laniatorean harvestmen. Zoomorphology 134:487–497.

Townsend Jr., V.R., D.N. Proud & M.K. Moore. 2008. Harvestmen (Arachnida: Opiliones) of Trinidad, West Indies. Living World, Journal of the Field Naturalist Club of Trinidad & Tobago 2008:53–65.

Townsend Jr., V.R., N.J. Rana, D.N. Proud, M.K. Moore, P. Rock & B.E. Felgenhauer. 2009. Morphological changes during postembryonic development in two species of Neotropical harvestmen (Opiliones, Laniatores, Cranaidae). Journal of Morphology 270:1055–1068.

Townsend Jr., V.R., M.H. Schaus, T. Zvonareva, J.J. Illinik & J.T. Evans. 2017. Leg injuries and wound repair among cosmetid harvestmen (Arachnida, Opiliones, Laniatores). Journal of Morphology 278:73–88.

Walker, E.A. & V.R. Townsend, Jr. 2014. Ovipositor morphology of cosmetid harvestmen (Arachnida, Opiliones, Laniatores): A new source of informative characters. Journal of Morphology 275:1376–1385.

Willemart, R.H. & E.A. Hebets. 2012. Sexual differences in the behavior of the harvestman *Leiobunum vittatum* (Opiliones, Sclerosomatidae). Journal of Insect Behavior 25:12–23.

Willemart, R.H., M.C. Chelini, R. De Andrade & P. Gnaspini. 2007. An ethological approach to a SEM survey on sensory structures and tegumental gland openings of two neotropical harvestmen (Arachnida, Opiliones, Gonyleptidae). Italian Journal of Zoology 74:39–54.

Willemart, R.H., J.P. Farine & P. Gnaspini. 2009. Sensory biology of Phalangida harvestmen (Arachnida, Opiliones): A review, with new morphological data on 18 species. Acta Zoologica 90:209–227.

Willemart, R.H., A. Pérez-González, J-P Farine & P. Gnaspini. 2010. Sexually dimorphic tegumental gland openings in Laniatores (Arachnida, Opiliones) with new data on 23 species. Journal of Morphology 271:641–653.

Wolff, J.O., A.L. Schönhofer, J. Martens, H. Wijnhoven, C.K. Taylor & S.N. Gorb. 2016. The evolution of pedipalps and glandular hairs as predatory devices in harvestmen (Arachnida, Opiliones). Zoological Journal of the Linnean Society 177:558–601.

Manuscript received 1 June 2017, revised 23 October 2017.

2018. Journal of Arachnology 46:62–68

Putative adhesive setae on the walking legs of the Paleotropical harvestman *Metibalonius* sp. (Arachnida: Opiliones: Podoctidae)

Guilherme Gainett[1,2], **Prashant P. Sharma**[2], **Gonzalo Giribet**[3] and **Rodrigo H. Willemart**[1,4,5]: [1] Laboratório de Ecologia Sensorial e Comportamento de Artrópodes, Escola de Artes, Ciências e Humanidades, Universidade de São Paulo, Rua Arlindo Béttio, 1000, Ermelino Matarazzo, São Paulo, SP 03828-000, Brazil; E-mail: guilherme.gainett@wisc.edu; [2] Department of Integrative Biology, University of Wisconsin-Madison, 352 Birge Hall, 430 Lincoln Drive, Madison, WI 53706 USA; [3] Museum of Comparative Zoology and Department of Organismic and Evolutionary Biology, Harvard University, 26 Oxford Street, Cambridge, MA 02138, USA; [4] Programa de Pós-Graduação em Zoologia, Instituto de Biociências, Universidade de São Paulo, Rua do Matão, 321, Travessa 14, São Paulo, SP 05508-090, Brazil; [5] Programa de Pós-Graduação em Ecologia e Evolução, Universidade Federal de São Paulo, Campus Diadema, Rua Professor Artur Riedel, 275, Jardim Eldorado, Diadema, SP 09972-270, Brazil.

Abstract. We provide a first scanning electron microscopy examination of the Paleotropical harvestman family Podoctidae (Opiliones: Laniatores), focusing on the distitarsus of the legs of *Metibalonius* sp. Distitarsi I and II are mostly equipped with olfactory sensilla chaetica with wall pores, while those of legs III and IV have gustatory sensilla chaetica with a tip pore, ventral trichomes with ovate tips (non-sensory) and a type of spatulate seta. Spatulate setae are present in adults of both sexes, with no apparent sexual dimorphism, but they are absent in the nymph. Seven of these setae are inserted on the frontal surface of the last tarsomere of legs III and IV, with the tips oriented ventrally. Each seta has an s-shaped socketed shaft, which terminates distally in a spatula-shaped structure. The distribution of spatulate setae, restricted to legs III and IV (walking legs), the position on the distitarsi, and the typical spatulate shape suggest an adhesive function for these structures. Morphology and position suggest that the socketed spatulate setae of *Metibalonius* sp. and the previously reported scopular spatulate setae of other harvestmen constitute two distinct types of adhesive structures, highlighting the diversity of adhesive structures in Laniatores. Future investigations about the natural history of this species and internal morphology of spatulate setae are necessary to test further functional hypotheses and to determine their behavioral role.

Keywords: Sensilla, Laniatores, spatulate setae, SEM, adhesion

Scanning electron microscopy surveys of integumental structures are inherently important for their potential to reveal informative characters for systematics, inspire engineering devices (e.g., bio-inspired adhesives) and give insights on the behavior of animals (Stork 1980; Gorb 2008; Wolff & Gorb 2016). Extensive SEM surveys have been conducted in insects, building a solid body of work on the diversity of forms and functions of the arthropod cuticle (e.g., Stork 1980; Beutel & Gorb 2001; Chapman 2013). In arachnids, most surveys have focused on spiders, mites and ticks (e.g., Alberti & Coons 1999; Coons & Alberti 1999; Ramírez 2014), but knowledge of the integument of other arachnid taxa, such as Opiliones (harvestmen or daddy-long-legs), remains relatively scarce (see below).

Studies in harvestmen have rapidly increased in the last decade, focusing mostly on the largest suborder, Laniatores, a group with approximately 30 families distributed worldwide (Kury 2013; Giribet & Sharma 2015). Researchers have mostly investigated the ultrastructure of the integument (Townsend et al. 2009; Rodriguez & Townsend 2015; Rodriguez et al. 2014a, b; Ramin et al. 2016), sensory organs (Willemart et al. 2007, 2009; Willemart & Giribet 2010; Gainett et al. 2014, 2017) and glands (Willemart et al. 2010; Gnaspini & Rodrigues 2011; Proud & Felgenhauer 2011, 2013; Gainett et al. 2014; Ramin et al. 2016). However, even in the better studied Laniatores, the members of a few families have never been closely investigated by SEM, Podoctidae being one of these. Podoctidae is a small family of Paleotropical harvestmen, whose precise sister-group relationship to other laniatorid families is still contentious (Fernández et al. 2017), and whose traditional systematics has recently been largely rearranged based on molecular evidence (Sharma et al. 2017). Therefore, knowledge about the integument of a podoctid could provide important information for the taxonomy and biology of this poorly known family. We thus used SEM to investigate the distitarsus of legs I–IV of the podoctid *Metibalonius* sp. (Fig. 1a–c), reporting a previously undescribed setal type.

METHODS

Metibalonius sp. is a small species, with a body length of 1.5 mm (Fig. 1). Specimens were obtained from the Invertebrate Zoology Collection in the Museum of Comparative Zoology, Harvard University. *Metibalonius* sp. individuals (MCZ-131275, available online at http://mczbase.mcz.harvard.edu/guid/MCZ:IZ:131275) were collected in Australia (Ella Bay N. P., Queensland; above waterfall, next to dirt road; 17° 28′ 39.3″ S, 145° 04′ 22.2″ E; collected by P.P. Sharma & R.M. Clouse, 1.V.2011). We sampled 3 males, 6 females, 1 nymph, and selected one male and one female for scanning electron microscopy (SEM). For SEM, legs of specimens were cleaned using a Branson 200 sonicator, in a 1:10 dilution of detergent, and subsequently in deionized water only. Some of the appendages were intentionally left uncleaned for the investigation of possible secretions. Cleaned appendages were dried in 100% acetone and mounted on 12 mm SEM stub mounts

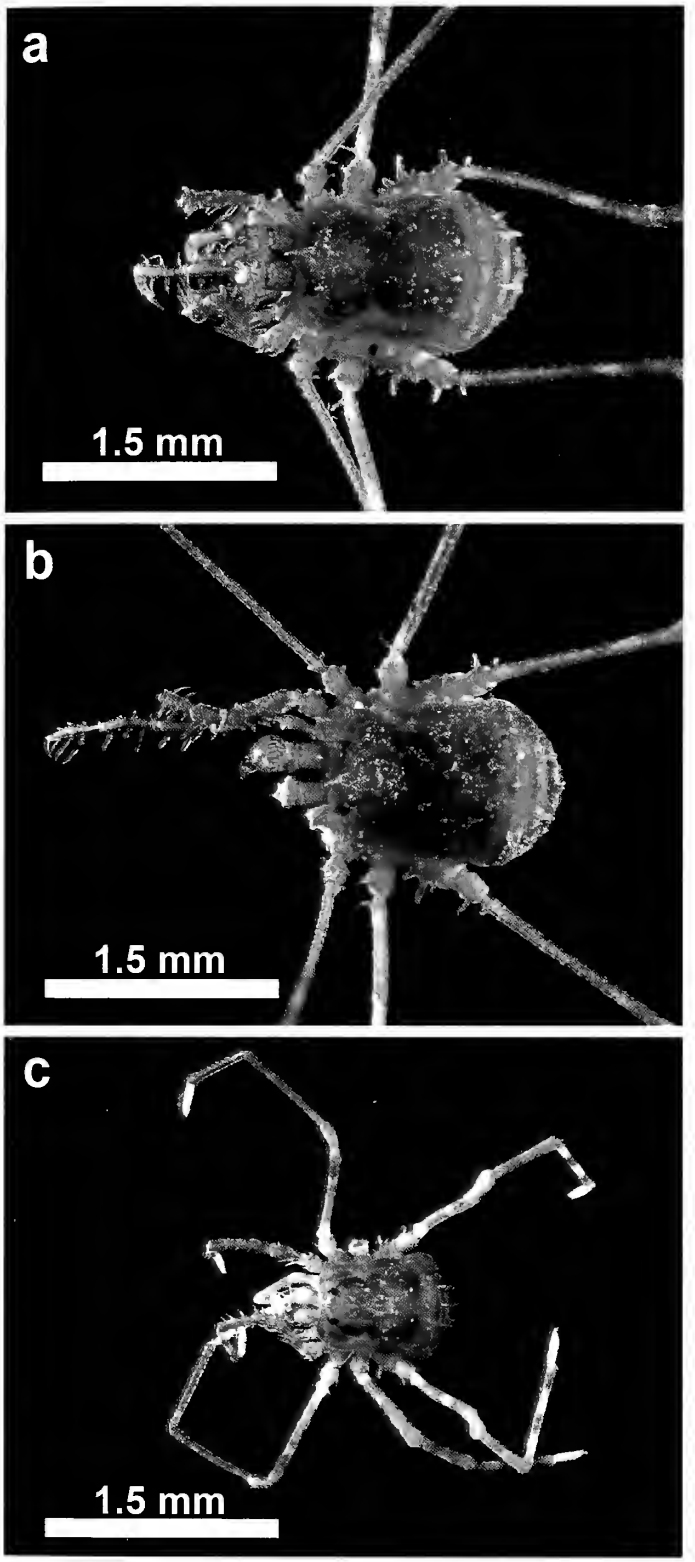

Figure 1.—Automontage pictures of individuals *Metibalonius* sp. (Podoctidae) in dorsal view. a: Adult female. b: Adult male. c: Nymph.

(Electron Microscopy Sciences) using Ultra-Smooth carbon adhesive tabs (Electron Microscopy Sciences). Samples were coated with Pt-Pd, using a Cressington 208HR sputter coater and imaged in a Zeiss Ultra-Plus (field emission scanning electron microscope; accelerating voltage: 5–6 kV) at the Center for Nanoscale Systems, Harvard University. Measurements were taken using the open source software ImageJ 1.48v (available online at https://imagej.nih.gov/ij).

RESULTS

Legs I and II differ from legs III and IV with respect to shape and setal composition (Figs. 2, 3). The distal tarsomeres of the anterior legs (I and II) are relatively more elongated than those in posterior legs (III and IV) (Figs. 2, 3). The most distal tarsomeres of the anterior legs have almost no trichomes and are mostly covered in sensilla chaetica with wall pores and some sensilla chaetica with a tip pore (Fig. 2a–c). On both legs, setae are evenly distributed on most tarsomeres, having a higher density only around the small single claw (Fig. 2). Legs I and II show a similar density and distribution of setae, with no evident sexual dimorphism (Fig. 2a–c). Distitarsi of posterior legs III and IV have trichomes along all surfaces of the tarsomeres, with higher density on the ventral side (Fig. 3b, c). Some of the distal ventral trichomes of the most distal tarsomeres III and IV of *Metibalonius* sp. have a curved shape ending in an expanded apex instead of tapering gradually toward the distal portion (Figs. 3b, c; 4f). The apex has an ovate shape of approximately 1.5 µm wide and 3.5 µm long. When broken, the shaft appears solid. These trichomes occur in specimens of both sexes, with no apparent sexual dimorphism. Posterior distitarsi also have sensilla chaetica with a tip pore (*sensu* Gainett et al. 2017) and a peculiar undescribed type of spatulate setae on the most distal tarsomeres.

These spatulate setae occur on the most distal part of the last tarsomere of legs III and IV of adults of both sexes, with no apparent sexual dimorphism (Fig. 3a–c). These structures are inserted in sockets on the frontal part of the tarsomere, three of them inserted retrolaterally and four prolaterally (Fig. 3a–c). The setae are sigmoidally curved towards the tip of the leg, with the tip of the setae facing down (Fig. 4a). The shaft is approximately 80 µm long. The proximal part of the shaft is cylindrical, with a diameter at the base of 5.8 µm (Fig. 4a). The wall of the shaft is externally smooth at this region. This cylindrical profile of the shaft becomes progressively flattened at 2/3 of its length towards the tip (Fig. 4a–d). Wall pores were not detected, and broken shafts reveal a lumen. The apex is expanded, flattened, and spatula-like, and the dorsal and ventral surfaces have different textures. The spatula is approximately 12 µm wide. The dorsal surface is similar in texture to the rest of the seta, but showing some ridges (Fig. 4b), while the ventral side of clean samples appears rough and wrinkled, bearing several microfolds (Fig. 4d, e). In uncleaned samples, this ventral surface is covered with particles, and a marked oval disc with clear margins was discernible (Fig. 4c, brackets). The particles were more concentrated in the ventral side of the spatula than in the rest of the shaft (Fig. 4c, brackets). The approximate area of the wrinkled ventral surface of the spatula is 90 μm^2, which implies a total contact surface of approximately 630 μm^2 per leg, and 2520 μm^2 for all walking legs (III and IV). Only the nymph (Fig. 1c) has an arolium on the frontal region of legs III and IV (absent on legs I and II), and lacks spatulate setae (See Supplementary Fig. 1, available online at http://dx.doi.org/101636/JoA-S-17-047.S1).

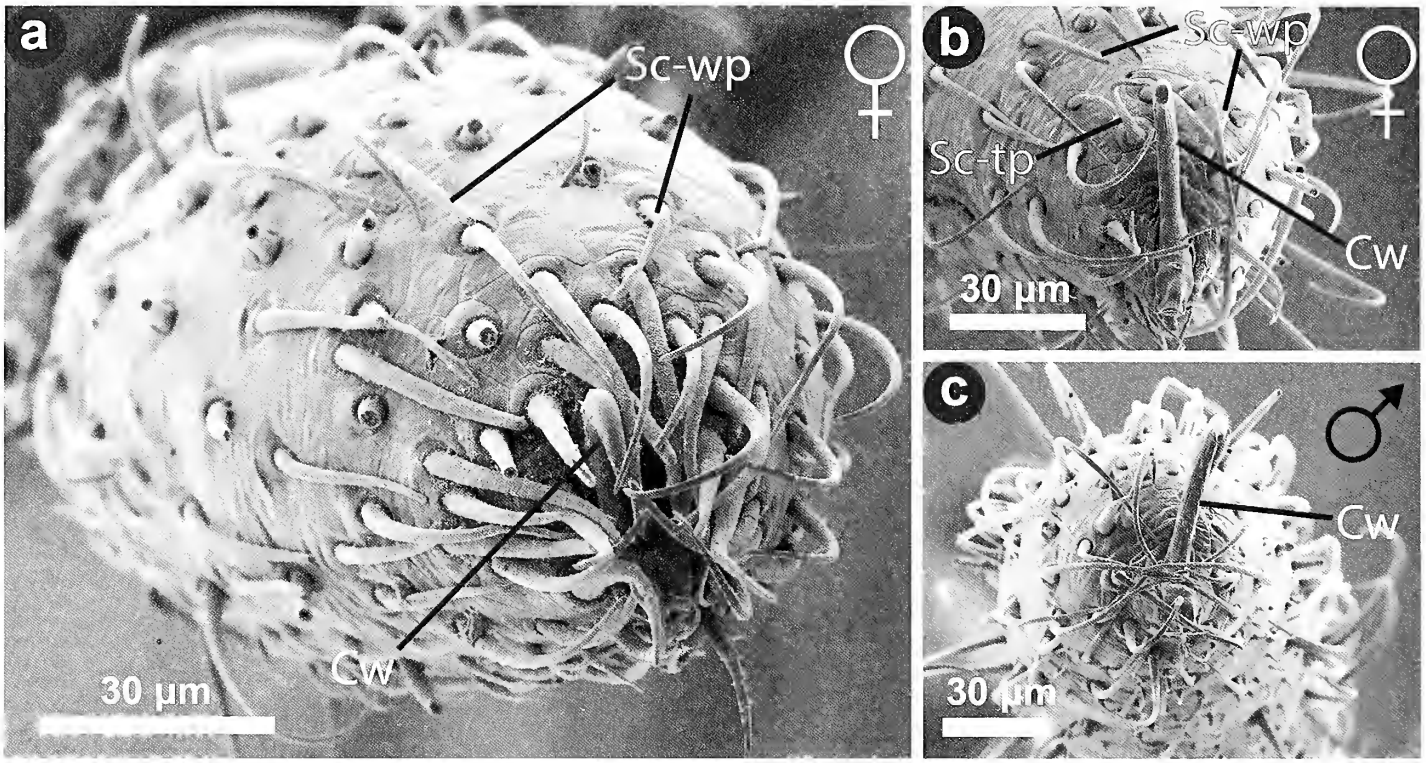

Figure 2.—Scanning electron micrographs of the frontal view of distitarsi I and II of *Metibalonius* sp. a: Leg I, female. b: Leg II, female. c: Leg II, male. Cw: claw; Se-tp: sensilla chaetica with a tip pore; Se-wp: sensilla chaetica with wall pores.

DISCUSSION

We have reported a distinctive socketed spatulate seta on the most distal tarsomeres III and IV of *Metibalonius* sp. The expanded spatulate tip clearly suggests an adhesive function. A spatulate shape is typical of adhesive setae and this shape has independently evolved in distantly related animal groups, including geckos, insects and arachnids (Foelix et al. 1984; Autumn et al. 2000; Beutel & Gorb 2001; Gorb 2001; Wolff & Gorb 2016). In comparison with blunt tips, spatulate structures increase the contact surface, which has been demonstrated both experimentally and theoretically to generate high adhesive forces (Autumn et al. 2000; Persson & Gorb 2003; Varenberg et al. 2010). Moreover, the spatulate setae in *Metibalonius* sp. have dorsal ridges and a lumen probably filled with liquid, features that have been observed in adhesive setae in insects (Gorb 1998). These features are thought to assist in stabilizing and spreading the contact zone over the substrate (Eimüller et al. 2008), conferring visco-elastic properties important for adhesion (Persson & Gorb 2003). In addition, the ventral surface of the spatula displays a wrinkled soft cuticle when dried. Similar ultrastructure has been reported in insects and could be explained by the presence of hydrated proteins (Peisker et al. 2013). In the ladybug beetle *Coccinella septempunctata*, it has been shown that the spatulate tips of adhesive setae have a high concentration of the protein resilin, which may be important to resist abrasion, and for optimizing contact zone and stability (Peisker et al. 2013).

The setae of *Metibalonius* sp. are also particularly similar in shape to the adhesive tenent setae observed in many beetle species (Stork 1980; Gnaspini et al. 2017). Even though the number of units of adhesive setae is usually higher than in the harvestman, some beetles may show comparable numbers. For instance, the beetle *Colenisia zelandica* (Leodidae) (body length: ~1.5 mm; Lesehen 1999) has only 8 large putative adhesive setae on each tarsus (Gnaspini et al. 2017). Therefore, an adhesive mechanism as seen in these insects, presumably relying on a liquid secretion and capillarity, seems plausible for the setae in this harvestman. Our scanning electron micrographs of spatulate setae of *Metibalonius* sp. show no slits or pores in the shaft and socket, but we cannot rule out that a liquid is secreted, as openings sometimes are only detectable with transmission electron microscopy. Nonetheless, some secretion-like material is clearly more concentrated on the putative adhesive surface of the spatula (Fig. 4c), which further supports this idea.

Setae presenting a single large terminal spatula and that rely on a liquid to adhere are very common in beetles and flies (Gorb 2001), but are relatively rare in Arachnida (reviewed in Wolff & Gorb 2016). In ricinuleids, a putative adhesive seta with spatulate tip has been shown to possess a secretory system that oozes at the base of the shaft (Talarico et al. 2006; Wolff & Gorb 2016). Other cases of setae with single terminal spatula in arachnids have only been reported for Opiliones of the suborder Laniatores (Rambla 1990; Wolff & Gorb 2016). They occur in the families Biantidae (Stenostygninae), Samoidae, Epedanidae, Stygnidae and Podoctidae ("Ibaloniinae" only), as a dense aggregation termed scopula (Rambla 1990; Pinto-da-Rocha et al. 2007; Wolff & Gorb 2016). Scopular setae also have some secretion-like material associated with the broadened tips (Wolff & Gorb 2016), similar to

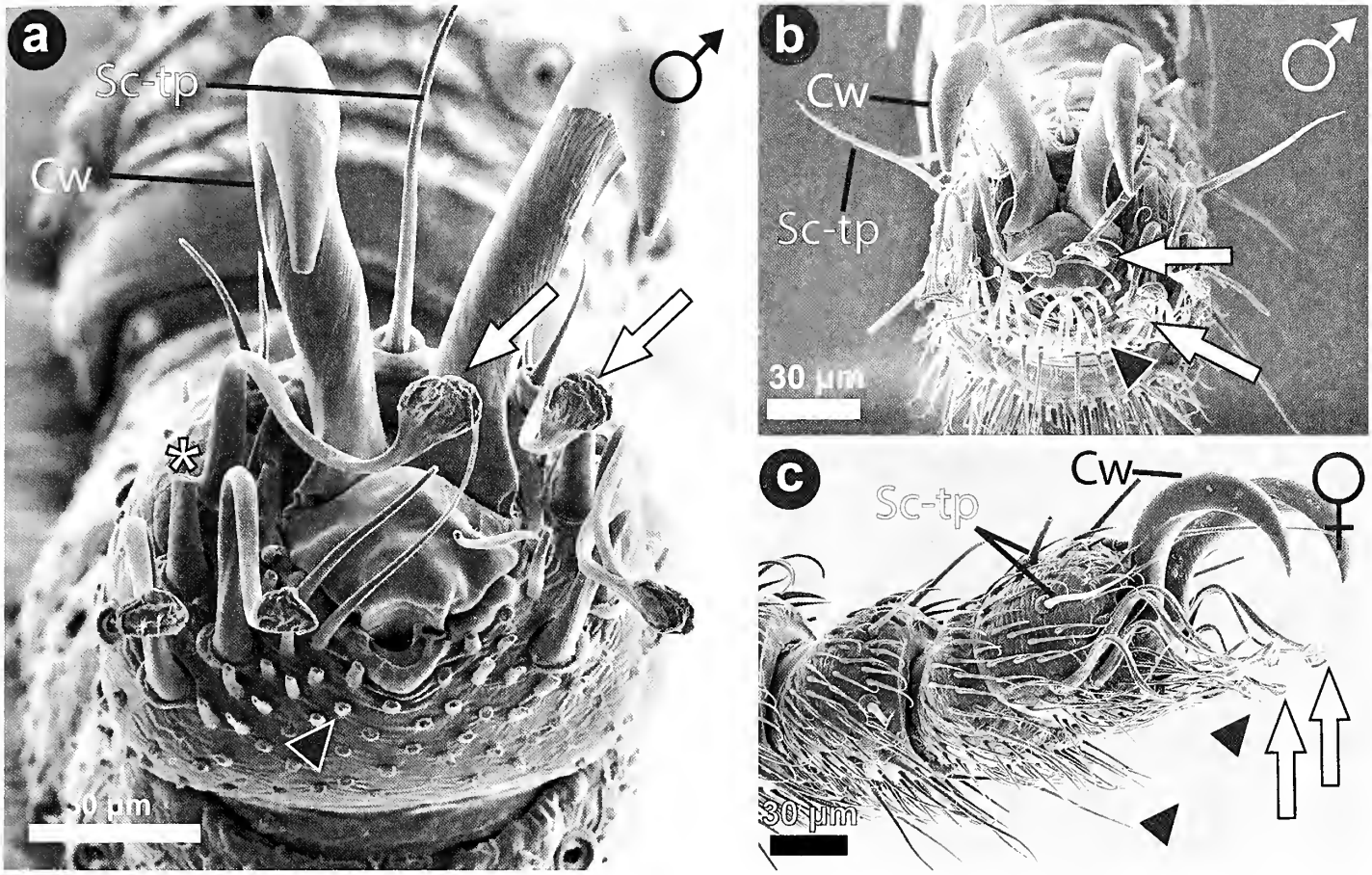

Figure 3.—Scanning electron micrographs of frontal (a, b) and lateral (c) views of distitarsi III and IV of *Metibalonius* sp. a: Male, leg III. Note that ventral trichomes (black arrowhead) are broken. b: Male, leg IV. c: Female, leg IV. Arrow: spatulate setae; Asterisk: broken spatulate seta; Black arrowhead: trichome with expanded tip; Cw: claw; Se-tp: sensilla chaetica with a tip pore.

what we observe in *Metibalonius* sp. However, scopular setae differ from the setae here described in some respects. The scopular setae occur in a much higher density, when compared to only 7 units of socketed spatulate setae per leg in *Metibalonius* sp. Also, described scopular spatulate setae have slender shafts, sometimes band-like flattened (e.g., *Metacrobunus* sp.; Epedanidae; Wolff & Gorb 2016), while the setae we report have tubular shafts proximally, with a lumen. Moreover, the tip of a scopular seta is either lanceolate or slightly broadened, and ranges from approximately 2 to 6 µm in width (Wolff & Gorb 2016), while the type of spatulate setae in *Metibalonius* sp. has a spatula-shaped tip with more than twice this size. The scopular setae morphology more closely resembles the ovate-tip trichomes herein reported, which co-occur with the socketed spatulate setae in *Metibalonius* sp. It is currently unknown if the described scopular setae have true sockets and shafts with a lumen, characteristics which would indicate similarity with the spatulate setae in *Metibalonius* sp. (see Rambla 1990; Wolff & Gorb 2016). Nonetheless, scopular setae have shaft dimensions and tip morphology resembling the ovate-tip trichomes, which have solid shafts and no apparent socket. Moreover, the density and distribution of scopular setae (ventral) in all reported cases in Laniatores (Wolff & Gorb 2016) is very similar to non-spatulate trichomes on the ventral surface of the most distal tarsomeres of other laniatorean harvestmen (Willemart & Gnaspini 2003), which suggests that they may be the same type of structure. Therefore, the socketed spatulate setae likely constitute a different type of adhesive setae in harvestmen. This observation and the fact that scopular spatulate setae have evolved multiple times in harvestmen (Wolff & Gorb 2016) further highlights the diversity of adhesive structures in these arachnids.

In other families of Laniatores, the corresponding region where socketed spatulate setae occur is equipped mainly with sensilla chaetica with a tip pore (Willemart et al. 2009; Gainett et al. 2017). In *Heteromitobates albiscriptus* (Mello-Leitão, 1932) (Gonyleptidae), six sensilla chaetica occur in this region, termed S1, S2 and S3 (pro- and retrolateral) (Ramin et al. 2016), and are precisely located in the correspondent position where spatulate setae occur in *Metibalonius* sp. Moreover, the morphology of the socket of spatulate setae in *Metibalonius* sp. is also similar to that of sensilla chaetica with a tip pore (compare in Fig. 4a). Therefore, socketed spatulate setae may be modified tip-pored sensilla chaetica, which are typical gustatory and touch-sensitive sensilla in harvestmen (Guffey et al. 2000; Willemart et al. 2009; Gainett et al. 2017). Modification of sensilla chaetica into setae with a new function has also been suggested for the glandular sensilla of some harvestmen (Wolff et al. 2016b).

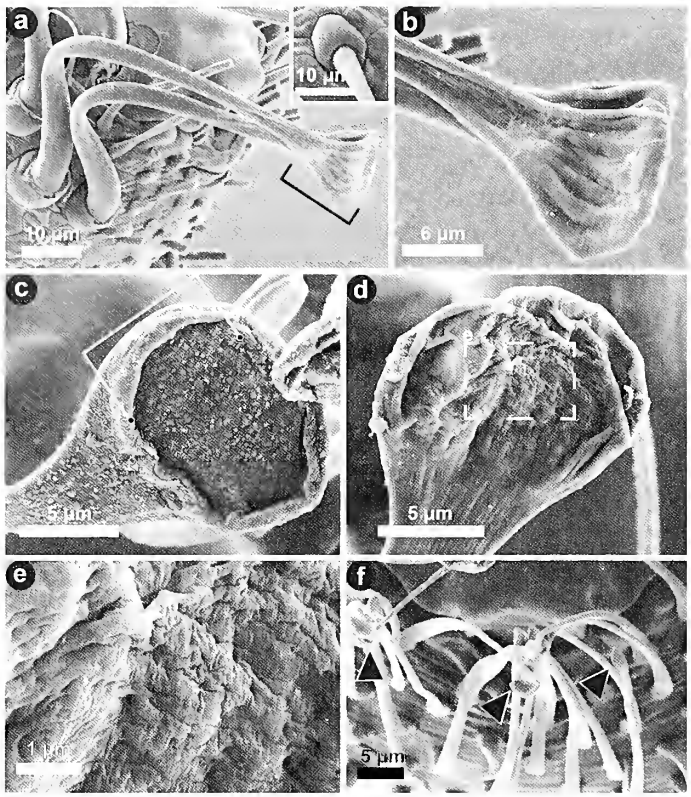

Figure 4.—Seanning electron micrographs of spatulate setae and trichomes on the most distal tarsomeres III and IV of *Metibalonius* sp. a: Lateral view of spatulate setae on the most distal tarsomere III, adult male. Bracket indicates the spatulate tips of two adjacent setae. Inset: socket of a sensillum chaeticum, leg III, male. b: Close-up of spatula tips shown in "a". c: Ventral surface of an uncleaned spatula, leg IV, female. Brackets indicate the limits of the oval disc with higher concentration of particles. d: Ventral surface of a cleaned spatula, leg III, male. e: Detail of the wrinkled surface of the spatula shown in "d" (dashed square). f: Frontal view of the ventral trichomes on the most distal tarsomere IV, male. Note the ovate shape of the tips (black arrowhead).

Apparent absence of terminal pores in spatulate setae disfavors chemoreception (Altner & Prillinger 1980; Keil & Steinbrecht 1984), but the presence of a hollow cuticular shaft inserted in a socket with articulating membrane is typical of mechanoreceptive sensilla of arachnids (Foelix 1985), and also of some adhesive setae in spiders (Foelix et al. 1984). On the other hand, legs I and II of *Metibalonius* sp. lack spatulate setae altogether, and are equipped with sensilla chaetica with wall pores (olfactory) (see also Gainett et al. 2017). This distribution is in accordance with what has been described for other laniatorean species: legs I and II (sensory appendages) concentrate the highest diversity of sensillar structures, including olfactory sensilla; and legs III and IV (walking legs) are equipped with trichomes (non-sensory) and a smaller diversity of sensilla, mostly touch detectors and contact-chemoreceptors (Willemart et al. 2009; Gainett et al. 2017).

Adhesion in arthropods may serve various functions, including prey capture, defense against predators and locomotion (Rovner 1980; Eisner & Aneshansley 2000; Betz & Kölsch 2004; Willemart et al. 2011; Wolff et al. 2015). For the spatulate setae here described, a role in prey capture, similar to glandular sensilla in other harvestmen (Wolff et al. 2014), seems unlikely, since spatulate setae occur on legs III and IV, the walking legs. The adhesive arolium of *Metibalonius* sp. nymph, as in other laniatorean harvestmen, occurs only on leg pairs III and IV and is absent in adults. Interestingly, spatulate setae are absent in the nymph, but occur on leg pairs III and IV of adults. The same pattern has also been reported for the arolium and scopular setae of *Hinzuanius flaviventris* Pocock, 1903 (Laniatores, Biantidae) (Wolff & Gorb 2016). These observations raise the question of why adults still need adhesion similar to immature individuals. It has been proposed that immature laniatorean harvestmen have arolia because they have to molt, which often requires being upside down (Gnaspini 1995, 2007). However, molting is generally assumed not to occur in adult harvestmen (Gnaspini 2007), so a general role of spatulate setae in substrate adhesion should be considered as more likely. Alternatively, emergence of spatulate setae only in the sexually mature stage of development may also indicate a sexual role (see Andersson 1994). Unfortunately, relatively little is known about the natural history of Podoctidae, and even less so for *Metibalonius*. Described features for other podoctids include the attachment of debris to the body (Martens 1993; Wolff et al. 2016a) and the iconic presence of eggs attached to legs IV of two male specimens of *Leytpodoctis oviger* Martens, 1993, indirectly suggesting paternal care (Martens 1993; but see Sharma et al. 2017). Therefore, basic natural history data on habitat use and biology of *Metibalonius* and other podoctids are needed to understand the behavioral role of these setae. Spatulate setae of similar morphology and in comparable numbers have also been observed in other species of the same genus, i.e., *Metibalonius esakii* Suzuki, 1941 (G. Machado, pers. comm.). Therefore, it would be interesting to inspect more species for the presence of these conspicuous setae, which can potentially reveal a new diagnostic character for the recently revised systematics of the family (Sharma et al. 2017).

ACKNOWLEDGMENTS

We thank Adam Graham and Dave Lange (Center for Nanoscale Systems, Harvard University) for assistance with SEM and Pedro Gnaspini and Glauco Machado for helpful discussions. Gabriel P. Murayama, Júlio M.G. Segovia and Thaiany M. Costa kindly revised the manuscript. This work was supported by FAPESP (Fundação de Amparo à Pesquisa do Estado de São Paulo) grant 2011/11527-4 to G. Gainett, grants 2010/00915-0 and 2015/01815-9 to R.H.W and internal funds of the MCZ to G. Giribet. Three anonymous reviewers and Associate Editor Peter Michalik provided constructive criticism that helped to improve this work.

LITERATURE CITED

Alberti, G. & L.B. Coons. 1999. Acari: Mites. Pp. 515–1265. *In* Microscopic Anatomy of Invertebrates, Volume 8B: Chelicerate Arthropoda (F. Harrison & R. Foelix, eds.). Wiley-Liss, New York.

Altner, H. & L. Prillinger. 1980. Ultrastructure of invertebrate chemo-, thermo-, and hygroreceptors and its functional significance. International Review of Cytology 67:69–139.

Andersson, M. 1994. Sexual Selection. Princeton University Press, Princeton.

Autumn, K., Y.A. Liang, S.T. Hsieh, W. Zesch, W.P. Chan, T.W. Kenny et al. 2000. Adhesive force of a single gecko foot-hair. Nature 405:681–685.

Betz, O. & G. Kölsch. 2004. The role of adhesion in prey capture and predator defence in arthropods. Arthropod Structure & Development 33:3–30.

Beutel, R.G. & S.N. Gorb. 2001. Ultrastructure of attachment specializations of hexapods (Arthropoda): evolutionary patterns inferred from a revised ordinal phylogeny. Journal of Zoological Systematics and Evolutionary Research 39:177–207.

Chapman, R. 2013. The Insects. Structure and Function. 5th edition. Cambridge University Press.

Coons, L.B. & G. Alberti. 1999. Acari: Ticks. Pp. 267–514. *In* Microscopic Anatomy of Invertebrates, Volume 8B: Chelicerate Arthropoda (F.W. Harrison & R.F. Foelix, eds.). Wiley-Liss, New York.

Eimüller, T., P. Guttmann & S.N. Gorb. 2008. Terminal contact elements of insect attachment devices studied by transmission X-ray microscopy. Journal of Experimental Biology 211:1958–1963.

Eisner, T. & D.J. Aneshansley. 2000. Defense by foot adhesion in a beetle (*Hemisphaerota cyanea*). Proceedings of the National Academy of Sciences of the United States of America 97:6568–6573.

Fernández, R., P. Sharma, A.L. Tourinho & G. Giribet. 2017. The Opiliones tree of life: shedding light on harvestmen relationships through transcriptomics. Proceedings of the Royal Society B: Biological Sciences 284:20162340.

Foelix, R.F. 1985. Mechano- and chemoreceptive sensilla. Pp. 118–134. *In* Neurobiology of Arachnids (F.G. Barth, ed.). Springer-Verlag, Berlin Heidelberg.

Foelix, R.F., R.R. Jackson, A. Henksmeyer & S. Hallas. 1984. Tarsal hairs specialized for prey capture in the salticid *Portia*. Revue Arachnologique 5:329–334.

Gainett, G., P. Michalik, C.H.G. Müller, G. Giribet, G. Talarico & R.H. Willemart. 2017. Ultrastructure of chemoreceptive tarsal sensilla in an armored harvestman and evidence of olfaction across Laniatores (Arachnida, Opiliones). Arthropod Structure & Development 46:178–195.

Gainett, G., P.P. Sharma, R. Pinto-da-Rocha, G. Giribet & R.H. Willemart. 2014. Walk it off: predictive power of appendicular characters toward inference of higher-level relationships in Laniatores (Arachnida: Opiliones). Cladistics 30:120–138.

Giribet, G. & P.P. Sharma. 2015. Evolutionary biology of harvestmen (Arachnida, Opiliones). Annual Review of Entomology 60:157–175.

Gnaspini, P. 1995. Reproduction and postembryonic development of *Gonyosoma spelaeum*, a cavernicolous harvestman from southeastern Brazil (Arachnida: Opiliones: Gonyleptidae). Invertebrate Reproduction & Development 28:137–151.

Gnaspini, P. 2007. Development. Pp. 455–472. *In* The Biology of Opiliones (R. Pinto-da-Rocha, G. Machado & G. Giribet, eds.). Harvard University Press, Cambridge, Massachusetts.

Gnaspini, P. & G.C.S. Rodrigues. 2011. Comparative study of the morphology of the gland opening area among Grassatores harvestmen (Arachnida, Opiliones, Laniatores). Journal of Zoological Systematics and Evolutionary Research 49:273–284.

Gnaspini, P., C. Antunes-Carvalho, A.F. Newton & R.A.B. Leschen. 2017. Show me your tenent setae and I tell you who you are – Telling the story of a neglected character complex with phylogenetic signals using Leiodidae (Coleoptera) as a case study. Arthropod Structure & Development 46:662–685.

Gorb, S.N. 1998. The design of the fly adhesive pad: distal tenent setae are adapted to the delivery of an adhesive secretion. Proceedings of the Royal Society B: Biological Sciences 265:747–752.

Gorb, S.N. 2001. Attachment Devices of Insect Cuticle. Kluwer Academic Publishers, Dordrecht.

Gorb, S.N. 2008. Biological attachment devices: exploring nature's diversity for biomimetics. Philosophical Transactions. Series A, Mathematical, Physical, and Engineering Sciences 366:1557–1574.

Guffey, C., V.R. Townsend & B.E. Felgenhauer. 2000. External morphology and ultrastructure of the prehensile region of the legs of *Leiobunum nigripes* (Arachnida, Opiliones). Journal of Arachnology 28:231–236.

Keil, T.A. & R.A. Steinbrecht. 1984. Mechanosensitive and Olfactory Sensilla. Pp. 477–516. *In* Insect Ultrastructure, Vol. 2 (R.C. King & H. Akai, eds.). Plenum Publishing Corporation, New York.

Kury, A.B. 2013. Order Opiliones Sundevall, 1833. Zootaxa 3703:27–33.

Leschen, R.A.B. 1999. *Pseudoliodini* (Coleoptera: Leiodidae: Leiodinae) of New Zealand. New Zealand Entomologist 22:33–44.

Martens, J. 1993. Further cases of paternal care in Opiliones (Arachnida). Tropical Zoology 6:97–107.

Peisker, H., J. Michels & S.N. Gorb. 2013. Evidence for a material gradient in the adhesive tarsal setae of the ladybird beetle *Coccinella septempunctata*. Nature Communications 4:1661.

Persson, B.N.J. & S. Gorb. 2003. The effect of surface roughness on the adhesion of elastic plates with application to biological systems. Journal of Chemical Physics 119:11437–11444.

Pinto-da-Rocha, R., G. Machado & G. Giribet. 2007. Harvestmen: The Biology of Opiliones. Harvard University Press, Cambridge, Massachusetts.

Proud, D.N. & B.E. Felgenhauer. 2011. Ultrastructure of the sexually dimorphic basitarsal glands of leg 1 in manaosbiid harvestmen (Opiliones, Laniatores). Journal of Morphology 272:872–882.

Proud, D.N. & B.E. Felgenhauer. 2013. Ultrastructure of the sexually dimorphic tarsal glands and tegumental glands in gonyleptoid harvestmen (Opiliones, Laniatores). Journal of Morphology 274:1203–1215.

Rambla, M. 1990. Les scopula des Opilions, différenees avec les scopula des Araignées (Arachnida, Opiliones, Araneae). Pp. 293–298. *In* Comptes rendus du XIIème Colloque européen d'Arachnologie. Bulletin de la Société européenne d'Arachnologie 1 (Supplement Volume) (M.L. Célérier, J. Heurtault & C. Rollard, eds.).

Ramin, A.Z., R.H. Willemart & P. Gnaspini. 2016. Changes in nymphal morphometric values and tarsal microstructures during postembryonic development in the Neotropical harvestman *Heteromitobates albiscriptus* (Opiliones: Gonyleptidae). Journal of Arachnology 44:330–346.

Ramírez, M.J. 2014. The morphology and phylogeny of dionychan spiders. Bulletin of the American Museum of Natural History 390:1–374.

Rodriguez, A.L. & V.R. Townsend. 2015. Survey of cuticular structures on leg IV of cosmetid harvestmen (Opiliones: Laniatores: Gonyleptoidea). Journal of Arachnology 43:194–206.

Rodriguez, A.L., V.R. Townsend, M.B. Johnson & T.B. White. 2014a. Interspecific variation in the microanatomy of cosmetid harvestmen (Arachnida, Opiliones, Laniatores). Journal of Morphology 20:1–20.

Rodriguez, A.L., V.R. Townsend & D.N. Proud. 2014b. Comparative study of the microanatomy of four species of harvestmen (Opiliones, Eupnoi). Annals of the Entomological Society of America 107:496–509.

Rovner, J.S. 1980. Morphological and ethological adaptations for prey capture in wolf spiders (Araneae, Lycosidae). Journal of Arachnology 8:201–215.

Sharma, P.P., M.A. Santiago, R. Kriebel, S.M. Lipps, P.A.C. Buenavente, A.C. Diesmos et al. 2017. A multilocus phylogeny of Podoctidae (Arachnida, Opiliones, Laniatores) and parametric shape analysis reveal the disutility of subfamilial nomenclature in

armored harvestman systematics. Molecular Phylogenetics and Evolution 106:164–173.

Stork, N.E. 1980. A scanning electron microscope study of tarsal adhesive setae in the Coleoptera. Zoological Journal of the Linnean Society 68:173–306.

Talarico, G., J.G. Palacios-Vargas, M.F. Silva & G. Alberti. 2006. Ultrastructure of tarsal sensilla and other integument structures of two *Pseudocellus* species (Ricinulei, Arachnida). Journal of Morphology 267:441–463.

Townsend, V.R., N.J. Rana, D.N. Proud, M.K. Moore, P. Rock, B.E. Felgenhauer et al. 2009. Morphological changes during postembryonic development in two species of Neotropical harvestmen (Opiliones, Laniatores, Cranaidae). Journal of Morphology 270:1055–1068.

Varenberg, M., N.M. Pugno & S.N. Gorb. 2010. Spatulate structures in biological fibrillar adhesion. Soft Matter 6:3269.

Willemart, R.H. & G. Giribet. 2010. A scanning electron microscopic survey of the cuticle in Cyphophthalmi (Arachnida, Opiliones) with the description of novel sensory and glandular structures. Zoomorphology 129:175–183.

Willemart, R.H. & P. Gnaspini. 2003. Comparative density of hair sensilla on the legs of cavernicolous and epigean harvestmen (Arachnida: Opiliones). Zoologischer Anzeiger 242:353–365.

Willemart, R.H., M.C. Chelini, R. de Andrade & P. Gnaspini. 2007. An ethological approach to a SEM survey on sensory structures and tegumental gland openings of two neotropical harvestmen (Arachnida, Opiliones, Gonyleptidae). Italian Journal of Zoology 74:39–54.

Willemart, R.H., J.P. Farine & P. Gnaspini. 2009. Sensory biology of Phalangida harvestmen (Arachnida, Opiliones): a review, with new morphological data on 18 species. Acta Zoologica 90:209–227.

Willemart, R.H., A. Pérez-González, J.P. Farine & P. Gnaspini. 2010. Sexually dimorphic tegumental gland openings in Laniatores (Arachnida, Opiliones), with new data on 23 species. Journal of Morphology 271:641–653.

Willemart, R.H., R.D. Santer, A.J. Spence & E.A. Hebets. 2011. A sticky situation: Solifugids (Arachnida, Solifugae) use adhesive organs on their pedipalps for prey capture. Journal of Ethology 29:177–180.

Wolff, J.O. & S.N. Gorb. 2016. Attachment Structures and Adhesive Secretions in Arachnids. Springer International Publishing, Cham.

Wolff, J.O., S. García-Hernández & S.N. Gorb. 2016a. Adhesive secretions in harvestmen (Arachnida: Opiliones). Pp. 285–305. *In* Biological Adhesives (A.M. Smith & J.A. Callow, eds.). Springer International Publishing, Switzerland.

Wolff, J.O., S.J. Huber & S.N. Gorb. 2015. How to stay on mummy's back: morphological and functional changes of the pretarsus in arachnid postembryonic stages. Arthropod Structure & Development 44:301–312.

Wolff, J.O., A.L. Schönhofer, J. Martens, H. Wijnhoven, C.K. Taylor & S.N. Gorb. 2016b. The evolution of pedipalps and glandular hairs as predatory devices in harvestmen (Arachnida, Opiliones). Zoological Journal of the Linnean Society 177:558–601.

Wolff, J.O., A.L. Schönhofer, C.F. Schaber & S.N. Gorb. 2014. Gluing the "unwettable": soil-dwelling harvestmen use viscoelastic fluids for capturing springtails. Journal of Experimental Biology 217:3535–3544.

Manuscript received 4 July 2017, revised 1 November 2017.

2018. Journal of Arachnology 46:69–80

The Opiliones of Iran with a description of a new genus and two new species

Nataly Yu. Snegovaya[1], **James C. Cokendolpher**[2] and **Fariba Mozaffarian**[3]: [1]Institute of Zoology, Azerbaijan Academy of Sciences, pr. 1128, kv. 504, Baku AZ1073, Azerbaijan; [2]Invertebrate Zoology, Natural Science Research Laboratory, Museum of Texas Tech University, Lubbock, Texas 79415, U.S.A. E-mail: james.cokendolpher@ttu.edu; [3]Insect Taxonomy Research Department, Iranian Research Institute of Plant Protection, Agricultural Research, Education and Extension Organization, P.O. Box 1454, 19395 Tehran, Iran.

Abstract. The 22 species of Opiliones recorded from Iran are known from four families: one species of Dicranolasmatidae, five species of Nemastomatidae, 15 species of Phalangiidae, and a single species of Sclerosomatidae. Five of these are recorded for the first time from the country: *Dicranolasma ponticum* Gruber, 1998, *Opilio nabozhenkoi* Snegovaya, 2010, *Phalangium armatum* Snegovaya, 2005, *Phalangium kopetdaghensis* Tchemeris & Snegovaya, 2010, and *Graecophalangium karakalensis* Tchemeris & Snegovaya, 2010. An additional unnamed *Rilaena* species is known from the literature, but not included in the total number of species from the country. One new genus and two new species are illustrated and described as new from Iran. The new species are *Opilio kakunini* and *Rilaena kasatkini*. *Goasheer*, a new genus, is described to hold the species "*Homolophus*" *iranus* Roewer, 1952.

Keywords: Taxonomy, Nemastomatidae, Dicranolasmatidae, Phalangiidae, Sclerosomatidae

ZooBank publication: http://zoobank.org:8080/references/urn:lsid:zoobank.org:pub:0B4D3C01-42BF-49FE-BC6F-BA91C77B0E5C

The first harvestmen named from Iran were by Thorell in 1876. His species *Egaenus oedipus* (Thorell, 1876) and *Opilio ejuncidus* (Thorell, 1876) were both discovered in Tehran. It was another 76 years before three other species were described from Iran by Roewer in 1952. Another five species were then recognized from Iran by Martens (2006) and a further two species and one new genus are described in the present publication. The remaining species now known from Iran were described from other counties and then more recently collected from Iran.

Opiliones are relatively unstudied from Iran. The number of specimens in university and other regional educational collections is uncertain. Judging from the geographic size and great variety of habitats from sandy deserts, mountains, forests, and vast shorelines of the Caspian Sea and Persian Gulf, many species are still to be discovered.

The present study provides a listing of all previously known species from the country as well as records of more recently studied collections. Hopefully, this will usher in a period of greater exploration of the Opiliones biodiversity of this region. Continued study of previously preserved museum collections is still a valuable source of unreported records; some in the present paper date back to 1914 from the Zoological Institute, St. Petersburg, Russia. We hope that it will serve as a guide to the fauna while other studies are undertaken to see what other specimens lie hidden in other institutional collections and hopefully will serve as a stimulus to students of arachnology to notice and collect new samples in as many situations as permitted.

METHODS

Specimens examined are from the collections of Agricultural Zoology Museum of Iran, (Iranian Research Institute of Plant Protection) Tehran (AZMI); Acarological Collection, Jalal Afshar Zoological Museum, Department of Plant Protection, Faculty of Agriculture, University of Tehran, Karaj, Iran (JAZM); Zoological Institute NAS of Azerbaijan, Baku (IZB); Senckenberg Museum Frankfurt am Main, Germany (SMF); Zoological Institute, St. Petersburg, Russia (ZIN); and the reference collection of Nataly Snegovaya, Baku, Azerbaijan (RCNS).

Specimens were analyzed and measured with a Nikon SMZ 1270 stereomicroscope with Sony DSC-P8 camera. Image processing was carried out in the Adobe Photoshop CS5 program. Specimens of *Homolophus iranus* Roewer, 1952 were similarly recorded in the 1980's with a Wild M5A stereomicroscope and an AO150 compound microscope with a camera lucida.

RESULTS AND DISCUSSION

Twenty-two species of Opiliones (one species of Dicranolasmatidae, five species of Nemastomatidae, 15 species of Phalangiidae, and a single species of Sclerosomatidae) are recorded from Iran. Five of these are listed for the first time from the country: *Dicranolasma ponticum* Gruber, 1998, *Opilio nabozhenkoi* Snegovaya, 2010, *Phalangium armatum* Snegovaya, 2005, *Phalangium kopetdaghensis* Tchemeris & Snegovaya, 2010, and *Graecophalangium karakalensis* Tchemeris & Snegovaya, 2010. An additional unnamed species of *Rilaena* Šilhavý, 1965 is known from the literature, but not included in the total number of species from the country.

Thus far, no Cyphophthalmi or Laniatores have been found in the country (or the nearby region of central Asia). Except for the wide-ranging (North America, Europe, Asia, and Tasmania) *Opilio parietinus* (DeGeer, 1778), most of the species are either endemic to Iran or the surrounding region. The other better-known tramp (synanthropic species) of Phalangiidae known from throughout the Northern Hemisphere and New Zealand, *Phalangium opilio* Linnaeus, 1758 is remarkably not recorded from Iran.

Species endemic to Iran are: *Mediostoma armatum* Martens, 2006, *Opilio kakunini* sp. nov., *Goasheer iranus* (Roewer, 1952), *Paranemastoma iranicum* Martens, 2006, *Rilaena kasatkini* sp. nov. and *Rilaena pusilla* (Roewer, 1952).

SYSTEMATICS

Family Dicranolasmatidae Simon, 1879

Dicranolasma ponticum Gruber, 1998

Dicranolasma ponticum Gruber 1998:513–521, figs. 54–81; Snegovaya & Chumachenko 2011:119; Snegovaya & Staręga 2011:48, 49, figs. 1–6; Schönhofer 2013:23.

Material examined.—IRAN: *Azarbaijan-e Gharbi Province*: 1 ♀, near Piranshahr, 16 May 2015, D. Kasatkin (RCNS).

Type locality.—Vilayet Ordu, ca. 5 km NE of Ulubey, Turkey.

Distribution.—Caucasus: Azerbaijan, Georgia, Iran (Fig. 5), Turkey.

Remarks.—The current record is the first from Iran.

Family Nemastomatidae Simon, 1872

Mediostoma variabile Martens, 2006

Mediostoma sp.: Snegovaya 2004:308, 309, figs. 9–13.
Mediostoma variabile Martens 2006:185–189, figs. 20, 23 a–h, 24 k–q, 25i–k; Schönhofer 2013:32; Snegovaya & Staręga 2011:48.

Material examined.—IRAN: *Gilan Province*: 1 ♀, Rostamabad District, near Hadjideh village, 29 May 2014, D. Kasatkin, I. Shokhin (RCNS).

Type locality.—Makidi near Kaleybar, Azarbaijan-e Sharghi Province, Iran.

Distribution.—Azerbaijan, Iran (Fig. 5).

Mediostoma armatum Martens, 2006

Mediostoma armatum Martens 2006:189, 190, figs. 20, 23i–n, 24f–i, 25c–d; Schönhofer 2013:31.

Type locality.—S of Alamdeh (Royan), Mazandaran Province, Iran.

Distribution.—Iran (Fig. 5).

Mediostoma nigrum Martens, 2006

Mediostoma nigrum Martens 2006:190–192, figs. 20, 23 o–q, 24 a–e, 25 a–b; Schönhofer 2013:31.

Type locality.—Seaside of Talysch Mountains, Gilan Province, Iran.

Distribution.—Azerbaijan, Iran (Fig. 5).

Paranemastoma filipes (Roewer, 1919)

Nemastoma quadripunctatum var. *filipes* Roewer 1919:144.
Nemastoma filipes: Roewer 1923:665; Redikorzev 1936:33.
Nemastoma (*Dromedostoma*) *filipes* Kratochvíl 1958:538.
Paranemastoma (*Paranemastoma*) *filipes*: Staręga 1978:204.
Paranemastoma filipes: Martens 2006:203, figs. 30 i–k, 31–32; Snegovaya & Staręga 2011:48; Schönhofer 2013:41.

Material examined.—IRAN: *Gilan Province*: 1 ♀, 16 km W. of Assalem, 13–14 May 2015, D. Kasatkin, S. Kakunin (RCNS).

Type locality.—Lenkoran, Azerbaijan.

Distribution.—Azerbaijan, Iran (Fig. 5).

Paranemastoma iranicum Martens, 2006

Paranemastoma iranicum Martens 2006:204–206, fig. 33; Schönhofer 2013:41.

Type locality.—11 km E Alasht, Mazandaran Province, Iran.

Distribution.—Iran (Fig. 5).

Family Phalangiidae Latreille, 1802
Subfamily Opilioninae C.L. Koch, 1839
Egaenus oedipus (Thorell, 1876)

Diabunus oedipus Thorell 1876:473–475; Roewer 1911:30, fig. 8; Roewer 1912a:212, fig. 6; Roewer 1923:829, fig. 1008; Redikorzev 1936:33.
Egaenus oedipus: Staręga 1978:222; Staręga 2003:95, 96, figs. 14–18.

Type locality.—Tehran, Tehran Province, Iran.

Distribution.—Iran (Fig. 5), Turkmenistan.

Remarks.—Females of this genus cannot currently be identified to species. We have examined such a specimen and give the record here: IRAN: *Markazi Province*: Sharra area, around Pol-e-Do Ab river, autumn, 2001, R. Vafaii, 1♀ (AZMI). It is hoped that this locality can be further collected and the identification established after the study of a male.

Staręga (1973:142, fig. 26) recorded and illustrated the seminal receptacle of a single specimen that he identified as *Egaenus lindbergi* (Roewer 1960). This female was collected from Iran: between "Siroft" and Deh Bakri, 2000 m, 3.IV.1965, leg. Mission d 'Iran and is housed at the Muséum national d'Histoire naturelle, Paris. Staręga thought that Siroft was probably Sisakht, 30°50′N, 51°30′E, but since this locality is rather distant to Dehbakari, we suggest that it is more likely Jiroft, which is a nearby community south of Dehbakari on Highway 91, both in Kerman Province. *Egaenus lindbergi is* otherwise only recorded from Afghanistan, Tadjikistan, and Turkmenistan (Šilhavý 1968, Staręga 2003). Until a male can be collected from this region, we cannot accurately identify the specimen.

Opilio afghanus Roewer, 1960

Opilio afghanus Roewer 1960:26; Šilhavý 1966:254–258, tab. II–III: Šilhavý 1968:317; Komposch 2002:99.
Opilio afganus (misspelling): Gritsenko 1979:35, fig. 27; Gritsenko 1980:557.

Material examined.—IRAN: *Golestan Province*: 1 ♂, Golestan National Park, 37° 22′ 46.33″N, 55° 51′ 54.56″E, 24–25 May 2016, D. Kasatkin (RCNS).

Type locality.—Qaisar, between Ghourmatch and Maimaneh, Afghanistan.

Distribution.—Afghanistan, Iran (Fig. 5), SW Russia.

Remarks.—Komposch (2002) recorded this species from northern Iran, but gave no specific locality.

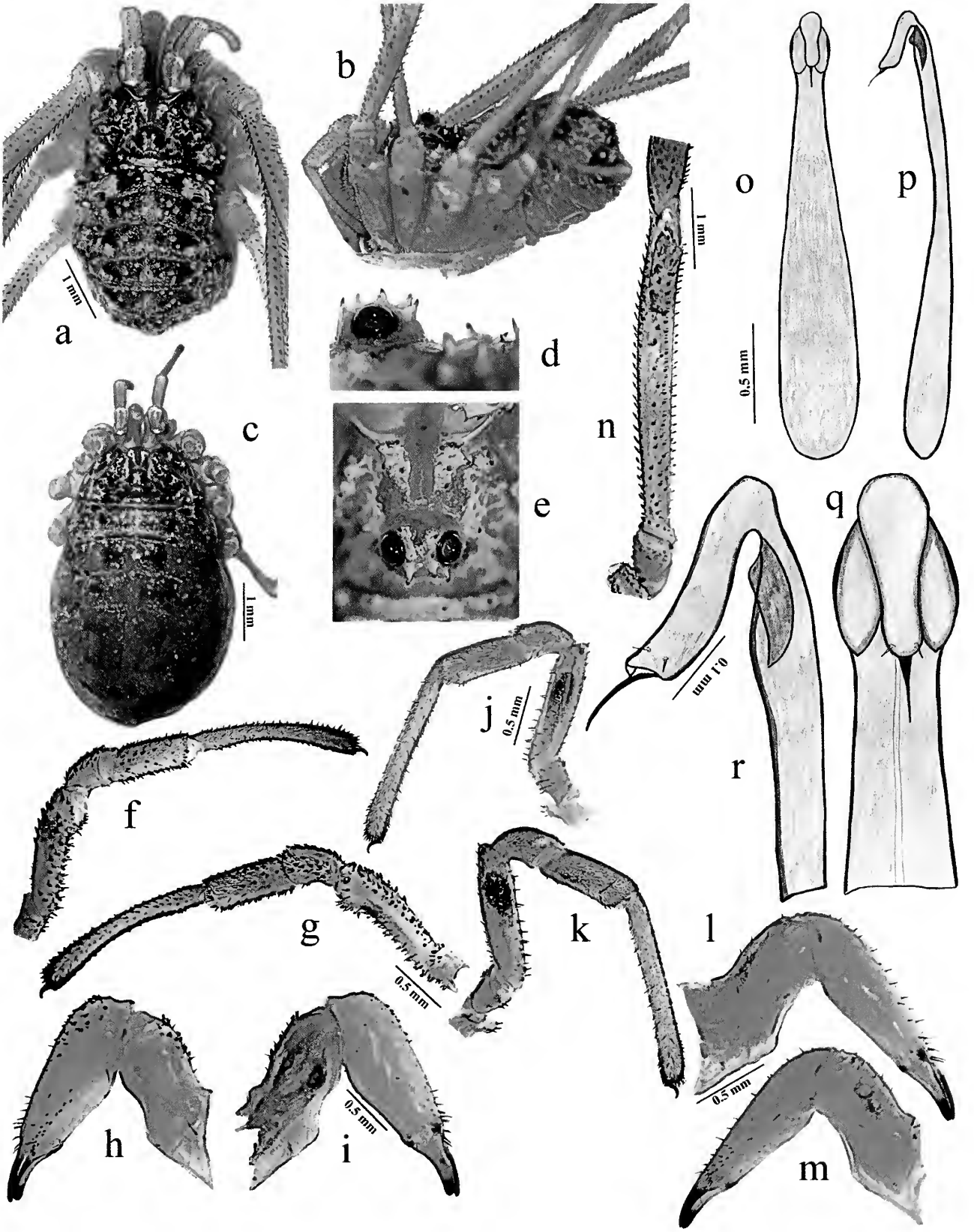

Figure 1.—*Opilio kakumini* sp. nov.: a. Male body, dorsal; b. Male body, lateral; c. Female body, dorsal; d. Male eye mound, lateral; e. Male eye mound, dorsal; f. Male pedipalp, mesolateral; g. Male pedipalp, ectolateral; h. Male chelicera, mesolateral; i. Male chelicera, ectolateral; j. Female pedipalp, mesolateral; k. Female pedipalp, ectolateral; l. Female chelicera, ectolateral; m. Female chelicera, mesolateral; n. Male femur I, lateral; o. Penis, dorsal; p. Penis, lateral; q. Penis dorsal, magnified distal end; r. Penis lateral, magnified distal end.

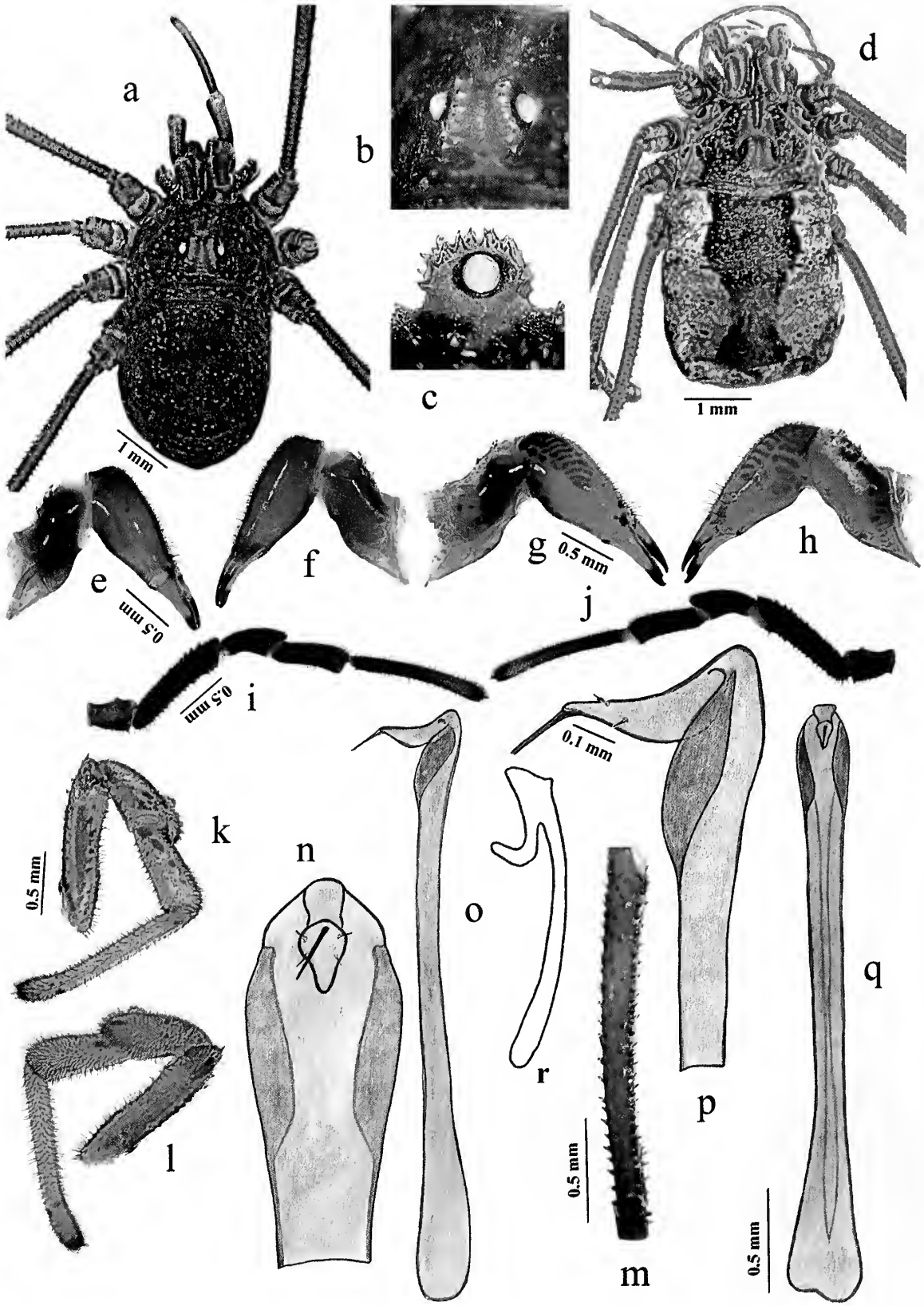

Figure 2.—*Rilaena kasatkini* n. sp: a. Male body dorsal; b. Male eye mound dorsal; c. Male eye mound lateral; d. Female body dorsal; e. Male chelicera ectolateral; f. Male chelicera mesolateral; g. Female chelicera ectolateral; h. Female chelicera mesolateral; i. Male pedipalp ectolateral; j. Male pedipalp mesolateral; k. Female pedipalp ectolateral; l. Female pedipalp mesolateral; m. Male femur I lateral; n. Penis dorsal magnified distal end; o. Penis lateral; p. Penis lateral magnified distal end; q. Penis dorsal; r. Seminal receptacle.

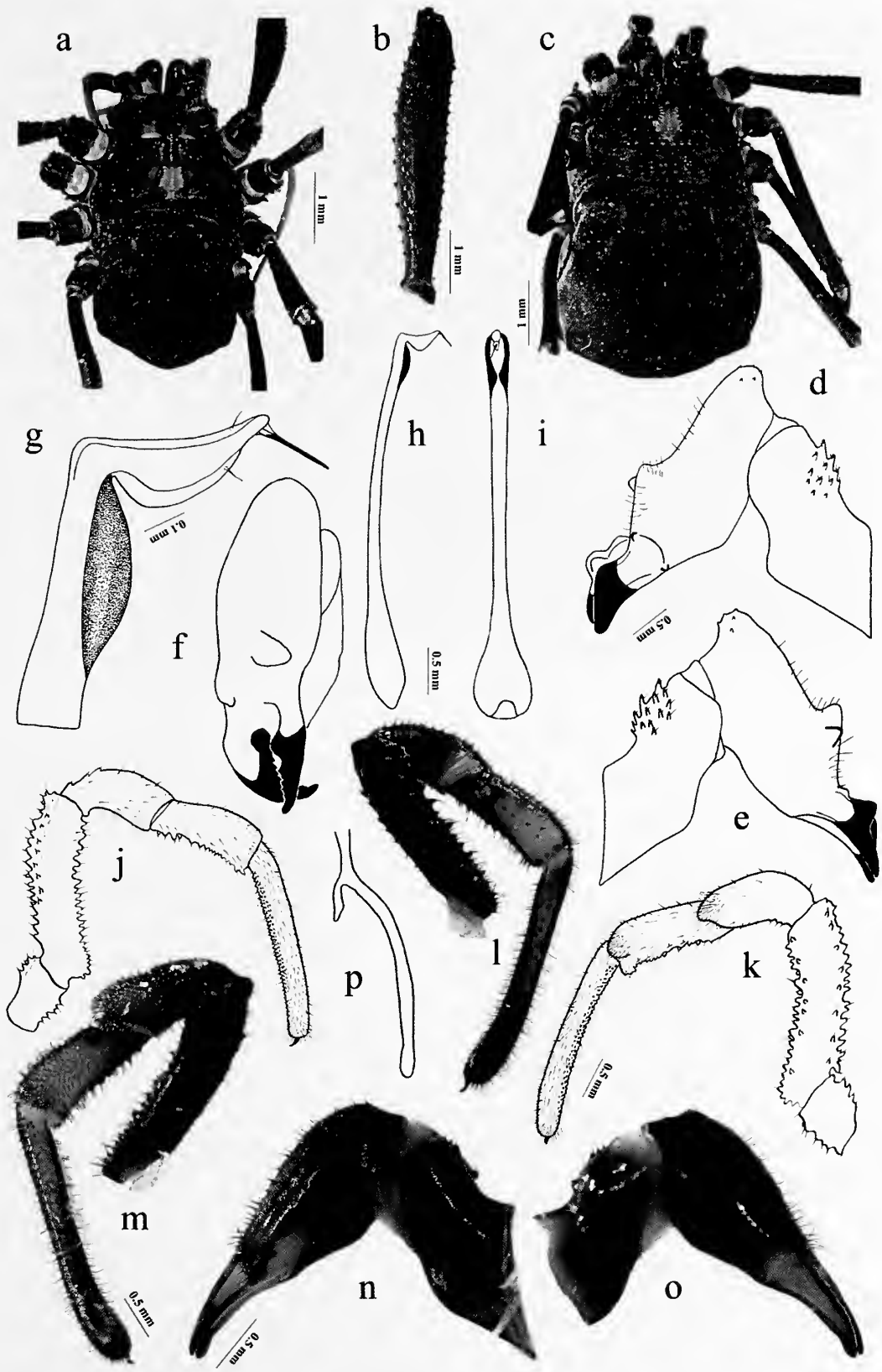

Figure 3.—*Rilaena pusilla*: a. Male body dorsal; b. Male femur I lateral; c. Female body dorsal; d. Male chelicera ectolateral; e. Male chelicera mesolateral; f. Male chelicera 2nd segment anterior; g. Penis lateral magnified distal end; h. Penis lateral; i. Penis dorsal; j. Male pedipalp ectolateral; k. Male pedipalp mesolateral; l. Female pedipalp ectolateral; m. Female pedipalp mesolateral; n. Female chelicera mesolateral; o. Female chelicera ectolateral; p. Seminal receptacle.

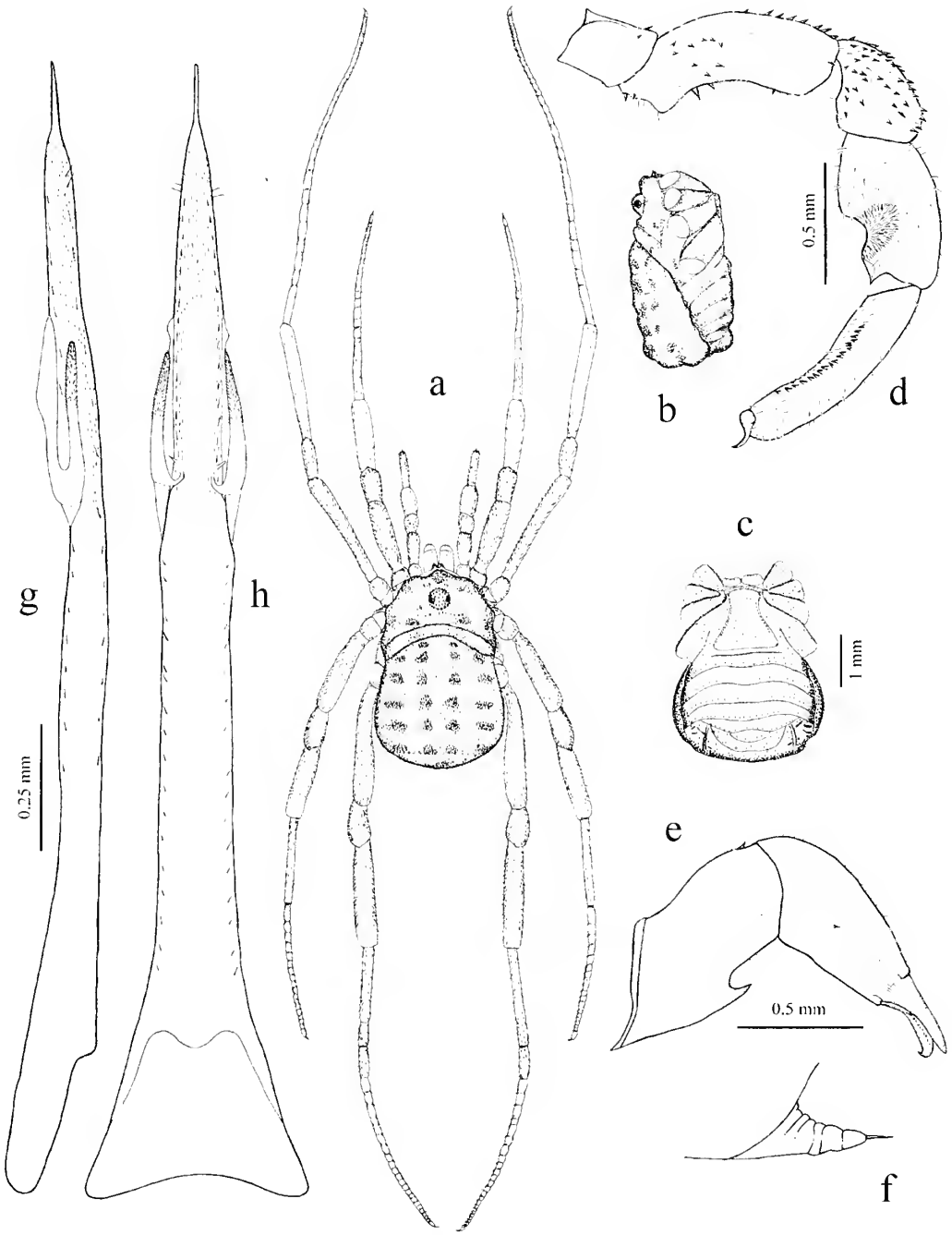

Figure 4.—*Goasheer iranus*: Male; a. Body dorsal; b. Body lateral; c. Body ventral; d. Pedipalp mesolateral; e. Chelicera ectolateral; f. Chelicera hook magnified; g. Penis lateral; h. Penis ventral.

Opilio ejuncidus (Thorell, 1876)

Phalangium ejuncidum Thorell 1876:475, 476.
Opilio ejuncidus: Roewer 1923:773, 774; Morin 1937:213, 218, 220; Bogachev 1951:406.
Opilio ?ejuncidus: Staręga 2003:96.

Type locality.—Tehran, Tehran Province, Iran.
Distribution.—Azerbaijan, Iran (Fig. 5).
Remarks.—Staręga (2003) was unaware of the record by Morin (1937) of this species in Bilasary village, Azerbaijan, when he stated that this species has never been collected again.

Opilio hemseni Roewer, 1952

Opilio hemseni Roewer 1952:512, 513, fig. 1a, b; Staręga 2003:97, 98, 101; Snegovaya 2010:5, figs. 10–19; Snegovaya & Staręga 2011:53, 54, figs. 17–20.
Opilio reginae Staręga 1966:404–406, figs. 19–21; Staręga 1978:227; Chevrizov 1979:26, fig. 149 (synonymized by Staręga 2003:98).
Homolophus azerbaijanicus Snegovaya & Staręga 2008:15–17, figs. 1–11 (synonymized by Snegovaya & Staręga 2011:53).

Material examined.—IRAN: *Gilan Province*: 1 ♂, 1 ♀,

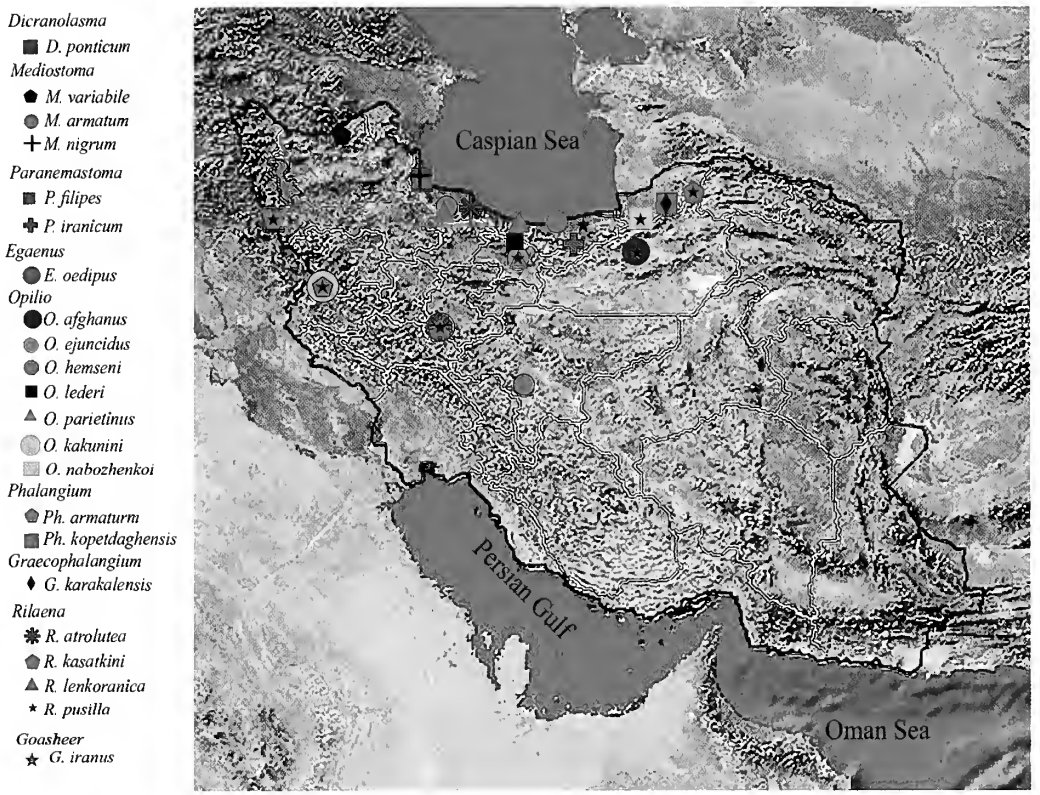

Figure 5.—Map showing the distribution of Opiliones in Iran.

Rasht District, near Dizkoh village, 36° 59′ 18.84″N, 49° 34′ 22.55″E, 5–6 June 2016, D. Kasatkin (RCNS).

Type localities.—Pir Bakran, Isfahan Province, Iran (*Opilio hemseni*); Suchumi, Republic of Abkhazia (*Opilio reginae*), Azfilial, Lenkoran, Azerbaijan (*Homolophus azerbaijanicus*).

Distribution.—Armenia, Azerbaijan, Georgia, Iran (Fig. 5), NE Turkey, SW Russia.

Opilio lederi Roewer, 1911

Opilio lederi Roewer 1911:45; Roewer 1912a:130; Roewer 1923:773, fig. 946; Staręga 1978:226; Chevrizov 1979:23, fig. 152; Staręga 2003:97; Snegovaya 2004:313; Snegovaya 2010:3–5, figs. 1–9; Snegovaya & Staręga 2011:53.

Phalangium coronatum: Redikorzev 1936:43, 44, fig. 15 (nec Fabricius 1779, misidentification).

Opilio redikorzevi Roewer 1956:294; Staręga 1978:227; Chevrizov 1979:26, figs. 144–146; Snegovaya 1999:455, figs. 19–23 (synonymized by Staręga 2003:97).

Material examined.—IRAN: *Alborz Province*: 2 ♂, 5 ♀, near Gachsar village, 2,330 m, 36° 6′ 42.19″N, 51° 20′ 7.74″E, 1–2 June 2016, D. Kasatkin (RCNS).

Type locality.—"Kussari", Caucasus = "Kusari" – Kusari district, now Gusar district, North Azerbaijan.

Distribution.—Armenia, Azerbaijan, Georgia, Iran (Fig. 5), Russia (North Ossetia-Alania, Daghestan), Ukraine (the Crimea).

Opilio parietinus (DeGeer, 1778)

Phalangium parietinum DeGeer 1778:116, fig. 35.

Opilio parietinus: Roewer 1923:770; Mkheidze 1959:113; Mkheidze 1962:185; Mkheidze 1964:120; Martens 1978:240–243, figs. 423–428; Staręga 1966:404; Staręga 1978:226; Chevrizov 1978:70, 71, figs. 1–12; Chevrizov 1979:26, figs. 141–143; Gritsenko 1979:35, fig. 26; Farzalieva & Esyunin 1999:194 195, figs. 79–86; Tchemeris, Logunov & Tsurusaki 1999:197, 198, figs. 43–48; Snegovaya 1999:455; Staręga 2003:96; Snegovaya 2004:313, 314, 316; Çorak & Bayram 2007:456; Snegovaya 2010:5, figs. 20–37; Snegovaya & Staręga 2011:53.

Material examined.—IRAN: *Tehran Province*: 1 ♂, Tehran, May 2012, A. Zamani (RCNS); 1 ♀, Tehran, Damarand, May 2014, A. Zamani (RCNS).

Type locality.—Sweden.

Distribution.—Azerbaijan, Georgia, Iran (Fig. 5), Kazakhstan, Turkey, western Siberia, and ?Afghanistan. Introduced many hundreds of years ago to many European countries and North America and presumably more recently to Tasmania.

Opilio kakunini sp. nov.

http://zoobank.org:8080/NomenclaturalActs/urn:lsid:zoobank.org:act:C9C53A69-D11C-4167-B0E8-1471D1AF5ABB

(Figs. 1a–r & 5)

Material examined.—*Holotype* ♂. IRAN: *Kermanshakh Province*: Shamshir village environs, 21 May 2015, D. Kasatkin, S. Kakunin (ZIN).

Paratypes. IRAN: *Kermanshakh Province*: 2 ♂, 1 ♀, collected with holotype (IZB).

Diagnosis and comparisons.—Body: oval in form (not quadrangular), covered with single transverse rows of black-tipped denticles. Eye mound: low, with 6 pairs large black-tipped denticles. Legs: long, femora I cylindrical, covered with large denticles. Pedipalps: medium-size (not enlarged), dorsally and ventrally with black-tipped denticles (not spine-tipped denticles). Chelicerae: medium-size (not large and strong), both segments dorsally with black-tipped denticles and no granules. Penis: short (less than 3 mm), small oval wings, glans oval form, long, not very wide.

Opilio kakunini sp. nov. is most similar to *Opilio lederi* Roewer, 1911 (Snegovaya 2010:3–5, figs. 1–9), *Opilio arborphilus* Snegovaya, 2010 (Snegovaya 2010:7, 9, 15, figs. 74–82) and *Opilio parietinus* (Snegovaya 2010:5, 8, 10, figs. 20–37). From *Opilio lederi*, it differs by having a smaller body size, longer legs, especially the femur of all legs, less developed chelicera and pedipalps, and by another form of penis (wings rounded versus straight, the shaft widened in the basal third, then tapers to the glans versus straight without expansion). From *Opilio arborphilus*, it differs by the more thickened Femur I, having stronger armament on chelicera, pedipalps and in front of the eye mound, the shorter penis, the broader and more rounded wings on the penis. From *Opilio parietinus*, it differs by smaller size of the body, shorter legs, and penis (wings on the penis smaller versus very wide wings).

Description.—Medium-size harvestmen, body length 4.5 mm, wide 2.7 mm, oval form, covered with transverse rows of black-tipped denticles (Fig. 1a–b). A group of merged large black-tipped denticles situated in front of eye mound. Eye mound low, covered with 6 pairs large black-tipped denticles (Fig. 1d–e). Body yellow with dark brown spots all over the body surface. Legs relatively long, covered with transverse rows of large denticles. Femora 1 cylindrical form (Fig. 1n). Length of legs (mm): I - 4 + 1.3 + 3.4 + 4.2 + 6.7 = 19.6, II - 4 + 2 + 6.6 + 5 + 18 = 35.6, III - 3.6 + 1.3 + 3.2 + 4.5 + 7.5 = 20.1, IV - 5.8 + 1.3 + 4.3 + 6.5 + 10.5 = 28.4. Chelicerae (Fig. 1h–i) small, basal and distal segments dorsally with small black-tipped denticles and setae. Basal segment of chelicera 1.7 mm, distal 1.8 mm. Pedipalps not very large, all segments, besides tarsus dorsally and ventrally densely covered with black-tipped denticles and setae (Fig. 1f–g). Tarsus covered only with setae and in male ventrally with microdenticles. Length of palpal segments: femur 1.4 mm, patella 0.5 mm, tibia 0.8 mm, tarsus 1.7 mm, total length 4.4 mm. Penis (Fig. 1o–r) medium-size, with oval wings, length 2.45 mm, glans length 0.35 mm; glans distally with two pairs of setae.

Female (paratype) (Fig. 1c). Body length 6 mm, width 3.5 mm. Basal segment of chelicera 1.3 mm, distal 1.6 mm. Length of palpal segments: femur 1.1 mm, patella 0.5 mm, tibia 0.8 mm, tarsus 1.5 mm, total length 3.9 mm. Legs missing on only specimen. Seminal receptacles not observed, damaged during processing for microscopical examination. Female differs from male by larger size, lack of black-tipped denticles on the pedipalps (Fig. 1j–k) and chelicerae (Fig. 1l–m).

Etymology.—The species is named in honor of the famous collector and photographer-entomologist, Mr. Sergei Kakunin (Krasnodar, Russia). He kindly provided material of the new *Opilio* and is further recognized for collecting the types as well as other interesting Opiliones of Iran.

Distribution.—The species is thus far known only from Kermanshakh Province, Iran (Fig. 5).

Opilio nabozhenkoi Snegovaya, 2010

Opilio nabozhenkoi Snegovaya 2010:9, 16, figs. 83–91.

Material examined.—IRAN: *Golestan Province*: 2 ♂, near Gorgan, Ziarat village, 36° 40′ 22.67″N, 54° 28′ 7.68″E, 27 May 2016, D. Kasatkin (RCNS).

Type locality.—North Ossetia-Alania, Russia.

Distribution.—Azerbaijan, Russia (North Ossetia-Alania). New for Iran (Fig. 5).

Family Phalangiidae Latreille, 1802
Subfamily Phalangiinae Latreille, 1802
Phalangium armatum Snegovaya, 2005

Phalangium savignyi: Snegovaya 1999:455, figs. 9–13; Snegovaya 2004:313, figs. 17–19 (nec *savignyi* Audouin 1826:182, misidentified).

Phalangium armatum Snegovaya 2005:22–26, figs. 17–34; Snegovaya & Staręga 2011:50; Kurt, Koç & Yağmur 2015:127, 129, 131–134.

Phalangium zuvandicum Snegovaya 2005:23, 26, figs. 35–45 (synonymized by Snegovaya & Staręga 2011:50).

Material examined.—IRAN: *Azarbaijan-e Gharbi Province*: 4 ♀, 4 juveniles, near Piranshahr, 16 May 2015, D. Kasatkin (RCNS); 1 ♂, 3 ♀, 3 juveniles, near Rajan village, 25–27 May 2014, D. Kasatkin, I. Shokhin (RCNS). *Kermanshah Province*: 1 ♀, Shamshir village environs, 21 May 2015, D. Kasatkin, S. Kakunin (RCNS).

Type localities.—Near Gosmalyan, Zuvand, Lerik District, Azerbaijan (*Phalangium armatum*); ca. 6 km. W of Gosmalyan, Zuvand, Azerbaijan (*Phalangium zuvandicum*).

Distribution.—Azerbaijan, Turkey. New for Iran (Fig. 5).

Phalangium kopetdaghensis Tchemeris & Snegovaya, 2010

Phalangium kopetdaghensis Tchemeris & Snegovaya 2010:70, 71, figs. 27–35.

Material examined.—IRAN: *Golestan Province*: 1 ♂, 1 ♀, road between Azad-Shahr and Shahorud, Khoshyeylag village, 15–16 May 2016, 36° 49′ 31.80″N, 55° 20′ 31.78″E, D. Kasatkin (RCNS).

Type locality.—SW Kopetdagh Mts., ca. 10 km SE of Kara-Kala (=Garrygala), Turkmenistan.

Distribution.—Turkmenistan. New for Iran (Fig. 5).

Graecophalangium karakalensis Tchemeris & Snegovaya, 2010

Graecophalangium karakalensis: Tchemeris & Snegovaya 2010:69, 70, figs. 10–26, 35; Murányi 2015:7.

Material examined.—IRAN: *Golestan Province*: 6 ♂, 3 ♀, road between Azad-Shahr and Shahrud, Khoshyeylag village, 15–16 May 2016, 36° 49′ 31.80″N, 55° 20′ 31.78″E, D. Kasatkin (RCNS).

Type locality.—South slopes of Isak Mt., N of Kara-Kala (=Garrygala), Turkmenistan.

Distribution.—Turkmenistan. New for Iran (Fig. 5).

Rilaena sp.

Rilaena sp.: Komposch 2002:99.

Distribution.—North Iran.

Remarks.—Komposch (2002) stated that this should be a new species, but that further taxonomic revision work is urgently needed at this point. We have not studied this material.

Staręga (1973:144) recorded *Rilaena lyrcana* (Thorell, 1876) as being distributed in Iraq, Iran, and Afghanistan, but Snegovaya & Staręga (2009) listed this name as *incertae sedis*.

Rilaena atrolutea (Roewer, 1915)

Metaplatybunus atroluteus Roewer 1915:133, 134; Roewer 1923:853, fig. 1024; Roewer 1956:271; Redikorzev 1936:33.

Metaplatybunus georgicus Mkheidze 1952:614; Mkheidze 1959:114; Mkheidze 1964:122 (synonymized by Staręga 1978:217).

Rilaena atrolutea: Staręga 1978:217; Snegovaya & Pkhakadze 2014:313, 316, 317, fig. 2.

Material examined.—IRAN: *Gilan Province*: 1 ♂, Lahijan, date? (pre-2001), R. Bastan (AZMI). *Markazi Province*: 1 ♀, Sharra area, around Pol-e-Do Ab river, Autumn 2001, R. Vafaii (AZMI).

Type locality.—Vladikavkaz, North Ossetia-Alania, Russia.

Distribution.—Iran (Fig. 5), Russia (North Ossetia-Alania and Daghestan).

Remarks.—Because the male and female reported above were not collected at the same location, we are not certain they represent the same species. Both are larger *Rilaena* specimens, with a distinctive saddle mark and longer legs. The male pedipalps and penis are like those illustrated for this species from Daghestan (Snegovaya & Pkhakadze 2014). Further collections from northwestern Iran will hopefully confirm these identifications. These are the first records of this species from Iran.

Rilaena kasatkini sp. nov.

http://zoobank.org:8080/NomenclaturalActs/urn:lsid:zoobank.org:act:F1AAC7F3-4EA8-4180-B1C4-E5D6B9045222

(Figs. 2a–q & 5)

Material examined.—*Holotype* ♂. IRAN: *Golestan Province*: Golestan National Park, 37° 22′ 46.33″N, 55° 51′ 54.56″E, 24–25 May 2016, D. Kasatkin (ZIN).

Paratypes. IRAN: *Golestan Province*: 1 ♀, collected with holotype (ZIN), 7 ♂, 6 ♀, collected with holotype (IZB).

Diagnosis and comparisons.—Body: oval form (not quadrangular), covered with denticles (not rounded granules). Legs: long, femora I fusiform (not longer than femur II), covered with large denticles. Pedipalps: femora dorsally with large denticles, ventrally with smaller denticles. Penis: with large black wings, glans banana-form (not triangular).

Rilaena kasatkini sp. nov. is most similar to *R. lenkoranica* Snegovaya, 2007 (Snegovaya 2007:90, 91, figs. 10–18) and *R. talishica* (Snegovaya, 2007) (Snegovaya 2007:88, 89, figs. 1–9). From *R. lenkoranica*, it differs by being smaller, more heavily armed (denticles on the body and legs are much larger and greater in number), armament on the chelicera (large teeth on the distal segment versus almost no denticles), armament on the femur of the pedipalp ventrally (the denticles are larger), in structure of the penis (more developed very dark wings versus weak light wings). From *R. talishica*, it differs by being larger, more darkly colored, more developed armament on the body (especially in front of the eye mound), segments of the legs are larger and more armed, denticles on the legs are more numerous, penis is longer and spoon is more developed, femur of the pedipalp ventrally without large teeth versus large spine-tipped teeth on *R. talishica*, less developed and less setose apophyses versus well-developed setose apophyses in *R. talishica*.

Description.—Males relatively large harvestmen, body length (holotype measurements) 5.3 mm, width 2.8 mm, rectangular in form, covered with transverse rows of small denticles near tergite borders (Fig. 2a). A group of similar denticles situated in front of eye mound and on each side of it. Eye mound (Fig. 2b–c) large, trapezoidal, covered with 8–9 pairs rather large black-tipped denticles. Body dark-brown, almost black with small light spots. Legs long, pair I slightly thickened. Femur I fusiform (Fig. 2m), femora and patella covered with transverse rows of large denticles. Lengths of palpal segments: femur 1.5 mm, patella 1.0 mm, tibia 1.0 mm, tarsus 1.9 mm, total length 5.4 mm. Lengths of legs (mm): I - 2.1 + 0.6 + 1.8 + 2.3 + 3.3 = 10.1, II - 3.5 + 0.8 + 2.8 + 4.3 + 7.1 = 18.5, III - 2.3 + 0.7 + 1.8 + 2.8 + 3.8 = 11.4, IV - 3.3 + 0.8 + 2.3 + 3.1 + 6. 0 = 15.5. Chelicerae (Fig. 2c–f) not very large, basal segment dorsally with small denticles, distal segment with only setae. Basal segment of chelicera 1.5 mm long, distal 2.0 mm. Pedipalps not enlarged (Fig. 2i–j). Femora dorsally with large denticles, ventrally with smaller denticles. Patella and tibia with small apophyses. Penis (Fig. 2n–q) with wide base, expanded to the glans, forming a spoon, with rather large black wings; glans narrow, banana-shaped with long stylus. Penis length 3.2 mm, stylus 0.4, glans 0.2.

Female (Fig. 2d) differs from the male by larger size and rounded form of body, shorter legs, lighter color, chelicerae (Fig. 2g–h) and pedipalps (Fig. 2k–l) less armed, pedipalp apophyses larger and more densely covered by setae. Female (paratype): body length 7.2 mm, width 3.4 mm. Basal segment of chelicera 1.7 mm, distal 2.0 mm long. Length of palpal segments: femur 1.7 mm, patella 1.1 mm, tibia 1.0 mm, tarsus 2.0 mm, total length 5.8 mm. Length of legs (mm): I - 4 + 1.3 + 3.3 + 4.3 + 6.2 = 19.1, II - 7.2 + 1.3 + 3.5 + 6.0 + 7.8 + 14.4 = 40.2, III - 4.0 + 1.3 + 3.5 + 5.5 + 6.8 = 21.1, IV - 6.5 + 1.7 + 1.8 + 9.0 + 8.6 = 27.6. Seminal receptacle as in Fig. 2r.

Etymology.—The species is named in honor of the famous Russian entomologist, Dr. Denis Kasatkin (Rostov-on-Don), who kindly provided material for study.

Distribution.—This species is thus far known only from Golestan Province, Iran (Fig. 5).

Rilaena lenkoranica Snegovaya, 2007

Rilaena pusilla: Staręga 1978:218; Snegovaya 1999:455, figs. 29–33; Snegovaya 2004:318, figs. 36–41 (nec Roewer 1952, misidentified).

Rilaena lenkoranica Snegovaya 2007:90–92, figs. 10–18; Snegovaya & Staręga 2011:52, figs. 12–16.

Lophopilio palpinalis: Noei, Saboori & Hajizadeh 2013:57, 59, 62 (nec Herbst 1799, misidentified).

Material examined.—IRAN: *Gilan Province*: 6 ♂, 2 ♀, 16 km W of Assalem, 13–14 May 2015, D. Kasatkin, S. Kakunin (RCNS); 1 ♂, Masooleh city, 19 July 2010 (JAZM); 25 ♂, 21 ♀, Rostamabad District, near Hajideh village, 29 May 2014, D. Kasatkin, I. Shokhin (RCNS). *Markazi Province*: 1 ♂, 8 ♀, 1 juvenile, Sharra area, around Pol-e-Do, Ab river, autumn 2001, R. Vafaii (AZMI). *Mazandaran Province*: 7 ♂, 11 ♀, Elburs Mts, near Chalus, elev. 200 m, 26 May 2015, D. Kasatkin, S. Kakunin (RCNS).

Type locality.—Lenkoran, Azerbaijan.

Distribution.—Azerbaijan, Iran (Fig. 5).

Rilaena pusilla (Roewer, 1952)
(Figs. 3a–o & 5)

Zacheus hyrcanus Redikorzev 1936:45, 46, figs. 18, 19 (nec Thorell 1876, synonymized by Staręga 1973:144).

Platybunus pusillus Roewer 1952:513; Roewer 1956:305.

Metadasylobus dentichelis Roewer 1956:268, 269, figs. 65–68 (synonymized by Staręga 1973:144).

Rilaena pusilla: Staręga 1973:143–146, figs. 31–33; Staręga 1978:218 (in part, not record from Azerbaijan); Komposch 2002:99.

Material examined.—*Holotype* ♂. IRAN: *Golestan Province*: Gorgan (listed on label as ancient city name Astrabad), 1914, A. Kirichenko (ZIN).

Paratype. IRAN: *Golestan Province*: 1 ♀, collected with holotype (ZIN).

Other material. IRAN: *Golestan Province*: 2 ♂, 1 ♀, Gorgan, 1914, A. Kirichenko (ZIN); 13 ♂, 5 ♀ Golestan National Park, 37° 22′ 46.33″N, 55° 51′ 54.56″E, 24–25 May 2016, D. Kasatkin, (RCNS); 8 ♀, near Gorgan, Ziarat village, 36° 40′ 22.67″N, 54° 28′ 7.68″E, 27 May 2016, D. Kasatkin (RCNS); 2 ♂, 3 ♀, Gorgan, wheat field, 30 March 2001, Mobasheri (AZMI). *Kermanshakh Province*: 1 ♀, Shamshir village environs, 21 May 2015, D. Kasatkin, S. Kakunin (RCNS); 1 ♂, 1 ♀, Mazandaran, Sari, April 2012, A. Zamani (RCNS); 1 ♀, Sari, Shahid Zare Forest Park, 25 April 2001, Abaii (AZMI). *Markazi Province*: 1 ♀, Sharra area, around Pol-e-Do, Ab river, autumn, 2001, R. Vafaii (AZMI). *Azarbaijan-e Gharbi Province*: 2 ♀, near Piranshahr, 16 May 2015, D. Kasatkin (RCNS).

Type localities.—Gorgan, Golestan Province, Iran (*Zacheus hyrcanus*); Lahidjan, Gilan Province, Iran (*Platybunus pusillus*); Tehran, Tehran Province, Iran (*Metadasylobus dentichelis*).

Remarks.—To aid in the recognition of this species, we have illustrated both sexes. Male body (Fig. 3a), femur I (Fig. 3b), chelicerae (Fig. 3d–f), pedipalps (Fig. 3j–k), penis (Fig. 3g–i). Female body (Fig. 3c), chelicerae (Fig. 3n–o), pedipalps (Fig. 3l–m), seminal receptacle (Fig. 3p).

Distribution.—Iran (Fig. 5).

Family Sclerosomatidae Simon, 1879
Subfamily Leiobuninae Banks, 1893
Goasheer gen. nov.
http://zoobank.org:8080/NomenclaturalActs/urn:lsid:zoobank.org:act:298B16E1-C4E5-4B3C-B11D-C3DF4CB45882

Homolophus: Roewer 1952:513–515; Roewer 1957:355 (in part); Roewer 1960:32 (in part); Cokendolpher 1985:397 (in part).

Microliobunum: Cokendolpher 1987:94 (in part).

Type species.—*Homolophus iranus* Roewer, 1952.

Diagnosis and comparisons.—Small sclerosomatids with all leg femora shorter than body length, no lateral abdominal sclerites, ozopores visible from above. Leg femora and tibiae without nodules or pseudosegments. Penis alate with lateral wings which narrow into bristly lobes. Male pedipalp with tibiae modified into groove on retrolateral margin; tarsi with ventral rows of tubercles, palpal claw smooth.

The new genus is most similar to *Microliobunum* Roewer, 1912b from the western coast of Lebanon and *Dilophiocara* Redikorzev 1931 from Uzbekistan. These three genera having species that are small (3–5 mm body lengths), short-legged (femora II less than body length) Leiobuninae without a palpal apophysis. The palpal claws are toothed in *Dilophiocara* and *Microliobunum*, but not *Goasheer*.

Description.—Small opilionids, 3.2–3.9 mm total length, with short legs; all femora less than body length. Coxae I–IV with rows of tri-pointed denticles, sometimes absent on posterior surfaces; femora and tibiae without pseudosegments or pseudoarticulary nodules. Male palpal tibiae modified into groove on retrolateral margin; tarsi with ventral rows of tubercles, claw smooth. Genital operculum with lateral rows of tri-pointed tubercles. Penis with long tapered shaft, ending in sharp tip, with median alate portion ventrally with lateral wings which narrow into bristly lobes. Eye mound low, covered with many small tubercles. Large preocular protuberance present, covered with many small single and tri-pointed tubercles. Ozopores small and slightly elongate, visible from above. Palpal tarsus with rows of small tubercles, claw simple and smooth. Chelicerae with hook on first segment ventrally. Supracheliceral lamellae in form of two plates, covered with denticles.

Etymology.—The new name, *Goasheer*, is the ancient name for the city of Kerman, now the capital of the Kerman Province and also another name for "Bardsir", where specimens of this genus are recorded. It is not formed from Latin or Greek so following the I.C.Z.N. code 30.2.2, we are specifying the gender to be masculine.

Distribution.—Known only from high mountains in central Iran (Fig. 5).

Goasheer iranus (Roewer, 1952), comb. nov.
(Figs. 4a–f & 5)

Homolophus iranus Roewer 1952:513–515, fig. 2; Roewer 1957:355; Roewer 1960:32; Cokendolpher 1985:399.

Microliobunum iranum: Cokendolpher 1987:94.

Material examined.—Holotype ♂. IRAN: *Kerman Province*: Bardsir, Lalezar Mountain (=Kūh-e-Lāleh Zār and Kūh-i-Laizar), 29° 24′ N, 56° 46′ E, 1949–1950, H. Löffler, F. Starmühlner, stream at about 3,000 m elev. (SMF cat. no. RII/10720). Chelicera, palpus, and first leg of holotype on microscope slide, SMF cat. no. RII/16119-RII/10720/13.

Paratype. IRAN: *Kerman Province*: 1 ♂, collected with holotype (SMF).

Diagnosis.—As for genus.

Description.—Male (measurements of holotype first) (Fig. 4a–c): Body small, total length 3.21–3.85, greatest width 2.56–2.98, maximum height 1.62–2.09; covered with small tubercles; cream yellow with light brown spots in four rows on dorsum of abdomen; dorsum flattened, coarsely granulate; venter and lateral surfaces finely granulate. Eye mound low, maximum height 0.21–0.24, greatest width 0.45–0.41, length 0.39–0.37; eyes black contrasting strongly with tubercle. Preocular protuberance prominent, height 0.18–0.24. Supracheliceral lamellae with many small tubercles on distal margin. Chelicerae (Fig. 4e–f) yellow, teeth black; spur on basal segment ending in sharp point. Genital operculum length 1.19–1.18, width at base 1.22–1.26, width at neck 0.51–0.58. Pedipalps (Fig. 4d) yellow, robust; all segments with spines; femora, patellae, and tibiae with few sharp tubercles; tibia with groove on retrolateral margin; tarsi with ventral rows of tubercles, claw smooth. Palpal segment lengths: femora 0.71–0.64, patellae 0.51–0.46, tibiae 0.59–0.59, tarsi 0.83–0.87. Legs yellow; femora, patellae, and tibiae with many spines and tubercles. Femora I–IV lengths (respectively): 1.39–1.42, 2.51–2.40, 1.62–1.61, 2.42–2.49. Tibiae I–IV lengths (respectively): 1.30–1.39, 2.30–2.27, 1.46–1.40, 2.13–1.89. Penis (Fig. 4g–h) with long shaft, tapered to a fine tip distally; alate portion small, with many small setae laterally; length 1.93–2.11, width at midpoint 0.14–0.14.

Distribution.—Kerman Province of Iran (Fig. 5).

ACKNOWLEDGMENTS

We thank Dr. Manfred Grasshoff of the Senckenberg Nature Museum for loan of Roewer's type specimens of *Homoloplus iranus* and specimens of comparative material of other short-legged Leiobuninae [*Dilophiocara, Eusclera, Microliobunum, Microuelima*, and *Scheukeliobunum*] from Asia and Dr. Reza Vafaii for donating some Opiliones specimens to AZMI which were studied among other specimens studied in this project. Dr. A. Krivokhatsky (St. Petersburg, Russia) for access to the material kept in the Zoological Institute of RAS, St.-Petersburg. Dr. D. Kasatkin (Rostov-on-Don, Russia), Mr. S. Kakunin (Krasnodar, Russia) and Dr. A. Zamani (Tehran, Iran) for help with collecting of Opiliones. We thank Dr. Javad Noei for the aid in studying the *Rilaena lenkoranica* from his Institute (Department of Plant Protection, Faculty of Agriculture, University of Birjand). That specimen of *R. lenkoranica* is now housed at the Acarological Collection, Jalal Afshar Zoological Museum (JAZM), Department of Plant Protection, Faculty of Agriculture, University of Tehran, Karaj, Iran.

LITERATURE CITED

Audouin, V. 1826. Explication sommaire des planches d'Arachnides de l'Égypte et de la Syrie, publiées par Jules-César Savigny, Membre de l'Institut; offrant un exposé des caractères naturelles des genres, avec la distinction des espèces. *In* J. C. Savigny, Description de l'Egypte, ou recueil des observations et des recherches qui ont été faites en Égypte pendant l'Expédition de l'armée française, publié par les ordes de sa majesté l'empereur Napoléon le Grand. Histoire Naturelle 1(4):99–186, pl. 1–9. Paris.

[Bogachev, A.A.] 1951. Opiliones. Pp. 405–406 *In* Zhivotniy mir Azerbaidzhana. [Animal World of Azerbaijan]. Academy of Sciences of the Azerbaijan Soviet Socialist Republic, Institute of Zoology. Baku [in Russian].

Chevrizov, B.P. 1978. [On the question of use of scanning electron microscope in harvestmen diagnostics (Opiliones)]. [Fine structural peculiarities of terrestrial arthropods.] [Proceedings of Sciences of the USSR, Proceedings of the Zoological Institute] 77:70–73 [+2 unnumbered pages at back of book, figures 1–12].

Chevrizov, B.P. 1979. [A brief key to the harvest-spiders (Opiliones) of the European territory of the USSR]. [The Fauna and Ecology of Arachnida]. Trudy Zoologicheskogo Instituta AN SSSR [Proceedings of the Zoological Institute Academy of Sciences of the USSR] 85:4–27 [in Russian].

Cokendolpher, J.C. 1985. Revision of the harvestman genus *Leptobunus* and dismantlement of the Leptobunidae (Arachnida: Opiliones: Palpatores). Journal of the New York Entomological Society 92:371–402.

Cokendolpher, J.C. 1987. On the identity of the genus *Homolophus*: a senior synonym of *Euphalangium* (Opiliones: Phalangiidae). Acta Arachnologica 35:89–96.

Çorak, İ. & A. Bayram. 2007. Harvestmen fauna of the Soğuksu National Park, Ankara (Arachnida: Opiliones). Munis Entomology & Zoology 2:455–460.

DeGeer, C. 1778. Mémoires pour servir à l'histoire des insects. Stockholm. Tome VII.

Fabricius, J.C. 1779. Reise nach Norwegen mit Bemerkungen aus der Naturhistorie und Oekonomie. Carl Ernst Bohn, Hamburg, pp. lxiv + 388 + [12].

Farzalieva, G. Sh. & S.L. Esyunin. 1999. The harvestman fauna of the Urals, Russia, with a key to the Ural species (Arachnida: Opiliones). Arthropoda Selecta 8(3):183–199.

Gritsenko, N.I. 1979. [The harvest-spiders (Opiliones) in the Asian territory of the USSR.]. [The Fauna and Ecology of Arachnida]. Trudy Zoologicheskogo Instituta AN SSSR [Proceedings of the Zoological Institute Academy of Sciences of the USSR] 85:28–38.

Gritsenko, N. I. 1980. [K faune senokostsev (Opiliones) Mongolii i sopredel'nykh rayonov Kitaya i SSSR = On the fauna of Opiliones of Mongolia and adjacent regions of China and the USSR]. Nasekomye Mongolii [Insects of Mongolia] (Sovmestnaya Sovetsko-Mongolskaya Kompleksnaya Biologicheskaya Ekspeditsiya) 7:553–565.

Gruber, J. 1998. Beiträge zur Systematik der Gattung *Dicranolasma* (Arachnida: Opiliones, Dieranolasmatidae). I. *Dicranolasma thracium* Staręga und verwandte Formen aus Südosteuropa und Südwestasien. Annalen des Naturhistorischen Museums in Wien. Serie B für Botanik und Zoologie 100:489–537.

Herbst, J.F.W. 1799. Natursystem der Ungeflügelten Insekten. III. Fortsetzung der Naturgeschichte der Insectengattung *Opilio*. G.A. Lange, Berlin.

Komposch, C. 2002. Spinnen, Weberknechte, Skorpione und Walzenspinnen aus dem Iran (Arachnida: Araneae, Opiliones, Scorpiones, Solifugae). Pp. 99–103. *In* Gutleb, B. & Ch. Wieser: Ergebnisse einer zoologischen Exkursion in den Nordiran, 2001. Carinthia II, 192/112:8–103.

Kratochvíl, J. 1958. Höhlenweberknechte Bulgariens (Palpatores-Nemastomatidae). Práce Brněnské základny Československé akademie věd, Brno 30:523–576.

Kurt, K., H. Koç & E.A. Yağmur 2015. Two new records for Turkish harvestmen fauna (Arachnida: Opiliones). Entomological News 125:127–135.

Martens, J. 1978. Spinnentiere, Arachnida: Weberknechte, Opiliones. Die Tierwelt Deutschlands. Vol. 64. G. Fischer Verlag, Jena.

Martens, J. 2006. Weberknechte aus dem Kaukasus (Arachnida,

Opiliones, Nemastomatidae). Senckenbergiana biologica 86:145–210.

[Mkheidze T.S.] 1952. [New species of Opiliones from Georgia]. [Report of Academy of Sciences Georgian SSR], Tbilisi, 13(10):613–616 [in Russian].

[Mkheidze, T.S.] 1959. [Materials by study of specific composition: spread of harvest-spiders in Georgian SSR]. [Trudy Tbilisskogo gosudarstvennogo Universiteta im. Stalina; Proceedings of Tbilisi University], Tbilisi, 70:109–117 [in Georgian with Russian summary].

[Mkheidze, T.S.] 1962. [A study of arachnids from Kharagauł district]. [Trudy Tbilisskogo Universiteta; Proceedings of Tbilisi University], Tbilisi, 82[1960]:183–189 [in Georgian].

[Mkheidze, T.S.] 1964. [Mtibavebi (Opiliones). Pp. 117–126 *In* Sakartvelos cchoveloa samgaro, 2. Peehsaehsrianebi. Tierwelt in Grusien - The animal world of Georgia, 2. Arthropoda]. Tbilisi [in Georgian].

Morin, S.M. 1937. Kaukasische Weberknechte (Opiliones). Trudi Odes'kogo Deržavnogo Universitetu, Biologia 2:209–222.

Murányi, D. 2015. First record of the genus *Graecophalangium* Roewer, 1923 (Opiliones: Phalangiidae) from Albania, with redescription of *G. militare* (C.L. Koch, 1839). Ecologica Montenegrina 4:4–13.

Noei, J., A. Saboori & J. Hajizadeh 2013. Redescription of the little known species, *Ralphaudyna iranensis* (Acari: Chyzeriidae). Persian Journal of Acarology 2:57–62.

Redikorzev, V.[V.] 1931. Ein neuer Weberknecht aus Buchara. Zoologischer Anzeiger 97:31–32.

Redikorzev, V.V. 1936. Beiträge zur Opilioniden-Fauna von U.S.S.R. Trudy Zoologiceskogo 3:33–57.

Roewer, C.F. 1911. Übersicht der Genera der Subfamilie der Phalangiini der Opiliones Palpatores nebst Beschreibung einiger neuer Gattungen und Arten. Archiv für Naturgeschichte, Berlin, Abteilung A, Original-Arbeiten, 77 (Supplementheft 2):1–106, plates 1–3.

Roewer, C.F. 1912a. Revision der Opiliones Palpatores (=Opiliones Plagiostethi) II. Teil: Familie der Phalangiidae. (Subfamilie: Selerosomini, Oligolophini, Phalangiini). Abhandlungen aus dem Gebiete der Naturwissenschaften, herausgegeben vom Naturwissenschaftlichen Verein in Hamburg 20(1):1–295, plates 1–4.

Roewer, C.F. 1912b. Einige neue Gattungen und arten der Opiliones Palpatores aus den subfamilien der Gagrellinae und Liobuninae der Familie der Phalangidae. Archiv für Naturgeschichte 78(A), Heft 1, pp. 27–59.

Roewer, C.F. 1915. 106 neue Opilioniden. Archiv für Naturgeschichte, Berlin, Abteilung A, Original-Arbeiten 81(3):1–152.

Roewer, C.F. 1919. Über Nemastomatiden und ihre Verbreitung. Archiv für Naturgeschichte 83(3):140–160.

Roewer, C.F. 1923. Die Weberknechte der Erde. Systematische Bearbeitung der bisher bekannten Opiliones. Gustav Fischer, Jena.

Roewer, C.F. 1952. Die Solfugen und Opilioniden der österreichischen Iran-Expedition 1949–1950. Sitzungsberichte und Anzeiger der Österreichische Akademie der Wissenschaften, Mathematisch-Naturwissenschaftliche Klasse, Wien, Abteilung I, Biologische Wissenschaften und Erdwissenschaften 161(7):509–516.

Roewer, C.F. 1956. Über Phalangiinae (Phalangiidae, Opiliones, Palpatores). (Weitere Weberknechte XIX.). Senckenbergiana biologica 37:247–318.

Roewer, C.F. 1957. Über Oligolophinae, Caddoinae, Selerosomatinae, Leiobuninae, Neopilioninae und Leptobuninae (Phalangiidae, Opiliones Palpatores). Senckenbergiana biologica 38:323–354.

Roewer, C.F. 1960. Solifugen und Opilioniden- Araneae, Orthognathae, Haplogynae und Entelegynae (Contribution l'étude de la fauna d'Afghanistan 23). Göteborgs Kungliche Vetenskaps- och Vitterhets Samhälles handlingar 6(8B7):1–53.

Schönhofer, A.L. 2013. A taxonomic catalogue of the Dyspnoi Hansen and Sorensen, 1904 (Arachnida: Opiliones). Zootaxa 3679:1–68.

Šilhavý, V. 1966. Beitrag zur Kenntnis der Opilioniden-fauna Afghanistans (Arachn.). Acta Musei Moraviae 51:251–258.

Šilhavý, V. 1968. Beitrag zur Kenntnis der Fauna Afghanistans (Sammelergebnisse von O. Jakeš 1963–64, D. Povolný 1965, D. Povolný & Fr. Tenora 1966, J. Šimek 1965–66, D. Povolný, J. Geisler, Z. Šebek & Fr. Tenora 1967). Opilionidea (Nachtrag). Časopis Moravského Musea 53:313–319.

Snegovaya, N. Yu. 1999. Contribution to the harvest spider (Arachnida, Opiliones) fauna of the Caucasus. Turkish Journal of Zoology 23:453–459.

Snegovaya, N. Yu. 2004. Preliminary notes on the harvestman fauna (Opiliones) of Azerbaijan. *In* Logunov, D.V. & Penney, D. (eds), European Arachnology 2003. Arthropoda Selecta (Special Issue No. 1):305–318.

Snegovaya, N. Yu. 2005. Four new harvestman species from Azerbaijan (Arachnida: Opiliones: Phalangiidae). Arthropoda Selecta 14:19–32.

Snegovaya, N. Yu. 2007. Two new harvestman species from Lenkoran, Azerbaijan (Arachnida: Opiliones: Phalangiidae). Bulletin of the British Arachnological Society 14:88–92.

Snegovaya, N. Yu. 2010. Further studies on harvestmen of the genus *Opilio* Herbst, 1798 (Arachnida: Opiliones: Phalangiidae) from the Caucasus. [Caucasian Entomological Bulletin] 6(1):3–18.

Snegovaya, N. Yu. & Yu. A. Chumachenko. 2011. Harvestmen (Arachnida: Opiliones) from the yew and box-tree grove of the Caucasian State Natural Biospheric Reserve, Russia. [Caucasian Entomological Bulletin] 7(2):115–124.

Snegovaya, N. Yu. & V.D. Pkhakadze. 2014. New species of the genus *Rilaena* (Opiliones, Phalangiidae) from the Mount Gyamish, Azerbaijan. Vestnik Zoologii 48:313–318.

Snegovaya, N. Yu. & W. Staręga. 2008. A new *Homolophus* species (Opiliones: Phalangiidae) from Lenkoran zone in Azerbaijan. Acta Arachnologica 57:15–17.

Snegovaya, N. Yu. & W. Staręga. 2009. *Taurolaena*, a new genus of Phalangiidae (Opiliones). Revista Ibérica de Aracnología 17:37–44.

Snegovaya, N. Yu. & W. Staręga. 2011. Harvestmen (Arachnida, Opiliones) from Talysh, with description of a new genus and other taxonomical changes. Fragmenta Faunistica 54:47–58.

Staręga, W. 1966. Beitrag zur Kenntnis der Weberknecht-Fauna (Opiliones) der Kaukasusländer. Annales Zoologici 23:387–411.

Staręga, W. 1973. Beitrag zur Kenntnis der Weberknechte (Opiliones) des Nahen Ostens. Annales Zoologici 30:129–153.

Staręga, W. 1978. Katalog der Weberknechte (Opiliones) der Sowjet-Union. Fragmenta Faunistica 23:197–234.

Staręga, W. 2003. On the identity and synonymies of some Asiatic Opilioninae (Opiliones: Phalangiidae). Revision of the Phalangiidae, IV. Acta Arachnologica 52:91–102.

Tchemeris, A.N. & N. Yu. Snegovaya. 2010. Three new species of Phalangiidae (Arachnida: Opiliones) from Turkmenistan. Acta Arachnologica 59:67–72.

Tchemeris, A.N., D.V. Logunov & N. Tsurusaki. 1999. A contribution to the knowledge of the harvestman fauna of Siberia (Arachnida: Opiliones). Arthropoda Selecta 7:189–199.

Thorell, T. 1876. Sopra alcuni Opilioni (Phalangidea) d'Europe e dell' Asia occidentale, con un quadro dei generi europei di quest' Ordine. Annali del Museo Civico di Storia Naturelle di Genova 8:452–508.

Manuscript received 12 February 2017, revised 21 June 2017.

2018. Journal of Arachnology 46:81–103

Five new hypogean *Occidenchthonius* (Pseudoscorpiones: Chthoniidae) from Portugal

Juan A. Zaragoza[1] and **Ana Sofia P.S. Reboleira**[2,3]: [1]Departamento de Ecología, Facultad de Ciencias, Universidad de Alicante, E-03690 Alicante, Spain. E-mail: ja.zaragoza@ua.es; [2]Natural History Museum of Denmark (Zoological Museum), University of Copenhagen, Universitetsparken 15, DK-2100 Kobenhavn Ø, Denmark; [3]Departamento de Biologia & CESAM, Universidade de Aveiro, Portugal.

Abstract. Five new species of the recently created genus *Occidenchthonius* Zaragoza, 2017 are described from caves of Portugal: *Occidenchthonius alandroalensis* sp. nov., *O. algharbicus* sp. nov., *O. dnecensis* sp. nov., *O. goncalvesi* sp. nov. and *O. vachoni* sp. nov. The species *Occidenchthonius cardosoi* (Zaragoza, 2012) and *Chthonius ischnocheles* (Hermann, 1804) are reported from new localities in different karst units of Portugal. New morphological characters are proposed for use in the Chthoniidae taxonomy. An updated key to the genus *Occidenchthonius* is given.

Key words: Pseudoscorpions, taxonomy, caves, karst, Iberian Peninsula.

ZooBank publication: http://zoobank.org:8080/References/A7261030-F4B4-4301-99F5-5C144C948245.

The pseudoscorpion genus *Occidenchthonius* Zaragoza, 2017 was recently created to accommodate some species previously assigned to the subgenus *Ephippiochthonius* Beier, 1930. It shares the presence of coxal spines in coxae II and III with the other *Chthonius*-related genera: *Cantabrochthonius* Zaragoza, 2017, *Chthonius* C.L. Koch, 1843, *Ephippiochthonius*, *Globochthonius* Beier, 1931, *Hesperochthonius* Muchmore, 1968, *Microchthonius* Hadži, 1933, *Neochthonius* Chamberlin, 1929 and *Spelyngochthonius* Beier, 1955 (as termed by Zaragoza 2017). However, *Occidenchthonius* is distinguished by a combination of characters that include: i) ephippiochthonian chelal form; ii) marked ventral hollow (*vh*) with thicker cuticle before base of movable finger; iii) absence of a medial protuberance between chelal condyles; iv) four setae at the proximal portion of chelal hand in adults and tritonymphs, seta ph_3 present; v) absence of paraxial dorsal seta ih_5 in some species; vi) third tooth of normal row (*mt*) of fixed finger modified in shape and orientation; vii) absence of a subdistal protuberance (*sp*) in the fixed chelal finger of males and tritonymphs; viii) base of movable chelal finger with a distinct enlarged condyle (*bc*), proximally with a sclerotized and well developed apodeme (*ap*); ix) absence of lyrifissures ma_1 and ma_2; x) presence of a bisetose intercoxal tubercle between coxae III and IV; xi) distal marginal seta of pedipalpal coxa disk (*dps*) distinctly longer than that of coxa I (*dcs*), exceptionally of same length; xii) sternite III in male and female usually with eight marginal macrosetae, close to the stigmata without lateral short seta on each side; and xiii) male genitalia without a median hiatus dividing each row of the guard-setae (Zaragoza 2017).

Occidenchthonius is mainly distributed in the Canary Islands and Southern Iberian Peninsula, currently being the most diverse genus of Chthoniini in both areas (Zaragoza 2017).

Intense fieldwork in caves of Portugal over the last decade provided surprising new genera and species of cave-adapted pseudoscorpion fauna (Reboleira et al. 2010, 2011, 2012, 2013a, b), including five new species of *Occidenchthonius* which are here described, as well as new localities for several previously known species.

METHODS

Specimens were obtained in deep insulated parts of caves along Portugal, using a combination of active and passive standardized collecting methods (see Reboleira 2012).

For scanning electron microscopy (SEM) study, specimens were transferred to absolute ethanol, critical point-dried in a Tousimis Autosamdi 815, serie A, mounted on aluminium stubs, coated with platinum/palladium and studied using a JEOL JSM-6335F scanning electron microscope.

Specimens were examined as temporary glycerine mounts in cavity slides after dissection of one chelicera and one pedipalp, of which the chela was also separated. Posteriorly they were preserved in 70% ethanol inside glass vials, with the dissected articles placed in a glass microvial. When necessary, some specimens were previously cleared by immersion in 60% lactic acid at room temperature for a few days. A trinocular Zeiss Axiolab light microscope was used for detailed study and measurements were taken with an ocular micrometer, using the reference points proposed by Chamberlin (1931).

Measurements are expressed in millimetres, followed by standard ratios in parentheses. The ratios given are length/width for carapace, chelicerae and pedipalps, except in the case of the chela and its hand, for which the depth was used instead of width (Mahnert 2011b). When two different articles are compared, the ratio is the length/length index; if only one measurement is given for an article it corresponds to the length. The general terminology follows Chamberlin (1931), including trichobothriotaxy, with modifications or additions proposed by Harvey (1992) and Judson (2007). The chaetotactic formulae of the carapace and chelicera follow Gabbutt & Vachon (1963). Terminology of setae on carapace, pedipalpal coxa and chelal hand, follows Zaragoza (2017). Lyrifissures terminology for pedipalpal chela and chelicera is as in Zaragoza (2017). Following data are given: lengths and ratio of the anteromedial (*ame*) and sublateral ocular setae (*osl*) of the carapace, unless lost; value of the angle formed by setae *dps-mps-lps* in the pedipalpal coxa disk; ratio chelal hand depth/seta ih_2; length of tactile setae on tergites IX and XI and sternite X.

Abbreviations used in the text: *Repositories*. DEUA: Departamento de Ecología, Universidad de Alicante, Spain; MCNB: Museu de Ciències Naturals de Barcelona; MHNG: Muséum d'Histoire Naturelle, Geneva; MNCN: Museo Nacional de Ciencias Naturales, Madrid; MNHN: Muséum national d'Histoire naturelle, Paris; NHMW: Naturhistorisches Museum Wien; ZMUC: Zoological Museum, Natural History Museum of Denmark. *Other abbreviations used in text*: *A*: angle coxal setae *dps-mps-lps*; *al*: anterolateral seta of carapace; *ame*: anteromedial seta of carapace; *an*: anterior setae row of carapace; *ap*: apodeme; *as*: antiaxial sensory setae; *bc*: basal condyle; *dcs*: distal marginal seta of coxa I; dh_1, dh_2, dh_3, dh_4: distal setae row of chelal hand; *di*: isolated subapical tooth; *dps*: distal marginal seta of pedipalpal coxa; *fa*: antiaxial lyrifissure of fixed chelal finger; *fb*: basal lyrifissure of fixed chelal finger; fd_1, fd_2, fd_3: dorsal lyrifissures of the fixed chelal finger; *fp*: paraxial lyrifissure of fixed chelal finger; *hd*: distal lyrifissure of chelal hand; *hp*: proximal lyrifissure of chelal hand; ih_1, ih_2, ih_3, ih_4, ih_5: intermediate setae row of chelal hand; *il*: intermedian lateral seta of carapace; *in*: intermedian setae row of carapace; *ldb*, *ldst*, *ldt*, *lvb*, *lve*, *lvt*: lyrifissures associated with cheliceral setae *db*, *dst*, *dt*, *vb*, *ve* and *vt*, respectively; *lps*: lateral marginal seta of pedipalpal coxa; *m*: microseta; ma_1, ma_2: antiaxial lyrifissures of movable chelal finger; *me*: median setae row of carapace; *ml*: median lateral seta of carapace; *mm*: median medial seta of carapace; *mms*: marginal microsetae coxa I; *mps*: medial seta of pedipalpal coxa; *mt*: modified tooth; mv_1, mv_2: ventral lyrifissures of movable chelal finger; *oc*: ocular setae row of carapace;*ol*: lateral ocular seta of carapace; *om*: medial ocular seta of carapace; *osl*: sublateral ocular seta of carapace; *pc*: coupled sensilla; ph_1, ph_2, ph_3, ph_4: proximal setae row of chelal hand; *pl*: posterolateral seta of carapace; *pm*: posteromedial seta of carapace; *po*: posterior setae row of carapace; *sp*: subdistal protuberance; T: tactile seta; *td*: accessory tooth; *vh*: ventral hollow in chelal hand.

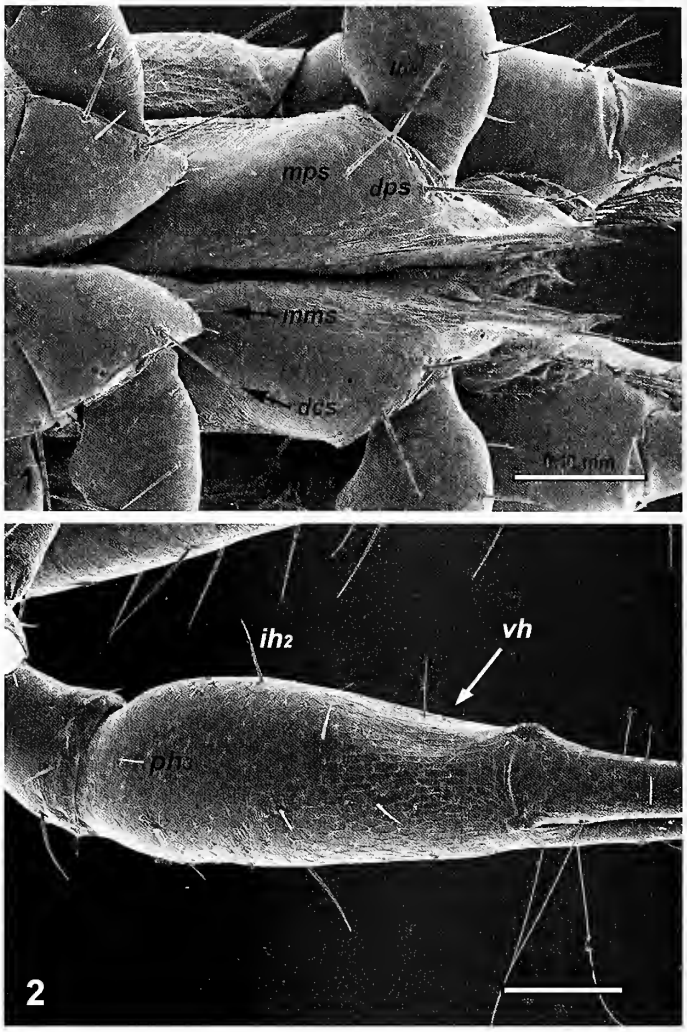

Figures 1–2.—*Occidenchthonius algharbicus* sp. nov., SEM pictures, female. (1) Pedipalpal coxae and coxae I, ventral view. (2) Left chelal hand, ventral view. See Methods for abbreviations.

SYSTEMATICS

Discussion of characters and terminology.—*Carapacal chaetotaxy:* Gabbut & Vachon (1963) considered that the carapacal setae in *Chthonius ischnocheles* (Hermann, 1804) were lying in five rows: *anterior*, *ocular*, *median*, *intermedian* and *posterior*, which they represented by the formula: 4-6-4-2-4. Some of the carapacal setae have been named by Zaragoza (2017) and are included in this study (Fig. 3). Lengths of some carapacal setae have been given in Chthoniidae descriptions (e.g., Mahnert 2011a; Gardini 2013; Zaragoza 2017), usually the anteromedial ones (*ame*), whose measurements may differ among species (Zaragoza et al. 2007). A character that should be pointed out and mentioned in descriptions is the posterolateral setae which, when they occur, are usually very short, of microsetae size, but sometimes longer (e.g., Zaragoza 2012, 2017). Sublateral ocular setae of carapace (*osl*) are rarely considerably or even extremely reduced in length in a few species (e.g., Mahnert 1993; Zaragoza 2017; this study); then, it is considered an important interspecific difference and, for a better quantification, the ratio *ame*/*osl* is useful.

Chelal hand chaetotaxy: a designation system was proposed by Zaragoza (2017) for the chaetotaxy of the chelal hand in Chthoniidae (Fig. 7). Presence/absence of seta ph_3 at the proximal row is a very important character in the diagnosis of the *Chthonius*-related genera; also the absence of seta ih_5 characterizes the *machadoi*-group within the genus *Occidenchthonius* (Zaragoza 2017). Other hand setae may show variation in their length, particularly in the genera *Ephippiochthonius* and *Occidenchthonius*, as occurs with seta ih_2 (Fig. 2) that may be short or as long as the hand depth, which is considered an interspecific variation of taxonomic importance and, for an accurate measure, the ratio hand depth/ih_2 length is proposed.

Pedipalp coxal setae: pedipalpal coxa bears three setae in the disk of most chthoniid genera, usually 2 marginal and 1 discal setae, being here named *dps*, *mps* and *lps* (Fig. 1). The importance of the length of the distal marginal seta (*dps*) of the pedipalpal coxa compared with the length of distal marginal seta (*dcs*) on coxa I was stated by Zaragoza (2017) for the diagnosis of genus *Cantabrochthonius*. The position of seta *mps* is usually extremely discal in comparison with the other two marginal setae; however, the position of *mps* may rarely be moved close to the line *dps-lps* in some few species, forming an angle higher than 100° [Mahnert 2011a described 2

marginal and 1 submarginal setae for the species *O. lopezi* (Mahnert, 2011); other Canarian species have the same pattern: *O. canariensis* (Beier, 1965), *O. dubius* (Mahnert, 1993) and *O. setosus* (Mahnert, 1993), J.A. Zaragoza, pers. obs.; also in Portuguese species: *O. duecensis* sp. nov. and *O. vachoni* sp. nov., this study], which is considered an important interspecific character. The angle formed by the areolar insertions of disk setae *dps-ups-lps* is given in descriptions and illustrated (Figs. 6, 36, 43).

TAXONOMY

Family Chthoniidae Daday, 1888
Subfamily Chthoniinae Daday, 1888
Tribe Chthoniini Daday, 1888
Genus *Occidenchthonius* Zaragoza, 2017

Occidenchthonius Zaragoza 2017:126–127.

Type species.—*Chthonius (Ephippiochthonius) machadoi* Vachon, 1940, by original designation.

KEY TO ADULTS OF THE *OCCIDENCHTHONIUS* SPECIES

1. Chelal hand chaetotactic formula 4:4:4, seta ih_5 absent. Cheliceral hand lyrifissure *ldb* present (*O. machadoi*-group) 2
   Chelal hand chaetotactic formula 4:5:4, seta ih_5 present. Cheliceral hand lyrifissure *ldb* present or absent..... 12
2. Epigean species. Well developed eyes, anterior and posterior eyes with convex lens 3
   Hypogean species. Eyeless or posterior eyes reduced to eye-spots..... 4
3. Fixed chelal finger with 12–16 teeth and movable with 7. Chela stouter: (♂) 4.5, (♀) 3.8–4.7 times longer than deep.... ..... *O. machadoi* (Vachon, 1940)
   Fixed chelal finger with 20–21 teeth, movable 9–10. Chela more slender: (♂) 5.1, (♀) 4.6–4.9 times longer than deep ... . *O. canariensis* (Beier, 1965)
4. Basal half of movable chelal finger with 5 or more rounded, partially fused, vestigial teeth, without canals, on raised lamina 5
   Basal half of movable chelal finger with only 1 rounded, vestigial teeth, without canal, on weak lamina..... ..... *O. alandroalensis* sp. nov.
5. Carapace with a total of 2–8 preocular and ocular microsetae..... 6
   Carapace with a total of 16 preocular and ocular microsetae..... *O. setosus* (Mahnert, 1993)
6. Posterior margin of carapace with 2 (exceptionally 3) setae..... 7
   Posterior margin of carapace with 4 (very exceptionally 3 or 5) setae..... 11
7. Anophthalmic..... *O. oromii* Zaragoza, 2017
   Eyes present, at least anterior eyes with weak lens, posterior eyes reduced to indistinct spots..... 8
8. Dorsal face of chelal hand without lyrifissure *hd*..... *O. gracilimanus* (Mahnert, 1997)
   Dorsal face of chelal hand with lyrifissure *hd* 9
9. Distal half of movable chelal finger with 9–10 pointed teeth up to slightly proximad of trichobothrium *st*, basal half with 8–12 rounded and fused vestigial teeth up to level slightly proximad of trichobothrium *sb* 10
   Distal half of movable chelal finger with 12–15 pointed teeth up to halfway between trichobothria *st* and *sb*, basal half with 10–12 rounded and fused vestigial teeth up to halfway between trichobothria *sb* and *b*..... ..... *O. malnerti* Zaragoza, 2017
10. Anterior medial margin of carapace prominent; cheliceral spinneret absent in male; stouter and smaller pedipalp: femur (♂) 6.0–6.1, (♀) 5.9 times longer than broad, length (♂) 0.53 mm, (♀) 0.53–0.58 mm; hand (♂) 2.2–2.3, (♀) 2.1 times longer than deep; chela (♂) 5.7–5.8, (♀) 5.0–5.2 times longer than deep, length (♂) 0.71–0.72 mm, (♀) 0.75–0.76 mm ..... *O. beieri* Zaragoza, 2017
    Anterior medial margin of carapace nearly straight; cheliceral spinneret present in male, hump like; pedipalp femur (♂) 6.8–7.2, (♀) 6.0–6.9 times longer than broad, length (♂) 0.62–0.65 mm, (♀) 0.63–0.72 mm, hand (♂) 2.4–2.6, (♀) 2.2–2.5 times longer than deep, chela (♂) 5.9–6.5, (♀) 5.5–6.2 times longer than deep, length (♂) 0.79–0.88 mm, (♀) 0.84–0.95 mm ..... *O. tamaran* (Mahnert, 2011)
11. Smaller, chela length (♀) 0.69 mm, 5.0–5.5 times longer than deep; trichobothrium *ist* slightly distad to *esb*..... ..... *O. lopezi* (Mahnert, 2011)
    Larger, chela length (♀) 1.08 mm, 6.1 times longer than deep; trichobothrium *ist* distinctly distad of *esb*..... ..... *O. tenerifae* (Mahnert, 2011)
12. Movable cheliceral finger with isolated subapical tooth (*di*)..... 13
    Movable cheliceral finger without isolated subapical tooth (*di*) 25
13. Posterior margin of carapace with 4 macrosetae..... 14
    Posterior margin of carapace with 2 macrosetae..... 16
14. Epigean species with normal eyes; carapace with 2 preocular microsetae on each side; fixed chelal finger with 12–16 triangular teeth (not including proximal rounded teeth); smaller: chela length (♂) 0.45–0.57 mm, (♀) 0.50–0.66 mm... 15
    Endogean or hypogean species, eyes reduced or absent; carapace with 1 preocular microseta on each side; fixed chelal finger with 17–21 triangular teeth (not including proximal rounded teeth); larger: chela length (♂) 0.89–1.12 mm, (♀) 0.84–1.37 mm ..... *O. cassolai* (Beier, 1973)

15. Proximal half of fixed chelal finger with 2–5 rounded teeth merging into an evident high bulge of marginal lamina... ..... *O. parmensis* (Beier, 1963)
Proximal half of fixed chelal finger with 2–5 rounded and spaced teeth, marginal lamina weakly raised .... *O. berninii* (Callaini, 1983)
16. Anophthalmic..... 17
With eyes, anterior pair with convex lens, posterior pair reduced to spots 24
17. Trichobothrium *ist* distinctly distad of *esb* 18
Trichobothrium *ist* proximad of *esb* .... *O. morenoi* (Carabajal Márquez, García Carrillo & Rodríguez Fernández, 2011)
18. Trichobothrium *ist* proximad of lyrifissure *fb* 19
Trichobothrium *ist* distinctly distad of lyrifissure *fb* 21
19. Larger and more slender: (♀) pedipalpal femur 7.5 times longer than broad, length 0.88 mm; chela (♀) 7.3 times longer than deep, length 1.23 mm ..... *O. sendrai* (Zaragoza, 1985)
Smaller and less slender: (♀) pedipalpal femur 5.8–6.5 times longer than broad, length 0.52–0.62 mm; chela (♀) 5.2–5.5 times longer than deep, length 0.70–0.86 mm 20
20. Chelicera with 6 setae and 4–5 lateral microsetae on hand..... *O. thaleri* (Gardini, 2009)
Chelicera with 6 setae and only 1 lateral microseta on hand..... *O. minutus* (Vachon, 1940)
21. Tergite 1 with 2 setae..... *O. ambrosiae* (Carabajal Márquez, García Carrillo & Rodríguez Fernández, 2012)
Tergite 1 with 4 setae..... 22
22. Cheliceral hand with 6 setae (excluding microsetae) 23
Cheliceral hand with 7–8 setae (excluding microsetae)..... ..... *O. bullonorum* (Carabajal Márquez, García Carrillo & Rodríguez Fernández, 2012)
23. Larger and slender: pedipalpal femur (♀) 7.5–7.7 times longer than broad, length (♀) 0.93–1.00 mm; chela (♀) 5.9–6.0 times longer than deep, length (♀) 1.27–1.37 mm ..... *O. felgueraorum* Zaragoza, 2017
Shorter and less slender: pedipalpal femur (♀) 5.5 times longer than broad, length 0.56 mm; chela (♀) 5.2 times longer than deep, length 0.78 mm ..... *O. villacarrillo* (Zaragoza & Pérez, 2013)
24. Lyrifissure *ldb* present on cheliceral hand, close to seta *db*. Trichobothrium *ist* slightly distad of *esb* and well proximad of lyrifissure *fb*..... *O. anae* Zaragoza, 2017
Lyrifissure *ldb* absent on cheliceral hand. Trichobothrium *ist* well distad of *esb* and slightly proximad of lyrifissure *fb* ..... *O. dubius* (Mahnert, 1993)
25. Posterior row of carapace with 2 macrosetae..... 26
Posterior row of carapace with 4 macrosetae..... *O. cardosoi* (Zaragoza, 2012)
26. Chelal hand lyrifissure *lp* absent..... 27
Chelal hand lyrifissure *lp* present..... 28
27. Carapace without preocular microsetae ..... (*O. verai*-group)...33
Carapace with 2 preocular microsetae on each side..... *O. pinai* (Zaragoza, 1985)
28. Epigean species with well developed eyes..... *O. serranoi* Zaragoza, 2017
Hypogean species anophthalmic 29
29. Chelal hand lyrifissure *lid* absent. Pedipalpal coxa setae *dps-mps-lps* forming an angle distinctly greater than 90° 30
Chelal hand lyrifissure *lid* present. Pedipalpal coxa setae *dps-mps-lps* forming an angle distinctly smaller than 90° 31
30. Carapacal sublateral ocular setae (*osl*) extremely reduced to microsetae size, ratio setae *ame*/*osl* 5.0–7.2..... ..... *O. vachoni* sp. nov.
Carapacal sublateral ocular seta (*osl*) not reduced to microsetae size, ratio setae *ame*/*osl* 1.9–2.5 .... *O. duecensis* sp. nov.
31. Smaller: pedipalp femur (♀) length 0.72–1.01 mm; chela (♀) length 0.94–1.29 mm..... 32
Larger: pedipalp femur (♀) length 1.28–1.30 mm; chela (♀) length 1.72–1.82 mm..... *O. ortunoi* Zaragoza, 2017
32. Trichobothrium *ist* distinctly proximad of lyrifissure *fb*; trichobothria *eb-esb-ist* in a straight line; femur (♀) 6.4–6.9 times longer than broad, length 0.72–0.79 mm; chela (♀) 5.6–5.8 (♀) times longer than deep, length 0.94–1.01 mm .... *O. algharbicus* sp. nov.
Trichobothrium *ist* close, slightly proximad, of lyrifissure *fb*; trichobothrium *ist* strongly distad of *eb-esb* and forming a distinct angle; femur (♀) 7.4–8.1 times longer than broad, length 0.89–1.01 mm; chela (♀) 6.8 (♀) times longer than deep, length 1.22–1.29 mm ..... *O. goncalvesi* sp. nov.
33. Subterranean species, anophthalmic..... 34
Epigean species with eyes, anterior pair with convex lens..... *O. gardinii* Zaragoza, 2017
34. Chelicera with 6 macrosetae and 1–2 (rarely 3) lateral microsetae. Trichobothrium *ist* distinctly distad of *esb* 35
Chelicera with 6 macrosetae and 4–5 lateral microsetae. Trichobothrium *ist* level with *esb* .... *O. giennensis* (Zaragoza & Pérez, 2013)
35. Smaller. Chela length about 0.70 mm or less..... 36
Larger. Chela length about 1.00 mm or more..... 37
36. Fixed chelal finger with 14–15 teeth; stouter and shorter pedipalp: femur (♂) length 0.39–0.42 mm, 4.8–5.0 times longer than broad, chela (♂) length 0.58–0.60 mm, 4.8–5.0 times longer than deep ..... *O. montagudi* Zaragoza, 2017
Fixed chelal finger with 19 teeth; more slender and longer pedipalp: femur (♂) length 0.54 mm, 6.0 times longer than broad, chela (♂) length 0.71 mm, 5.7 times longer than deep..... *O. lencinai* Zaragoza, 2017

37. Trichobothrium *ist* proximad of or level with lyrifissure *fb*; smaller species, pedipalpal femur (♀) 5.7–7.5 times longer than broad, length 0.66–0.94 mm, chela (♀) length 0.94–1.29 mm 38
Trichobothrium *ist* distinctly distad of lyrifissure *fb*; larger species, pedipalpal femur (♀) 7.9–8.6 times longer than broad, length about 1.10 mm, chela (♀) length 1.40–1.53 mm 46
38. Movable chelal finger with 3–8 rounded vestigial teeth without dental canals in its basal half 39
Movable chelal finger with 9–12 rounded vestigial teeth without dental canals in its basal half 42
39. Trichobothrium *ist* distinctly proximad of lyrifissure *fb* 40
Trichobothrium *ist* level with lyrifissure *fb* ..... *O. riopar* Zaragoza, 2017
40. Lyrifissure *ldb* present on cheliceral hand .... *O. cazorlensis* Carabajal Márquez, García Carrillo & Rodríguez Fernández, 2001
Lyrifissure *ldb* absent on cheliceral hand 41
41. More slender species, pedipalpal femur (♀) 6.9–7.1 times longer than broad ..... *O. mateui* Zaragoza, 2017
Stouter species, pedipalpal femur (♀) 6.1 times longer than broad ..... *O. hoerwegi* Zaragoza, 2017
42. Cheliceral fixed finger with 2 large distal teeth 43
Cheliceral fixed finger with only 1 large distal tooth ..... *O. torreniarinae* (Carabajal Márquez, García Carrillo & Rodríguez Fernández, 2012)
43. Smaller: (♀) pedipalpal femur length 0.66–0.75 mm, 5.7–6.4 times longer than broad; chela (♀) length 0.94–1.10 mm, 5.2–5.5 times longer than deep ..... *O. perezi* (Carabajal Márquez, García Carrillo & Rodríguez Fernández, 2011)
Larger: (♀) pedipalpal femur length 0.80–0.99 mm, 6.4–7.5 times longer than broad; chela (♀) length 1.06–1.38 mm, 5.7–6.5 times longer than deep 44
44. Male spinneret prominent ..... *O. verai* (Zaragoza, 1985)
Male spinneret absent or strongly reduced 45
45. Lyrifissure *ldb* of cheliceral hand present ..... *O. ventalloi* (Beier, 1939)
Lyrifissure *ldb* of cheliceral hand absent ..... *O. espanyoli* (Zaragoza & Pérez, 2013)
46. Movable chelal finger with 14 vestigial teeth without dental canals in basal half ..... *O. murcia* Zaragoza, 2017
Movable chelal finger with only 6–8 vestigial teeth without dental canals in basal half 47
47. Lyrifissure *ldb* of cheliceral hand present ..... *O. ruizporteroae* (Carabajal Márquez, García Carrillo & Rodríguez Fernández, 2001)
Lyrifissure *ldb* of cheliceral hand absent ..... *O. ebo* Zaragoza, 2017

Occidenchthonius cardosoi (Zaragoza, 2012)
(Figs. 3–9)

Chthonius (*Ephippiochthonius*) *cardosoi* Zaragoza 2012:26–27, figs 1–9.

Chthonius cardosoi Zaragoza: Reboleira 2012:162, 164, 331; NECA & Associação de Municípios da Região de Setúbal 2015:299, 2 unnumbered figures; NECA 2016:59, 1 unnumbered figure; Reboleira & Correia 2016:48, fig. 71.

Chthonius (E.) cardosoi Zaragoza: Reboleira 2012:212.

Occidenchthonius cardosoi (Zaragoza): Zaragoza 2017:140–143, fig. 229.

Type locality.—PORTUGAL: Arrábida karst massif, Setúbal district, Sesimbra municipality, Gruta do Fumo (38°26′03″N, 09°08′39″W; 209 m a.s.l.).

Material examined.—PORTUGAL: Lisboa district, Montejunto massif, Cadaval municipality, Lamas e Cercal, Algar do Javali (39°12′36″N, 9°02′12″W; 380 m a.s.l.), 1 ♀, 5 April 2009; 1 ♀, 6 June 2009; 1 ♀, 19 November 2009; 1 ♂, 3 ♀, 2 tritonymphs (DEUA), 24 December 2009; all them A.S.P.S. Reboleira. Leiria district, Cesaredas Plateau, Peniche municipality, Bolhos, Gruta dos Bolhos (synonym of Gruta do Casal da Lebre, 39°18′31″N, 9°16′37″W; 145 m a.s.l.), 1 ♀ (DEUA), 18 November 2009, A.S.P.S. Reboleira.

Diagnosis.—Modified from Zaragoza (2017). *Occidenchthonius cardosoi* is a medium-sized hypogean species, weakly troglomorphic. Movable cheliceral finger without isolated subapical tooth (*di*) and spinneret moderately prominent in females, extremely reduced in males, cheliceral lyrifissure *ldb* present. Anophthalmic, anterior margin of carapace with 1–2 preocular microsetae on each side, posterior margin with 4 macrosetae. Pedipalp coxa setae *dps-mps-lps* forming a 50–65° angle; chelal hand distinctly depressed at level of *ib*/*isb*, with short and very low rounded hump distad of *ib*/*isb* and very gentle slope between trichobothria *ib*/*isb* and *eb*; fixed chelal finger with 16–18 teeth; two-thirds distal parts of movable chelal finger with 12–14 pointed teeth with dental canals, basal third of movable chelal finger with 4–6 rounded, partially fused, vestigial teeth without canals on raised lamina; pedipalpal femur (♂) 6.1, (♀) 5.8–6.2 times longer than broad, length (♂) 0.49 mm, (♀) 0.63–0.66 mm; chela (♂) 5.5, (♀) 5.0–5.5 times longer than deep, length (♂) 0.66 mm, (♀) 0.85–0.89 mm; ratio movable chelal finger/chelal hand (♂) 1.5, (♀) 1.4; lacking lyrifissures ma_1 and ma_2, all the other chelal patterns and their standard number are present.

Description (adults from Algar do Javali and Gruta dos Bolhos).—Data that coincide with type specimens (Zaragoza 2012, 2017) are omitted. *Carapace*: subquadrate, slightly longer than broad, constricted posteriorly; medial part of anterior margin strongly prominent, with rudimentary epistome, and strongly dentate, showing variability in its development (Figs. 4a, b, c). Anophthalmic. Chaetotaxy: 20 macrosetae, with 1–2 preocular microsetae on each side, macrosetae formula 4:6:4:2:4; anteromedial setae (*ame*) 0.08–0.11 mm long, sublateral ocular setae (*osl*) 0.05–0.08 mm, ratio setae *ame*/*osl* 1.2–1.7; posteromedial setae slightly longer than the posterolateral ones.

Chelicera: hand with 6 setae and 1 lateral microseta (1 female 2 lateral microsetae), seta *vb* short (0.025–0.040 mm long), microseta 0.015–0.025 mm. Fixed finger (Fig. 5a) with 7–9 teeth proximally decreasing in size, 2–3 proximal microtubercles, two distal teeth distinctly larger than others. Movable finger (Fig. 5b) without an isolated subapical tooth (*di*), with 5–8 teeth

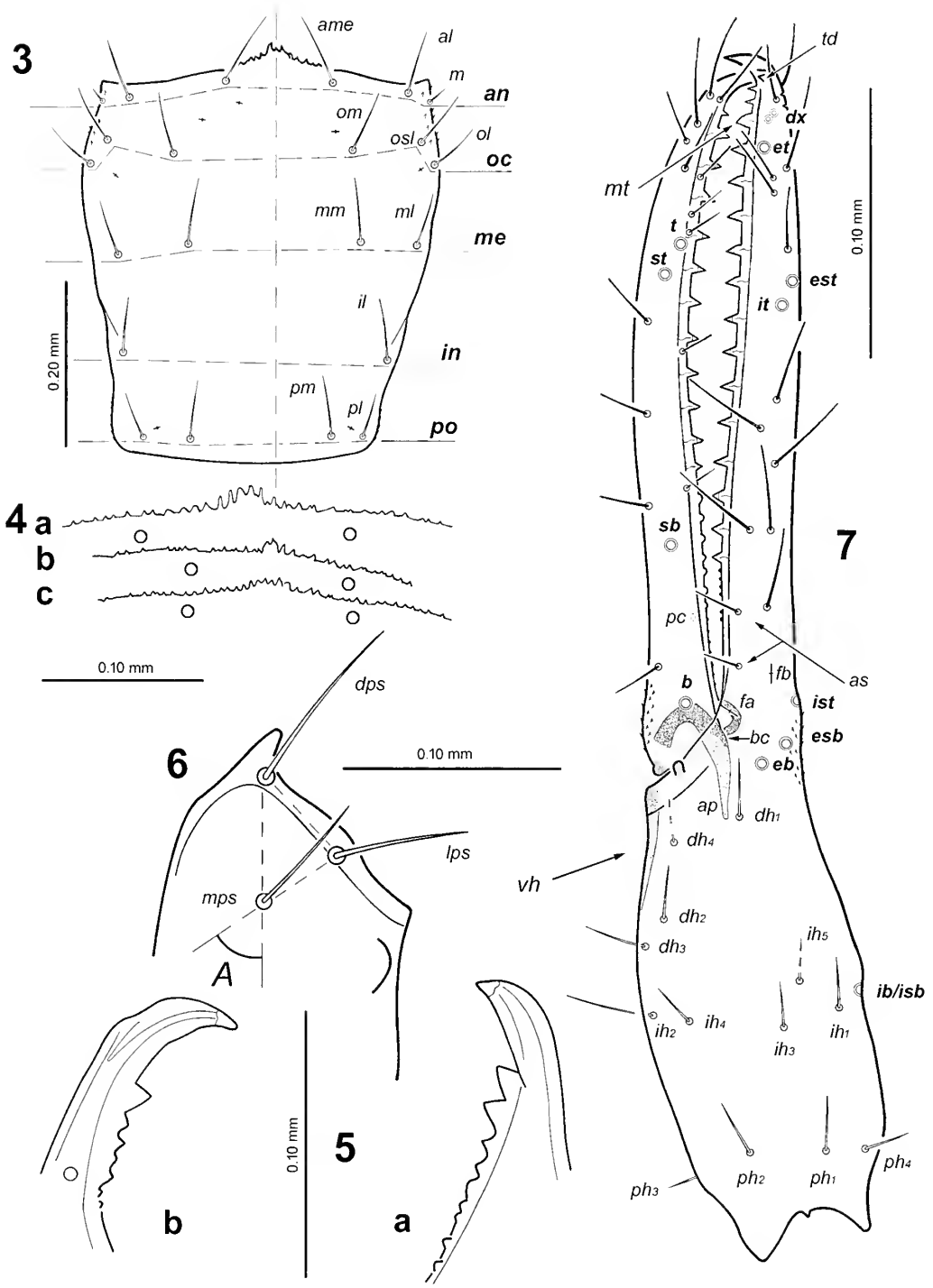

Figures 3–7.—*Occidenchthonius cardosoi* (Zaragoza), female holotype and dorsal views, unless stated otherwise. (3) Carapace (modified from Zaragoza 2012). (4) Anterior margin of carapace, partial view, (a) female from Algar do Javali, (b) male from Algar do Javali, (c) female Gruta dos Bolhos. (5) Fingers of left chelicera, male from Algar do Javali, partial view, (a) fixed finger, (b) movable finger. (6) Left pedipalpal coxa, female from Algar do Javali, partial view. (7) Left chela, antiaxial view (modified from Zaragoza 2017). See Methods for abbreviations.

proximally decreasing in size, 1–2 proximal microtubercles, the distal tooth larger than others; spinneret moderately prominent and apically rounded in female, vestigial and almost absent in male (Fig. 5b); seta *gl* 0.50–0.55 from base of movable finger. Rallum with 11 blades. Serrula exterior with 14–15 blades, serrula interior with 12 blades.

Abdomen: Tergites IX and XI with 2 sublateral tactile setae on each one (0.16–0.18 and 0.18–0.24 mm long respectively). Chaetotaxy of sternites II–III 8–10:(3)7–8(3):(2)6–7(2):8, sternite X with 2 submedial tactile setae (0.12–0.21 mm long), genital notch of males flanked by 6–7 setae on each side and 4+4 internal glandular setae.

Coxae: Pedipalpal coxa with distal marginal seta of the disk (*dps*) 0.06–0.10 mm long, areolar insertions of disk setae *dps-mps-lps* forming a 50–53° angle (Fig. 6) (59–65° in female types); coxa I 3–4 + 3 marginal microsetae, distal marginal seta (*dcs*) 0.03–0.07

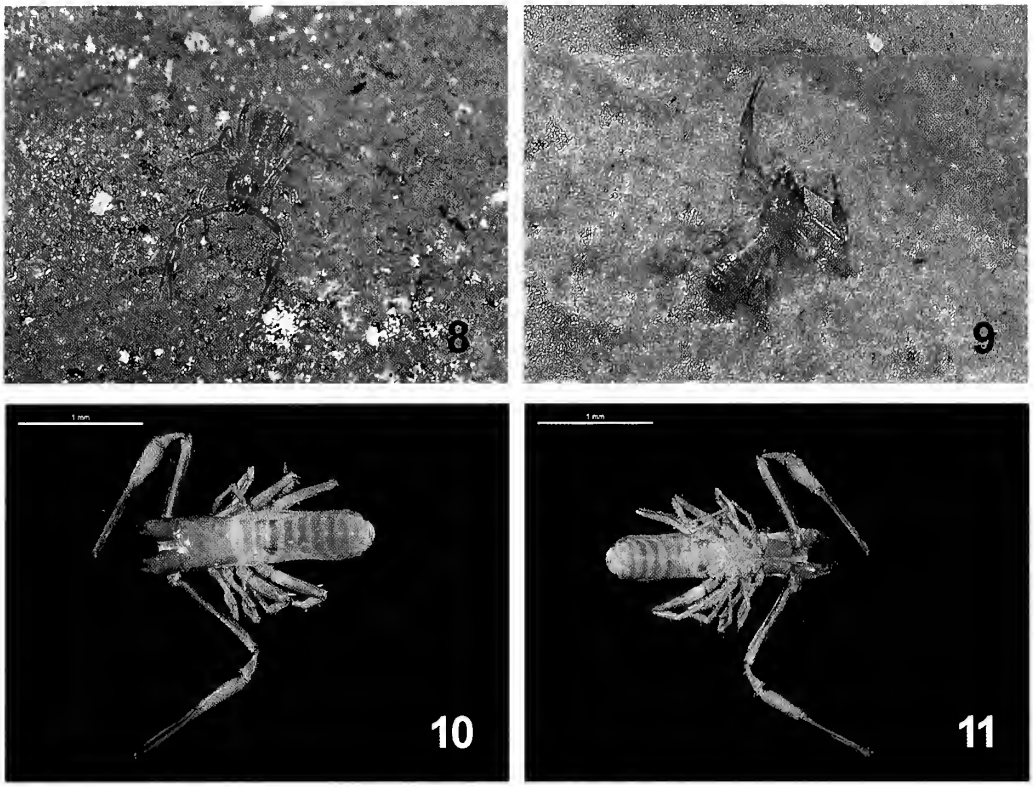

Figures 8–11.—Habitus of specimens of *Occidenchthonius* species from Portugal. (8 & 9) *Occidenchthonius cardosoi* (Zaragoza, 2012), Gruta do Fumo, photograph: Francisco Luís Rasteiro. (10 &11) *Occidenchthonius goncalvesi* sp. nov., female in dorsal and ventral view, Algarão do Remexido.

mm long, seta *dps* distinctly longer than seta *dcs*; II 4 + 5–9 bipinnate coxal spines, III 5+4–5 bipinnate coxal spines and IV 6.

Pedipalp: femoral chaetotaxy 3:5–6:3:5–6:1. Chelal hand seta ih_2 distinctly thinner and longer than other hand setae (0.050–0.075 mm long, ratio hand depth/ih_2 length 1.9–2.7) (0.063–0.065 mm long, ratio 2.8 in female types). Fixed finger with 16–18 mostly pointed teeth and with dental canals, two first distal teeth small, third subdistal tooth (*mt*) of the fixed finger distinctly modified in shape and deviated in orientation with respect to the others, dental row reaching up to slightly proximad to trichobothrium *sb*, usually level sensilla *pc*, 6–10 proximal microtubercles; tip of fixed chelal finger of male with a weak hollow on paraxial face, without subdistal protuberance (*sp*); one pair of long antiaxial sensory setae (*as*) at the base, one level and other strongly distad of lyrifissure *fb*, 0.025–0.040 mm long, distance between them 0.032–0.045 mm, fixed finger depth at the base 0.045–0.058 mm; 4–5 teeth at level of *est*/*it* occupying 0.1 mm, distance between apices 0.020–0.028 mm. Two-thirds distal parts of movable finger with 12–14 pointed teeth with dental canals that reach up to proximad of halfway between trichobothria *st* and *sb*, two proximal teeth reduced in size, 1–2 distal teeth tiny; third basal part of movable chelal finger with 4–6 rounded, partially fused, vestigial teeth without canals on raised and short lamina, dental row reaching up to level of sensilla *pc*, 6 proximal microtubercles. Trichobothrium *ist* distinctly distad of *esb* and slightly proximad of lyrifissure *fb*; distance between *st-sb* 1.5–1.8 times longer than that between *sb-b*.

Measurements and ratios: Specimens from Algar do Javali: male, followed by females in square brackets, when different: Body 1.00 [1.16–1.36]. Carapace 0.35/0.31 (1.1) [0.45–0.47/0.41–0.43 (1.1)]. Chelicera 0.30/0.15 (2.0) [0.41/0.19 (2.1–2.2)], movable finger 0.16 [0.20–0.21]. Pedipalp: femur 0.49/0.08 (6.1) [0.65–0.66/0.11 (6.1–6.2)], patella 0.20/0.10 (2.0) [0.27–0.28/0.13–0.14 (2.0–2.1)], chela 0.66/0.12 (5.5) [0.85–0.87/0.17–0.18 (5.0)], hand 0.26 (2.2) [0.35–0.36 (2.1)], movable finger 0.39 [0.50]; ratio movable finger/hand 1.5 [1.4], femur/movable finger 1.3, femur/carapace 1.4, chela/carapace 1.9, chela/femur 1.3. *Female from Gruta dos Bolhos:* Body 1.0. Carapace 0.42/0.40 (1.0). Chelicera 0.36/0.17 (2.1), movable finger 0.18. Pedipalp: femur 0.52/0.10 (5.5), patella 0.22/0.11 (2.0), chela 0.72/0.14 (5.3), hand 0.30 (2.2), movable finger 0.41; ratio movable finger/hand 1.4, femur/movable finger 1.3, femur/carapace 1.2, chela/carapace 1.7, chela/femur 1.4.

Description (tritonymphs).—Carapace slightly longer than broad; medial part of anterior margin moderately prominent and strongly dentate; anophthalmic; macrochaetotaxy as in adult, only one preocular microseta on each side; anteromedial setae (*ame*) 0.075 mm long, sublateral ocular setae (*osl*) 0.040–0.050 mm long, ratio setae *ame*/*osl* 1.5–1.9; 4 lyrifissures anteriorly and 2 posteriorly. Cheliceral hand with 5 setae (lacks seta *it* respect to adults) and 1 lateral microseta; fixed finger with 7–8 teeth, two distal teeth larger than others; movable finger without an isolated subapical tooth (*di*), with 5–6 teeth, the distal one larger than others; spinneret moderately prominent, as in adult females; seta *gl* 0.55 from base of movable finger; lyrifissures patterns as in adults. Chaetotaxy of tergites as in adults; sternites 5–7:(2)6(2):(1)6(1–2):7–8:6:6:6:6:1T2T1:0:2. Pedipalpal coxa 5 setae (including 2 on manducatory process), distal marginal seta of the disk (*dps*)

0.050–0.055 mm long, areolar insertions of disk setae *dps-mps-lps* forming a 50–54° angle; coxa I 3 + 2 marginal microsetae, distal marginal seta (*dcs*) 0.035–0.040 mm long; II 4 + 6–7 bipinnate coxal spines, III 5 + 4 bipinnate coxal spines and IV 5; intercoxal tubercle bisetose. Pedipalp with femoral chaetotaxy 3:5:2:4:1; chelal hand chaetotaxy 4:5:4, seta ih_2 0.050 mm long, ratio hand depth/ih_2 length 2.2–2.3; trichobothrium *ist* forming a straight line with *eb-esb*, and strongly proximad of lyrifissure *fb*; fixed finger with 13–14 mostly pointed teeth with dental canals, two first distal teeth small, third subdistal tooth modified (*mt*), 5–6 teeth at level of *est*/*it* occupying 0.1 mm, distance between apices 0.018–0.020 mm; fixed finger with an unique antiaxial sensory setae (*as*) at the finger base, at level of lyrifissure *fb*; distal half of movable finger with 10 pointed teeth with dental canals, distal one tiny, subdistal small; proximal half of finger with 4–5 rounded, vestigial teeth on raised lamina; coupled sensilla *pc* distad of trichobothrium *b*; lacking lyrifissures fd_3, ma_1 and ma_2.

Measurements and ratios (tritonymphs): Body 0.90–0.94. Carapace 0.33–0.34/0.29 (1.1–1.2). Chelicera 0.28/0.14 (2.0), movable finger 0.15–0.16. Pedipalp: femur 0.40–0.42/0.07–0.08 (5.3–5.5), patella 0.17–0.18/0.10 (1.8), chela 0.55–0.57/0.11–0.12 (4.9–5.0), hand 0.22–0.24 (2.0–2.1), movable finger 0.32–0.33; ratio movable finger/hand 1.3–1.4, femur/movable finger 1.2–1.3, femur/carapace 1.2, chela/carapace 1.7, chela/femur 1.4.

Remarks.—*Occidenchthonius cardosoi* (Zaragoza, 2012) is not included in a recognized species-group within the genus. *O. cardosoi* is the only species of the genus without isolated subapical tooth (*di*) on the cheliceral movable finger, which has 4 setae in the posterior row of the carapace (Fig. 3). Additionally to the type locality, two other populations were found in other caves from two different karst units: Montejunto and Cesaredas (Reboleira 2012), considerably increasing its distribution area. The original species description (Zaragoza 2012; redescribed Zaragoza 2017) was based on two females and new material is now incorporated in the diagnosis, including the previously unknown male and tritonymphs. The female from Gruta dos Bolhos (Cesaredas karst) mostly coincide with the *O. cardosoi* description, but it has a distinctly smaller and stouter pedipalp than the types and the specimens from Algar do Javali (Montejunto karst), so its measurement data are not included in the diagnosis until confirmation with new material from the same locality.

Distribution.—PORTUGAL: Arrábida, Montejunto and Cesaredas karst areas.

Occidenchthonius alandroalensis sp. nov.
http://zoobank.org:8080/NomenclaturalActs/E13093D3-9BC9-44FD-B0A8-2D2454E146CD (Figs. 12–18)

Chthonius n. sp. 5: Reboleira 2012: 161.

Material examined.—*Holotype female*. PORTUGAL: Alentejo region, Évora district, Alandroal municipality, Algar de Santo António (38°42′14″N, 7°23′59″W; 370 m a.s.l.), 30 December 2009, A.S.P.S. Reboleira (DEUA).

Paratypes. PORTUGAL: 3 ♀ (DEUA, MNCN, MCNB), 1 tritonymph, 1 deutonymph (DEUA), same locality, 30 December 2009, A.S.P.S. Reboleira.

Diagnosis (female).—*Occidenchthonius alandroalensis* sp. nov. is a medium-sized, hypogean species included in the *machadoi*-group. Movable cheliceral finger without isolated subapical tooth (*di*) and with moderately prominent spinneret in females, unknown in males; cheliceral lyrifissure *ldb* present. Anophthalmic, anterior margin of carapace without preocular microsetae on each side, posterior margin with 2 macrosetae. Pedipalpal coxa setae *dps-mps-lps* forming a 51–54° angle; chelal hand weakly depressed at level of *ib*/*isb*, with a low hump distad of *ib*/*isb* and very gentle slope between trichobothria *ib*/*isb* and *eb*, chaetotaxy 4:4:4, seta ih_5 absent; fixed chelal finger with 18–19 teeth; movable chelal finger with 16–18 pointed teeth with dental canals, proximally with only one rounded tooth without dental canal on weak lamina; pedipalpal femur (♀) 7.0–7.5 times longer than broad, length (♀) 0.95–1.01 mm; chela (♀) 5.7–5.9 times longer than deep, length (♀) 1.28–1.36 mm; ratio movable chelal finger/chelal hand (♀) 1.3–1.4; lacking lyrifissures ma_1 and ma_2, all the other chelal patterns and their standard number are present.

Description (female).—*Body:* medium-sized hypogean species, moderately troglomorphic with depigmented integument; weak hispid granulation on lateral surfaces of carapace, on the cheliceral hand and almost absent on the base of chelal fingers.

Carapace (Fig. 12): subquadrate, weakly constricted posteriorly; medial part of anterior margin (Fig. 13) strongly prominent and dentate, with a rudimentary epistome. Anophthalmic. Chaetotaxy: 18 setae, without preocular microsetae on each side, 2 setae in posterior row, formula 4:6:4:2:2, anteromedial setae (*ame*) 0.14–0.15 mm long, sublateral ocular setae (*osl*) 0.07–0.09 mm, ratio setae *ame*/*osl* 1.8–2.1; 4 lyrifissures anteriorly and 2 posteriorly.

Chelicera (Fig. 14): hand with 6 setae and 2 lateral microsetae, seta *vb* short (0.055–0.070 mm long), microsetae 0.025–0.035 mm; hand with 5 dorsal lyrifissures and one ventral, lyrifissure *ldb* and all the others (*ldst*, *ldt*, *lvb*, *lve*, *lvt*) present. Fixed finger (Fig. 15a) with 10–11 teeth proximally decreasing in size, two distal teeth distinctly larger than others, 2–3 proximal microtubercles. Movable finger (Fig. 15b) without an isolated subapical tooth (*di*), with 8–9 teeth proximally decreasing in size, the distal tooth larger than others, 0–2 proximal microtubercles; spinneret small and apically rounded in females, unknown in males; seta *gl* 0.55–0.58 from base of movable finger. Rallum with 11 blades. Serrula exterior with 15–17 blades, serrula interior 13–14 blades.

Abdomen: chaetotaxy of tergites 4:4:4:4:6:6:6:6:1T2T1:4:1T2T1:0, tergites IX and XI with 2 sublateral tactile setae on each one (0.22–0.27 and 0.30–0.31 mm long respectively). Chaetotaxy of sternites 9–10:(3)8–9(3):(2)6–7(2):7–8:6:6:6:6:2T1T2:0:2, lateral setae on sternite III macrosetae size, sternite X with 2 submedial tactile setae (0.23 mm long).

Coxae: pedipalpal coxa with 5 setae (including 2 on manducatory process), distal marginal seta of the disk (*dps*) 0.125–0.130 mm long, areolar insertions of disk setae *dps-mps-lps* forming a 51–54° angle (Fig. 16); coxa I 3 + 3 marginal microsetae (holotype 3 + 2 in one coxa, normal in the other), distal marginal seta (*dcs*) 0.075–0.080 mm long, seta *dps* distinctly longer than seta *dcs*; II 4 + 10–12 bipinnate coxal spines, III 5 + 7–11 bipinnate coxal spines and IV 6; intercoxal tubercle bisetose.

Pedipalp: femoral chaetotaxy 3:6:3:5:1. Chela (Fig. 17) with the hand weakly depressed at level of *ib*/*isb*, with a low hump distad of *ib*/*isb* and very gentle slope between trichobothria *ib*/*isb* and *eb*; weak ventral hollow (*vh*) before the base of the movable

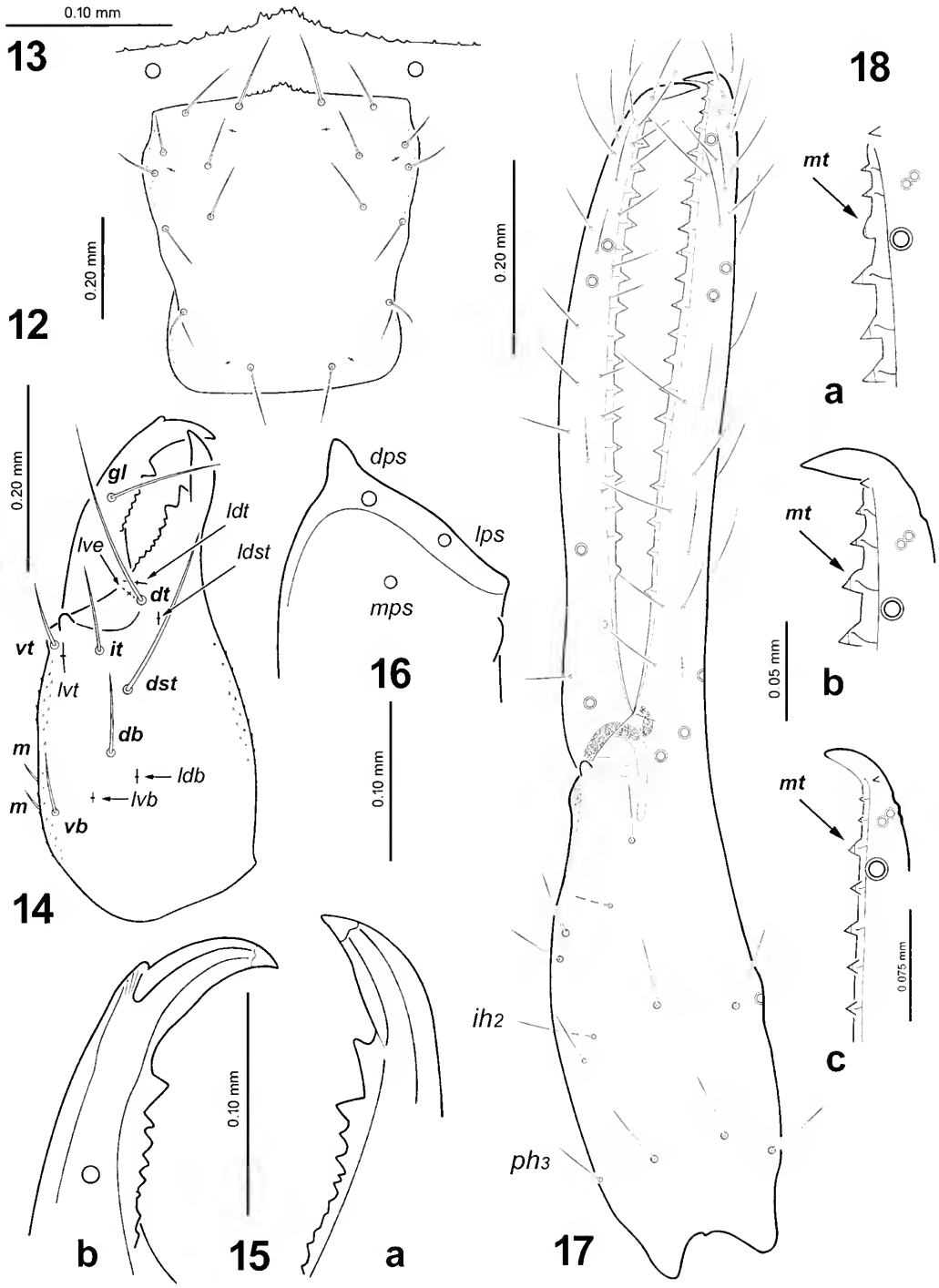

Figures 12–18.—*Occidenchthonius alandroalensis* sp. nov., female holotype and dorsal views, unless stated otherwise. (12) Carapace. (13) Anterior margin of carapace, partial view. (14) Left chelicera. (15) Fingers of left chelicera, partial view, (a) fixed finger, (b) movable finger. (16) Left pedipalpal coxa, partial view. (17) Left chela, antiaxial view. (18) Distal portion of fixed chelal finger, (a) female holotype, antiaxial view, (b) female paratype, antiaxial view, (c) female paratype, antiaxio-ventral view. See Methods for abbreviations.

finger with thicker cuticle; width slightly shorter than depth, maximum width slightly proximad to *ib*/*isb*; chaetotaxy 4:4:4, seta ih_5 absent, seta ph_3 present, setae dh_2 and dh_3 removed to halfway between the distal and the intermediary setal rows, seta ih_2 distinctly thinner and longer than other hand setae (0.11–0.12 mm long, ratio hand depth/ih_2 length 1.9–2.0); distal end of the hand and base of the chelal fingers with sclerotized condylar complex. Fixed finger with 18–19 pointed teeth and with dental canals, two first distal teeth small, third subdistal tooth (*mt*) distinctly modified in shape and deviated in orientation with respect to the others, apically rounded in holotype (Fig. 18a) and one paratype (apparently worn), pointed in the other paratypes (Fig. 18b), distal half with saw-like shape (Fig. 18c), dental row reaching up to level or proximad to trichobothrium *sb* and distad to sensilla *pc*, towards the base smooth or with some extremely tiny proximal microtubercles; tip of fixed finger with a modified

accessory tooth (*td*) on antiaxial face; one pair of long antiaxial sensory setae (*as*) at the base, one level and the other distad of lyrifissure *fb*, 0.050–0.060 mm long, distance between them 0.055–0.063 mm, fixed finger depth at the base 0.070–0.075 mm; 4 teeth at level of *est*/*it* occupying 0.1 mm, distance between apices 0.025–0.030 mm. Movable finger with 16–18 pointed teeth with dental canals, one tiny distal tooth, dental row reaching up to approximately level trichobothrium *sb*, followed by only one rounded vestigial teeth without dental canal on weak lamina, 4–6 proximal microtubercles; basal condyle (*bc*) present, basal apodeme long and apically narrowed; coupled sensilla *pc* halfway between *sb* and *b* or slightly closer to *b*. Trichobothria as in Fig. 17; trichobothrium *ist* strongly distad of *esb* and level lyrifissure *fb*; trichobothria *ib*/*isb* equidistant between *esb* and the base of the hand; distance between *st-sb* 1.7–2.0 times longer than that between *sb-b*. Lacking lyrifissures ma_1 and ma_2, all the other chelal patterns and their standard number are present: *fa*, *fb*, *fp*, *hd*, *hp*, fd_1, fd_2, fd_3, mv_1 and mv_2 (mv_2 can be absent in some chelae).

Measurements and ratios: female holotype, followed by female paratypes in square brackets, when different: Body 1.84 [2.12–2.20]. Carapace 0.61/0.55 (1.1) [0.62–0.66/0.56 (1.1–1.2)]. Chelicera 0.53/0.24 (2.2) [0.54–0.56/0.25–0.26 (2.2)], movable finger 0.25 [0.27–0.28]. Pedipalp: femur 0.97/0.13 (7.5) [0.95–1.01/0.14 (7.0–7.2)], patella 0.38/0.16 (2.3) [0.39–0.41/0.17 (2.3–2.5)], chela 1.28/0.22 (5.7) [1.32–1.36/0.23 (5.9)], hand 0.55 (2.5) [0.56–0.57 (2.4–2.5)], movable finger 0.72 [0.75–0.78]; ratio movable finger/hand 1.3 [1.3–1.4], femur/movable finger 1.4 [1.3], femur/carapace 1.6 [1.5], chela/carapace 2.1, chela/femur 1.3 [1.3–1.4].

Description (tritonymph).—Carapace distinctly longer than broad; medial part of anterior margin distinctly prominent and strongly dentate; anophthalmic; macrochaetotaxy as in adult, without preocular microseta on each side; anteromedial setae (*ame*) 0.07 mm long, sublateral ocular setae (*osl*) 0.04 mm long, ratio setae *ame*/*osl* 2.0; 4 lyrifissures anteriorly and 2 posteriorly. Cheliceral hand with 5 setae (lacks seta *it* respect to adults) and 1 lateral microseta; fixed finger with 6 teeth, two distal teeth larger than others; movable finger without an isolated subapical tooth (*di*), with 5 teeth, the distal one larger than others; spinneret prominent as in adult females; seta *gl* 0.59 from base of movable finger; lyrifissures patterns as in adults. Chaetotaxy of tergites as in adults; sternites 7:(2)6(2):(1)5(1):6:6:6:6:6:1T2T1:0:2. Pedipalpal coxa 5 setae (including 2 on manducatory process), distal marginal seta of the disk (*dps*) 0.070 mm long, areolar insertions of disk setae *dps-mps-lps* forming a 68° angle; coxa I 3 + 2 marginal microsetae, distal marginal seta (*dcs*) 0.040 mm long, seta *dps* distinctly longer than seta *dcs*; II 4–5 + 5–8 bipinnate coxal spines, III 5 + 6–8 bipinnate coxal spines and IV 5; intercoxal tubercle bisetose. Pedipalp with femoral chaetotaxy 3:5:2:5:1; chelal hand chaetotaxy 4:3:4 (lack setae ih_3 and ih_5), seta ih_2 0.060 mm long, ratio hand depth/ih_2 length 2.0; trichobothrium *ist* strongly distad of *esb*, and level lyrifissure *fb*; fixed finger with 15 pointed teeth with dental canals, two first distal teeth small, third subdistal tooth modified (*mt*), 5 teeth at level of *est*/*it* occupying 0.1 mm, distance between apices 0.023–0.025 mm; movable finger with 12 pointed teeth with dental canals, one tiny distal tooth, only two rounded vestigial teeth without dental canals on weak lamina; coupled sensilla *pc* distad of trichobothrium *b*; lacking lyrifissures fd_3, mv_2, ma_1 and ma_2.

Measurements and ratios (tritonymph paratypes): Body 1.06. Carapace 0.37/0.31 (1.2). Chelicera 0.30/0.14 (2.2), movable finger 0.14. Pedipalp: femur 0.53/0.08 (6.6), patella 0.21/0.10 (2.2), chela 0.72/0.12 (6.0), hand 0.30 (2.4), movable finger 0.42; ratio movable finger/hand 1.4, femur/movable finger 1.3, femur/carapace 1.4, chela/carapace 1.9, chela/femur 1.4.

Description (deutonymph).—Carapace without eyes; chaetotaxy: 4:6:4:2:2, without preocular microsetae. Cheliceral hand with 4 setae (lack setae *db* and *it* respect to adults) and without lateral microsetae, only three lyrifissures present: *lve*, *ldt* and *lvt*; fixed finger with 7 teeth, two distal teeth larger than others; movable finger without an isolated subapical tooth (*di*), with 4 teeth, the distal one larger than others; spinneret prominent as in adult females; seta *gl* 0.59 from base of movable finger. Chaetotaxy of tergites as in adults. Pedipalpal coxa 5 setae (including 2 on manducatory process), distal marginal seta of the disk (*dps*) 0.065 mm long, areolar insertions of disk setae *dps-mps-lps* forming a 54° angle; coxa I 2 + 1 marginal microseta, distal marginal seta (*dcs*) 0.040 mm long, seta *dps* distinctly longer than seta *dcs*; II 3 + 7 bipinnate coxal spines, III 3 + 6 bipinnate coxal spines and IV 3; intercoxal tubercle bisetose. Pedipalp: chelal hand chaetotaxy 4:2:3 (lack setae ih_3, ih_4, ih_5 and ph_2 respect to adults), seta ih_2 0.045 mm long, ratio hand depth/ih_2 length 2.4; fixed pedipalpal finger with 12 teeth, two distal teeth small, third subdistal tooth modified (*mt*), 5 teeth at level of *est*/*it* occupying 0.1 mm, distance between apices 0.0175–0.0225 mm; movable finger with 10 pointed teeth with dental canals and only two rounded vestigial teeth without dental canals on weak lamina; coupled sensilla *pc* in subbasal position along the movable finger; lyrifissures *fa*, *fp*, *fb*, fd_1 and mv_1 present, lacking all the others.

Measurements and ratios (deutonymph paratype): Body 1.02. Carapace 0.34/0.25 (1.3). Chelicera 0.26/0.12 (2.1). Pedipalp: femur 0.41/0.08 (5.5), patella 0.18/0.09 (1.9), chela 0.57/0.11 (5.3), hand 0.23 (2.1), movable finger 0.34; ratio movable finger/hand 1.5, femur/movable finger 1.2, femur/carapace 1.2, chela/carapace 1.7, chela/femur 1.4.

Remarks.—*Occidenchthonius alandroalensis* sp. nov. is an anophthalmic species that is here tentatively assigned to the *machadoi*-group by the absence of the chelal hand seta ih_5, despite not sharing some other characteristics of the group, as the presence of an isolated subapical tooth (*di*) on chelicera and preocular microsetae on carapace, as stated in Zaragoza (2017). Additionally, the shape of the basal lamina on movable chelal finger with only one rounded vestigial teeth (2 in nymphs) without dental canal on weak lamina in *O. alandroalensis* sp. nov., configures unique characteristics for this species within *Occidenchthonius*.

Distribution.—PORTUGAL: Alentejo Region.

Etymology.—The species epithet is a Latin adjective referring to the locality where the type cave is located, Alandroal.

Occidenchthonius algharbicus sp. nov.
http://zoobank.org:8080/NomenclaturalActs/C26DF4AB-94F1-40BC-9F7C-6C80AA1C320E
(Figs. 19–24)

Chthonius af. n. sp.1: Reboleira 2012: 161.
Chthonius n. sp. 1: Reboleira 2012: 162.

Material examined.—*Holotype female*. PORTUGAL: Algarve region, Faro district, Olhão municipality, Moncarapa-

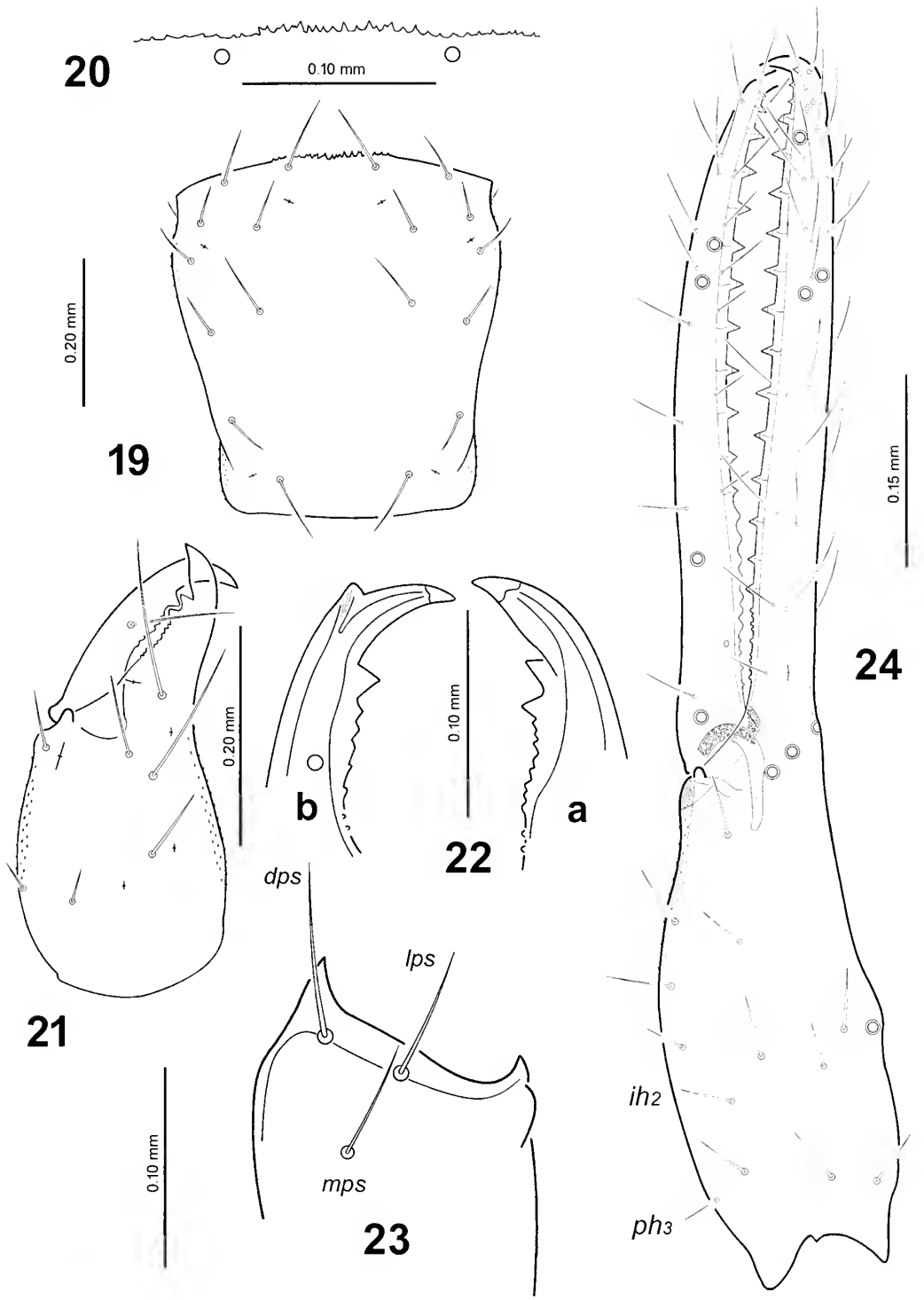

Figures 19–24.—*Occidenchthonius algharbicus* sp. nov., female holotype and dorsal views, unless stated otherwise: (19) Carapace. (20) Anterior margin of carapace, partial view. (21) Left chelicera (22) Fingers of left chelicera, partial view, (a) fixed finger, (b) movable finger. (23) Left pedipalpal coxa, partial view. (24) Left chela, antiaxial view. See Methods for abbreviations.

cho, Gruta da Senhora (37°06′20″N, 7°46′35″W; 85 m a.s.l.), 3 July 2011, A.S.P.S. Reboleira (DEUA).

Paratypes. PORTUGAL: 1 ♀ (MNCN), same locality, 14 March 2009; 1 ♀ (MCNB), 06 September 2009; 1 ♀, 1 tritonymph (DEUA), 29 December 2009; 1 ♀ (ZMUC), 3 July 2011; 1 ♀ (MHNG), 18 May 2013; A.S.P.S. Reboleira.

Other material. PORTUGAL: Algarve region, Faro district, Loulé municipality, Vale Telheiro, Gruta do Vale Telheiro (37°10′13″N, 8°02′05″W; 239 m a.s.l.), 1 ♀ , 24.V.2009; 1 ♀ , 29 December 2009; all A.S.P.S. Reboleira (DEUA).

Diagnosis.—*Occidenchthonius algharbicus* sp. nov. is a medium-sized hypogean species, weakly troglomorphic. Mov-

able cheliceral finger without isolated subapical tooth (*di*) and with well developed spinneret in females, unknown in males; lyrifissure *ldb* and all the others present. Anophthalmic, anterior margin of carapace with one preocular microseta on each side, posterior margin with 2 macrosetae. Pedipalp coxa setae *dps-mps-lps* forming an angle of 46–59°; chelal hand distinctly depressed at level of *ib/isb*, with low and long hump distad of *ib/isb* and gentle slope between trichobothria *ib/isb* and *eb*; fixed chelal finger with 14–15 teeth; two-thirds distal parts of movable chelal finger with 10–12 pointed teeth with dental canals, third basal part with 6–7 rounded teeth without canals on raised lamina; pedipalpal femur (♀) 6.4–6.9 times longer than broad, length (♀) 0.72–0.79 mm; chela (♀) 5.6–5.8 times longer than deep, length (♀) 0.94–1.01 mm; ratio movable chelal finger/chelal hand (♀) 1.4–1.5; lacking lyrifissures ma_1, and ma_2, all the other chelal patterns and their standard number are present.

Description (female).—*Body:* medium-sized hypogean species with weak troglomorphic facies and depigmented integument; weak hispid granulation on lateral surfaces of carapace, on cheliceral hand, on base of fixed chelal finger and distally on ventral part of chelal hand.

Carapace (Fig. 19): subquadrate, weakly constricted posteriorly; medial part of anterior margin very weakly prominent or straight and strongly dentate (Fig. 20). Anophthalmic. Chaetotaxy: 18 setae, with one preocular microseta on each side (two female paratypes 0–1, lacking one microseta or lost), 2 setae in posterior row, formula 4:6:4:2:2, anteromedial setae (*ame*) 0.08–0.09 mm long, sublateral ocular setae (*osl*) 0.04–0.07 mm, ratio setae *ame/osl* 1.3–2.3; 4 lyrifissures anteriorly and 2 posteriorly.

Chelicera (Fig. 21): with 6 setae and one lateral microseta on hand, seta *vb* short (0.03–0.04 mm long), microsetae 0.02–0.03 mm; hand with 5 dorsal lyrifissures and one ventral, lyrifissure *ldb* present. Fixed finger (Fig. 22a) with 9–10 teeth proximally decreasing in size, two distal teeth distinctly larger than others, 1–3 proximal microtubercles. Movable finger (Fig. 22b) without an isolated subapical tooth (*di*), with 6–8 teeth proximally decreasing in size, the distal tooth larger than others, 1–2 proximal microtubercles; spinneret prominent and well developed in females, unknown in males; seta *gl* 0.52–0.55 from base of movable finger. Rallum with 11 blades. Serrula exterior with 14 blades, serrula interior 11–12 blades.

Abdomen: Chaetotaxy of tergites 4:4:4:4:6:6:6:6:1T2T1:4:1T2T1:0, tergites IX and XI with 2 sublateral tactile setae on each one (0.16–0.18 and 0.21–0.23 mm long respectively). Chaetotaxy of sternites 8–10:(3)6(3):(2)6(2):7–8:6:6:6:6:2T1T2:0:2, lateral setae on sternite III macrosetae size, sternite X with 2 submedial tactile setae (0.15–0.22 mm long).

Coxae: pedipalpal coxa with 5 setae (including 2 on manducatory process), distal marginal seta of the disk (*dps*) 0.08–0.09 mm long, areolar insertions of disk setae *dps-mps-lps* forming an angle of 46–59° (Fig. 23); coxa I 3 + 3 marginal microsetae, distal marginal seta (*dcs*) 0.055–0.065 mm long, seta *dps* distinctly longer than seta *dcs*; II 4 + 7–11 bipinnate coxal spines, III 5 + 4–5 bipinnate coxal spines and IV 6; intercoxal tubercle bisetose.

Pedipalp: femoral chaetotaxy 3:6:3:5–6:1. Chela (Fig. 24) with hand distinctly depressed at level of *ib/isb*, with low and long hump distad of *ib/isb* and gentle slope between trichobothria *ib/isb* and *eb*; weak hollow before base of movable finger with thicker cuticle; width approximately equal to depth, maximum width slightly proximad of *ib/isb*; chaetotaxy 4:5:4, seta ph_3 present, seta dl_3 removed to halfway between the distal and the intermediary setal rows, seta ih_2 same size as others (0.05 mm long, ratio hand depth/ih_2 length 3.5); distal end of the hand and base of the chelal fingers with sclerotized condylar complex. Fixed finger with 14–15 pointed teeth and with dental canals, two first distal teeth small, third subdistal tooth (*mt*) distinctly modified in shape and deviated in orientation with respect to the others, dental row reaching up to proximad of trichobothrium *sb* and distad to sensilla *pc*, 4–9 proximal microtubercles; tip of fixed finger with a modified accessory tooth (*td*) on antiaxial face; one pair of long antiaxial sensory setae (*as*) at the base, one level with and the other distad of lyrifissure *fb*, 0.040–0.055 mm long, distance between them 0.040–0.060 mm, fixed finger depth at the base 0.050–0.060 mm; 3–4 teeth at level of *est/it* occupying 0.1 mm, distance between apices 0.025–0.035 mm. Two-thirds distal parts of movable finger with 10–12 pointed teeth with dental canals that reach up to distinctly proximad of halfway between trichobothria *st* and *sb*, distal tooth tiny, subdistal tooth small; third basal part of movable chelal finger with 6–7 rounded (rarely 4), partially fused, vestigial teeth without canals on raised lamina; dental row reaching proximad of *sb*, approximately level sensilla *pc*, 1–5 proximal microtubercles; basal condyle (*bc*) present, basal apodeme long and apically indented; coupled sensilla *pc* halfway between trichobothria *sb* and *b* or slightly closer to *b*. Trichobothria as in Fig. 24; trichobothrium *ist* forming a straight line with *eb-esb* and strongly proximad of lyrifissure *fb*; distance between *ib/isb* and the base of the hand slightly shorter than that between *ib/isb* and *esb*; distance between *st-sb* 1.7–1.9 times longer than that between *sb-b*. Lacking lyrifissures ma_1 and ma_2, all the other chelal patterns and their standard number are present (one female lacks mv_2 in one chela).

Measurements and ratios: female holotype, followed by female paratypes, when different: Body 1.55 [1.38–1.44]. Carapace 0.49/0.45 (1.1) [0.48–0.50/0.41–0.44 (1.1–1.2). Chelicera 0.43/0.19 (2.2) [0.42–0.45/0.19–0.20 (2.2)], movable finger 0.20 [0.21–0.22]. Pedipalp: femur 0.79/0.12 (6.9) [0.72–0.74/0.11–0.12 (6.4–6.5)], patella 0.29/0.14 (2.1) [0.28–0.29/0.13 (2.1–2.2)], chela 0.98/0.18 (5.6) [0.94–1.01/0.17–0.18 (5.7–5.8)], hand 0.41 (2.3) [0.38–0.41], movable finger 0.56 [0.54–0.60]; ratio movable finger/hand 1.4 [1.4–1.5], femur/movable finger 1.4 [1.2–1.3], femur/carapace 1.6 [1.5], chela/carapace 2.0, chela/femur 1.2 [1.3–1.4]. *Females from Gruta do Vale Telheiro:* Body 0.89–1.10. Carapace 0.41–0.43/0.35 (1.2). Chelicera 0.35–0.38/0.16–0.17 (2.1–2.2). Pedipalp: femur 0.54–0.59/0.10 (5.6–6.1), patella 0.21–0.24/0.11–0.12 (2.0), chela 0.74–0.79/0.14–0.15 (5.2–5.3), hand 0.29–0.32 (2.0–2.1), movable finger 0.53–0.55; ratio movable finger/hand 1.5, femur/movable finger 1.2, femur/carapace 1.3–1.4, chela/carapace 1.8, chela/femur 1.3–1.4.

Description (tritonymph paratype).—Carapace slightly longer than broad; medial part of anterior margin almost straight and strongly dentate; anophthalmic; macrochaetotaxy as in adult, only one preocular microseta on one side, absent in the other; anteromedial setae (*ame*) 0.055 mm long, sublateral ocular setae (*osl*) 0.035 mm long, ratio setae *ame/osl* 1.6; 4

lyrifissures anteriorly and 2 posteriorly. Cheliceral hand with 5 setae (lacks seta *it* respect to adults) and 1 lateral microseta; fixed finger with 6 teeth, two distal teeth larger than others; movable finger without an isolated subapical tooth (*di*), with 5 teeth, the distal one larger than others; spinneret prominent as in adult females; seta *gl* 0.54 from base of movable finger; lyrifissures patterns as in adults. Chaetotaxy of tergites as in adults; sternites 5:(2)5(2):(1)5(1–2):7:6:6:6:6:1T2T1:0:2. Pedipalpal coxa 5 setae (including 2 on manducatory process), distal marginal seta of the disk (*dps*) 0.050 mm long, areolar insertions of disk setae *dps-mps-lps* forming a 62° angle; coxa I 3 + 2 marginal microsetae, distal marginal seta (*dcs*) 0.030 mm long; II 4 + 5 bipinnate coxal spines, III 5 + 4 bipinnate coxal spines and IV 5; intercoxal tubercle bisetose. Pedipalp with femoral chaetotaxy 3:5:2:5:1; chelal hand chaetotaxy 4:5:4, seta ih_2 0.025 mm long, ratio hand depth/ih_2 length 4.0; trichobothrium *ist* forming a straight line with *eb-esb*, and strongly proximad of lyrifissure *fb*; fixed finger with 14 mostly pointed teeth with dental canals, two first distal teeth small, third subdistal tooth modified (*mt*), 5 teeth at level of *est*/*it* occupying 0.1 mm, distance between apices 0.023 mm; fixed finger with an unique antiaxial sensory setae (*as*) at the finger base, at level of lyrifissure *fb*; distal half of movable finger with 10 pointed teeth with dental canals, distal one tiny, subdistal small; proximal half of finger with 5 rounded, vestigial teeth on raised lamina; coupled sensilla *pc* distad of trichobothrium *b*; lacking lyrifissures fd_3, ma_1 and ma_2.

Measurements and ratios (tritonymph paratype): Body 1.04. Carapace 0.33/0.28 (1.2). Chelicera 0.27/0.12 (2.1), movable finger 0.14. Pedipalp: femur 0.41/0.07 (5.7), patella 0.16/0.09 (1.8), chela 0.58/0.10 (5.8), hand 0.23 (2.2), movable finger 0.35; ratio movable finger/hand 1.5, femur/movable finger 1.2, femur/carapace 1.2, chela/carapace 1.8, chela/femur 1.4.

Remarks.—*Occidenchthonius algharbicus* sp. nov. does not belong to either of the species-groups recognized within the genus. *O. algharbicus* sp. nov. shares with the species *O. goncalvesi* sp. nov. and *O. ortunoi* Zaragoza, 2017, the hypogean life, absence of an isolated subapical tooth on chelicera, posterior row of carapace with 2 macrosetae, presence of preocular microsetae, presence of chelal hand lyrifissures *hd* and *hp* and pedipalpal coxa setae *dps-mps-lps* forming an angle distinctly smaller than 90°. The new species has smaller and stouter pedipalp than *O. ortunoi* [pedipalpal femur (♀) 6.4–6.9 times longer than broad, length 0.72–0.79 mm; chela 5.6–5.8 times longer than deep, length 0.94–1.01 mm in *O. algharbicus* sp. nov. versus pedipalp femur (♀) 8.7–8.8 times longer than broad, length 1.28–1.30; chela 7.5–7.9 times longer than deep, length 1.72–1.82 in *O. ortunoi*]. *O. algharbicus* sp. nov. is closer in measurements to *O. goncalvesi* sp. nov., but differs in the position of trichobothrium *ist*, strongly proximad of lyrifissure *fb* and close, forming a straight line, of eb-esb in *O. algharbicus* sp. nov. versus close, slightly proximad, of lyrifissure *fb* and strongly distad, forming a distinct angle, of *eb-esb* in *O. goncalvesi* sp. nov. Specimens from Gruta do Vale Telheiro cohabit in the same cave with specimens of the species *O. goncalvesi* sp. nov., but are easily distinguished by the characteristics discussed above; syntopy of pseudoscorpions in caves is not frequent but occurs (e.g., Zaragoza 2000; 2007).

Distribution.—PORTUGAL: Algarve Region.

Etymology.—Named after the Arabic name *Al-Gharb*, the origin of Algarve, the southernmost province of Portugal, where the species is endemic.

Occidenchthonius duecensis sp. nov.
http://zoobank.org:8080/NomenclaturalActs/74147FB4-190B-4B47-9783-FD457BEFD3A6
(Figs. 25–30)

Chthonius n. sp. 2: Reboleira 2012: 165.

Material examined.—*Holotype female*. PORTUGAL: Centro region, Sicó Massif, Coimbra district, Penela municipality, Taliscas, Dueça Cave System, Gruta do Soprador do Carvalho (39°59′10″N, 8°22′58″W; 200 m a.s.l.), 30.VIII.2009, A.S.P.S. Reboleira (DEUA).

Paratypes. PORTUGAL: 1 ♀ (DEUA), same locality, 21.III.2009, 2 ♀ paratypes (MCNB, MNCN), 30.VIII.2009, A.S.P.S. Reboleira.

Diagnosis (female).—*Occidenchthonius duecensis* sp. nov. is a medium-sized hypogean species, weakly troglomorphic. Movable cheliceral finger without isolated subapical tooth (*di*) and with moderately prominent spinneret in females, unknown in males; all the standard cheliceral lyrifissures present. Anophthalmic, anterior margin of carapace with 2 preocular microsetae on each side, posterior margin with 2 macrosetae. Pedipalp coxa setae *dps-mps-lps* forming an angle of 113–132°; chelal hand distinctly depressed at level of *ib*/*isb*, with distinct and short hump distad of *ib*/*isb* and gentle slope between trichobothria *ib*/*isb* and *eb*; fixed chelal finger with 18 teeth; distal half of movable chelal finger with 10–11 pointed teeth with dental canals, basal half with 7–8 rounded teeth without canals on raised lamina; pedipalpal femur (♀) 5.6–6.0 times longer than broad, length (♀) 0.59–0.63 mm; chela (♀) 5.9–6.5 times longer than deep, length (♀) 0.84–0.91 mm; ratio movable chelal finger/chelal hand (♀) 1.5–1.7; lacking lyrifissures ma_1, ma_2 and *hd*, all the other chelal patterns and their standard number are present.

Description (female).—*Body:* medium-sized hypogean species of weak troglomorphic facies and depigmented integument; weak hispid granulation on lateral surfaces of carapace, on cheliceral hand and on bases of chelal fingers.

Carapace (Fig. 25): subquadrate, weakly constricted posteriorly; medial part of anterior margin weakly prominent and strongly dentate (Fig. 26). Anophthalmic. Chaetotaxy: 18 setae, with 2 (one female paratype with 2–3) preocular microsetae on each side, 2 setae in posterior row, formula 4: 6:4:2:2, anteromedial setae (*ame*) 0.10–0.11 mm long, sublateral ocular setae (*osl*) 0.04–0.06 mm, ratio setae *ame*/*osl* 1.9–2.5; 4 lyrifissures anteriorly and 2 posteriorly.

Chelicera (Fig. 27): hand with 6 setae and usually 2 (one female paratype 3–4) lateral microsetae, seta *vb* short (0.03–0.04 mm long), microsetae 0.02–0.03 mm; hand with 5 dorsal lyrifissures and one ventral, lyrifissure *ldb* and all the others present. Fixed finger (Fig. 28a) with 9–11 teeth proximally decreasing in size, two distal teeth distinctly larger than others, 2–4 proximal microtubercles. Movable finger (Fig. 28b) without an isolated subapical tooth (*di*), with 8–11 teeth proximally decreasing in size, the distal tooth larger than others; spinneret moderately prominent and apically rounded in females, unknown in males; seta *gl* 0.52–0.56 from base of

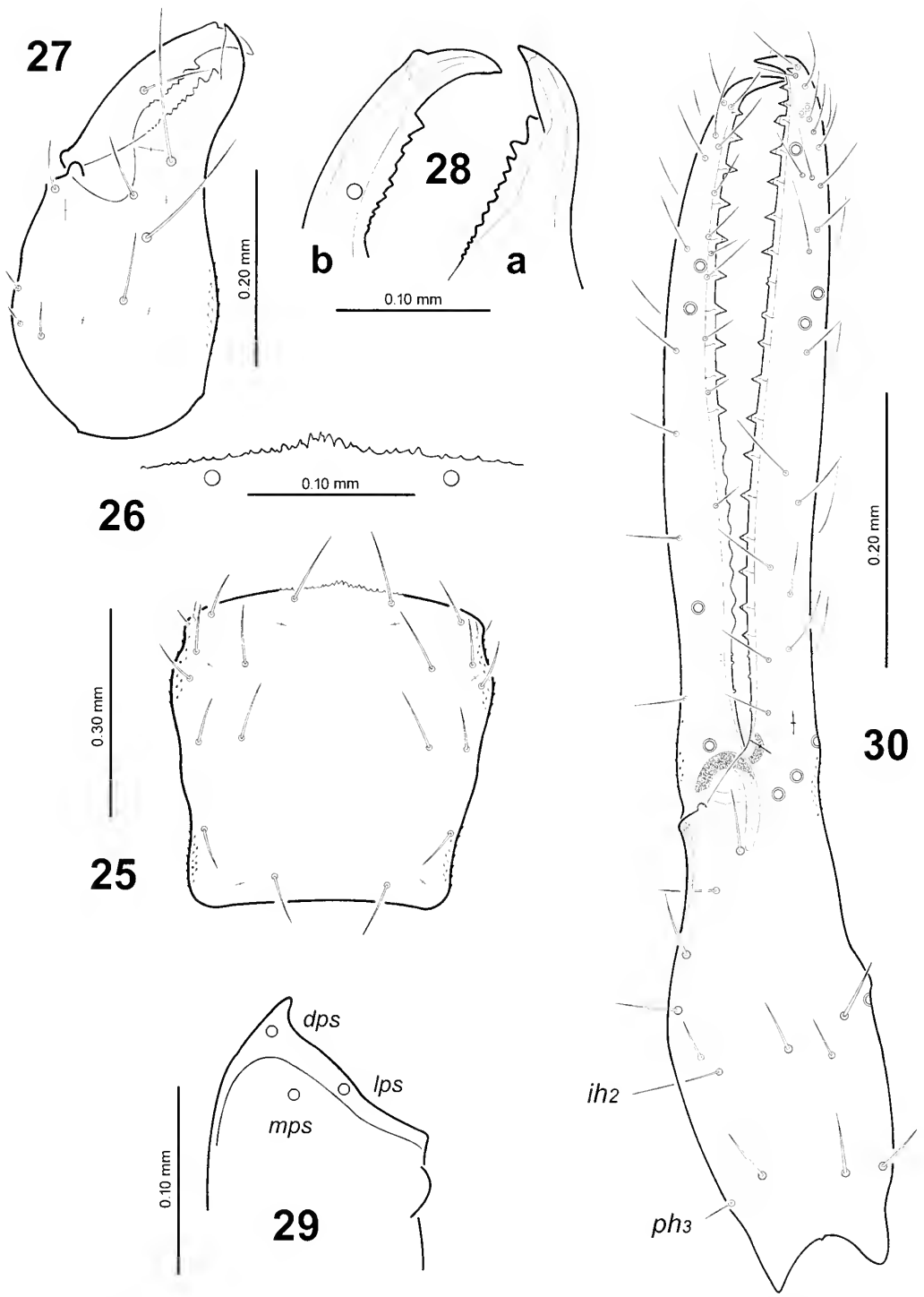

Figures 25–30.—*Occidenchthonius duecensis* sp. nov., female holotype and dorsal views, unless stated otherwise: (25) Carapace. (26) Anterior margin of carapace, partial view. (27) Left chelicera. (28). Fingers of left chelicera, partial view, (a) fixed finger, (b) movable finger. (29) Left pedipalpal coxa, partial view. (30) Left chela, antiaxial view. See Methods for abbreviations.

movable finger. Rallum with 11 blades. Serrula exterior with 15 blades, serrula interior 11–12 blades.

Abdomen: Chaetotaxy of tergites 4:4:4:4:6:6:6:6:1T2T1:4:1T2T1:0, tergites IX and XI with 2 sublateral tactile setae on each one (0.22 and 0.22–0.24 mm long respectively). Chaetotaxy of sternites 10:(3)8(3):(2)7(2):7–8:6:6:6:6:2T1T2:0:2, lateral setae on sternite III macrosetae size, sternite X with 2 submedial tactile setae (0.16–0.19 mm long).

Coxae: pedipalpal coxa with 5 setae (including 2 on manducatory process), distal marginal seta of the disk (*dps*) 0.065–0.070 mm long, areolar insertions of disk setae *dps-mps-lps* forming a 113–132° angle (Fig. 29); coxa I 3 + 3 marginal microsetae, distal marginal seta (*dcs*) 0.050–0.065 mm long,

seta *dps* distinctly longer than seta *dcs*; II 4 + 7–9 bipinnate coxal spines, III 5 + 3–4 bipinnate coxal spines and IV 6; intercoxal tubercle bisetose.

Pedipalp: femoral chaetotaxy 3:6–7:3:5:1. Chela (Fig. 30) with hand distinctly depressed at level of *ib*/*isb*, with distinct, short hump distad of *ib*/*isb* and gentle slope between trichobothria *ib*/*isb* and *eb*; weak hollow before base of movable finger with thicker cuticle; width approximately equal than depth, maximum width slightly proximad of *ib*/*isb*; chaetotaxy 4:5:4, seta ph_3 present, seta dh_3 removed to halfway between the distal and the intermediary setal rows, seta ih_2 distinctly thinner and longer than other hand setae (0.65–0.070 mm long, ratio hand depth/ih_2 length 2.0–2.4); distal end of the hand and base of the chelal fingers with sclerotized condylar complex. Fixed finger with 18 pointed teeth and with dental canals, two first distal teeth small, third subdistal tooth (*mt*) distinctly modified in shape and deviated in orientation with respect to the others, dental row reaching up to proximad to trichobothrium *sb* and level or distad to sensilla *pc*, 4–6 proximal microtubercles; tip of fixed finger with a modified accessory tooth (*td*) on antiaxial face; one pair of long antiaxial sensory setae (*as*) at the base, one level and the other distad of lyrifissure *fb*, 0.030–0.040 mm long, distance between them 0.036–0.042 mm, fixed finger depth at the base 0.045–0.050 mm; 5 teeth at level of *est*/*it* occupying 0.1 mm, distance between apices 0.023–0.025 mm. Distal half of movable finger with 10–11 pointed teeth with dental canals that reach up to distad or halfway between trichobothria *st* and *sb*, two distal teeth small; basal half of movable chelal finger with 7–8 rounded, partially fused, vestigial teeth without canals on raised lamina; dental row reaching slightly proximad to *sb* or level sensilla *pc*, 3 proximal microtubercles; basal condyle (*bc*) present, basal apodeme long and apically narrowed; coupled sensilla *pc* slightly proximad to trichobothrium *sb* or halfway between *sb* and *b*. Trichobothria as in Fig. 30; trichobothrium *ist* distinct or slightly distad of *esb* and distinct proximad of lyrifissure *fb*; distance between *ib*/*isb* and the base of the hand slightly longer than that between *ib*/*isb* and *esb*; distance between *st*-*sb* 1.9–2.2 times longer than that between *sb*-*b*. Lacking lyrifissures ma_1, ma_2 and *hd*, all the other chelal patterns and most of their standard number are present.

Measurements and ratios: female holotype, followed by female paratypes in square brackets, when different: Body 1.60 [1.00–1.36]. Carapace 0.49/0.47 (1.0) [0.43–0.46/0.42–0.44]. Chelicera 0.45/0.22 (2.1) [0.39–0.41/0.19–0.20], movable finger 0.23 [0.20–0.21]. Pedipalp: femur 0.63/0.11 (5.6) [0.59–0.60/0.10–0.11 (5.6–6.0)], patella 0.26/0.13 (2.1) [0.25–0.27/0.12 (2.1–2.3)], chela 0.91/0.16 (5.9) [0.84–0.85/0.13–0.14 (5.9–6.5)], hand 0.35 (2.3) [0.31–0.33 (2.3–2.4)], movable finger 0.55 [0.50–0.53]; ratio movable finger/hand 1.6 [1.5–1.7], femur/movable finger 1.1 [1.1–1.2], femur/carapace 1.3 [1.3–1.4], chela/carapace 1.9 [1.8–2.0], chela/femur 1.4.

Remarks.—*Occidenchthonius duecensis* sp. nov. is not included in a recognized species-group within the genus. It shares with *O. vachoni* sp. nov. the hypogean life-style, absence of an isolated subapical tooth on chelicera, posterior row of carapace with 2 macrosetae, presence of preocular microsetae, chelal hand lyrifissure *hd* absent and pedipalpal coxa setae *dps*-*mps*-*lps* forming an angle distinctly greater than 90°. Both species differ by the size of the carapacal sublateral ocular setae (*osl*), not shortened in *O. duecensis* sp. nov. (ratio *ame*/*osl* 1.9–2.5) and extremely reduced to microsetae size in *O. vachoni* sp. nov. (ratio *ame*/*osl* 5.0–7.2); additionally, cheliceral lyrifissure *lvb* is present in *O. duecensis* sp. nov. and absent in *O. vachoni* sp. nov.

Distribution.—PORTUGAL: Centro Region.

Etymology.—The species epithet is a Latin adjective referring to the type locality, the spring of the Dueça River and the major cave of the Dueça Cave System.

Occidenchthonius goncalvesi sp. nov.
http://zoobank.org:8080/NomenclaturalActs/E734737B-8C49-4FC2-BE35-32EC293770D7
(Figs. 10–11, 31–37)

Cluthonius n. sp. 4: Reboleira 2012: 161, 162.

Type locality.—PORTUGAL: Algarve region, Faro district, Silves municipality, São Bartolomeu de Messines, Algarão do Remexido (37°14′29″N, 8°16′36″W; 131 m a.s.l.).

Material examined.—*Holotype male*. PORTUGAL: Algarve region, Faro district, Silves municipality, São Bartolomeu de Messines, Algarão do Remexido (37°14′29″N, 8°16′36″W; 131 m a.s.l.), 5 September 2009, A.S.P.S. Reboleira (DEUA).

Paratypes. PORTUGAL: 1 ♂, 7 ♀, 1 tritonymph [1 ♂, 1 ♀, 1 tritonymph (DEUA), 1 ♀ (MCNB), 1 ♀ (MNCN), 1 ♀ (MHNG), 1 ♀ (MNHN), 1 ♀ (NHMW), 1 ♀ (ZMUC)], 15 March 2009; 3 ♂ [(MCNB), (MHNG), (MNHN)], 1 ♀, 1 tritonymph (DEUA), same locality, 23 May 2009; 2 ♂, 2 ♀, 1 tritonymph, 1 deutonymph (DEUA), same locality, 5 September 2009; 5 ♀, 1 tritonymph (DEUA), same locality, 29 December 2009. Faro district, Loulé municipality, Vale Telheiro, Gruta do Vale Telheiro (37°10′13″N, 8°02′05″W; 239 m a.s.l.), paratypes: 1 ♂ (DEUA), same locality, 30 January 2009; 2 ♀ (DEUA), 24 May 2009; 1 ♀, 1 tritonymph (DEUA), same locality, 29 December 2009. All paratypes A.S.P.S. Reboleira.

Diagnosis.—*Occidenchthonius goncalvesi* sp. nov. is a medium-large hypogean species, distinctly troglomorphic. Movable cheliceral finger without isolated subapical tooth (*di*) and with moderately prominent spinneret in females, almost absent in males; cheliceral lyrifissure *ldb* present. Anophthalmic, anterior margin of carapace with one preocular microseta on each side, posterior margin with 2 macrosetae. Pedipalp coxa setae *dps*-*mps*-*lps* forming a 46–52° angle; chelal hand weakly depressed at level of *ib*/*isb*, with low, almost indistinct hump distad of *ib*/*isb* and very gentle slope between trichobothria *ib*/*isb* and *eb*; fixed chelal finger with 17–18 teeth; two-thirds distal parts of movable chelal finger with 12–14 pointed teeth with dental canals, basal third with 5–7 rounded teeth without canals on raised lamina; pedipalpal femur (♂) 7.9, (♀) 7.4–8.1 times longer than broad, length (♂) 0.76–0.91 mm, (♀) 0.89–1.01 mm; chela (♂) 6.8–7.4, (♀) 6.8 times longer than deep, length (♂) 0.98–1.23, (♀) 1.22–1.29 mm; ratio movable chelal finger/chelal hand (♂) 1.5–1.6, (♀) 1.4; lacking lyrifissures ma_1 and ma_2, all the other chelal patterns and their standard number are present.

Description (adults).—*Body:* moderately large, hypogean species with troglomorphic facies and depigmented integu-

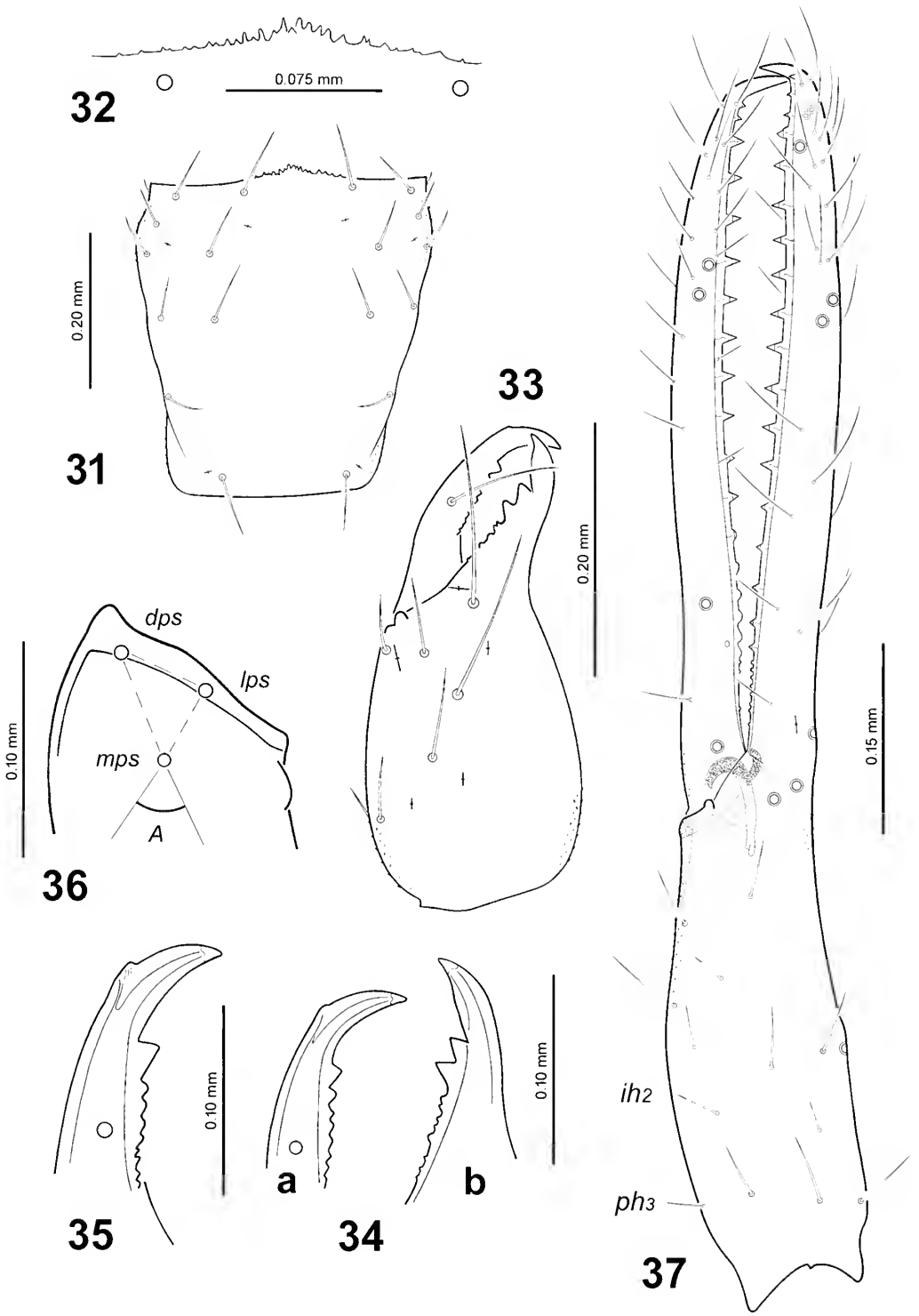

Figures 31–37.—*Occidenchthonius goncalvesi* sp. nov., male holotype and dorsal views, unless stated otherwise: (31) Carapace. (32) Anterior margin of carapace, partial view. (33) Left chelicera. (34) Fingers of left chelicera, partial view, (a) fixed finger, (b) movable finger. (35) Movable cheliceral finger, female paratype, partial view. (36) Left pedipalpal coxa, partial view. (37) Left chela, antiaxial view. See Methods for abbreviations.

ment; weak hispid granulation on lateral surfaces of carapace, on cheliceral hand, on base of movable chelal finger and on distal part of chelal hand.

Carapace (Fig. 31): subquadrate, distinctly longer than broad, weakly constricted posteriorly; medial part of anterior margin prominent, without a well-defined epistome and strongly dentate (Fig. 32). Anophthalmic. Chaetotaxy: 18 setae, with one preocular microsetae on each side (absent or lost in some adults), 2 setae in posterior row, formula 4:6:4:2: 2, anteromedial setae (*ame*) 0.090–0.13 mm long, sublateral

ocular setae (*osl*) 0.030–0.070 mm long, ratio setae *ame*/*osl* 1.8–2.9; 4 lyrifissures anteriorly and 2 posteriorly.

Chelicera (Fig. 33): with 6 setae and one lateral microseta on hand, seta *vb* short (0.035–0.055 mm long), microseta 0.025–0.035 mm; hand with 5 dorsal lyrifissures and one ventral, lyrifissure *ldb* present. Fixed finger (Fig. 34a) with 8–13 teeth proximally decreasing in size, two distal teeth distinctly larger than others, 1–2 proximal microtubercles. Movable finger (Fig. 34b) without an isolated subapical tooth (*di*), with 6–7 teeth proximally decreasing in size, the distal tooth larger than others, 2 proximal microtubercles; spinneret extremely reduced, almost absent, in males (Fig. 34b) and moderately prominent in females (Fig. 35); seta *gl* 0.55–0.61 from base of movable finger. Rallum with 11 blades. Serrula exterior with 15 blades, serrula interior 13 blades.

Abdomen: Chaetotaxy of tergites 4:4:4:4:6:6:6:6:1T2T1:4:1T2T1:0, tergites IX and XI with 2 sublateral tactile setae on each one (0.22–0.26 and 0.24–0.30 mm long respectively). Chaetotaxy of sternites 9–11:(3)6–8(3):(2)6–7(2):7–9:6–7:6:6:6:2T1T2:0:2, lateral setae on sternite III macrosetae size, sternite X with 2 submedial tactile setae (0.21–0.25 mm long); moreover, genital notch of males flanked by 5–8 setae on each side and 4+4 internal glandular setae.

Coxae: pedipalpal coxa with 5 setae (including 2 on manducatory process), distal marginal seta of the disk (*dps*) 0.10–0.13 mm long, areolar insertions of disk setae *dps-mps-lps* forming a 46–52° angle (Fig. 36); coxa I 3 + 3 marginal microsetae, distal marginal seta (*dcs*) 0.07–0.09 mm long, seta *dps* distinctly longer than seta *dcs*; II 4 + 6–10 bipinnate coxal spines, III 5 + 4–6 bipinnate coxal spines and IV 5–6; intercoxal tubercle bisetose.

Pedipalp: femoral chaetotaxy 3:6:3:5:1 (rarely 3:5–6:2–4:5–7:1). Chela (Fig. 37) with hand weakly depressed at level of *ib*/*isb*, with low, almost indistinct hump distad of *ib*/*isb* and very gentle slope between trichobothria *ib*/*isb* and *eb*; weak hollow before base of movable finger with thicker cuticle; width approximately equal than depth, maximum width distinctly proximad of *ib*/*isb*; chaetotaxy 4:5:4, seta ph_3 present, setae dh_3 removed close to the intermediary setal row, seta ih_2 slightly longer than other hand setae (0.055–0.075 mm long, ratio hand depth/ih_2 length 2.4–3.3); distal end of the hand and base of the chelal fingers with sclerotized condylar complex. Fixed finger with 17–18 mostly pointed teeth and with dental canals, two first distal teeth small, third subdistal tooth (*mt*) distinctly modified in shape and deviated in orientation with respect to the others, 0–3 proximal teeth slightly smaller than the others and apically rounded, dental row reaching up to approximately level sensilla *pc*, 8–10 proximal microtubercles; tip of fixed finger with a modified accessory tooth (*td*) on antiaxial face; tip of fixed chelal finger of male with a weak hollow on paraxial face, without subdistal protuberance (*sp*); one pair of long antiaxial sensory setae (*as*) at the base, one level and the other distad of lyrifissure *fb*, (0.040–0.085 mm long), distance between them 0.060–0.110 mm, fixed finger depth at the base 0.052–0.067 mm; 3–4 teeth at level of *est*/*it* occupying 0.1 mm, distance between apices 0.027–0.38 mm. Two-thirds distal parts of movable finger with 12–14 pointed teeth with dental canals that reach up to distinctly proximad halfway between trichobothria *st* and *sb*, two distal teeth tiny; third basal part of movable chelal finger with 5–7 rounded, partially fused, vestigial teeth without canals on raised lamina; dental row reaching proximad of *sb*, often level sensilla *pc*, 3–8 proximal microtubercles; basal condyle (*bc*) present, basal apodeme long and apically indented; coupled sensilla *pc* distad halfway between *sb* and *b*, usually slightly proximad to trichobothrium *sb*. Trichobothria as in Fig. 37; trichobothrium *ist* strongly distad of *esb* and slightly proximad of lyrifissure *fb*; distance between *ib*/*isb* and the base of the hand equal or slightly shorter than that between *ib*/*isb* and *esb*; distance between *st*-*sb* 1.8–2.3 times longer than that between *sb*-*b*. Lacking lyrifissures ma_1 and ma_2, all the other chelal patterns and their standard number are present.

Measurements and ratios: male holotype, followed by male paratypes in square brackets, when different: body 1.33 [1.08–1.36]. Carapace 0.44/0.39 (1.1) [0.43–0.49/0.39–0.46 (1.1)]. Chelicera 0.36/0.17 (2.1) [0.39–0.46/0.18–0.20 (2.2–2.3)], movable finger 0.18 [0.19–0.24]. Pedipalp: femur 0.76/0.10 (7.9) [0.76–0.91/0.10–0.12 (7.9)], patella 0.29/0.12 (2.4) [0.28–0.35/0.12–0.13 (2.3–2.7)], chela 0.98/0.14 (7.0) [1.00–1.23/0.14–0.16 (6.8–7.4)], hand 0.39 (2.8) [0.38–0.47 (2.6–2.8)], movable finger 0.58 [0.60–0.75]; ratio movable finger/hand 1.5 [1.6], femur/movable finger 1.3 [1.2–1.3], femur/carapace 1.7 [1.7–1.9], chela/carapace 2.2 [2.3–2.5], chela/femur 1.3 [1.3–1.4]. *Female paratypes*: body 1.64–1.86. Carapace 0.52–0.53/0.46–0.50 (1.1). Chelicera 0.49–0.50/0.22 (2.2–2.3). Pedipalp: femur 0.89–1.01/0.12–013 (7.4–8.1), patella 0.35/0.15 (2.4), chela 1.22–1.29/0.18–0.19 (6.8), hand 0.50–0.54 (2.8), movable finger 0.70–0.74; ratio movable finger/hand 1.4, femur/movable finger 1.3–1.4, femur/carapace 1.7–1.9, chela/carapace 2.3–2.4, chela/femur 1.3–1.4.

Description (tritonymph paratypes).—Carapace distinctly longer than broad; medial part of anterior margin very weakly prominent and strongly dentate; anophthalmic; macrochaetotaxy as in adult, without preocular microseta on each side; anteromedial setae (*ame*) 0.10–0.11 mm long, sublateral ocular setae (*osl*) 0.03–0.04 mm long, ratio setae *ame*/*osl* 2.8–3.3; 4 lyrifissures anteriorly and 2 posteriorly. Cheliceral hand with 5 setae (lacks seta *it* respect to adults) and 1 lateral microseta; fixed finger with 8–9 teeth, two distal teeth larger than others; movable finger without an isolated subapical tooth (*di*), with 4–7 teeth, the distal one larger than others; spinneret prominent as in female adults; seta *gl* 0.54–0.56 from base of movable finger; lyrifissures patterns as in adults. Chaetotaxy of tergites as in adults; sternites 5:(2)5(2):(1)5(1):7:6:6:6:6:1T2T1:0:2. Pedipalpal coxa 5 setae (including 2 on the manducatory process), distal marginal seta of the disk (*dps*) 0.090–0.095 mm long, areolar insertions of disk setae *dps-mps-lps* forming a 52° angle; coxa I 3 + 2 marginal microsetae; II 4 + 6–8 bipinnate coxal spines, III 5 + 4 bipinnate coxal spines and IV 5; intercoxal tubercle bisetose. Pedipalp with femoral chaetotaxy 2–3:5:2:4–5:1; chelal hand chaetotaxy 4:5:4; trichobothrium *ist* distinctly distad of *esb*, and distinctly proximad of lyrifissure *fb*; fixed finger with 14–15 pointed teeth with dental canals, two first distal teeth small, third subdistal tooth modified (*mt*), 4 teeth at the level of *est*/*it* occupying 0.1 mm, distance between apices 0.030–0.033 mm; distal half of movable finger with 11 pointed teeth with dental canals, 2 tiny distal ones; proximal half of finger with 4–5 rounded vestigial

teeth on raised lamina; coupled sensilla *pc* distad of trichobothrium *b*; lacking lyrifissures fd_3, ma_1 and ma_2.

Measurements and ratios (tritonymph paratypes): body 1.10–1.12. Carapace 0.41–0.43/0.34–0.37 (1.2). Chelicera 0.36–0.38/0.16–0.18 (2.2–2.3), movable finger 0.18. Pedipalp: femur 0.65–0.66/0.10 (6.6–6.8), patella 0.26/0.12 (2.1–2.2), chela 0.83–0.88/0.13–0.14 (6.1–6.3), hand 0.34–0.35 (2.5–2.6), movable finger 0.48–0.52; ratio movable finger/hand 1.4–1.5, femur/movable finger 1.3–1.4, femur/carapace 1.5–1.6, chela/carapace 2.0, chela/femur 1.3.

Description (deutonymph paratype).—Carapace distinctly longer than broad; anophthalmic; chaetotaxy: 4:6:4:2:2, without preocular microsetae. Cheliceral hand with 4 setae (lack setae *db* and *it* respect to adults) and without lateral microsetae, only three lyrifissures present: *ldt*, *lve* and *lvt*; fixed finger with 9 teeth, two distal teeth larger than others; movable finger without an isolated subapical tooth (*di*), with 5 teeth, the distal one larger than others; spinneret prominent as in adult females; seta *gl* 0.55 from base of movable finger. Chaetotaxy of tergites as in adults; sternites 2:4:(1)4(1):6:6:6:6:6:1TT1:0:2. Pedipalpal coxa 5 setae (including 2 on the manducatory process), distal marginal seta of the disk (*dps*) 0.055 mm long, areolar insertions of disk setae *dps-mps-lps* forming a 58° angle; coxa I 2 + 1 marginal microseta; II 3 + 3 bipinnate coxal spines, III 3 + 2 bipinnate coxal spines and IV 3; intercoxal tubercle bisetose. Chelal hand chaetotaxy 4:3:4 (lack setae ih_3 and ih_4 respect to adults); fixed pedipalpal finger with 12 teeth, first distal tooth small, second subdistal tooth modified (*mt*), 5 teeth at level of *est*/*it* occupying 0.1 mm, distance between apices 0.0225–0.0250 mm; movable finger with 9 pointed teeth and 4 rounded, vestigial teeth on weak lamina; coupled sensilla *pc* in subbasal position along the movable finger; lyrifissures *fa*, *fp*, *fb*, fd_1 and mv_1 present, absent all the others.

Measurements and ratios (deutonymph paratype): body 0.68. Carapace 0.28/0.19 (1.4). Chelicera 0.22/0.11 (2.1). Pedipalp: femur 0.34/0.07 (5.2), patella 0.15/0.08 (1.9), chela 0.51/0.09 (5.8), hand 0.21 (2.3), movable finger 0.31; ratio movable finger/hand 1.5, femur/movable finger 1.1, femur/carapace 1.2, chela/carapace 1.9, chela/femur 1.5.

Remarks.—*Occidenchthonius goncalvesi* sp. nov. is not included in any of the recognized species-groups within the genus. *O. goncalvesi* sp. nov. is similar to *O. algharbicus* sp. nov. and *O. ortunoi*, but differs from *O. algharbicus* sp. nov. by position of trichobothrium *ist* and has distinctly smaller and stouter pedipalp than *O. ortunoi*, as compared in the key and in the description of *O. algharbicus* sp. nov.

Distribution.—PORTUGAL: Algarve region.

Etymology.—This species is named after Professor Fernando Gonçalves, University of Aveiro, in recognition of his constribution to the study of subterranean biology in Portugal.

Occidenchthonius vachoni sp. nov.
http://zoobank.org:8080/NomenclaturalActs/DDADC044-02F5-455A-ACA1-6A5EAEDB50C4
(Figs. 38–45)

Chthonius n. sp. 3: Reboleira 2012: 164.

Material examined.—*Holotype male.* PORTUGAL: Centro region, Sicó Massif, Leiria district, Pombal municipality, Redinha, Gruta da Senhora da Estrela (synonym Gruta da Serra-do-Poio) (39°55′41″N, 8°32′59″W; 380 m a.s.l.), 29 August 2009, A.S.P.S. Reboleira (DEUA).

Paratypes. PORTUGAL: 2 ♀ (DEUA), same locality, 11 June 2009; 1 ♀ (DEUA), same locality, 20 November 2009; 4 ♂, 13 ♀, 7 tritonymph [7♀, 1 tritonymph (DEUA), 1♂, 1♀, 1 tritonymph (MCNB), 1♂, 1♀, 1 tritonymph (MNHN), 1♂, 1♀, 1 tritonymph (MHNG), 1♂, 1♀, 1 tritonymph (NHMW), 1♀, 1 tritonymph (MNCN), 1♀, 1 tritonymph (ZMUC)], same locality, 29 August 2009. Leiria district, Ansião municipality, Santiago da Guarda, Gruta da Cerâmica (39°55′37″N, 8°31′04″W; 355 m a.s.l.): 2 ♂, 3 ♀, 1 tritonymph paratypes [DEUA], 28 November 2009; 2 ♀, 3 tritonymph, 1 deutonymph paratypes [DEUA], same locality, 21 March 2010. All paratypes A.S.P.S. Reboleira.

Diagnosis.—*Occidenchthonius vachoni* sp. nov. is a medium-sized hypogean species, weakly troglomorphic. Movable cheliceral finger without isolated subapical tooth (*di*) and with moderately prominent spinneret in females, lacking in males; cheliceral lyrifissure *lvb* absent. Anophthalmic, anterior margin of carapace with 2 preocular microsetae on each side, sublateral ocular setae (*osl*) reduced to microsetae size, posterior margin with 2 macrosetae. Pedipalp coxa setae *dps-mps-lps* forming a 141–153° angle; chelal hand distinctly depressed at level of *ib*/*isb*, with distinct hump distad of *ib*/*isb* and gentle slope between trichobothria *ib*/*isb* and *eb*; fixed chelal finger with 16–18 teeth; two-thirds distal parts of movable chelal finger with 10–13 pointed teeth with dental canals, basal third with 4–6 rounded teeth without canals on raised lamina; pedipalpal femur (♂) 6.6–6.8, (♀) 7.2 times longer than broad, length (♂) 0.52–0.54 mm, (♀) 0.76–0.79 mm; chela (♂) 6.3–6.8, (♀) 5.9–6.0 times longer than deep, length (♂) 0.70–0.72, (♀) 1.00–1.05 mm; ratio movable chelal finger/chelal hand (♂) 1.5–1.6, (♀) 1.5; lacking lyrifissures ma_1, ma_2 and *hd*, all the other chelal patterns and most of their standard number are present.

Description (adults).—*Body:* Medium-sized hypogean species of weak troglomorphic facies and depigmented integument; weak hispid granulation on lateral surfaces of carapace, on the cheliceral hand and on base of chelal fingers.

Carapace (Fig. 38): ubquadrate, distinctly longer than broad, weakly constricted posteriorly; medial part of anterior margin weakly prominent, without a well-defined epistome and strongly dentate (Fig. 39). Anophthalmic. Chaetotaxy: 18 setae, with 2 (one female paratype 1–2) preocular microsetae on each side, 2 setae in posterior row, formula 4:6:4:2:2, anteromedial setae (*ame*) 0.090–0.13 mm long, 0.0040–0.0050 mm wide, sublateral ocular setae (*osl*) reduced to microsetae size: 0.0137–0.0250 mm long, 0.0017–0.0025 mm wide, preocular microsetae 0.0125–0.0175 mm long, 0.0017–0.0020 mm wide, ratio setae *ame*/*osl* 5.0–7.2; 4 lyrifissures anteriorly and 2 posteriorly.

Chelicera (Fig. 40): with 6 setae and 2 lateral microsetae on hand, seta *vb* very short (0.0125–0.0325 mm long), microsetae 0.0075–0.0225 mm; hand with 4 dorsal lyrifissures and one ventral, lyrifissure *lvb* absent, *ldb* and all the others present. Fixed finger (Fig. 41a) with 6–8 teeth proximally decreasing in size, two distal teeth distinctly larger than others, 1–3 proximal microtubercles. Movable finger (Fig. 41b) without an isolated subapical tooth (*di*), with 5–8 teeth proximally decreasing in size, the distal tooth larger than others, 1–5

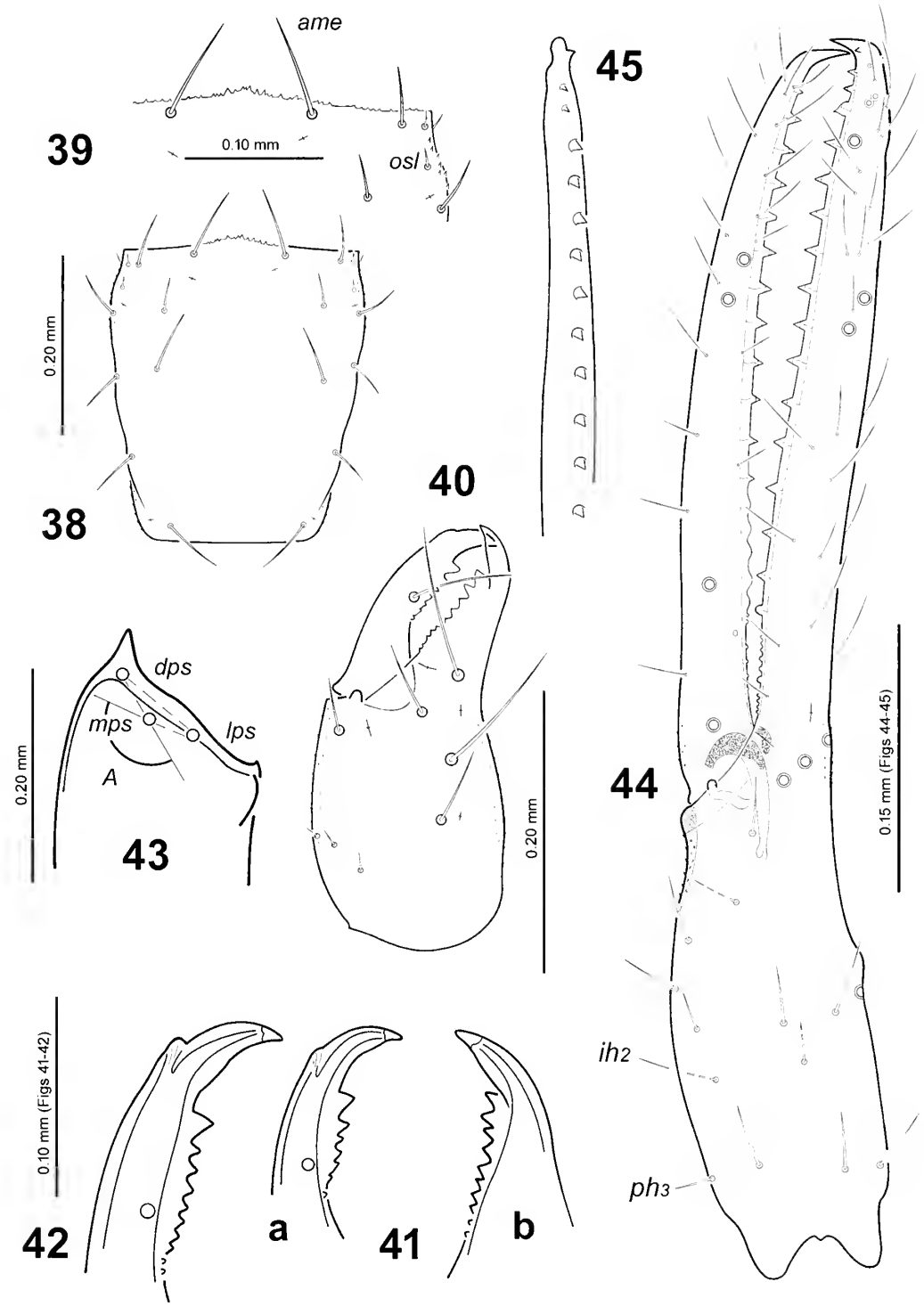

Figures 38–45.—*Occidenchthonius vachoni* sp. nov., male holotype and dorsal views, unless stated otherwise: (38) Carapace. (39) Anterior margin of carapace, partial view. (40) Left chelicera. (41) Fingers of left chelicera, partial view, (a) fixed finger, (b) movable finger. (42) Movable cheliceral finger, female paratype from Gruta da Senhora da Estrela, partial view. (43) Left pedipalpal coxa, partial view. (44) Left chela, antiaxial view. (45) Distal portion of fixed chelal finger, ventral view. See Methods for abbreviations.

proximal microtubercles; spinneret extremely reduced, almost absent, in males (Fig. 41b) and moderately prominent in females (Fig. 42); seta *gl* 0.54–0.60 from base of movable finger. Rallum with 11 blades. Serrula exterior with 14 blades, serrula interior 12 blades.

Abdomen: chaetotaxy of tergites 4:4:4:4:6:6:6:6:1T2T1:4:1T2T1:0, tergites IX and XI with 2 sublateral tactile setae on each one (0.21–0.22 and 0.26–0.29 mm long respectively). Chaetotaxy of sternites 9–10:(3)6–8(3):(2)6–7(2):6–7:6:6:6:6:2T1T2:0:2, lateral setae on sternite III macrosetae size, sternite

X with 2 submedial tactile setae (0.18 mm long); moreover, genital notch of males flanked by 7–9 setae on each side and 4+4 internal glandular setae.

Coxae: pedipalpal coxa with 5 setae (including 2 on manducatory process), distal marginal seta of the disk (*dps*) 0.055–0.090 mm long, areolar insertions of disk setae *dps-mps-lps* forming an angle of 141–153° (Fig. 43); coxa I 3 + 3 marginal microsetae, distal marginal seta (*dcs*) 0.045–0.075 mm long, seta *dps* distinctly longer than seta *dcs*; II 4 + 7–13 bipinnate coxal spines, III 5 + 4–6 bipinnate coxal spines and IV 6; intercoxal tubercle bisetose.

Pedipalp: femoral chaetotaxy 3:6:3:5–6:1. Chela (Fig. 44) with hand distinctly depressed at level of *ib*/*isb*, with distinct hump distad of *ib*/*isb* and gentle slope between trichobothria *ib*/*isb* and *eb*; weak hollow before base of movable finger with thicker cuticle; width slightly longer or equal than depth, maximum width distinctly proximad to *ib*/*isb*; chaetotaxy 4:5:4, seta ph_3 present, setae dh_3 removed close to the intermediary setal row, seta ih_2 distinctly thinner and longer than other hand setae (0.050–0.085 mm long, ratio hand depth/ih_2 length 1.6–2.7); distal end of the hand and base of the chelal fingers with sclerotized condylar complex. Fixed finger with 16–18 pointed teeth and with dental canals, two first distal teeth small, third subdistal tooth (*mt*) distinctly modified in shape and deviated in orientation with respect to the others, distal half with saw-like shape (Fig. 45), most proximal tooth slightly smaller than the others and apically rounded, dental row reaching up to level sensilla *pc*, 5–10 proximal microtubercles; tip of fixed finger with a modified accessory tooth (*td*) on antiaxial face; tip of fixed chelal finger of male with a weak hollow on paraxial face, without subdistal protuberance (*sp*); one pair of long antiaxial sensory setae (*as*) at the base, one level and the other distad of lyrifissure *fb*, 0.025–0.050 mm long, distance between them 0.026–0.040 mm, fixed finger depth at the base 0.043–0.060 mm; 4–5 teeth at level of *est*/*it* occupying 0.1 mm, distance between apices 0.020–0.028 mm. Two-thirds distal parts of movable finger with 10–13 pointed teeth with dental canals that reach up to proximad halfway between trichobothria *st* and *sb*, distal tooth tiny or absent and reduced to a protuberance; third basal part of movable chelal finger with 4–6 rounded, partially fused, vestigial teeth without canals on raised lamina; dental row reaching proximad of *sb*, level sensilla *pc*, 3–6 proximal microtubercles; basal condyle (*bc*) present, basal apodeme long and apically indented; coupled sensilla *pc* distad halfway between *sb* and *b*, slightly proximad to trichobothrium *sb*. Trichobothria as in Fig. 44; trichobothrium *ist* distinct or slightly distad of *esb*, usually forming almost a straight line with *eb-esb*, and distinctly proximad of lyrifissure *fb*; distance between *ib*/*isb* and the base of the hand slightly longer than that between *ib*/*isb* and *esb*; distance between *st-sb* 1.7–2.0 times longer than that between *sb-b*. Lacking lyrifissures ma_1, ma_2 and *hd*, all the other chelal patterns and most of their standard number are present.

Measurements and ratios: male holotype, followed by male paratypes in square brackets, when different: body 0.99 [1.10–1.12]. Carapace 0.35/0.30 (1.2) [0.37–0.40/0.31–0.32 (1.2–1.3)]. Chelicera 0.31/0.14 (2.2), movable finger 0.15 [0.16]. Pedipalp: femur 0.52/0.08 (6.8) [0.52–0.54/0.08 (6.6–6.7)], patella 0.19/0.09 (2.1) [0.21/0.10 (2.1–2.2)], chela 0.70/0.11 (6.4) [0.71–0.72/0.11–0.12 (6.3–6.8)], hand 0.27 (2.5) [0.28 (2.4–2.5)], movable finger 0.43 [0.42–0.43]; ratio movable finger/hand 1.6 [1.5–1.6], femur/movable finger 1.2 [1.2–1.3], femur/carapace 1.5 [1.4], chela/carapace 2.0 [1.8–1.9], chela/femur 1.3 [1.3–1.4]. *Female paratypes:* body 1.42–1.62. Carapace 0.52–0.54/0.46–0.48 (1.1). Chelicera 0.43–0.46/0.19–0.21 (2.2). Pedipalp: femur 0.76–0.79/0.11 (7.2), patella 0.30–0.31/0.14 (2.2–2.3), chela 1.00–1.05/0.17–0.18 (5.9–6.0), hand 0.40–0.42 (2.4), movable finger 0.59–0.62; ratio movable finger/hand 1.5, femur/movable finger 1.3, femur/carapace 1.5, chela/carapace 1.9, chela/femur 1.3.

Description (tritonymph paratypes).—Carapace slightly longer than broad; medial part of anterior margin weakly prominent and strongly dentate; anophthalmic; macrochaetotaxy as in adult, only one preocular microseta on each side; anteromedial setae (*ame*) 0.095 mm long, 0.0032 mm wide, sublateral ocular setae (*osl*) microsetae size: 0.0175 mm long, 0.0017 mm wide, preocular microsetae 0.0150 mm long, 0.0017 mm wide, ratio setae *ame*/ *osl* 5.4; 4 lyrifissures anteriorly and 2 posteriorly. Cheliceral hand with 5 setae (lacks seta *it* respect to adults) and 1 lateral microseta; fixed finger with 7–8 teeth, two distal teeth larger than others; movable finger without an isolated subapical tooth (*di*), with 6–7 teeth, the distal one larger than others; spinneret prominent as in adult female adults; seta *gl* 0.55–0.56 from base of movable finger; lyrifissures patterns as in adults. Chaetotaxy of tergites as in adults; sternites 5:(2)6(2):(1)5(1):6:6:6:6:6:1T2T1:0:2. Pedipalpal coxa 5 setae (including 2 on manducatory process), distal marginal seta of the disk (*dps*) 0.060–0.070 mm long, areolar insertions of disk setae *dps-mps-lps* forming an angle of 104–118°; coxa I 3 + 2 marginal microsetae, distal marginal seta (*dcs*) 0.050 mm long, seta *dps* distinctly longer than seta *dcs*; II 4 + 6–10 bipinnate coxal spines, III 5 + 4–6 bipinnate coxal spines and IV 5; intercoxal tubercle bisetose. Pedipalp with femoral chaetotaxy 3:5:2:4–5:1; chelal hand chaetotaxy 4:5:4, seta ih_2 distinctly thinner and longer than others (0.040–0.045 mm long, ratio hand depth/ih_2 length 2.0–2.7); trichobothrium *ist* forming a straight line with *eb-esb*, and distinctly proximad of lyrifissure *fb*; fixed finger with 15 pointed teeth with dental canals, two first distal teeth small, third subdistal tooth modified (*mt*), distal half with saw-like shape; 5 teeth at level of *est*/*it* occupying 0.1 mm, distance between apices 0.020–0.025 mm; fixed finger with an unique antiaxial sensory setae (*as*) at the finger base, at level of lyrifissure *fb*; distal half of movable finger with 10 pointed teeth with dental canals, 0–1 tiny distal ones; proximal half of finger with 4–5 rounded vestigial teeth on raised lamina; coupled sensilla *pc* distad of trichobothrium *b*; lacking lyrifissures fd_3, *hd*, ma_1 and ma_2.

Measurements and ratios (tritonymph paratypes): body 0.96–1.10. Carapace 0.36–0.39/0.31–0.32 (1.2). Chelicera 0.31–0.32/0.15 (2.1), movable finger 0.17. Pedipalp: femur 0.50/0.09 (5.9), patella 0.20–0.21/0.10 (2.0), chela 0.67/0.13 (5.4), hand 0.27–0.28 (2.1–2.2), movable finger 0.38–0.40; ratio movable finger/hand 1.4–1.5, femur/movable finger 1.3, femur/carapace 1.3–1.4, chela/carapace 1.7–1.9, chela/femur 1.3.

Description (deutonymph paratype).—Carapace almost as long as broad; anophthalmic; chaetotaxy: 4:6:4:2:2, without preocular microsetae. Cheliceral hand with 4 setae (lack setae

db and *it* respect to adults) and without lateral microsetae, anteromedial setae (*ame*) 0.068 mm long, sublateral ocular setae (*osl*) microsetae size: 0.0075 mm long, ratio setae *ame*/*osl* 9.0, only three lyrifissures present: *ldt*, *lve* and *lvt*; fixed finger with 5 teeth, two distal teeth larger than others; movable finger without an isolated subapical tooth (*di*), with 4 teeth, the distal one larger than others; spinneret prominent as in adult females; seta *gl* 0.55 from base of movable finger. Chaetotaxy of tergites as in adults; sternites 2:4:4:6:6:6:6:6:1TT1:0:2, stigmatal microsetae apparently absent. Pedipalpal coxa 5 setae (including 2 on manducatory process), distal marginal seta of the disk (*dps*) 0.045 mm long, areolar insertions of disk setae *dps-mps-lps* forming a 123° angle; coxa I 2 + 1 marginal microseta, distal marginal seta (*dcs*) 0.050 mm long; II 3 + 5–6 bipinnate coxal spines, III 3 + 3 bipinnate coxal spines and IV 3; intercoxal tubercle bisetose. Fixed pedipalpal finger with 12 teeth, two first distal teeth small, third subdistal tooth modified (*mt*), distal half with saw-like shape, 7 teeth at level of *est*/*it* occupying 0.1 mm, distance between apices 0.014–0.016 mm; movable finger with 8 pointed teeth and 4 rounded, vestigial teeth on weak lamina; coupled sensilla *pc* in subbasal position along the movable finger; lyrifissures *fa*, *fp*, *fb*, fd_1 and mv_1 present, absent all the others.

Measurements and ratios (deutonymph paratype): body 0.58. Carapace 0.25/0.23 (1.1). Chelicera 0.21/0.10 (2.1). Pedipalp: femur 0.30/0.12 (5.1), patella 0.14/0.07 (1.9), chela 0.42/0.09 (4.9), hand 0.17 (1.9), movable finger 0.25; ratio movable finger/hand 1.5, femur/movable finger 1.2, femur/carapace 1.2, chela/carapace 1.7, chela/femur 1.4.

Remarks.—*Occidenchthonius vachoni* sp. nov. is not included in any of the recognized species-groups of the genus. *O. vachoni* sp. nov. shares many characters with *O. duecensis* sp. nov., as discussed in the description of the latter species. Additionally, *O. vachoni* sp. nov. has slender and longer pedipalps than *O. duecensis* sp. nov.: (♀) femur 7.2 times longer than broad, length 0.76–0.79 mm, chela 5.9–6.0 times longer than deep, length 1.00–1.05 mm, ratio chela/femur 1.3 in *O. vachoni* sp. nov. versus (♀) femur 5.6–6.0 times longer than broad, length 0.59–0.63 mm, chela 5.9–6.5 times longer than deep, length 0.84–0.91 mm, ratio chela/femur 1.4 in *O. duecensis* sp. nov.

Distribution.—PORTUGAL: Centro region.

Etymology.—This species is dedicated to the memory of Prof. Max Vachon (1908–1991), for his great contribution to the study of pseudoscorpion fauna and particularly those from Portugal.

Genus *Chthonius* C.L. Koch, 1843
Chthonius ischnocheles (Hermann, 1804)

Material examined.—PORTUGAL: Sicó Massif, Coimbra district, Penela municipality, Taliscas, Dueça Cave System, Soprador do Carvalho (39°59′10″N, 8°22′58″W; 200 m a.s.l.), 1 ♂, 21 March 2009; 1 ♂, 9 ♀, 2 tritonymphs (DEUA), 30 August 2009; all A.S.P.S. Reboleira. Portugal, Coimbra district, Cantanhede municipality, Portunhos, Gruta d'el Rey (40°17′39″N, 8°32′49″W; 70 m a.s.l.), 4 ♀ (DEUA), 19 May 2009; 2 ♂, 3 ♀, 2 tritonymphs (DEUA), 8 October 2009; all A.S.P.S. Reboleira.

Remarks.—*Chthonius ischnocheles* inhabits leaf litter, in humid habitats and in moss; in southern Mediterranean regions, it is often found in cave entrances, exhibiting a trogloxene life-style with some populations showing weak hypogean adaptations, usually with the reduction of the posterior pair of eyes (e.g., Mahnert 1977), not observed in the specimens of this study.

The species is widespread in Europe and adjacent areas (Harvey 2013): Andorra, Austria, Belgium, Bulgaria, Croatia, Czech Republic, Croatia, Denmark, France (mainland and Corsica), Germany, Great Britain, Greece, Ireland, Italy (mainland, Sardinia and Sicily), Madeira, Malta, Netherlands, Norway, Poland, Portugal (Azores, Madeira archipelagos), Romania, Serbia, Spain (mainland, Balearic and Canarian archipelagos), Sweden, Switzerland and Turkey. It has been introduced to Saint Helena Island (South Atlantic Ocean) and several Atlantic Coast and Upper Midwestern states in the U.S.A. In Portugal, this species is only known in the middle of the country (Zaragoza 2007; this study).

DISCUSSION

Currently, three Chthoniidae genera occur in mainland Portugal: *Chthonius* (3 spp): *C. halberti* Kew, 1916, *C. ischnocheles* and *C. jonicus* Beier, 1931, *Ephippiochthonius* (3 spp.): *E. gibbus* (Beier, 1952), *E. portugalensis* Zaragoza, 2017 and *E. tetrachelatus* (Preyssler, 1790), and *Occidenchthonius* (9 spp): *O. alandroalensis* sp. nov., *O. algharbicus* sp. nov., *O. cardosoi*, *O. duecensis* sp. nov., *O. goncalvesi* sp. nov., *O. machadoi* (Vachon, 1940), *O. minutus* (Vachon, 1940), *O. serranoi* Zaragoza, 2017 and *O. vachoni* sp. nov. (Fig. 46). Portuguese species of the genera *Chthonius* and *Ephippiochthonius* are scarce and all epigean, whereas the genus *Occidenchthonius* is more diverse and mostly represented by troglobiont species.

Occidenchthonius is distributed mostly in Southern Iberian Peninsula: mainland Portugal (Coimbra, Évora, Faro, Leiria, Lisboa and Setúbal districts) and mainland Spain (Andalusia, Castilla-La Mancha, Murcia and Valencian Community regions). Outside of the Iberian Peninsula, only four species are known: *O. berninii* (Callaini, 1983) and *O. cassolai* (Beier, 1973), both from Sardinia, *O. thaleri* (Gardini, 2009) from mainland Italy (Veneto) and *O. parmensis* (Beier, 1963) which is widespread in Austria, Croatia, Germany, Italy, Slovenia and Switzerland.

Occidenchthonius is a genus that frequently inhabits hidden subterranean ecosystems, i.e., endogean habitats in microcaverns within the soil, or hypogean habitats in meso and macrocaverns below the soil, and shows a high degree of endemicity. It has also been found at the surface, though up to now such records are scarce (Zaragoza 2017). Due to its small size, we should not dismiss the possibility that the lack of *Occidenchthonius* in surface ecosystems might be a result of overlooking them during sampling. The discovery of five new *Occidenchthonius* species in caves of Portugal with micro-endemic patterns increases to 48 the number of currently known species of the genus (Zaragoza 2017).

Hypogean pseudoscorpions in mainland Portugal are represented by four families, Chthoniidae (*Occidenchthonius*), Neobisiidae (*Roncocreagris* Mahnert, 1976) and two remarkable relict monospecific genera: *Titanobochica* Zaragoza & Reboleira, 2010 (the species name is here changed from *Titanobochica magna* to *Titanobochica magnus*, since the suffix

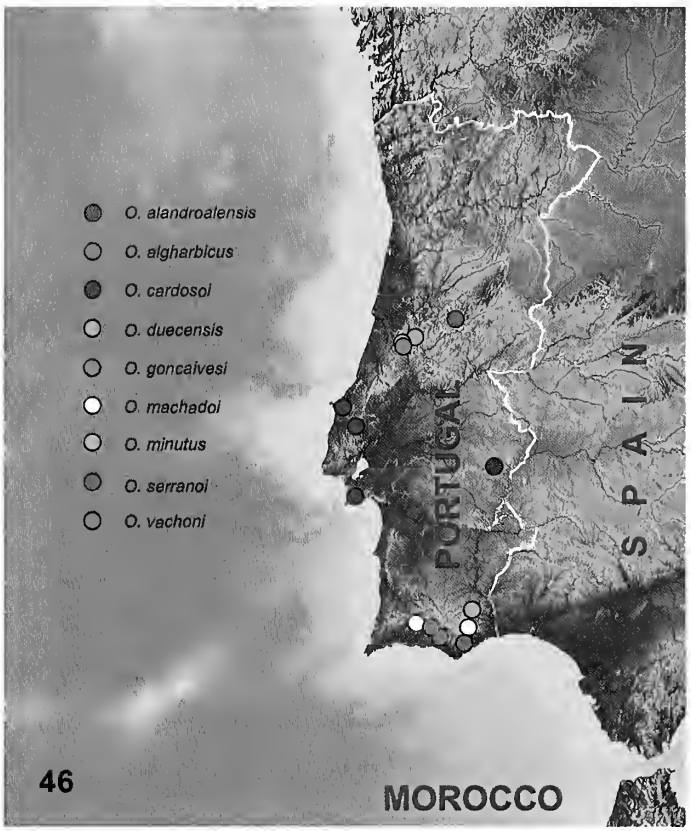

Figure 46.—Distribution map of *Occidenchthonius* spp. in Portugal.

Bochica corresponds to the name of an Amerindian God, masculine in gender) and *Lusoblothrus* Zaragoza & Reboleira, 2012, of the families Bochicidae and Syarinidae respectively. Pseudoscorpions are now the second most diversified group of troglobionts in mainland Portugal; only terrestrial isopods are richer in mainland Portugal (Reboleira et al. 2015).

ACKNOWLEDGMENTS

We are grateful to Francisco Luís Rasteiro, who kindly provided habitus pictures of *Occidenchthonius cardosoi*. ASR was supported by the FCT Portugal (grant ref. SFRH/BPD/110000/2015) and by a research grant (15471) from VILLUM FONDEN. Our gratitude to two anonymous referees for their helpful comments and suggestions on the manuscript.

LITERATURE CITED

Chamberlin, J.C. 1931. The arachnid order Chelonethida. Stanford University Publications, Biological Sciences 7(1):1–284.

Gabbutt, P.D. & M. Vachon. 1963. The external morphology and life history of the pseudoscorpion *Chthonius ischnocheles* (Hermann). Proceedings of the Zoological Society of London 140:75–98.

Gardini, G. 2013. A revision of the species of the pseudoscorpion subgenus *Chthonius* (*Ephippiochthonius*) (Arachnida, Pseudoscorpiones, Chthoniidae) from Italy and neighbouring areas. Zootaxa 3655:1–151.

Harvey, M.S. 1992. The phylogeny and classification of the Pseudoscorpionida (Chelicerata: Arachnida). Invertebrate Taxonomy 6:1373–1435.

Harvey, M.S. 2013. Pseudoscorpions of the World, version 3.0. Western Australian Museum, Perth. Available from: http://www.museum.wa.gov.au/catalogues-beta/pseudoscorpions (accessed 30 December 2016).

Judson, M.L.I. 2007. A new and endangered pseudoscorpion of the genus *Lagynochthonius* (Arachnida, Chelonethi, Chthoniidae) from a cave in Vietnam, with notes on chelal morphology and the composition of the Tyrannochthoniini. Zootaxa 1627:53–68.

Mahnert, V. 1977. Spanische Höhlenpseudoskorpione. Miscelanea Zoologica 4:61–104.

Mahnert, V. 1993. Pseudoskorpione (Arachnida: Pseudoscorpiones) von Inseln des Mittelmeers und des Atlantiks (Balearen, Kanarische Inseln, Madeira, Ascensión), mit Vorwiegend subterraner Lebensweise. Revue suisse de Zoologie 100:971–992.

Mahnert, V. 2011a. A nature's treasury: Pseudoscorpion diversity of the Canary Islands, with the description of nine new species (Pseudoscorpiones, Chthoniidae, Cheiridiidae) and new records. Revista Ibérica de Aracnología 19:27–45.

Mahnert, V. 2011b. New records of pseudoscorpions from the Juan Fernandez Islands (Chile), with the description of a new genus and three new species of Chernetidae (Arachnida: Pseudoscorpiones). Revue suisse de Zoologie 118:17–29.

NECA (Núcleo de Espeleologia da Costa Azul) & Associação de Municípios da Região de Setúbal. 2015. Sistema do Frade. Classificação dos espeleotemas e contribuições para o conhecimento do carso da Arrábida ocidental, Associação de Municípios da Região de Setúbal. Setúbal: 1–332.

NECA (Núcleo de Espeleologia da Costa Azul). 2016. Arrábida "per fora e por dentro". Guia do Património Natural no Concelho de Sesimbra, Núcleo de Espeleologia da Costa Azul, Sesimbra. 1–107.

Reboleira, A.S.P.S. 2012. Biodiversity and conservation of subterranean fauna of Portuguese karst. PhD Thesis, University of Aveiro, Portugal. 1–333.

Reboleira, A.S.P.S. & F. Correia. 2016. Sesimbra, por fora e por dentro, as grutas, a fauna cavernícola e a sua ecologia. Edições Afrontamento Coleção Biologicando 11:1–172.

Reboleira, A.S.P.S., P. Borges, F. Gonçalves, A. Serrano & P. Oromí. 2011. The subterranean fauna of a biodiversity hotspot region - Portugal: an overview and its conservation. International Journal of Speleology 40:23–37.

Reboleira, A.S.P.S., F. Gonçalves & P. Oromí. 2013a. Literature survey, bibliographic analysis and a taxonomic catalogue of subterranean fauna from Portugal. Subterranean Biology 10:51–60.

Reboleira, A.S.P.S., F. Gonçalves, P. Oromí & S. Taiti. 2015. The cavernicolous Oniscidea (Crustacea: Isopoda) of Portugal. European Journal of Taxonomy 161:1–61.

Reboleira A.S.P.S., F. Gonçalves, P. Oromí & J.A. Zaragoza. 2010. *Titanobochica*, surprising discovery of a new cave-dwelling genus from southern Portugal (Arachnida: Pseudoscorpiones: Bochiciidae). Zootaxa 2681:1–19.

Reboleira, A.S.P.S., J.A. Zaragoza, F. Gonçalves & P. Oromí. 2012. *Lusoblothrus*, a new syarinid pseudoscorpion genus (Arachnida) from Portugal, occupying an enigmatic position within the Holarctic fauna. Zootaxa 3544:52–62.

Reboleira, A.S.P.S., J.A. Zaragoza, F. Gonçalves & P. Oromí. 2013b. On hypogean *Roucocreagris* (Arachnida: Pseudoscorpiones: Neobisiidae) from Portugal, with descriptions of three new species. Zootaxa 3670:283–299.

Zaragoza, J.A. 2000. Pseudoscorpiones cavernícoles de Asturias, Cantabria y País Vasco (Arachnida). Mediterránea, Série de Estudios Biológicos 17:5–17.

Zaragoza, J.A. 2007. Catálogo de los pseudoescorpiones de la Península Ibérica e Islas Baleares (Arachnida: Pseudoscorpiones). Revista Ibérica de Aracnología 13:3–91.

Zaragoza, J.A. 2012. *Chthonius (Ephippiochthonius) cardosoi*, nueva especie hipogea de Portugal (Pseudoscorpiones: Chthoniidae). Revista Ibérica de Aracnología 20:25–30.

Zaragoza, J.A. 2017. Revision of the *Ephippiochthonius* complex (Pseudoscorpiones, Chthoniidae) in the Iberian Peninsula, Balearic Islands and Macaronesia, with proposed changes to the status of the *Chthonius* subgenera. Zootaxa 4246:1–221.

Zaragoza, J.A., E. de Mas & C. Ribera 2007. Pseudoescorpiones del Parque Natural del Cadí-Moixeró (Pirineo Catalán): estudio ecológico, faunístico y taxonómico (Arachnida: Pseudoscorpiones). Revista Ibérica de Aracnología 14:69–95.

Manuscript received 1 May 2017, revised 28 June 2017.

2018. Journal of Arachnology 46:104–113

Phoretic or not? Phylogeography of the pseudoscorpion *Chernes hahnii* (Pseudoscorpiones: Chernetidae)

Vera Opatova[1,2] and **František Šťáhlavský**[1]: [1]Department of Zoology, Faculty of Science, Charles University in Prague, Viničná 7, CZ – 128 44 Prague, Czech Republic; [2]Department of Biological Sciences and Auburn University Museum of Natural History, Auburn University, Auburn, AL 36849, USA. E-mail: vzo0003@auburn.edu

Abstract. An organism's ability to respond to ecological changes at its currently inhabited location, and to colonize a new one, is particularly important for organisms inhabiting ephemeral habitats. Phoresy, which involves attaching of a non-vagile individual to a selected carrier of a different species, is used by a wide variety of taxa, but surprisingly little is known about the genetic structure of phoretic species. A better understanding of their genetic structure would help elucidate the efficacy of this manner of dispersal. In this study, we analyse the phylogeographic patterns of the pseudoscorpion *Chernes hahnii* (C.L. Koch, 1839) across a 1830 km range, encompassing most of the species' distribution range in Europe. The lack of geographic structure and low divergences within the two main clades suggest that *C. hahnii* disperses by phoresy. Individuals shared haplotypes at localities 350 km apart and very little divergence was detected between localities over 1450 km away from each other, indicating that phoresy is a very efficient manner of dispersal in this species. We also detected highly divergent populations within *C. hahnii*; however, more material and additional data would be necessary in order to evaluate the potential existence of cryptic diversity within this species.

Keywords: Arachnida; dispersal; Europe; lack of geographic structure; phoresy

An organism's dispersal capability plays a key role in colonizing new habitats and is one of the main factors behind the distribution patterns of individual taxa (Bernatchez & Wilson 1998; Michalak et al. 2010; Gittenberger 2012; Wahlberg & Johanson 2014). The ability to leave a currently inhabited site and find a new one after unfavourable ecological changes or habitat degradation is particularly important for organisms living in temporary habitats such as decomposing wood, animal carrion, faeces, ephemeral streams, vernal pools, or host organisms as in the case for parasites. Many organisms with low dispersal capability evolved different strategies of colonizing new habitats by means of passive transportation (Hulsmans et al. 2007; Macchioni 2007; Vanschoenwinkel et al. 2008). Phoresy (Beier 1948) is a type of passive transportation that involves attachment of a non-vagile individual to a selected carrier from a different species. Phoresy is used by a wide variety of animal groups; e.g., nematodes (Okumura & Yoshiga 2014; Pimentel et al. 2014), crustaceans (Brochet et al. 2010; Sabagh et al. 2011), bryozoans (Brochet et al. 2010), mollusks (Gittenberger 2012), insects (Bartlow et al. 2016; Hastriter et al. 2017) and arachnids. Among arachnids it is particularly common in mites (Barton et al. 2014; Hastriter & Bush 2014; Keum et al. 2016; Pfammatter et al. 2016) and pseudoscorpions (Muchmore 1971; Poinar et al. 1998), but there are also records for spiders (Camargo et al. 2015) and ticks (Saloña-Bordas et al. 2015). Surprisingly, there is very little information about the genetic structure of phoretic organisms (Wilcox et al. 1997; Zeh et al. 2003; Pfeiler et al. 2009; Harvey et al. 2015); however, this information would help evaluate the efficacy of this manner of dispersal.

Phoresy is known from at least 10 pseudoscorpion families (Poinar et al. 1998), where the most common hosts are Coleoptera and Diptera (Poinar et al. 1998). There are also records of phoretic dispersal of pseudoscorpions on vertebrate carriers such as birds (Harvey et al. 2015) and bats (Finlayson et al. 2015), which may play an important role in colonization of cave systems (Moulds et al. 2007). The carrier host specificity varies depending on the species. Most species use multiple carriers, for example a variety of different beetle or fly species, or a combination of both (Poinar et al. 1998), but some species appear to be ecologically linked to a specific carrier host (Zeh & Zeh 1992a, b). Pseudoscorpions usually attach themselves to their carrier's appendages (e.g., legs, wing bases, antennae) (Poinar et al. 1998) or crawl underneath the elytra in the case of beetles (Zeh & Zeh 1992b). Phylogeographic patterns have been studied in several phoretic pseudoscorpion species (Wilcox et al. 1997; Ranius & Douwes 2002; Zeh et al. 2003; Pfeiler et al. 2009). In some species, the populations showed significant structuring (Wilcox et al. 1997; Zeh et al. 2003; Pfeiler et al. 2009), while other species displayed very little genetic variation across populations (Ranius & Douwes 2002; Harvey et al. 2015). However, it is difficult to make assumptions about the efficacy of phoretic dispersal from these results. Deep structuring in some species was likely caused by the presence of cryptic diversity (Wilcox et al. 1997; Zeh et al. 2003), a relatively small area was sampled (Ranius & Douwes 2002), the species naturally occurs in a specific type of habitat that likely limits the species' distribution (Pfeiler et al. 2009), or the study involved only a couple of populations (Harvey et al. 2015).

Chernes hahnii (C.L. Koch, 1839) (Fig. 1) belongs to the family Chernetidae, one of the most diverse pseudoscorpion families with a cosmopolitan distribution (Harvey 2013). Its representatives can be found in a large variety of terrestrial habitats, and many species are specialized to patchy ephemeral habitats such as tree hollows or decaying plant material (Weygoldt 1969). *Chernes hahnii* is a medium sized pseudoscorpion (2.2 – 2.7 mm) with a wide distribution, ranging from Central Europe, northern parts of southern Europe to Caucasus and Central Asia, with sporadic records from eastern China (Fig. 1) (Harvey 2013). There are few records in the literature suggesting an even wider distribution; however, these may correspond to the congeneric species *C. cimicoides* (Fabricius, 1793) that is morphologically very similar to *C. hahnii* and misidentifications were likely until

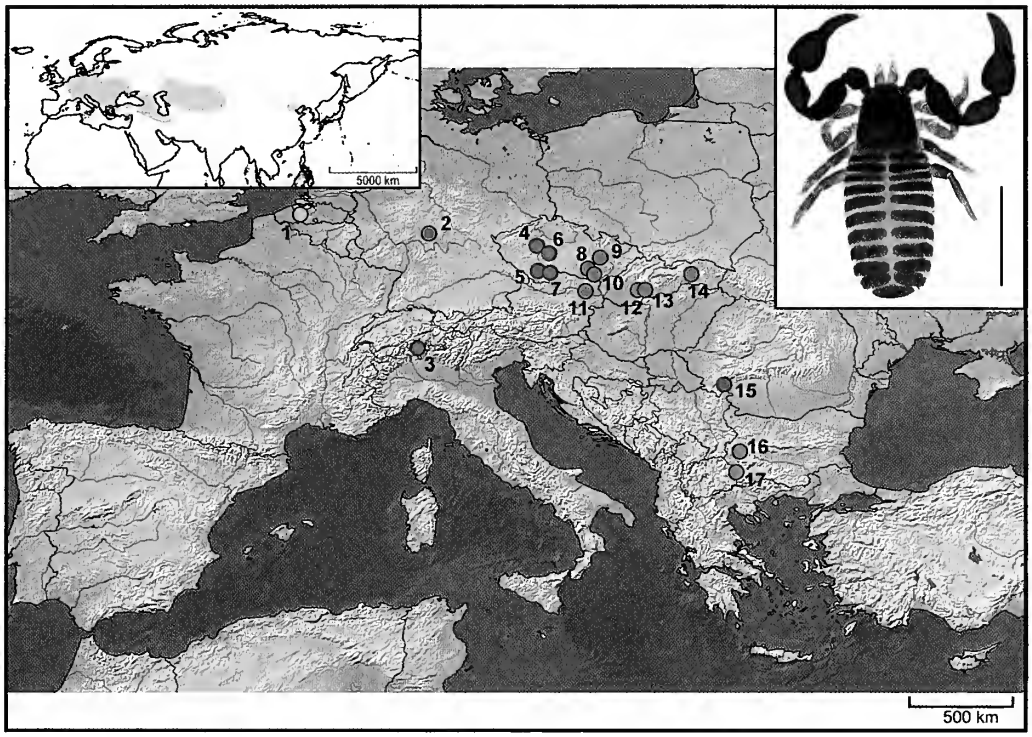

Figure 1.—Map showing sampling locations of *C. hahnii*. Upper left corner insert shows the distribution of species according to the Pseudoscorpions of the World catalogue (Harvey 2013), only references after species redescription by Beier (1960) are considered. Both maps were created with the help of online version of SimpleMappr (Shorthouse 2010). Upper right corner insert shows adult male of *C. hahnii* (bar = 1mm).

diagnostic characters were redefined in both species (Beier 1960). *Chernes hahnii* is mostly found under the bark of various deciduous trees, in tree hollows, in bird nests and nest boxes (Koch 1873; Beier 1948; Christophoryová et al. 2017). There is little information available about phoresy in *C. hahnii* and the earliest record (Schiner 1872) is possibly a misidentification (Beier 1948). However, the combination of the wide distribution range of the species and its presence under tree bark, in tree hollows and nests; i.e., the habitat typical for phoretic species, suggests that *C. hahnii* uses phoresy as a manner of dispersal. Alternatively, *C. hahnii* could also represent a species-complex harbouring multiple cryptic lineages that are geographically isolated, but unrecognizable on the basis of morphological characters. In this study, we analyse the phylogeographic patterns of *C. hahnii* from Central and Eastern Europe using mitochondrial data in order to establish whether the species uses phoretic dispersal, and to test its efficiency.

METHODS

Taxonomic sampling, PCR amplification, sequencing and sequence alignment.—The 33 individuals of *Chernes hahnii* used in this study were hand collected from under tree bark at 17 different locations across Europe, covering most of the species' known distribution range in this region (Fig. 1). *Chernes nigrimanus* Ellingsen, 1897 and *Dinocheirus panzeri* (C.L. Koch, 1837) (Chernetidae) were used as outgroups in the phylogenetic analyses. The outgroups were selected based on the results of an ongoing project focusing on diversity of European chernetids. In this project, we did not detect any ancestrally shared haplotypes/alleles between *C. hahnii* and any other *Chernes* taxa (Opatova et al. unpublished). Detailed locality information and Genbank accession numbers are provided in Table 1. The vouchers were deposited in the collections of the Department of Zoology, Faculty of Science, Charles University in Prague, Czech Republic.

Whole genomic DNA was extracted from the samples using the DNeasy Tissue Kit (Qiagen), according to the manufacturer's guidelines. A partial fragment of the mitochondrial gene Cytochrome oxidase I (*cox1*) (the animal barcode) was amplified for all individuals with the primer pair C1-J-1490/C1-N-2198 (Folmer et al. 1994). Partial fragments of two nuclear genes—28S rDNA (*28S*) and Histone H3 (*H3*)—were amplified for a small number of *C. hahnii* individuals (4 and 2 respectively) from different localities in order to assess the amount of variability of the gene fragments and their potential informativeness for the phylogenetic analyses. The fragments were amplified with the following primer combinations: 28SpsF1/28SpsR1 (Murienne et al. 2008) for *28S*, and H3a F/H3a R (Colgan et al. 1998) for *H3*. PCR conditions followed the protocol described in Opatova & Arnedo (2014), the PCR products were then purified using MinElute PCR Purification Kit (Qiagen) and sequenced in both directions by Macrogen Inc. (Seoul, South Korea). The chromatograms were assembled and edited in Geneious v. 5.3.6 (Drummond et al. 2010). The alignment of all three fragments (*cox1*, *28S*, *H3*) was trivial since no length polymorphism due to indel mutations was observed.

Phylogenetic analysis.—The best partitioning scheme and evolutionary models for each codon position of the *cox1* dataset were selected using the greedy algorithm in the

Table 1.—Locality data and GenBank accession numbers for the specimens sequenced in this study.

Species	Locality Name (Number)	Country	Lat/Long	Sample code	*cox1*
Dinocheirus panzeri	Hlohovec	Czech Republic	48.7738N 16.7822E	DINP1	MF538664
Chernes nigrimanus	Cervene Blato	Czech Republic	48.8560N 14.8016E	CHERN1	MF538665
Chernes hahnii	Litovelske Pomoravi I (9)	Czech Republic	49.7781N 16.9712E	8581	MF538666
Chernes hahnii	Litovelske Pomoravi II (9)	Czech Republic	49.7102N 17.0468E	8584	MF538667
Chernes hahnii	Litovelske Pomoravi III (9)	Czech Republic	49.7196N 17.0298E	8585	MF538668
Chernes hahnii	Magadino (3)	Switzerland	46.1549N 08.8629E	AlpenF1	MF538669
Chernes hahnii	Magadino (3)	Switzerland	46.1549N 08.8629E	AlpenF2	MF538670
Chernes hahnii	Magadino (3)	Switzerland	46.1549N 08.8629E	AlpenF3	MF538671
Chernes hahnii	Lilyanovo (17)	Bulgaria	41.6135N 23.3133E	BG2	MF538672
Chernes hahnii	Sofia (16)	Bulgaria	42.6960N 23.3280E	BG22	MF538673
Chernes hahnii	Prague I (4)	Czech Republic	50.0689N 14.4290E	Ch53	MF538674
Chernes hahnii	Prague I (4)	Czech Republic	50.0689N 14.4290E	Ch54	MF538675
Chernes hahnii	Prague I (4)	Czech Republic	50.0689N 14.4290E	Ch55	MF538676
Chernes hahnii	Prague II (4)	Czech Republic	50.0734N 14.4247E	Ch58	MF538677
Chernes hahnii	Prague II (4)	Czech Republic	50.0734N 14.4247E	Ch59	MF538678
Chernes hahnii	Brno (8)	Czech Republic	49.2515N 16.5750E	Ch60	MF538679
Chernes hahnii	Ceske Budejovice (5)	Czech Republic	48.974N 14.47817E	Ch64	MF538680
Chernes hahnii	Ceske Budejovice (5)	Czech Republic	48.974N 14.47817E	Ch65	MF538681
Chernes hahnii	Konopiste (6)	Czech Republic	49.7803N 14.6619E	CHERH1	MF538682
Chernes hahnii	Bad Hersfeld (2)	Germany	50.8684N 09.7011E	CHERH3	MF538683
Chernes hahnii	Modry kamen – Rieeky (12)	Slovakia	48.2774N 19.3150E	GSK336	MF538684
Chernes hahnii	Filakovske Kovaee (13)	Slovakia	48.2816N 19.7962E	GSK337	MF538685
Chernes hahnii	Kosiee (14)	Slovakia	48.7224N 21.2641E	GSK338	MF538686
Chernes hahnii	Kosiee (14)	Slovakia	48.7224N 21.2641E	GSK339	MF538687
Chernes hahnii	Kosiee (14)	Slovakia	48.7224N 21.2641E	GSK358	MF538688
Chernes hahnii	Vienna (11)	Austria	48.2047N 16.3626E	M1	MF538689
Chernes hahnii	Vienna (11)	Austria	48.2047N 16.3626E	M2	MF538690
Chernes hahnii	Konopiste (6)	Czech Republic	49.7803N 14.6619E	M3	MF538691
Chernes hahnii	Beile Herculane (15)	Romania	44.8819N 22.4143E	M117	MF538692
Chernes hahnii	Ghent (1)	Belgium	51.0389N 03.7240E	M124	MF538693
Chernes hahnii	Ghent (1)	Belgium	51.0389N 03.7240E	M125	MF538694
Chernes hahnii	Lednice na Morave (10)	Czech Republic	48.8044N 16.8077E	M174	MF538695
Chernes hahnii	Lednice na Morave (10)	Czech Republic	48.8044N 16.8077E	M175	MF538696
Chernes hahnii	Bad Hersfeld (2)	Germany	50.8684N 09.7011E	M178	MF538697
Chernes hahnii	Straz nad Nezarkou (7)	Czech Republic	49.0692N 14.9094E	M184	MF538698

program PartionFinder v. 1.0.1 (Lanfear et al. 2012). The Bayesian inference (BI) analyses were conducted in MrBayes v. 3.2.6 (Ronquist & Huelsenbeck 2003) and run remotely at the CIPRES Science gateway v 3.3 (Miller et al. 2010). An independent evolutionary model (see Results) was defined for each codon position. Two independent runs of $5x10^7$ generations with 8 MCMC (Markov Chain Monte Carlo) chains each, starting from random trees and resampling each 1000 generations, were run simultaneously. The first 20% of the generations were discarded as a *burn-in* for the analyses. Convergence and chain mixing was assessed by standard deviation of split frequencies (<0.01) and ESS values summarized in TRACER v. 1.5 (Rambaut & Drummond 2009). Maximum Likelihood (ML) analyses were conducted in RaxML v.7.4.2 (Stamatakis 2006). An independent GTR+G substitution model was assigned to each codon position. The best maximum likelihood tree was selected from 1000 searches, while support of the nodes was assessed with 1000 replicates of bootstrap resampling. All trees were visualized and manipulated with the program FigTree v. 1.3.1 (Rambaut 2009).

Estimation of divergence times.—Divergence times were estimated for the full *C. hahnii cox1* dataset using the program BEAST v. 1.8.4. (Drummond et al. 2012). Because of the lack of relevant biogeographic events and no fossil record for the genus *Chernes*, we used the general arthropod mitochondrial substitution rate of 2.3% (Brower 1994). A lognormal prior was assigned to the ucld.mean parameter of the lognormal relaxed clock for *cox1* with an initial and mean value of 0.0115, each. A Coalescent – constant size model was set as a tree prior. A corresponding evolutionary model selected by PartionFinder was assigned to the *cox1* dataset, which was treated as a single partition.

Genetic divergence and haplotype network.—Genetic distances were calculated for the *cox1* dataset in MEGA 7 (Kumar et al. 2016) via both the uncorrected p-distance and the Tamura – Nei distance model (Tamura & Nei 1993; Tamura & Kumar 2002). Standard genetic diversity indices, including the nucleotide (π) and haplotype diversity (Hd) indices, were calculated in DnaSP 5.10.1 (Librado & Rozas 2009). The genetic distances and diversity indices were calculated for the entire *C. hahnii* dataset, the two main clades recovered in the Bayesian analyses and between them. Genetic distances using the Tamura – Nei distance model were also calculated among all sampled localities. The haplotype network was constructed with the program PopART (available online at http://popart.otago.ac.nz/) using the TCS method (Clement et al. 2000). Geographic distances among sampled locations were obtained in Geographic Matrix

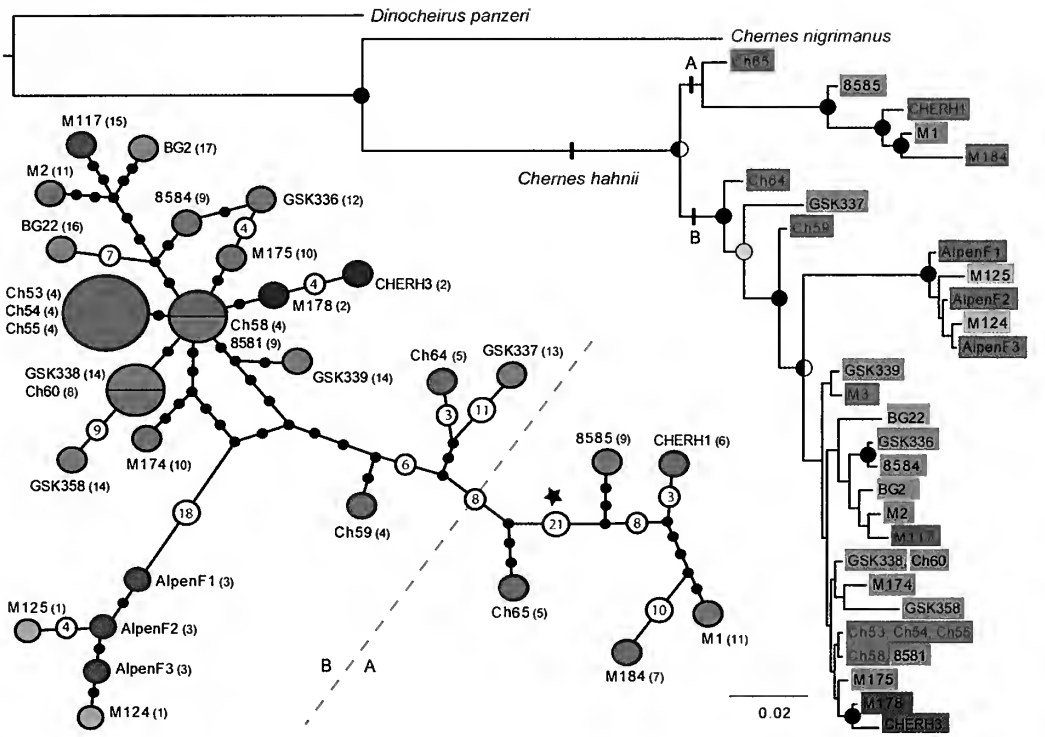

Figure 2.—Upper right corner shows topology obtained in the Bayesian analyses. Dots on nodes denote support as follows: right semi-circles are Bayesian posterior probabilities (PP) and left semi-circles are maximum likelihood bootstraps, black= PP> 0.95, ML bootstrap support > 70%, grey= same topology but with lower support values than thresholds above, white= topology not recovered in ML, nodes without dots= topology not recovered in ML and BI support lower than threshold. Left corner shows the haplotype network obtained by the TCS method. Four and more mutational steps between haplotypes or reticulation are depicted as numbers. Doted grey line corresponds to the clades recovered in BI analyses. Star marks the division in ML analyses. Haplotypes are colour-corded according to the sampling locations in Fig. 1 in both cases.

Distance Generator v 1.2.3. (Ersts, available online at http://biodiversityinformatics.amnh.org/open_source/gdmg).

RESULTS

A total of 35 specimens (33 *C. hahnii* samples, 2 outgroups) was used in this study (Table 1), sampled from the localities shown in Fig. 1. The sequence length for each gene fragment was as follows: *cox1:* 608bp *28S*: 1126bp and *H3:* 371bp. Thirty-one unique haplotypes (including outgroups) identified within the *cox1* dataset were used in ML and BI analyses. No variability was detected in the *28S* and *H3* datasets, therefore these gene fragments were not amplified for the entire *C. hahnii* sample and were not included in the analyses. Independent nucleotide substitution models selected by PartitionFinder for each codon position within the *cox1* dataset in BI were defined as follows: HKY+G was assigned to both 1st and 3rd positions and F81+I to 2nd position. HKY+G model was assigned to *cox1* in divergence time estimation analyses in BEAST.

In both maximum likelihood (-lnL=2121.852) and Bayesian analyses (Fig. 2), a large portion of the tree lacked support. Overall BI yielded support for a higher number of nodes. The topology was similar between the two methods in supported nodes, but differed in unsupported ones. Both methods recovered the monophyly of *C. hahnii* and supported its division into two main clades (clade A and clade B). The placement of the individual Ch65 differed between the analyses. In the BI, the individual belonged to clade A (as shown in Fig. 2), while in the ML it was placed as sister to all individuals in clade B. Successive branching of the individuals Ch64, GSK337, Ch59 at the base of clade B was recovered by both methods. Bayesian analyses further supported a division between a lineage comprising five individuals from Belgium and Switzerland (AlpenF1-F3, M124, M125) and all the remaining *C. hahnii* individuals with unresolved relationships. Haplotypes were shared by individuals from different localities in two instances (see details below), while individuals from both A and B clades co-occurred at three localities: individuals M1, M2 at loc. 11 in Austria, and loc. 6 (individuals CHERH1, M3) and loc. 9 (individuals 8584, 8585) in the Czech Republic.

Divergence time estimation analyses conducted in BEAST also yielded a poorly supported tree (Fig. 3). The overall topology was similar to the topology obtained in BI and the topology of the supported clades was similar to both BI and ML results. The basal split between the two *C. hahnii* clades was dated approximately to 0.09 Million years ago (Ma) (95% highest posterior density (HPD): 0.5644 – 0.0017). Clade A started diversifying at 0.035 Ma (0.23 – 0.0006), although this node was not supported, two supported nodes from clade A dated back to 0.018 Ma (0.122 – 0.0003) and 0.008 Ma (0.05 – 0.001). Clade B started diversifying at 0.044 Ma (0.257 – 0.0009) (unsupported node), the only supported deeper node from clade B dated to 0.027 Ma (0.171 – 0.0004).

We observed a lack of geographic structure in the haplotype network (Fig. 2). Nine individuals from Central Europe

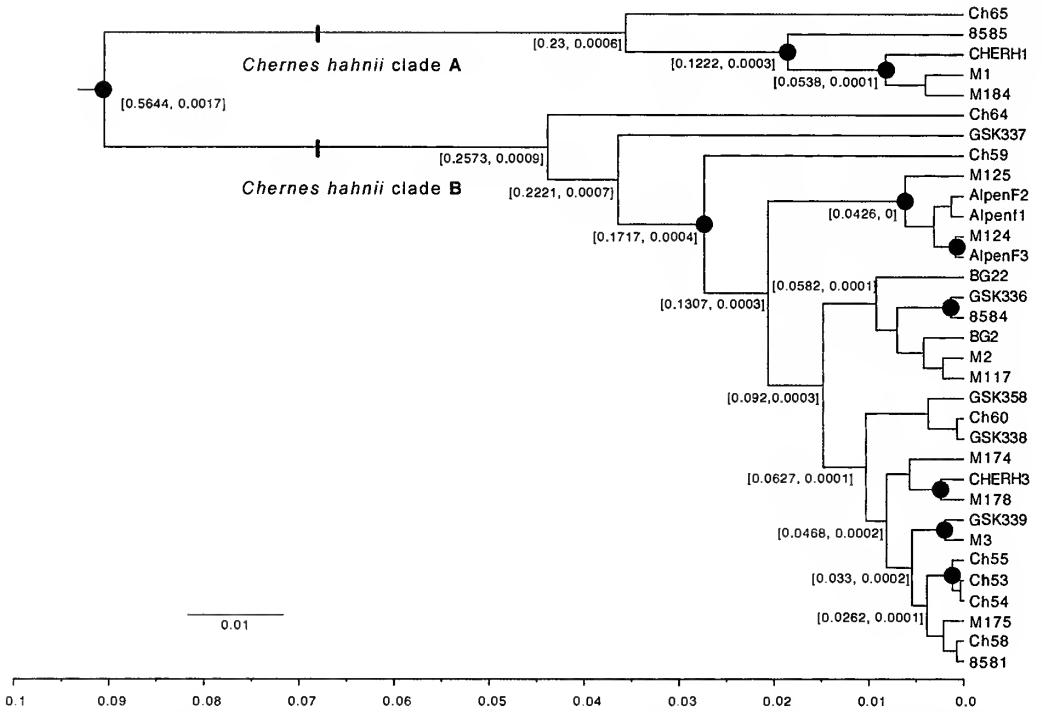

Figure 3.—Chronograms obtained in BEAST analyses. Dots on nodes denote Bayesian posterior probabilities above 0.95. Numbers in square braekets indicate the 95% HPD confidenee intervals of the divergenee time. The x-axis is time in million years (My).

presented very similar haplotypes. The centrally connected haplotype involving individuals Ch58 and 8581 from localities 4 and 9 in Czech Republic (185 km apart), respectively, connected with up to three mutational steps to another shared haplotype by individuals Ch60 and GSK338 from Czech Republic (loc. 8) and eastern Slovakia (loc. 14, 348 km apart), respectively. Furthermore, other individuals from Germany, Czech Republic and Slovakia were also connected with up to three different mutational steps. Haplotypes 7–9 steps away from the central haplotype belonged to samples that were either geographically distant (e.g., individuals from Bulgaria and Romania) or proximate (e.g., individuals from Austria and Slovakia). Individuals from Belgium and Switzerland were connected to the central haplotype by 24 – 31 mutational steps, while the distantly related samples that were placed into the same clade as the central haplotype (clade B) in the phylogenetic inference were up to 28 steps away. The samples from Czech Republic and Austria placed into clade A were 26 – 68 (BI) and 48 – 68 (ML) steps away from the central haplotype. The values of the diversity indices and haplotype distances within the *C. hahnii* dataset are reported in Table 2; distances calculated among the localities are reported in Table 3.

DISCUSSION

Pseudoscorpions can be found practically in all types of terrestrial habitats, but they are particularly abundant in leaf litter, tree hollows and under tree bark (Weygoldt 1969). Their dispersal capability by walking is very low and species that do not use phoresy for their dispersal, typically those inhabiting leaf litter, tend to have limited distributions and show tendencies to short-range endemism (Gardini 2013; Gardini 2014; Harrison et al. 2014; Cosgrove et al. 2016), where chromosomal differentiation within one population may constitute a reproductive barrier even on a relatively small geographic scale (Kotrbová et al. 2016). On the other hand, pseudoscorpions inhabiting temporary habitats, or those found under tree bark, compensate for their low vagility by dispersal via phoresy (Poinar et al. 1998). These species tend to have wider distributions (Harvey 2013) and previously conducted studies that employed molecular markers found in some cases relatively subtle population structuring (Ranius & Douwes 2002; Harvey et al. 2015) or haplotype sharing among localities (Zeh et al. 2003). Deep phylogeographic breaks were detected in some phoretic species (Wilcox et al. 1997; Zeh et al. 2003); however, the divergences were mostly attributed to the previously unrecognized cryptic diversity within these taxa (Wilcox et al. 1997; Zeh et al. 2003).

In this study, we sequenced *C. hahnii* individuals across an approximately 1830 km range, encompassing most of the European species' distribution in order to establish whether this species uses phoresy and how efficient is this manner of dispersal in arthropods. We uncovered surprisingly high haplotype diversity, but no clear geographic patterns were detected within the sampled area. Unfortunately, low supports of most of the internal nodes hamper the interpretation of the results of the phylogenetic analyses; however, fine-grain relationships among individuals can still be assessed from the haplotype network.

We detected shared haplotypes between Central European localities that were up to 350 km apart, and when calculating the distances among all combination pairs of sampled localities, we found less than 2% divergence in 35 pairs, which constitutes 28% of the whole. Populations that were furthest away from each other (1465 km) were from Bad Hersfeld (loc.

Table 2.—Uncorrected p-distances, Tamura – Nei genetic distances and diversity indices within *C. hahnii* dataset and the main clades recovered in Bayesian Analyses. N_{ind}: number of individuals π: nucleotide diversity, H: number of haplotypes, Hd: Haplotype diversity, S.E: Standard error, S.D: Standard deviation

C. hahnii	N_{ind}	p-distance [S.E]	Tamura – Nei [S.E]	π [S.D]	h	Hd [S.D]
Overall *cox1* dataset	33	0.039 [0.004]	0.038 [0.005]	0.036 [0.005]	29	0.991 [0.011]
Clade A	5	0.035 [0.005]	0.036 [0.006]	0.035 [0.008]	5	1.0 [0.126]
Clade B	28	0.025 [0.003]	0.026 [0.004]	0.023 [0.004]	23	0.987 [0.014]
Clade A vs. B	—	0.042 [0.006]	0.047 [0.007]	—	—	—

2) in Germany and Lilyanovo (loc. 17) in Bulgaria. Similar divergences that were considered "low" (2.6%), were found over the span of 1200 km between *Cordylochernes scorpioides* (Linnaeus, 1758) populations from Trinidad and French Guiana (Wilcox et al. 1997), shared haplotypes and low divergences were detected in another *C. scorpioides* lineage from Panama that was sampled across a 418 km span (Zeh et al. 2003). Even less divergence (1.1%) has been found between two populations of newly described pseudoscorpion species *Sociochelifer metoecus* (Harvey, 2015) (Cheliferidae) which has been collected in plumage and nests of the sociable weaver bird *Philetairus socius* (Latham, 1790) over a 440 km span in southern Africa (Harvey et al. 2015). Little geographic structuring was also detected in 2 allozyme loci in pseudoscorpion species *Allochernes wideri* (L.C. Koch, 1843) (Chernetidae) and *Larca lata* (Hansen, 1884) (Larcidae) sampled across 900 km in southern Sweden (Ranius & Douwes 2002). The patterns observed in the mitochondrial data of *C. hahnii* do not show the deep structuring typical for non-vagile pseudoscorpions (Harrison et al. 2014; Cosgrove et al. 2016), or the general lack of the haplotype diversity within populations documented from other sedentary arachnids (Opatova & Arnedo 2014). On the other hand, our results show similarities with the patterns reported from known phoretic species, such as low divergences among geographically distant localities (Wilcox et al. 1997; Ranius & Douwes 2002; Harvey et al. 2015). The combination of the above-mentioned features substantiates our hypothesis, that *C. hahnii* is not sedentary and likely disperses via phoresy.

The observed patterns (i.e., wide distribution, lack of geographic structure and haplotype sharing) could also be produced by accidental human-mediated introduction. Cases of introduction of other arachnids casually transported with trees are known from the Mediterranean (Pantini & Isaia 2008) and trading of infested timber, or its usage for packaging, can result in alien species' introduction over long distances (Meng et al. 2015). However, the ecological preferences of *C. hahnii* make the species an unlikely candidate for human-mediated dispersal. *Chernes hahnii* is known to prefer large deciduous trees in parks or open landscape (Beier 1960; Šťáhlavský 2001, 2011; Šťáhlavský & Chytil 2013) that are not of primary interest of commercial logging. The different structure and the absence of bark layering in young trees, essential for pseudoscorpions inhabiting the tree bark, also makes the species unlikely to be present on young trees (Šťáhlavský & Hörweg, pers. obs.) that are primarily used for park or urban landscaping. The wood of large deciduous trees was certainly logged in the past, but the means of transporting lumber were not as efficient as in modern day. The travelling time is one of the key aspects determining the success of a potential introduction. As logs become dryer over time, the survival of organisms associated with them decreases (Kobelt & Nentwig 2008). Successful introduction would also have to be followed by finding a new suitable microhabitat either by walking or hitchhiking on locally available carriers, which

Table 3.—Pairwise Tamura – Nei genetic distances based on cox1 mtDNA (above diagonal) and standard errors (below diagonal) among the sampled localities.

	Loc. 1	Loc. 2	Loc. 3	Loc. 4	Loc. 5	Loc. 6	Loc. 7	Loc. 8	Loc. 9	Loc. 10	Loc. 11	Loc. 12	Loc. 13	Loc. 14	Loc. 15	Loc. 17	Loc. 16
Loc. 1		0.051	0.006	0.044	0.057	0.079	0.078	0.045	0.06	0.043	0.073	0.047	0.071	0.049	0.047	0.045	0.047
Loc. 2	0.01		0.049	0.01	0.037	0.061	0.089	0.008	0.037	0.011	0.06	0.015	0.043	0.014	0.019	0.015	0.021
Loc. 3	0.002	0.009		0.042	0.055	0.078	0.076	0.043	0.059	0.042	0.072	0.047	0.068	0.046	0.047	0.043	0.045
Loc. 4	0.009	0.003	0.008		0.031	0.057	0.085	0.005	0.033	0.007	0.056	0.011	0.035	0.01	0.015	0.011	0.016
Loc. 5	0.01	0.007	0.01	0.006		0.053	0.061	0.029	0.04	0.035	0.054	0.035	0.029	0.031	0.042	0.039	0.039
Loc. 6	0.011	0.009	0.011	0.008	0.007		0.06	0.056	0.057	0.061	0.059	0.061	0.06	0.058	0.067	0.063	0.069
Loc. 7	0.013	0.014	0.013	0.014	0.011	0.009		0.089	0.072	0.085	0.054	0.089	0.075	0.086	0.098	0.093	0.096
Loc. 8	0.009	0.003	0.009	0.002	0.006	0.008	0.014		0.032	0.006	0.055	0.01	0.033	0.007	0.013	0.01	0.015
Loc. 9	0.009	0.006	0.009	0.005	0.006	0.008	0.011	0.005		0.034	0.057	0.032	0.046	0.035	0.038	0.036	0.041
Loc. 10	0.009	0.003	0.009	0.002	0.007	0.009	0.014	0.002	0.005		0.059	0.009	0.038	0.011	0.014	0.013	0.018
Loc. 11	0.01	0.009	0.01	0.008	0.007	0.008	0.008	0.008	0.008	0.009		0.057	0.059	0.057	0.06	0.058	0.064
Loc. 12	0.009	0.005	0.009	0.004	0.007	0.009	0.014	0.004	0.005	0.003	0.008		0.041	0.016	0.01	0.01	0.015
Loc. 13	0.012	0.009	0.012	0.008	0.007	0.009	0.013	0.008	0.007	0.008	0.008	0.009		0.034	0.044	0.041	0.047
Loc. 14	0.009	0.004	0.009	0.002	0.006	0.008	0.014	0.002	0.005	0.003	0.008	0.004	0.008		0.019	0.016	0.021
Loc. 15	0.009	0.005	0.009	0.005	0.008	0.009	0.015	0.005	0.006	0.004	0.009	0.004	0.009	0.005		0.007	0.019
Loc. 17	0.009	0.005	0.009	0.004	0.007	0.009	0.015	0.004	0.006	0.004	0.009	0.004	0.008	0.004	0.003		0.019
Loc. 16	0.009	0.006	0.009	0.005	0.008	0.011	0.016	0.005	0.007	0.005	0.01	0.005	0.01	0.006	0.006	0.006	

further limits the potential survival of the individuals. Human mediated introduction thus seems unlikely to play an important role in shaping the current distribution of *C. hahnii*.

There are differences in geographic patterns or distribution sizes among phoretic species (Wilcox et al. 1997; Zeh et al. 2003; Pfeiler et al. 2009) that could be related to the dispersal ability of the carrier species or its ecological preferences (Pfeiler & Markow 2011). In this case, the widest ranges and most homogeneous populations would be expected in species phoretic on birds. *Chernes hahnii* is known to inhabit bird boxes and nests (Turienzo et al. 2010; Christophoryová et al. 2011, 2017) and using birds as carriers could offer a better explanation for the species' reported presence in eastern China and Sakhalin Island (Schawaller 1995a, b), rather than hitchhiking on flies or beetles. However, there is no record about the species' presence in bird plumage so far. The results of this study suggest that the phoretic dispersal in *C. hahnii* is similarly or slightly more effective than in other species that hitchhike on beetles or flies (Wilcox et al. 1997; Ranius & Douwes 2002; Zeh et al. 2003; Pfeiler et al. 2009). In this respect, a thorough analysis of phylogeographic patterns of bird-phoretic species like *S. metoecus* would allow us to evaluate if the efficacy of phoretic dispersal could be as variable as for example in the aerial dispersal (i.e., ballooning) of spiders (Pedersen & Loeschcke 2001; Krehenwinkel & Tautz 2013; Opatova et al. 2016).

The phylogenetic analyses supported the division of *C. hahnii* into two main clades (clade A and B) with a sympatric distribution separated by a mean genetic distance (*d*) between 4.2% (uncorrected p-distance) and 4.7% (Tamura – Nei distance). The pseudoscorpions are a taxonomically challenging group and some widely distributed species may actually constitute cryptic species complexes that could be characterized by deep molecular divergences but otherwise display morphological stasis (Wilcox et al. 1997). Intraspecific divergences reported in the literature for putative cryptic species in two chernetid pseudoscorpions range from 2.6% in *Dinocheirus arizonensis* (Banks, 1901), where the main clades are referred to as "independent lineages" (Pfeiler et al. 2009) up to 13.4% in *C. scorpioides* species complex (Wilcox et al. 1997; Zeh et al. 2003). The sympatric occurrence and deeper divergence between clades A and B may be indicative of the presence of unrecognized diversity within *C. hahnii*, despite the fact that no morphological differences were observed between the two clades. The distances between some pairs of localities belonging to the different clades were particularly high. The highest divergences were found between Straz nad Nezarkou (loc. 7) in Czech Republic and localities in Bulgaria and Romania: Sofia (loc. 16, 9.6%, 962 km from Straz nad Nezarkou), Lilyanovo (loc. 17, 9.3%, 1057 km from Straz nad Nezarkou) and Biele Herculane (loc. 15, 9.8%, 735 km from Straz nad Nezarkou). Experimental crosses among populations of *C. scorpioides* revealed a postzygotic reproductive barrier among populations that showed sequence divergence of 11% (Zeh & Zeh 1994; Wilcox et al. 1997), which is much higher than the overall divergence value between clade A and B, but relatively close to the values of divergence among the above-mentioned populations. It is possible that individuals from these particular localities may potentially experience some degree of reproductive isolation as part of the speciation processes (Wilcox et al. 1997), while the reproduction between individuals from other localities could be unaffected. However, delimiting species solely based on *cox1* genetic divergence would most likely lead to taxa over splitting (Kekkonen & Hebert 2014). Additional material as well as ecological and behaviour data (or potentially crossbreeding experiments) would be necessary to confirm the presence of cryptic diversity.

Despite the poorly supported tree recovered in the divergence time analyses, the basal split of *C. hahnii* (dated to approximately 90,000 years ago (ya)), and the two oldest supported nodes in both clades (Clade A, 18,000 ya and Clade B, 27,000 ya) date to the most recent Quaternary glaciation. This glaciation began approximately 110,000 ya, reached its maximum in Europe around 22,000–25,000 ya and ended 11,500 ya, marking the beginning of the Holocene, which was characterized by sporadic local glacial advancements (Ivy-Ochs et al. 2009; Federici et al. 2017; Zens et al. 2017). The cold and dry climate during glaciation would cause thermophilic taxa to retreat to refugia with more suitable climatic conditions, typically located in the Mediterranean region and Caucasus (Hewitt 1996). Furthermore, the long-term isolation and smaller sizes of populations would facilitate fixation of genetic differences by genetic drift (Hewitt 1996, 2000, 2004; Bálint et al. 2008; Scheel & Hausdorf 2012). In the case of *C. hahnii*, it is possible that the species survived glaciation in multiple refugia and subsequently colonized the currently inhabited area. Similar cases are known from both vertebrate (Bernatchez & Wilson 1998; Taberlet et al. 1998) and invertebrate taxa (Habel et al. 2005). There is also an increasing amount of evidence that some taxa (including invertebrates) were able to survive glaciations in small local refugia outside of the Mediterranean region (Pauls et al. 2006; Provan & Bennett 2008; Tzedakis et al. 2013; Copilaş-Ciocianu et al. 2017). Dispersal via phoresy from multiple refugia across Europe and partial interbreeding among the formerly isolated population could potentially explain the lack of geographic structure we observe in the *C. hahnii cox1* data and the lack of variability in nuclear markers (data not shown, but see Results). A similar scenario has been put forward to explain the phylogeographic patterns observed in the pseudoscorpion *D. arizonensis*. In this case, the glacial cycles could have isolated the population on the Baja California Peninsula from the mainland one and the current overlap of their lineages could be a result of a secondary contact after area expansion via phoresy (Pfeiler et al. 2009).

CONCLUSIONS

The lack of geographic structuring and low divergences across a large portion of the *C. hahnii* distribution suggests that *C. hahnii* is a phoretic species and that phoresy in pseudoscorpions can be a very efficient manner of dispersal on larger geographic scales. Despite the poorly supported results of divergence time analyses, most of the deeper splits of *C. hahnii* dated back to the last glaciation. We hypothesize that the species survived the glaciation in multiple refugia and subsequently colonized the currently inhabited region, which could explain the existence of some highly divergent populations. However, more material and additional data concerning the biology of these populations is necessary in order to

evaluate the potential existence of cryptic diversity within *C. hahnii*.

ACKNOWLEDGMENTS

We would like to thank H. Hendrickx for kindly providing us with the samples M124, M125 and to E. Kosnicki for grammatical review of the manuscript. We would also like to thank two anonymous reviewers for their insightful comments that improved the final version of the manuscript. This project was funded by the Charles University Grant Agency project GAUK 36908 to VO.

LITERATURE CITED

Bálint, M., P. Barnard, T. Schmitt, L. Ujvárosi & O. Popescu. 2008. Differentiation and speciation in mountain streams: a case study in the caddisfly *Rhyacophila aquitanica* (Trichoptera). Journal of Zoological Systematics and Evolutionary Research 46:340–345.

Bartlow, A.W., S.M. Villa, M.W. Thompson & S.E. Bush. 2016. Walk or ride? Phoretic behaviour of amblyceran and ischnoceran lice. International Journal for Parasitology 46:221–227.

Barton, P.S., H.J. Weaver & A.D. Manning. 2014. Contrasting diversity dynamics of phoretic mites and beetles associated with vertebrate carrion. Experimental and Applied Acarology 63:1–13.

Beier, M. 1948. Phoresie und Phagophilie bei Pseudoscorpionen. Österreichische Zoologische Zeitschrift 1:441–497.

Beier, M. 1960. *Chernes cimicoides* (F.) und *Chernes hahni* (L.C. Koch), zwei gut unterschiedene Arten. Zeitschrift der Arbaitsgemeinschaft Österreichischer Entomologen 12:100–102.

Bernatchez, L. & C.C. Wilson. 1998. Comparative phylogeography of nearctic and palearctic fishes. Molecular Ecology 7:431–452.

Brochet, A.-L., M. Gauthier-Clerc, M. Guillemain, H. Fritz, A. Waterkeyn, Á. Baltanás et al. 2010. Field evidence of dispersal of branchiopods, ostracods and bryozoans by teal (*Anas crecca*) in the Camargue (southern France). Hydrobiologia 637:255.

Brower, A.V.Z. 1994. Rapid morphological radiation and convergence among races of the butterfly *Heliconius erato* inferred from patterns of mitochondrial DNA evolution. Proceedings of the National Academy of Sciences, USA 91:6491–6495.

Camargo, R.d.S., L.C. Forti, C.A.O. de Matos & A.D. Brescovit. 2015. Phoretic behaviour of *Attacobius attarum* (Roewer, 1935) (Araneae: Corinnidae: Corininae) dispersion not associated with predation? Journal of Natural History 49:1653–1658.

Christophoryová, J., D. Grul'a & K. Krajčovičová. 2017. New records of pseudoscorpions (Arachnida: Pseudoscorpiones) associated with animals and human habitats in Slovakia and the Czech Republic. Arachnologische Mitteilungen 53:67–76.

Christophoryová, J., Z. Krumpálová, J. Krištofík & Z. Országhová. 2011. Association of pseudoscorpions with different types of bird nests. Biologia 66:669–677.

Clement, M., D. Posada & K.A. Crandall. 2000. TCS: a computer program to estimate gene genealogies. Molecular Ecology 9:1657–1660.

Colgan, D.J., A. McLauchlan, G.D.F. Wilson, S.P. Livingston, G.D. Edgecombe, J. Macaranas et al. 1998. Histone H3 and U2 snRNA DNA sequences and arthropod molecular evolution. Australian Journal of Zoology 46:419–437.

Copilaş-Ciocianu, D., T. Rutová, P. Pařil & A. Petrusek. 2017. Epigean gammarids survived millions of years of severe climatic fluctuations in high latitude refugia throughout the Western Carpathians. Molecular Phylogenetics and Evolution 112:218–229.

Cosgrove, J.G., I. Agnarsson, M.S. Harvey & G.J. Binford. 2016. Pseudoscorpion diversity and distribution in the West Indies: sequence data confirm single island endemism for some clades, but not others. Journal of Arachnology 44:257–271.

Drummond, A., B. Ashton, M. Cheung, J. Heled, M. Kearse, R. Moir et al. 2010. Geneious v.5.3. Available online at http://www.geneious.com/

Drummond, A.J., M.A. Suchard, D. Xie & A. Rambaut. 2012. Bayesian phylogenetics with BEAUti and the BEAST 1.7. Molecular Biology and Evolution 29:1969–1973.

Ersts, P.J.A. Geographic Distance Matrix Generator (version 1.2.3). American Museum of Natural History, Center for Biodiversity and Conservation. Available online at http://biodiversityinformatics.amnh.org/open_source/gdmg Accessed on 2017-5-6.

Federici, P.R., A. Ribolini & M. Spagnolo. 2017. Glacial history of the Maritime Alps from the Last Glacial Maximum to the Little Ice Age. Geological Society, London, Special Publications 433:137–159.

Finlayson, G., G. Madani, G. Dennis & M. Harvey. 2015. First reported observation of phoresy of pseudoscorpions on an endemic New Zealand mammal, the lesser short-tailed bat, *Mystacina tuberculata*. New Zealand Journal of Zoology 42:298–301.

Folmer, O., M. Black, W. Hoeh, R. Lutz & R. Vrijenhoek. 1994. DNA primers for amplification of mitochondrial cytochrome c oxidase subunit 1 from diverse metazoan invertebrates. Molecular Marine Biology and Biotechnology 3:294–299.

Gardini, G. 2013. A revision of the species of the pseudoscorpion subgenus *Chthonius* (*Ephippiochthonius*) (Arachnida, Pseudoscorpiones, Chthoniidae) from Italy and neighbouring areas. Zootaxa 3655:1–151.

Gardini, G. 2014. The species of the *Chtonius heterodactylus* group from the eastern Alps and the Carpathians. Zootaxa 3887:101–137.

Gittenberger, E. 2012. Long-distance dispersal of molluses: 'Their distribution at first perplexed me much'. Journal of Biogeography 39:10–11.

Habel, J.C., T. Schmitt & P. Müller. 2005. The fourth paradigm pattern of post-glacial range expansion of European terrestrial species: the phylogeography of the Marbled White butterfly (Satyrinae, Lepidoptera). Journal of Biogeography 32:1489–1497.

Harrison, S.E., M.T. Guzik, M.S. Harvey & A.D. Austin. 2014. Molecular phylogenetic analysis of Western Australian troglobitic chthoniid pseudoscorpions (Pseudoscorpiones: Chthoniidae) points to multiple independent subterranean clades. Invertebrate Systematics 28:386–400.

Harvey, M.S. 2013. Pseudoscorpions of the World, version 3.0. Western Australian Museum, Perth. Available online at http://www.museum.wa.gov.au/catalogues/pseudoscorpions

Harvey, M.S., P.C. Lopes, G.R. Goldsmith, A. Halajian, M.J. Hillyer & J.A. Huey. 2015. A novel symbiotic relationship between sociable weaver birds (*Philetairus socius*) and a new cheliferid pseudoscorpion (Pseudoscorpiones: Cheliferidae) in southern Africa. Invertebrate Systematics 29:444–456.

Hastriter, M.W. & S.E. Bush. 2014. Description of *Medwayella independencia* (Siphonaptera, Stivaliidae), a new species of flea from Mindanao Island, the Philippines and their phoretic mites, and miscellaneous flea records from the Malay Archipelago. ZooKeys 408:107–123.

Hastriter, M.W., K.B. Miller, G.J. Svenson, G.J. Martin & M.F. Whiting. 2017. New record of a phoretic flea associated with earwigs (Dermaptera, Arixeniidae) and a redescription of the bat flea *Lagaropsylla signata* (Siphonaptera, Ischnopsyllidae). ZooKeys 657:67–79.

Hewitt, G. 1996. Some genetic consequences of ice ages, and their role in divergence and speciation. Biological Journal of the Linnean Society 58:247–276.

Hewitt, G. 2000. The genetic legacy of the Quaternary ice ages. Nature 405:907–913.

Hewitt, G. 2004. The structure of biodiversity - insights from molecular phylogeography. Frontiers in Zoology 1:4.

Hulsmans, A., K. Moreau, L. De Meester, B.J. Riddoch & L. Brendonck. 2007. Direct and indirect measures of dispersal in the fairy shrimp *Branchipodopsis wolfi* indicate a small scale isolation-by-distance pattern. Limnology and Oceanography 52:676–684.

Ivy-Ochs, S., H. Kerschner, M. Maisch, M. Christl, P.W. Kubik & C. Schlüchter. 2009. Latest Pleistocene and Holocene glacier variations in the European Alps. Quaternary Science Reviews 28:2137–2149.

Kekkonen, M. & P.D. Hebert. 2014. DNA barcode-based delineation of putative species: efficient start for taxonomic workflows. Molecular Ecology Resources 14:706–715.

Keum, E., G. Takaku, K. Lee & C. Jung. 2016. New records of phoretic mites (Acari: Mesostigmata) associated with dung beetles (Coleoptera: Scarabaeidae) in Korea and their ecological implication. Journal of Asia-Pacific Entomology 19:353–357.

Kobelt, M. & W. Nentwig. 2008. Alien spider introductions to Europe supported by global trade. Diversity and Distributions 14:273–280.

Koch, L. 1873. Uebersichtliche Darstellung der europäischen Chernetiden (Pseudoscorpione). Bauer & Raspe, Nürnberg.

Kotrbová, J., V. Opatova, G. Gardini & F. Šťáhlavský. 2016. Karyotype diversity of pseudoscorpions of the genus *Chthonius* (Pseudoscorpiones, Chthoniidae) in the Alps. Comparative Cytogenetics 10:325–345.

Krehenwinkel, H. & D. Tautz. 2013. Northern range expansion of European populations of the wasp spider *Argiope bruennichi* is associated with global warming-correlated genetic admixture and population-specific temperature adaptations. Molecular Ecology 22:2232–2248.

Kumar, S., G. Stecher & K. Tamura. 2016. MEGA7: Molecular Evolutionary Genetics Analysis version 7.0 for bigger datasets. Molecular Biology and Evolution 33:1870–1874.

Lanfear, R., B. Calcott, S.Y.W. Ho & S. Guindon. 2012. PartitionFinder: combined selection of partitioning schemes and substitution models for phylogenetic analyses. Molecular Biology and Evolution 29:1695–1701.

Librado, P. & J. Rozas. 2009. DnaSP v5: a software for comprehensive analysis of DNA polymorphism data. Bioinformatics 25:1451–1452.

Macchioni, F. 2007. Importance of phoresy in the transmission of Acarina. Parassitologia 49:17–22.

Meng, P., K. Hoover & M. Keena. 2015. Asian longhorned beetle (Coleoptera: Cerambycidae), an introduced pest of maple and other hardwood trees in North America and Europe. Journal of Integrated Pest Management 6:4. DOI: 10.1093/jipm/pmv003

Michalak, I., L.-B. Zhang & S.S. Renner. 2010. Trans-Atlantic, trans-Pacific and trans-Indian Ocean dispersal in the small Gondwanan Laurales family Hernandiaceae. Journal of Biogeography 37:1214–1226.

Miller, M.A., W. Pfeiffer & T. Schwartz. 2010. Creating the CIPRES Science Gateway for inference of large phylogenetic trees, pp. 1–8. Proceedings of the Gateway Computing Environments Workshop (GCE), New Orleans, LA.

Moulds, T.A., N. Murphy, M. Adams, T. Reardon, M.S. Harvey, J. Jennings et al. 2007. Phylogeography of cave pseudoscorpions in southern Australia. Journal of Biogeography 34:951–962.

Muchmore, W. 1971. On phoresy in pseudoscorpions. Bulletin of the British Arachnological Society 2:38.

Murienne, J., M.S. Harvey & G. Giribet. 2008. First molecular phylogeny of the major clades of Pseudoscorpiones (Arthropoda: Chelicerata). Molecular Phylogenetics and Evolution 49:170–184.

Okumura, E. & T. Yoshiga. 2014. Host orientation using volatiles in the phoretic nematode *Caenorhabditis japonica*. Journal of Experimental Biology 217:3197–3199.

Opatova, V. & M.A. Arnedo. 2014. Spiders on a hot volcanic roof: colonisation pathways and phylogeography of the Canary Islands endemic trap-door spider *Titanidiops canariensis* (Araneae, Idiopidae). PLoS ONE 9:e115078. doi:115010.111371/journal.pone.0115078.

Opatova, V., J.E. Bond & M.A. Arnedo. 2016. Uncovering the role of the Western Mediterranean tectonics in shaping the diversity and distribution of the trap-door spider genus *Ummidia* (Araneae, Ctenizidae). Journal of Biogeography 43:1955–1966.

Pantini, P. & M. Isaia. 2008. New records for the Italian spider fauna (Arachnida, Araneae). Arthropoda Selecta. 17:133–144.

Pauls, S.U., H.T. Lumbsch & P. Haase. 2006. Phylogeography of the montane caddisfly *Drusus discolor*: evidence for multiple refugia and periglacial survival. Molecular Ecology 15:2153–2169.

Pedersen, A.A. & V. Loeschcke. 2001. Conservation genetics of peripheral populations of the mygalomorph spider *Atypus affinis* (Atypidae) in northern Europe. Molecular Ecology 10:1133–1142.

Pfammatter, J.A., D.R. Coyle, K.J. Gandhi, N. Hernandez, R.W. Hofstetter, J.C. Moser et al. 2016. Structure of phoretic mite assemblages across subcortical beetle species at a regional scale. Environmental Entomology 45:53–65.

Pfeiler, E. & T.A. Markow. 2011. Phylogeography of the cactophilic *Drosophila* and other arthropods associated with cactus resources in the Sonoran Desert. Insects 2:218–231.

Pfeiler, E., B.G. Bitler, S. Castrezana, L.M. Matzkin & T.A. Markow. 2009. Genetic diversification and demographic history of the cactophilic pseudoscorpion *Dinocheirus arizonensis* from the Sonoran Desert. Molecular Phylogenetics and Evolution 52:133–141.

Pimentel, C.S., M.P. Ayres, E. Vallery, C. Young & D.A. Streett. 2014. Geographical variation in seasonality and life history of pine sawyer beetles *Monochamus* spp: its relationship with phoresy by the pinewood nematode *Bursaphelenchus xylophilus*. Agricultural and Forest Entomology 16:196–206.

Poinar, G.O., B.P. Cureie & J.C. Cokendolpher. 1998. Arthropod phoresy involving pseudoscorpions in the past and present. Acta Arachnologica 47:79–96.

PopART. Available online at http://popart.otago.ac.nz/

Provan, J. & K. Bennett. 2008. Phylogeographic insights into cryptic glacial refugia. Trends in Ecology & Evolution 23:564–571.

Rambaut, A. 2009. FigTree v. 1.3.1

Rambaut, A. & A.J. Drummond. 2009. TRACER v.1.5. Available online at http://tree.bio.ed.ac.uk/software/tracer/ (accessed on December 1st, 2009).

Ranius, T. & P. Douwes. 2002. Genetic structure of two pseudoscorpion species living in tree hollows in Sweden. Animal Biodiversity and Conservation 25:67–74.

Ronquist, F. & J. Huelsenbeck. 2003. MrBayes 3: Bayesian phylogenetic inference under mixed models. Bioinformatics 19:1572–1574.

Sabagh, L.T., R.J.P. Dias, C.W. Branco & C.F. Rocha. 2011. New records of phoresy and hyperphoresy among treefrogs, ostracods, and ciliates in bromeliad of Atlantic forest. Biodiversity and Conservation 20:1837–1841.

Saloña-Bordas, M.I., P.B. de la Puebla, B.D. Martín, J. Sumner & M.A. Perotti. 2015. *Ixodes ricinus* (Ixodidae), an occasional phoront on necrophagous and coprophagous beetles in Europe. Experimental and Applied Acarology 65:243–248.

Schawaller, W. 1995a. Review of the pseudoscorpion fauna of China (Arachnida: Pseudoscorpionida). Revue Suisse de Zoologie 102:1045–1063.

Schawaller, W. 1995b. Review of the pseudoscorpion fauna of the Far

East of Russia (Arachnida Pseudoscorpionida). Arthropoda Selecta 3:123–126.

Scheel, B.M. & B. Hausdorf. 2012. Survival and differentiation of subspecies of the land snail *Charpentieria itala* in mountain refuges in the Southern Alps. Molecular Ecology 21:3794–3808.

Schiner, T. 1872. Miscellen. Vorkommen von Chelifer an Fliegen. Verhandlungen der K. K. Zoologischen-Botanischen Gesellschaft in Wien 22:75–76.

Shorthouse, D.P. 2010. SimpleMappr, an online tool to produce publication-quality point maps. [Retrieved from http://www.simplemappr.net/ Accessed May 2017].

Šťáhlavský, F. 2001. Pseudoscorpions of Prague. In Czech, with English Summary. Klapalekiana 37:73–121.

Šťáhlavský, F. 2011. Pseudoscorpions (Arachnida: Pseudoscorpiones) of the Třeboňsko Protected Landscape Area and the adjacent area. In Czech, with English Summary. Klapalekiana 47:247–258.

Šťáhlavský, F. & J. Chytil. 2013. Štírci (Arachnida: Pseudoscorpiones) Biosférické rezervace Dolní Morava a okolí (Česká republika). In Czech, with English summary. Klapalekiana 49:73–88.

Stamatakis, A. 2006. RAxML-VI-HPC: maximum likelihood-based phylogenetic analyses with thousands of taxa and mixed models. Bioinformatics 22:2688–2690.

Taberlet, P., L. Fumagalli, A.G. Wust-Saucy & J.F. Cosson. 1998. Comparative phylogeography and postglacial colonization routes in Europe. Molecular Ecology 7:453–464.

Tamura, K. & S. Kumar. 2002. Evolutionary distance estimation under heterogeneous substitution pattern among lineages. Molecular Biology and Evolution 19:1727–1736.

Tamura, K. & M. Nei. 1993. Estimation of the number of nucleotide substitutions in the control region of mitochondrial DNA in humans and chimpanzees. Molecular Biology and Evolution 10:512–526.

Turienzo, P., O. Di Iorio & V. Mahnert. 2010. Global checklist of pseudoscorpions (Arachnida) found in birds' nests. Revue Suisse de Zoologie 117:557–598.

Tzedakis, P., B. Emerson & G. Hewitt. 2013. Cryptic or mystic? Glacial tree refugia in northern Europe. Trends in Ecology & Evolution 28:696–704.

Vanschoenwinkel, B., S. Gielen, M. Seaman & L. Brendonck. 2008. Any way the wind blows-frequent wind dispersal drives species sorting in ephemeral aquatic communities. Oikos 117:125–134.

Wahlberg, E. & K.A. Johanson. 2014. The age, ancestral distribution and radiation of *Chimarra* (Trichoptera: Philopotamidae) using molecular methods. Molecular Phylogenetics and Evolution 79:433–442.

Weygoldt, P. 1969. The Biology of Pseudoscorpions. Harvard University Press, Cambridge, MA.

Wilcox, T.P., L. Hugg, J.A. Zeh & D.W. Zeh. 1997. Mitochondrial DNA sequencing reveals extreme genetic differentiation in a cryptic species complex of neotropical pseudoscorpions. Molecular Phylogenetics and Evolution 7:208–216.

Zeh, D.W. & J.A. Zeh. 1992a. Dispersal-generated sexual selection in a beetle-riding pseudoscorpion. Behavioral Ecology and Sociobiology 30:135–142.

Zeh, D.W. & J.A. Zeh. 1992b. On the function of harlequin beetle-riding in the pseudoscorpion, *Cordylochernes scorpioides* (Pseudoscorpionida: Chernetidae). Journal of Arachnology 20:47–51.

Zeh, D.W. & J.A. Zeh. 1994. When morphology misleads - interpopulation uniformity in sexual selection masks genetic divergence in harlequin beetle-riding pseudoscorpion populations. Evolution 48:1168–1182.

Zeh, J., D. Zeh & M. Bonilla. 2003. Phylogeography of the harlequin beetle-riding pseudoscorpion and the rise of the Isthmus of Panamá. Molecular Ecology 12:2759–2769.

Zens, J., C. Zeeden, W. Römer, M. Fuchs, N. Klasen & F. Lehmkuhl. 2017. The Eltville Tephra (Western Europe) age revised: Integrating stratigraphic and dating information from different Last Glacial loess localities. Palaeogeography, Palaeoclimatology, Palaeoecology 466:240–251.

Manuscript received 13 June 2017, revised 15 August 2017.

2018. Journal of Arachnology 46:114–132

New morphological data for the order Ricinulei with the description of two new species of *Pseudocellus* (Arachnida: Ricinulei: Ricinoididae) from Mexico

Alejandro Valdez-Mondragón*[1,2], **Oscar F. Francke**[2] and **Ricardo Botero-Trujillo**[3,4]: [1]CONACYT Research Fellow. Laboratory of Arachnology (LATLAX), Laboratorio Regional de Biodiversidad y Cultivo de Tejidos Vegetales (LBCTV), Instituto de Biología, Universidad Nacional Autónoma de México (UNAM), sede Tlaxcala, Ex-Fábrica San Manuel, San Miguel Contla, 90640 Santa Cruz Tlaxcala, Tlaxcala, Mexico. *E-mail: lat_mactans@yahoo.com.mx; [2]Colección Nacional de Arácnidos (CNAN), Departamento de Zoología, Instituto de Biología, Universidad Nacional Autónoma de México (UNAM), Ciudad Universitaria, Apartado Postal 04510, Coyoacán, Mexico City, Mexico. [3]División Aracnología, Museo Argentino de Ciencias Naturales "Bernardino Rivadavia", Avenida Ángel Gallardo 470, CP: 1405DJR, C.A.B.A., Buenos Aires, Argentina. [4]Associate Researcher. Laboratorio de Entomología, Unidad de Ecología y Sistemática–UNESIS, Departamento de Biología, Pontificia Universidad Javeriana, Bogotá, Colombia.

Abstract. Two new species of ricinuleids of the genus *Pseudocellus* Platnick, 1980 are described based on adult males and females from Mexico: *Pseudocellus quetzalcoatl* sp. nov. and *Pseudocellus olmeca* sp. nov. from the same type locality in the state of Veracruz. The two new species represent the first record of two sympatric epigean species of ricinuleids for North America. The total number of described species of *Pseudocellus* from Mexico increases to 18, holding first place in terms of number of known ricinuleid species worldwide. With the two new species described herein, Veracruz, with four species, is the second state of Mexico with higher diversity after Chiapas, which has five recorded species. We describe for the first time, for any ricinuleids, pores on the membrane below the spermatheeae, revealed using a staining technique. The function of these pores is unknown, although it is possible that these could be secretion glands for some kind of substance during the reproductive process. A taxonomic key for identification of males of species from Mexico and the southern United States is provided.

Keywords: Taxonomy, sympatry, glands, Veracruz, new data

Ricinulei is the second least diverse order of Arachnida, comprising 89 extant (including the two new species herein described) and 22 fossil species. Suborders Palaeoricinulei Selden, 1992 and Neoricinulei Selden, 1992, each gathering extinct and living taxa, respectively, were traditionally recognized (Selden 1992; Harvey 2003). A few years ago, the classification scheme was modified by Wunderlich (2012, 2015). This author proposed that all previously known species be placed in suborder Posteriorricinulei Wunderlich, 2015, while a newly discovered fossil, *Primoricinuleus pugio* Wunderlich, 2015, was assigned to suborder Primoricinulei Wunderlich, 2015 on account of it presumably being the sister taxon to all other ricinuleids. More recently (Wunderlich 2017), two new monogeneric families of extinct ricinuleids were described into the Primoricinulei: Hirsutisomidae Wunderlich, 2017 and Monooculricinuleidae Wunderlich, 2017.

The Superfamily Ricinoidoidea Ewing, 1929 comprises the genera *Cryptocellus* Westwood, 1874, *Pseudocellus* Platnick, 1980 and *Ricinoides* Ewing, 1929, each with 42, 34 and 11 previously known species, respectively. Of these, only *Ricinoides* occurs in the Old World, having thus far remained restricted to western and central African countries (Tuxen 1974; Naskrecki 2008; Penney et al. 2009). In contrast, *Pseudocellus* and *Cryptocellus* are exclusive New World elements; the former is primarily distributed in North and Central America, with some species having been described from Caribbean islands, whereas *Cryptocellus* is predominantly South American, the distribution of both overlapping in the Central American region (Harvey 2003; Tourinho & Azevedo 2007; Botero-Trujillo & Pérez 2008, 2009; Teruel & Armas 2008; Tourinho & Saturnino 2010; Tourinho et al. 2010, 2014; Valdez-Mondragón & Francke 2011, 2013; Pinto-da-Rocha & Andrade 2012; Botero-Trujillo 2014; Armas & Agreda 2016; Botero-Trujillo & Valdez-Mondragón 2016; Armas 2017; Botero-Trujillo & Flórez, 2017).

Ricinuleids are typically found in the soil of lowland tropical rainforests (i.e., in the leaf litter and underlying layers) as well as under rocks and rotten logs (Platnick 2002; Harvey 2003). Many species, all belonging to *Pseudocellus*, are cave inhabitants and frequently true troglobites with distinct troglomorphisms. Mexico holds first place in number of known ricinuleid species, with 16 out of 33 currently recognized valid *Pseudocellus* species (not including the two new species described herein). Many works have contributed to the knowledge of the ricinuleid fauna of Mexican natural subterranean systems (Bolívar y Pieltain 1946; Gertsch 1971, 1977; Pittard & Mitchell 1972; Brignoli 1974; Reddell 1981; Cokendolpher & Enríquez 2004; Valdez-Mondragón & Francke 2011). Mexico is also the country with the largest number of known troglobitic ricinuleids, eight thus far: *Pseudocellus bolivari* (Gertsch, 1971), *P. boneti* (Bolívar y Pieltain, 1942), *P. monjarazi* Valdez-Mondragón & Francke, 2013, *P. osorioi* (Bolívar y Pieltain, 1946), *P. oztotl* Valdez-Mondragón & Francke, 2011, *P. platnicki* Valdez-Mondragón & Francke, 2011, *P. reddelli* (Gertsch, 1971) and *P. sbordonii* (Brignoli, 1974).

Species of Ricinulei generally exhibit narrow geographical distributions and normally no more than one species is known to occur in a given area. *Cryptocellus lampeli* Cooke, 1967 and

Cryptocellus albosquamatus Cooke, 1967 were described from Amatuk, British Guiana; this became the first case of sympatric ricinuleid species to be documented, and thus far remains the only one to our knowledge.

In this contribution, we describe two new *Pseudocellus* species from a single locality of tropical rainforest in the state of Veracruz, Mexico. The Jaguaroundi Ecological Park is a natural reserve, embedded within a large petrochemical complex administered by the Mexican oil company PEMEX (Fig. 90). Specimens of *P. quetzalcoatl* sp. nov. were collected in the ground, all under the same boulder which was about 80 cm in diameter. Specimens of *P. olmeca* sp. nov. were found by digging in the ground, close to the roots of some plants. The collection points where the two species were found are separated from each other by only some 200 m or less. Also, a taxonomic key for identification of males of species from Mexico and the southern United States is provided.

METHODS

All the material is deposited in the Colección Nacional de Arácnidos (CNAN) (Curator: Dr. Oscar F. Francke), Instituto de Biología, Universidad Nacional Autónoma de México (CNAN-IBUNAM), Mexico City. Specimens were examined in a Zeiss DiscoveryV8 stereomicroscope. Photographs were obtained with a Zeiss Axiocam 506 digital camera attached to a Zeiss AXIO ZoomV16 stereomicroscope. Photography was conducted with specimens and structures submerged into commercial-use gel alcohol (to hold them in the appropriate position), and the preparation completely covered with 80% ethanol. Spermathecae were stained using a drop of chlorazol (1%) for a few seconds followed by wash with 80% ethanol. Images were edited in Adobe Photoshop CS6. The map was produced using SimpleMappr (Shorthouse 2010). Measurements, in millimeters, were obtained using the methodology outlined by Cooke & Shadab (1973). Terminology used for referring to leg segments follows Gertsch (1971), whereas that used for the copulatory structures follows Pittard & Mitchell (1972) and Botero-Trujillo & Valdez-Mondragón (2016). The length/diameter (l/d) ratio of femur II of males was calculated in prolateral view. We use the following abbreviations for some cuticular structures on the male copulatory apparatus following Salvatierra & Tourinho (2016): *BS*, barbed setae; *CS*, clubbed setae; *FD*, flat depressions; *Lct*, long curved-tip setae; *OS*, ordinary setae; *Sct*, sculptured surface tubercles. The following abbreviations are used for some copulatory structures following Botero-Trujillo & Valdez-Mondragón (2016): *ac*, accessory piece of the male copulatory apparatus; *Lc*, lamina cyathiformis; *MT*, metatarsus; *mP*, metatarsal process; *st*, spermatheca; *tP*, tarsal process.

RESULTS

TAXONOMY

Family Ricinoididae Ewing, 1929
Genus *Pseudocellus* Platnick, 1980

Type species.—*Pseudocellus dorotheae* (Gertsch & Mulaik, 1939).

KEY TO ADULT MALES OF *PSEUDOCELLUS* SPECIES FROM MEXICO AND THE USA

1. Troglomorphic species with elongated legs (e.g., Valdez-Mondragón & Francke 2013: fig. 14): femur II at least 1.5 times longer than carapace; tibia II longer than carapace 2
   Edaphomorphic species with short appendages (e.g., Figs. 1, 40): femur II less than 1.5 times the carapace length; tibia II shorter than carapace 9
2. Femur II length/width ratio greater than 9; femur II more than twice longer than carapace 3
   Femur II length/width ratio less than 9; femur II less than twice longer than carapace 6
3. Cheliceral fingers with 5 teeth ..... *P. reddelli* (Durango, Mexico)
   Cheliceral fingers with more than 5 teeth 4
4. Leg formula 2413; tibia II twice as long as patella II ..... *P. sbordonii* (Chiapas, Mexico)
   Leg formula 2431; tibia II less than twice as long as longer than patella II 5
5. Tibia I with distinct ventral hump (Valdez-Mondragón & Francke 2011: figs. 24, 26); tibia and tarsus of leg II unarmed ..... *P. platnicki* (Coahuila, Mexico)
   Tibia I without distinct ventral hump (Valdez-Mondragón & Francke 2011: fig. 17); tibia and tarsus of leg II with distinct proventral and retroventral rows of spines (Valdez-Mondragón & Francke 2011: fig. 19) ..... *P. oztotl* (Puebla, Mexico)
6. Leg formula 2341; cheliceral fixed finger with 4 teeth; tarsal claws asymmetrical and somewhat spatulate ..... *P. bolivari* (Chiapas, Mexico)
   Leg formula 2431; cheliceral fixed finger with 5 or 6 teeth; tarsal claws symmetrical, none spatulate 7
7. Tibia II elongated, about 11 times longer than wide, with scattered spines or granules ventrally; cheliceral movable finger with basal tooth not distinctly larger than the others 8
   Tibia II short, about 6 times longer than wide, with two distinct rows of spines ventrally; cheliceral movable finger with basal tooth distinctly larger than the others ..... *P. boneti* (Guerrero, Mexico)
8. Tibia II with few scattered spines ventrally; cheliceral movable finger with teeth uniform in size ..... *P. osorioi* (San Luis Potosí, Mexico)
   Tibia II without scattered spines, but with numerous granules ventrally (Valdez-Mondragón & Francke 2013: fig. 17); cheliceral movable finger with teeth progressively decreasing in length distally ..... *P. moujarazi* (Chiapas, Mexico)
9. Tibia II armed ventrally with one or two distinct apophyses (e.g., Figs. 52, 53) 10
   Tibia II without distinct ventral apophyses (e.g., Figs. 11, 12) 13

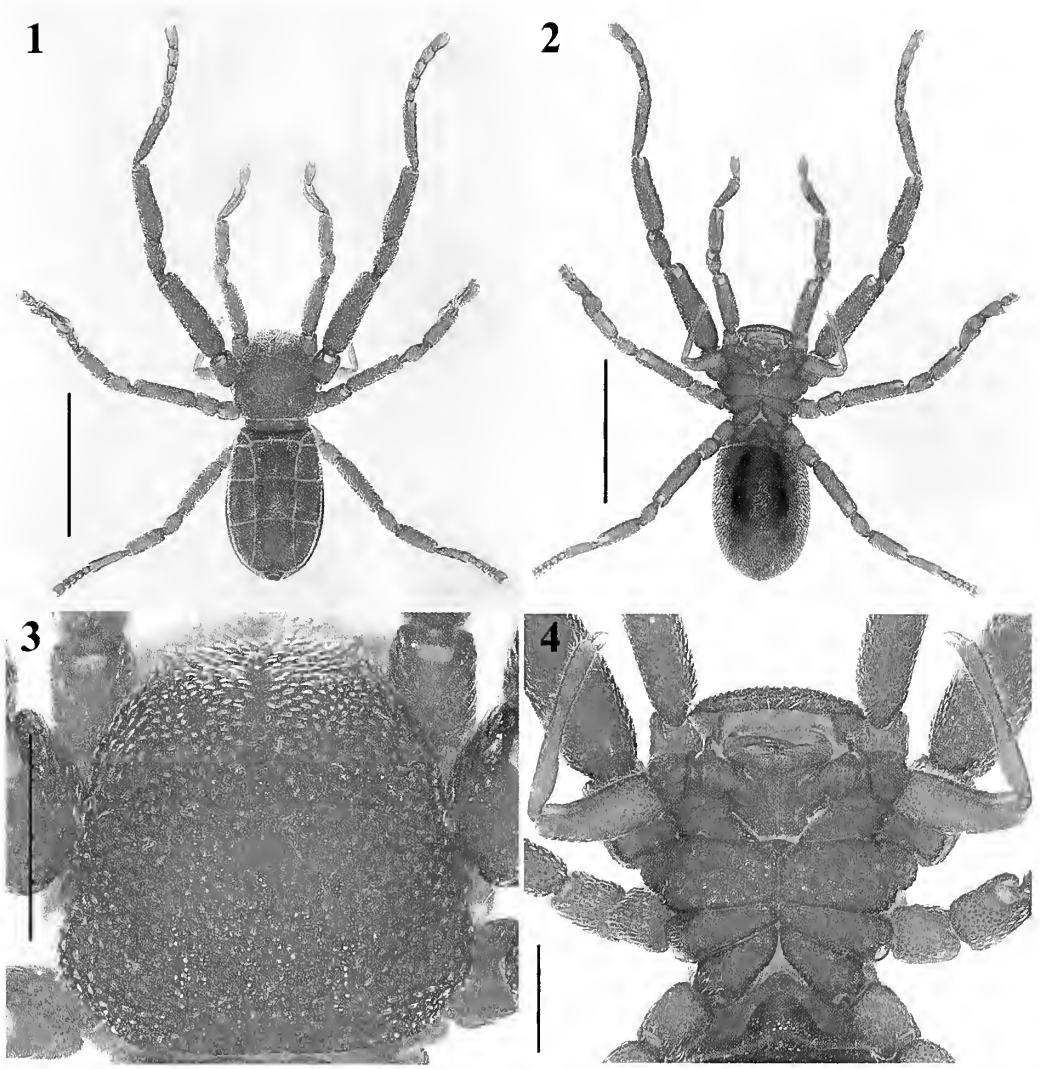

Figures 1–4.—*Pseudocellus quetzalcoatl* sp. nov. Male holotype: 1–2. Habitus, dorsal and ventral views. 3. Carapace, dorsal view. 4. Prosoma, ventral view showing coxosternal region. Scale bars: 0.5 mm (Figs. 3–4), 2 mm (Figs. 1, 2).

10. Femur II moderately thickened, 4 times longer than wide; tibia II with a single proventral tubercle, lacking a distinct retroventral tubercle ..... *P. pearsei* (Yucatán, Mexico)
    Femur II strongly thickened, less than 2.5 times longer than wide; tibia II with proventral and retroventral apophyses subequal in size 11
11. Femur II shorter than carapace; tibia II with small proventral and retroventral apophyses placed at same level, medially on segment ..... *P. spinotibialis* (Chiapas, Mexico)
    Femur II distinctly longer than carapace; tibia II with long and stout apophyses not aligned to each other on segment (e.g., Figs. 52, 53) 12
12. Femur II 2.4 times longer than wide. Ventral apophyses of tibia II more robust than those of *P. olmeca* (Valdez-Mondragón & Francke 2011, figs. 1, 3). Tarsal process (*tP*) of leg III in prolateral view slightly sigmoidal in distal half (Valdez-Mondragón & Francke 2011: fig. 5). Metatarsal process (*mP*) long and predominantly straight (Valdez-Mondragón & Francke 2011: fig. 4) ..... *P. chankin* (Chiapas, Mexico; Petén, Guatemala)
    Femur II 2.6 times longer than wide (Figs. 50, 51). Ventral apophyses of tibia II weaker (Figs. 40, 41, 52, 53). Tarsal process (*tP*) of leg III in prolateral view curved in distal half (Figs. 58, 61, 64, 65). Metatarsal process (*mP*) short and slightly sigmoidal (Figs. 58, 59, 64, 70) ..... *P. olmeca* sp. nov. (Veracruz, Mexico)
13. Leg formula 2431; carapace and opisthosoma distinctly and evenly pitted 14
    Leg formula 2341; integument not distinctly pitted 15
14. Adult 3.2 mm in total length; tibia II slightly more than 0.5 times the carapace length; patella and tibia of leg II subequal in length ..... *P. dorotheae* (Texas, USA)
    Adult 5.0 mm in total length; tibia II almost as long as carapace as long as carapace; tibia II 1.5 times longer than patella II ..... *P. mitchelli* (Durango, Mexico)

15. Femora I and IV markedly bulky, at least 1.5 times thicker than other segments ..... *P. gertschi* (Veracruz, Mexico)
    Femora I and IV not remarkably bulky, about same thickness as other segments (e.g., Valdez-Mondragón & Francke, 2013: fig. 1) 16
16. Femur II thickened (Valdez-Mondragón & Francke, 2013: fig. 1), about 2.5 times longer than wide; tibia II at least 1.5 times the length of patella II 17
    Femur II not thickened, slightly more than 4 times longer than wide; tibia II 1.2 times the length of patella II ..... *P. pelaezi* (San Luis Potosí, Mexico)
17. Tarsal process of the copulatory apparatus narrow, apically with two tips or lobes (Valdez-Mondragón & Francke 2011: figs. 13, 14) ..... *P. jarocho* (Veracruz, Mexico)
    Tarsal process of the copulatory apparatus wide, apically with one or three tips or lobes (Figs. 21–23) 18
18. Tarsal process of the copulatory apparatus ending in a single, long, thin and sharp tip (Valdez-Mondragón & Francke, 2013: figs. 10–12) ..... *P. cruzlopezi* (Oaxaca, Mexico)
    Tarsal process of the copulatory apparatus ending in three rounded and conspicuous tips or lobes (tripod-shaped) (Figs. 21–26) ..... *P. quetzalcoatl* sp. nov. (Veracruz, Mexico)

Pseudocellus quetzalcoatl sp. nov.
Figs. 1–39

Type material.—*Holotype male.* MEXICO: *Veracruz:* Parque Ecológico Jaguaroundi, camino al Ejidal Cangrejera Uno (18.11196°N, 94.35796°W; 25 m elev.), Municipio Coatzacoalcos, 6 July 2016, A. Valdez, E. Briones, M. Cortez, J. Valerdi (daytime collection) (CNAN-T1172).

Paratypes: MEXICO: *Veracruz:* 1 ♀, same collection data as holotype (CNAN-T1173); 1 ♂, 1 ♀, 1 deutonymph, 1 tritonymph, same collection data as holotype (CNAN-T1174).

Diagnosis.—Males can be distinguished by the following combination of features: (1) the rounded edges of the cucullus (Fig. 9); (2) two ventral rows of small conical spines on tibia II, which are the same size (Figs. 11, 12); (3) the scattered spines on metatarsus II (Figs. 13, 14); (4) the robust femur II, 3.2 times longer than wide (Figs. 1, 2, 15); (5) tarsal process (*tP*) of the copulatory apparatus wide, canoe-shaped in prolateral view, ventrally curved and stout (Figs. 18, 21, 24, 25); (6) *tP* with dorsal carina on distal half (Figs. 22, 23); (7) *tP* apically with three rounded and conspicuous tips or lobes (Figs. 21–26); (8) *tP* with additional inconspicuous lobe (Fig. 23); and (9) accessory piece (*ac*) simple, curved and thin, with sharp tip (Figs. 21, 26). Females can be distinguished by the spermathecae slightly oval apically, and with two long lobules on each side: one large and curved in an upside-down J-shape, and other smaller and straight (Figs. 33–35). Also, the spermathecae have a pale medial region below (Figs. 33, 35).

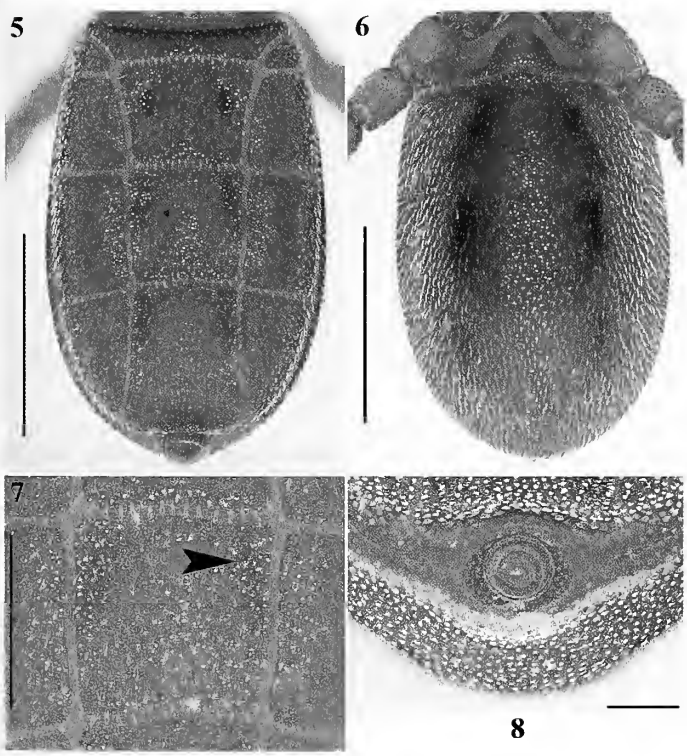

Figures 5–8.—*Pseudocellus quetzalcoatl* sp. nov. Male holotype: 5–6. Opisthosoma, dorsal and ventral views. 7. Tergite XII median plate (arrow indicates the depression). 8. Pygidium, posterior view. Scale bars: 0.2 mm (Fig. 8), 0.5 mm (Fig. 7), 1 mm (Figs. 5–6).

Description (male holotype).—*Coloration.* Cucullus, carapace and sternal region reddish (Figs. 3, 4, 9). Pedipalps, leg I, III and IV lighter reddish than leg II, which is darker; metatarsus and tarsus of legs I, III and IV paler reddish than other segments (Figs. 1–2). Opisthosoma brownish dorsally, darker ventrally (Figs. 5, 6).

Carapace (Fig. 3). Slightly longer than wide, trapezoidal, widest at posterior margin near coxae III. Tegument covered with abundant, fine translucent setae and rounded granules. Anterior margin straight, lateral margins not parallel, narrowing anteriorly; posterior margin procurved. Translucent areas completely absent. Carapace with six depressions: median longitudinal depression, ¾ the length of carapace; two small circular depressions at level of coxae II; three depressions on each side, close to posterior margin.

Cucullus (Fig. 9). Wider than long, widest distally; anterior margin straight, lateral margins rounded on anterior corners, where widest. Tegument covered with abundant translucent setae and granules similar to those on carapace; granules become larger and more conspicuous distally; depressions and cuticular pits absent. Distal margin with long, translucent setae; with shallow concavity in dorsal view.

Chelicera (Fig. 10). Fixed finger with six teeth, distalmost slightly larger than others, which are subequal in size. Movable finger with eight teeth: basalmost smallest, 3rd basal tooth largest; 4th to 7th of intermediate size; distalmost (8th) slightly smaller than 3rd.

Sternal region (Figs. 2, 4). Coxae covered with abundant translucent setae and granules similar to those on carapace. Coxa I rhomboidal, II sub-rectangular, III and IV conical. Coxa II considerably larger than others; coxa IV smallest.

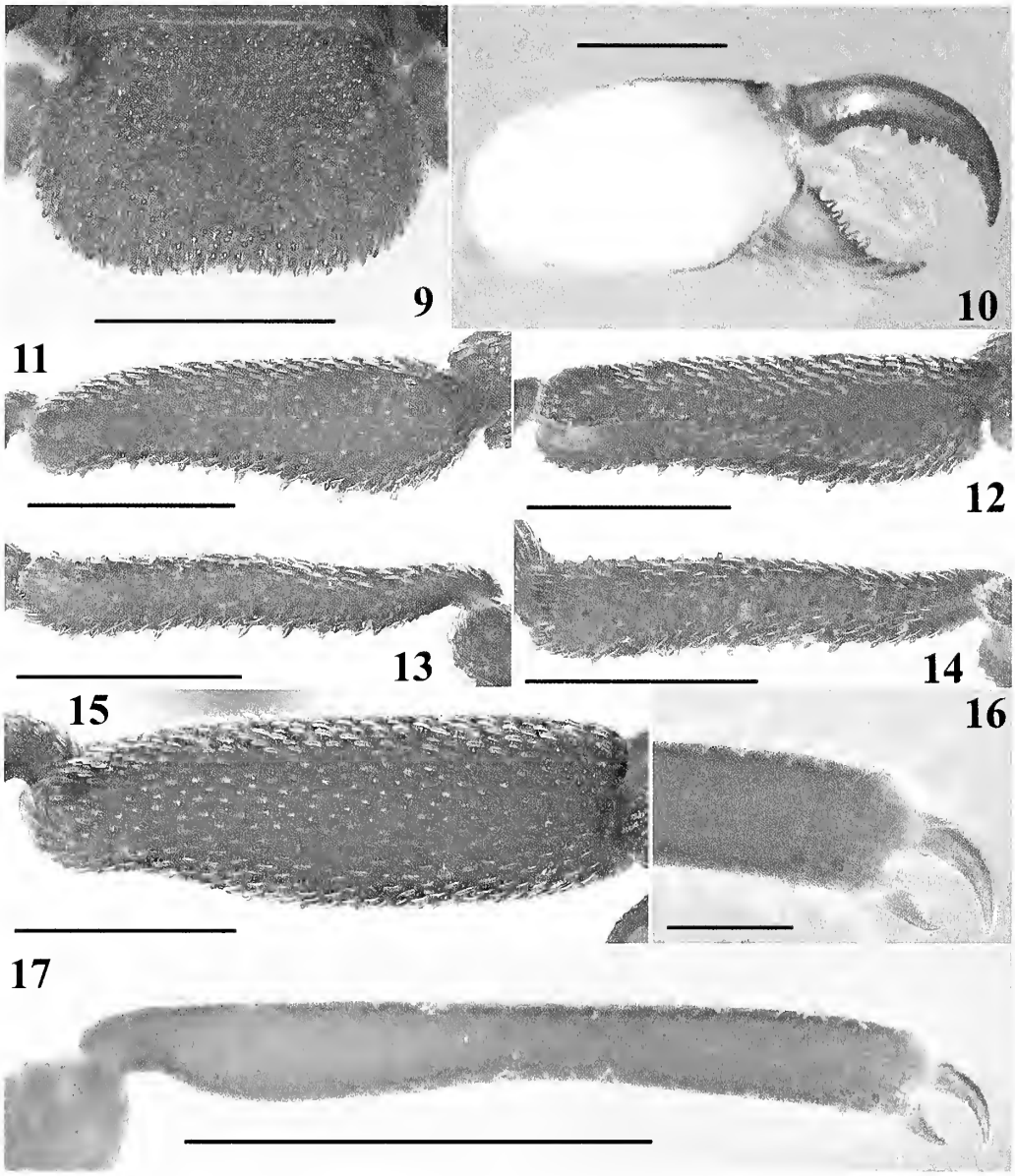

Figures 9–17.—*Pseudocellus quetzalcoatl* sp. nov. Male holotype: 9. Cueullus, dorsal view. 10. Left chelicerae, dorsal view. 11–12. Right tibia II, prolateral and proventral views. 13–14. Right metatarsus II, prolateral and proventral views. 15. Right femur II, prolateral view. 16. Detail of the movable and fixed claws of right pedipalp, retrolateral view. 17. Right pedipalp tibia, retrolateral view. Scale bars: 0.1 mm (Fig. 16), 0.2 mm (Fig. 10), 0.5 mm (Figs. 9, 11–15, 17).

Coxae I not meeting tritosternum; coxa II meeting tritosternum along 1/3 of its length. Coxae II anterior and posterior margins perpendicular to median axis of prosoma; coxae III slightly oblique, their posterior margins forming an obtuse angle (>90°) with each other; coxae IV oblique, their posterior margins forming an acute angle (<90°) with each other.

Opisthosoma (Figs. 5, 6). Longer than wide, widest at level of tergite XII. Tegument covered with abundant setae and granules similar to those on carapace; cuticular pits absent. Median plates of tergites XI–XIII with paired longitudinal depressions, those of tergite XI being the smallest. Tergite X widest and shortest. Median tergite XI trapezoidal, wider than long; XII as wide as long; median tergite XIII markedly longer than wide with posterior corners pointed, protruding laterally. Lateral tergites in oblique position; X smallest, XII and XIII largest. Lateral tergites XI trapezoidal, XII square and XIII triangular. Sternites XI–XIII with paired depressions. Sternites XI and XII dark medially. Pygidium segments without notch (Fig. 8).

Pedipalps (Figs. 4, 16, 17). Coxa without cuticular pits, with fine translucent setae and rounded granules on posterior half. Trochanter 1 rounded, with sparse fine translucent setae and granules restricted to ventrodistal half, and with small distal protuberance; trochanter 2 conical, ventrally with basal setae and granules (similar to those on 1st). Femur curved and wider proximally, with deep prolateral concavity distally close to the tibial joint; tegument with abundant translucent setae, which are thinner and longer in the prolateral surface. Femur with granules restricted to basal third of segment. Tibia predominantly straight, slightly concave medially in ventral view, with

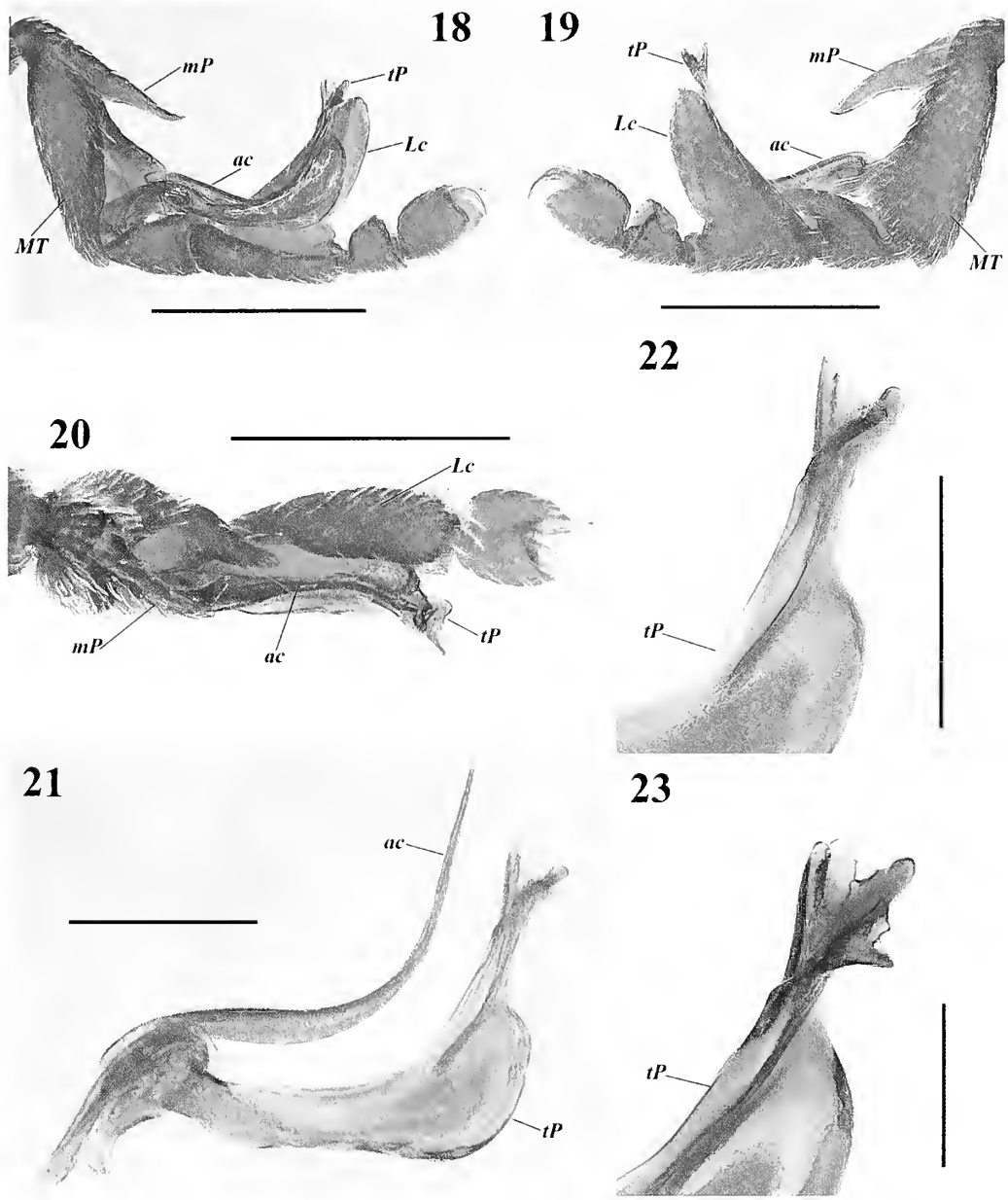

Figures 18–23.—*Pseudocellus quetzalcoatl* sp. nov. Male holotype: 18–20. Left leg III (copulatory apparatus), prolateral, retrolateral and dorsal views. 21. Copulatory apparatus, prolateral view. 22. Tarsal process, distal half, prolateral view. 23. Tarsal process, distal half, prodorsal view. Scale bars: 0.1 mm (Fig. 23), 0.2 mm (Figs. 21–22), 0.5 mm (Figs. 18–20).

numerous thin translucent setae which are longer on distal half of segment. Movable claw longer than fixed claw.

Legs. Without cuticular pits but with translucent setae and rounded granules on all segments (Figs. 1, 2). Leg II noticeably longer (Fig. 2). Femur II wider and longer than the others, femur and patella II ventrally with some sharp-tipped granules distally (Fig. 15). Tibia II ventrally with two longitudinal rows of curved spines (Figs. 11, 12). Metatarsus II with scattered sharp-tipped granules, not forming rows, dorsal ones smaller than ventral (Figs. 13, 14). Tarsomeres of leg II dorsally with sharp-tipped granules, tarsomeres 4 and 5 have fewer granules. Femora I, III and IV ventrally with few sharp-tipped granules. Patellae I, III and IV with normal granules. Tibiae I, III and IV ventrally with few sharp-tipped granules distally. All metatarsi dorsally with V-shaped invaginations distally; metatarsus I ventrally with numerous granules, metatarsus III without granules, metatarsus IV without granules ventrally, only few slightly sharp-tipped granules dorso distally. Tarsomere of leg I without granules, tarsomeres of legs III and IV with few granules apically.

Leg III and copulatory apparatus. Metatarsus conical, with numerous translucent setae; metatarsal process (*mP*) long and sigmoidal (Figs. 18, 24). Lamina cyathiformis (*Lc*) of tarsomere 2 conical, with a notch basally on retrolateral view (Fig. 19), with long translucent setae throughout. All tarsomeres ventrally with long curved-tip setae (*Lct*), more numerous and longer on tarsomere 4 (Figs. 24, 27). Tarsomere 3 with several sculptured surface tubercles (*Sct*) on distal

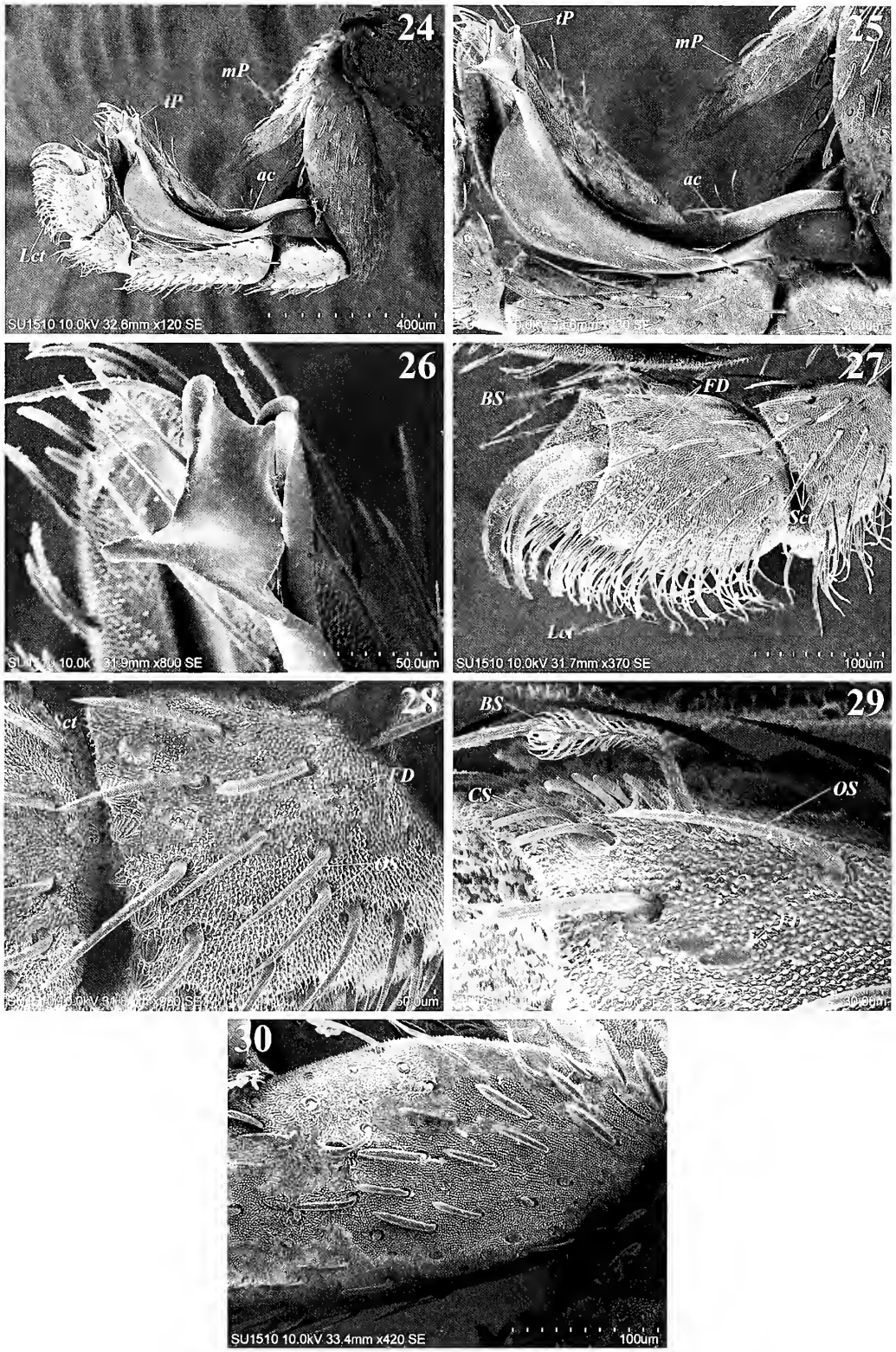

Figures 24–30.—*Pseudocellus quetzalcoatl* sp. nov. Male holotype: 24. Right leg III (copulatory apparatus), prolateral view. 25. Detail of copulatory apparatus, prolateral view. 26. Distal end of the copulatory apparatus, showing the apices of the tarsal process and accessory piece. 27. Distalmost tarsomere and tarsal claws of the right leg III, prolateral view. 28. Third tarsomere of the right leg III, prolateral view. 29. Detail of the dorsal setae on the fourth tarsomere of the right leg III. 30. Metatarsus of the right leg III, prolateral view.

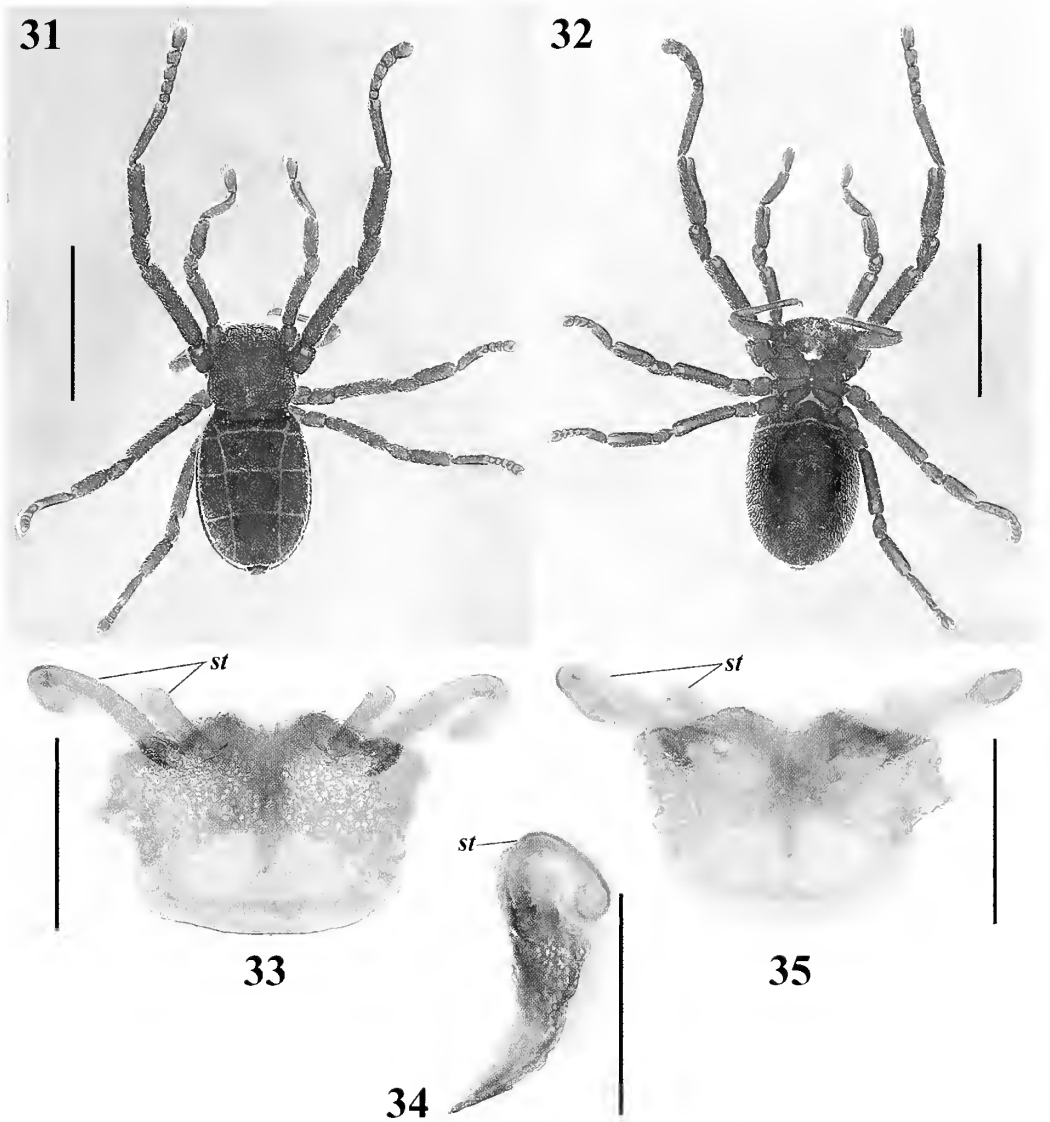

Figures 31–35.—*Pseudocellus quetzalcoatl* sp. nov. Female paratype: 31–32. Habitus, dorsal and ventral views. 33–35. Spermathecae, anterior, lateral and posterior views, respectively. Scale bars: 0.2 mm (Figs. 33–35), 2 mm (Figs. 31–32).

region (Figs. 27, 28). Tarsomere 4 with two curved claws (Fig. 27); dorsally with barbed setae (*BS*) and flat depressions (*FD*) (Figs. 27–29).

Measurements (in mm). Total length (carapace + opisthosoma including pygidium) 3.45. Carapace 1.18 long, 1.15 wide (widest part). Cucullus 0.54 long, 0.83 wide. Opisthosoma 2.13 long (not including pygidium), 1.38 wide (widest part). Femur II length/diameter (l/d): 3.11. Legs tarsal formula (leg I to IV): 1-5-4-5. Leg lengths; I: coxa 0.56/ trochanter 1 0.33/ trochanter 2 -/ femur 0.86/ patella 0.44/ tibia 0.60/ metatarsus 0.70/ tarsus 0.38/ total 3.87; II: 0.67/ 0.43/ -/ 1.38/ 0.66/ 1.08/ 1.06/ 1.20/ 6.48; III: 0.52/ 0.33/ 0.41/ 0.92/ 0.50/ 0.61/ 0.60/ 0.86/ 4.75; IV: 0.49/ 0.33/ 0.34/ 0.95/ 0.47/ 0.64/ 0.63/ 0.65/ 4.50. Leg length formula: 2341.

Female (paratype).—Differs from male as follows: Carapace darker reddish, median longitudinal depression deeper than on male. Coxa II smaller and femur II less robust than those on male. Tibia II without the two longitudinal rows of curved spines, only with few sharp-tipped granules. Metatarsus II with the scattered sharp-tipped granules smaller than those on male. Opisthosoma wider, higher and shorter than in male; darker reddish (Figs. 31, 32). Median tergites XI and XII wider than those on male (Fig. 31). Spermathecae with widespread tiny pores throughout (Figs. 33–35).

Measurements: Total length 3.24. Carapace 1.16 long, 1.14 wide. Cucullus 0.51 long, 0.80 wide. Opisthosoma 1.98 long, 1.50 wide. Femur II length/diameter (l/d): 4.27. Legs tarsal formula (leg I to IV): 1-5-4-5. Leg lengths; I: coxa 0.49/ trochanter 1 0.28/ trochanter 2 -/ femur 0.76/ patella 0.37/ tibia 0.54/ metatarsus 0.63/ tarsus 0.33/ total 3.40; II: 0.65/ 0.40/ -/ 1.22/ 0.58/ 0.96 / 0.94/ 1.12/ 5.87; III: 0.52/ 0.32/ 0.34/ 0.83/ 0.44/ 0.56/ 0.58/ 0.50/ 4.09; IV: 0.48/ 0.33/ 0.31/ 0.87/ 0.41/ 0.63/ 0.55/ 0.52/ 4.10. Leg length formula: 2431.

Deutonymph (Figs. 36, 37).—Appendages and body coloration pale orange, darker on carapace and mainly on opisthosoma; distal half of pedipalp tibia brown. Carapace slightly longer than wide, trapezoidal, with five pits dorsally: two on each side medially, two on each side posteriorly and

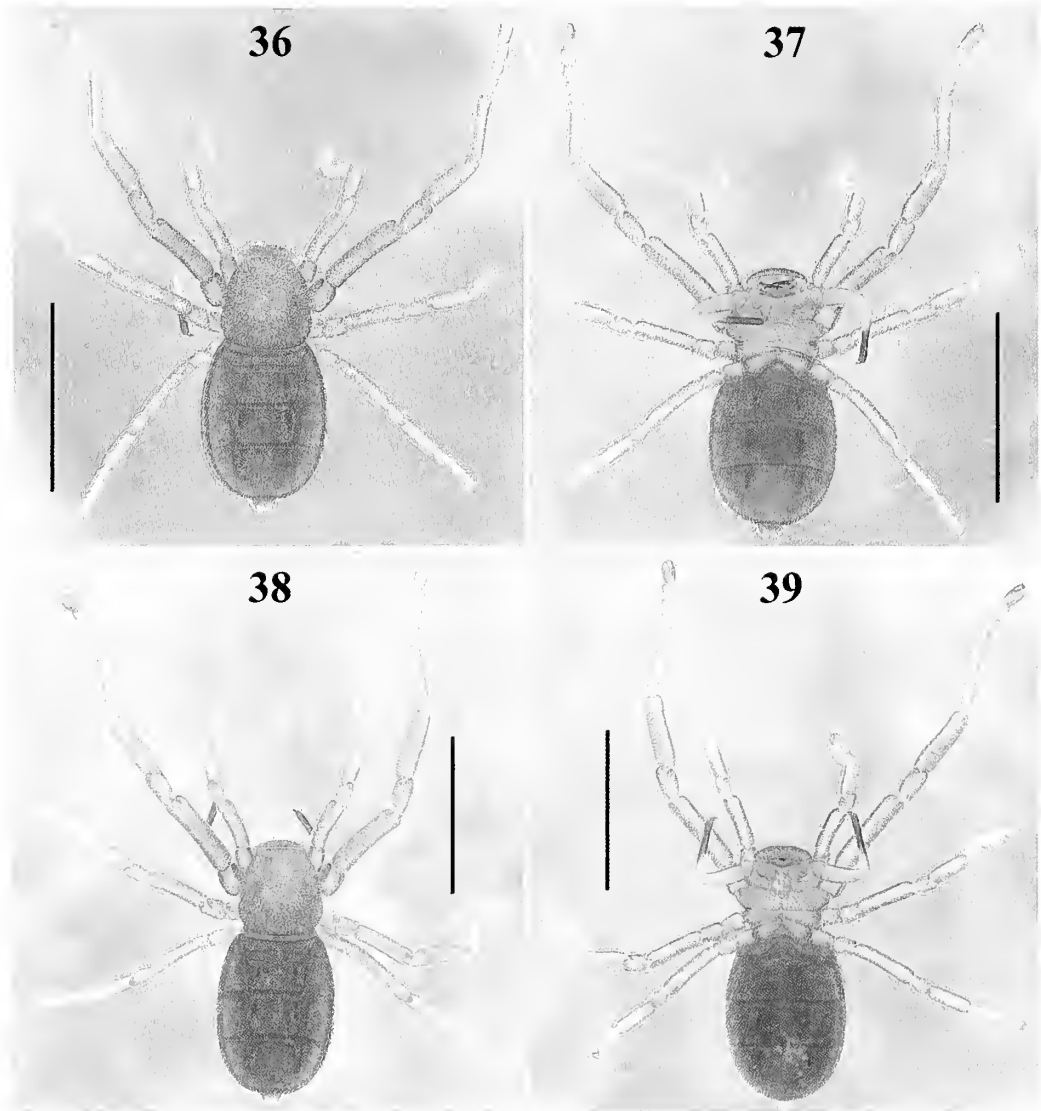

Figures 36–39.—*Pseudocellus quetzalcoatl* sp. nov. Deutonymph: 36–37. Habitus, dorsal and ventral views. Tritonymph: 38–39. Habitus, dorsal and ventral views. Scale bars: 2 mm.

one longer centrally. Cucullus wider than long, distal margin with long translucent setae like the adults. Cucullus, carapace, sternal region, legs and opisthosoma covered with abundant, fine translucent setae and rounded granules, except pedipalps with sparse rounded granules. Opisthosoma longer than wide, widest at level of tergite XII, median tergites X–XIII wider than long. Lateral tergite X smallest, XII and XIII largest. Lateral tergites: XI trapezoidal, XII square and XIII triangular. All tergites widely separated from each other in comparison to adults. Sternites X–XIII distinct and not fused in comparison to adults. Pygidium segments without notch. *Measurements*: Total length 2.77. Carapace 1.00 long, 0.96 wide (widest part). Cucullus 0.42 long, 0.65 wide. Opisthosoma 1.75 long, 1.30 wide. Legs tarsal formula (leg I to IV): 1-5-4-4.

Tritonymph (Figs. 38, 39).—Same appendages and body coloration pale orange like deutonymph but slightly darker, mainly in opisthosoma, distal half of pedipalp tibia brown. Carapace slightly longer than wide, trapezoidal, with five pits dorsally like deutonymph. Cucullus wider than long, distal margin with long translucent setae like the adults and deutonymph. Opisthosoma longer than wide, widest at the level of tergite XII, median tergites X–XII wider than long, tergite XIII as long as wide. Lateral tergite X smallest, lateral tergites XII and XIII largest, XI trapezoidal; XII square and XIII triangular. Sternites X–XIII widely separated from each other like deutonymph. Sternites X–XIII distinct like deutonymph, not fused in comparison to adults. Pygidium segments without notch. *Measurements*: Total length 3.32. Carapace 1.10 long, 1.08 (widest part). Cucullus 0.47 long, 0.70 wide. Opisthosoma 2.09 long, 1.46 wide. Legs tarsal formula (leg I to IV): 1-5-4-5.

Related species.—*Pseudocellus quetzalcoatl* sp. nov. is similar to *Pseudocellus cruzlopezi* Valdez-Mondragón & Francke, 2013 from Cerro Caballero, San José Tenango, Oaxaca, Mexico. Males resemble each other in overall body shape, proportions of femur II and the shape of the ventral spines of tibia II and metatarsus II. However, several

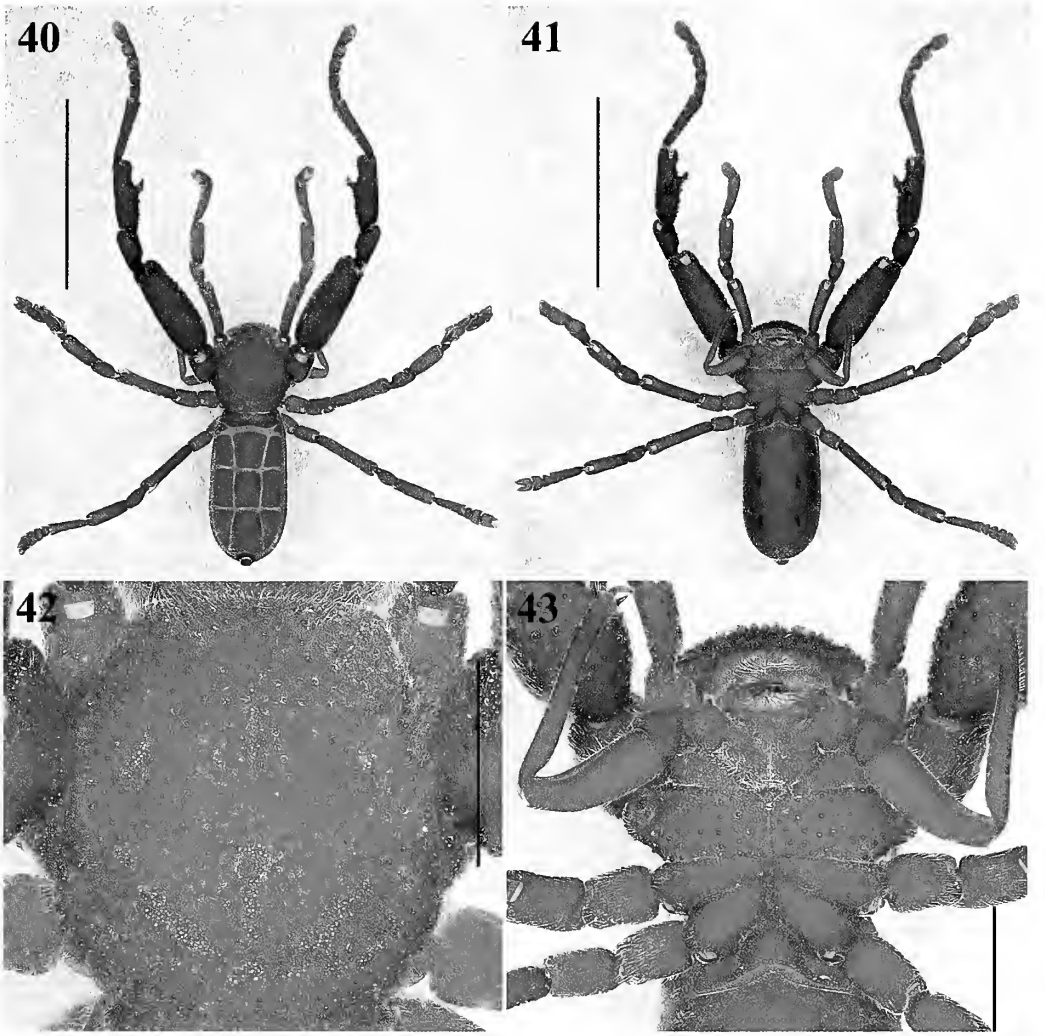

Figures 40–43.—*Pseudocellus olmeca* sp. nov. Male holotype: 40–41. Habitus, dorsal and ventral views. 42. Carapace. 43. Prosoma, ventral view showing coxosternal region. Scale bars: 1 mm (Figs. 42–43), 5 mm (Figs. 40–41).

morphological characters separate them; lateral margins of cucullus are more rounded in *P. quetzalcoatl* (Fig. 9) than in *P. cruzlopezi* (Valdez-Mondragón & Francke 2013: fig. 3). *Pseudocellus quetzalcoatl* has the ventral spines of tibia II (Figs. 11, 12) smaller and evenly sized, whereas those of *P. cruzlopezi* are larger and have different sizes (Valdez-Mondragón & Francke 2013: figs. 4, 5). The accessory piece (*ac*) of the *tP* is simple in *P. quetzalcoatl* (Fig. 21), whereas that of *P. cruzlopezi* is bifid (Valdez-Mondragón & Francke 2013: figs. 10, 11, 13). As for the females, the spermathecae of *P. quetzalcoatl* have two distinct pairs of lobes each of which is slightly oval apically, one is large and curved (i.e., J-shaped), and other is small and straight (Figs. 33–35); whereas in *P. cruzlopezi* the spermathecae have only one distinct pair of lobules, which are long, curved, and horn-shaped, with the apex evidently rounded (Valdez-Mondragón & Francke 2013: figs. 6, 7).

Etymology.—The specific name is a noun in apposition dedicated to the Aztec and Mesoamerican deity *Quetzalcoatl*, which in the mythology and in terms from the Nahuatl language means "feathered snake".

Pseudocellus olmeca sp. nov.
Figs. 40–85, 86, 87

Type material.—*Holotype male:* MEXICO: *Veracruz:* Parque Ecológico Jaguaroundi, camino al Ejidal Cangrejera Uno (18.11196°N, 94.35796°W; 25 m elev.), Municipio Coatzacoalcos, 7 July 2016, A. Valdez, E. Briones, M. Cortez, J. Valerdi (daytime collection) (CNAN-T1175).

Paratypes: MEXICO: *Veracruz:* 1 ♀, same data as holotype (CNAN-T1176), 1 ♂, 1 protonymph, 3 deutonymphs, 4 tritonymphs, same data as holotype (CNAN-T1177).

Other material examined.—MEXICO: *Veracruz:* 1 ♀, same locality as holotype, 30 April 2012, A. Reyna (CNAN-Ri0030).

Diagnosis.—Males can be distinguished by the following combination of features: (1) a pair of long, conical, pro- and retroventral apophyses in tibia II; covered with rounded granules throughout (Figs. 52, 53); (2) the scattered spines on metatarsus II (Figs. 54, 55); (3) the very robust femur II (Figs. 50, 51), 2.6 times longer than wide; (4) tarsal process (*tP*) of copulatory apparatus of leg III thin and arc-shaped in prolateral view (Figs. 58, 61, 64, 65), sigmoidal in dorsal and

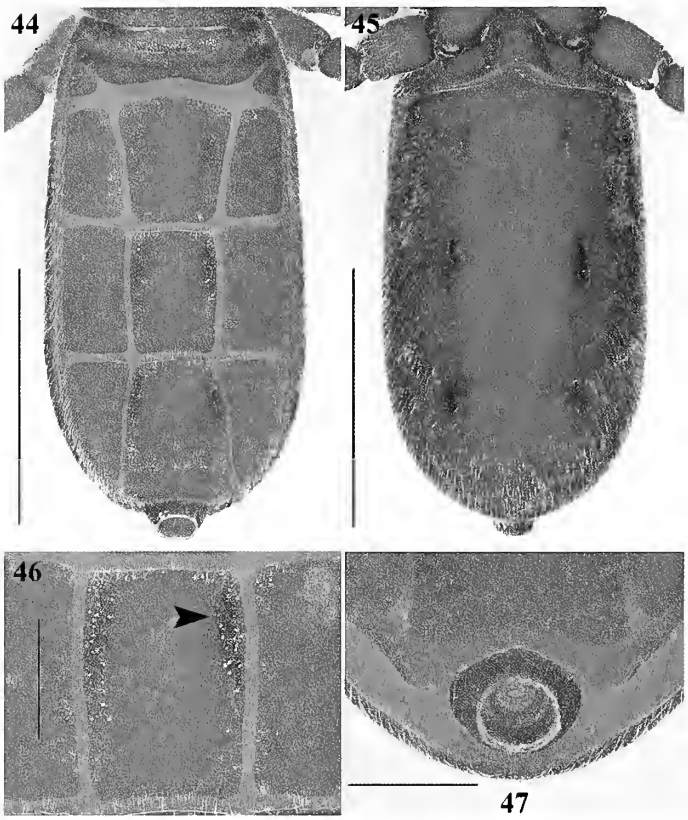

Figures 44–47.—*Pseudocellus olmeca* sp. nov. Male holotype: 44–45. Opisthosoma, dorsal and ventral views. 46. Tergite XII median plate (arrow indicates the depression). 47. Pygidium, posterior view. Scale bars: 0.5 mm (Figs. 46–47), 2 mm (Figs. 44–45).

prodorsal views (Fig. 63), conical apically (Figs. 62, 65, 66); 5) the accessory piece (*ac*) is thin and bifurcated distally (Fig. 61). Females can be distinguished by the two small paired apophysis ventrally on tibia II, homologous to those in the male (Figs. 75, 76); and by the spermathecae with two lobules on each side, one long, wide and S-shaped and the other one smaller, below the first one (Figs. 77–79).

Description (male holotype).—*Coloration.* Body coloration reddish, darker in carapace and leg II; pedipalps, legs and opisthosoma lighter reddish (Figs. 40, 41, 86, 87).

Carapace (Fig. 42). Longer than wide, trapezoidal, widest at posterior margin near level of coxae III. Tegument covered with abundant, long and fine translucent setae and rounded granules, which are more abundant posteriorly. Anterior margin straight; lateral margins not parallel, narrowing anteriorly; posterior margin procurved. Conspicuous elongated translucent areas, located at level of coxae II. Carapace with pits: three median longitudinal, one long, another circular at median part, and last upside down V-shaped close to posterior margin; two lateral and small at level of coxae I; two lateral bigger at level of coxae II; and two lateral pairs in oblique position close to posterior margin.

Cucullus (Fig. 48). Wider than long, widest distally; anterior margin straight, lateral margins rounded on anterior corners, where widest. Tegument covered with abundant translucent setae, longer distally; rounded granules similar to those on carapace, becoming bigger distally. Depressions and cuticular pits absent. Distal margin with shallow concavity in dorsal view.

Chelicera (Fig. 49). Fixed finger with six teeth, distalmost largest than others, which are subequal in size. Movable finger with ten teeth: the two basal smallest, 3rd basal tooth largest; 4th–10th subequal in size.

Sternal region (Fig. 43). Coxae covered with abundant translucent setae, without pits. Granules similar to those on carapace, considerably more numerous on coxae I and II. Coxa I triangular, II sub-rectangular, III conical and IV trapezoidal. Coxa II considerably larger than others; coxa IV smallest. Coxa I meeting tritosternum; coxa II meeting tritosternum along 1/4 of its length. Coxa II anterior and posterior margins perpendicular to the median axis of the prosoma; coxae III slightly oblique, their posterior margins forming an obtuse angle (>90°) with each other; coxae IV oblique, their posterior margins forming an acute angle (<90°) with each other.

Opisthosoma (Figs. 44, 45). Longer than wide, widest at level between tergites XII and XIII. Tegument covered with small and abundant translucent setae. Tergites X with rounded granules on middle and sides. Tergites XI–XIII with granule-containing cuticular pits along lateral margins of median plates and on internal margin of lateral plates; median plates XI–XIII with paired longitudinal depressions (Figs. 44, 46). Tergite X widest and shortest. Median tergite XI trapezoidal, wider than long. Median tergite XII longer than wide, median tergite XIII trapezoidal, longer than wide with posterior corners pointed, protruding laterally. Lateral tergites in oblique position; lateral tergites X smallest, lateral tergites XII and XIII largest. Lateral tergites XI trapezoidal; XII square and XIII triangular. Pygidium segments without notch (Figs. 44, 47). Sternites XI–XIII with paired depressions.

Pedipalps (Figs. 43, 56, 57). Coxa without cuticular pits, with fine translucent setae and rounded granules near the joint. Trochanter 1 rounded, with fine translucent setae and sparse rounded granules ventrally; trochanter 2 conical with rounded granules basally. Femur curved and wider proximally, with deep prolateral concavity close to joint with tibia, tegument with abundant translucent setae, which are thinner and longer on the prolateral surface. Femur without granules. Tibia predominantly straight, slightly concave at ¾ of its length, with numerous thin translucent setae which are longer on distal half of segment. Conspicuous oval granules close to chelae. Movable claw longer than fixed claw.

Legs. Without cuticular pits but with translucent setae and rounded granules on all segments (Figs. 50–55). Leg II noticeably long (Figs. 40, 41). Femur II wider and longer than the others (Figs. 40, 41, 50, 51), femur and patella II ventrally with numerous sharp-tipped granules (Figs. 50, 51). Tibia II ventrally with two long, conical paired apophysis, covered with rounded granules (Figs. 52, 53). Metatarsus II with scattered sharp-tipped granules throughout, not forming rows, dorsal ones smaller than ventral ones (Figs. 54, 55). Tarsomeres of leg II dorsally with sharp-tipped granules, tarsomere 5 without granules. Femora I, III and IV ventrally with few sharp-tipped granules. Patella I with few normal granules, patellae II and IV without granules. Tibia I ventrally with few sharp-tipped granules distally, tibiae III and IV without granules. All metatarsi dorsally with V-shaped

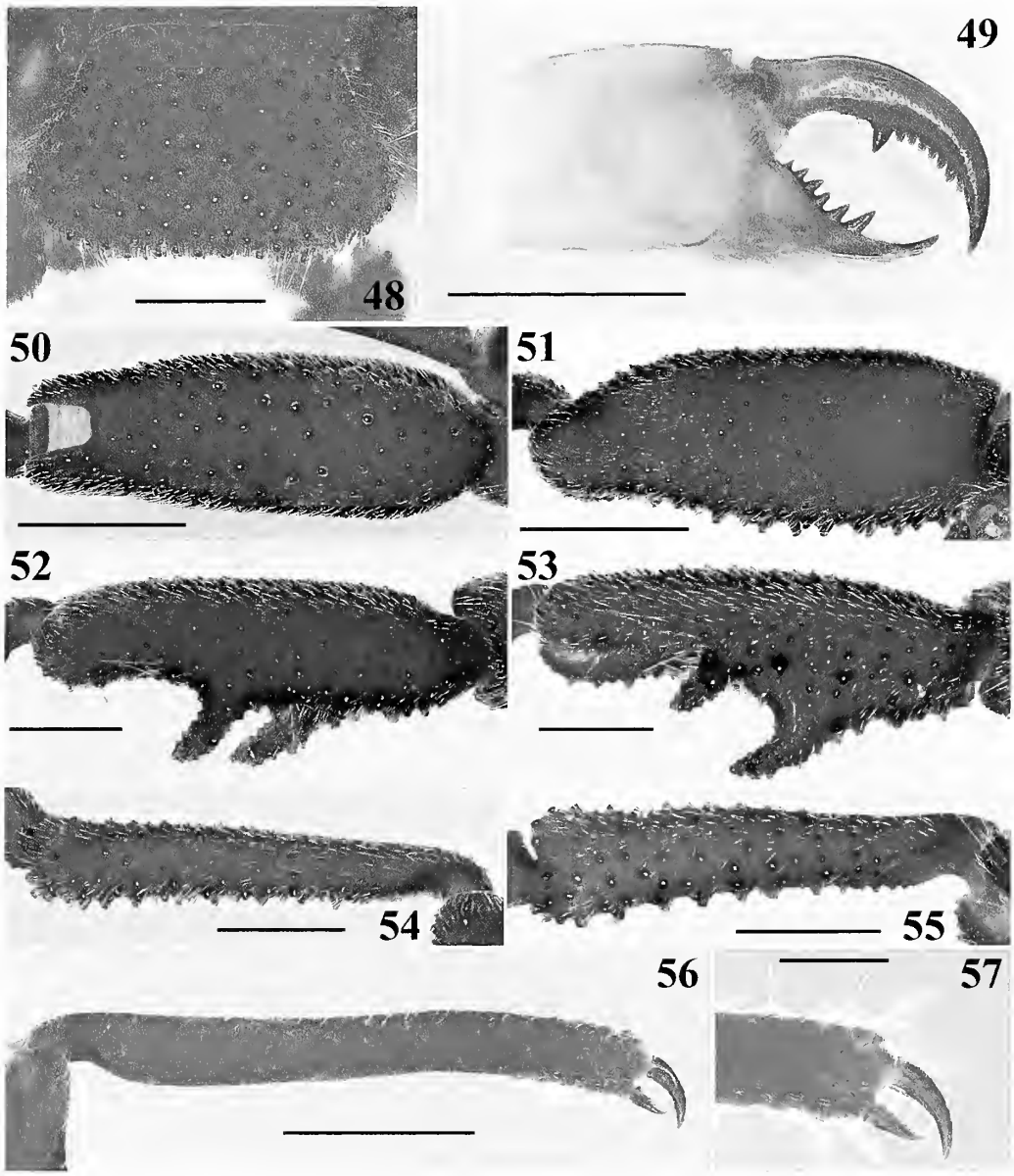

Figures 48–57.—*Pseudocellus olmeca* sp. nov. Male holotype: 48. Cucullus, dorsal view. 49. Left chelicera, dorsal view. 50–51. Right femur II, ventral and prolateral views. 52–53. Right tibia II, prolateral and proventral views. 54–55. Right metatarsus II, prolateral and proventral views. 56. Right pedipalp tibia, retrolateral view. 57. Detail of the movable and fixed claws of right pedipalp, retrolateral view. Scale bars: 0.2 mm (Fig. 57), 0.5 mm (Figs. 48–49, 52–56), 1 mm (Figs. 50–51).

invaginations distally; metatarsus I ventrally with few granules, metatarsi III and IV without granules. Tarsomeres of leg I, III and IV without granules.

Leg III and copulatory apparatus. Metatarsus conical, with long translucent setae; metatarsal process (*mP*) long and slightly sigmoidal (Figs. 58, 59, 64, 70). Lamina cyathiformis (*Lc*) of tarsomere 2 conical and curved dorsally, with a small notch basally in retrolateral view (Figs. 58, 59, 64), with long translucent setae throughout. All tarsomeres ventrally with long curved-tip setae (*Lct*) (Figs. 58, 59, 64), more abundant and longer on tarsomere 4 (Fig. 67). Tarsomere 3 with several sculptured surface tubercles (*Sct*) distally (Figs. 67, 68), with some flat depressions (*FD*) (Fig. 68). Tarsomere 4 with two curved claws (Fig. 67). Tarsomere 4 with barbed setae dorsally (*BS*) and *FD* (Figs. 67, 69).

Measurements (in mm). Total length (carapace + opisthosoma including pygidium) 5.90. Carapace 2.00 long, 1.85 wide (widest part). Cucullus 0.90 long, 1.44 wide. Opisthosoma 3.90 long (not including pygidium), 2.05 wide (widest part). Femur II length/diameter (l/d): 2.65. Legs tarsal formula (leg I to IV): I-5-4-5. Leg lengths; I: coxa 0.87/ trochanter 1 0.53/ trochanter 2 -/ femur 1.56/ patella 0.80/ tibia 1.09 / metatarsus 1.31 / tarsus 0.59/ total 6.75; II: 1.10/ 0.90/ -/ 2.80/ 1.21/ 1.88/ 1.76/ 2.12/ 11.77; III: 0.92/ 0.60/ 0.75/ 1.72/ 0.87/ 1.00/ 1.12/ 1.53/ 8.51; IV: 0.85/ 0.65/ 0.65/ 1.81/ 0.78/ 1.12/ 1.25/ 1.00/ 8.11. Leg length formula: 2341.

Female (paratype).—Differs from male as follows: Body coloration lighter, more reddish than the male (Figs. 71, 72). Coxa II and femur II smaller than those of male. Femur II less robust than on male, ventrally with sharp-tipped granules

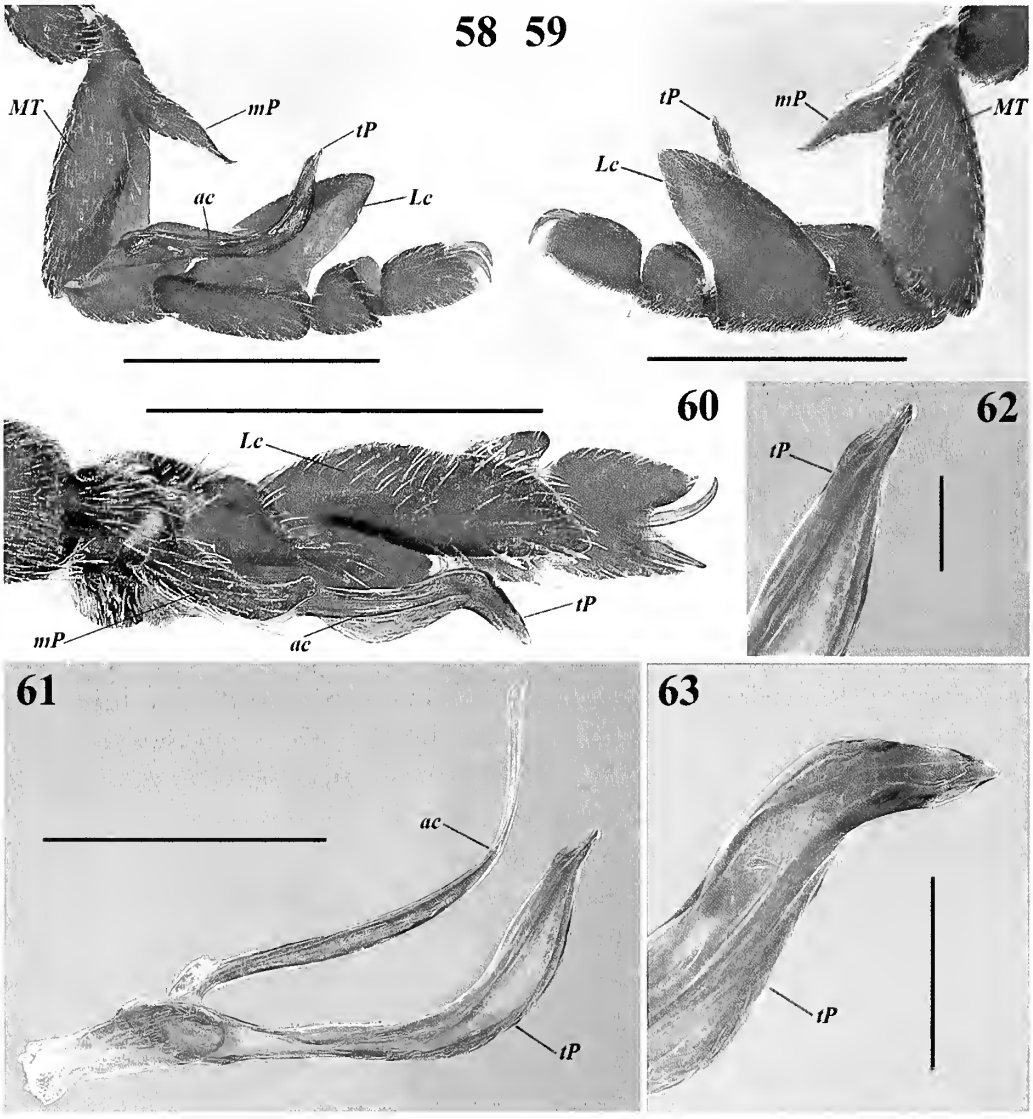

Figures 58–63.—*Pseudocellus olmeca* sp. nov. Male holotype: 58–60. Left leg III (copulatory apparatus), prolateral, retrolateral and dorsal views. 61, Copulatory apparatus, prolateral view. 62. Tarsal process, apex, prolateral view. 63. Tarsal process, apex, prodorsal view. Scale bars: 0.1 mm (Fig. 62), 0.2 mm (Fig. 63), 0.5 mm (Fig. 61), 1 mm (Figs. 58–60).

(Figs. 71–74). Tibia II with numerous sharp-tipped granules, and two small apophyses ventrally (arrows Figs. 75, 76). Metatarsus II with scattered, sharp-tipped granules, smaller than those on male. Opisthosoma shorter than in the male (Figs. 71, 72). Tergite XI wider than long (Fig. 71).

Measurements: (in mm). Total length (carapace + opisthosoma including pygidium) 6.1. Carapace 2.00 long, 1.95 wide (widest part). Cucullus 0.93 long, 1.50 wide. Opisthosoma 3.90 long (not including pygidium), 2.40 wide (widest part). Femur II length/diameter (l/d): 3.60. Legs tarsal formula (leg I to IV): 1-5-4-5. Leg lengths; I: coxa 0.93/ trochanter 1 0.52/ trochanter 2 -/ femur 1.44/ patella 0.68/ tibia 1.00/ metatarsus 1.24/ tarsus 0.57/ total 6.38; II: 1.15/ 0.75/ -/ 2.50/ 1.13/ 1.81/ 1.78/ 2.00/ 11.12; III: 0.90/ 0.54/ 0.63/ 1.56/ 0.75/ 1.00/ 1.13/ 0.96/ 7.47; IV: 0.84/ 0.60/ 0.60/ 1.70/ 0.75/ 1.06/ 1.18/ 0.93/ 7.66. Leg length formula: 2431.

Protonymph (Figs. 80, 81).—Appendages and body coloration pale orange, darker in distal part of cucullus; distal half of pedipalp tibia brown. Carapace as long as wide, trapezoidal, with rounded corners, with five pits dorsally: two on each side medially, two on each side posteriorly, and one longer centrally. Cucullus wider than long, distal margin with long translucent setae like the adults. Cucullus, carapace, sternal region, legs and opisthosoma covered with abundant, fine translucent setae and rounded granules, except pedipalps where granules are absent. Opisthosoma longer than wide, widest at the level between tergites XI and XII, tergites X–XIII wider than long. Tergites XI–XIII with paired long pits. Lateral tergite X smallest, lateral tergites XI–XIII largest. Lateral tergites XI trapezoidal; XII square and XIII triangular. All tergites widely separated from each other. Sternites X–XIII clearly visible and widely separated from each other, not fused in comparison to adults. Sternites XI–XIII with paired long pits. Pygidium segments without notch. *Measurements*: Total length 3.16. Carapace 1.04 long, 1.04 wide (widest part).

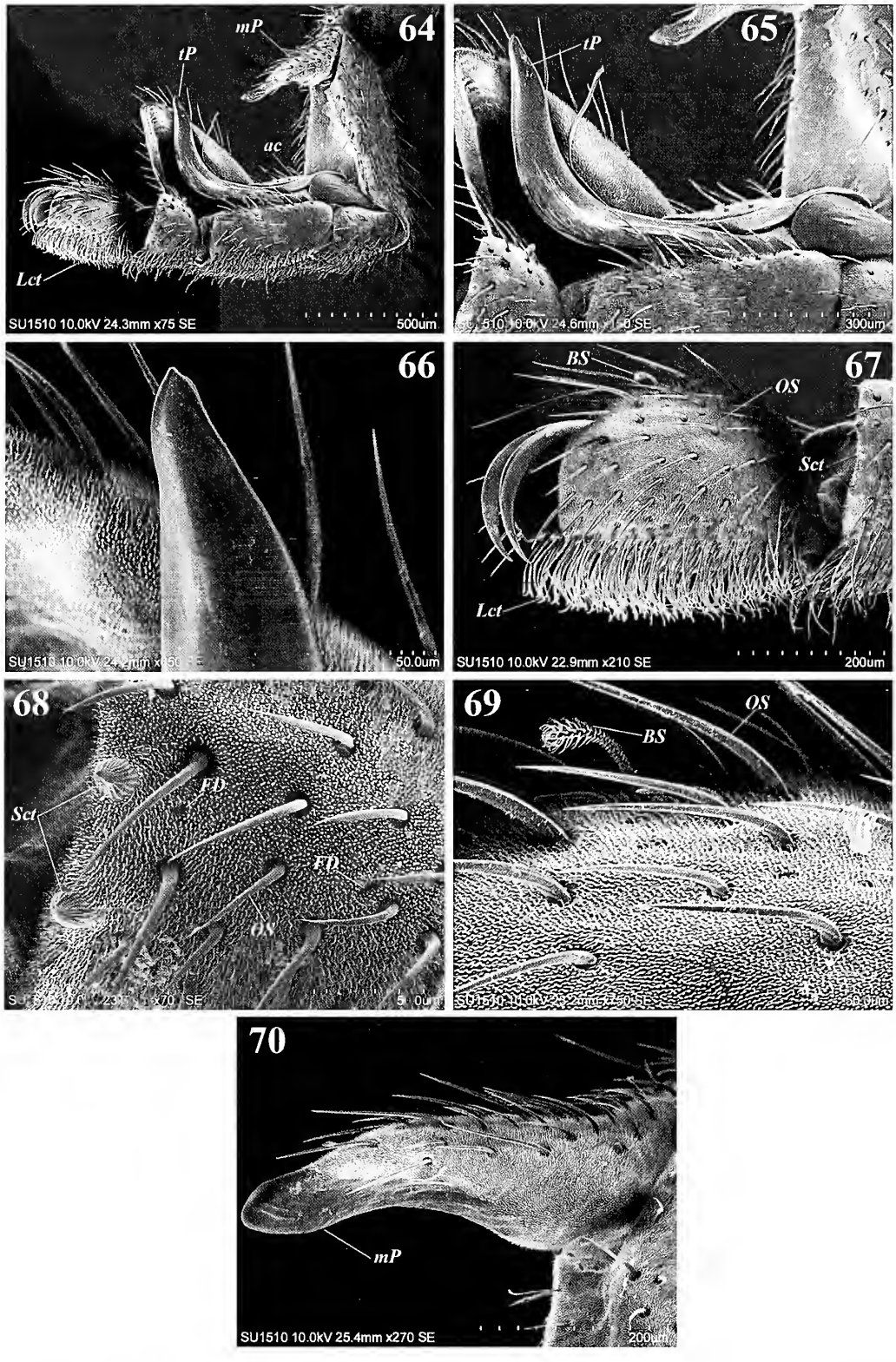

Figures 64–70.—*Pseudocellus olmeca* sp. nov. Male holotype: 64. Right leg III (copulatory apparatus), prolateral view. 65. Detail of copulatory apparatus, prolateral view. 66. Apex of tarsal process of the copulatory apparatus, prolateral view. 67. Distalmost tarsomere and tarsal claws of right leg III, prolateral view. 68. Third tarsomere of right leg III, prolateral view. 69. Detail of setae on dorsal surface of right leg III fourth tarsomere. 70. Metatarsal process of right leg III, prolateral view.

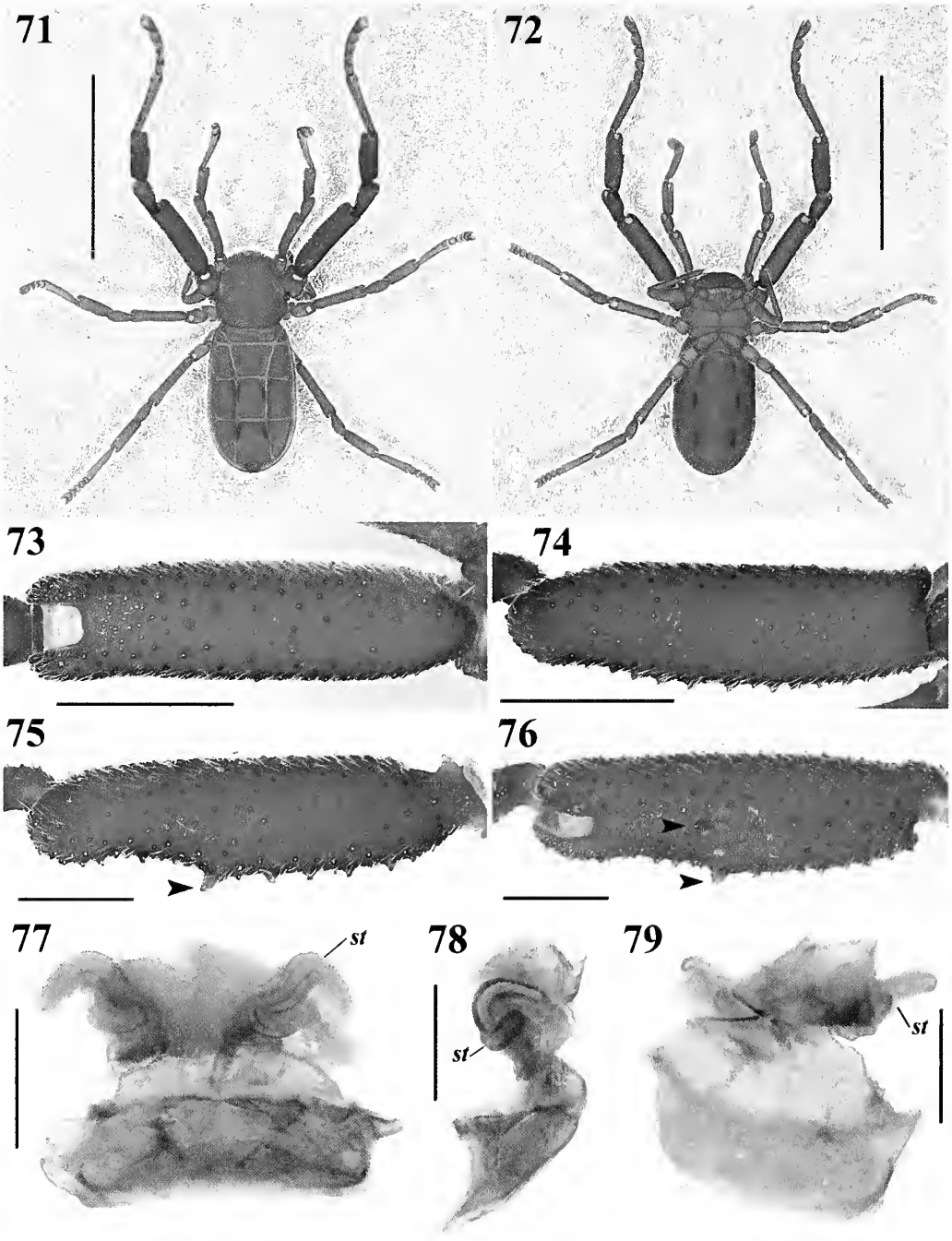

Figures 71–79.—*Pseudocellus olmeca* sp. nov. Female paratype: 71–72, Habitus, dorsal and ventral views. 73–74. Right femur II, ventral and prolateral views. 75–76. Right tibia II, prolateral and proventral views (arrows indicate the two small spines). 77–79. Spermathecae, anterior, lateral and posterior views, respectively. Scale bars: 0.2 mm (Figs. 77–79), 0.5 mm (Figs. 75–76), 1 mm (Figs. 73–74), 5 mm (Figs. 71–72).

Cucullus 0.47 long, 0.69 wide. Opisthosoma 1.96 long, 1.54 wide. Legs tarsal formula (leg I to IV): 1-4-3-2.

Deutonymph (Figs. 82, 83).—Appendages and body coloration darker orange than the protonymph, leg II darker orange than other legs, dark orange in distal part of cucullus, distal half of pedipalp tibia brown. Legs II wider than those on protonymph. Carapace as long as wide, trapezoidal, with rounded corners, with the same five pits dorsally as the protonymph, but more conspicuous. Cucullus wider than long, distal margin with long translucent setae like protonymph. Cucullus, carapace, sternal region, legs and opisthosoma covered with abundant, fine translucent setae and rounded granules, except pedipalps where granules are absent; the granules are more conspicuous than those on the protonymph. Opisthosoma longer than wide, longer than on protonymph, widest at the level of tergite XII; tergites X–XIII wider than long. Tergites XI–XIII with long paired pits, more marked than on protonymph. Lateral tergite X smallest, lateral tergites XI–XIII largest. Lateral tergites XI trapezoidal; XII square and XIII triangular. All tergites less widely separated from each other in comparison to protonymph. Sternites X–XIII clearly visible and less separated from each

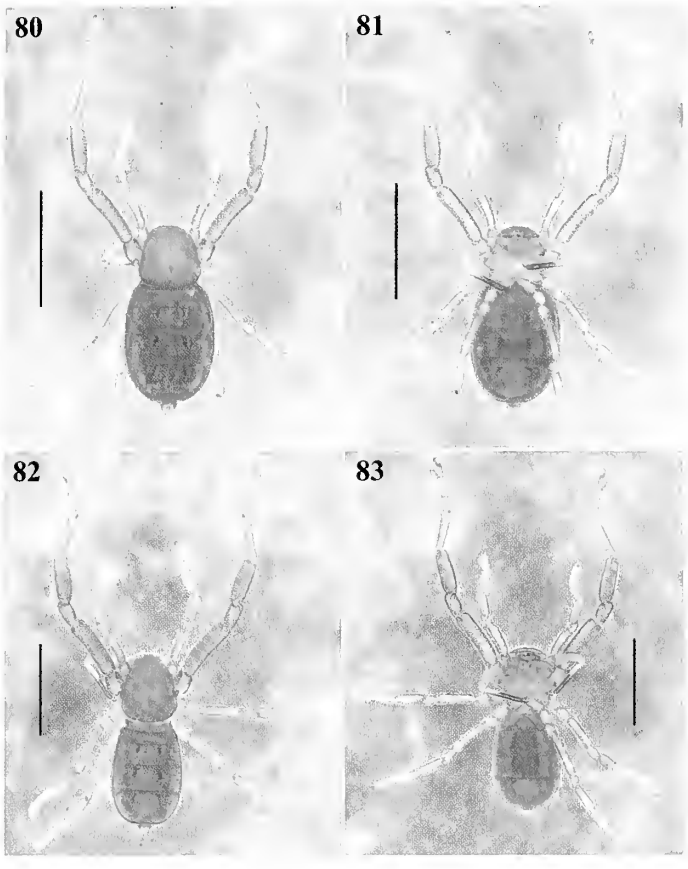

Figures 80–83.—*Pseudocellus olmeca* sp. nov. Protonymph: 80–81. Habitus, dorsal and ventral views. Deutonymph: 82–83. Habitus, dorsal and ventral views respectively. Scale bars: 2 mm.

other in comparison to protonymph; sternites XI and XII dark medially. Sternites XI–XIII with long paired pits more conspicuous than those in the protonymph. Pygidium segments without notch. *Measurements*: Total length 3.67. Carapace 1.37 long, 1.32 wide (widest part). Cucullus 0.64 long, 0.94 wide. Opisthosoma 2.32 long, 1.72 wide. Legs tarsal formula (leg I to IV): 1-5-4-4.

Tritonymph (Figs. 84, 85, 88, 89).—Appendages and body coloration darker orange than the deutonymph, leg II darker orange than other legs, having the same coloration as cucullus, carapace and opisthosoma. Cucullus uniformly dark orange. The distal half of pedipalp tibia is darker brown than on deutonymph. Legs II wider than those on deutonymph, with more rounded granules. Carapace as long as wide, trapezoidal, with rounded corners, with the same five pits dorsally as the deutonymph but less marked than those on deutonymph. Cucullus wider than long, distal margin with long translucent setae like deutonymph. Cucullus, carapace, sternal region, legs and opisthosoma covered with abundant, fine translucent setae and rounded granules, except pedipalps where granules are absent; the granules are more conspicuous than those on the deutonymph. Opisthosoma longer than wide, longer than on deutonymph, widest at the level between tergites XII and XIII, tergites X–XIII wider than long. Tergites XI–XIII with long paired pits, more conspicuous than on deutonymph. Lateral tergites X smallest, lateral tergites XI–XIII largest. Lateral tergites XI trapezoidal; XII square and XIII triangular. All tergites widely separated as those in the protonymph. Sternites X–XIII clearly visible and separated as those in the deutonymph, sternites XI–XIII with the same coloration, dark orange. Sternites XI–XIII with long paired pits less marked than those in the deutonymph. Pygidium segments without notch. *Measurements*: Total length 4.88. Carapace 1.68 long, 1.64 wide (widest part). Cucullus 0.78 long, 1.20 wide. Opisthosoma 3.15 long, 2.10 wide. Legs tarsal formula (leg I to IV): 1-5-4-5.

Related species.—*Pseudocellus olmeca* sp. nov. is similar to *Pseudocellus chankin* Valdez-Mondragón & Francke, 2011 from Cueva Kolem-chen "Cueva Grande," Reserva Chan-kin, Municipio Ocosingo, Chiapas, Mexico. The species resemble each other in overall body shape, proportions of femur II, and

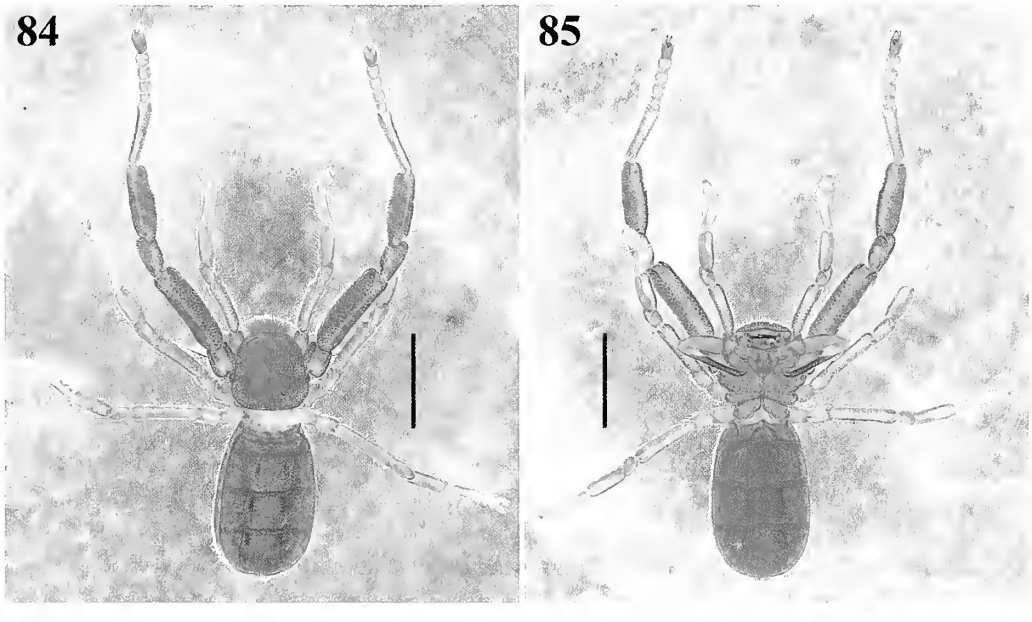

Figures 84–85.—*Pseudocellus olmeca* sp. nov. Tritonymph. Habitus, dorsal and ventral views. Scale bars: 2 mm.

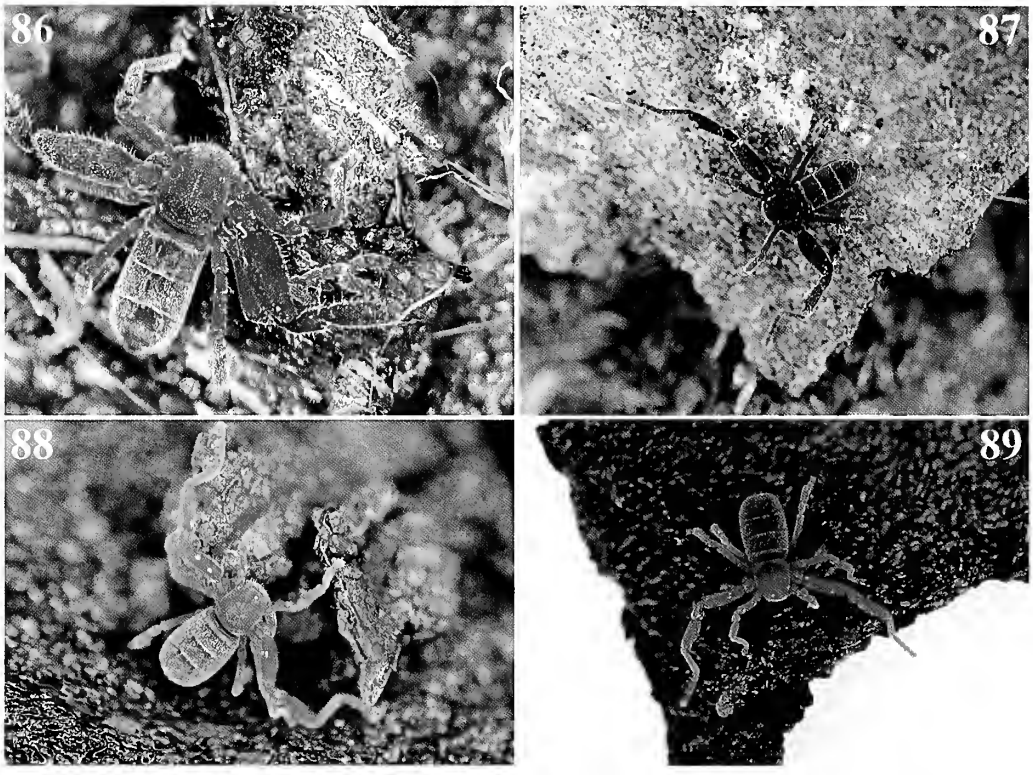

Figures 86–89.—Living specimens of *Pseudocellus olmeca* sp. nov. 86–87, Male holotype. 88–89, Tritonymph. Photos by A. Valdez-Mondragón.

shape of the paired apophyses on tibia II of males. However, several morphological differences distinguish both species. The carapace of the male of *P. olmeca* is somewhat quadrangular (Fig. 42), whereas that of *P. chankin* is more trapezoidal, with lateral margins more distinctly narrowing anteriorly (Valdez-Mondragón & Francke, 2011: fig. 1; Botero-Trujillo & Valdez-Mondragón, 2016: fig. 53). The opisthosoma of the male of *P. olmeca* (Figs. 40, 41, 44, 45) is oval, whereas that of *P. chankin* is somewhat truncated posteriorly (Valdez-Mondragón & Francke, 2011: fig. 1). Males of *P. olmeca* have the femur of leg II thinner than that of *P. chankin*, such that it is 2.6 and 2.4 times longer than

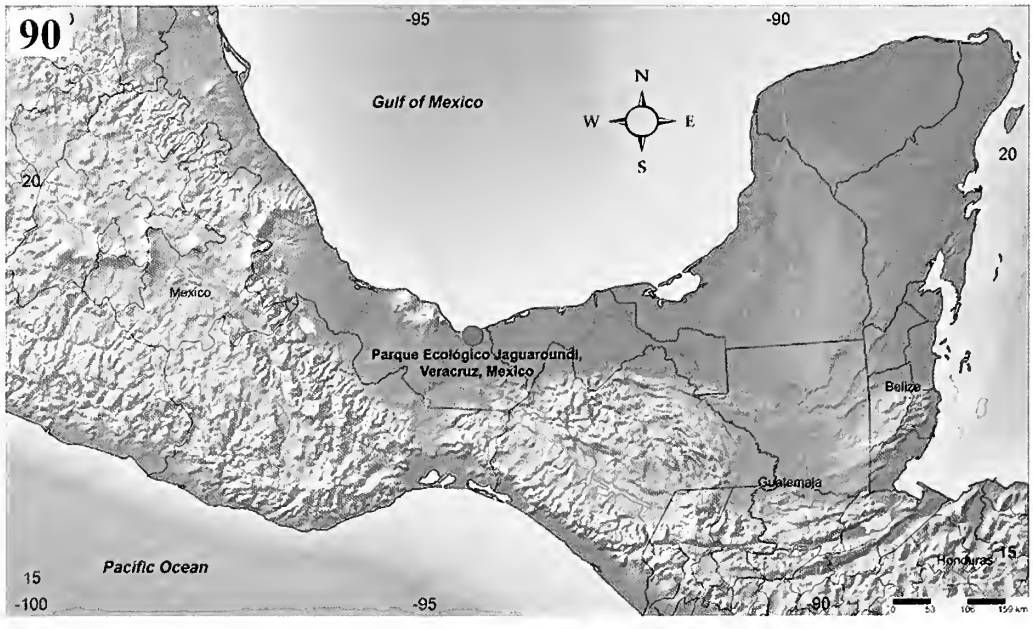

Figure 90.—Location of the Parque Ecológico Jaguaroundi, Veracruz, Mexico; type locality and known records for *Pseudocellus quetzalcoatl* sp. nov. and *Pseudocellus olmeca* sp. nov.

wide, respectively (Figs. 50, 51; Valdez-Mondragón & Francke, 2011: fig. 1). The paired apophyses of tibia II of males are thinner and smaller in *P. olmeca* (Figs. 40, 41, 52, 53) than in *P. chankin* (Valdez-Mondragón & Francke, 2011: fig. 3). The tarsal process (*tP*) of male leg III of *P. olmeca* is curved in the distal half on prolateral view (Figs. 58, 61, 64, 65), whereas the *tP* of *P. chankin* is slightly sigmoidal distally (Valdez-Mondragón & Francke 2011: fig. 5). The metatarsal process (*mP*) of males of *P. olmeca* is wider, shorter and more sigmoidal (Figs. 58, 59, 64, 70) than that of *P. chankin*, where the *mP* is almost straight (Valdez-Mondragón & Francke 2011: fig. 4). As for the females, the lobules of the spermathecae of *P. olmeca* (Figs. 77–79) are larger and more distinctly curved than those of *P. chankin* (Valdez-Mondragón & Francke 2011: figs. 6, 7).

Etymology.—The specific name is a noun in apposition dedicated to the Olmec people, the first major civilization which flourished in Mesoamerica's formative period, dating from as early as 1500 b. c. to about 400 b. c. The Olmecs occupied the state of Veracruz, where the type locality is located.

DISCUSSION

According to the previous records of other species of the genus *Pseudocellus* from North America, the troglobitic species *Pseudocellus osorioi* and *Pseudocellus pelaezi* Corona-do-Gutierrez, 1970 have been found in the same cave system in the North of Mexico, in the states of San Luis Potosi and Tamaulipas (Reddell 1981). Both species could be considered sympatric because they share the same cave system; however, more research is needed to prove if both species share the same microhabitat in those caves to be considered as sympatric species.

The case here reported is a well-documented record of sympatry for epigean species from North America for the genus *Pseudocellus*. The most important evidence to prove the sympatry between both species is that a tritonymph (CNAN-T1177) of *P. olmeca* sp. nov. (Figs. 88, 89) was found in the same microhabitat, under a big rock on the ground where all the specimens of *P. quetzalcoatl* sp. nov. were collected as well. Although species identification based on immatures specimens is often impossible, the size of specimens within each instar (larva, protonymph, deutonymph and tritonymph) is remarkably invariable for a given ricinuleid species. Likewise, each of the three nymphal stages is characterized by a unique combination of tarsomere counts for each of the four pairs of legs, whereas the larva is six-legged (Platnick 2002). Upon examination, the tritonymph specimen of *P. olmeca*, found in the same collection event and under the very same boulder as *P. quetzalcoatl*, was recognized as different from *P. quetzalcoatl*, because it was noticeably larger (*P. olmeca* total length 4.88 mm, against *P. quetzalcoatl* total length 3.32 mm); similarly, adults of *P. olmeca* are larger than the adults of *P. quetzalcoatl*.

The staining technique with clorazol (1%) was used for the first time with ricinuleids, revealing new morphological information of the order: the presence of numerous tiny pores on the membrane below the spermathecae of the female (Figs. 33–35, 77–79). The function of these pores is unknown, but it is possible that these could be the opening of some kind of secretory glands. Additional studies are needed to determine the function of these pores, as well as to evaluate if these are present in other ricinuleid taxa (*Cryptocellus* and *Ricinoides*), where this morphological characteristic has been unexplored thus far.

ACKNOWLEDGMENTS

AVM wishes to thank the program "Cátedras CONACyT", Consejo Nacional de Ciencia y Tecnología (CONACyT), Mexico for the scientific support for project No. 59: "Laboratorio Regional de Biodiversidad y Cultivo de Tejidos Vegetales (LBCTV) del Instituto de Biología (IBUNAM), Tlaxcala". We thank Mayra R. Cortez Roldán, Jose Cruz Valerdi Tlachi and Eduardo Briones Osorno, students of the Laboratory of Arachnology (LATLAX) of the LBCTV, IBUNAM, Tlaxcala, Mexico for their help in the collection of the specimens in the field. To the Secretaría de Fomento Agropecuario del Estado de Tlaxcala (SEFOA) and the Government of the state of Tlaxcala for the facilities and support to this research. To M.Sc. Berenit Mendoza Gárfias for the photographs taken with the scanning electron microscope (SEM). To the staff, responsible persons, and workers of PEMEX and of the Jaguaroundi Ecological Park, Veracruz, Mexico for the facilities and logistical help in the fieldwork. The specimens were collected under Scientific Collector Permit FAUT-0309 from Secretaría de Medio Ambiente y Recursos Naturales (SEMARNAT) to the first author (AVM). RBT was initially supported by a 3-year Doctoral Fellowship associated to PICT 2011-01007 from the "Fondo para la Investigación Científica y Tecnológica–FONCyT", Argentina, and currently by a 2-year Doctoral Fellowship from the "Consejo Nacional de Investigaciones Científicas y Técnicas–CONICET", Argentina.

LITERATURE CITED

Armas, L.F. 2017. Cuatro especies nuevas de *Pseudocellus* de Cuba (Arachnida: Ricinulei). Revista Ibérica de Aracnología 30:87–99.

Armas, L.F. & E.O. Agreda. 2016. Una nueva especie de *Pseudocellus* (Ricinulei: Ricinoididae) del Suroeste de Guatemala. Revista Ibérica de Aracnología 28:79–83.

Bolívar y Pieltain, C. 1942. Estudio de un Ricinulideo de la Caverna de Cacahuamilpa, Guerrero, Mex. Revista de la Sociedad Mexicana de Historia Natural 2:197–209.

Bolívar y Pieltain, C. 1946. Hallazgo de un nuevo Ricinulideo en el Mexico Central (Arach.). Ciencia, México 7:24–28.

Botero-Trujillo, R. 2014. A new Colombian species of *Cryptocellus* (Arachnida, Ricinulei), with notes on the taxonomy of the genus. Zootaxa 3814:121–132.

Botero-Trujillo, R. & D.E. Flórez. 2017. Two new ricinuleid species from Ecuador and Colombia belonging to the *peckorum* species-group of *Cryptocellus* Westwood (Arachnida, Ricinulei). Zootaxa 4286:483–498.

Botero-Trujillo, R. & G.A. Pérez. 2008. A new species of *Cryptocellus* (Arachnida, Ricinulei) from northwestern Colombia. Journal of Arachnology 36:468–471.

Botero-Trujillo, R. & G.A. Pérez. 2009. A new species of *Cryptocellus* (Arachnida, Ricinulei) from the Kófan Territory in southwestern Colombia. Zootaxa 2050:56–64.

Botero-Trujillo, R. & A. Valdez-Mondragón. 2016. A remarkable new species of the *magnus* species-group of *Cryptocellus* (Arachnida, Ricinulei) from Ecuador, with observations on the taxonomy of the New World genera. Zootaxa 4107:321–337.

Brignoli, P.M. 1974. On some Ricinulei of Mexico with notes of the morphology of the female genital apparatus (Arachnida, Ricinulei). Quaderno Accademia Nazionale dei Lincei 171:153–174.

Cokendolpher, J.C. & T. Enríquez. 2004. A new species and records of *Pseudocellus* (Arachnida: Ricinulei: Ricinoididae) from caves in Yucatán, Mexico and Belize. Texas Memorial Museum, Speleological Monographs 6:95–99.

Cooke, J.W. 1967. Observations on the biology of Ricinulei (Arachnida) with descriptions of two new species of *Cryptocellus*. Journal of Zoology 151:31–42.

Cooke, J.A.L. & M.U. Shadab. 1973. New and little known ricinuleids of the genus *Cryptocellus* (Arachnida, Ricinulei). American Museum Novitates 2530:1–25.

Ewing, H.E. 1929. A synopsis of the American arachnids of the primitive order Ricinulei. Annals of the Entomological Society of America 22:583–600.

Gertsch, W.J. 1971. Three new ricinuleids from Mexican caves (Arachnida, Ricinulei). Bulletin of the Association for Mexican Cave Studies 4:127–135.

Gertsch, W.J. 1977. On two ricinuleids from the Yucatan Peninsula (Arachnida: Ricinulei). Bulletin of the Association for Mexican Cave Studies 6:133–138.

Harvey, M.S. 2003. Catalogue of the Smaller Arachnid Orders of the World. CSIRO Publishing, Collinwood, Victoria, Australia.

Naskrecki, P. 2008. A new ricinuleid of the genus *Ricinoides* Ewing (Arachnida, Ricinulei) from Ghana. Zootaxa 1698:57–64.

Penney, D., Y. Marusik, C.P. Wheater & A.M. Langan. 2009. First Gambian Ricinulei (Arachnida: Ricinoididae): northernmost African record for the order. Zootaxa 2021:66–68.

Pinto-da-Rocha, R. & R. Andrade. 2012. A new *Cryptocellus* (Arachnida: Ricinulei) from Eastern Amazonia. Zoologia 29:474–478.

Pittard, K. & R.W. Mitchell. 1972. Comparative morphology of the life stages of *Cryptocellus pelaezi* (Arachnida, Ricinulei). Graduate Studies Texas Tech University 1:1–77.

Platnick, N.I. 1980. On the phylogeny of Ricinulei. Pp. 349–353. *In* Verhandlungen des 8. Internationalen Arachnologen-Kongress, Wien. (J. Gruber (ed.)). H. Egermann, Wien.

Platnick, N.I. 2002. Ricinulei. Pp. 381–386. *In* Amazonian Arachnida and Myriapoda. (J. Adis (ed.)). PENSOFT Publishers, Sofia-Moscow.

Reddell, J.R. 1981. A review of the cavernicole fauna of Mexico, Guatemala and Belize. Bulletin of the Texas Memorial Museum 27:1–327.

Salvatierra, L. & A.L. Tourinho. 2016. The integumentary ultrastructure of *Cryptocellus bordoni* Dumitresco and Juvara-Bals, 1976 (Arachnida, Ricinulei). Micron 81:1–19.

Selden, P.A. 1992. Revision of the fossil ricinuleids. Transactions of the Royal Society of Edinburgh: Earth Sciences 83:595–634.

Shorthouse, D.P. 2010. SimpleMappr, an online tool to produce publication-quality point maps. Available online at http://www.simplemappr.net (Accessed 14 August 2017).

Teruel, R. & L.F. Armas. 2008. Nuevo *Pseudocellus* Platnick 1980 de Cuba oriental y nuevos registros de *Pseudocellus paradoxus* (Cooke 1972) (Ricinulei: Ricinoididae). Boletín de la Sociedad Entomológica Aragonesa 43:29–33.

Tourinho, A.L. & C.S. Azevedo. 2007. A new Amazonian *Cryptocellus* Westwood (Arachnida, Ricinulei). Zootaxa 1540:55–60.

Tourinho, A.L. & R. Saturnino. 2010. On the *Cryptocellus peckorum* and *Cryptocellus adisi* groups, and description of a new species of *Cryptocellus* from Brazil (Arachnida: Ricinulei). Journal of Arachnology 38:425–432.

Tourinho, A.L., N.F. Lo Man-Hung & A.B. Bonaldo. 2010. A new species of Ricinulei of the genus *Cryptocellus* Westwood (Arachnida) from northern Brazil. Zootaxa 2684:63–68.

Tourinho, A.L., N.F. Lo Man-Hung & L. Salvatierra. 2014. A new Amazonian species of *Cryptocellus* (Arachnida, Ricinulei), with descriptions of its integumental structures and all free-living life stages. Zootaxa 3814:81–95.

Tuxen, S.L. 1974. The African genus *Ricinoides* (Arachnida, Ricinulei). Journal of Arachnology 1:85–106.

Valdez-Mondragón, A. & O.F. Francke. 2011. Four new species of the genus *Pseudocellus* (Arachnida: Ricinulei: Ricinoididae) from Mexico. Journal of Arachnology 39:365–377.

Valdez-Mondragón, A. & O.F. Francke. 2013. Two new species of ricinuleids of the genus *Pseudocellus* (Arachnida: Ricinulei: Ricinoididae) from southern Mexico. Zootaxa 3635:545–556.

Westwood, J.O. 1874. Thesaurus Entomologicus Oxoniensis. Clarendon Press, Oxford, United Kingdom.

Wunderlich, J. 2012. Description of the first fossil Ricinulei in amber from Burma (Myanmar), the first report of this arachnid order from the Mesozoic and from Asia, with notes on the related extinct order Trigonotarbida. Pp. 233–244. *In* Beiträge zur Araneologie 7: Fifteen papers on extant and fossil spiders (Araneae). (J. Wunderlich (ed.)). Joerg Wunderlich, Hirschberg, Germany.

Wunderlich, J. 2015. New and rare fossil Arachnida in Cretaceous Burmese amber (Amblypygi, Ricinulei and Uropygi: Thelephonida). Pp. 409–436. *In* Beiträge zur Araneologie 9: Spinnen des erdmittelalters. (J. Wunderlich (ed.)). Joerg Wunderlich, Hirschberg, Germany.

Wunderlich, J. 2017. New extinct taxa of the arachnid order Ricinulei, based on new fossils preserved in Mid Cretaceous Burmese amber. Pp. 48–71. *In* Beiträge zur Araneologie 10: Spinnen des erdmittelalters. (J. Wunderlich (ed.)). Joerg Wunderlich, Hirschberg, Germany.

Manuscript received 20 July 2017, revised 20 October 2017.

2018. Journal of Arachnology 46:133–154

Systematics of the spiny trapdoor spiders of the genus *Eucanippe* (Mygalomorphae: Idiopidae: Aganippini) from south-western Australia: documenting a poorly-known lineage from Australia's biodiversity hotspot

Michael G. Rix[1,2,3], **Barbara Y. Main**[4], **Robert J. Raven**[1] and **Mark S. Harvey**[3,4,5]: [1]Biodiversity and Geosciences Program, Queensland Museum, South Brisbane, Queensland 4101, Australia. E-mail: michael.rix@qm.qld.gov.au; [2]Australian Centre for Evolutionary Biology and Department of Ecology and Evolutionary Biology, School of Biological Sciences, The University of Adelaide, Adelaide, South Australia 5005, Australia; [3]Department of Terrestrial Zoology, Western Australian Museum, Welshpool, Western Australia 6106, Australia; [4]School of Biological Sciences, The University of Western Australia, Crawley, Western Australia 6009, Australia; [5]School of Natural Sciences, Edith Cowan University, Joondalup, Western Australia 6027, Australia

Abstract. The aganippine spiny trapdoor spiders of the genus *Eucanippe* Rix, Main, Raven & Harvey, 2017 are revised, and six new species from south-western Australia's biodiversity hotspot are described: *E. absita* sp. nov., *E. agastachys* sp. nov., *E. eucla* sp. nov., *E. mallee* sp. nov., *E. mouldsi* sp. nov., and *E. nemestrina* sp. nov. Species of *Eucanippe* are among the most enigmatic of Australia's Mygalomorphae, with most taxa known only from pitfall-trapped male specimens. Little is known of their biology, natural history or burrow morphology, and a female specimen was unknown prior to targeted field work in 2017. This revision documents the known diversity of *Eucanippe* in Australia, and reveals a fauna dominated by species with restricted and largely non-overlapping distributions in the heavily-cleared agricultural zone of Australia's south-west.

Keywords: Taxonomy, new species, arid zone, biogeography

ZooBank publication: http://zoobank.org/?lsid=urn:lsid:zoobank.org:pub:277920E5-CB4C-4EDC-9483-57476BA84100

The spiny trapdoor spiders of the Western Australian endemic genus *Eucanippe* Rix, Main, Raven & Harvey, 2017 (Figs. 1–4) are among the most enigmatic of Australia's Mygalomorphae. The genus was only recently formally described (Rix et al. 2017d) following its phylogenetic delimitation by Rix et al. (2017b), and a female specimen (Fig. 3) was unknown prior to targeted field work in 2017. Males were also rare in collections prior to the 'Salinity Action Plan Survey' (later 'State Salinity Strategy') of the Western Australian agricultural zone, conducted by the then Department of Conservation and Land Management (CALM) between 1997 and 2000 (Harvey et al. 2004; Keighery 2004). This ground-breaking survey of much of the threatened south-western Australian biodiversity hotspot (see Myers et al. 2000; Rix et al. 2015) was a whole of Government approach to combating the devastating effects of dryland salinity on the heavily fragmented habitats of the region (Keighery 2004). Due to the scale of the survey, both geographically and temporally, and the use of wet pitfall traps at over 300 sampling sites, the distribution and diversity of *Eucanippe* (and numerous other mygalomorph genera) were revealed in considerable detail.

We now know that species of *Eucanippe* are largely restricted to the Mallee, central and southern Wheatbelt and Esperance Plains IBRA (Interim Biogeographic Regionalisation of Australia) bioregions, with only a limited number of records from the Murchison, Coolgardie, Hampton and Jarrah Forest bioregions (Fig. 11). This distribution is thus centered on one of the most heavily-cleared landscapes in Australia (Laurance et al. 2011; Bradshaw 2012), and extant populations of most species are now severely fragmented. Given the declines being experienced by idiopid populations across arid and semi-arid temperate Australia (Rix et al. 2017c), the documentation of this diversity is an urgent undertaking. This paper is now the third in a series of revisionary works to describe the region's known species of *Eucanippe*, *Bungulla* Rix, Main, Raven & Harvey, 2017 (see Rix et al. 2017d), *Cataxia* Rainbow, 1914 (see Rix et al. 2017a), *Eucyrtops* Pocock, 1897, *Euoplos* Rainbow, 1914, *Gaius* Rainbow, 1914 and *Idiosoma* Ausserer, 1871 (see Rix et al. 2017d). Six new species are here described, taking the total number of species in the genus to seven.

METHODS

Morphological methods, including the format of species descriptions, follow Rix et al. (2017d). Specimens were examined using a Zeiss Stemi SV11 stereomicroscope, and female genitalia were cleared in 100% lactic acid at room temperature. Measurements (in millimeters, to one decimal place) and digital automontage images were taken using a Leica M165C stereomicroscope with mounted DFC425 digital camera, and processed using Leica Application Suite Version 3.7 software. Species are presented in this paper in alphabetical order (following the generic type species), and leg segments were measured along the dorsal prolateral edge, in prolateral view. Total body length measurements include the chelicerae, in dorsal view. Most available male specimens of *Eucanippe* were illustrated for this study, either within the primary numbered plates or, for additional (non-holotype) specimens, as an 'Atlas' series of more rapidly assembled single-shot images in four standard views (see Supplementary

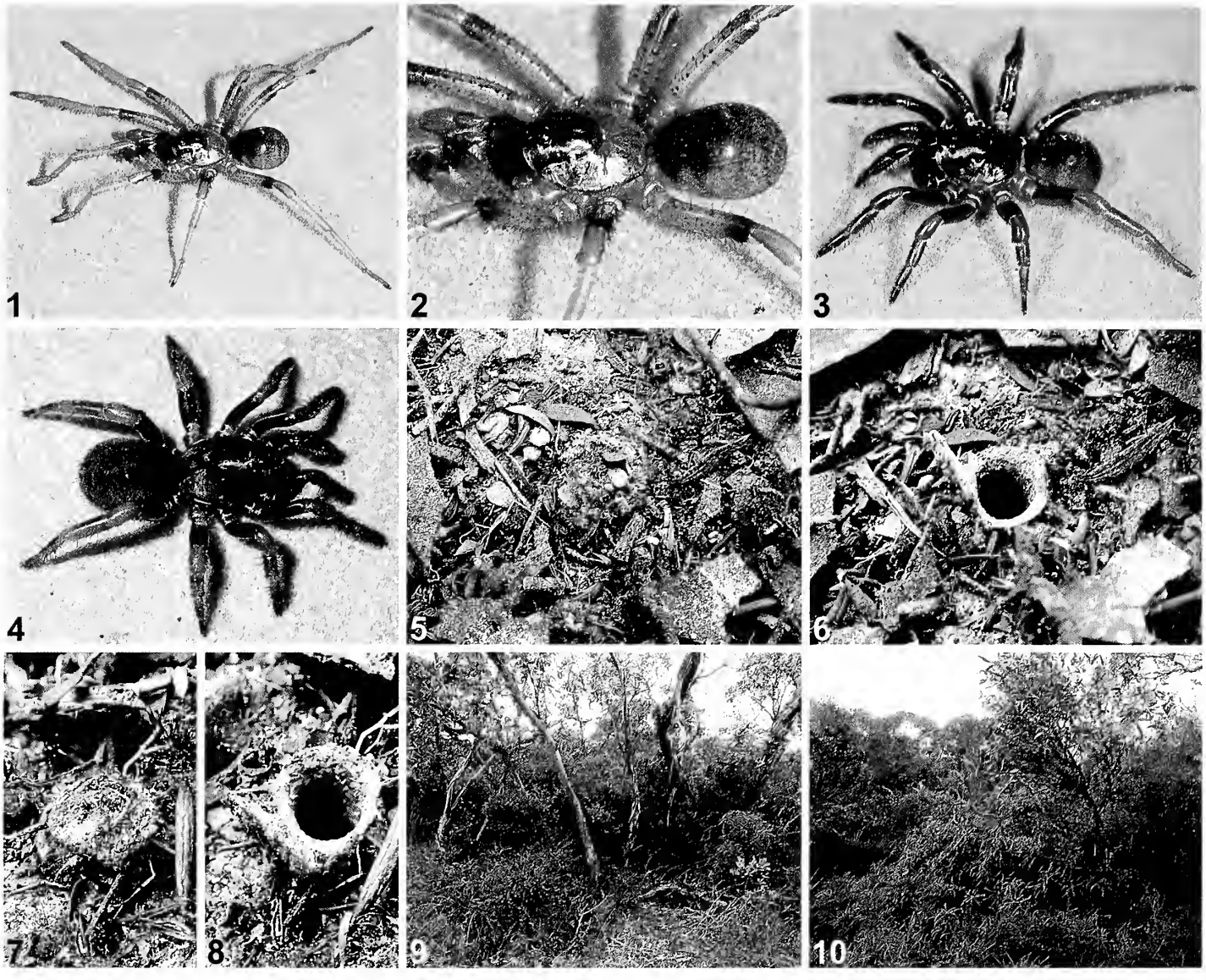

Figures 1–10.—Live habitus images, burrows and habitats of *Eucanippe* from south-western Australia. 1–3, 5–10, *E. mouldsi* sp. nov. from near Wellstead: 1–2, paratype male (WAM T132002) habitus; 3, paratype female (WAM T143003) habitus; 5–8, images of two burrows with lids open (5, 7) and closed (6, 8); 9–10, mallee eucalypt and *Banksia* woodland at the type locality (April 2017). 4, Habitus image of subadult (likely penultimate) female *E. agastachys* sp. nov. (WAM T143012) from Hopkins Nature Reserve, near Kulin. Note the sculptured, highly camouflaged lid, the slightly raised hinge and broad lower lip typical of burrows of *E. mouldsi* sp. nov. at the type locality. Images 1–3, 9 by M. Harvey; 4–8, 10 by M. Rix.

File 1, online at http://dx.doi.org/10.1636/JoA-S-17-030.s1). The latter are included for ease of comparison to the type specimens, to directly illustrate the subtle morphological variation in key characters typical of Mygalomorphae, and to provide a comprehensive digital compendium of the material available in collections. For records with multiple specimens per vial, in most cases only a single exemplar specimen was imaged.

Specimens are lodged at the Western Australian Museum, Perth (WAM), and the following abbreviations are used throughout the text: ALE, anterior lateral eye/s; AME, anterior median eye/s; IBRA, Interim Biogeographic Regionalisation of Australia Version 7 (online at https://www.environment.gov.au/land/nrs/science/ibra); PLE, posterior lateral eye/s; PME, posterior median eye/s; RTA, retrolateral tibial apophysis (of male pedipalp).

SYSTEMATICS

Family Idiopidae Simon, 1889
Subfamily Arbanitinae Simon, 1903
Tribe Aganippini Simon, 1903
Genus *Eucanippe* Rix, Main, Raven & Harvey, 2017

Eucanippe Rix, Main Raven & Harvey, 2017 in Rix et al., 2017d: 607.

Type species.—*Eucanippe bifida* Rix, Main, Raven & Harvey, 2017, by original designation.

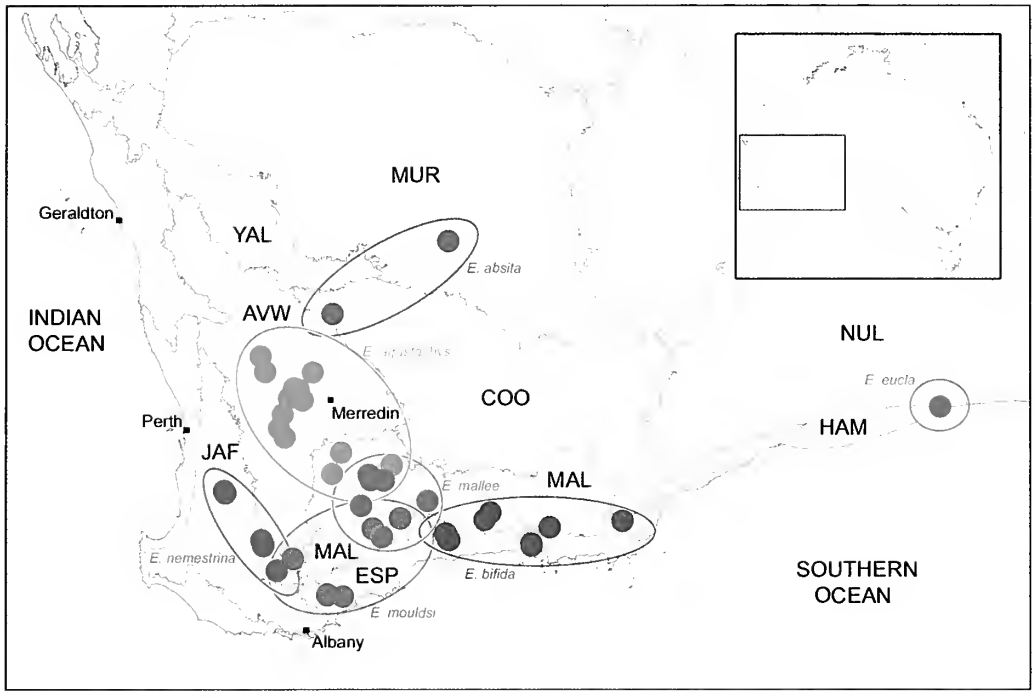

Figure 11.—Map showing collection records of *Eucanippe* from south-western Australia. Select metropolitan centers are labeled, and relevant IBRA 7.0 bioregional acronyms are as follows: AVW, Avon Wheatbelt; COO, Coolgardie; ESP, Esperance Plains; HAM, Hampton; JAF, Jarrah Forest; MAL, Mallee; MUR, Murchison; NUL, Nullarbor; YAL, Yalgoo.

Diagnosis.—Species of *Eucanippe* can be distinguished from all other Arbanitinae by the presence of a forked embolus on the male pedipalp (Fig. 12) (Rix et al. 2017d), and by the unusual aciniform morphology of the female spermathecae (at least in *E. mouldsi* sp. nov.; Fig. 107). They are also the only Idiopidae in Australia, other than *Idiosoma*, to possess a pair of sclerotized sigilla on the dorsal abdomen (Figs. 2–4, 27, 40, 87, 100).

Description.—See Rix et al. (2017d). For a description of the only known adult female specimen of this genus, see *E. mouldsi* sp. nov. (Figs. 99–107).

Distribution.—The genus *Eucanippe* is endemic to south-western Australia, with a distribution centered on the semi-arid Mallee, Esperance Plains and Wheatbelt bioregions (Fig. 11). Outside of these areas they extend marginally west into the south-eastern Jarrah Forest bioregion, east to the western Coolgardie and Hampton bioregions, and north-east to the southern Murchison bioregion. The greatest diversity of species occurs in the western Mallee bioregion, where the ranges of three species intersect (Fig. 11).

Composition and remarks.—*Eucanippe* was found to be the sister-genus to *Idiosoma* by Rix et al. (2017b) (Fig. 12), and together they share the synapomorphic presence of sclerotized dorsal abdominal sigilla (Figs. 2–4, 27, 40, 87, 100). *Eucanippe* includes seven species, six of which are newly described in this study. Specimens are rare in collections, and only a single adult female is known (Figs. 3, 99–107). Burrows of *E. mouldsi* sp. nov. are small and highly camouflaged, with a slightly raised hinge and broad lower lip (Figs. 5–8), and at the type locality these burrows are situated in dense mallee eucalypt and *Banksia* woodland (Figs. 9, 10). Little else is known of the biology or natural history of these spiders, other than that males wander in search of females in late autumn, winter (predominantly) or early spring, and a recently molted adult male of *E. mouldsi* sp. nov. (Figs. 1, 2) was collected from its burrow in mid-April.

KEY TO THE AUSTRALIAN SPECIES OF *EUCANIPPE* (MALES ONLY)

NB. Females of all species except *E. mouldsi* sp. nov. are unknown. See also Supplementary File 1 for additional images of relevant character states (online at http://dx.doi.org/10.1636/JoA-S-17-030.s1).

1. Tibia of leg I with pair of opposing prolateral clasping spurs (Figs. 20–22, 33–35) 2
– Tibia of leg I without pair of opposing prolateral clasping spurs (Figs. 68, 69) ..... ***E. eucla*** sp. nov.
2. RTA short and relatively rounded distally, without prominent distal process (Figs. 23, 24); proximal-most clasping spur on prolateral tibia I with 2–3 modified, similarly-sized setae (Figs. 20, 21) ... ***E. bifida*** Rix, Main, Raven & Harvey, 2017
– RTA longer, more strongly pointed distally and usually with prominent (often aspinose) distal process (Figs. 36, 49, 83, 96, 118); proximal-most clasping spur on prolateral tibia I with 1–3 modified setae (Figs. 34, 47, 81, 94, 116) 3
3. RTA of intermediate length, with only a short distal process (Figs. 83, 84); proximal-most clasping spur on prolateral tibia I with just one enlarged spur-like seta (Figs. 80, 81) (if >1 seta rarely present, spur-like seta remains the largest) ..... ***E. mallee*** sp. nov.

– RTA longer, with large and pointed (usually aspinose) distal process (Figs. 36, 49, 96, 118); proximal-most clasping spur on prolateral tibia I with 1–3 modified setae (Figs. 34, 47, 94, 116) 4

4. Body size relatively small (carapace length < 3.5; Fig. 26); abdomen ornate, with prominent bi-colored pattern (Fig. 27); RTA with slightly curved aspinose distal process and dense, triangular-shaped field of spinules in retrolateral view (Fig. 36) ..... ***E. absita*** sp. nov.

– Body size usually larger; RTA with porrect distal process in retrolateral view (Figs. 49, 96, 118) 5

5. Palpal tibia relatively stout in lateral profile (ca. 1.8 x longer than wide), with proximal mid-point of RTA-base projecting from lower half of tibia (Fig. 49); RTA directed relatively anteriorly, with ventral edge only marginally angled away from ventral face of proximal tibia in retrolateral view (Fig. 49) ..... ***E. agastachys*** sp. nov.

– Palpal tibia less stout in lateral profile (ca. 2.0 x longer than wide), with basal mid-point of RTA projecting from near middle of tibia (Figs. 96, 118); RTA directed away from ventral face of tibia in more strongly oblique ventral orientation (Figs. 96, 118) 6

6. Cephalic region of the carapace and abdomen heavily pigmented (Figs. 86, 87); stiff, porrect black setae on dorsal abdomen with large, strongly-sclerotized sclerotic bases (Fig. 87) ..... ***E. mouldsi*** sp. nov.

– Carapace and abdomen paler (Figs. 108, 109); sclerotic bases of stiff, porrect abdominal setae slightly smaller and less heavily sclerotized (Fig. 109) ..... ***E. nemestrina*** sp. nov.

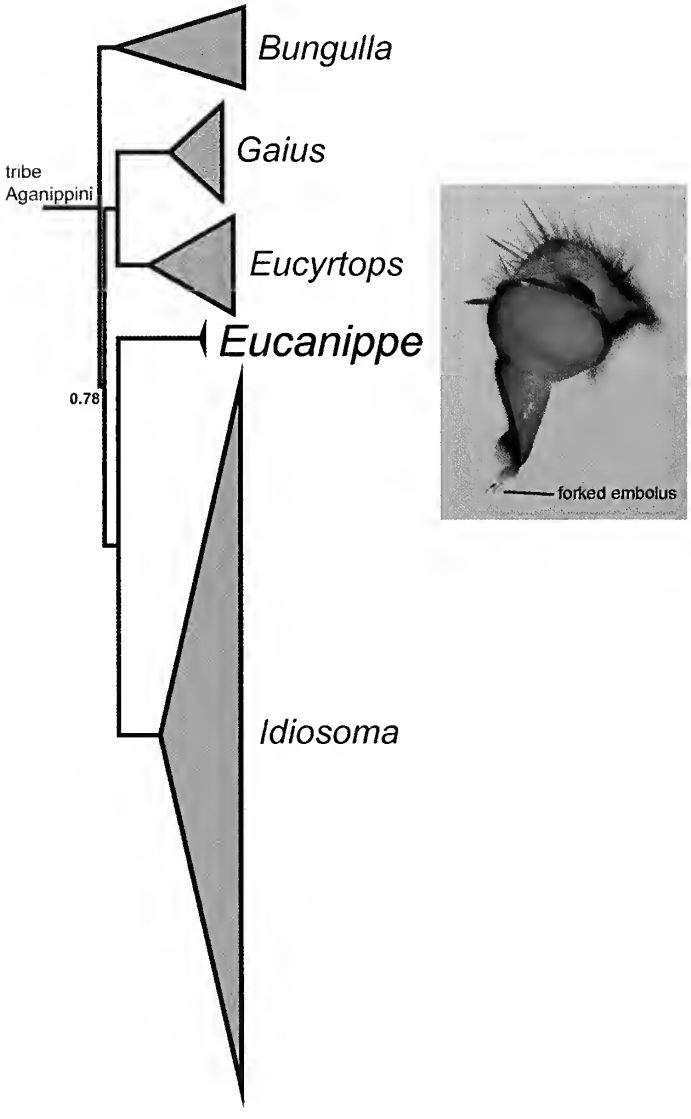

Figure 12.—Summary phylogeny of the tribe Aganippini, from the 'FULL' 12-gene Bayesian analysis of Rix et al. (2017a). Note the sister-group relationship between the genera *Eucanippe* and *Idiosoma*. Inset image shows the pro-distal cymbium and bulb of *E. absita* sp. nov., and the distinctive, finely-forked embolus characteristic of all *Eucanippe*.

Eucanippe bifida Rix, Main, Raven & Harvey, 2017
(Figs. 11, 13–25)

Eucanippe bifida Rix, Main Raven & Harvey, 2017 in Rix et al., 2017d: 609, figs. 180, 191–204.

Type material.—*Holotype male*. AUSTRALIA: *Western Australia*: 24.3 km E. of Ravensthorpe, site RNOCTS1 (IBRA_ESP), 33°34′45″S, 120°18′37″E, dry pitfall, 26 August 2005, R. Teale, Z. Hamilton (WAM T72649; examined).

Paratypes. AUSTRALIA: *Western Australia*: 1 ♂, 25.5 km E. of Ravensthorpe, site RNOCTS3 (IBRA_ESP), 33°34′06″S, 120°19′11″E, dry pitfall, 25 August 2005, R. Teale, Z. Hamilton (WAM T72656); 1 ♂, same data (WAM T72657); 1 ♂, same data (WAM T72655); 1 ♂, same data (WAM T72658); 1 ♂, same data (WAM T72654).

Other material examined.—AUSTRALIA: *Western Australia*: 1 ♂, Western Australia: 25.5 km E. of Ravensthorpe, site RNOCTS3 (IBRA_ESP), 33°34′06″S, 120°19′11″E, dry pitfall, 24 August 2005, R. Teale, Z. Hamilton (WAM T72659); 1 ♂, same data except 26 August 2005 (WAM T72653); 1 ♂, same data (WAM T72660); 1 ♂, same data except 24.4 km E. of Ravensthorpe, site RNOCTS2, 33°34′22″S, 120°18′28″E, 25 August 2005 (WAM T72650); 1 ♂, same data (WAM T72651); 1 ♂, same data except 24.6 km E. of Ravensthorpe, site RNOCTS1, 33°34′45″S, 120°18′37″E, 26 August 2005 (WAM T72669); 1 ♂, same data except 30.1 km SE. of Ravensthorpe, site CMS4, 33°39′30″S, 120°21′30″E, 26 August 2005 (WAM T72671); 1 ♂, same data except ca. 37 km SE. of Ravensthorpe, site CMS2, 33°39′46″S, 120°22′40″E, 23–28 August 2005 (WAM T72670); 1 ♂, N. of Edwards Rd, SE. of Lake King, site GP 2 (IBRA_MAL), 33°22′01″S, 120°59′43″E, wet pitfalls, 15 October 1999–1 November 2000, P. Van Heurck, CALM Survey (WAM T139585); 1 ♂, same data (WAM T139586); 1 ♂, Junana Rock, Cape Arid National Park, NW. of Mount Ragged, site 3 (IBRA_MAL), 33°23′S, 123°24′E, 5 April–23 May 1986, B.Y. Main (WAM T139584); 1 ♂, Lake Morgan, Helms Arboretum Reserve, site ES 3 (IBRA_ESP), 33°43′09″S, 121°48′29″E, 15 October 1999–1 November 2000, P. Van Heurck, CALM Survey (WAM T139588); 1 ♂, Norwoods Rd, Wittenoom Hill Nature Reserve, site ES 7 (IBRA_MAL), 33°28′29″S, 122°07′17″E, wet pitfalls, 15 October 1999–1 November 2000, B. Durrant,

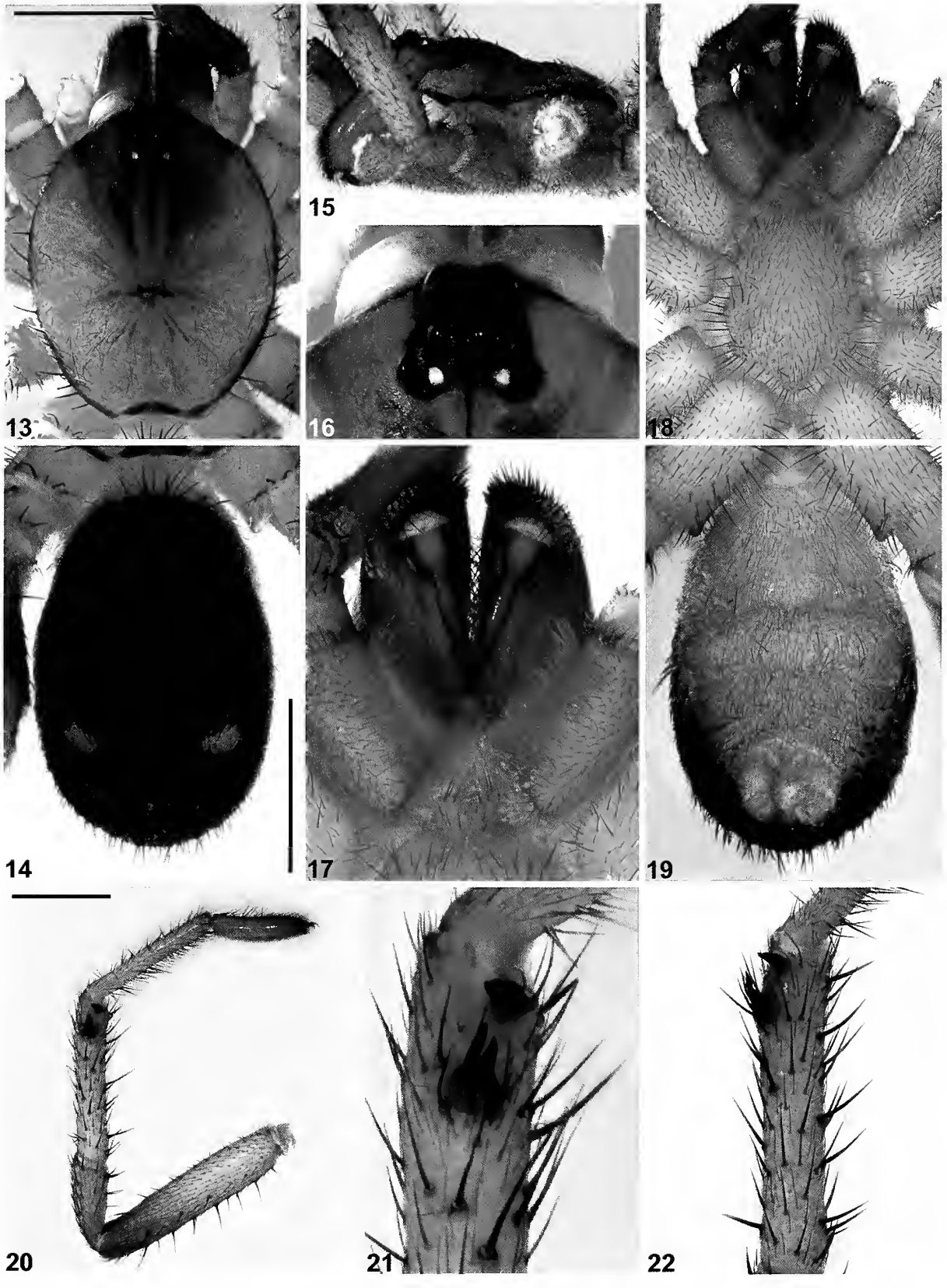

Figures 13–22.—*Eucanippe bifida* Rix, Main, Raven & Harvey, 2017, male holotype (WAM T72649) from E. of Ravensthorpe (Western Australia; ESP), somatic morphology: 13–14, carapace and abdomen, dorsal view; 15, cephalothorax, lateral view; 16, eyes, dorsal view; 17, mouthparts, ventral view; 18–19, cephalothorax and abdomen, ventral view; 20, leg I, prolateral view; 21, leg I tibia, clasping spurs, prolateral view; 22, leg I tibia, pro-ventral view. Scale bars = 2.0.

Figures 23–25.—*Eucanippe bifida* Rix, Main, Raven & Harvey, 2017, male holotype (WAM T72649) from E. of Ravensthorpe (Western Australia; ESP), pedipalp: 23, retrolateral view; 24, retro-ventral view; 25, prolateral view. Scale bar = 2.0.

CALM Survey (WAM T143013); 1 ♂, same data (WAM T143014); 1 ♂, Shark Lake Rd, Helms Arboretum Reserve, site ES 1 (IBRA_ESP), 33°44′49″S, 121°48′55″E, wet pitfalls, 15 October 1999–1 November 2000, P. Van Heurck, CALM Survey (WAM T139587); 1 ♂, same data (WAM T139590); 1 ♂, N. of Rollond Rd, near junction with Neds Corner Rd, site GP 3 (IBRA_MAL), 33°15′28″S, 121°05′47″E, wet pitfalls, 15 October 1999–1 November 2000, P. Van Heurck, CALM Survey (WAM T139589).

Diagnosis.—Males of *Eucanippe bifida* can be distinguished from all other known congeners by the shape of the RTA, which is short and relatively rounded distally, without a prominent distal process (Figs. 23, 24; cf. Figs. 36, 49, 70, 83, 96, 118). This species can be further distinguished from the similar species *E. mallee* sp. nov. by the presence of 2 (or rarely 3) modified prolateral setae on the proximal-most leg 1 clasping spur, each of a similar size and usually with a relatively straight profile in prolateral view (Figs. 20, 21; cf. Figs. 80, 81).

Description (male holotype).—See Rix et al. (2017d).

Distribution and remarks.—*Eucanippe bifida* has a relatively restricted distribution in the Esperance Plains and south-eastern Mallee bioregions of south-western Australia, from the Ravensthorpe Range east to Cape Arid National Park (Rix et al. 2017d) (Fig. 11). The Cape Arid (Junana Rock) specimen is tentatively assigned to this species, on the basis of its short RTA, however the distribution of RTA spinules is unlike all other specimens of *E. bifida* (see Supplementary File 1, online at http://dx.doi.org/10.1636/JoA-S-17-030.s1). Thus, while it is possible that the Cape Arid record is another undescribed species, we refrain from separating it here until additional specimens or sequence data become available. Nothing is known of the biology of this species, other than that the known male specimens were collected wandering in search of females in late autumn and winter. Females are unknown.

Eucanippe absita sp. nov.
http://zoobank.org/?lsid=urn:lsid:zoobank.org:act:FA1DCBBB-9ADC-4683-8B11-77A0F60C58EE
(Figs. 11, 12, 26–38)

Eucanippe sp. 'Mount Mason' Rix et al., 2017d: 608, figs. 176, 177, 181, 185, 186.

Type material.—*Holotype male.* AUSTRALIA: *Western Australia*: Mt Mason, 100 km WSW. of Leonora, site MM-1-1J (IBRA_MUR), 29°06′56.4″S, 120°21′40.8″E, pitfall trap, 29 July 2008, M. Quinn, G. Murray (WAM T110226).

Other material examined.—AUSTRALIA: *Western Australia*: 1 ♂, Vermin Proof Fence, E. of Beacon, site BE 2 (IBRA_COO), 30°14′17″S, 118°20′09″E, wet pitfalls, 15 September 1998–25 October 1999, P. Van Heurck, CALM Survey (WAM T143015).

Etymology.—The specific epithet is derived from the Latin 'absitus' (adjective: 'distant', 'apart' or 'remote'; see Brown 1956), in reference to the disjunct distribution of this species in the remote Coolgardie and Murchison bioregions.

Diagnosis.—Males of *Eucanippe absita* sp. nov. can be distinguished from all other known congeners by the ornate and markedly bi-colored abdominal pattern (Fig. 27; cf. Figs. 14, 40, 62, 74, 87, 109); combined with the shape of the RTA, which has a slightly curved aspinose distal process and a dense, triangular-shaped field of spinules in retrolateral view (Fig. 36; cf. Figs. 23, 49, 70, 83, 96, 118). *Eucanippe absita* sp.

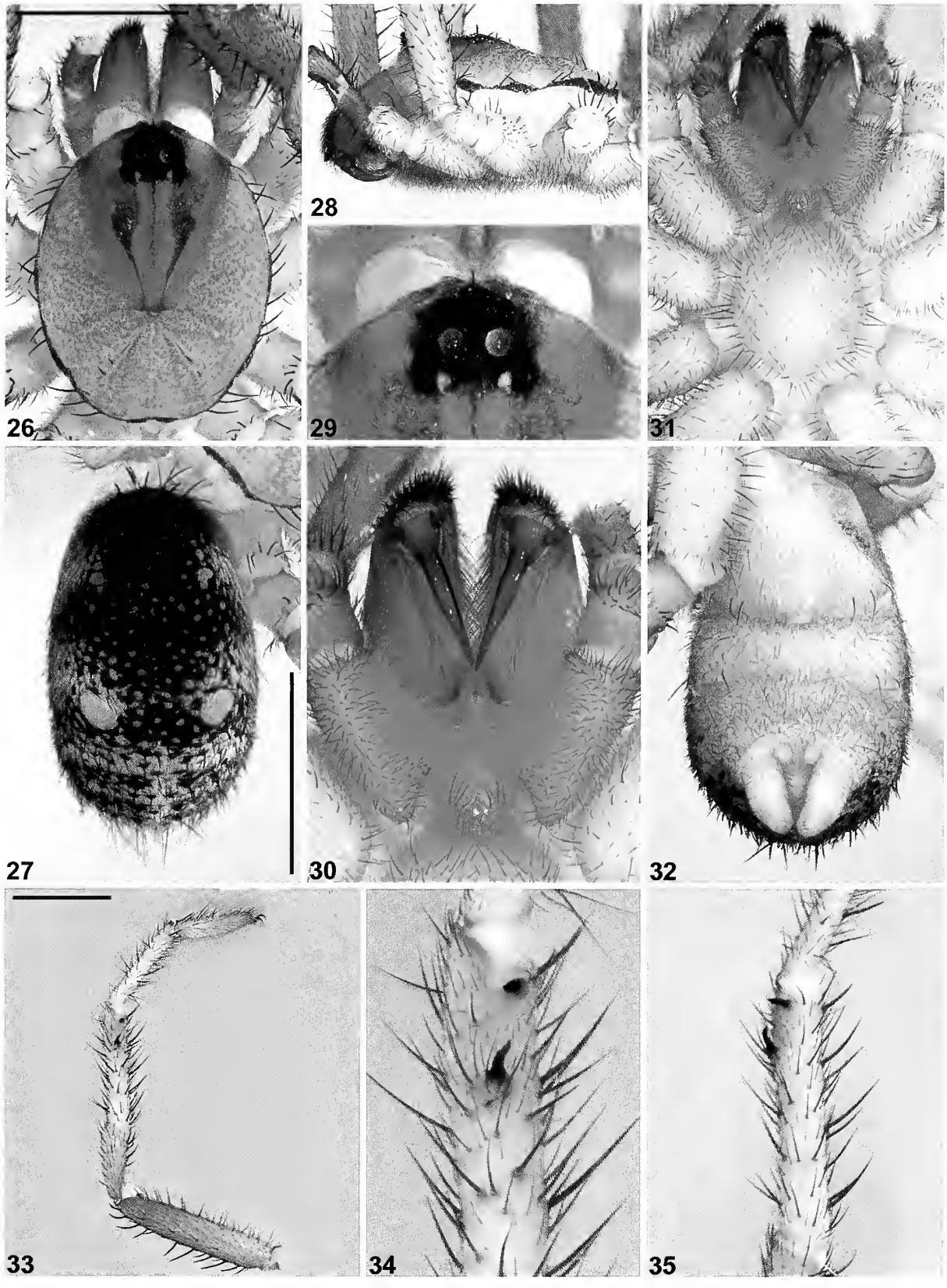

Figures 26–35.—*Eucanippe absita* sp. nov., male holotype (WAM T110226) from Mount Mason (Western Australia: MUR), somatic morphology: 26–27, carapace and abdomen, dorsal view; 28, cephalothorax, lateral view; 29, eyes, dorsal view; 30, mouthparts, ventral view; 31–32, cephalothorax and abdomen, ventral view; 33, leg I, prolateral view; 34, leg I tibia, clasping spurs, prolateral view; 35, leg I tibia, pro-ventral view. Scale bars = 2.0.

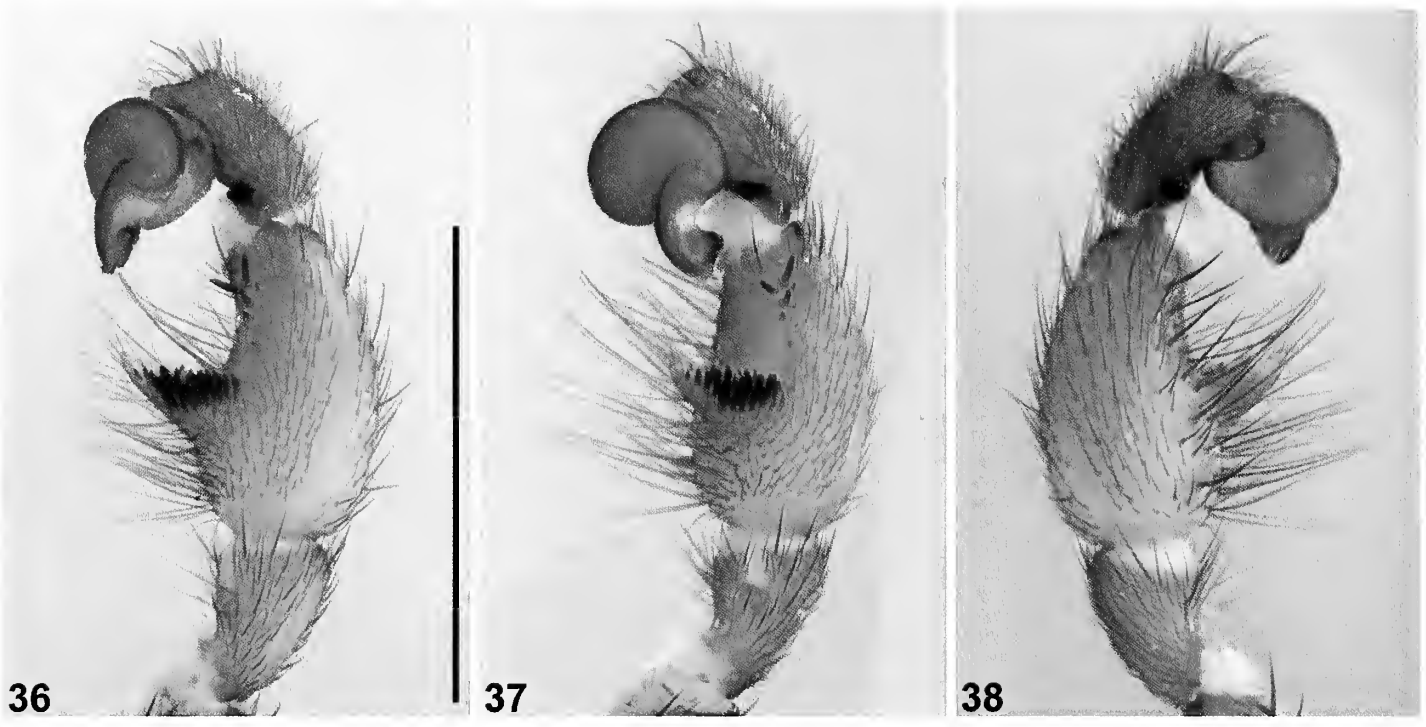

Figures 36–38.—*Eucanippe absita* sp. nov., male holotype (WAM T110226) from Mount Mason (Western Australia; MUR), pedipalp: 36, retrolateral view; 37, retro-ventral view; 38, prolateral view. Scale bar = 2.0.

nov. is the smallest known species of *Eucanippe*, with a male carapace length of < 3.5 (Fig. 26).

Description (male holotype).—Total length 7.9. Carapace 3.4 long, 2.7 wide. Abdomen 3.4 long, 2.1 wide. Carapace (Fig. 26) mottled tan, with darker pars cephalica, black ocular region, dark brown lyre-like pattern on pars cephalica and black rim; lateral margins with sparse, irregularly-spaced fringe of porrect black setae; fovea slightly procurved. Eye group (Fig. 29) trapezoidal (anterior eye row strongly procurved), 0.9 x as long as wide, PLE–PLE/ALE–ALE ratio 1.7; ALE almost contiguous, angled antero-laterally; AME separated by slightly less than half their own diameter; PME separated by ca. 3.0 x their own diameter; PME and PLE separated by diameter of PME, PME positioned in line with level of PLE. Maxillae with field of cuspules confined to inner corner (Fig. 30); labium without cuspules. Abdomen (Figs. 27, 32) oval, dark grey-brown in dorsal view with beige-tan mottling, two pairs of prominent beige-tan sigilla spots, beige dorso-lateral markings adjacent to sigilla pairs 1 and 2, and thick beige banding posteriorly. Dorsal surface of abdomen (Fig. 27) covered with stiff, porrect black setae, each with slightly raised, dark brown sclerotic base, the latter largest medially; single pair of large, lightly sclerotized oval sigilla present (sigilla pair 2), separated by nearly 3.0 x their own width. Legs (Figs. 33–35) variable shades of pale tan, with light scopulae on tarsi I–II; tibia I bearing small prolateral clasping spurs; proximal-most clasping spur with single, spur-like macroseta. Leg I: femur 3.4; patella 1.6; tibia 2.4; metatarsus 2.1; tarsus 1.7; total 11.2. Leg I femur–tarsus/carapace length ratio 3.3. Pedipalpal tibia (Figs. 36–38) 1.8 x longer than wide; RTA relatively large, triangular in retro-lateral view, with slightly curved aspinose distal process and dense, triangular-shaped field of retrolateral spinules; tibia also with field of spinules extending along curved retroventral edge (distal to base of RTA), consisting of 2 large and 4 smaller spinules. Cymbium (Figs. 36–38) setose, with only a few long spinules anteriorly. Embolus (Figs. 12, 36–38) ca. 1.5 x length of bulb, sharply tapering distally, with broad twisted morphology, sub-distal flange and finely bifurcate tip; embolic apophysis absent.

Distribution and remarks.—*Eucanippe absita* (formerly known by WAM identification code 'MYG262') is known from only two widely separated locations in the arid inland of south-western Australia: at Mount Mason, in the southern Murchison bioregion; and 51 km north-east of Beacon, in the western Coolgardie bioregion (Fig. 11). The Beacon specimen is poorly preserved and highly discolored, and the pedipalp is damaged (see Supplementary File 1, online at http://dx.doi.org/10.1636/JoA-S-17-030.s1); this specimen is therefore tentatively assigned to the species based on its size, the shape of the RTA and the apparent coloration of the abdomen, on which the diagnostic pale lateral markings seem faintly visible. Nothing is known of the biology of this species, other than that the holotype male specimen was collected wandering in search of females in mid-winter. Females are unknown.

Eucanippe agastachys sp. nov.
http://zoobank.org/?lsid=urn:lsid:zoobank.org:act:C40E62C6-83A8-4760-B4FF-104D62E866FF
(Figs. 4, 11, 39–60)

Type material.—*Holotype male.* AUSTRALIA: *Western Australia*: Durokoppin Nature Reserve, NW. tip, Transect G100 (IBRA_AVW), 31°24′S, 117°45′E, pitfall trap, 23 June–4 August 1987, B.Y. Main (WAM T139546).

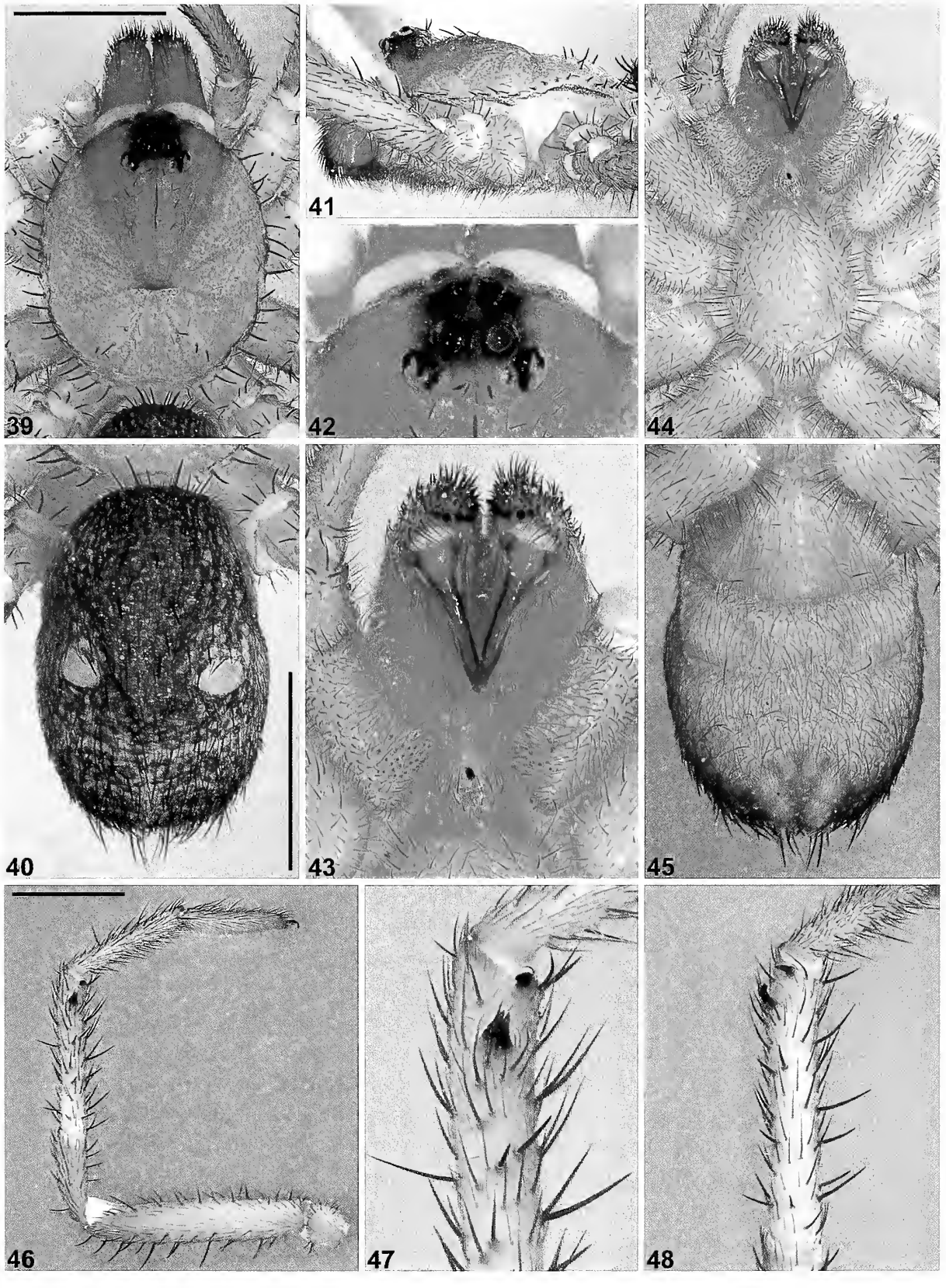

Figures 39–48.—*Eucanippe agastachys* sp. nov., male holotype (WAM T139546) from Durokoppin Nature Reserve (Western Australia; AVW), somatic morphology: 39–40, carapace and abdomen, dorsal view; 41, cephalothorax, lateral view; 42, eyes, dorsal view; 43, mouthparts, ventral view; 44–45, cephalothorax and abdomen, ventral view; 46, leg I, prolateral view; 47, leg I tibia, clasping spurs, prolateral view; 48, leg I tibia, pro-ventral view. Scale bars = 2.0.

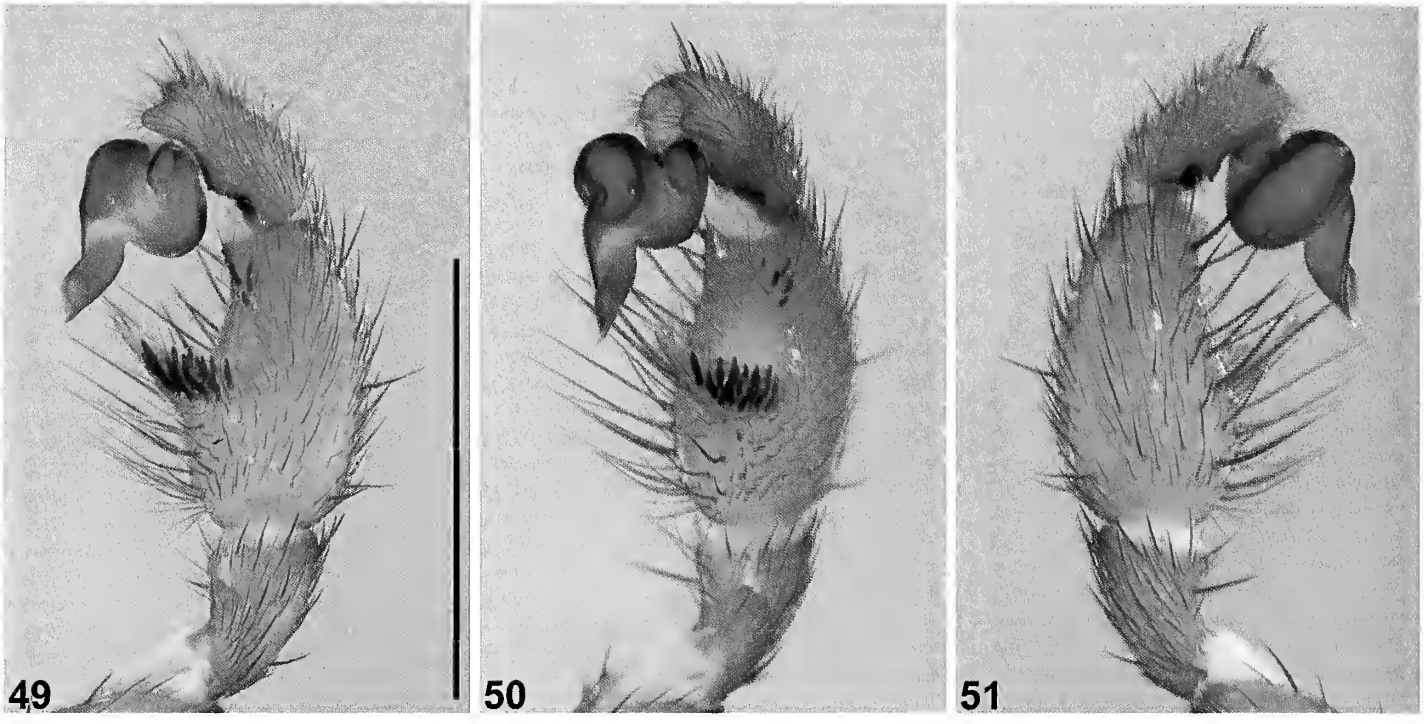

Figures 49–51.—*Eucanippe agastachys* sp. nov., male holotype (WAM T139546) from Durokoppin Nature Reserve (Western Australia: AVW), pedipalp: 49, retrolateral view; 50, retro-ventral view; 51, prolateral view. Scale bar = 2.0.

Paratypes. AUSTRALIA: *Western Australia*: 2 ♂, Durokoppin Nature Reserve, NW. tip, Transect D (IBRA_AVW), 31°24′S, 117°45′E, pitfall trap, 3 May–25 June 1988, B.Y. Main (WAM T139544); 1 ♂, same data exeept 20 July–11 August 1990 (WAM T139551); 2 ♂, same data except Transect E, 3 May–25 June 1988 (WAM T139545); 1 ♂, same data except 9 July–20 September 1989 (WAM T139547); 1 ♂, same data except 20 July–11 August 1990 (WAM T139549); 1 ♂, same data except 4 June–19 July 1990 (WAM T139550); 1 ♂, same data except Transect F (WAM T139543); 1 ♂, same data except Transect G (WAM T139548); 1 ♂, same data except Transect F100, 6–27 May 1987 (WAM T139542).

Other material examined.—AUSTRALIA: *Western Australia*: 1 ♂, Bendering Reserve Road, site KN 11 (IBRA_MAL), 32°21′27″S, 118°29′46″E, wet pitfalls, 30 October 1997–19 May 1998, P. Van Heurck, N. Guthrie, CALM Survey (WAM T143016); 1 ♂, ca. 16 km N. of Doodlakine, bushland remnant K46A NE. (IBRA_AVW), 31°34′S, 117°49′E, pitfall, July 1992, G. Smith et al. (WAM T57305); 1 ♂, East Yorkrakine Nature Reserve, EYR K2 (IBRA_AVW), 31°23′S, 117°40′E, wet pitfall traps, 15–25 September 1989, G. Friend et al. (WAM T44165); 1 ♂, Gardner Reserve Road, north, NE. of Quairading, site QU 3 (IBRA_AVW), 31°46′45″S, 117°28′22″E, wet pitfalls, 30 October 1997–27 May 1998, E. Ladhams, CALM Survey (WAM T139662); 1 ♂, same data (WAM T139664); 1 juvenile (subadult), Hopkins Nature Reserve, SE. of Kulin (IBRA_MAL), 32°43′15″S, 118°16′59″E, hand collected, litter brushing under shrub, 12 April 2017, M. Rix, M. Harvey, J. Cosgrove (WAM T143012); 1 ♂, Jilakin Lake, site KN 1 (IBRA_MAL), 32°40′29″S, 118°20′10″E, wet pitfalls, 30 October 1997–15 May 1998, L. King, CALM Survey (WAM T143017); 1 ♂, Kwelkan (IBRA_AVW), 31°08′21″S, 117°59′43″E, wet pitfall trap, 29 June–7 September 1999, B.Y. Main, J.M. Waldock (WAM T40014); 1 ♂, same data (WAM T39678); 1 ♂, Lake Hurlstone Nature Reserve, site HY 12 (IBRA_MAL), 32°32′32″S, 119°22′42″E, wet pitfalls, 30 October 1997–20 May 1998, P. Van Heurck, N. Guthrie, CALM Survey (WAM T143018); 1 ♂, same data (WAM T143019); 1 ♂, Manmanning Nature Reserve, NW., site WH 10 (IBRA_AVW), 30°53′32″S, 117°05′17″E, wet pitfalls, 15 September 1998–25 October 1999, P. Van Heurck, CALM Survey (WAM T139659); 1 ♂, W. of Minnivale (IBRA_AVW), 31°07′58″S, 117°10′13″E, wet pitfall trap, 21 May–16 September 1996, M.S. Harvey, J.M. Waldock (WAM T38503); 1 ♂, Mt Stirling Road, site QU 10 (IBRA_AVW), 31°59′27″S, 117°24′19″E, wet pitfalls, 30 October 1997–27 May 1998, P. Van Heurck, N. Guthrie, CALM Survey (WAM T139665); 1 ♂, same data (WAM T143020); 1 ♂, North Bungulla Nature Reserve (IBRA_AVW), 31°32′S, 117°35′E, pitfall trap, 22 June–1 August 1983, B.Y. Main (WAM T139658); 1 ♂, Wamenusking Nature Reserve, site QU 6 (IBRA_AVW), 32°07′34″S, 117°30′31″E, wet pitfalls, 26 May–5 October 1998, N. Guthrie, CALM Survey (WAM T143021).

Etymology.—The specific epithet is derived from the Greek 'agastachys' (adjective: 'rich in grain' or 'many ears of grain'; see Brown 1956), in reference to the distribution of this species in the Wheatbelt and north-western Mallee agricultural zones of south-western Australia.

Diagnosis.—Males of *Eucanippe agastachys* sp. nov. can be distinguished from all other known congeners by the combined presence of prolateral clasping spurs on tibia I (Figs. 46–48) (spurs absent in *E. eucla* sp. nov.; Fig. 69); by the presenee of a large RTA with a long and aspinose distal

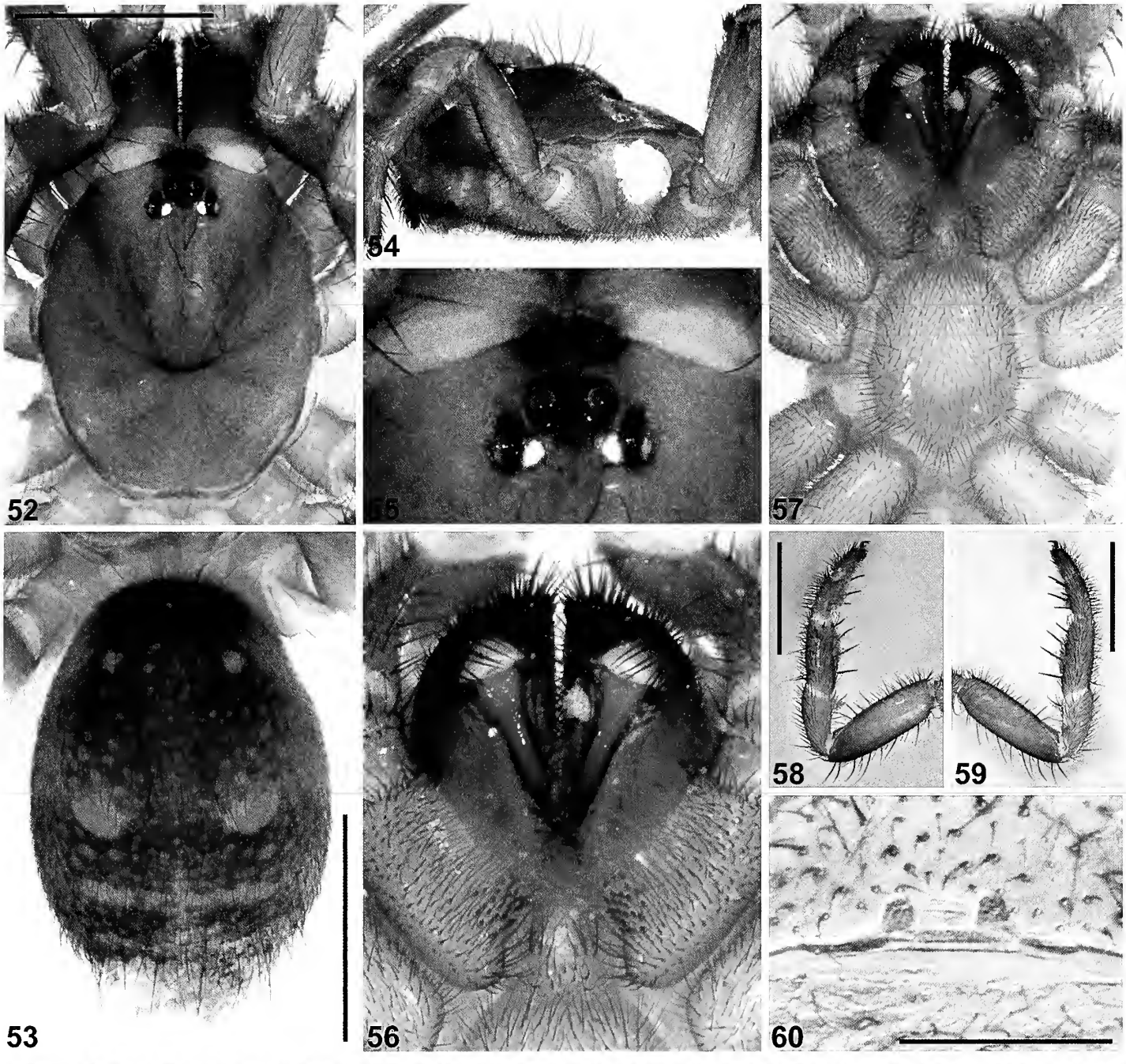

Figures 52–60.—*Eucanippe agastachys* sp. nov., subadult (likely penultimate) female (WAM T143012) from Hopkins Nature Reserve (Western Australia; MAL): 52–53, carapace and abdomen, dorsal view; 54, cephalothorax, lateral view; 55, eyes, dorsal view; 56, mouthparts, ventral view; 57, cephalothorax, ventral view; 58, leg 1, prolateral view; 59, leg 1, retrolateral view; 60, rudimentary spermathecae, dorsal view. Scale bars = 2.0 (52–53, 58–59), 0.5 (60).

process (Figs. 49, 50) (distal process smaller or absent in *E. bifida* and *E. mallee* sp. nov.; Figs. 23, 83); by the dorsal color pattern of the abdomen, which is not ornately patterned (Fig. 40) (abdomen markedly bi-colored in *E. absita*; Fig. 27); and by the position and shape of the RTA, the proximal mid-point of which projects from the lower half of the palpal tibia, and which is directed away from the ventral face of the tibia in a relatively anterior orientation (Fig. 49) (RTA directed more ventrally in *E. mouldsi* sp. nov. and *E. nemestrina* sp. nov.; Figs. 96, 118).

Description (male holotype).—Total length 8.1. Carapace 3.6 long, 3.0 wide. Abdomen 3.5 long, 2.3 wide. Carapace (Fig. 39) mottled tan, with darker pars cephalica, mostly black ocular region, faint brown lyre-like pattern on pars cephalica and grey-black rim; lateral margins with uniformly-spaced fringe of porrect black setae; fovea slightly procurved. Eye group (Fig. 42) trapezoidal (anterior eye row strongly procurved), 0.9 x as long as wide, PLE–PLE, ALE–ALE ratio 1.5; ALE contiguous, angled antero-laterally; AME separated by slightly less than half their own diameter; PME separated

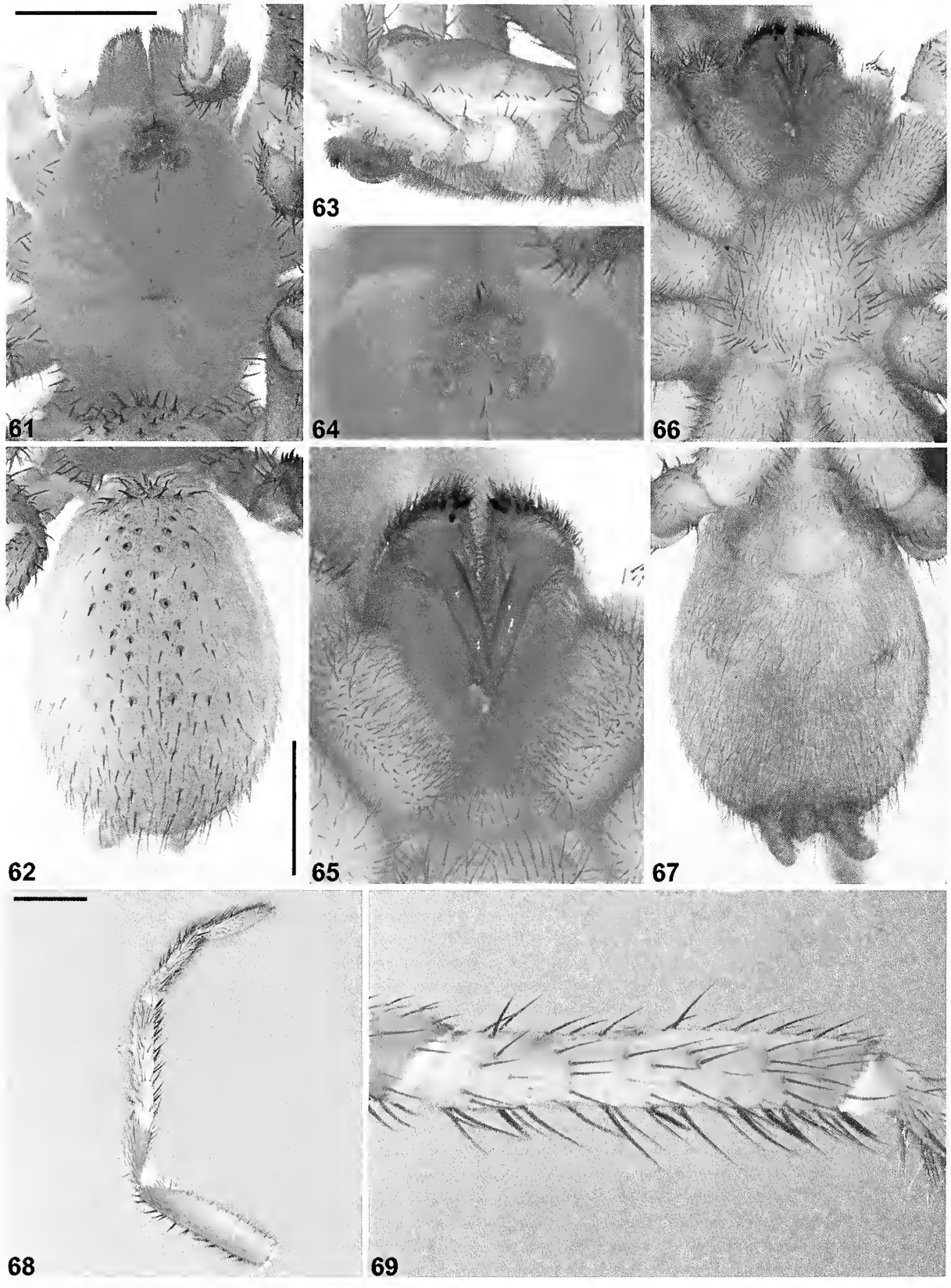

Figures 61–69.—*Eucampe cucla* sp. nov., male holotype (WAM T139649) from E. of Eucla (Western Australia; HAM), somatic morphology: 61–62, carapace and abdomen, dorsal view; 63, cephalothorax, lateral view; 64, eyes, dorsal view; 65, mouthparts, ventral view; 66–67, cephalothorax and abdomen, ventral view; 68, leg I, prolateral view; 69, leg I tibia, prolateral view. Scale bars = 2.0.

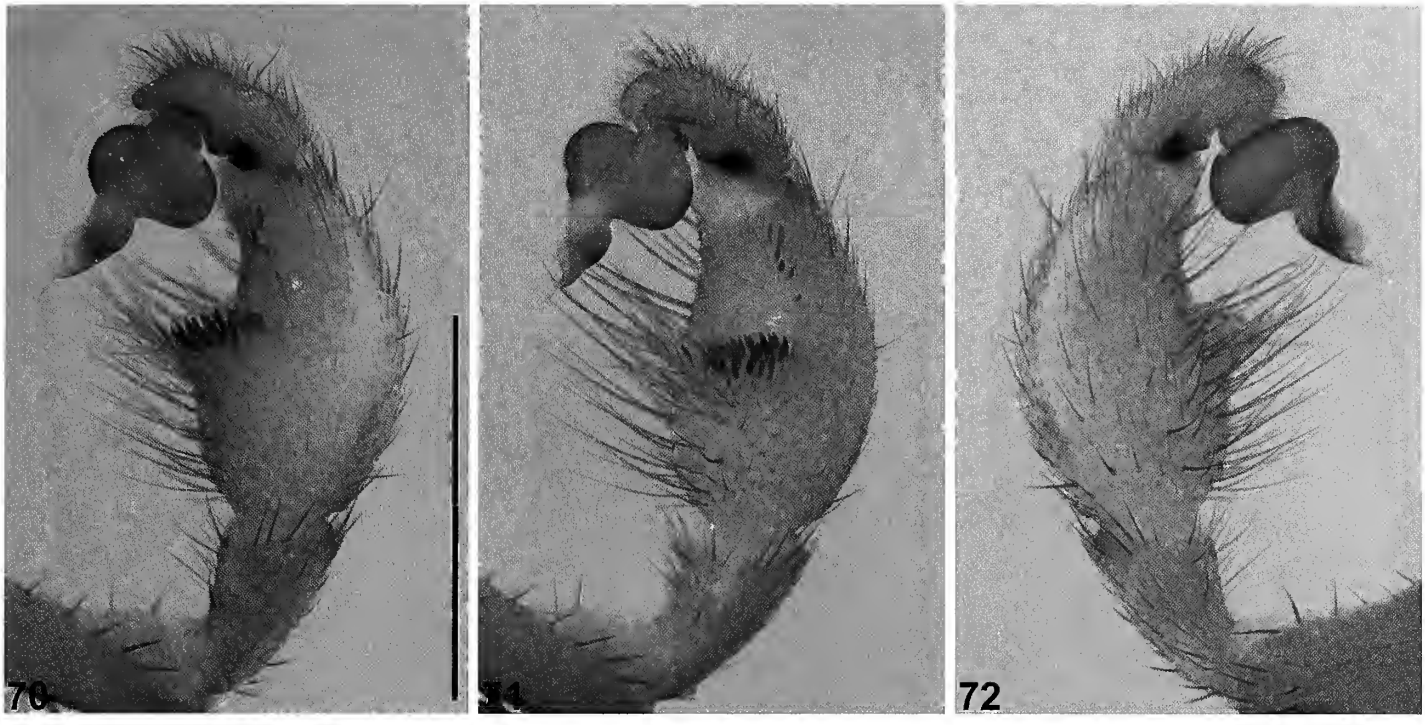

Figures 70–72.—*Eucanippe eucla* sp. nov., male holotype (WAM T139649) from E. of Eucla (Western Australia; HAM), pedipalp: 70, retrolateral view; 71, retro-ventral view; 72, prolateral view. Scale bar = 2.0.

by ca. 3.0 x their own diameter; PME and PLE separated by diameter of PME, PME positioned in line with level of PLE. Maxillae with field of cuspules confined to inner corner (Fig. 43); labium without cuspules. Abdomen (Figs. 40, 45) oval, grey-brown in dorsal view with tan mottling, pair of prominent beige-tan sigilla spots, and faint tan banding posteriorly. Dorsal surface of abdomen (Fig. 40) covered with stiff, porrect black setae, each with slightly raised, dark brown sclerotic base, the latter largest medially; single pair of large, lightly sclerotized oval sigilla present (sigilla pair 2), separated by nearly 3.0 x their own width. Legs (Figs. 46–48) variable shades of tan, with light scopulae on tarsi I–II; tibia I bearing small prolateral clasping spurs; proximal-most clasping spur with two similarly-sized macrosetae. Leg I: femur 3.9; patella 1.8; tibia 2.9; metatarsus 2.4; tarsus 1.8; total 12.7. Leg I femur–tarsus/carapace length ratio 3.5. Pedipalpal tibia (Figs. 49–51) 1.8 x longer than wide; RTA relatively large, acutely triangular in retrolateral view, with porrect aspinose distal process and sparse field of retrolateral spinules; tibia also with distal field of spinules along curved retroventral edge (distal to base of RTA), consisting of 4 large and 2 smaller spinules. Cymbium (Figs. 49–51) setose, with only a few long spinules anteriorly. Embolus (Figs. 49–51) ca. 1.5 x length of bulb, sharply tapering distally, with broad twisted morphology, sub-distal flange and finely bifurcate tip; embolic apophysis absent.

Distribution and remarks.—*Eucanippe agastachys* has a relatively restricted distribution in the central Wheatbelt and north-western Mallee bioregions of south-western Australia, from Manmanning Nature Reserve and Kwelkan in the north, south to Kulin and Lake Hurlstone (Fig. 11). At Hopkins Nature Reserve (near Kulin), a burrow of a single subadult (likely penultimate) specimen (Figs. 4, 52–60) – linked here based on distribution and color pattern – was revealed by brushing compact leaf litter under a low myrtaceous shrub in open sandy heathland. Little else is known of the biology of this species, other than that the known male specimens were collected wandering in search of females in late autumn, winter and early spring. Adult females are unknown, although the subadult female from near Kulin is illustrated here (Figs. 52–60) for comparative purposes.

Eucanippe eucla sp. nov.
http://zoobank.org/?lsid=urn:lsid:zoobank.org:act:5A72F843-C35C-4E3A-A4DF-FC0C9B8F968F
(Figs. 11, 61–72)

Type material.—*Holotype male*. AUSTRALIA: *Western Australia*: 5 km E. of Eucla, site 10 (IBRA_HAM), 31°40′S, 128°56′E, pitfall trap, 21 May 1986, B.Y. Main (WAM T139649).

Etymology.—The specific epithet is a noun in apposition, in reference to the type locality of this species near the town of Eucla.

Diagnosis.—Males of *Eucanippe eucla* sp. nov. can be distinguished from all other known congeners by the absence of prolateral clasping spurs on tibia I (Figs. 68, 69; cf. Figs. 21, 34, 47, 81, 94, 116).

Description (male holotype).—Total length 10.8. Carapace 4.4 long, 3.6 wide. Abdomen 5.3 long, 3.7 wide. Carapace (Fig. 61) very pale (faded) mottled tan, with darker pars cephalica and darker ocular region; lateral margins with uniformly-spaced fringe of porrect black setae; fovea slightly procurved. Eye group (Fig. 64) trapezoidal (anterior eye row strongly procurved), 0.9 x as long as wide, PLE–PLE/ALE–ALE ratio 1.8; ALE almost contiguous, angled antero-

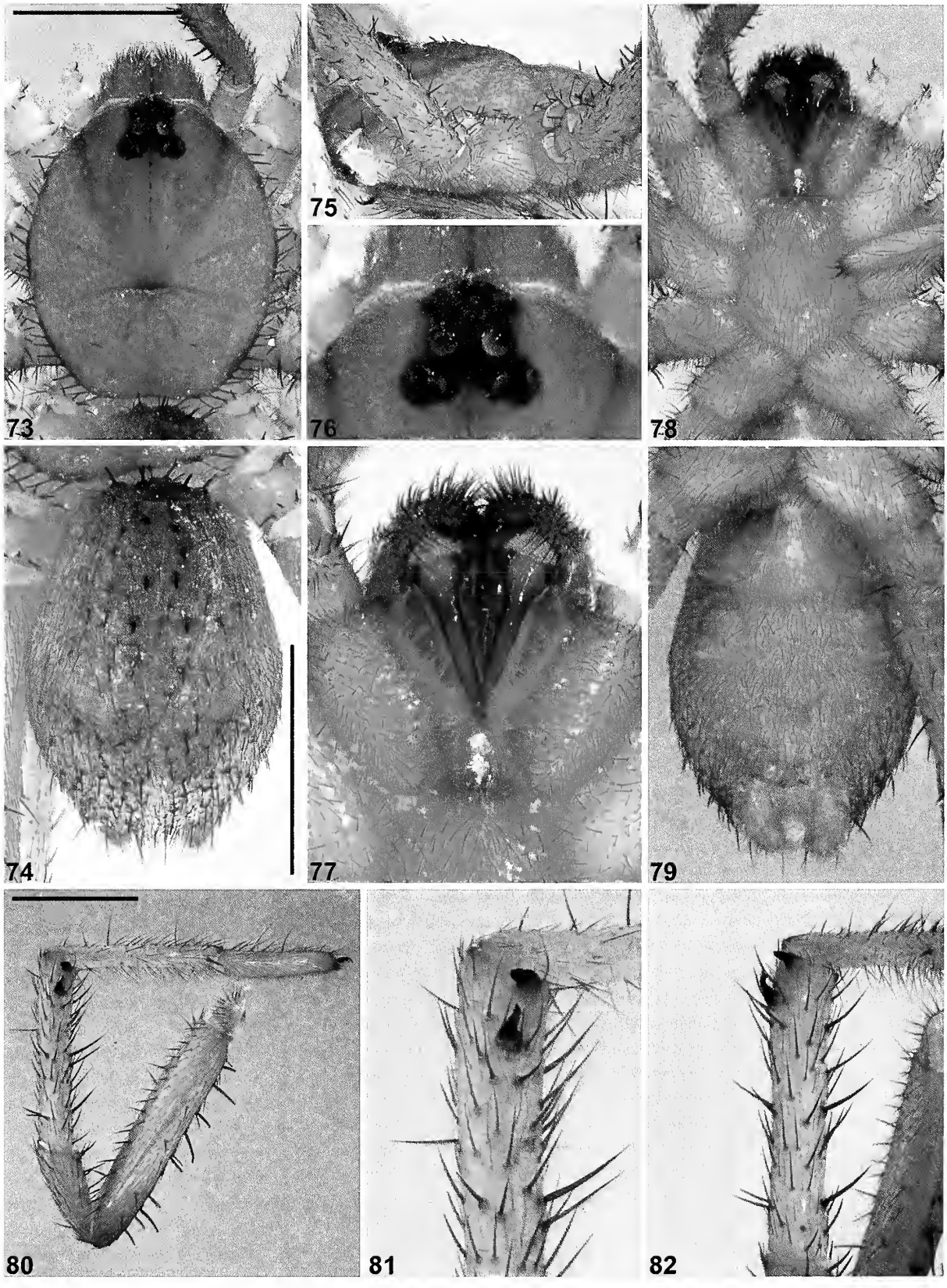

Figures 73–82.—*Eucanippe mallee* sp. nov., male holotype (WAM T143025) from north of Lake King-Norseman Rd (Western Australia: MAL), somatic morphology: 73–74, carapace and abdomen, dorsal view; 75, cephalothorax, lateral view; 76, eyes, dorsal view; 77, mouthparts, ventral view; 78–79, cephalothorax and abdomen, ventral view; 80, leg I, prolateral view; 81, leg I tibia, clasping spurs, prolateral view; 82, leg I tibia, pro-ventral view. Scale bars = 2.0.

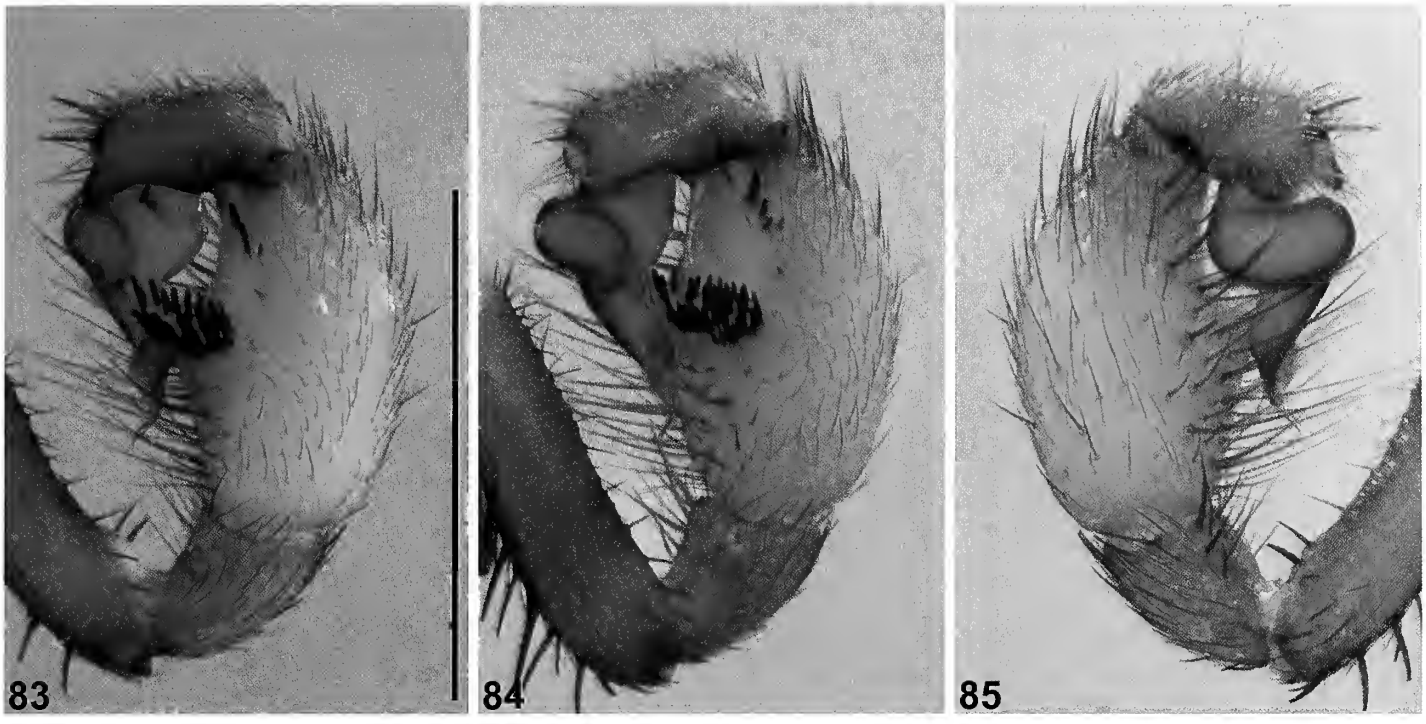

Figures 83–85.—*Eucanippe mallee* sp. nov., male holotype (WAM T143025) from north of Lake King-Norseman Rd (Western Australia: MAL), pedipalp: 83, retrolateral view; 84, retro-ventral view; 85, prolateral view. Scale bar = 2.0.

laterally; AME separated by slightly less than half their own diameter; PME separated by slightly more than 3.0 x their own diameter; PME and PLE separated by diameter of PME, PME positioned slightly posterior to level of PLE. Maxillae with field of cuspules confined to inner corner (Fig. 65); labium without cuspules. Abdomen (Figs. 62, 67) oval, very pale (faded) beige in dorsal view. Dorsal surface of abdomen (Fig. 62) covered with stiff, porrect black setae, each with slightly raised, dark brown sclerotic base, the latter largest medially; single pair of large, lightly sclerotized oval sigilla present (sigilla pair 2), separated by ca. 4.0 x their own width. Legs (Figs. 68, 69) variable shades of pale (faded) tan, with light scopulae on tarsi I–II; tibia I unmodified, without prolateral clasping spurs or distal macrosetae. Leg I: femur 4.1; patella 2.0; tibia 3.2; metatarsus 2.5; tarsus 2.0; total 13.8. Leg I femur–tarsus/carapace length ratio 3.2. Pedipalpal tibia (Figs. 70–72) 1.8 x longer than wide; RTA relatively large, with porrect aspinose distal process and relatively sparse field of retrolateral spinules; tibia also with field of spinules extending along curved retroventral edge (distal to base of RTA), consisting of 1 large and 5 increasingly smaller spinules. Cymbium (Figs. 70–72) setose, with only a few long spinules anteriorly. Embolus (Figs. 70–72) ca. 1.5 x length of bulb, sharply tapering distally, with broad twisted morphology, sub-distal flange and finely bifurcate tip; embolic apophysis absent.

Distribution and remarks.—*Eucanippe eucla* is known only from east of Eucla in southern Western Australia, near the Western Australian/South Australian border (Fig. 11). Nothing is known of the biology of this species, other than that the holotype male specimen was collected wandering in search of females in late autumn. Females are unknown.

Eucanippe mallee sp. nov.
http://zoobank.org/?lsid=urn:lsid:zoobank.org:act:7E75FFE0-937C-499A-B2FC-8A37A5A02FFC
(Figs. 11, 73–85)

Type material.—*Holotype male.* AUSTRALIA: *Western Australia*: N. of Lake King-Norseman Rd, site LK 13 (IBRA_MAL), 33°04′54″S, 119°59′53″E, wet pitfalls, 15 October 1999–20 October 2000, N. Guthrie, CALM Survey (WAM T143025).

Other material examined.—AUSTRALIA: *Western Australia*: 1 ♂, Dragon Rocks Nature Reserve, northern end, site HY 4 (IBRA_MAL), 32°41′27″S, 118°58′30″E, wet pitfalls, 30 October 1997–20 May 1998, N. Guthrie, CALM Survey (WAM T143022); 2 ♂, Lake Magenta Nature Reserve (E. Central), east, site PI 11 (IBRA_MAL), 33°36′59″S, 119°11′58″E, wet pitfalls, 15 October 1999–1 November 2000, P. Van Heurck, CALM Survey (WAM T143023); 1 ♂, Mount Vernon, site HY 7 (IBRA_MAL), 32°46′40″S, 119°14′01″E, wet pitfalls, 30 October 1997–20 May 1998, P. Van Heurck, N. Guthrie, CALM Survey (WAM T143024); 3 ♂, Pingaring-Varley Road Sth, Dragon Rocks Nature Reserve, site HY 6 (IBRA_MAL), 32°46′10″S, 119°00′32″E, wet pitfalls, 30 October 1997–20 May 1998, P. Van Heurck, N. Guthrie, CALM Survey (WAM T139663); 2 ♂, same data (WAM T143026); 1 ♂, Silver Wattle Hill Nature Reserve site PI 1 (IBRA_MAL), 33°08′56″S, 118°49′46″E, wet pitfalls, 15 October 1999–1 November 2000, P. Van Heurck, CALM Survey (WAM T139660); 1 ♂, same data (WAM T143027); 1 ♂, same data (WAM T143028).

Etymology.—The specific epithet is a noun in apposition, in reference to the distribution of this species in the Mallee bioregion of Western Australia.

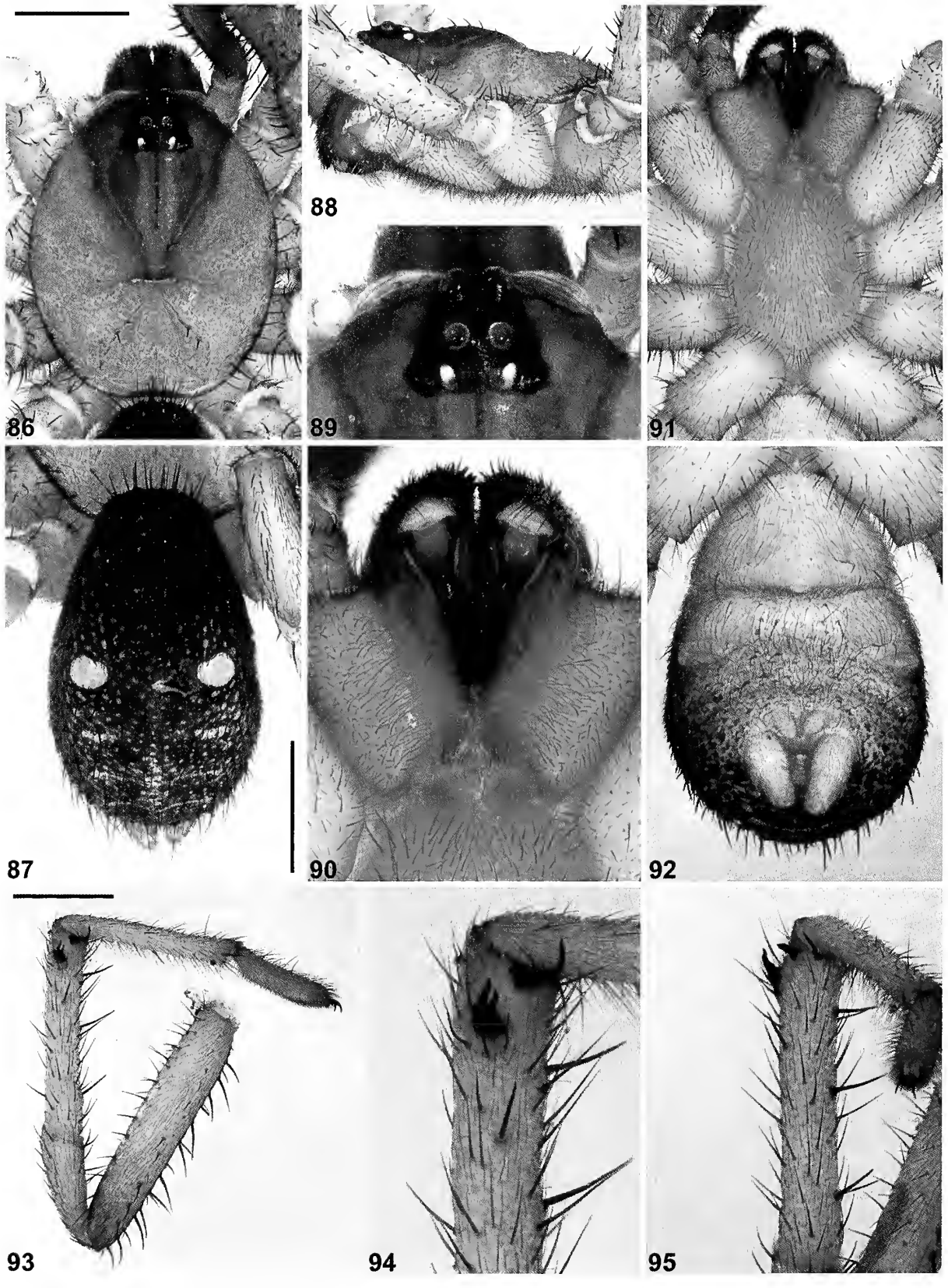

Figures 86–95.—*Eucanippe mouldsi* sp. nov., male holotype (WAM T117264) from near Wellstead (Western Australia; ESP), somatic morphology: 86–87, carapace and abdomen, dorsal view; 88, cephalothorax, lateral view; 89, eyes, dorsal view; 90, mouthparts, ventral view; 91–92, cephalothorax and abdomen, ventral view; 93, leg I, prolateral view; 94, leg I tibia, clasping spurs, prolateral view; 95, leg I tibia, pro-ventral view. Scale bars = 2.0.

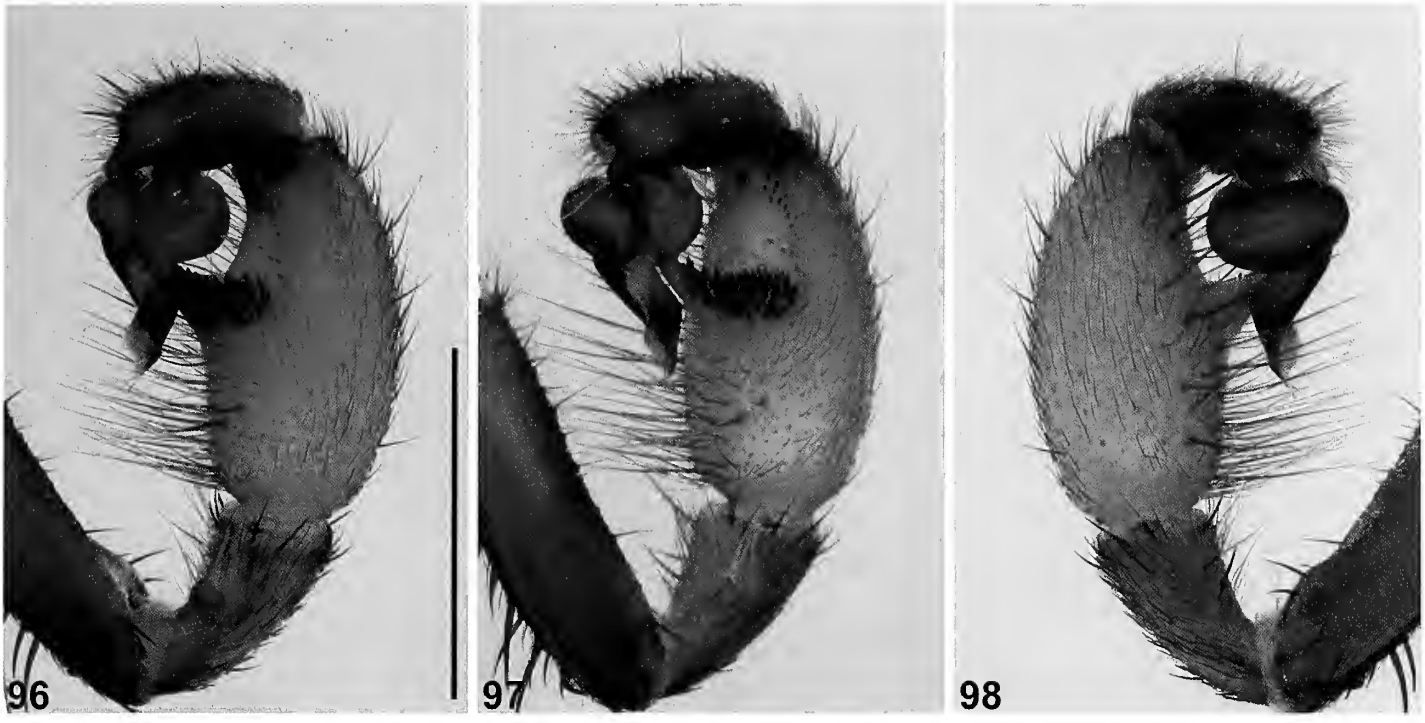

Figures 96–98.—*Eucanippe mouldsi* sp. nov., male holotype (WAM T117264) from near Wellstead (Western Australia: ESP), pedipalp: 96, retrolateral view; 97, retro-ventral view; 98, prolateral view. Scale bar = 2.0.

Diagnosis.—Males of *Eucanippe mallee* sp. nov. can be distinguished from all other known congeners by the shape of the RTA, which is of an intermediate length, with only a short distal process (Figs. 83, 84; cf. Figs. 23, 36, 49, 70, 96, 118). This species can be further distinguished from the similar species *E. bifida* by the presence of just 1 enlarged spur-like seta on the proximal-most leg I clasping spur (Figs. 80, 81; cf. Fig. 21) (if >1 seta is rarely present, the spur-like seta remains the largest).

Description (male holotype).—Total length 7.2. Carapace 3.6 long, 3.0 wide. Abdomen 3.1 long, 2.2 wide. Carapace (Fig. 73) mottled dark tan, with darker pars cephalica, black ocular region, and dark brown-black rim; lateral margins with uniformly-spaced fringe of porrect black setae; fovea slightly procurved. Eye group (Fig. 76) trapezoidal (anterior eye row strongly procurved), 0.9 x as long as wide, PLE–PLE/ALE–ALE ratio 1.5; ALE contiguous, angled antero-laterally; AME separated by slightly less than half their own diameter; PME separated by ca. 2.0 x their own diameter; PME and PLE separated by slightly less than diameter of PME, PME positioned in line with level of PLE. Maxillae with field of cuspules confined to inner corner (Fig. 77); labium without cuspules. Abdomen (Figs. 74, 79) oval, light brown in dorsal view, palest posteriorly, with pair of prominent light brown sigilla spots. Dorsal surface of abdomen (Fig. 74) covered with stiff, porrect black setae, each with slightly raised, dark brown sclerotic base, the latter largest medially; single pair of large, lightly sclerotized oval sigilla present (sigilla pair 2), separated by slightly more than 3.0 x their own width. Legs (Figs. 80–82) variable shades of tan, with light scopulae on tarsi I–II; tibia I bearing small prolateral clasping spurs; proximal-most clasping spur with single, spur-like macroseta. Leg I: femur 4.0; patella 1.9; tibia 3.0; metatarsus 2.8; tarsus 1.8; total 13.5. Leg I femur–tarsus/carapace length ratio 3.7. Pedipalpal tibia (Figs. 83–85) 1.8 x longer than wide; RTA of intermediate length, roundly-pointed distally, with short distal process and sparse field of retrolateral spinules extending along length of RTA; tibia also with field of spinules along curved retroventral edge (distal to base of RTA), consisting of 1 large and 4 smaller spinules. Cymbium (Figs. 83–85) setose, with only a few long spinules anteriorly. Embolus (Figs. 83–85) ca. 2.0 x length of bulb, sharply tapering distally, with broad twisted morphology, sub-distal flange and finely bifurcate tip; embolic apophysis absent.

Distribution and remarks.—*Eucanippe mallee* has a restricted distribution in the western Mallee bioregion of south-western Australia, from the Silver Wattle Hill and Dragon Rocks Nature Reserves, east to Frank Hann National Park and south to Lake Magenta Nature Reserve (Fig. 11). Nothing is known of the biology of this species, and females are unknown.

Eucanippe mouldsi sp. nov.
http://zoobank.org/?lsid=urn:lsid:zoobank.org:act:0129A99C-C6E9-4A05-AD69-69F9E67D7426
(Figs. 1–3, 11, 86–107)

Eucanippe sp. 'Stirling Range National Park' Rix et al., 2017d: 608, figs. 178–179, 184, 187.
Eucanippe sp. 'Wellstead' Rix et al., 2017d: 608, figs. 182, 188.

Type material.—*Holotype male.* AUSTRALIA: *Western Australia*: Wellstead, Gnowellan Road (IBRA_ESP), 34°30′07.5″S, 118°31′22.5″E, pitfall trap, 13–18 August 2011, T. Moulds, G. Owen (WAM T117264).

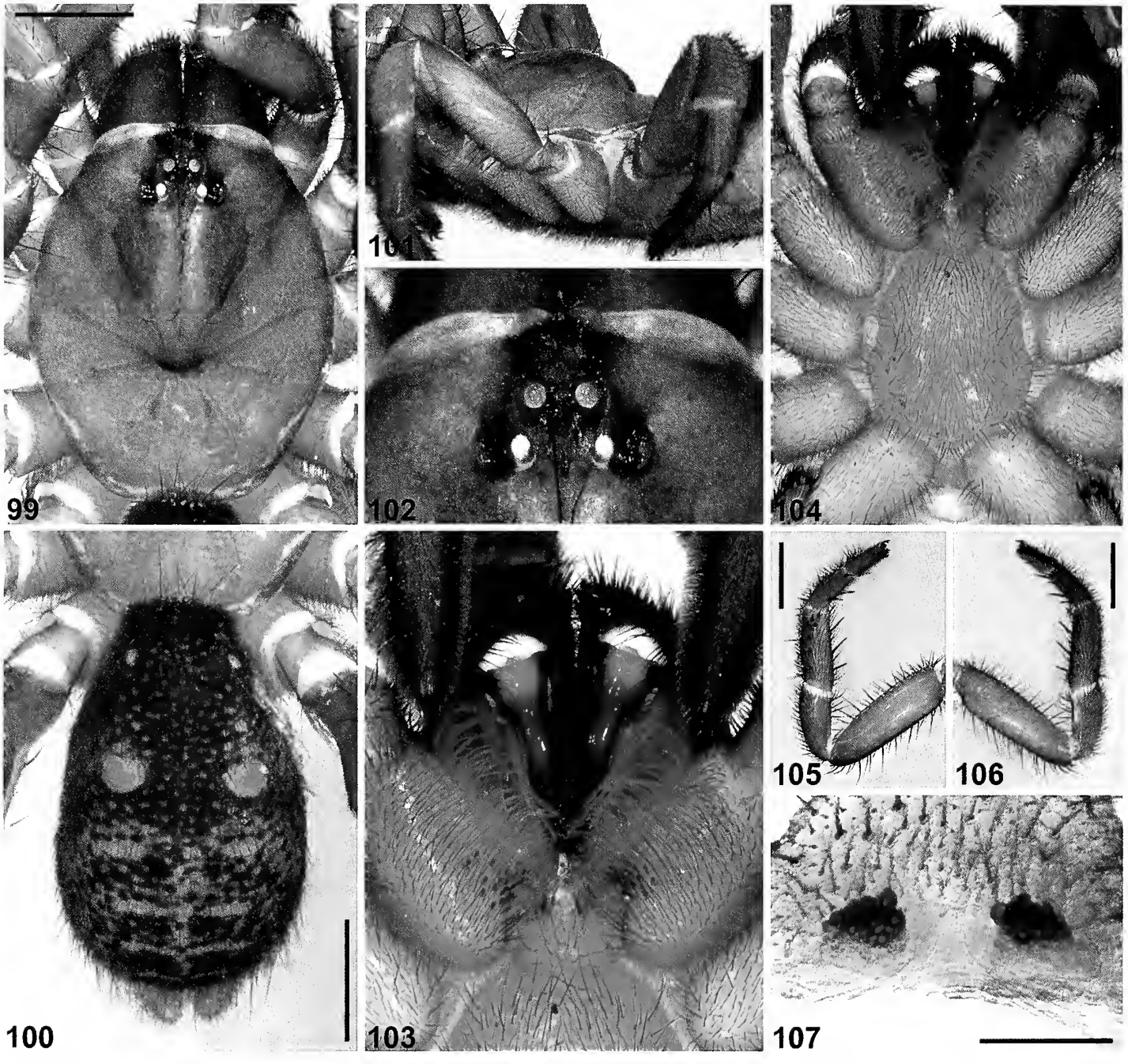

Figures 99–107.—*Eucampipe mouldsi* sp. nov., female paratype (WAM T143003) from near Wellstead (Western Australia; ESP): 99–100, carapace and abdomen, dorsal view; 101, cephalothorax, lateral view; 102, eyes, dorsal view; 103, mouthparts, ventral view; 104, cephalothorax, ventral view; 105, leg 1, prolateral view; 106, leg 1, retrolateral view; 107, spermathecae, dorsal view. Scale bars = 2.0 (99–100, 105–106), 0.5 (107).

Paratypes. AUSTRALIA: *Western Australia*: 1 ♂, same data as holotype except hand collected from burrow, 9 April 2017, M. Rix, M. Harvey, J. Cosgrove (WAM T143002); 1 ♀, same data (WAM T143003).

Other material examined. –AUSTRALIA: *Western Australia*: 1 juvenile, Wellstead, Gnowellan Road (IBRA_ESP), 34°30′07.5″S, 118°31′22.5″E, hand collected from burrow, 9 April 2017, M. Rix, M. Harvey, J. Cosgrove (WAM T143004); 1 juvenile, same data (WAM T143005); 1 ♂, Dunn Rock Nature Reserve, E. of Dunn Rock, site LK 8 (IBRA_MAL), 33°20′37″S, 119°31′30″E, wet pitfalls, 15 October 1999–20 October 2000, N. Guthrie, CALM Survey (WAM T139666); 1 ♂, same data (WAM T143029); 1 ♂, Lake Magenta Nature Reserve (N. Central), west, site PI 7 (IBRA_MAL), 33°29′41″S, 119°02′53″E, wet pitfalls, 15 October 1999–1 November 2000, P. Van Heurek, CALM Survey (WAM T139661); 1 ♂, Peringillup Nature Reserve, site ST 12 (IBRA_AVW), 33°56′37″S, 117°38′41″E, wet pitfalls, 15 October 1999–1 November 2000, P. Van Heurek, CALM Survey (WAM T143030); 1 ♂, Stirling Range National Park, NW. of Two Mile Lake (STR 5b-4) (IBRA_ESP), 34°28′S, 118°15′E, pitfalls, 10–20 September 1990, G. Friend et al.

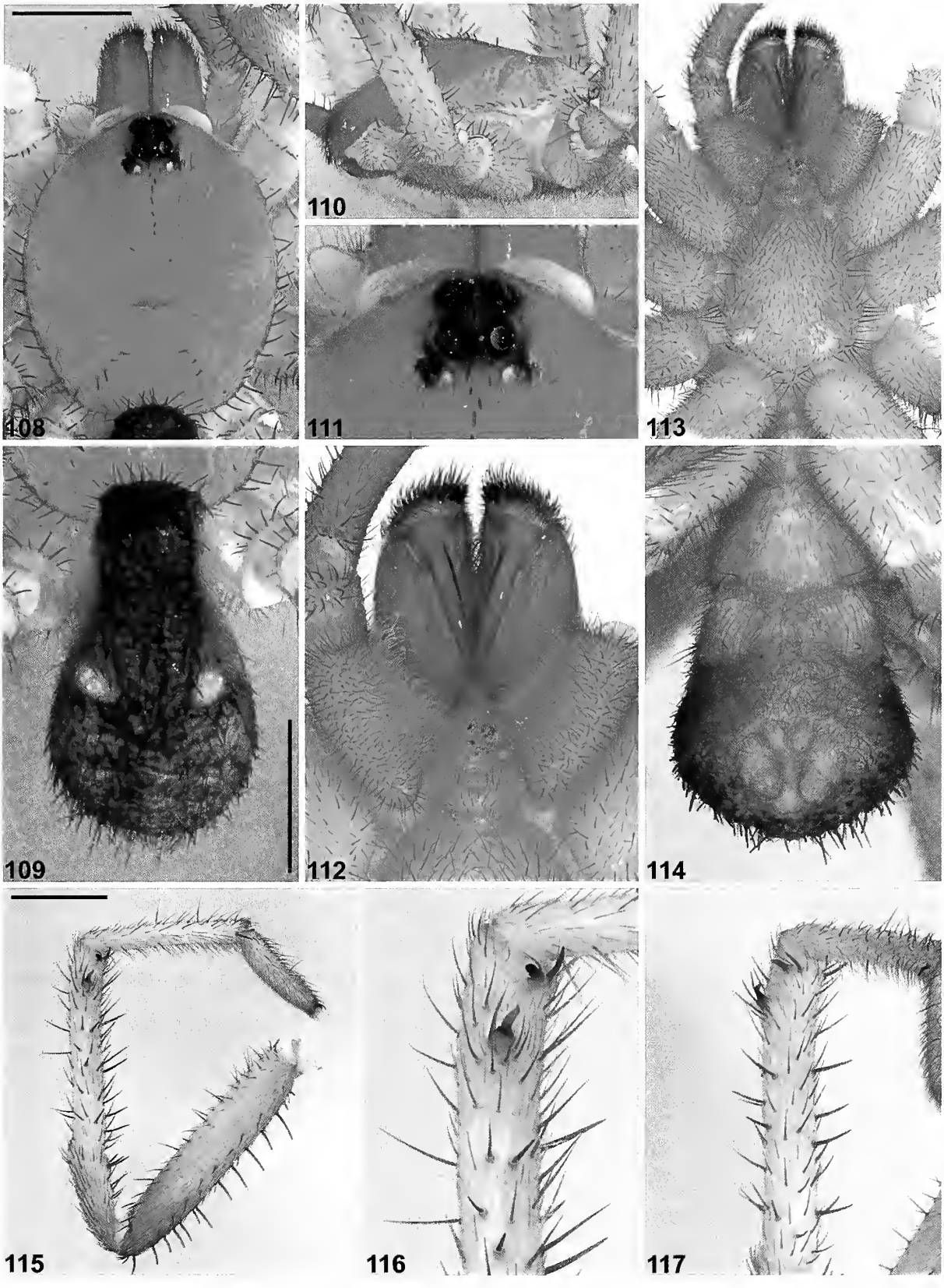

Figures 108–117.—*Eucamippe nemestrina* sp. nov., male holotype (WAM T139657) from Mount Saddleback (Western Australia; JAF), somatic morphology; 108–109, carapace and abdomen, dorsal view; 110, cephalothorax, lateral view; 111, eyes, dorsal view; 112, mouthparts, ventral view; 113–114, cephalothorax and abdomen, ventral view; 115, leg I, prolateral view; 116, leg I tibia, clasping spurs, prolateral view; 117, leg I tibia, pro-ventral view. Scale bars = 2.0.

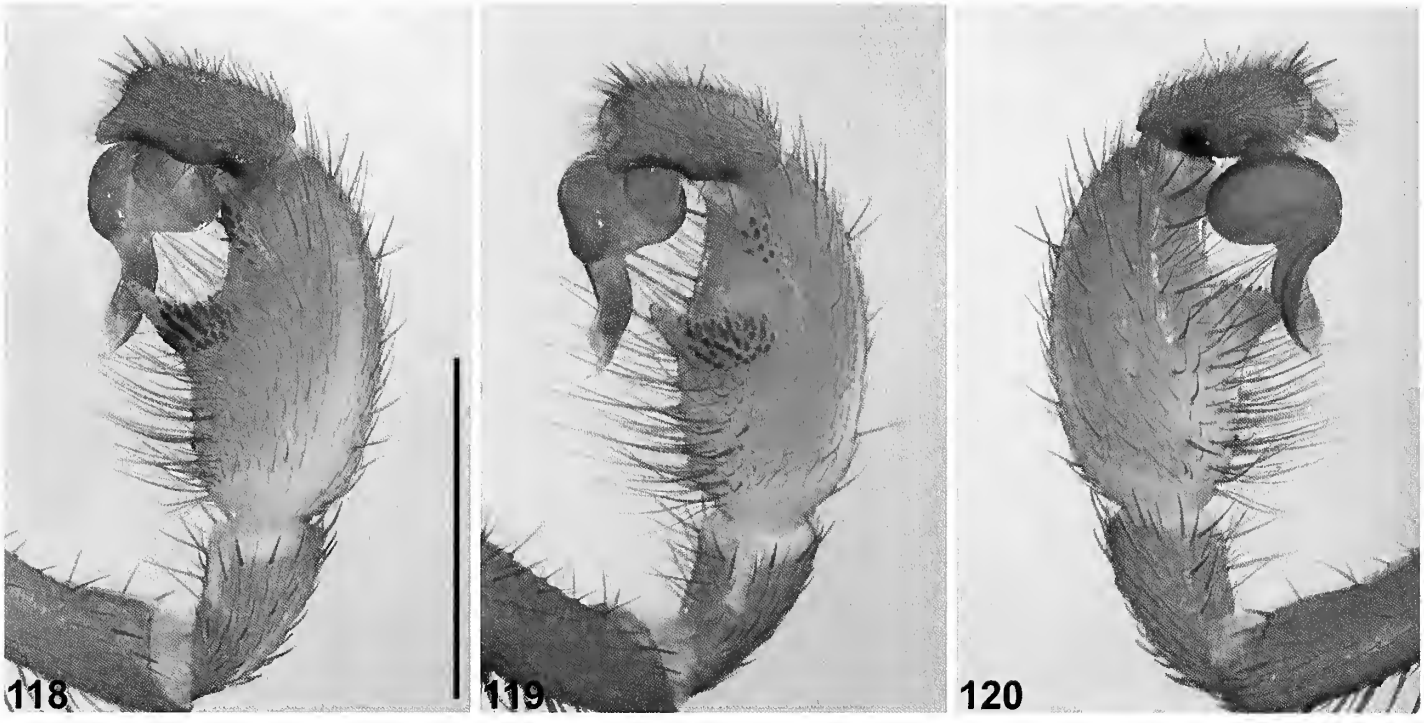

Figures 118–120.—*Eucanippe nemestrina* sp. nov., male holotype (WAM T139657) from Mount Saddleback (Western Australia; JAF), pedipalp: 118, retrolateral view; 119, retro-ventral view; 120, prolateral view. Scale bar = 2.0.

(WAM T44163); 1 ♂, Stirling Range National Park, W. of Two Mile Lake (STR 1-4) (IBRA_ESP), 34°29′S, 118°15′E, pitfall trap, 10–20 September 1990, G. Friend et al. (WAM T41782).

Etymology.—The specific epithet is a patronym in honor of Tim Moulds, in recognition of his contributions to zoology and for collecting the holotype male of this species in 2011.

Diagnosis.—Males of *Eucanippe mouldsi* sp. nov. can be distinguished from all other known congeners except *E. nemestrina* sp. nov. by the combined presence of prolateral clasping spurs on tibia I (Figs. 93–95) (spurs absent in *E. eucla*; Fig. 69); by the presence of a large RTA with a long and usually aspinose distal process (Figs. 96, 97) (distal process smaller or absent in *E. bifida* and *E. mallee* sp. nov.; Figs. 23, 83); by the dorsal color pattern of the abdomen, which is not ornately patterned (Fig. 87) (abdomen markedly bi-colored in *E. absita*; Fig. 27); and by the position and shape of the RTA, the proximal mid-point of which projects from near the middle of the palpal tibia, and which is directed away from the ventral face of the tibia in an antero-ventral orientation (Fig. 96) (RTA directed more anteriorly in *E. agastachys*; Fig. 49). *Eucanippe mouldsi* sp. nov. can be distinguished from *E. nemestrina* sp. nov. by the darker coloration of the carapace and abdomen, which are both heavily pigmented (Figs. 86, 87; cf. Figs. 108–109), combined with the presence of stiff, porrect black setae on the dorsal abdomen which have slightly larger, more strongly-sclerotized sclerotic bases (Fig. 87; cf. Fig. 109).

Description (male holotype).—Total length 11.3. Carapace 5.4 long, 4.4 wide. Abdomen 5.1 long, 3.2 wide. Carapace (Fig. 86) mottled dark tan, with darker brown pars cephalica, black ocular region, dark brown lyre-like pattern on pars cephalica and black rim; lateral margins with uniformly-spaced fringe of porrect black setae; fovea slightly procurved. Eye group (Fig. 89) trapezoidal (anterior eye row strongly procurved), 0.9 x as long as wide, PLE–PLE/ALE–ALE ratio 1.8; ALE almost contiguous, angled antero-laterally; AME separated by slightly less than half their own diameter; PME separated by ca. 3.0 x their own diameter; PME and PLE separated by diameter of PME, PME positioned in line with level of PLE. Maxillae with field of cuspules confined to inner corner (Fig. 90); labium without cuspules. Abdomen (Figs. 87, 92) oval, black and dark charcoal-brown in dorsal view with beige-tan mottling, a pair of prominent beige-tan sigilla spots, and three pairs of thin beige bands posteriorly. Dorsal surface of abdomen (Fig. 87) covered with stiff, porrect black setae, each with slightly raised, dark brown sclerotic base; the latter largest medially; single pair of large, lightly sclerotized oval sigilla present (sigilla pair 2), separated by slightly more than 3.0 x their own width. Legs (Figs. 93–95) variable shades of tan, with light scopulae on tarsi I–II; tibia I bearing small prolateral clasping spurs; proximal-most clasping spur with two similarly-sized macrosetae. Leg I: femur 5.3; patella 2.7; tibia 4.1; metatarsus 3.8; tarsus 2.1; total 17.9. Leg I femur–tarsus/carapace length ratio 3.3. Pedipalpal tibia (Figs. 96–98) nearly 2.0 x longer than wide; RTA relatively large, triangular in retrolateral view, with pointed aspinose distal process and dense field of retrolateral spinules; tibia also with field of spinules extending along curved retroventral edge (distal to base of RTA), consisting of ca. 19 spinules of varying length, the latter longest distally. Cymbium (Figs. 96–98) setose, with only a few long spinules anteriorly. Embolus (Figs. 96–98) ca. 1.5 x length of bulb, sharply tapering distally, with broad twisted morphology, sub-distal flange and finely bifurcate tip; embolic apophysis absent.

Description (female paratype, WAM T143003).—Total length 14.2. Carapace 6.2 long, 5.1 wide. Abdomen 6.4 long, 4.1 wide. Carapace (Fig. 99) dark olive-brown (dark brown-black in life; Fig. 3), with slightly darker pars cephalica, mostly black ocular region, dark brown lyre-like pattern on pars cephalica and dark brown rim; fovea procurved. Eye group (Fig. 102) trapezoidal (anterior eye row strongly procurved), 0.9 x as long as wide, PLE–PLE/ALE–ALE ratio 1.9; ALE almost contiguous, angled antero-laterally; AME separated by slightly less than half their own diameter; PME separated by ca. 3.0 x their own diameter; PME and PLE separated by diameter of PME, PME positioned in line with level of PLE. Maxillae with field of cuspules confined to inner corner (Fig. 103); labium without cuspules. Abdomen (Fig. 100) oval, dark brown in dorsal view with beige-tan mottling, a pair of prominent tan sigilla spots, and four pairs of beige-tan bands posteriorly; single pair of large, sclerotized oval sigilla present (sigilla pair 2), separated by slightly less than 3.0 x their own width. Legs (Figs. 105, 106) variable shades of olive-brown (darker brown-black in life with contrasting red-brown patellae; Fig. 3); scopulae present on tarsi and metatarsi I–II; tibia I with 8 stout prolateral macrosetae, 4 ventral spine-like macrosetae and 7 stout retrolateral macrosetae; metatarsus I with 2 stout prolateral macrosetae and 6 longer retrolateral macrosetae. Leg I: femur 4.1; patella 2.5; tibia 2.3; metatarsus 1.7; tarsus 1.4; total 11.9. Leg I femur–tarsus/carapace length ratio 1.9. Pedipalp olive-brown, spinose on tibia and retrolateral tarsus, with thick tarsal scopula. Genitalia (Fig. 107) with pair of short aciniform spermathecae.

Distribution and remarks.—*Eucanippe mouldsi* has a relatively restricted distribution in the 'Great Southern' region of south-western Australia, from the Dunn Rock and Lake Magenta Nature Reserves, west to Peringillup Nature Reserve and south to the Stirling Range and Wellstead (Fig. 11). As a result of dedicated field work conducted in April 2017, this species is now the best known *Eucanippe*, and the only species for which an adult female specimen and burrow data are available. Burrows of *E. mouldsi* sp. nov. are small and highly camouflaged, less than 30 cm deep, with a slightly raised hinge and broad lower lip (Figs. 5–8). At the type locality near Wellstead, these burrows are situated in dense mallee eucalypt and *Banksia* woodland (Figs. 9, 10) on loamy sand soil. Little else is known of the biology of this species, other than that the known male specimens were collected wandering in search of females in late winter and early spring, and a newly-molted adult male (Figs. 1, 2) was collected from its burrow in mid-April.

Eucanippe nemestrina sp. nov.
http://zoobank.org/?lsid=urn:lsid:zoobank.org:act:F49F061A-5B44-4438-BFF5-4B5A530CDD6C
(Figs. 11, 108–120)

Aganippe raphiduca Rainbow & Pulleine: Main, 1957: 435, fig. 13a, b (in part, "aberrant" specimen B.M. 56/174 from Albany Highway).

Eucanippe sp. 'Kojonup' Rix et al., 2017d: 608, figs. 183, 189.

Type material.—*Holotype male.* AUSTRALIA: *Western Australia*: Mount Saddleback, Worsley Alumina Project (IBRA_JAF), 32°58′S, 116°28′E, pitfall trap, 27 July 1980, A. Weston (WAM T139657).

Other material examined.—AUSTRALIA: *Western Australia*: 1 ♂, Albany Highway, 164 Mile Peg [ca. Tunney, S. of Kojonup] (IBRA_AVW), 34°07′S, 117°22′E, 25 March 1956, B.Y. Main (WAM T139650); 1 ♂, 20 km S. of Beaufort River tavern on Albany Highway, site A [ca. Watts Road] (IBRA_JAF), 33°45′S, 117°08′E, pitfall trap, 4 July 1980, B.Y. Main (WAM T139655); 1 ♂, same data except 14 September 1980 (WAM T139651); 1 ♂, same data except 29 September 1980 (WAM T139652); 2 ♂, Boddington, Murray River, Worsley Alumina Project, trap 5 (IBRA_JAF), 32°56′S, 116°27′E, pitfall trap, wandoo forest, 14 July 1980, J. Taylor (WAM T139656); 1 ♂, Crapella Road, quarry site, N. of Kojonup (IBRA_JAF), 33°40′S, 117°06′E, pitfall trap, sandy heath with wandoo, 17 July 1983, B.Y. Main (WAM T139654); 1 ♂, 10 km N. of Kojonup, Albany Highway site F [ca. Watts Road] (IBRA_JAF), 33°45′S, 117°08′E, pitfall trap, 8 January 1981, B.Y. Main (WAM T139596); 1 ♂, same data except 27 September 1981 (WAM T139653).

Etymology.—The specific epithet is derived from the Latin 'nemestrinus' (adjective: 'inhabiting groves or forests'), in reference to the distribution of this species in the heavily wooded Jarrah Forest bioregion.

Diagnosis.— Males of *Eucanippe nemestrina* sp. nov. can be distinguished from all other known congeners except *E. mouldsi* by the combined presence of prolateral clasping spurs on tibia I (Figs. 115–117) (spurs absent in *E. eucla*; Fig. 69); by the presence of a large RTA with a long and usually aspinose distal process (Figs. 118, 119) (distal process smaller or absent in *E. bifida* and *E. mallee* sp. nov.; Figs. 23, 83); by the dorsal color pattern of the abdomen, which is not ornately patterned (Fig. 109) (abdomen markedly bi-colored in *E. absita*; Fig. 27); and by the position and shape of the RTA, the proximal midpoint of which projects from near the middle of the palpal tibia, and which is directed away from the ventral face of the tibia in an antero-ventral orientation (Fig. 118) (RTA directed more anteriorly in *E. agastachys*; Fig. 49). *Eucanippe nemestrina* sp. nov. can be distinguished from *E. mouldsi* by the paler coloration of the carapace and abdomen (Figs. 108, 109; cf. Figs. 86, 87), combined with the presence of stiff, porrect black setae on the dorsal abdomen which have slightly smaller, less strongly-sclerotized sclerotic bases (Fig. 109; cf. Fig. 87).

Description (male holotype).—Total length 11.2. Carapace 5.1 long, 4.3 wide. Abdomen 4.6 long, 2.7 wide. Carapace (Fig. 108) mottled tan, with darker pars cephalica, mostly black ocular region, faint brown lyre-like pattern on pars cephalica and dark grey rim; lateral margins with uniformly-spaced fringe of porrect black setae; fovea slightly procurved. Eye group (Fig. 111) trapezoidal (anterior eye row strongly procurved), 0.9 x as long as wide, PLE–PLE/ALE–ALE ratio 1.5; ALE almost contiguous, angled antero-laterally; AME separated by slightly less than half their own diameter; PME separated by slightly less than 3.0 x their own diameter; PME and PLE separated by slightly less than diameter of PME, PME positioned in line with level of PLE. Maxillae with field of cuspules confined to inner corner (Fig. 112); labium without cuspules. Abdomen (Figs. 109, 114) oval but somewhat shrivelled anteriorly, dark brown in dorsal view with tan

mottling, a pair of prominent beige sigilla spots, and faint tan banding posteriorly. Dorsal surface of abdomen (Fig. 109) covered with stiff, porrect black setae, each with slightly raised, dark brown sclerotic base; the latter largest medially; single pair of large, lightly sclerotized oval sigilla present (sigilla pair 2), separated by slightly less than 3.0 x their own width. Legs (Figs. 115–117) variable shades of tan, with light scopulae on tarsi I–II; tibia I bearing small prolateral clasping spurs; proximal-most clasping spur with single spur-like macroseta. Leg I: femur 5.4; patella 2.6; tibia 4.2; metatarsus 3.6; tarsus 2.1; total 17.9. Leg I femur–tarsus/carapace length ratio 3.5. Pedipalpal tibia (Figs. 118–120) nearly 2.0 x longer than wide; RTA relatively large, triangular in retrolateral view, with pointed aspinose distal process and sparse field of retrolateral spinules; tibia also with field of spinules extending along curved retroventral edge (distal to base of RTA), consisting of 12 spinules of varying length. Cymbium (Figs. 118–120) setose, with only a few long spinules anteriorly. Embolus (Figs. 118–120) ca. 1.5 x length of bulb, sharply tapering distally, with broad twisted morphology, sub-distal flange and finely bifurcate tip; embolic apophysis absent.

Distribution and remarks.—*Eucanippe nemestrina* has a relatively restricted distribution in the south-eastern Jarrah Forest bioregion of south-western Australia, from south of Kojonup north to Boddington (Fig. 11). Nothing is known of the biology of this species, other than that the known male specimens were collected wandering in search of females in autumn, winter and early spring, with an outlying record (possibly mislabeled) from mid-summer. Females are unknown.

ACKNOWLEDGMENTS

This work would have been impossible without the priceless collections provided by the then CALM (Department of Conservation and Land Management) 'Salinity Action Plan Survey' (later 'State Salinity Strategy') of the Western Australian agricultural zone, run from 1997–2000. This comprehensive biological survey of one of the most diverse yet threatened landscapes in Australia provided numerous new records of *Eucanippe*, from areas where no specimens had previously been collected. Other important specimens were provided by Roy Teale, Zoe Hamilton and Gordon Friend, during their respective surveys of the Ravensthorpe Range and Wheatbelt. We would like especially to thank Andy Austin, Steve Cooper and Sophie Harrison for their contributions to the sister-project on Australian Idiopidae (Australian Research Council Linkage Grant No. LP120200092), which resulted in the phylogenetic delimitation and formal description of this genus, and Jeremy Wilson for his contribution to the development of the 'Atlas' approach to mygalomorph systematics. This work was funded by an Australian Biological Resources Study (ABRS) Taxonomy Research Grant (No. RF21506) to MGR, RJR and MSH.

LITERATURE CITED

Bradshaw, C.J.A. 2012. Little left to lose: deforestation and forest degradation in Australia since European colonization. Journal of Plant Ecology 5:109–120.

Brown, R.W. 1956. Composition of Scientific Words: A Manual of Methods and a Lexicon of Materials for the Practice of Logotechnics. Smithsonian Books, Washington, D.C.

Harvey, M.S., J.M. Waldock, N.A. Guthrie, B.J. Durrant & N.L. McKenzie. 2004. Patterns of composition of ground-dwelling araneomorph spider communities in the Western Australian wheatbelt. Records of the Western Australian Museum Supplement 67:257–291.

Keighery, G.J. 2004. State Salinity Strategy biological survey of the Western Australian wheatbelt: background. Records of the Western Australian Museum Supplement 67:1–6.

Laurance, W.F., B. Dell, S.M. Turton, M.J. Lawes, L.B. Hutley, H. McCallum, et al. 2011. The ten Australian ecosystems most vulnerable to tipping points. Biological Conservation 144:1472–1480.

Main, B.Y. 1957. Biology of aganippine trapdoor spiders (Mygalomorphae: Ctenizidae). Australian Journal of Zoology 5:402–473.

Myers, N., R.A. Mittermeier, C.G. Mittermeier, G.A.B. da Fonseca & J. Kent. 2000. Biodiversity hotspots for conservation priorities. Nature 403:853–858.

Rix, M.G., K. Bain, B.Y. Main, R.J. Raven, A.D. Austin, S.J.B. Cooper et al. 2017a. Systematics of the spiny trapdoor spiders of the genus *Cataxia* (Mygalomorphae: Idiopidae) from south-western Australia: documenting a threatened fauna in a sky-island landscape. Journal of Arachnology 45:395–423.

Rix, M.G., S.J.B. Cooper, K. Meusemann, S. Klopfstein, S.E. Harrison, M.S. Harvey et al. 2017b. Post-Eocene climate change across continental Australia and the diversification of Australasian spiny trapdoor spiders (Idiopidae). Molecular Phylogenetics and Evolution 109:302–320.

Rix, M.G., D.L. Edwards, M. Byrne, M.S. Harvey, L. Joseph & J.D. Roberts. 2015. Biogeography and speciation of terrestrial fauna in the south-western Australian biodiversity hotspot. Biological Reviews 90:762–793.

Rix, M.G., J. Huey, B.Y. Main, J.M. Waldock, S.E. Harrison, S. Comer, et al. 2017c. Where have all the spiders gone? The decline of a poorly known invertebrate fauna in the agricultural and arid zones of southern Australia. Austral Entomology 56:14–22.

Rix, M.G., R.J. Raven, B.Y. Main, S.E. Harrison, A.D. Austin, S.J.B. Cooper et al. 2017d. The Australasian spiny trapdoor spiders of the family Idiopidae (Mygalomorphae: Arbanitinae): a relimitation and revision at the generic level. Invertebrate Systematics 31:566–634, doi: 10.1071/IS16065.

Manuscript received 21 April 2017, revised 29 May 2017.

2018. Journal of Arachnology 46:155–158

SHORT COMMUNICATION

Notes on the behavior and the pendulous egg-sacs of *Viridasius* sp. (Araneae: Viridasiidae)

Tobias Bauer, **Florian Raub** and **Hubert Höfer**: Staatliches Museum für Naturkunde Karlsruhe, Erbprinzenstr. 13, 76133 Karlsruhe, Germany. E-mail: tobias.bauer@smnk.de

Abstract. The natural history and biology of the recently erected family Viridasiidae is virtually unknown, although members of *Viridasius* Simon, 1889 are frequently used in cladistical or toxicological studies. Therefore, we report on laboratory observations made of the feeding and mating behavior and describe the egg-sac of a species tentatively assigned to *Viridasius*. The spiders were mostly nocturnal and built a large, silken retreat for molting. Females built pendulum-like egg sacs consisting of a silken, string-like stalk and an oval repository. The egg-sacs were covered actively with substrate by the female. Our observations corroborate the positioning of the Viridasiidae outside of the Ctenidae, because pendulous and camouflaged egg-sacs are not known from any ctenid species to date.

Keywords: Ctenidae, reproduction, silk, trait

The taxon Viridasiinae was introduced as a subfamily of the Ctenidae by Lehtinen (1967) for several species of *Viridasius* Simon, 1889 (but not *Vulsor* Simon, 1889) from Madagascar. This classification was maintained until recently Polotow et al. (2015) revealed that Viridasiinae are probably Dionycha and arose independently from other ctenids. Consequently, the clade comprising the two genera *Viridasius* and *Vulsor* was raised to family status (corroborated by Bayer & Schönhofer (2013) and Henrard & Jocqué (2017)). The occurrence of the family is restricted to Madagascar (Polotow et al. 2015). However, both genera were never formally revised, although (probably undescribed) members of *Viridasius* and *Vulsor* were frequently used in cladistical or toxicological studies (e.g., Silva Dávila 2003; Bayer & Schönhofer 2013; Eggs et al. 2015; Polotow et al. 2015; Oldrati et al. 2017). Although nothing is published about the natural history or biology of *Viridasius*, the genus is bred in captivity by laboratories and pet owners. However, reproduction behavior, natural history and mating experiments can contribute significantly to species separation (Barth & Schmitt 1991; Dahlem et al. 1987; Töpfer-Hofmann et al. 2000) and different traits related to reproduction behavior are often used in cladistical analyses, e.g., egg-sac deposition (e.g., Ramirez 2014; Polotow et al. 2015).

Especially in the Ctenidae and other Lycosoidea, egg-sac treatment and deposition varies. In Amazonian species of the still poorly defined genus *Ctenus* Walckenaer, 1805, spiders were observed carrying their egg-sac in the chelicerae (*Ctenus amphora* Mello-Leitão, 1930, *Ctenus crulsi* Mello-Leitão, 1930, *Ctenus manauara* Höfer, Brescovit & Gasnier, 1994; photos of *C. crulsi* available online at www.wandering-spiders.net), while at least one species, *Ctenus villasboasi* Mello-Leitão, 1949, attaches its egg-sac to the ground surface and guards it (Höfer et al. 1994), similar to *Phoneutria* Perty, 1833 (Hazzi 2014; pers. obs.; photo available online at www.wandering-spiders.net). The recently described *Californctenus cacachilensis* Jiménez, Berrian, Polotow & Palacios-Cardiel, 2017 was observed producing whitish egg-sacs, which were also attached to corners or sides of their terrarium and not carried around (Jiménez et al. 2017). All species of *Ancylometes* Bertkau, 1880 for which breeding behavior is known carry their egg-sac, which is covered by a thick layer of hard and purplish-brown silk, in the chelicerae (Höfer & Brescovit 2000; photo available online at www.wandering-spiders.net), whereas in *Cupiennius salei* (Keyserling, 1877) the white egg sac is attached to the spinnerets of the female, similar to Lycosidae (Barth 2002, own observations). In Dionycha, egg sacs are carried in the chelicerae by members of Sparassidae (Ross et al. 1982; Jäger 2003), but observations on members of other families suggest that most species in some way or the other deposit their eggs, often guarded directly by the female (e.g., Pollard 1983; Jocqué & Dippenaar-Schoeman 2006; Ramirez 2014). However, no such observations were made for the genus *Viridasius*. Therefore, our intention is to describe the form and structure of an egg-sac built by a species of *Viridasius* together with a report on some observations of their behavior in captivity. Additionally, we provide photographs of the genitalia to allow a future identification of our material after a revision of the genus.

Three specimens of a possibly undescribed *Viridasius* species (Figs. 1 & 2) were bought as juveniles from an exotic pet exhibition in July 2016. The specimens were kept in small plastic boxes of 15 x 10 x 15 cm at room temperature until their final molt and then transferred to larger boxes (approximately 20 x 20 x 25 cm) with cork rear panels. The spiders were fed with two or three crickets of adequate size once a week. The substrate used was a mixture of unfertilized potting soil and red sand. The sand covered the bottom of the terrarium to drain humidity; the potting soil formed a continuous layer above. A curved piece of thin bark (200 mm x 50 mm; diameter 4–5 mm) was placed on the bottom of each container as a retreat. Photographs of the genitalia were made with Software Automontage © (Syncroscopy, Cambridge, UK) and a Leica DFC 495 Digital camera, connected to a Leica Z6 APO (Leica Microsystems, Wetzlar, Germany). Specimens are deposited in the collection of the Staatliche Museum für Naturkunde, Karlsruhe (collection number SMNK-ARA 14750).

During the day, all three specimens could be found under the curved piece of bark and became mostly active in the night. After its final molt, the male started to wander around in the daytime as well. Subadult and adult specimens often disregarded prey which was transferred to their box in the daytime and hunted only during the dawn or night, while younger stages voraciously went after prey as soon as it was introduced into their boxes. Before molting the first time in our care, the spiders produced a large silken retreat, consisting of a very strong and tear-resistant silk, under the piece of bark. The retreat was large enough to contain the spider including the legs and was often incrusted with substrate. It was also used for hiding at daytime and was consequently expanded for following molts. When we destroyed the silken retreat, a new one was only built for molting. Two specimens (one male, one female) reached adulthood in November/December 2016, the second female finally molted in late January 2017 and reached a considerably larger body size of about 25 mm compared to about 20 mm of the other female. The male was transferred to the box of the smaller female on 24 January 2017 at around 3 pm. The male approached the female very slowly, under constant tapping and moving of his forelegs. The female showed no

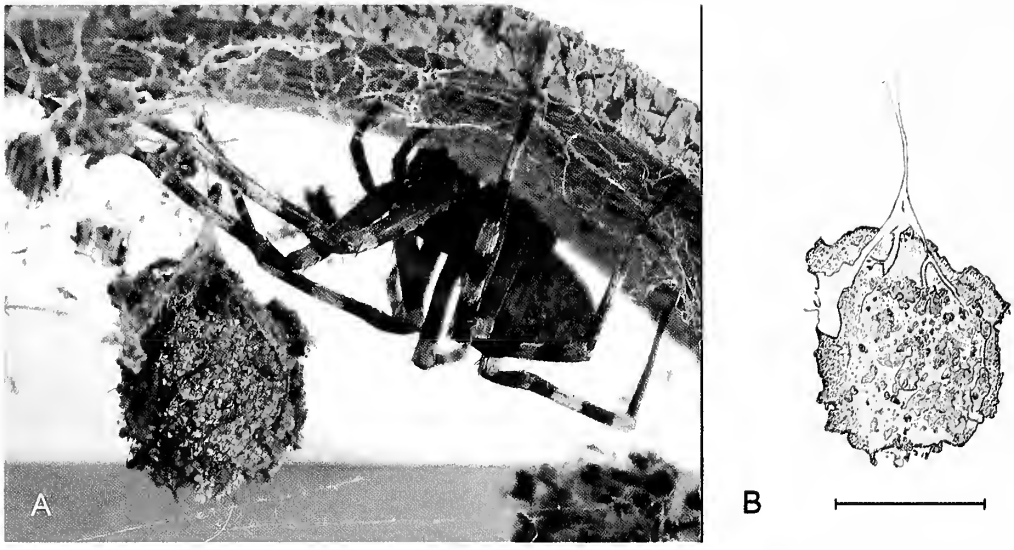

Figure 1.—*Viridasius* sp., Egg-sac camouflaged with sand and earth. A. Female with egg-sac, B. Drawing (scale line = 10 mm).

sign of aggression, but moved towards the male and started to lift the forelegs alternately, while getting repeatedly tapped on the body and legs by the male. After about two minutes, the male suddenly moved over the body of the female. The mating position and procedure corresponded well to descriptions by Foelix (2011, Fig. 7.27C) and Stratton et al. (1996). The entire mating took place at the rear panel of cork installed in the terrarium. The female showed no sign of aggression during and shortly after the copulation and remained passive throughout the whole procedure, which typically resulted in a nearly horizontal positioning of its body due to the copulation activities of the male, while some of its legs were still attached to the rear panel (see video S1, available online at http://dx.doi.org/10.1636/JoA-S-17-058.S1). The male showed pronounced epigynal scratching before and between insertions. At least once, it seems like the male performed multiple insertions with one palp. Insertions lasted for about 20–30 seconds. The entire mating process, including the approach and the courtship behavior, took place in about 30 minutes. Afterwards, the male was chased away by the female and removed by us from the terrarium. The male lived for several more weeks and died on 17 April 2017. In the following months after the mating the female produced three egg-sacs, two of which contained eggs. All three egg-sacs were attached to the underside of the curved piece of bark in the silken retreat (first and second) or the upper glass panel of the terrarium. The egg-sacs consisted of a silken, string-like stalk of about 15 mm length and an egg-shaped repository of 15–18 mm length and 12–14 mm width (Fig. 1). All egg sacs, including the third one without eggs, were actively camouflaged by the female with substrate, such that nearly no silk (except for the silken stalk) was visible when we found the egg-sacs. Because the red sand (visible on the egg-sac in Fig. 1A) was covered by a thin layer of potting-earth, the female had to move considerable amounts of substrate. The silk of the egg-sac was strong and was not torn apart easily, but was easily penetrable with a needle and not stiff or paper-like, but flexible. From both egg sacs 30–35 spiderlings emerged, approximately 4–5 weeks after deposition. After emergence, no unfertilized eggs were found. Because the egg-sacs were removed and opened by us to prevent cannibalistic feedings on the eggs or the spiderlings by their mother, we are not able to report on the release mechanism. Some cannibalism was observed soon after the dispersal of the spiderlings, so the original number was possibly somewhat higher. However, most of the time until separation, the spiderlings behaved peacefully. The female died on 29 June 2017. The unmated female was still alive during the preparation of the manuscript.

With respect to recent phylogenetic results (Polotow et al. 2015; Henrard & Jocqué 2017), it is not entirely surprising that females of *Viridasius* construct egg-sacs which would be very atypical for a ctenid spider. The construction of a pendulous and well camouflaged egg-sac was, to the best of our knowledge, never reported for a species of Ctenidae, particularly African genera (e.g., Henrard & Jocqué 2017, see also introduction) and could be a special attribute of the Family Viridasiidae. However, similar pendulous egg-sacs are built by *Tamopsis* Baehr & Baehr, 1987 (Hersiliidae) (Baehr & Baehr 1987), *Agroeca* Westring, 1861 (Lioeranidae), the pirate spiders of the genus *Ero* C.L. Koch, 1836 (Mimetidae), *Theridiosoma gemmosum* (L. Koch, 1877) (Theridiosomatidae) and the cave-dwelling genus *Meta* C.L. Koch, 1836 (Tetragnathidae) (Roberts 1995). Nielsen (1932) reported on intraspecific variation of egg-sac deposition in an agelenid species, which builds pendulous as well as attached egg sacs, showing that this trait should be used with care in phylogenetic analyses, especially in agelenid species or related families. We could not observe any significant variations in the architecture of the egg-sacs built by *Viridasius* sp., and even the third egg-sac, which contained no eggs, was pendulous and covered with earth and sand. To our knowledge, differing egg-sacs within one species were also never observed in other free-hunting spiders. However, because our observations were made on a single female, we cannot exclude the possibility that egg-sac variations occur within the natural population of this species or under different ecological parameters.

The female was often found nearby the first two egg-sacs (Figs. 1 & 2), but was easily chased away by us. Because both were built in their retreat, the position of the female near the egg-sacs could be an artefact of captivity, and we suppose females may abandon their well-camouflaged egg-sacs in nature. We can only speculate about the function of the pendulum-like form. Egg-sacs are a barrier for egg-predators and parasitoids and costly for the spider (Austin 1985). It is feasible that a hanging, camouflaged egg-sac is harder to locate for both types of antagonists, not only visually, but on a tactile level as well. However, the pendulous egg-sacs of *Ero* are frequently parasitized by different parasitoids, as are egg-sacs of *Agroeca* (Fitch 2005), so the intense camouflaging could be a result of an evolutionary arms race between *Viridasius* and different parasitoids, possibly not only masking the egg-sac, but also serving as a sort of protection. We are not able to say if the constant incrustations with substrate observed on the surface of the retreats serve as camouflage or were an artefact of captivity; nevertheless, in some cases, the covering was dense and showed similarities to the camouflage of the

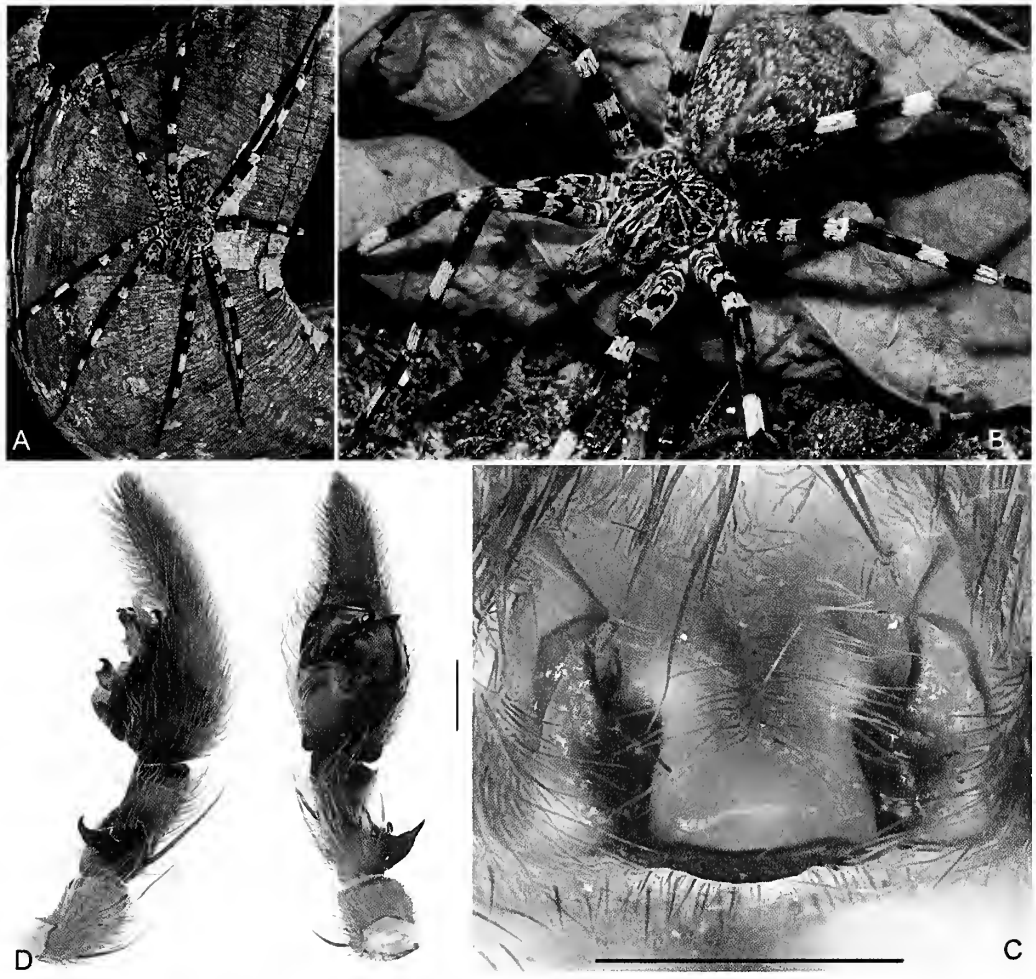

Figure 2.—*Viridasius* sp.: A. Living male; B. Living female; C. Epigyne; D. Male pedipalpus (retrolateral, ventral); Scale lines = 1 mm.

egg-sac. It is also possible that our observations on the egg numbers are biased by the small size of the mated female, and that larger females are able to produce more eggs per clutch, as observed by Eberhard (1979) or Skow & Jacob (2003).

We hope that our observations facilitate the description of egg-sacs in other genera, especially other Viridasiidae, and a revision of *Viridasius*, since Madagascar is traditionally affected by heavy deforestation and good taxonomical knowledge is urgently needed to provide conservation managements for these stunning and fascinating spiders. We are very thankful to Rainer Breitling (Manchester, United Kingdom) for help with literature and to two anonymous reviewers and the editor Thomas C. Jones for their constructive and helpful comments which greatly improved the article.

LITERATURE CITED

Austin, A.D. 1985. The function of spider egg sacs in relation to parasitoids and predators, with special reference to the Australian fauna. Journal of Natural History 19:359–376.

Baehr, B.C. & M. Baehr. 1987. The Australian Hersiliidae (Arachnida: Araneae): taxonomy, phylogeny, zoogeography. Invertebrate Taxonomy 1:351–438.

Barth, F.G. 2002. A Spider's World: Senses and Behavior. Springer, Berlin.

Barth, F.G. & A. Schmitt. 1991. Species recognition and species isolation in wandering spiders (*Cupiennius* spp.; Ctenidae). Behavioral Ecology and Sociobiology 29:333–339.

Bayer, S. & A.L. Schönhofer. 2013. Phylogenetic relationships of the spider family Psechridae inferred from molecular data, with comments on the Lycosoidea (Arachnida: Araneae). Invertebrate Systematics 27:53–80.

Dahlem, B., C. Gack & J. Martens. 1987. Balzverhalten von Wolfspinnen der Gattung *Alopecosa* (Arachnida: Lycosidae). Zoologische Beiträge (N. F.) 31: 151–164

Eberhard, W.G. 1979. Rate of egg production by tropical spiders in the field. Biotropica 11:292–300.

Eggs, B., J.O. Wolff, L. Kuhn-Nentwig, S.N. Gorb & W. Nentwig. 2015. Hunting without a web: how lycosoid spiders subdue their prey. Ethology 121:1166–1177.

Finch, O.D. 2005. The parasitoid complex and parasitoid-induced mortality of spiders (Araneae) in a Central European woodland. Journal of Natural History 39:2339–2354.

Foelix, R.F. 2011. Biology of Spiders. 3rd ed., Oxford University Press. Oxford.

Hazzi, N.A. 2014. Natural history of *Phoneutria boliviensis* (Araneae: Ctenidae): habitats, reproductive behavior, postembryonic development and prey-wrapping. Journal of Arachnology 42:303–310.

Henrard, A. & R. Jocqué. 2017. Morphological and molecular evidence for new genera in the Afrotropical Cteninae (Araneae, Ctenidae) complex. Zoological Journal of the Linnean Society 180:82–154.

Höfer, H. & A.D. Brescovit. 2000. A revision of the Neotropical

spider genus *Ancylometes* Bertkau (Araneae: Pisauridae). Insect Systematics & Evolution 31:323–360.

Höfer, H., A.D. Brescovit & T.R. Gasnier. 1994. The wandering spiders of the genus *Ctenus* (Ctenidae, Araneae) of Reserva Ducke, a rainforest reserve in central Amazonia. Andrias 13:81–98.

Jäger, P. 2003. A study of the character "palpal claw" in the spider subfamily Heteropodinae (Araneae: Sparassidae). Arthropoda Selecta Special Issue 1 2004:107–125.

Jiménez, M.L., J.E. Berrian, D. Polotow & C. Palacios-Cardiel. 2017. Description of *Californctenus* (Cteninae, Ctenidae, Araneae), a new spider genus from Mexico. Zootaxa 4238:97–108.

Jocqué, R. & A. Dippenaar-Schoeman. 2006. Spider Families of the World. Musée Royal de l'Afrique Central, Tervuren.

Lehtinen, P.T. 1967. Classification of the cribellate spiders and some allied families with notes on the evolution of the suborder Arancomorpha. Annales Zoologici Fennici 4:199–467.

Nielsen, E. 1932. The Biology of Spiders. Levin and Munksgaard, Copenhagen, Denmark.

Oldrati, V., D. Koua, P.M. Allard, N. Hulo, M. Arrell, W. Nentwig, et al. 2017. Peptidomic and transcriptomic profiling of four distinct spider venoms. PLoS ONE 12:1–18.

Pollard, S.D. 1983. Egg guarding by *Clubiona cambridgei* (Araneae, Clubionidae) against conspecific predators. Journal of Arachnology 11:323–326.

Polotow, D., A. Carmichael & C.E. Griswold 2015. Total evidence analysis of the phylogenetic relationships of Lycosoidea spiders (Araneae, Entelegynae). Invertebrate Systematics 29:124–163.

Ramírez, M.J. 2014. The morphology and phylogeny of dionychan spiders (Araneae, Araneomorphae). Bulletin of the American Museum of Natural History 390:1–374.

Roberts, M.J. 1995. Collins Field Guide. Spiders of Britain & Northern Europe. Harper Collins, London.

Ross, J., D.B. Richman, F. Mansour, A. Trambarulo & W.H. Whitcomb. 1982. The life cycle of *Heteropoda venatoria* (Linnaeus) (Araneae: Heteropodidae). Psyche 89:297–306.

Silva Dávila, D. 2003. Higher-level relationships of the spider family Ctenidae (Araneae: Ctenoidea). Bulletin of the American Museum of Natural History 274:1–86.

Skow, C.D. & E.M. Jacob 2003. Effect of maternal body size on clutch size and egg weight in a pholcid spider. Journal of Arachnology 31:305–308.

Stratton, G.E., E.A. Hebets, P.R. Miller & G.L. Miller. 1996. Pattern and duration of copulation in wolf spiders (Araneae, Lycosidae). Journal of Arachnology 24:186–200.

Töpfer-Hofmann, G., D. Cordes & O.V. Helversen. 2000. Cryptic species and behavioural isolation in the *Pardosa lugubris* group (Araneae, Lycosidae), with description of two new species. Bulletin of the British Arachnological Society 11:257–274.

Manuscript received 27 July 2017, revised 10 October 2017.

2018. Journal of Arachnology 46:159–161

SHORT COMMUNICATION

Dissection of silk glands in the Western black widow *Latrodectus hesperus*

R. Crystal Chaw[1,2] and **Cheryl Y. Hayashi**[1,3]: [1]Department of Evolution, Ecology and Organismal Biology, University of California at Riverside, 900 University Avenue, Riverside, California 92521, USA; E-mail: rocrystalchaw@gmail.com; [2]Current address: Advanced Light Microscopy Core, Department of Neurology, Oregon Health & Science University, 3181 SW Sam Jackson Park Rd., Portland, OR 97239; [3]Current address: Division of Invertebrate Zoology and Sackler Institute for Comparative Genomics, American Museum of Natural History, Central Park West at 79th St. New York, NY 10024

Abstract. The silk glands of the Western black widow *Latrodectus hesperus* Chamberlin & Ivie, 1935 are morphologically and functionally distinct. Studies of spider silk glands often show only high magnification images of sections or drawings of glands, making differentiation of dissected glands difficult. We dissect all of the gland types from *L. hesperus* females and show their gross morphology with light microscopy. Our micrographs portray the distinct morphologies and relative sizes of each silk gland type, consistent with prior descriptions of the silk apparatus of *Latrodectus* spiders. Notably, we verify the presence of two differentiated pairs of aggregate silk glands and spigots, thus resolving a discrepancy in the literature.

Keywords: Theridiidae, morphology, spinneret, spigot

Black widow spiders (Theridiidae) have hundreds of silk glands. Based on morphology, these silk glands can be grouped into seven general types: aciniform, aggregate, flagelliform, major ampullate, minor ampullate, pyriform, and tubuliform (Kovoor 1987). The multiple pairs of aggregate glands can be further subdivided into "anterior" or "posterior" aggregate glands, synonymous with "typical" or "atypical" aggregate glands, respectively. Although the morphology of silk glands is used to determine silk gland identity for dissection, the gross morphology of black widow silk glands is rarely depicted; most studies show drawings of glands or sections of glands at high magnification (e.g., Kovoor 1977; Moon et al. 1998; Townley & Tillinghast 2013). The identification of black widow silk glands has become increasingly important given the growing literature on the biomechanics of widow spider silks and transcriptomics of their silk glands (e.g., Lawrence et al. 2004; Argintean et al. 2005; Garb et al. 2010; Clarke et al. 2015).

One recent study of black widows includes a video of a dissection focusing on the gross morphology of silk glands (Jeffery et al. 2011). However, some of the results of this study conflict with other descriptions of silk gland morphology for *Latrodectus* spiders (Kovoor 1977, 1987; Townley & Tillinghast 2013). Spiders that use aggregate silk glue have two pairs of aggregate silk glands (Townley & Tillinghast 2013). In theridiids, the aggregate silk gland pairs have differentiated from each other in morphology and function (Kovoor 1977, 1987). However, in their study of silk glands from black widows, Jeffrey et al. (2011) identify only one pair of aggregate silk glands.

To clarify the silk gland types present in widow spiders, we reinvestigated the silk glands from the Western black widow, *Latrodectus hesperus* Chamberlin & Ivie, 1935. We documented all of the general silk gland types and their relative sizes and morphologies. Furthermore, we found two pairs of aggregate silk glands that are differentiated from each other. Our data are consistent with descriptions of theridiid silk gland types that predate the Jeffery et al. (2011) video study.

We collected adult female Western black widow *L. hesperus* spiders in June and July of 2016 (Riverside, Riverside County, CA, 33.9737° N, 117.3281° W). Spiders were anesthetized with CO_2 gas prior to dissection. Silk glands were dissected with sharpened Dumont #5 forceps in Saline Sodium Citrate (0.15 M sodium chloride, 0.015M sodium citrate). Micrograph images of four individuals were taken through a Leica EC3 camera with Leica Application Suite (LAS) software, v. 4.6.

Seven general types of silk glands were identified: aciniform, aggregate, flagelliform, major ampullate, minor ampullate, pyriform, and tubuliform (Fig.1). The sizes and shapes of the glands are consistent with other descriptions of theridiid silk glands. The major ampullate gland is the largest, and features a long tail that can be stretched to many mm in length (Fig. 1A; Casem et al. 2002). In comparison, the minor ampullate glands are dwarfed ampulla-shaped glands that have much shorter tails (Fig. 1B). Both major and minor ampullate glands have three parts: a tail, an ampulla-shaped storage sac, and a zig-zag duct.

Like the ampullate glands, we found two pairs of aggregate glands that are morphologically distinct from each other (Figs. 1C,D & 2C). Both pairs of aggregate glands are multi-lobed. However, the anterior aggregate gland has a wavy duct covered in a removable, nodulated sheath, while the posterior aggregate gland has a short, wide, duct that does not have a nodulated sheath (Fig. 1C,D; sheath indicated by bracket in Fig. 2C).

The long, noodle-shaped tubuliform glands are smooth and have a gradient of brown coloration that darkens toward the duct. The duct is a tight curl (Fig. 1E). We presume that the tubuliform glands are brown as a result of the silk dope; *L. hesperus* egg sacs are pale yellow to light tan and tubuliform silk is the main component of egg-case covering.

The aciniform, flagelliform, and pyriform glands are the smallest glands (Fig. 1F–H). Aciniform (Fig. 1F) and pyriform (Fig. 1G) silk glands are numerous, having multiple pairs and numbering in the hundreds, whereas only one pair of flagelliform glands (Fig. 1H) is present. Compared to the pyriform glands, the finger-like aciniform glands and ampulla-shaped flagelliform glands are larger and more easily separable. The pyriform glands are tightly associated with each other in fan-like formations that do not easily divide into individual glands (Fig. 1G). Both aciniform and pyriform silk glands have extremely fine, hair-like ducts, and neither gland type has a tail. In contrast, flagelliform glands have a distinct tail and a more robust duct (Figs. 1H & 2E).

Overall, our dissections were consistent with descriptions of theridiid silk glands (e.g., Kovoor 1977; Moon et al. 1998; Townley

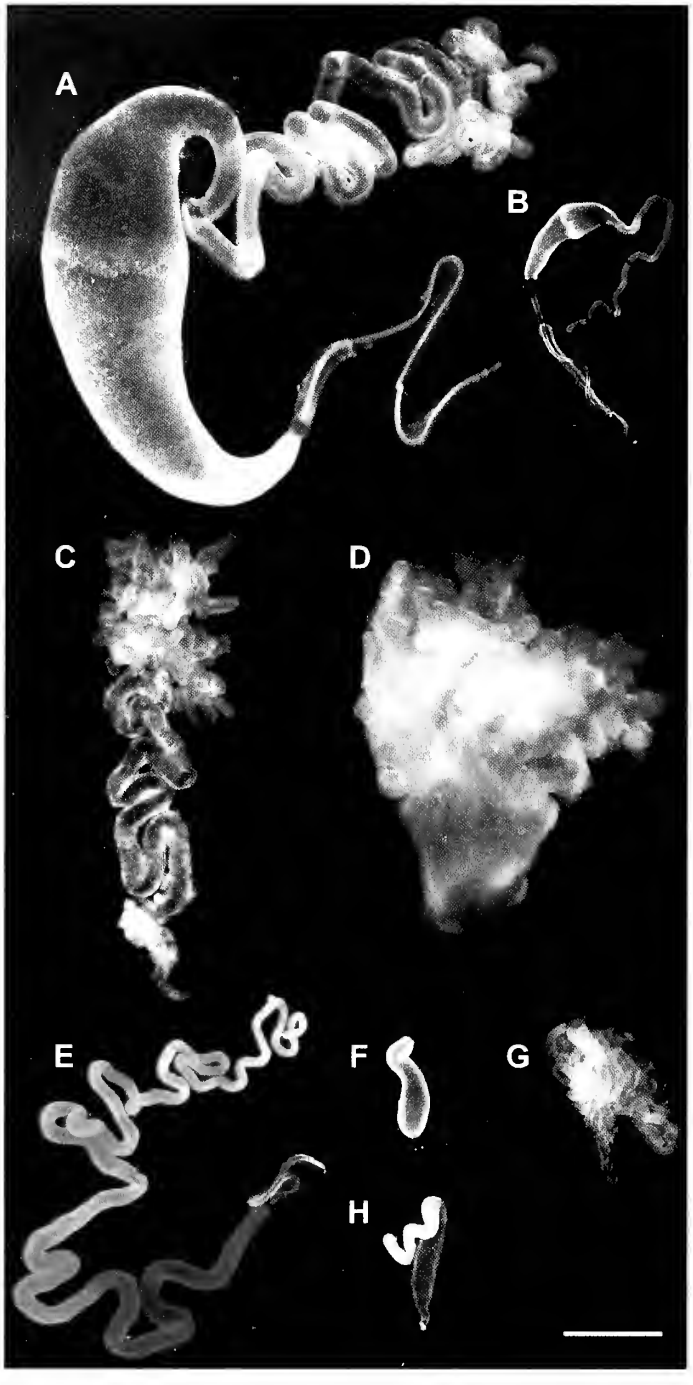

Figure 1.—Silk glands of *Latrodectus hesperus*. A. Major ampullate. Storage sac is to the left, tail (up) and duct (bottom) extend to the right. B. Minor ampullate, oriented as A. C. Anterior aggregate. Body (top) of gland is a cluster of branched lobes. D. Posterior aggregate. Body (top) of gland is lobed and globular. Duct (bottom) is wide and straight. E. Tubuliform, F. Aciniform, G. Group of approximately 20 pyriform glands, H. Flagelliform. With the exception of tubuliform, aciniform, and pyriform silk glands, all silk glands are paired in the spider and only one is depicted. There are three pairs of tubuliform glands in *L. hesperus*, a single gland is shown (E). There are hundreds of aciniform glands, and one is shown (F). Pyriform glands group into tightly associated clusters, a single cluster of approximately twenty glands is shown (G). Scale bar = 1mm.

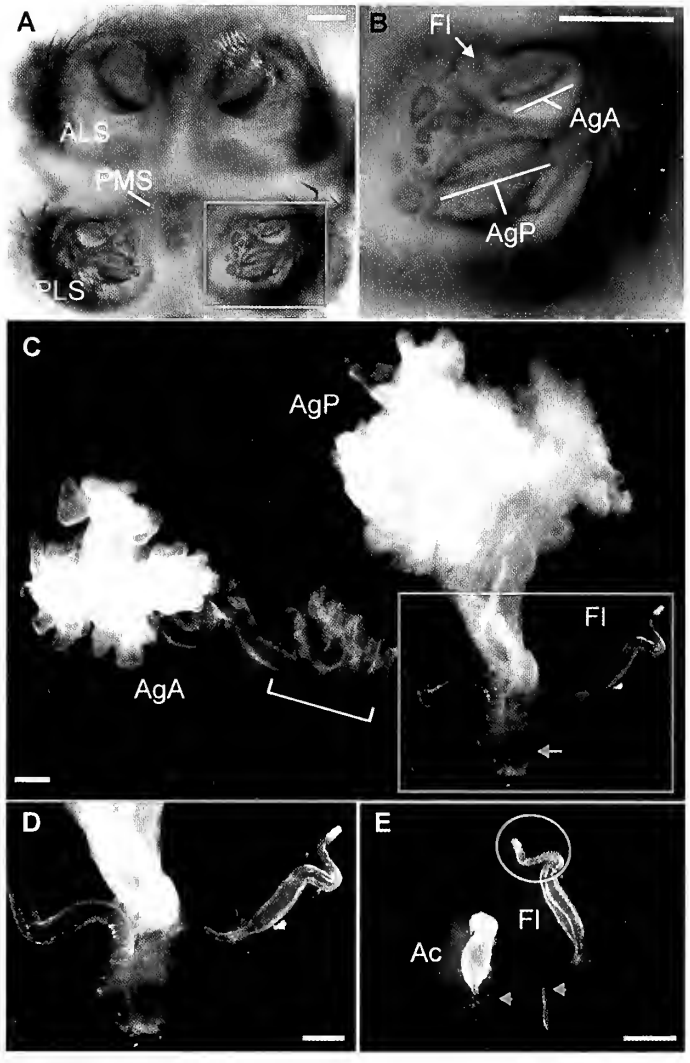

Figure 2.—A, B. Spinnerets of *Latrodectus hesperus*. A. The anterior lateral spinnerets (ALS), posterior median spinnerets (PMS) and posterior lateral spinnerets (PLS) of *Latrodectus hesperus*. Boxed area is shown in (B). B. Left posterior lateral spinneret. Flagelliform (Fl), anterior aggregate (AgA) and posterior aggregate (AgP) spigots are indicated. C E. Aggregate and flagelliform silk glands of *Latrodectus hesperus*. C. Anterior aggregate (AgA), posterior aggregate (AgP), and putative flagelliform (Fl) silk glands are shown attached to the left posterior lateral spinneret (arrow). Bracket indicates nodulated area on remaining sheath. Aciniform glands have been removed for clarity. Boxed area shown in (D). D. The ducts of all three glands go to the posterior lateral spinneret. E. An aciniform silk gland (left) next to a flagelliform silk gland (right). The flagelliform silk gland has a tail (circle) and a wider duct (arrowheads) than the aciniform silk gland. Scale bars = 250 μm.

and Tillinghast 2013). However, Jeffery et al. (2011) did not describe silk glands that match the pair of flagelliform glands that we identify. To verify our description, we looked for a triad of spigots on the posterior lateral spinnerets. Known as the aggregate and flagelliform triad, two of these spigots are relatively enormous, and one spigot is much smaller than the other two (Fig. 2A,B). This triad matches descriptions of the aggregate and flagelliform triad in the southern black widow *Latrodectus mactans* (Fabricius, 1775) by Moon et al. (1998). We found that the long, thin duct of the flagelliform gland is connected to the small spigot near the anterior of the two large, wide

spigots on the posterior lateral spinnerets (Fig. 2C,D). Although comparable in size and shape to aciniform glands, we identified the flagelliform glands by their more pronounced tails and longer, more robust ducts as compared to aciniform glands (Fig. 2E).

Based on morphology and spigot position, we propose that the silk glands defined as flagelliform and aggregate by Jeffery et al. (2011) instead correspond to the anterior and posterior aggregate silk glands of *L. hesperus*, respectively. The flagelliform glands described in the 2011 study are similar in size, shape (multi-lobed body) and duct morphology (long, wavy, nodulated) as the glands that we and other researchers have identified as anterior aggregate glands (e.g., Townley & Tillinghast 2013). Furthermore, the glands referred to as flagelliform by Jeffrey et al. (2011) greatly differ from previous descriptions of theridiid flagelliform silk glands (Kovoor 1987) as well as our flagelliform glands (Fig. 1H). In our dissections, we were able to track the wavy, nodulated duct of the putative anterior aggregate silk glands to the more anterior widened spigot on the posterior lateral spinnerets. Consistently, the large, short duct of the posterior aggregate silk glands led to the larger, more posterior spigot of the aggregate/flagelliform triad (Fig. 2A,B).

We depict the gross morphology of the full complement of silk glands from *L. hesperus*. Our results resolve the conflict between a recent study of black widow silk glands (Jefferey et al. 2011) and prior descriptions of aggregate and flagelliform silk glands in theridiids (Kovoor 1977; Moon et al. 1998). Although loss of aggregate silk glands has occurred in some theridiid species, losses are accompanied by a corresponding loss of silk gland spigots (Coddington 1989; Schütt 1995; Agnarsson 2004). We confirm that *L. hesperus* spiders possess two aggregate gland spigots and one flagelliform gland spigot on each of the posterior lateral spinnerets, and we found two aggregate silk gland pairs and one flagelliform silk gland pair in *L. hesperus*. Future studies could confirm the identity of each of the glands using gene expression or biochemical methods.

ACKNOWLEDGMENTS

The authors thank Nadia Ayoub, Jonathan Coddington, and Milan Rezác for helpful discussions. This work was supported by the Army Research Office W911NF-15-1-0099 to R.C.C. and C.Y.H.

LITERATURE CITED

Agnarsson, I. 2004. Morphological phylogeny of cobweb spiders and their relatives (Araneae, Araneoidea, Theridiidae). Zoological Journal of the Linnean Society 141:447–626.

Argintean, S., J. Chen, M. Kim & A.M.F. Moore. 2005. Resilient silk captures prey in black widow cobwebs. Applied Physics A 82:235–241.

Casem, M.L., L.P.P. Tran & A.M.F. Moore. 2002. Ultrastructure of the major ampullate gland of the black widow spider, *Latrodectus hesperus*. Tissue Cell 34:427–436.

Chamberlin, R.V. & W. Ivie. 1935. The black widow spider and its varieties in the United States. Bulletin of the University of Utah 25:1–29.

Clarke, T.H., J.E. Garb, C.Y. Hayashi, P. Arensburger & N.A. Ayoub. 2015. Spider transcriptomes identify ancient large-scale gene duplication event potentially important in silk gland evolution. Genome Biology & Evolution 7:1856–1870.

Coddington, J.A. 1989. Spinneret silk spigot morphology: evidence for the monophyly of orbweaving spiders, Cyrtophorinae (Araneidae), and the group Theridiidae plus Nesticidae. Journal of Arachnology 17:71–95.

Fabricius, J.C. 1775. Systema Entomologiae, Sistens Insectorum Classes, Ordines, Genera, Species, Adiectis, Synonymis, Locis Descriptionibus Observationibus. Flensburg and Lipsiae.

Garb, J.E., N.A. Ayoub & C.Y. Hayashi. 2010. Untangling spider silk evolution with spidroin terminal domains. BioMed Central Evolutionary Biology 10:243.

Jeffery, F., C. La Mattina, T. Tuton-Blasingame, Y. Hsia, E. Gnesa, L. Zhao et al. 2011. Microdissection of black widow spider silk-producing glands. Journal of Visual Experiments 47:e2382.

Kovoor, J. 1977. Donnees histochimiques sur les glandes serieigenes de la veuve noire *Latrodectus mactans* Fabr.(Araneae, Theridiidae). Annales des Sciences Naturelles Zoologie et Biologie Animale 19:63–87.

Kovoor, J. 1987. Comparative structure and histochemistry of silk-producing organs in arachnids. Pp. 160–186. *In* Ecophysiology of Spiders. (W. Nentwig, ed.) Springer Berlin Heidelberg.

Lawrence, B.A., C.A. Vierra & A.M.F. Moore. 2004. Molecular and mechanical properties of major ampullate silk of the black widow spider, *Latrodectus hesperus*. Biomacromolecules 5:689–695.

Moon, M.J., M.A. Townley & E.K. Tillinghast. 1998. Fine structural analysis of secretory silk production in the black widow spider, *Latrodectus mactans*. Korean Journal of Biological Sciences 2:145–152.

Schütt, K. 1995. *Drapetisca socialis* (Araneae: Linyphiidae): Web reduction-ethological and morphological adaptations. European Journal of Entomology 95:553–563.

Townley, M.A. & E.K. Tillinghast. 2013. Aggregate silk gland secretions of araneoid spiders. Pp. 283–302. *In* Spider Ecophysiology. (W. Nentwig, ed.) Springer Berlin Heidelberg.

Manuscript received 23 September 2016, revised 24 July 2017.

2018. Journal of Araehnology 46:162–164

SHORT COMMUNICATION

Are multiple copulations harmful? Damage to male pedipalps in the funnel-web wolf spider *Aglaoctenus lagotis* (Araneae: Lycosidae)

Macarena González: Laboratorio de Etología, Ecología y Evolución, Instituto de Investigaciones Biológicas Clemente Estable, Montevideo, Uruguay; E-mail: mmgonzalez@iibce.edu.uy

Abstract. Damage to genital struetures during eopulation has been reported in about twenty spider families, but never in Lyeosidae. *Aglaoctenus lagotis* (Holmberg, 1876), a South Ameriean wolf spider, is one of the few that live their whole lives in funnel-webs. This work reports on the damage to pedipalpal bulbs observed in males of the "southern Uruguay" form of *A. lagotis* with multiple eopulations. Observed damage eonsists of the irreversible expansion of the hematodoeha and even its explosion. A high eopulation cost resulting from multiple and long-lasting eopulations eould be eausing this damage, affeeting the mechanism of sperm transferenee in a definitive way. This is the first report of pedipalp damage in lyeosids, and also the first report of damage involving the hematodoeha in spiders.

Keywords: Copulation eost, expansion, explosion, hematodoeha, re-eopulation

Damage to genital struetures during eopulation has been reported in speeies from about twenty spider families (Uhl et al. 2010), of the 113 families eurrently known (World Spider Catalog 2017). These struetures are almost always from the male (but see Nakata 2016), and consist of pieees of the embolus or the entire pedipalp that the male leaves attached to or inside the female's genitalia, forming a mating plug (Uhl et al. 2014). These plugs are usually assoeiated with a monogynous mating system (Uhl et al. 2010). Among the spiders of the family Lyeosidae, genital damage during mating has never been reported (Fernández-Montraveta & Ortega 1990; Norton & Uetz 2005; Jiao et al. 2011; Fernández-Montraveta & Cuadrado 2013). And, although studies reporting the number of copulations that males can achieve (and their associated eosts) are searee, polygamy is likely the most widespread mating system (Huber 2005).

Aglaoctenus lagotis (Holmberg, 1876) is one of the few lyeosid spiders that, instead of having the eharaeteristie wandering habit of the family, lives its whole life in funnel-webs (Santos & Breseovit 2001). Only males leave their webs, in order to seareh for mates (Sordi 1996). The geographie distribution of the speeies is Neotropieal, from Uruguay to Venezuela, although there is a historieal taxonomie eontroversy that questions whether this is a single speeies (Santos & Breseovit 2001; González et al. 2015). In faet, two "forms" of *A. lagotis*, differing in sexual behaviour, body eoloration patterns, and phenology, are eurrently reported and have been suggested as different speeies (González et al. 2015). One differenee between the two forms is eopulation duration: long copulations (averaging 60 minutes) in the "southern Uruguay" form (SU form) and short eopulations (averaging 8 minutes) in the "eentral Argentina" form (CA form) (González et al. 2013). Other studies related to the reproductive biology of the speeies are searee (Stefani et al. 2011; González et al. 2015), and there are no reports regarding mating systems or the funetioning of sexual struetures during mating.

During observations performed to deseribe the sexual behavior of the speeies, I had oeeasionally observed a male of the SU form with a lax, white membrane, the hematodoeha, hanging from one of his pedipalpal bulbs (heneeforth referred to as "bulb") after copulation. Therefore, I deeided to quantify the oeeurrenee of this pedipalp damage in males of this form of *A. lagotis* under laboratory conditions. As I have not found previous references regarding damage in spiders involving the hematodoeha, or data about genital damage in the lyeosids, this would be the first report about them.

Forty-eight subadult individuals of *A. lagotis* were eolleeted in Piedras de Afilar, Canelones, Uruguay (34°43′44″ S, 55°30′46″ W) during Mareh and April 2016. Spiders were individually maintained in Petri dishes (9.5 em diam. x 1.5 em height), with cotton moistened with water. Individuals were fed two times a week with mealworms (*Tenebrio molitor*, Coleoptera, Tenebrionidae) and fruit flies (*Drosophila melanogaster*, Diptera, Drosophilidae), until reaehing adulthood. Room temperature during the breeding and trials period averaged 21.6 ± 3.6 °C (mean ± SD).

I exposed seven virgin males to eonseeutive randomly assigned virgin females and eheeked male palpal bulbs after eaeh sexual eneounter. Eaeh male was exposed to a new female every three days. Copulations and their eharaeteristies were reeorded with a Sony DCR-SR85 digital video eamera. Bulb observations were performed under an Olympus Stereoscopie mieroseope with a reeessed digital eamera. Males were exposed to females until they did not eourt for two eonseeutive trials. Experimental trials were earried out in glass eages (length 30 em x width 16 em x height 20 em) following previous work with the speeies (e.g., González et al. 2013). I plaeed a layer of 2 em of sand and 2 em of wood-ehips as substrate, simulating leaf litter, and Y-shaped small plant branehes were added as refuge and for web support. Eneounters were promoted on female's webs, so I plaeed eaeh virgin female in the arena five days before the trial to allow funnel-web eonstruction. Males were earefully introdueed into the margin of eaeh web and removed after 30 min if there was no eourtship, after 60 min if males eourted but did not eopulate, or after the end of eopulation. Experimental males were used between 10–15 days after reaehing adulthood; females were at least 10 days of adult age. Females were not reused. Cephalothorax width, a eommon measure of body size in spiders (Eberhard et al. 1998), and body weight of individuals were measured. Voueher speeimens were deposited in the araehnologieal eolleetion of Seeeión Entomología, Faeultad de Cieneias, Montevideo, Uruguay.

In three of the seven males evaluated (43%), damage appeared in bulbs during sueeessive sexual exposures (Table 1); irreversible expansions of the hematodoeha were observed in two eases (males A and D) and an explosion of the hematodoeha (male F) from the left bulb in another ease (Fig. 1). The three eases of irreversible damage were observed after the seeond, fourth and fifth eopulation, respectively (Table 1). The explosion of the hematodoeha was aeeompanied by the spill of transparent drops (eoming from the same bulb), probably hemolymph (see video S1, Supplemental

Table 1.—Copulations characteristics and body measurements of the experimental males.

Male	N° copulations	Cephalothorax width (mm)	Body weight (g)	Pedipalp damage	Attacks (by females)
A	2	4.7	0.203	yes	yes
B	2	4.7	0.205	no	yes
C	2	4.9	0.251	no	yes
D	4	4.7	0.224	yes	no
E	4	4.9	0.256	no	no
F	6	4.6	0.207	yes	yes
G	6	5.1	0.277	no	no

material, online at http://dx.doi.org/10.1636/JoA-S-17-017.s1, and video caption S2, online at http://dx.doi.org/10.1636/JoA-S-17-017.s2). The damage was always more accentuated in one of the male bulbs than in the other, generating asymmetries in the number of ejaculations performed, but males continued inserting both pedipalps until the end of copulation. I had already observed that the males with four and five copulations had brought their pedipalps to the mouth constantly after their previous copulation, and that their hematodochae had remained somewhat expanded even after the copulation was finished, returning to the resting position few minutes later. After the occurrence of two events of irreversible damage, females attacked males at the dismounting. However, attacks (always during dismounting) were also recorded in two other males that did not damage their bulbs (Table 1). Despite the small sample size, it is worth noting that males that achieved several copulations but did not damage their bulbs were larger and heavier to those which incurred damage.

The present study suggests that the occurrence of damage in bulbs of the males of the SU form of *A. lagotis* would occur when they copulate multiple times (lycosids always used both pedipalps during copulation). No male damaged his bulbs during the first copulation. Additionally, damage would be more frequent in smaller, lighter weight males. Therefore, considering all mentioned above, and the fact that copulations last an hour on average (longer than in the other form of the species and other lycosids, González et al. 2013), I suggest that the alteration in the functioning of the bulbs is produced by a high copulation cost, associated with extreme fatigue in pedipalps use (Rovner & Wright 1975), and that individuals with better body condition are better able to cope with this stress.

Reported events of damage in male bulbs are usually related to their functions as mating plugs, and involve parts of the embolus (Fromhage & Schneider 2006), the whole pedipalp (Ramírez & González 1999) or the entire body of the male (Andrade 1996; Foellmer & Fairbairn 2003), but no hematodochae damage, as happens in *A. lagotis*. Furthermore, within the Lycosidae family, reports of plugs are scarce (Kronestedt 1987; Szinetár et al. 2005) and do not involve parts of the body, but substances adhering to the females' epigynes. As the only two reports are based on collection data collection, is difficult to know how the plugs were produced.

I have not found references to the type of pedipalp damage reported here for other spiders. I have also not found reports about the relation between genital damage and polygyny (but see Lynam et al. 2006). Among the few species of lycosids for which there are data regarding male mating systems, *Schizocosa ocreata* (Hentz, 1844) exhibits polygamous males and long copulations (155 min on average) (Norton & Uetz 2005), but pedipalp damage is not observed. Pedipalp damage is also absent in the CA form of *A. lagotis*, although males copulate with several females (a greater number than in the SU form studied here) (Peretti et al. 2016). However, copulations are significantly shorter (8 min) (González et al. 2013), perhaps with less energetic costs per copulation and associated to a different sexual strategy, related to populations density. Finally, the experimental design employed here probably favored males' copulations, even with over enforced bulbs, as males were repeatedly exposed to virgin females, but the same procedure has been followed for the CA form without producing similar damage.

Studying the copulatory mechanism and functional morphology of *A. lagotis* pedipalps during copulation, as well as female receptivity and the amount of sperm in their spermatheehae after copulating with damaged and undamaged males, will be of interest to better understand the implications of the present report. Also, expanding research on the sexual history of males to additional families will clarify how widespread this type of genital damage is in spiders.

ACKNOWLEDGMENTS

I thank Anita Aisenberg and Fernando G. Costa for encouraging me to write this note. I am very grateful to Carlos A. Toscano-Gadea for his unconditional collaboration in field collections of individuals and the critical reading of this manuscript. I acknowledge Karen Churches for the revision of the English and the institutional support provided by PEDECIBA, UdelaR, and the ANII, Uruguay. I also thank Matthias Foellmer and another anonymous reviewer for their comments and suggestions that substantially improved the manuscript.

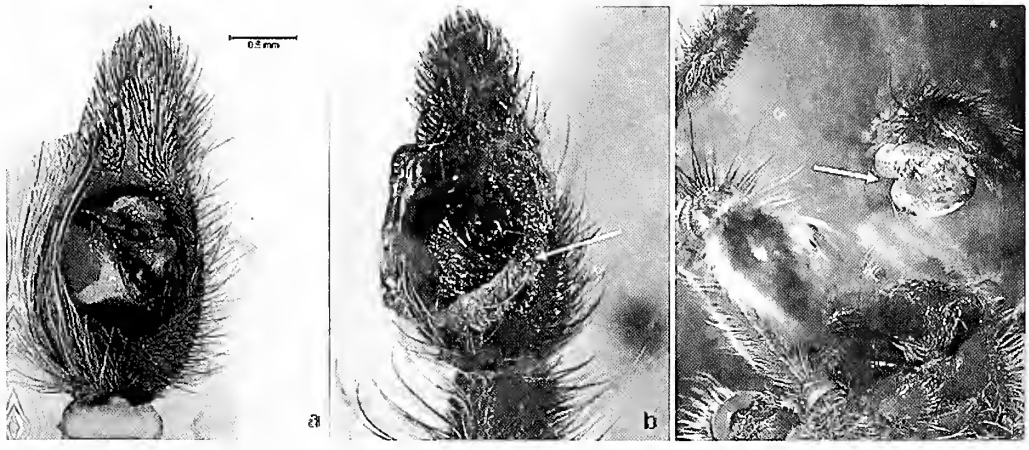

Figure 1.—Bulbs of the SU form of *A. lagotis* with damage found after copulations. (a) Normal bulb in the resting position; (b) Bulb observed with the hematodocha torn and loose ("exploded bulb"); (c) Pedipalps of a male with the left bulb irreversibly expanded.

LITERATURE CITED

Andrade, M.C.B. 1996. Sexual selection for male sacrifice in the Australian redback spider. Science 271:70–72.

Eberhard, W.G., B.A. Huber, S.R.L. Rodríguez, R.D. Briceño, L. Salas & V. Rodríguez. 1998. One size fits all? Relationships between the size and degree of variation in genitalia and other body parts in twenty species of insects and spiders. Evolution 52:415–431.

Fernández-Montraveta, C. & M. Cuadrado. 2013. *Hogna radiata* males do not deplete their sperm in a single mating. Journal of Arachnology 41:102–107.

Fernández-Montraveta, C. & J. Ortega. 1990. Some aspects of the reproductive behavior of *Lycosa tarentula fasciiventris* (Araneae, Lycosidae). Journal of Arachnology 18:257–262.

Foellmer, M.W. & D.J. Fairbairn. 2003. Spontaneous male death during copulation in an orb-weaving spider. Proceedings of the Royal Society of London B 270 (Suppl.):183–185.

Fromhage, L. & J.M. Schneider. 2006. Emasculation to plug up females: the significance of pedipalp damage in *Nephila fenestrata*. Behavioral Ecology 17:353–357.

González, M., A.V. Peretti & F.G. Costa. 2015. Reproductive isolation between two populations of *Aglaoctenus lagotis*, a funnel-web wolf spider. Biological Journal of the Linnean Society 114:646–658.

González, M., A.V. Peretti, C. Vieira & F.G. Costa. 2013. Differences in sexual behavior of two distant populations of the funnel-web wolf spider *Aglaoctenus lagotis*. Journal of Ethology 31:175–184.

Huber, B.A. 2005. Sexual selection research on spiders: progress and biases. Biological Revue 80:363–385.

Jiao, X., Z. Chen, J. Wu, H. Du, F. Liu, J. Chen et al. 2011. Male remating and female fitness in the wolf spider *Pardosa astrigera*: the role of male mating history. Behavioral Ecology and Sociobiology 65:325–332.

Kronestedt, T. 1987. On some African and Oriental wolf spiders (Araneae, Lycosidae): Redescription of *Pardosa oucka* Lawrence from Africa, with notes on its generic position. Journal of Natural History 21:967–976.

Lynam, E.C., J.C. Owens & M.H. Persons. 2006. The influence of pedipalp autotomy on the courtship and mating behavior of *Pardosa milvina* (Araneae: Lycosidae). Journal of Insect Behavior 19:63–75.

Nakata, K. 2016. Female genital mutilation and monandry in an orb-web spider. Biology Letters 2(2):12: 20150912. Online at http://dx.doi.org/10.1098/rsbl.2015.0912.

Norton, S. & G.W. Uetz. 2005. Mating frequency in *Schizocosa ocreata* (Hentz) wolf spider: Evidence for a mating system with female monandry and male polygyny. The Journal of Arachnology 33:16–24.

Peretti, A.V., M. González & D. Abregú. 2016. Level of polygyny and associated reproductive costs in a funnel-web lycosid. 20th International Congress of Arachnology, Golden, Colorado EEUU:149–150.

Ramírez, M.J. & A. González. 1999. New or little-known species of the genus *Echinotheridion* Levi (Araneae, Theridiidae). Bulletin of the British Arachnological Society 11:195–198.

Rovner, J. & E.E. Wright. 1975. Copulation in spiders: experimental evidence for fatigue effects and bilateral control of palpal insertions. Animal Behavior 23:233–236.

Santos, A.J. & A.D. Brescovit. 2001. A revision of the South American spider genus *Aglaoctenus* Tullgren, 1905 (Araneae, Lycosidae, Sosippinae). Andrias 15:75–90.

Sordi, S. 1996. Ecologia de populaçoes da aranha *Porrinosa lagotis* (Lycosidae) nas reservas Mata de Santa Genebra, Campinas (SP) e Serra do Japi, Jundai (SP). PhD Thesis, Universidade Estadual de Campinas, Sao Paulo, Brasil.

Stefani, V., K. Del-Claro, L.A. Silva, B. Guimaraes & E. Tizo-Pedroso. 2011. Mating behavior and maternal care in the tropical savanna funnel-web spider *Aglaoctenus lagotis* Holmberg (Araneae: Lycosidae). Journal of Natural History 45:1119–1129.

Szinetár, C., J. Eichardt & R. Horváth. 2005. Data on the biology of *Alopecosa psammophila* Buchar 2001 (Araneae, Lycosidae). Journal of Arachnology 33:384–389.

Uhl, G., K. Kunz, O. Vocking & E. Lipke. 2014. A spider mating plug: origin and constraints of production. Biological Journal of the Linnean Society 113:345–354.

Uhl, G., S.H. Nessler & J.M. Schneider. 2010. Securing paternity in spiders? A review on occurrence and effects of mating plugs and male genital mutilation. Genetica 138:75–104.

World Spider Catalog. 2017. World Spider Catalog. Natural History Museum Bern, online at http://wsc.nmbe.ch, version 18.0, accessed 3 February 2017.

Manuscript received 7 March 2017, revised 21 June 2017.

2018. Journal of Arachnology 46:165–169

Convergent fighting behavior in two species of Neotropical harvestmen (Opiliones): insights on the evolution of maternal care and resource defense polygyny

Solimary García-Hernández[1] and **Glauco Machado**[2]: [1]Programa de Pós-graduação em Ecologia, Instituto de Biociências, Universidade de São Paulo, São Paulo, Brazil. [2]LAGE do Departamento de Ecologia, Instituto de Biociências, Universidade de São Paulo, São Paulo, SP, 05.508-090, Brazil. E-mail: glaucom@ib.usp.br

Abstract. Males of several harvestman species fight for the possession of oviposition sites. Usually, males use spines and elongated appendages as weapons in these fights. Although males of many cranaids have spines that could be used as weapons, there is no report of male-male fights in this family. Here we describe the first case of a male-male fight in cranaids. Males of *Phareicranaus* aff. *spinulatus* face each other, extend their second pair of legs laterally, and use them to hit the second legs of the opponent. Pedipalps are kept above the chelicerae and not used to strike the opponent. The fighting behavior is remarkably similar to that described for Goniosomatinae (Gonyleptidae). We interpret morphological and behavioral similarities between cranaids and goniosomatines as convergences. Moreover, we suggest that body/egg size and predation pressure may have influenced the evolution of parental care and resource defense polygyny in these two harvestman clades.

Keywords: Cranaidae, egg-attendance, Goniosomatinae, mating system, body size

Males of several harvestman species fight each other for the possession of oviposition sites used by egg-bearing females (reviewed in Buzatto & Machado 2014). Different parts of the males' body may be modified and used as weapons in intrasexual fights. Among some species of Neopilionidae (suborder Eupnoi), for instance, males have enlarged chelicerae that are used to hit and grab the rivals (Painting et al. 2015). Among many species of the family Gonyleptidae (suborder Laniatores), males use spines on the fourth pair of legs (mainly on the coxa, trochanter, and femur) to pinch the opponent (Willemart et al. 2009; Buzatto et al. 2014). In some gonyleptid species belonging to the subfamily Goniosomatinae, males fight using their elongated second pair of legs. Fights begin with males facing each other, holding their elongated second pair of legs laterally extended, the first pair of legs retracted above the dorsal scute, and the pedipalps raised or extended forward (Fig. 1A, B). In this position, males hit each other on the tip of their second legs several times and intercalate these sequences of hits with periods of immobility. Males may also attack the opponent's first pair of legs with rapid pedipalp strikes. In most of the fights, one male runs away after some rounds of hits and the winner holds the territory, where females oviposit and remain attending the eggs (Buzatto & Machado 2008).

Although many species of Cranaidae (Laniatores) show marked sexual dimorphism (Pinto-da-Rocha & Kury 2007), and males have many spines and tubercles that could be used as weapons, there is no report of male-male fights in this family. Several cranaid species also show maternal egg attendance (García-Hernández & Machado 2017), and in some of them egg-tending females are found close to each other, suggesting the existence of harems, which are likely to be defended by territorial males (S. García-Hernández & G. Machado unpublished data). Here we describe for the first time intrasexual fights between males of an undescribed cranaid species, the Colombian *Phareicranaus* aff. *spinulatus* (Cranainae). The fighting behavior is remarkably similar to that described for goniosomatine harvestmen, and male-male fights also seem to be related to the possession of territories where females lay eggs. Considering that cranaids and goniosomatines are not closely related taxa (Pinto-da-Rocha et al. 2014; see also Fernández et al. 2017), we interpret the similarities as convergences between these two clades of Neotropical harvestmen, and discuss the selective pressures that may have favored the evolution of a mating system based on territory defense.

On December 11, 2011, we conducted a field trip to the rural zone of Santa Rita, municipality of Carmen de Viboral, Antioquia, Colombia (5°53′48.40″N, 75°12′44.96″W, 1743 m altitude). The site has high precipitation levels throughout the year (nearly 100 mm of rain per month), and is covered by pristine cloud forest. Close to the entrance of an artificial cave formerly used as a gold mining site, we found two males of *P.* aff. *spinulatus* approaching each other. We filmed and photographed the interaction between them and the descriptions we provide below are based mostly on the footage (Supplementary Material 1, available online at http://dx.doi.org/10.1636/JoA-S-17-070.s1). On July 20, 2013, we conducted a second field trip to the same site, aiming at recording other fights and gathering additional behavioral information. Although we did not find any male-male interactions in this second trip, we gathered behavioral information on female egg attendance, which is also provided here. We deposited two males of *P.* aff. *spinulatus* as voucher specimens at the Museu Nacional do Rio de Janeiro, Rio de Janeiro, Brazil (MNRJ 4283).

When we approached the cave entrance in our first field trip, we found two males of *P.* aff. *spinulatus* close together (ca. 10 cm) and facing each other on a rock wall. The males approached each other and stopped with the frontal part of their bodies nearly 2-3 cm apart (Fig. 1C, D). In this position, the first pair of legs of both males was retracted above the dorsal scute (Fig. 1C). The second pair of legs was widely extended laterally and, during most part of the interaction, both males performed fast frontward-backward movements with these legs (Figs, 1C, D). With the fast movements, the tips

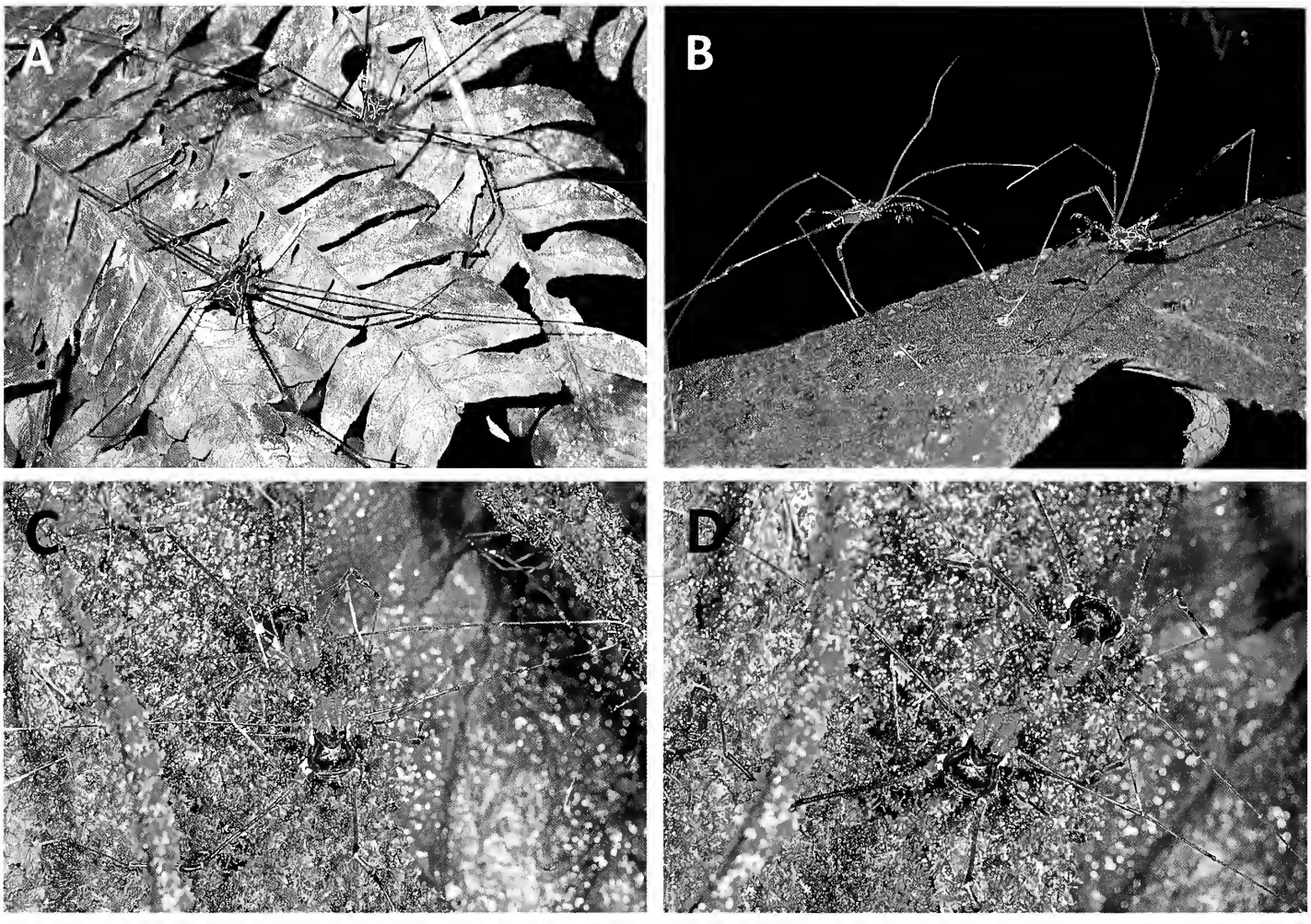

Figure 1.—(A & B) Males of the harvestman *Serracutisoma proximum* (Gonyleptidae: Goniosomatinae) fighting on the vegetation in the Atlantic Forest, São Paulo, Brazil (photos: Bruno A. Buzatto). During the fight, the males face each other, keep their second pair of legs extended laterally, and use these legs to hit the legs of the opponent. Note that in (A) the first pair of legs of both males is retracted above the dorsal scute and in (B) these legs are gently touching each other. During the fight, males rarely use these legs to touch each other, but their pedipalps are stretched frontwards and occasionally used to strike the front legs of the opponent. (C & D) Males of the harvestman *Phareicranaus* aff. *spinulatus* (Cranaidae) fighting on a rock in a Colombian cloud forest (photos: Sebastián Vieira-Uribe). The general posture and the behavior of the fighting males is remarkably similar to those described for *S. proximum*. The main differences are that pedipalps are not stretched frontwards (C & D), and the first pair of legs is not retracted above the dorsal scute in *P.* aff. *spinulatus* — instead, these legs are used to touch and tap the pedipalps and front legs of the opponent (D).

of the second pair of legs (mostly the tibia, tarsus, and metatarsus) of both males whipped each other. The hitting with the second pair of legs was intercalated with brief periods of immobility. Occasionally, the first pair of legs was extended forward and used to touch or quickly tap the pedipalps, first and second pair of legs of the opponent (Fig. 1D). During the entire interaction, the pedipalps of both males were kept retracted above the chelicerae, and were not used to strike the opponent (Fig. 1C, D). The interaction lasted 15 min, from 15:50 h to 16:05 h, after which the males were probably disturbed by the light of our flashes and left the place. We found no females close to the place where we observed the two males fighting, but there was another conspecific male nearly 0.5 m from the fighting males.

In our second field trip, we did not find males fighting each other, but found two females of *P.* aff. *spinulatus* attending their eggs in a damp pocket of a roadside bank (Fig. 2A). They were both prostrated on a clutch of eggs, in the typical egg-tending posture observed in many species of Laniatores (Machado & Macías-Ordóñez 2007). Eggs were laid in a single layer on the substrate, and in both clutches, the eggs had a small amount of debris attached to their surface (Fig. 2B). The mean egg diameter was 2.75 mm (SD = 0.08 mm; $n = 8$), representing 24% of the female's dorsal scute length (Fig. 2B). The number of eggs in one of the clutches was 22, and the distance between the two egg-tending females was nearly 2 m (Fig. 2A). The other clutch was inside a crack, so that it was not possible to count the eggs. In between the two egg-tending females, we found an adult male. In this trip, we also found another adult male in a similar damp pocket several meters away in another roadside bank. No female or egg clutch was found close to this male.

In a recent molecular phylogeny, the family Cranaidae appears within the family Gonyleptidae, as the sister group to

Figure 2.—(A) Damp pocket in a roadside bank where we found two egg-tending females (F) and a large adult male (M) of *Pharecranaus* aff. *spinulatus*. Only one female is visible in the photo (circle); the other female and the male were inside a rock crack and below roots and vines, respectively, but their positions are indicated by arrows (photo: Sebastián Vieira-Uribe). Scale bar = 0.5 m. (B) Egg-tending female of *P.* aff. *spinulatus* prostrated on a clutch containing 22 large eggs in early stages of embryonic development. Note that the eggs are covered by debris, which is probably attached to the egg surface by the egg-tending female (photo: Sebastián Vieira-Uribe).

the subfamily Ampycinae, and closely related to the clade K92 and the subfamily Manaosbiinae (Pinto-da-Rocha et al. 2014). The subfamily Goniosomatinae is located far from the clade including the Cranaidae (Pinto-da-Rocha et al. 2014). Although the phylogenetic position of the Cranaidae as a clade within the Gonyleptidae still deserves further investigation, cranaids and goniosomatines clearly do not share a recent common ancestor. Moreover, whereas cranaids occur mostly in the northern region of South America, along the Andes and Amazon Basin up to Panama (Pinto-da-Rocha & Kury 2007), goniosomatines are restricted to the Atlantic forest, from southern to northeastern Brazil (DaSilva & Gnaspini 2009). Despite the distant phylogenetic relationship between cranaids and goniosomatines, it is remarkable that they show so many convergences. Pinto-da-Rocha & Kury (2003) were the first to point out some morphological convergences between them, including large body size, stout and long legs bearing few spines, and robust and heavily armed pedipalps. Three years later, Machado & Warfel (2006) added other convergent traits related to behavior, such as maternal egg attendance of large eggs laid mostly on rock walls and damp pockets in roadside banks. The findings reported here extend the number of behavioral convergences to several traits of the mating system, which will be discussed below.

The general fighting behavior of *P.* aff. *spinulatus* is very similar to that described for the goniosomatine *Serracutisoma proximum* (Mello-Leitão, 1922) (Buzatto & Machado 2008; Fig. 1A, B), and has no parallel with other harvestmen for which fights have already been described (see Buzatto & Machado 2008 and Painting et al. 2015). Males of both species face each other, keep their first pair of legs retracted above the body, and hit the second pair of legs of the opponent using their own second pair of legs (see video in Supplementary Material 1, online at http://dx.doi.org/10.1636/JoA-S-17-070.s1). One difference is that males of *S. proximum* use their pedipalps to strike the opponent and grasp his pedipalps or first pair of legs. After that, the grasped appendage may be chewed on and amputated by the chelicerae of the attacking male (Buzatto & Machado 2008). In *P.* aff. *spinulatus*, males keep the pedipalps retracted above the chelicerae during the entire fight, and they did not extend them frontwards or use them to grasp the opponent (compare pedipalpal posture between Fig. 1A, B and 1C-D). Probably as a consequence of the pedipalpal strikes, the first pair of legs in *S. proximum* is rarely used to touch the first pair of legs of the opponent (e.g., Fig. 1B). In *P.* aff. *spinulatus*, however, the first pair of legs is frequently used to touch and tap the opponent (Supplementary Material 1) — perhaps to acquire information on his posture and/or strength because cranaids, like most harvestman species, are unable to form visual images (Acosta & Machado 2007).

Male-male fights in *P.* aff. *spinulatus* are probably related to the possession of a territory that is used by females as oviposition site. Our suggestion is based mainly on the fact that males were fighting without any conspecific female around. This is a pattern typically observed in resource defense polygynies, a mating system in which males defend territories that attract females due to the presence of food, shelter or oviposition sites (Ostfeld 1987). The presence of an adult male close to egg-tending females is also a pattern commonly reported for many other harvestman species exhibiting a resource defense mating system (Machado et al. 2015). As it occurs with all goniosomatines studied so far (Machado 2002), females of *P.* aff. *spinulatus* seem to attend eggs inside the males' territories, and the putative harem we found had two egg-tending females. In some harem-defending harvestman species, there are two male morphs with different mating tactics. Large and heavily-armed males (majors) usually defend territories and guard their mates for as much as two days after mating, whereas small and poorly-armed males (minors) rely mostly on harem invasion, sneak copulations, and very rarely

exhibit mate guarding (Buzatto & Machado 2014). This is the case of *S. proximum*, in which majors have a second pair of legs almost twice as long as those of minors and females, probably because these legs are used as weapons in territorial fights and only majors fight for territory possession (Buzatto et al. 2011). Unfortunately, we do not have many individuals of *P.* aff. *spinulatus* deposited in museums to test whether their second pair of legs is also sexually and intra-sexually dimorphic. Though, according to our view, the existence of two male morphs with different mating tactics in *P.* aff. *spinulatus* would not be surprising.

Why are there so many morphological and behavioral convergences between cranaids and goniosomatines? Whereas goniosomatines are relatively well-studied harvestmen, the same is not true for cranaids, and this lack of basic biological knowledge hampers a strongly supported answer for this question. However, it is reasonable to say that species of these two clades are ecological equivalents, defined as non-closely related taxa that occupy similar habitats, belong to the same guild, and perform similar ecological functions in different biomes (Pianka 1974; Gitay et al. 1996). Cranaid and goniosomatine species live mostly in tropical forests, where they are found foraging mainly on the vegetation at night (e.g., Acosta & Machado 2007; Proud et al. 2012; Caetano & Machado 2013; Colmenares & Tourinho 2014). Moreover, both in the Atlantic and in the Amazon forest, species of these two clades are the largest representatives of the harvestmen community, feeding mostly on large prey, such as cockroaches, moths, beetles, and even frogs (Table S1 in Supplementary Material 2, available online at http://dx.doi.org/10.1636/JoA-S-17-070.s2, and Figure S1 in Supplementary Material 3, available online at http://dx.doi.org/10.1636/JoA-S-17-070.s3). Some species of the two clades can also be found inside caves, where they also feed mostly on large prey, including earthworms, cave crickets, and wandering spiders (Table S1 in Supplementary Material 2). Considering that the sister groups to both cranaids and goniosomatines are composed mostly of small-bodied, short-legged, and ground-dwelling species (Pinto-da-Rocha et al. 2014), we argue that three morphological traits found in these two clades, namely large body size, long legs, and heavily armed pedipalps, evolved convergently under selection for the use of large prey and/or a greater spectrum of prey sizes living on the vegetation (see further discussion on leg length and vegetation use in Curtis & Machado 2007 and Caetano & Machado 2013).

In a comparative study with insects, a positive relationship has been found between female and egg sizes (Gilbert & Manica 2010). Another comparative study with frogs found an association between parental care and large egg size, and showed that the evolution of large egg size precedes the evolution of parental care (Summers et al. 2006). Based on these life-history patterns found for terrestrial ectotherms, we propose a hypothetical evolutionary scenario that accounts for many behavioral convergences between cranaids and goniosomatines. First, natural selection favoring large body size in species of both clades may have promoted a side effect: large females tend to lay large eggs, which have proportionately lower respiratory and metabolic rates, and slower development rate (Sargent et at. 1987). Assuming that instantaneous egg mortality is constant throughout embryonic development, the longer the development, the higher is offspring mortality. If parental presence reduces mortality risk of eggs with slow development (as it is the case in harvestmen, see review in Santos et al. 2017), theory predicts that parental care should evolve (Klug & Bonsall 2009). Once parental care has evolved, the next step should be the evolution of oviposition site selection, because inadequate sites may expose both the eggs and the parents to unfavorable biotic and abiotic conditions (Mousseau & Fox 1998). Females of several predatory species living on the vegetation and exhibiting maternal care indeed select oviposition sites (Osses et al. 2008 and references therein). Finally, whenever the preferred oviposition sites can be economically defended by males, we should expect the evolution of a resource defense polygyny mating system (Emlen & Oring 1977). This evolutionary scenario explains why cranaids and goniosomatines are so large, lay large eggs, exhibit maternal egg attendance, and have a mating system based on resource defense, in which males fight for the possession of oviposition sites. Our hypothetical scenario also proposes a series of evolutionary transitions that could be formally tested when the availability of basic information on the biology of a larger set of cranaid and gonyleptid species allows comprehensive comparative studies.

ACKNOWLEDGMENTS

We thank Sebastián Vieira-Uribe and Luis Pérez for shooting the video, taking the photos of the male-male fight and the egg-tending females in *Phareicranaus*, and for providing us all these material to write this note, Bruno A. Buzatto for taking the photos of the male-male fight in *Serracutisoma* and for commenting an early version of the manuscript, Abel Pérez González, John A. Uribe, Louise M. Alissa, Margy Green, and Paul Bertner for allowing us to use the photos included in Fig. S1 of the Supplementary Material, Osvaldo Villareal-Manzanilla for identifying several cranaid species mentioned here, and Alexandre V. Palaoro and two anonymous reviewers for comments on the manuscript. SGH is supported by a student grant from São Paulo Research Foundation (FAPESP 2017/05283-1), and GM is support by research grants from São Paulo Research Foundation (FAPESP 2015/10448-4) and National Counsel of Technological and Scientific Development (CNPq 306550/2014-8).

LITERATURE CITED

Acosta, L.E. & G. Machado. 2007. Diet and foraging. Pp. 309–338. *In* Harvestmen: The Biology of Opiliones (R. Pinto-da-Rocha, G. Machado & G. Giribet, eds.). Harvard University Press, Cambridge, MA.

Buzatto, B.A. & G. Machado. 2008. Resource defense polygyny shifts to female defense polygyny over the course of the reproductive season of a Neotropical harvestman. Behavioral Ecology and Sociobiology 63:85–94. doi:10.1007/s00265-008-0638-9.

Buzatto, B.A. & G. Machado. 2014. Male dimorphism and alternative reproductive tactics in harvestmen (Arachnida: Opiliones). Behavioural Processes 109A:2–13. doi:10.1016/j.beproc.2014.06.008.

Buzatto, B.A., G.S. Requena, R.S. Lourenço & G. Machado. 2011. Conditional male dimorphism and alternative reproductive tactics in a Neotropical arachnid (Opiliones). Evolutionary Ecology 25:331–349. doi:10.1007/s10682-010-9431-0.

Buzatto, B.A., J.L. Tomkins, L.W. Simmons & G. Machado. 2014. Correlated evolution of sexual dimorphism and male dimorphism in a clade of Neotropical harvestmen. Evolution 68:1671–1686. doi:10.1111/evo.12395.

Cactano, D.S. & G. Machado 2013. The ecological tale of Gonyleptidae (Arachnida, Opiliones) evolution: phylogeny of a Neotropical lineage of armoured harvestmen using ecological, behavioural and chemical characters. Cladistics 29:589–609. doi:10.1111/cla.12009.

Colmenares, P.A. & A.N. Tourinho. 2014. Two new species of *Phareicranaus* Roewer, 1913 (Opiliones: Laniatores: Cranaidae), with notes on gregarious behavior and maternal care in *Phareicranaus manamara*. Zootaxa 3768:59–72. doi:10.11646/zootaxa.3768.1.4.

Curtis, D.J. & G. Machado. 2007. Ecology. Pp. 280–308. *In* Harvestmen: The Biology of Opiliones (R. Pinto-da-Rocha, G. Machado & G. Giribet, eds.). Harvard University Press, Cambridge, MA.

DaSilva, M.B. & P. Gnaspini. 2009. A systematic revision of Goniosomatinae (Arachnida: Opiliones: Gonyleptidae), with a cladistic analysis and biogeographical notes. Invertebrate Systematics 23:530–624. doi:10.1071/IS09022.

Emlen, S.T. & L.W. Oring. 1977. Ecology, sexual selection, and the evolution of mating systems. Science 197:215–223.

Fernández, R., P.P. Sharma, A.L. Tourinho & G. Giribet. 2017. The Opiliones tree of life: shedding light on harvestmen relationships through transcriptomics. Proceedings of the Royal Society of London, Biological Series 284:20162340. doi:10.1098/rspb.2016.2340.

García-Hernández, S. & G. Machado. 2017. Effectiveness of maternal egg attendance in an exclusively cave-dwelling harvestman (Arachnida: Opiliones). Journal of Zoology 302:228–235. doi:10.1111/jzo.12452.

Gilbert, J.D.J. & A. Manica. 2010. Parental care trade-offs and life-history relationships in insects. American Naturalist 176:212–226. doi:10.1086/653661.

Gitay, H.G., J.B. Wilson & W.G. Lee. 1996. Species redundancy: a redundant concept? Journal of Ecology 84:121–124. doi:10.2307/2261706.

Klug, H. & M.B. Bonsall. 2009. Life history and the evolution of parental care. Evolution 64:823–835. doi:10.1111/j.1558-5646.2009.00854.x.

Machado, G. 2002. Maternal care, defensive behavior, and sociality in Neotropical *Goniosoma* harvestmen (Arachnida, Opiliones). Insectes Sociaux 49:388–393. doi:0020-1812/02/040388-06.

Machado, G. & R. Macías-Ordóñez. 2007. Reproduction. Pp. 414–454. *In* Harvestmen: The Biology of Opiliones (R. Pinto-da-Rocha, G. Machado & G. Giribet, eds.). Harvard University Press, Cambridge, MA.

Machado, G. & J. Warfel. 2006. First case of maternal care in the family Cranaidae (Opiliones, Laniatores). Journal of Arachnology 34:269–272. doi:10.1636/S04-63.1.

Machado, G., G.S. Requena, C. Toscano-Gadea, E. Stanley & R. Macías-Ordóñez. 2015. Male and female mate choice in harvestmen: general patterns and inferences on the underlying processes. Pp. 169–201. *In* Cryptic Female Choice in Arthropods: Patterns, Mechanisms and Prospects (A.V. Peretti & A. Aisenberg, eds.). Springer, Switzerland.

Mousseau, T.A. & C.W. Fox. 1998. The adaptive significance of maternal effects. Trends in Ecology and Evolution 13:403–407. doi:10.1016/S0169-5347(98)01472-4.

Osses, F., E.G. Martins & G. Machado. 2008. Oviposition site selection by the bromeliad-dweller harvestman *Bourguyia hamata* (Arachnida: Opiliones). Journal of Ethology 26:233–241. doi:10.1007/s10164-007-0054-z.

Ostfeld, R.S. 1987. On the distinction between female defense and resource defense polygyny. Oikos 48:238–240. doi:10.2307/3565861.

Painting, C.J., A.F. Probert, D.J. Townsend & G.I. Holwell. 2015. Multiple exaggerated weapon morphs: a novel form of male polymorphism in harvestmen. Scientific Reports 5:16368. doi:10.1038/srep16368.

Pianka, E.R. 1974. Evolutionary Ecology. Harper & Row, New York, NY.

Pinto-da-Rocha, R. & A.B. Kury. 2003. Phylogenetic analysis of *Santinezia* with description of five new species (Opiliones, Laniatores, Cranaidae). Journal of Arachnology 31:173–208. doi:10.1636/0161-8202(2003)031[0173:PAOSWD]2.0.CO;2.

Pinto-da-Rocha, R. & A.B. Kury. 2007. Cranaidae. Pp. 185–188. *In* Harvestmen: The Biology of Opiliones (R. Pinto-da-Rocha, G. Machado & G. Giribet, eds.). Harvard University Press, Cambridge, MA.

Pinto-da-Rocha, R., C. Bragagnolo, F.P.L. Marques & M.A. Junior 2014. Phylogeny of harvestmen family Gonyleptidae inferred from a multilocus approach (Arachnida: Opiliones). Cladistics 30:519–539. doi:10.1111/cla.12065.

Proud, D.N., B.E. Felgenhauer, V.R. Townsend Jr., D.O. Osula, W.O. Gilmore III, Z.L. Napier et al.2012. Diversity and habitat use of Neotropical harvestmen (Arachnida: Opiliones) in a Costa Rican rainforest. ISRN Zoology 2012:ID 549765. doi:10.5402/2012/549765.

Santos, E.S.A., P.P. Bueno, J.D.J. Gilbert & G. Machado. 2017. Macroecology of parental care in arthropods: higher mortality risk leads to higher benefits of offspring protection in tropical climates. Biological Reviews 92:1688–1701. doi:10.1111/brv.12303.

Santos-Silva, N.F. & R.H. Willemart. 2015. Foraging, oviposition sites and notes on the natural history of the harvestman *Heteromitobates discolor* (Opiliones, Gonyleptidae). Biota Neotropica 15(3): e20140186. doi:10.1590/1676-06032015018614.

Sargent, R.C., P.D. Taylor & M.R. Gross. 1987. Parental care and the evolution of egg size in fishes. American Naturalist 129:32–46. doi:10.1086/284621.

Summers, K., C.S. McKeon & H. Heying. 2006. The evolution of parental care and egg size: a comparative analysis in frogs. Proceedings of the Royal Society of London, Biological Series 273:687–692. doi:10.1098/rspb.2005.3368.

Willemart, R.H., F. Osses, M.C. Chelini, R. Macías-Ordóñez & G. Machado. 2009. Sexually dimorphic legs in a Neotropical harvestman (Arachnida, Opiliones): ornament or weapon? Behavioural Processes 80:51–59. doi:10.1016/j.beproc.2008.09.006.

Manuscript received 21 August 2017, revised 1 October 2017.

2018. Journal of Arachnology 46:170–171

INSTRUCTIONS TO AUTHORS

(revised January 2018)

All manuscripts are submitted online at
http://www.editorialmanager.com/arachno

General: The *Journal of Arachnology* publishes scientific articles reporting novel and significant observations and data regarding any aspect of the biology of arachnid groups. Articles must be scientifically rigorous and report substantially new information. Submissions that are overly narrow in focus (e.g., local faunal lists, descriptions of a second sex or of a single species without additional discussion of the significance of this information), that have poorly substantiated observational data, or that present no new information will not be considered. Book reviews will not be published.

Manuscripts must be in English and should use the active voice throughout. Authors should consult a recent issue of the *Journal of Arachnology* for additional points of style. Manuscripts longer than three printed journal pages (12 or more double-spaced manuscript pages) should be prepared as Feature Articles, shorter papers as Short Communications. Invited Reviews will be published from time to time and unsolicited reviews are also welcomed. All reviews will be subject to the same review process as other submissions.

Submission: Manuscripts should be prepared in Microsoft Word and submitted electronically via our online system, *PeerTrack* (http://www.editorialmanager.com/arachno). *PeerTrack* will guide you through the step-by-step process including uploading the manuscript and all of its parts. The paper can be uploaded as one piece, with tables, figures, and appendices embedded, or as text, then tables, figures, and appendices, each uploaded individually. Ultimately, *PeerTrack* will assemble all parts of the paper into a PDF that you, as corresponding author, will need to approve before the submission process can be completed. Supplemental Materials (see below) can also be uploaded, but they are not bundled into the PDF. If the manuscript is accepted for publication, authors are responsible for ensuring that all figures are submitted as individual image files that meet the required resolution and dimensions (see "**Illustrations**" below). These may be submitted to *PeerTrack* or directly to the editor-in-chief.

Voucher Specimens: Specimens of species used in your research should be deposited in a recognized scientific institution. All type material *must* be deposited in a recognized collection/institution and the identity of the collection must be given in the text of the manuscript.

Checklist—Common Formatting Errors is available as a PDF at http://www.americanarachnology.org/JOA.html# instructions

FEATURED ARTICLES

Title page.—The title page includes the complete name, address, and e-mail address of the corresponding author; the title in bold text and sentence case; each author's name and address; and the running head.

Running head.—This should be in all capital letters, not exceeding 60 characters and spaces, and placed at the top of the title page. It should be composed of the authors' surnames and a short title. Examples: SMITH—SALTICIDS OF PANAMA; SMITH & CRUZ—SALTICIDS... ; SMITH ET AL.—SALTICIDS...

Abstract.—Length: ≤ 250 words for Feature Articles; ≤ 150 words for Short Communications.

Keywords.—Give 3–5 appropriate keywords or phrases following the abstract. *Keywords should not duplicate words in the title.*

Text.—Double-space text, tables, legends, etc. throughout. Except for titles and headers, all text should be left-justified. Do not add line numbers—they are automatically added by *PeerTrack*. Three levels of heads are used.

- The first level (METHODS, RESULTS, etc.) is typed in capitals and centered on a separate line.
- The second level head begins a paragraph with an indent, is in bold type, and is separated from the text by a period and a dash.
- The third level may or may not begin a paragraph but is italicized and separated from the text by a colon.

Use only the metric system unless quoting text or referencing collection data. If English measurements are used when referencing collection data, then metric equivalents should also be included parenthetically. All decimal fractions are indicated by a period (e.g., 3.141). Include geographic coordinates for collecting locales if possible, using one of the following formats: 0°12′32″S, 29°52′17″E or 0.2089°S, 29.8714°E.

Citation of references in the text: Cite only papers already published or in press. Include within parentheses the surname of the author followed by the date of publication. A comma separates multiple citations by the same author(s) and a semicolon separates citations by different authors, e.g., (Smith 1970), (Jones 1988; Smith 1993), (Smith & Jones 1986, 1987; Jones et al. 1989). Include a letter of permission from any person who is cited as providing unpublished data in the form of a personal communication.

Citation of taxa in the text: Include the complete taxonomic citation (author, year) for each arachnid genus and/or species name when it first appears in the abstract and text proper. For example, *Araneus diadematus* Clerck, 1757. For Araneae, this information can be found online at www.wsc.nmbe.ch. Citations for scorpions can be found in the *Catalog of the Scorpions of the World (1758–1998)* by V. Fet, W.D. Sissom, G. Lowe & M.E. Braunwalder. Citations for the smaller arachnid orders (pseudoscorpions, solifuges, whip scorpions, whip spiders, schizomids, ricinuleids and palpigrades) can be found at museum.wa.gov.au/catalogues-beta/. Citations for some species of Opiliones can be found in the *Annotated Catalogue of the Laniatores of the New World (Arachnida,Opiliones)* by A.B. Kury.

Literature cited.—Use the following style and formatting exactly as illustrated; include the full unabbreviated journal title.

Personal web pages should not be included in Literature Cited. These can be cited within the text as (John Doe, pers. website) without the URL. Institutional websites may be included in Literature Cited. If a citation includes more than six authors, list the first six and add "et al." to represent the others.

Binford, G. 2013. The evolution of a toxic enzyme in sicariid spiders. Pp. 229–240. *In* Spider Ecophysiology. (W. Nentwig, ed.). Springer-Verlag, Heidelberg.

Cushing, P.E., P. Casto, E.D. Knowlton, S. Royer, D. Laudier, D.D. Gaffin et al. 2014. Comparative morphology and functional significance of setae called papillae on the pedipalps of male camel spiders (Arachnida, Solifugae). Annals of the Entomological Society of America 107:510–520.

Harvey, M.S. & G. Du Preez. 2014. A new troglobitic ideoroncid pseudoscorpion (Pseudoscorpiones: Ideoroncidae) from southern Africa. Journal of Arachnology 42:105–110.

World Spider Catalog. 2015. World Spider Catalog. Version 16. Natural History Museum, Bern. Online at http://wsc.nmbe.ch/

Roewer, C.F. 1954. Katalog der Araneae, Volume 2a. Institut Royal des Sciences Naturelles de Belgique, Bruxelles.

Rubio, G.D., M.O. Arbino & P.E. Cushing. 2013. Ant mimicry in the spider *Myrmecotypus iguazu* (Araneae: Corinnidae), with notes about myrmecomorphy in spiders. Journal of Arachnology 41:395–399.

Footnotes.—Footnotes are permitted on the first page, only to give current address or other author information, and at the bottom of tables (see below).

Taxonomic articles.—Consult a recent taxonomic article in the *Journal of Arachnology* for style or contact a Subject Editor for Systematics. Papers containing original descriptions of focal arachnid taxa should be listed in the Literature Cited section.

Tables.—Each table, with the legend above, should be placed on a separate manuscript page. Only horizontal lines (usually no more than three) should be included. When necessary, tables may have footnotes, for example, to specify the meanings of symbols about particular data.

Illustrations.—Original illustrations include photographs, line drawings, maps, and other graphic representations. All should be considered figures and numbered consecutively with other figures. You should ensure that all illustrations, at submission, are at high enough resolution to be useful to editors and reviewers; 300 dpi is usually sufficient. When preparing images, consider the final dimensions of the image on a printed page. Images may be printed at a width of one column (20.8 picas, 3.45 inches or 8.8 cm), one and a half columns (31.3 picas, 5.2 inches or 13.25 cm) or two columns (43.3 picas, 7.2 inches or 18.3 cm). Maximum height for all printed images is 49.8 picas, 8.3 inches or 21.08 cm. Thus, if a figure must be printed two columns wide to be legible, its corresponding vertical dimension cannot be greater than 21.08 cm.

At the discretion of the Editor-in-Chief, a figure can be rendered in color in the online version but in monochrome in the journal's printed version, or in color in both versions if warranted by the figure's context and content. Address all questions concerning illustrations to the Editor-in-Chief of the *Journal of Arachnology*: **Deborah R. Smith, Editor-in-Chief** [*E-mail:* debsmith@ku.edu].

Legends for illustrations should be placed together on the same page(s). Each plate must have only one legend, as indicated below:

Figures 1–4. *A-us x-us*, male from Timbuktu: 1. Left leg. 2. Right chelicera. 3. Dorsal aspect of genitalia. 4. Ventral aspect of abdomen.

The following alternate Figure numbering is also acceptable:

Figure 1a–e. *A-us x-us*, male from Timbuktu: a. Left leg. b. Right chelicera. c. Dorsal aspect of genitalia. d. Ventral aspect of abdomen.

Assemble manuscript.—The manuscript should be assembled in the following sequence: title page, abstract, text, tables with legends, figure legends, figures. As noted above, at the time of submission the paper can be uploaded as one piece, with tables, figures, and appendices embedded, or as text, then tables, figures, and appendices, each uploaded individually. However, if manuscripts are accepted for publication, figures (or plates) must be provided in individual files.

Supplemental materials.—Authors may submit materials for online publication that importantly augment the contents of a manuscript. These may be audio files (e.g., .mp3, .m4a, .aif, .wav), video files (e.g., .mov, .m4v, .flv, .avi), or Word documents (e.g., .doc, .docx) for large tables of data. Consult with the Editor-in-Chief if you are considering submitting other kinds of files. Audio and video files should be carefully edited before submission to eliminate leaders, trailers, and other extraneous content. Individual files may not exceed 10MB; no more than five files may be included as supplemental materials for a manuscript.

Supplemental materials will be considered by reviewers and therefore must be included at the time of manuscript submission. Supplemental materials are published online at the discretion of the editors.

SHORT COMMUNICATIONS

Short Communications are usually limited to 3–4 journal pages, including tables and figures (11 or fewer double-spaced manuscript pages including Literature Cited; no more than 2 figures or tables). Internal headings (METHODS, RESULTS, etc.) are omitted. Short communications must include an abstract and keywords.

Page charges.—Page charges are voluntary, but authors who are not members of the American Arachnological Society are strongly encouraged to pay in full or in part for their articles ($75 per journal page).

Proofs.—The Journal's expectation is that the final revision of a manuscript, the one that is ultimately accepted for publication, will not require substantive changes. Accordingly, the corresponding author will be charged for excessive numbers of changes made in the proofs.

Reprints.—PDFs of papers published in the *Journal of Arachnology* are available to AAS members at the society's web site. They are also available through BioOne (www.bioone.org) and JSTOR (www.jstor.org) if you or your institution is a member of BioOne or JSTOR. PDFs of articles older than one year are freely available from the AAS website.

COVER ARTWORK

Authors are encouraged to send high quality color photographs to the Editor-in-Chief to be considered for use on the cover. Images should be at least 300 dpi.

The following individuals contributed to the quality of the *Journal of Arachnology* in 2017 by serving as reviewers. Their labors are gratefully acknowledged.

Miquel Arnedo
Gilbert Barrantes
Tobias Bauer
Suresh Benjamin
Tharina Bird
Klaus Birkhofer
Alexandre Bonaldo
Dries Bonte
Antonio Brescovit
Chris Brown
Philip Brownell
Roman Bucher
Bruno Buzatto
Alan Cady
Ronald Clouse
Julia Cosgrove
Paula E. Cushing
Anne Danielson-Francois
Jean-Francois David
Gary Dodson
Michael L.Draney
Jason Dunlop
Nadine Dupérré
G. B. Edwards
Mark Elgar
Lauren Esposito
Nelson Ferretti
Matthias Foellmer
Stefan Foord
Volker Framenau
Oscar Francke
Guilherme Gainett
Gonzalo Giribet
Marco Gottardo
Jose Guadanucci
Ambros Hänggi
Brent Hendrixson
Joh Henschel
Mariella Herberstein
Volker Herzig
H. Hofer
Bernhard A. Huber
Joel Huey
Rudy Jocqué
Carl Kloock
Matjaž Kuntner
Witold Lapinski
Skye Long
Glauco Machado
Wayne Maddison
Volker Mahnert
Stefano Mammola
Jochen Martens
Susan Masta
Amanda Mendes
Florian Menzel
Plamen Mitov
Liliana M. Mola
Jordi Moya-Larano
Kensuke Nakata
Wolfgang Nentwig
Martin Nyffeler
Hirostugu Ono
Vera Opatova
Brent Opell
Stano Pekar
Alfredo Peretti
Abel Perez Gonzalez
Fernando Pérez-Miles
Matthew Persons
Luis Piacentini
Malayka S. Picchi
Ricardo Pinto-da-Rocha
Simon Pollard
Lorenzo Prendini
Daniel Proud
Jonathan N. Pruitt
Jessica Purcell
Robert Raven
Sarah Reed-Guy
Ann Rypstra
Alexander Sánchez-Ruiz
Jutta M. Schneider
Steven Schwartz
Peter Schwendinger
Catherine Scott
Michael Seiter
Andrew Sensenig
Jeff Shultz
Migugel Simo
Kamiel Spoelstra
James Starrett
Robert Suter
Támas Szüts
Søren Toft
Victor R. Townsend
Gabriele Uhl
Arie van der Meijen
Cor Vink
J. Colton Watts
Dustin J. Wilgers
Rodrigo H. Willmart
Jonas Wolff
Juan Zaragoza

CONTENTS

Journal of Arachnology

Volume 46 **Number 1**

Featured Articles

Short Communications